

Book of Abstracts

# 10<sup>th</sup> EUROPEAN LS-DYNA CONFERENCE

---

15 - 17 JUNE 2015 – WÜRZBURG, GERMANY



Courtesy of Daimler AG

Platinum Sponsors



Microsoft Azure



Book of Abstracts

# 10<sup>th</sup> EUROPEAN LS-DYNA CONFERENCE

---

15 – 17 June 2015, Würzburg, Germany

The conference is organized by



in association with



## Copyright

Copyright © 2015 by DYNAMore GmbH. Permission to reproduce any papers contained herein is granted provided that credit is given to DYNAMore, the author, and his/her company. Authors retain their respective copyrights.

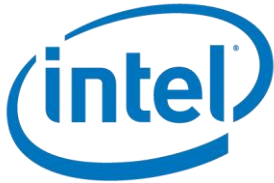
DYNAMore GmbH, Industriestr. 2, D-70565 Stuttgart, Germany  
Tel. +49 (0)711 - 459600 – 0, E-Mail: [info@dynamore.de](mailto:info@dynamore.de), Web: [www.dynamore.de](http://www.dynamore.de)

ISBN 978-3-9816215-2-5



Sponsors

Platinum



Microsoft Azure

Gold



Silver





---

**PLENARY AND KEYNOTE PRESENTATIONS I** **PAGES 23 - 30**

Plenary Presentations, Monday 15 June, 13:00 – 15:00 Page

---

**Recent Developments in LS-DYNA – Part I + 2**

J. O. Hallquist, B. Wainscott and other developers (LSTC) ..... 25

**Crash CAE in the all New Volvo XC90 and SPA Platform**

A. Sandahl, J. Jergeus, O. Centeno, D. Macri, A. Ericsson, W. Wu, E. Claesson,  
P. A. Eggertsen, M. Retzlaff, M. Khoo (Volvo Car) ..... 27

**Modeling the Press Hardening Process**

Prof. M. Oldenburg (Luleå University of Technology) ..... 28

**Big Compute/HPC in Microsoft Azure**

T. Karmarkar (Microsoft)..... 30

---

**PLENARY AND KEYNOTE PRESENTATIONS II** **PAGES 31 - 36**

Plenary Presentations, Tuesday 16 June, 13:30 – 15:15 Page

---

**Stochastic Simulations for Crash Worthiness and Occupant Protection**

T. Yasuki (Toyota Motor) ..... 33

**Dummy-Positioning for a Whiplash Load Case using LS-DYNA Implicit**

A. Hirth (Daimler); A. Gromer (DYNAmore); T. Borrvall (DYNAmore Nordic)..... 34

**Usage of LS-DYNA in Metal Forming**

M. Fleischer, A. Lipp, J. Meinhardt, P. Hippchen, I. Heinle, A. Ickes, T. Senner (BMW Group)..... 35

**Enabling Effective and Easy to Access Simulation**

E. Schnepf (Fujitsu Technology Solutions); S. Gillich (Intel) ..... 36

---

**PLENARY AND KEYNOTE PRESENTATIONS III** **PAGES 37 - 44**

Plenary Presentations, Wednesday 17 June, 13:40 – 16:40 Page

---

**Under Body Vulnerability and Design Loads Prediction using LS-DYNA at Jaguar Land Rover**

P. Khapane (Jaguar Land Rover)..... 39

**CAE and Testing Dreams for 2020**

C. Lemaitre (Faurecia)..... 40

**Joint Analytical/Experimental Constitutive and Failure Model Development**

P. Du Bois (Consultant); J. Seidt (Ohio State University) ..... 41

**Nonlinear Analysis 1980 - 2020**

M. Lawson (Rolls-Royce) ..... 43

**CRASH I – FAILURE****PAGES 45 - 52**

Room 1, Monday, 15 June, 15:40 – 16:55

Page

**Prediction of Dynamic Material Failure – Part I: Strain Rate Dependent Plastic Yielding**M. Feucht (Daimler); R. Böhm (Karls-ruher Institut für Technologie); P. Du Bois (Consultant);  
F. Andrade, A. Haufe (DYNAmore) ..... 47**Prediction of Dynamic Material Failure – Part II: Application with GISSMO in LS-DYNA**F. Andrade, A. Haufe (DYNAmore); M. Feucht (Daimler); R. Böhm  
(Karlsruher Institut für Technologie); P. Du Bois (Consultant) ..... 48**Modeling of Strain-Rate Dependence of Deformation and Damage Behavior of HSS- and UHSS at Different Loading States**

A. Trondl, D. Sun (Fraunhofer IWM) ..... 49

**CRASH II – FAILURE****PAGES 53 - 60**

Room 1, Monday, 15 June, 17:30 – 18:45

Page

**Development of an Anisotropic Material Model for the Simulation of Extruded Aluminum under Transient Dynamic Loads**

A. Smith (Honda R&amp;D Americas); P. Du Bois (Consultant); T. Borrvall (DYNAmore Nordic) ..... 55

**The Numerical Failure Prediction by the Damage Model GISSMO in Various Materials of Sheet Metal**

S. Chinzei, J. Naito (KOBE Steel) ..... 57

**An Investigation of Modeling Approaches for Material Instability of Aluminum Sheet Metal using the GISSMO-Model**

G. Falkinger (Leichtmetallkompetenz-zentrum Ranshofen LKR); P. Simon (AMAG Rolling) ..... 59

**CRASH III – CONNECTION****PAGES 61 - 68**

Room 1, Tuesday, 16 June, 15:45 – 17:00

Page

**Modeling Adhesively Bonded Joints with \*MAT252 and \*MAT\_ADD\_COHESIVE for Practical Applications**

F. Burbulla (Dr. Ing. h.c. F. Porsche); A. Matzenmiller, U. Kroll (University of Kassel) ..... 63

**Practical Failure Criterion of Spot Weld for Crash Simulation**

J.-H. Lim, J. Ha, C.-Y. Oh (Posco) ..... 65

**Macroscopic Modeling of Flow Drill Screw Connections**

J. K. Sønstabø, D. Morin, M. Langseth (Norwegian University of Science and Technology) ..... 67



**CRASH IV – CONNECTION/MISCELLANEOUS****PAGES 69 - 70**

Room 1, Tuesday, 16 June, 17:25 – 18:40

Page

**Modeling of Self-Piercing Riveted Joints for Crash Simulation  
– State of the Art and Future Topics**

M. Bier, S. Sommer (Fraunhofer IWM)..... 71

**Challenges in Tire Modeling for Small Overlap Crashworthiness**

S. Bala (LSTC) ..... 72

**On Automatic Crash Model Translation**

E. Di Pasquale (SimTech/ Université de Valenciennes) ..... 73

**CRASH V – SHIPS/PLANES****PAGES 71 - 82**

Room 1, Wednesday, 17 June, 08:30 – 10:10

Page

**Highly Advanced M&S System for Marine Accident Cause Investigation  
using FSI Analysis Technique**

S.-G. Lee, J.-S. Lee, H.-S. Lee (Korea Maritime and Ocean University) ..... 77

**Use of Forming Limit Curve as a Failure Criterion in Maritime Crash Analysis**

B. Atli-Veltin, L. Vredeveltdt (TNO)..... 79

**Non-Structural Mass Modeling in Aircraft Impact Analysis using  
Smooth Particle Hydrodynamics**

M. Kostov, M. Miloshev, Z. Nikolov, I. Klecherov (Risk Engineering) ..... 81

**CRASH VI – MATERIAL****PAGES 83 - 92**

Room 1, Wednesday, 17 June, 10:40 – 12:20

Page

**Ductile Fracture Prediction with Forming Effects Mapping of Press Hardened Steels**L. Knoerr, T. Faath, S. Sikora (ThyssenKrupp Steel NA);  
P. Woelke, B. Benowitz, B. Hiriyur (Weidlinger Associates) ..... 85**Probabilistic Analysis of Process Chain “Forming to Crash“ Regarding  
Failure Prediction**B. Özarmut, H. Richter (ThyssenKrupp Steel Europe);  
A. Brosius (Technical University Dresden)..... 86**Development of a Fully-Tabulated, Anisotropic and Asymmetric  
Material Model for LS-DYNA (\*MAT\_264)**

S. Haight, C.-D. Kan (George Mason University); P. Du Bois (Consultant) ..... 87

**Comparison of Crash Models for Ductile Plastics**

B. Croop, M. Lobdell, H. Lobo (DatapointLabs) ..... 90

---

**PROCESS I – METAL FORMING** **PAGES 93 - 100**

 Room 4, Monday, 15 June, 15:40 – 16:55 Page


---

**Simulation Aspects for the Application of High Strength Steel Materials  
in Forming Processes**

L. Keßler, T. Beier, H. Richter (ThyssenKrupp Steel Europe) ..... 95

**A Combined Technological Proofing Method for Deep Drawing and  
Stretch Forming of Sheet Metal Materials**

R. Hennig (Aleris Rolled Products Germany) ..... 96

**Developments in LS-DYNA for Metal Forming Simulations**

X. Zhu, L. Zhang (LSTC) ..... 97

**PROCESS II – METAL FORMING** **PAGES 101 - 108**

 Room 4, Monday, 15 June, 17:30 – 18:45 Page


---

**Comprehensive Correlation of Seat Track Assembly – From Forming to Assembly Test**

S. Sinne, H. Klose, V. J. Dura Brisa, P. Partheymüller (Brose Fahrzeugteile) ..... 103

**Creation and Validation of Material Cards for Aluminium Sheet Metal Materials**

R. Hennig (Aleris Rolled Products Germany) ..... 105

**Evaluation of Kinematic Hardening Models for Multiple Stress Reversals  
under Continuous Cyclic Shearing and Multi-Step Bending**

S. Suttner, M. Rosenschon, Prof. M. Merklein (University of Erlangen-Nürnberg) ..... 106

**PROCESS III – METAL FORMING** **PAGES 109 - 116**

 Room 4, Tuesday, 16 June, 08:20 – 10:00 Page


---

**Parameter Identification for Forming Simulations of High-Strength Steels**

M. Thomisch, Prof. M. Kley (University Aalen) ..... 111

**ACP Process Integrated 3B Forming Optimization**

A. Farahani, D. Mittal (Engineering Technology Associates); J. Shaw (US Steel) ..... 112

**Influence of Variations in a Mechanical Framing Station on the  
Shape Accuracy of S-Rail Assemblies**

K. Wiegand, T. Konrad, (Daimler); M. Merklein (University of Erlangen-Nürnberg) ..... 114

**Structural Analysis of an Automotive Forming Tool for Large Presses Using LS-DYNA**

 K. Swidergal, Prof. M. Wagner (OTH Regensburg); C. Lubeseder, I. von Wurmb, J. Meinhardt  
(BMW Group); S. Marburg (University of the Federal Armed Forces) ..... 115

**PROCESS IV– COMPOSITES****PAGES 117 - 126**

Room 4, Tuesday, 16 June, 10:30 – 12:10

Page

**Simulation of Forming of Paperboard Packaging using LS-DYNA**

M. Schill, J. Karlsson (DYNAmore Nordic); J. Tryding (Tetra Pak) ..... 119

**Forming Simulation of Textile Composites Using LS-DYNA**

M. Nishi, T. Hirashima (JSOL)..... 120

**A Graphical User Interface for Simulating Resin-Transfer-Molding  
Combining LS-DYNA and OpenFOAM**

M. Wagner, M. Martins-Wagner (OTH Regensburg); A. Haufe, C. Liebold (DYNAmore) ..... 122

**Modeling Non-Isothermal Thermoforming of Fabric-Reinforced  
Thermoplastic Composites**

D. Schommer, M. Duhovic, J. Hausmann (University of Kaiserslautern) ..... 124

**PROCESS V – MISCELLANEOUS****PAGES 127 - 134**

Room 4, Tuesday, 16 June, 15:45 – 17:00

Page

**RollerPaG – a Tool for the Automatic Path Generation for Roller Hemming  
Simulation using LS-DYNA**

B. Boll (DYNAmore); O. Ghouati (Ford Research &amp; Advanced Engineering)..... 129

**Simulation of the Manufacturing Process of Self-Piercing Rivets with LS-DYNA  
with Focus on Failure Prediction for Sheets and Rivet**

M. Buckley (Jaguar Land Rover); H. Gese, M. Reissner, G. Oberhofer (Matfem Partnerschaft) .. 130

**Towards Location Specific Statistical Fracture Prediction in High Pressure  
Die Castings**R. Watson, W. Griffiths (University of Birmingham); T. Zeguer (Jaguar Land Rover);  
S. Ruffle (JVM Castings) ..... 132**PROCESS VI – DEEP DRAWING****PAGES 135 - 142**

Room 4, Tuesday, 16 June, 17:25 – 18:40

Page

**Numerical Analysis of Multistep Ironing of Thin-Wall Aluminium Drawpiece**L. Brodawka, M. Kociolek, M. Siedlik, R. Budzyn, A. Furman (Can-Pack);  
A. Rekas, T. Latos (AGH University of Science and Technology) ..... 137**Numerical Analysis of Relationship between Height and Geometry of Bottom of a  
Beverage Can and its Resistance to Increase in Internal Pressure**L. Brodawka, M. Kociolek, M. Siedlik, R. Budzyn, M. Fijalkowski (Can-Pack);  
T. Latos, A. Rekas (AGH University of Science and Technology) ..... 139**Optimization of the Blank Holder Stiffness in Deep Drawing Processes by using FEA**

R. Radonjic, Prof. M. Liewald, F. Han ..... 141

**PROCESS VII – WELDING****PAGES 143 - 150**

Room 5, Tuesday, 16 June, 15:45 – 17:00

Page

**SimWeld and DynaWeld Software Tools to Setup Simulation Models for the Analysis of Welded Structures with LS-DYNA**

T. Loose (Ingenieurbüro Tobias Loose); O. Mokrov (RWTH Aachen) ..... 145

**A Finite Element Investigation Into the Continuous Induction Welding of Dissimilar Material Joints**

M. Duhovic, J. Hausmann (Institut für Verbundwerkstoffe); P. L´Eplattenier, I. Caldichoury (LSTC) ..... 147

**Simulating the Induction Spot Welding of Hybrid Material Joints**

M. Didi, D. Wind, M. Duhovic, J. Hausmann (Technical University Kaiserslautern) ..... 149

**PROCESS VIII – WELDING****PAGES 151 - 158**

Room 5, Tuesday, 16 June, 17:25 – 18:40

Page

**Numerical Simulation of Impact Welding Processes with LS-DYNA**

C. Pabst, P. Groche (Technical University Darmstadt) ..... 153

**Evaluation of Electromagnetism Capabilities of LS-DYNA: Alternative Heating Processes**

E. Gripon, T. Senart, V. Lapoujade (DynaS+) ..... 155

**Cohesive Contact Modeling in Thermoforming Simulations of Metal-CRFP-Metal Sandwich Sheets**

Ö. Cebeci (Consultant); A. Zeiser (Inpro Innovationsellschaft für fortgeschrittene Produktionssysteme in der Fahrzeugindustrie); M. von Scheven (University of Stuttgart) ..... 157

**PROCESS IX – CUTTING/MODEL REDUCTION****PAGES 159 - 168**

Room 4, Wednesday, 17 June, 08:30 – 10:10

Page

**The Influence of Johnson-Cook Parameters on SPH modeling of Orthogonal Cutting of AISI 316L**

A. A. Olleak, H. El-Hofy (Egypt-Japan University of Science and Technology); M. N. A. Nasr (Alexandria University) ..... 161

**SPH Modeling of Cutting Forces while Turning of Ti6Al4V Alloy**

A. A. Olleak, H. El-Hofy (Egypt-Japan University of Science and Technology) ..... 163

**Simulation of Circular Sawing Processes**

H. Vazquez Martinez (Fraunhofer IPA) ..... 165

**Model Reduction Techniques for LS-DYNA ALE and Crash Applications**

K. Kayvantash, A.-T. Thiam (CADLM); Ryckelynck (Mines Paris Tech); S. B. Chaabane, J. Touzeau, P. Ravier (Silkan) ..... 167

**MATERIALS I – PLASTICS** **PAGES 169 - 178**Room 3, Monday, 15 June, 15:40 – 16:55 Page**Failure of Thermoplastics – Part 1: Characterization and Testing**

A. Fertschej, P. Reithofer, M. Rollant (4a engineering)..... 171

**Failure of Thermoplastics – Part 2 Material Modeling and Simulation**

A. Fertschej, P. Reithofer, M. Rollant (4a engineering)..... 173

**Macroscopic Modeling of Flow-Drill Screw Connections**

J. K. Sønstabø, D. Morin, M. Langseth (Norwegian University of Science and Technology) ..... 176

**MATERIALS II – ENDLESS FIBERS** **PAGES 179 - 188**Room 3, Tuesday, 16 June, 08:20 – 10:00 Page**Textile and Composite Modeling on a Near Micro-Scale: Possibilities and Benefits**

O. Döbrich, T. Gereke, C. Cherif (Technical University Dresden)..... 181

**Micro-Meso Draping Modeling of Non-Crimp Fabrics**

O. Vorobiov, T. Bischoff, A. Tulke (FTA Forschungsgesellschaft für Textiltechnik Albstadt) ..... 182

**Numerical Investigation of Carbon Braided Composites at the Mesoscale:  
Using Computer Tomography as a Validation Tool**

M. Vinot, M. Holzapfel, R. Jemmali (German Aerospace Center)..... 184

**Modeling of Thick UD Composites for Type IV Pressure Vessels**

R. Matheis, H. Murnisya (fka Aachen); T. Johansson (DYNAmore Nordic)..... 186

**MATERIALS III – SHORT/LONG FIBER** **PAGES 189 - 198**Room 3, Tuesday, 16 June, 10:30 – 12:10 Page**Digmat Material Model for Short Fiber Reinforced Plastics at Volvo  
Car Corporation**

M. Landervik (DYNAmore Nordic); J. Jergeus (Volvo Car)..... 191

**Simplified Integrative Simulation of Short Fibre Reinforced Polymers under  
Varying Thermal Conditions**

C. Witzgall, Prof. S. Wartzack (University of Erlangen-Nürnberg) ..... 192

**Recent Enhancements on Short-Fiber Reinforced Plastics Modeling in LS-DYNA**

C. Liebold, A. Erhart (DYNAmore) ..... 194

**Short and Long Fiber Reinforced Thermoplastics Material Models in LS-DYNA**

S. Hartmann, T. Erhart, A. Haufe (DYNAmore); P. Reithofer, B. Jilka (4a engineering) ..... 196

**MATERIALS IV – ADHESIVES/FAILURE****PAGES 199 - 208**

Room 3, Tuesday, 16 June, 15:45 – 17:00

Page

**Strain-Rate Dependant Damage Material Model for Layered Fabric Composites with Delamination Prediction for Impact Simulations**S. Treutenaere, F. Lauro, B. Bennani (University of Valenciennes and Hainaut Cambrésis);  
T. Matsumoto, E. Mottola (Toyota Motor Europe) ..... 201**Predicting Mechanical Behaviour of Reinforced Plastic and Composite Parts**

S. Calmels (e-Xstream engineering) ..... 203

**Implementation of Peridynamic Theory to LS-DYNA for Prediction of Crack Propagation in a Composite Lamina**T. Kahraman (MAN Turkey/ TOBB University of Economics and Technology);  
U. Yolum, M. A. Guler (TOBB University of Economics and Technology) ..... 206**MATERIALS V – COMPOSITES****PAGES 209 - 214**

Room 3, Tuesday, 16 June, 17:25 – 18:40

Page

**Damage in Rubber-Toughened Polymers – Modeling and Experiments**

M. Helbig (DYNAmore); T. Seelig (Karlsruhe Institute of Technology) ..... 211

**Calculation and Validation of Material Tests with Specimens Made out of Filled Elastomers**P. Thumann, K. Swidergal,  
Prof. M. Wagner (OTH Regensburg) ..... 213**OCCUPANT SAFETY I – AIRBAGS****PAGES 215 - 222**

Room 2, Monday, 15 June, 15:40 – 16:55

Page

**Numerical Simulation of the Laser Scoring Line Behavior in Airbag Deployment**M. Nutini, M. Vitali (Basell Poliolefine Italia); S. Bianco, D. Brancadoro, A. Luera,  
D. Marino (FCA); M. Olivero (CRF) ..... 217**CAE Analysis of Passenger Airbag Bursting through Instrumental Panel Based on Corpuscular Particle Method**

Y. Feng, M. Beadle (Jaguar Land Rover) ..... 218

**Using JFOLD & LS-DYNA to Study the Effects of Folding on Airbag Deployment**

R. Taylor (Arup), S. Hayashi (JSOL) ..... 220

---

**OCCUPANT SAFETY II – DUMMIES** **PAGES 223 - 230**

 Room 2, Tuesday, 16 June, 08:20 – 10:00 Page


---

**Optimal Forces for the Deceleration of the ES-2 Dummy**  
 J. Fehr, J. Köhler, C. Kleinbach (University of Stuttgart)..... 225

**Assessment of Motorcycle Helmet Chin Bar Design Criteria with Respect to Basilar Skull Fracture Using FEM**  
 S. Farajzadeh Khosroshahi, M. Ghajari (Imperial College London);  
 U. Galvanetto (University of Padova) ..... 227

**CAE Validation Study of a Side Window Impact using Plexiglas Materials**  
 D. Lopez Ruiz (Tecosim Technische Simulation); A. Rühl, Prof. S. Kolling (THM Giessen);  
 E. Ruban, B. Kiese-wetter, S. Ulzheimer (Evonik Industries) ..... 229

**Agile Dummy Model Development Illustrated by Refinement Activities of the WorldSID Shoulder Model**  
 R. Brown, G. Stokes (Jaguar Land Rover); U. Franz, S. Stahlschmidt (DYNAmore) ..... 230

**OCCUPANT SAFETY III – DUMMIES** **PAGES 231 - 238**

 Room 2, Tuesday, 16 June, 10:30 – 12:10 Page


---

**LS-DYNA Model Development of the THOR-M**  
 I. Maatouki, P. Lemmen (Humanetics Europe); Z. Zhou (Humanetics Innovative Solutions) ..... 233

**LS-DYNA Model Development of the Harmonized Hybrid III 05F Crash Test Dummy to Meet the Euro NCAP Testing Protocol Requirements**  
 R. Kant, P. Lemmen (Humanetics Europe); C. Shah (Humanetics Innovative Solutions) ..... 234

**H-Point Machine and Head Restraint Measurement Device Positioning Tools – Extended Capabilities**  
 B. Walker, L. Cowlam, J. Dennis (Arup); S. Albery, N. Leblanc (Futuris) ..... 235

**Investigation of Seat Modeling for Sled Analysis and Seat Comfort Analysis with J-SEATdesigner**  
 N. Ichinose, H. Yagi (JSOL) ..... 236

**HUMAN MODELS** **PAGES 239 - 248**

 Room 2, Monday, 15 June, 17:30 – 18:45 Page


---

**The Effects of Active Muscle Contraction into Pedestrian Kinematics and Injury During Vehicle-Pedestrian Collision**  
 I. Putra, J. Carmai, S. Koetnyom (King Mongkut's University of North Bangkok);  
 B. Markert (RWTH Aachen/University of Agder) ..... 241

**Stability and Sensitivity of THUMS Pedestrian Model and its Trauma Response to a Real-Life Accident**  
 L. Wen, C. Bastien, M. Blundell, C. Neal-Surgess (Coventry University);  
 K. Kayvantash (CADLM) ..... 243

**The CASIMIR Model for Simulation in Seating Comfort Applications – A Status Update for LS-DYNA**  
 N. Lazarov, D. Fressmann (DYNAmore); A. Siefert (Wölfel Beratende Ingenieure)..... 246

---

**SIMULATION I – MULTIPHYSICS****PAGES 249 - 260**

Room 5, Monday, 15 June, 15:40 – 16:55

Page

**Simulation of the Electromagnetic Flux Compression using LS-DYNA Multi-Physics Capability**

K. Takekoshi (Terrabyte) ..... 251

**Numerical Methodology for Thermal-mechanical Analysis of Fire Doors**

A. Bozzolo, C. Ferrando (D'Appolonia - RINA Group); A. Tonelli, E. Cabella (RINA Group) ..... 253

**A Contribution to CESE Method Validation in LS-DYNA**

E. Gripon, N. Van Dorsselaer, V. Lapoujade (DynaS+) ..... 257

**SIMULATION II – IMPACT/CRACKS****PAGES 261 - 266**

Room 5, Monday, 15 June, 17:30 – 18:45

Page

**Hail Impact Problem in Aeronautical Field**

A. Prato, M. Anghileri, L. Castelletti (Politecnico di Milano) ..... 263

**Simulation of Bird Strike on Airplane Wings by Using SPH Methodology**

M. Guler (TOBB University of Economics and Technology); T. Kiper Elibol (Turkish Aerospace); I. Uslan (Gazi University); M. Buyuk (Turkish Standards Institution) ..... 265

**SIMULATION III – BLAST/PENETRATION****PAGES 267 - 278**

Room 3, Wednesday, 17 June, 08:30 – 10:10

Page

**An Advanced Identification Procedure for Material Model Parameters based on Image Analysis**

L. Peroni, M. Scapin, C. Fichera (Politecnico di Torino) ..... 269

**Model Based Design of Pressure Profiles for Pyrotechnic Actuator using SPH Method & LS-OPT Solution**

E. Kantor, Y. Lev (Rafael) ..... 271

**LS-DYNA Air Blast Techniques: Comparisons with Experiments for Close-in Charges**

L. Schwer (Schwer Engineering); H. Teng (LSTC); M. Souli (University of Lille) ..... 273

**ALE/FSI AirBlast Modeling: On the Way to one Billion Elements**

N. Van Dorsselaer, V. Lapoujade (DynaS+) ..... 276



---

**SIMULATION IV – BLAST/PENETRATION** **PAGES 279 - 290**

 Room 3, Wednesday, 17 June, 10:40 – 12:20 Page


---

**An Assessment of ALE Mapping Technique for Buried Charge Simulations**  
 I. Kurtoğlu (FNSS Savunma Sistemleri) ..... 281

**An Investigation of AA7075-T651 Plate Perforation Using Different Projectile Nose Shapes**  
 B. Balaban, İ. Kurtoğlu (FNSS Savunma Sistemleri) ..... 283

**Modeling of Ballistic Impact of Fragment Simulating Projectiles against Aluminum Plates**  
 T. Fras, L. Colard, B. Reck (French-German Research Institute of Saint-Louis)..... 286

**Shock Response Analysis of Blast Hardened Bulkhead in Naval Ship under Internal Blast**  
 S.-G. Lee, H.-S. Lee, J.-S. Lee (Korea Maritime & Ocean University);  
 Y. Y. Kim, G. G. Choi (Korea Advanced Institute of Science and Technology) ..... 288

**SIMULATION V – MATERIALS** **PAGES 291 - 298**

 Room 5, Wednesday, 17 June, 08:30 – 10:10 Page


---

**Mechanical Response Modeling of Different Porous Metal Materials**  
 Prof. M. Vesenjāk, M. Borovinšek, A. Kovačič, M. Ulbin, Z. Ren (University of Maribor) ..... 293

**Development of a Tool for Automatic Calibration of Material Models in LS-DYNA**  
 A. Mardalizad (Polytechnic University of Turin); E. Sadeghipour,  
 M. Lienkamp (Technical University Munich)..... 294

**Verification of the Part-Composite Approach for Modeling the Multi-Layered Structure of a Rolling Truck Tire**  
 S. Shokouhfar, S. Rakheja (Concordia University); M. El-Gindy (UOIT) ..... 296

**SIMULATION VI – CRACKS** **PAGES 299 - 308**

 Room 4, Wednesday, 17 June, 10:40 – 12:20 Page


---

**Three-Point Bending Crack Propagation Analysis of Beam Subjected to Eccentric Impact Loading by X-FEM**  
 T. Tsuda, Y. Ohnishi, R. Ohtagaki (Itochu Techno-Solutions);  
 K. Cho, T. Fujimoto (Kobe University) ..... 301

**Keep the Material Model Simple with Input from Elements that Predict the Correct Deformation Mode**  
 Prof. T. Tryland (Sintef Raufoss Manufacturing); T. Berstad (Norwegian University of Science and Technology) ..... 303

**Damping Modeling in Woven Lattice Materials**  
 S. Szyniszewski (University of Surrey); S. Ryan, S. Ha, Y. Zhang, T. Weihs,  
 K. Hemker, J.K. Guest (The Johns Hopkins University Baltimore) ..... 305

**Solving of Crash Problems of the Fuel Supply Modules in the Fuel Tank**  
 M. Dobeš, J. Navratil (Robert Bosch)..... 307

---

**SIMULATION VII – DROP TEST/BIO** **PAGES 309- 316**Room 5, Wednesday, 17 June, 10:40 – 12:20 Page

<b>Drop Test Simulation and Verification of a Dishwasher Mechanical Structure</b> O. Mulkoglu, M. A. Guler (TOBB University of Economics and Technology); H. Demirbag (Arcelik) .....	311
<b>Impact Simulations on Home Appliances to Optimize Packaging Protection: A Case Study on a Refrigerator</b> D. Hailoua Blanco, A. Ortalda (Engin-soft); F. Clementi (Electrolux Italia) .....	313
<b>A Variable Finite Element Model of the Overall Human Masticatory System for Evaluation of Stress Distributions During Biting and Bruxism</b> S. Martinez, J. Lenz, Prof. K. Schweizer-hof (Karlsruhe Institute of Technology); Prof. H. Schindler (University of Heidelberg).....	314

**OPTIMIZATION I – ROBUSTNESS** **PAGES 317 - 324**Room 1, Tuesday, 16 June, 08:20 – 10:00 Page

<b>Recent Advances on Surrogate Modeling for Robustness Assessment of Structures with Respect to Crashworthiness Requirements</b> Prof. F. Duddeck, E. Wehrle (Technical University Munich) .....	319
<b>Robustness Analysis of a Vehicle Front Structure Using Statistical Approach</b> M. Okamura (JSOL) .....	320
<b>Improving Robustness of Chevrolet Silverado with Exemplary Design Adaptations Based on Identified Scatter Sources</b> D. Borsotto, R. Strickstock, C. A. Thole (Sidact).....	322
<b>Classification-based Optimization and Reliability Assessment using LS-OPT</b> A. Basudhar, I. Gandikota, N. Stander (LSTC); A. Svedin, C. Belestam (DYNAmore Nordic); K. Witowski (DYNAmore) .....	323

**OPTIMIZATION II – GENERAL** **PAGES 325 - 332**Room 1, Tuesday, 16 June, 10:30 – 12:10 Page

<b>Some LS-OPT Applications in the CAE Development of Injection Molded Thermoplastic Parts</b> A. Wüst (BASF) .....	327
<b>Optimization of a Lower Bumper Support Regarding Pedestrian Protection Requirements using ANSA and LS-OPT</b> I. Wetzstein, B. Lauterbach, N. Erzgräber, L. Harzheim (Adam Opel).....	328
<b>X760 Bumper Automation and Optimization Process</b> T. Zeguer (Jaguar Land Rover).....	330
<b>Multi-Scale Material Parameter Identification using LS-DYNA and LS-OPT</b> N. Stander, A. Basudhar, U. Basu, I. Gandikota (LSTC); V. Savic (General Motors Company); X. Sun, K. Sil Choi, X. Hu (Pacific Northwest National Labora-tory); Prof. F. Pourboghrat, T. Park, A. Mapar (Michigan State University); S. Kumar, H. Ghassemi-Armaki (Brown University); F. Abu-Farha (Clemson University).....	331

**OPTIMIZATION III – TOPOLOGY** **PAGES 333 - 340**Room 2, Tuesday, 16 June, 15:45 – 17:00 Page**A Weight Balanced Multi-Objective Topology Optimization for Automotive Development**N. Aulig, S. Menzel (Honda Research Institute Europe); E. Nutwell (Ohio State University);  
D. Detwiler (Honda R&D) ..... 335**Topometry and Shape Optimization of a Hood**

Y. H. Han (Hyundai Motor Group); K. Witowski, N. Lazarov, K. Anakiev (DYNAmore) ..... 337

**Meta-Model Based Optimization of Spot-welded Crash Box using Differential Evolution Algorithm**A. Serdar Önal (Beyçelik Gestamp Kalip ve Oto Yan San. Paz. ve Tic.);  
N. Kaya (Uludağ University) ..... 339**OPTIMIZATION IV– TOPOLOGY** **PAGES 341 - 348**Room 2, Tuesday, 16 June, 17:25 – 18:40 Page**Topology Optimization of Transient Nonlinear Structures – A Comparative Assessment of Methods**

E. J. Wehrle, F. Duddeck (Technical University Munich); Y. H. Han (Hyundai Motor Group) ..... 343

**Multidisciplinary Design Optimisation Strategies for Lightweight Vehicle Structures**

A. Prem, C. Bastien, M. Dickson (Coventry University) ..... 345

**Optimization of Turbine Blade Fir Tree Root Geometry Utilizing LS-PrePost in Pre- and Postprocessing**

J. Jankovec (Research and Testing Institute Plzen) ..... 348

**MULTIPHYSICS I – CFD/FSI** **PAGES 349 - 354**Room 2, Wednesday, 17 June, 08:30 – 10:10 Page**A Numerical Investigation of Turbulent Flow in Circular U-Bend**

A. Miloud, M. Aounallah, O. Imine, M. Guen (University of Science and Technology of Oran Algeria) ..... 351

**Numerical Investigation of the Nozzle Number on the Performance of Conical Vortex Tube**

M. Guen, O. Imine, A. Miloud (University of Science and Technology of Oran Algeria) ..... 352

**Validation of Fluid Analysis Capabilities in LS-DYNA Based on Experimental Result**

S. Tokura (Tokura Simulation Research) ..... 353

**MULTIPHYSICS II – CFD/FSI****PAGES 355 - 362**

Room 2, Wednesday, 17 June, 10:40 – 12:20

Page

**Analysis of Unsteady Aerodynamics of a Car Model with Radiator in Dynamic Pitching Motion using LS-DYNA**

Y. Nakae, J. Takamitsu, H. Tanaka, T. Yasuki (Toyota Motor) ..... 357

**Analysis of an Automobile Roof Panel under Strongly Coupled Fluid Structure Interaction using LS-DYNA**

D. Detwiler (Honda R&amp;D Americas) ..... 359

**Ground Vehicle Aerodynamics using LS-DYNA**

F. Del Pin, R. R. Paz, I. Caldichoury (LSTC)..... 360

**PARTICLE METHODS – SPH/DEM****PAGES 363 - 370**

Room 7, Tuesday, 16 June, 10:30 – 12:10

Page

**Application of the SPH Finite Element Method to Evaluate Pipeline Response to Slope Instability and Landslides**

A. Fredj, A. Dinovitzer (BMT Fleet Technology); M. Sen (Enbridge Pipelines)..... 365

**Modeling the Behavior of Dry Sand with DEM for Improved Impact Prediction**

S. Sridhar, S. K. Vishwakarma (Whirlpool of India)..... 366

**Volume-Averaged Stress States for Idealized Granular Materials using Unbonded Discrete Spheres in LS-DYNA**

M. T. Davidson, J. H. Chung, V. Le (Bridge Software Institute); H. Teng, Z. Han (LSTC) ..... 368

**Discrete Element Analysis of Idealized Granular Geometric Packing Subjected to Gravity**

M. Faraone, J. Chung, M. Davidson (University of Florida, Bridge Software Institute)..... 369

**DEVELOPER I – FREQUENCY DOMAIN****PAGES 371 - 376**

Room 3, Monday, 15 June, 17:30 – 18:45

Page

**Recent Updates in LS-DYNA Frequency Domain Solvers**

Y. Huang, Z. Cui (LSTC) ..... 373

**Statistical Energy Acoustic for High Frequencies Analysis**M. Souli, R. Messahel (University Lille); Y. T. Zeguer (Jaguar Land Rover);  
Y. Huang (LSTC)..... 375

**DEVELOPER II – PREPOST/MAPPING****PAGES 377 - 386**

Room 6, Tuesday, 16 June, 15:45 – 17:00

Page

**Current Status of LS-PrePost and the New Features in Version 4.2**

P. Ho (LSTC) ..... 379

**Non-Linear Fracture Mechanics in LS-DYNA and LS-PrePost**P. Lindström (University West/DNV GL Materials Laboratory); A. Jonsson,  
A. Jernberg (DYNAmore Nordic); E. Østby (DNV GL Materials Laboratory) ..... 381**A Fabric Material Model with Stress Map Functionality in LS-DYNA**

T. Borrvall (DYNAmore Nordic); C. Ehle, T. Stratton (Autoliv OTC) ..... 384

**DEVELOPER III – MULTIPHYSICS****PAGES 387 - 394**

Room 6, Tuesday, 16 June, 17:25 – 18:40

Page

**Generalized Anisotropic/Isotropic Porous Media Flows in LS-DYNA**

R. R. Paz, F. Del Pin, I. Caldichoury (LSTC); H. G. Castro (Conicet) ..... 389

**Chemically Reactive Flows in Airbag Inflator Chambers**

K. Im, G. Cook Jr., Z. Zhang (LSTC) ..... 391

**Recent Developments in the Electromagnetic Module:****A New 2D Axi-Symmetric EM Solver**

P. L'Eplattenier, I. Çaldichoury (LSTC) ..... 392

**DEVELOPER IV – MISCELLANEOUS****PAGES 395 - 402**

Room 6, Wednesday, 17 June, 08:30 – 10:10

Page

**LS-TaSC Product Status**

K. Witowski, P. Schumacher (DYNAmore); W. Roux (LSTC) ..... 397

**Recent Developments for Thermo-Mechanically Coupled Simulations  
in LS-DYNA with Focus on Welding Processes**

T. Klöppel (DYNAmore); T. Loose (Ingenieurbüro Tobias Loose) ..... 398

**Improvements to LS-DYNA Implicit Mechanics**

R. Grimes (LSTC) ..... 400

**MPP Contact: Options and Recommendations**

B. Wainscott (LSTC) ..... 402

**DEVELOPER V – ELEMENTS** **PAGES 403 - 410**Room 6, Wednesday, 17 June, 10:40 – 12:20 Page**Edge-to-Edge Cohesive Shell Elements in LS-DYNA**

J. Karlsson (DYNAmore Nordic); M. Fagerström (Chalmers University) ..... 405

**A New Feature to Model Shell-Like Structures with Stacked Elements**

T. Erhart (DYNAmore) ..... 406

**Isogeometric Analysis in LS-DYNA: Using CAD-Geometry for Numerical Simulation**Prof. D. Benson (University of California), D. Bhalsod, P. Ho, L. Li, W. Li, A. Nagy,  
I. Yeh (LSTC); S. Hartmann (DYNAmore) ..... 408**IT PERFORMANCE/SCALABILITY I** **PAGES 411 - 418**Room 6, Monday, 15 June, 15:40 – 16:55 Page**Improvement of Domain Decomposition of LS-DYNA R7 and R8**

M. Makino (Dynapower) ..... 413

**Performance Optimizations for LS-DYNA with Mellanox HPC-X Scalable Software Toolkit**

P. Lui, D. Cho, G. Shainer, S. Schultz, B. Klaff (Mellanox Technologies) ..... 415

**Characterizing LS-DYNA Performance on SGI Systems using SGI MPInside MPI Profiling Tool**

T. DeVarco, O. Schreiber, A. Altman, S. Shaw (Silicon Graphics) ..... 416

**IT PERFORMANCE/SCALABILITY II** **PAGES 419 - 424**Room 6, Monday, 15 June, 17:30 – 18:45 Page**Fast Road Barrier Car Safety Calculations on a Cray XC**

J. Cholewinski, A. Findling, G. Clifford (Cray); M. Piechnik (Stalprodukt) ..... 421

**Cost-Effective Sizing of Your HPC Cluster for CAE Simulations**

N. Henkel, S. Treiber (GNS Systems) ..... 422

**Cloud-Enabled CAE Solutions: Requirements, Basic Concepts and Usability**

A. Heine (CPU 24/7) ..... 423

**IT – CLOUD I****PAGES 425 - 432**

Room 6, Tuesday, 16 June, 08:30 – 10:00

Page

**Collaboration for Future HPC-based Simulation Technologies**

A. Walser (Automotive Simulation Center Stuttgart) ..... 427

**CAE as a Service as Cloud Platform for the Full LS-DYNA Simulation Process**

A. Geiger, K.-H. Hierholz, C. Neimöck (T-Systems) ..... 429

**Experiences with LS-DYNA on Cloud-like Infrastructure**

Prof. U. Göhner (DYNAmore) ..... 431

**CAE Cluster in Microsoft Azure**

T. Karmarkar, N. Greising (Microsoft); S. Bala (LSTC) ..... 432

**IT – CLOUD II****PAGES 433 - 440**

Room 6, Tuesday, 16 June, 10:30 – 12:10

Page

**Making HPC Accessible for SMEs**

A. Wierse (Sicos BW) ..... 435

**Scaling LS-DYNA on Rescale – HPC Cloud Simulation Platform**

J. Poort, I. Graedel (Rescale) ..... 437

**HPC on the Cloud: Gcompute Support for LS-DYNA Simulations**

I. Fernandez, R. Díaz (Gridcore) ..... 439

**Smart Manufacturing: CAE as a Service, in the Cloud**

W. Gentsch (The UberCloud) ..... 440

**CAE PROCESSES****PAGES 441 - 450**

Room 5, Tuesday, 16 June, 08:20 – 10:00

Page

**Crashworthy Design of Composite Structures Using CAE Process Chain**

M. Chatiri (Cadfem); T. Schütz (Adam Opel); Prof. A. Matzenmiller (University of Kassel) ..... 443

**New Technologies for Side Impact Model Set-Up**

T. Fokilidis, A. Lioras (BETA CAE Systems) ..... 445

**Speeding up the Pedestrian Protection CAE Process**

G. Newlands, C. Archer (Arup) ..... 447

**Increasing Efficiency of the Design Process with an Isogeometric Analysis  
Plugin for Siemens NX by Analyzing the CAD Model Directly**M. Breitenberger, B. Philipp, R. Wüchner, K.-U. Bletzinger (Technical University Munich);  
S. Hartmann, A. Haufe (DYNAmore) ..... 449

**SDM & MODEL REDUCTION****PAGES 451 - 460**

Room 5, Tuesday, 16 June, 10:30 – 12:10

Page

**Using LoCo for Multi Run Simulations**

R. Luijckx (AUDI); M.Thiele (SCALE)..... 453

**New Developments in LoCo – The Innovative SDM System**

M. Thiele, T. Landschoff (SCALE)..... 455

**Machine Learning Approaches for Repositories of Numerical Simulation Results**

Prof. J. Garcke, R. Iza Teran (Fraunhofer SCAI) ..... 457

**Small-Overlap Crash Simulation Challenges and Solutions**

S. R. M. Arepalli, G. Kini, A. Gittens (ESI Group)..... 459

**WORKSHOPS****PAGE 461 - 463****Setting up an ICFD Simulation in LS-DYNA**

Room 7, Monday, 15 June, 15:40 – 16:55

**Material Parameter Identification with LS-OPT**

Room 8, Monday, 15 June, 15:40 – 16:55

**Setting up an EM Simulation in LS-DYNA**

Room 7, Monday, 15 June, 17:30 – 18:45

**Meshing and Postprocessing with LS-PrePost**

Room 8, Monday, 15 June, 17:30 – 18:45

**Material Failure using GISSMO**

Room 8, Tuesday, 16 June, 08:20 – 10:00

**Creating Forming Simulations with OpenForm**

Room 8, Tuesday, 16 June, 10:30 – 12:10

**DEM Modeling in LS-DYNA**

Room 7, Tuesday, 16 June, 15:45 – 17:00

**New Developments in LoCo– The innovative SDM Solution**

Room 8, Tuesday, 16 June, 15:45 – 17:00

**Setting up an Implicit Simulation in LS-DYNA**

Room 8, Tuesday, 16 June, 17:25 – 18:40

**Dynamics Plastic Material Characterization with the 4a/Impetus Pendulum**

Room 7, Wednesday, 17 June, 08:30 – 10:10

**Welding and Heat Treatment with LS-DYNA**

Room 7, Wednesday, 17 June, 10:40 – 12:20

**Sheet Metal Forming Simulation with eta/DYNAFORM**

Room 8, Wednesday, 17 June, 08:30 – 10:10

**Modeling Composites in LS-DYNA**

Room 8, Wednesday, 17 June, 10:40 – 12:20



# **PLENARY AND KEYNOTE PRESENTATIONS I**



---

# Recent Developments in LS-DYNA

John Hallquist, [Brian Wainscott](#), Jason Wang,  
and many other developers

Livermore Software Technology Corporation (LSTC), Livermore, USA

## 1 Introduction

The goal of this presentation is to provide an overview of some recent, ongoing and future developments in LS-DYNA, which is the general-purpose finite-element program of the Livermore Software Technology Corporation (LSTC). LSTC's strategy is to combine multi-physics capabilities into one scalable code for solving highly nonlinear transient problems to enable the solution of coupled multi-physics and multi-stage problems. These coupling capabilities are of great importance when approaching real world problems, as there is no single solution method available that is suitable to solve all applications. Thus, LS-DYNA provides multiple formulations and features, which include

- Explicit and Implicit time integration
- Manifold of 1-d, 2-d and 3-d finite-element discretizations
- ALE & Mesh Free, i.e., EFG, SPH, Particle methods
- Discrete Element Method
- Acoustics, Frequency Response, Modal Methods
- Compressible and Incompressible Fluids
- Electromagnetics
- Over 250 Material models
- Capabilities to parameterize loads and supports
- Strong contact formulations
- Heat Transfer
- User Interface

In addition to being the world leader in automotive crash and manufacturing, LS-DYNA provides the tools to solve applications like

- Tire Hydroplaning
- Airbags
- Hot Forging and stamping
- Bird Strike on Engine
- Drop testing
- Can and shipping container design
- Electronic component design
- Glass forming
- Plastics, mold, and blow forming
- Biomedical
- Metal cutting
- Earthquake engineering
- Failure analysis
- Sports equipment (golf clubs, golf balls, baseball bats, helmets)
- Civil engineering (offshore platforms, pavement design)

LS-DYNA provides two parallel solution methods that are suitable for shared and distributed memory machines, respectively. The distributed memory solver for massively parallel processing (MPP) provides very short turnaround times on Unix, Linux and Windows clusters. To take advantage of new processor architectures, the two approaches have been combined into a hybrid version, that combines the power of shared memory parallelization (SMP) and MPP. This feature improves the scalability of LS-DYNA to more than 10K cores.

In addition to LS-DYNA, LSTC develops sophisticated tools to support model creation and simulation processes of large deformable structures. In particular, these are

- LS-PrePost: Pre- and postprocessing
- LS-Opt: Optimization and Workflow
- LS-TaSC: Topology optimization

## 2 Examples

This is a small selection of the many capabilities that have been implemented in LS-DYNA.

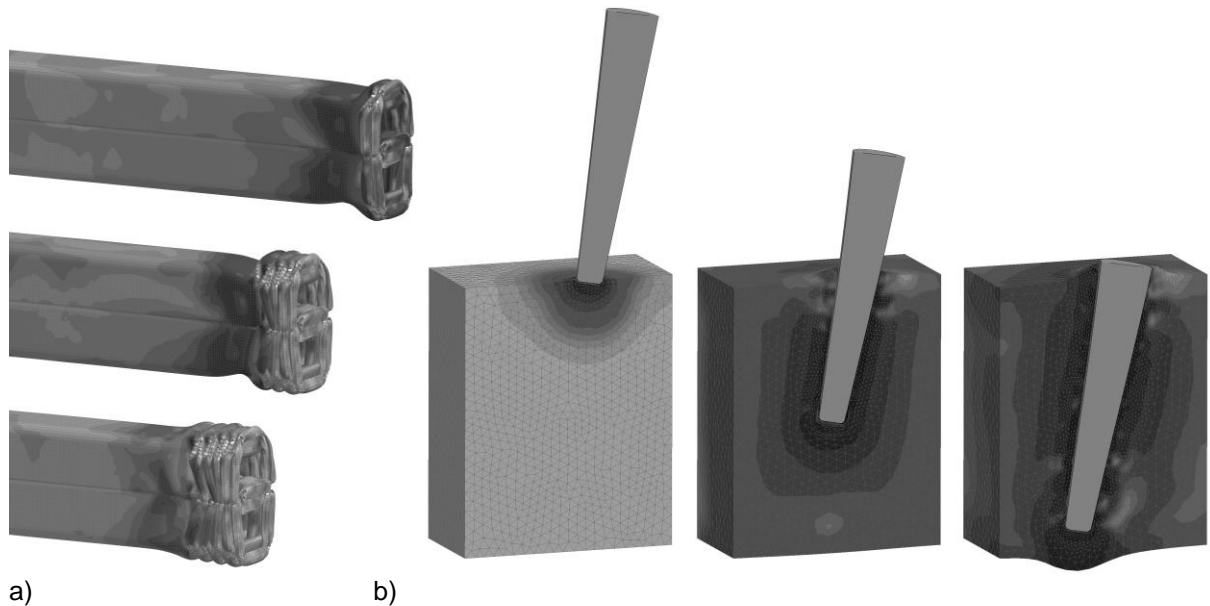


Fig.1: Improvements on a) the failure modeling of steel materials and on b) the adaptive meshfree methods (EFG).



Fig.2: Improvements on a) free surface flows, b) fluid-structure interaction on moving reference frames and c) on coupled simulations of different physical fields, i.e. fluid, solid, electro-magnetism and temperature..

## 3 Historical Review

LSTC was founded in 1987 by John O. Hallquist to commercialize as LS-DYNA the public domain code that originated as DYNA3D. DYNA3D was developed at the Lawrence Livermore National Laboratory, by LSTC's founder, John Hallquist.

# Crash CAE in the all New Volvo XC90 and SPA Platform

A. Sandahl

J. Jergeus, O. Centeno, D. Macri, A. Ericsson, W. Wu, E. Claesson,  
P. A. Eggertsen, M. Retzlaff, M. Khoo

Volvo Car, Sweden

---

# Modeling the Press Hardening Process

Mats Oldenburg

Luleå University of Technology, Sweden

## 1 Introduction

Simultaneous forming and quenching is a current manufacturing process for low weight and ultra-high strength components. The process is often referred to as *hot stamping* or *press hardening* and is mainly used for producing safety related components for the automotive industry, such as side impact beams, bumper beams and different types of structural components. The use of press hardened components has increased exponentially in the automotive industry during the last two decades. The driving forces behind this development are concern for the environment and passenger safety. The use of ultra-high strength components enables design of low weight vehicle structures with maintained or increased passenger safety. Currently and in a foreseeable future, the press hardening is the dominating technology on the market for low weight design of automotive structures.

The hot stamping process uses boron steel blanks which are first austenitized at a temperature of approximately 900 °C. The blank is then formed and quenched in cold tools to obtain martensitic ultra-high strength material. The forming operation at elevated temperatures allows complex geometries to be obtained due to the high formability of the hot material.

A material model for simulation of the thermo-mechanical press hardening process, MAT\_UHS\_STEEL (MAT\_244), has been implemented in LS-Dyna [1]. The model is based on research and developments within the Solid Mechanics research group at Luleå University of Technology.

## 2 Model development

The development of simulation methods for the analysis of the press hardening process has been carried out in several research projects including studies of several phenomena related to the process and several development steps since the middle of the 1990'ies including:

- The development of a new finite element shell formulation for thermo-mechanical analysis of sheet metal forming. The use of quadratic interpolation functions for temperatures in the thickness direction makes it possible to model one- or two-sided cooling in the press hardening process. The linear interpolation in the plane of the shell maintains compatibility between thermal expansion and other mechanical fields. The formulation was implemented in the public dyna3d code together with an explicit thermal solver [2].
- Investigation of the material properties of a boron alloyed steel used in press hardening manufacturing process. The study gives input for material modelling of the thermo-mechanical process of forming and hardening of boron steel. One important part of the study shows the influence of straining in high temperatures on the microstructure and on the transformation plasticity. This study is used as a base for modelling of the microstructure evolution and transformation plasticity [3].
- The use of inverse modelling and innovative experiments for material characterisation. In this work, it is shown that it is possible to evaluate experimental data for conditions that can not be established physically. Iso-thermal data for deformation of the austenite phase of boron steel has been evaluated by continuous cooling and deformation experiments combined with inverse modelling. The procedure is due to that there are only 10 seconds available until the austenite transforms to other phases [4].

- The development of a complete thermo-mechanical constitutive model for simulation of press hardening and similar processes. The model accounts for and establishes time dependent and time-independent phase transformations, mechanical and thermal properties as well as transformation plasticity during the complete cooling and deformation process from 900 °C to room temperature [5],[6].

### 3 Ongoing research

There are several completed and ongoing research projects at the Solid Mechanics research group at LTU that concern refinement of the simulation methods or make use of the model capabilities. Examples of such research tracks are:

- Studies of processes for manufacturing of components with spatially varying microstructure, i.e. components with tailored material properties, such as soft zones [7],[8]
- Experimental studies and model developments for pressure and temperature dependent heat transfer coefficient in the contact between the blank and tool,[9].
- Development of ductile failure models for multi-phase materials such as press hardened components with spatially varying micro-structure, [10],[11].

### 4 Acknowledgments

Former PhD-students and coworkers carrying out most of the research work concerning the development of simulation methods for analyses of the press hardening process are gratefully acknowledged. These persons are found in the reference list below. The fruitful cooperation with several companies such as Gestamp Hardtech (former SSAB Hardtech), Volvo Car Corporation and Ford Motor Company is also gratefully acknowledged.

### 5 References

- [1] Olsson, T.: An LS-DYNA material model for simulations of hot stamping processes of ultra high strength steels, in: Hot sheet metal forming of high-performance steel, CHS2: 2nd int. conf., June 15-17, 2009, Luleå, Sweden, Verlag Wissenschaftliche Scripten, 2009. 229-237
- [2] Bergman, G., Oldenburg, M.: A finite element model for thermo-mechanical analysis of sheet-metal forming, Int. J. Numer. Meth. Eng. 59, 2004, 1167–1186
- [3] Somani, M.C., Karjalainen L.P., Oldenburg, M. and Eriksson, M.: Effects of plastic deformation and stresses on dilatation during martensitic transformation in a B-bearing steel, J. Mater. Sci. Technol., vol. 17, No 2, 2001, 203-206
- [4] Åkerström, P., Wikman, B. and Oldenburg, M.: Material parameter estimation for boron steel from simultaneous cooling and compression experiments, Modelling Simul. Mater. Sci. Eng. 13, 2005, 1291-1308
- [5] Åkerström, P., Oldenburg, M.: Austenite decomposition during press hardening of Boron steel - computer simulation and test, Journal of Materials Processing technology 174, 2006, 399-406
- [6] Åkerström, P., Bergman, G., Oldenburg, M.: Numerical implementation of a constitutive model for simulation of hot stamping. Modelling Simul. Mater. Sci. Eng. 15, 2007, 105–119
- [7] Oldenburg M, Lindkvist G.: Tool thermal conditions for tailored material properties, HTM: Journal of Heat Treatment and Materials: Zeitschrift für Werkstoffe, Wärmebehandlungv Fertigung, 66(6), 2011, 329-334.
- [8] Oldenburg M.: Warm forming of steels for tailored microstructure, in: Hetnarski R, Ed., Encyclopedia of Thermal Stresses, Springer, 2014, 6469-6479.
- [9] Salomonsson P., Oldenburg M., Åkerström P., Bergman G.: Experimental and numerical evaluation of the heat transfer coefficient in press hardening, Steel Research International, 80(11), 2009, 841-845.
- [10] Östlund R, Oldenburg M, Häggblad H-Å, Berglund D.: Evaluation of localization and failure of boron alloyed steels with different microstructure compositions”, Journal of Materials Processing Technology, 214(3), 2014, 592–598
- [11] Östlund R, Oldenburg M, Häggblad H-Å, Berglund D.: Numerical failure analysis of steel sheets using a localization enhanced element and a stress based fracture criterion”, International Journal of Solids and Structures. 56, 2015, 1-10.

# **Big Compute/HPC in Microsoft Azure**

T. Karmarkar

Microsoft, USA



## **PLENARY AND KEYNOTE PRESENTATIONS II**



# Stochastic Simulations for Crash Worthiness and Occupant Protection

Tsuyoshi Yasuki Ph.D.  
Project general manager, Advanced CAE Division

Toyota Motor Corporation, Japan

Reduction of mass of vehicle is a high priority of design targets in automotive industries. To achieve the design targets, several quality control methods are employed in crashworthiness and occupant simulations by LS-DYNA at Toyota Motor Corporation. Some topics using quality control methods in the simulations including LS-TASC are introduced, and its effectiveness and limitations are discussed.

# Dummy-Positioning for a Whiplash Load Case using LS-DYNA Implicit

A. Hirth  
Daimler AG, Germany

A. Gromer  
DYNAmore GmbH, Germany

T. Borrvall  
DYNAmore Nordic AB, Sweden

---

## Usage of LS-DYNA in Metal Forming

Dr. Michael Fleischer, A. Lipp, Dr. J. Meinhardt, Dr. P. Hippchen, Dr. I. Heinle, A. Ickes, T. Senner

BMW Group, Germany

The use of finite element simulations for a virtual validation of the forming process for sheet metal parts is used since the mid 1990s and is state of the art in the automotive industry today. Two challenging tasks for determining whether a tool design and its process parameters are feasible are the prediction of the material behavior during the forming process and the springback of the final part.

For improving the predictive accuracy of the forming simulation, the levels of detail have increased steadily regarding many aspects of the simulation model. For example, the material behavior during drawing is influenced by the preceding trimming operation. The latter causes damage at the trimmed edge. Furthermore, during the drawing the pressure distribution between the blank and the blank holder may vary significantly due to the deflection of the tool and the press. This can result in a disadvantageous restraining behavior. Considering these effects may lead to a further improvement of the simulation's accuracy.

In addition to the well-established cold-forming processes, new production technologies were introduced in the automotive industry. If the part is manufactured in a hot forming process the material model has also to consider the phase transformation of the steel for an accurate prediction of the final part geometry. Another example for a new forming technology is the use of carbon fiber reinforced plastic parts.

As a result, the increase in size and level of detail of the finite element models as well as the growing complexity of the material models poses a challenge for the future simulation infrastructure with respect to computing resources, licenses, etc.

The above examples were all for the simulation of production of single parts of a body in white. However the actual body in white consists of assemblies such as the doors, which itself contains multiple single parts. Predicting the geometry of the final assemblies, as well as the virtual validation of these assemblies, pose a future challenge.

# Enabling Effective and Easy to Access Simulation

E. Schnepf  
Fujitsu Technology Solutions

S. Gillich  
Intel

**PLENARY AND  
KEYNOTE PRESENTATIONS III**





# **Under Body Vulnerability and Design Loads Prediction using LS-DYNA at Jaguar Land Rover**

P. Khapane

Jaguar Land Rover, United Kingdom

# CAE and Testing Dreams for 2020

C. Lemaitre

Faurecia, France

# Joint Analytical/Experimental Constitutive and Failure Model Development

Jeremy Seidt<sup>1</sup>, Paul Du Bois<sup>2</sup>

<sup>1</sup> Ohio State University

<sup>2</sup> Consulting Engineer, Northville, MI

## 1 Introduction

The prediction of failure is without any doubt the decisive ingredient of any numerical simulation performed within the framework of safety analysis. Whereas this has always been true for aeronautical and defense applications, it became so in automotive crash more recently through the introduction of lightweight materials. There is definitely no shortage of failure models in the LS-DYNA software and the wide range of applications has driven many of these models towards ever increasing generality including a strong tendency towards tabulated input formats. This has the advantage of a high predictive potential provided that 1/ the necessary experimental data are available, 2/ the model has been carefully calibrated with respect to these data and 3/ the data cover the entire range of temperatures, stress states, strain rates a.s.o. , that the structure might be subjected to in a real life application. In other words, the experimental program must be carefully designed keeping the actual application in mind. This is the first level where a close cooperation between analysts and experimentalist is absolutely crucial.

## 2 Experimental techniques ; DIC

Digital Image Correlation (DIC) is an optical, non-contact technique to measure full-field deformation on the surface of a work piece. One camera can be used to measure planar displacements and strains on flat objects. Three dimensional DIC measurements are necessary for specimens with 3D geometric features or where significant out of plane deformation is expected. 3D measurements can be made with two cameras in a calibrated stereo rig. DIC measurements can be made in static tests and dynamic tests at strain rates ranging from  $1E-4 \text{ s}^{-1}$  to  $5000 \text{ s}^{-1}$ . The technique is only limited by the camera hardware used in the experiment. 3D DIC can be used for servohydraulic load frame and split Hopkinson bar (SHB) experiments. In addition, 3D DIC can be used to measure specimen deformation at elevated temperatures (up to 860 deg C) with a custom designed furnace.

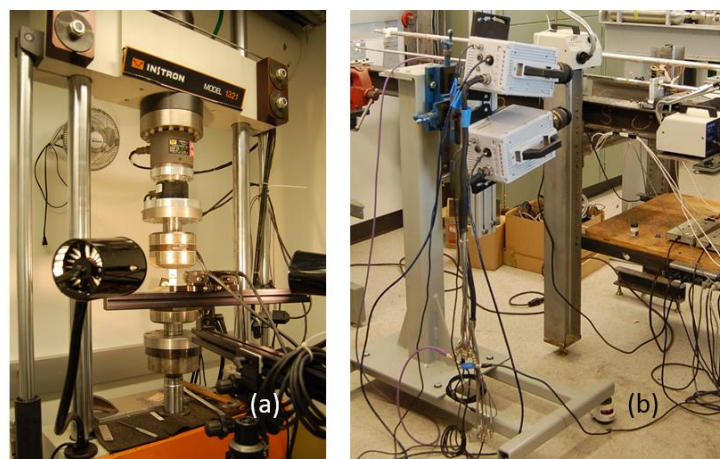


Fig.1: 3D DIC experimental setups: (a) typical low strain rate setup on a load frame, (b) dynamic setup with a tension SHB apparatus.

### 3 Direct Benefits to the CAE implementation

As the DIC can output full strain fields for any chosen base length ( virtual strain gage length ) and these strain fields can be directly compared to numerical results obtained with a similar mesh size ( element characteristic length ), the potential for numerical modeling is obvious. As shown in Figure 2 the maximum strains recorded prior to failure in experiments corresponding to different stress states can be used to generate a first estimate of the failure curve for any material. The curve remains a first guess as the experimentalist cannot measure stresses and the exact value of the stress triaxiality therefore remains unknown.

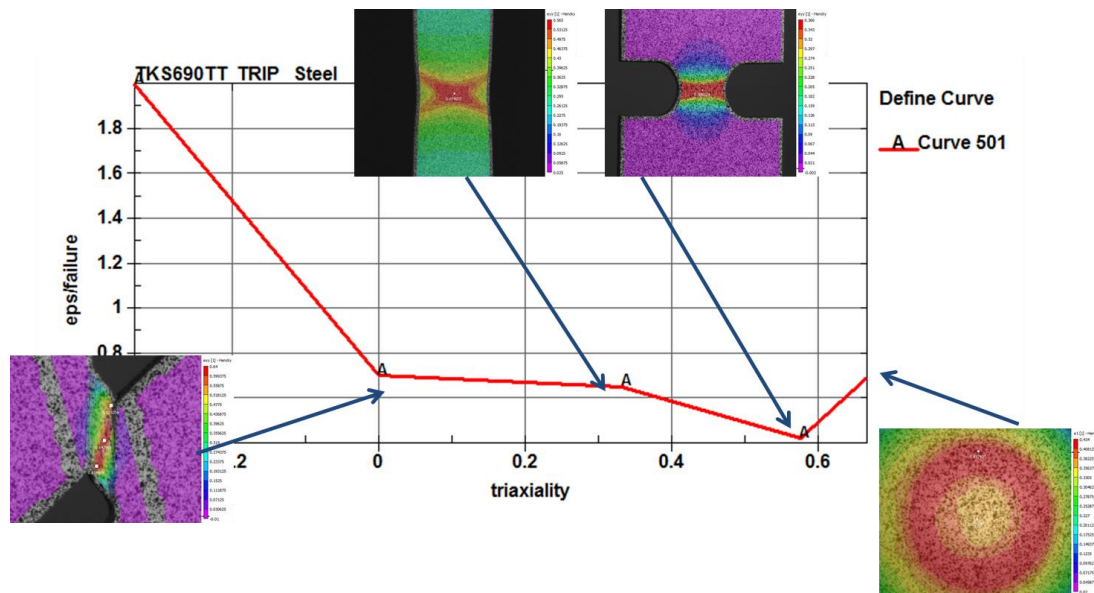


Fig.2: First estimate of a failure curve based on DIC data

Similarly, as strain fields can be output from the same test for different values of the virtual strain gage length, this can be used to construct a first guess of regularization curves , primarily in uniaxial and biaxial testing where larger gage lengths are physically possible ( this is typically not the case in a shear test )

### 4 Summary

The generation of a predictive material and failure model depends upon the close cooperation between the analyst and the test lab. This cooperation does not stop with the test report but continues with discussions during the model development process to deepen both sides' understanding of the results that were obtained. In particular the introduction of DIC has allowed to reduce lead times for the development of GISSMO and/or MAT\_224 datasets from 6 to 2 weeks with a considerable increase in confidence levels of the models.

### 5 Literature

- [1] Sengoz, K.: " Development of A Generalized Isotropic Yield Surface for Pressure Insensitive Metal Plasticity Considering Yield Strength Differential Effect in Tension, Compression and Shear Stress States", Doctoral Dissertation (The George Washington University), 2015
- [2] Buyuk, M. : " Development of A Tabulated Thermo-Viscoplastic Material Model with Regularized Failure for Dynamic Ductile Failure Prediction of Structures under Impact loading", Doctoral Dissertation (The George Washington University), 2013
- [3] Seidt, J.: "Plastic Deformation and Ductile Fracture of 2024-T351 Aluminum under Various Loading Conditions", Doctoral Dissertation (The Ohio State University), 2010.
- [4] Hammer, J.: "Plastic Deformation and Ductile Fracture of Ti-6Al-4V under Various Loading Conditions", Thesis (The Ohio State University), 2012.

# Nonlinear Analysis 1980 – 2020

M. Lawson

Rolls-Royce, United Kingdom



**CRASH I**

**FAILURE**





# Prediction of Dynamic Material Failure – Part I: Strain Rate Dependent Plastic Yielding

M. Feucht<sup>1</sup>, R. Böhm<sup>2</sup>, F. Andrade<sup>3</sup>, P. DuBois<sup>4</sup>, A. Haufe<sup>3</sup>

<sup>1</sup>Daimler AG, Sindelfingen, Germany

<sup>2</sup>KIT, Karlsruhe, Germany

<sup>3</sup>DYNAmore GmbH, Stuttgart, Germany

<sup>4</sup>Consultant, Offenbach, Germany

The dynamic behavior of materials plays a major role in crashworthiness. During a high speed crash event, the material undergoes different strain rates that may affect its constitutive behavior. For instance, in the first milliseconds of such an event, the strain rates near the contact region between the impacting and the impacted areas are extremely high. The strain rate then tends to rapidly decrease as energy is progressively dissipated during the crash. In the case of metallic materials, this means that the material is experiencing a viscoplastic regime under non-constant strain rate. The viscoplastic deformation process causes adiabatic heating at high strain rates where this heating tends to soften the material. At the same time, as the strain rate decreases, the heat caused by plastic deformation is then transferred to the surroundings and therefore the material behaves in a different fashion than at the beginning of the crash. For an accurate description of the material deformation under such conditions, the aspects involving plastic straining and adiabatic heating have to be somehow taken into account if one aims to have relevant simulation results. In this contribution, we address this question by firstly numerically calibrating the viscoplastic behavior for two modern steel alloys using \*MAT\_224 in fully coupled thermo-mechanical simulations in LS-DYNA. In this manner, we are able to correctly consider the thermal effect associated with the different strain rates. However, coupled thermo-mechanical simulations are unfortunately prohibitive when simulating a full vehicle collision as it would require extremely long simulation times. Therefore, two alternative approaches are assessed in this paper. In the first one, we make use of a pseudo-thermal analysis where the material heating is estimated from the plastic work by using Taylor-Quinney's coefficient in \*MAT\_224. In the second approach, effective yield curves, which inherently take into account the softening effects of adiabatic heating, are calibrated for classical von Mises plasticity through \*MAT\_024 in LS-DYNA. A true viscoplastic formulation is also considered here. In this case, the resulting strain rate dependent yield curves may have to cross each other in order to correctly match experimental data under different strain rates. As could be expected, the crossing of yield curves poses an algorithmic challenge which has been further investigated during this work and whose results will be presented. Furthermore, the calibration of such strain rate dependent yield curves is quite difficult using classical extrapolation functions. Therefore, we propose in this contribution an extended version of Hockett-Sherby's extrapolation where strain rate dependent parameters are incorporated. The results show that the newly proposed extrapolation scheme is able to generate dynamic yield curves for \*MAT\_024 that match experimental data under different strain rates.

# Prediction of Dynamic Material Failure – Part II: Application with GISSMO in LS-DYNA

F. Andrade<sup>1</sup>, M. Feucht<sup>2</sup>, R. Böhm<sup>3</sup>, P. DuBois<sup>4</sup>, A. Haufe<sup>1</sup>

<sup>1</sup>DYNAmore GmbH, Stuttgart, Germany

<sup>2</sup>Daimler AG, Sindelfingen, Germany

<sup>3</sup>KIT, Karlsruhe, Germany

<sup>4</sup>Consultant, Offenbach, Germany

As alluded in the first part of the present contribution, strain rate effects are quite relevant during a high speed crash event. If one intends to accurately predict failure under such conditions, it is important to properly understand and depict the underlying phenomena involved in such a scenario. For instance, the adiabatic heating that takes place during the plastic deformation process at high strain rates softens the material in such manner that the local plastic strain increases in critical zones. Also, localization is more pronounced in such critical zones due to the softening caused by adiabatic heating. On the other hand, the failure of metallic materials depends on innumerable factors such as stress state, strain path, non-proportionality of loading but also on the plastic strain. Therefore, it is quite important to properly model the plastic straining under the different strain rates if one aims to predict failure in full car crash simulations. In this respect, the first part of this contribution has proposed a methodology to deal with the description of viscoplasticity by using effective yield curves with \*MAT\_024. As a consequence, the local plastic strain at critical zones is more accurate, which means that the definition of a failure criterion for ductile fracture can be done properly. In this work, we use the so-called GISSMO damage/failure model available in LS-DYNA through the keyword \*MAT\_ADD\_EROSION. GISSMO allows the definition of a fracture curve which is used for the nonlinear accumulation of scalar damage. This kind of accumulation inherently takes into account the effects of strain path change during plastic deformation, a very important effect in crash simulation. Furthermore, strain localization is predicted by accumulating an instability measure, which activates element fading by affecting the stress tensor with the damage variable. GISSMO also has a simple regularization tool which scales the fracture curve in order to take spurious mesh dependence into account. These features of GISSMO have been tested when adopting the dynamic yield curves calibrated for different strain rates with \*MAT\_024. The associated GISSMO calibration for two modern steel alloys is presented in the present contribution. It is shown that, for these two materials, a single fracture curve can be used with reasonable results, i.e., the simulation of specimens under different stress states and different strain rates could reproduce experimental data with good accuracy. The effects of strain rate dependence on the regularization methodology of GISSMO have also been focus of the present study. Numerical investigation conducted by the authors suggests that the different strain rates require different regularization factors. This effect is more pronounced for coarser (5mm > Le > 10mm) than for finer (1mm > Le > 3mm) mesh refinements. In fact, up to an element size of 3mm the already existing regularization method provides satisfactory results. Therefore, for such mesh refinements, the calibration of a strain rate dependent GISSMO card seems somewhat similar to the quasi-static case. Nevertheless, further investigation is still needed in order to better understand the consequences of such modeling technique.

# Modelling of Strain-Rate Dependence of Deformation and Damage Behavior of HSS- and UHSS at Different Loading States

Andreas Trondl<sup>1</sup>, Dong-Zhi Sun<sup>1</sup>

<sup>1</sup>Fraunhofer Institute for Mechanics of Materials IWM

## 1 Abstract

The predictive capability of crash simulation concerning material failure is still in need of improvement due to the coupled complex influences of triaxiality, strain rate and temperature. Because of their lower ductility the use of high- and ultra-high strength steels (HSS&UHSS) requires a more accurate prediction of failure. This subject commonly leads to more complicated material- and failure models to describe complex interactions between deformation, strain rate and temperature, which usually results in longer computational time. On the other hand, due to the high complexity of crash simulation structures, simpler and less time-consuming material models and numerical methods are required to keep simulation times in an acceptable frame. For this reasons, a material model which considers the influences of strain rates and adiabatic effects was suggested and applied to simulate different testing scenarios. To avoid the time-consuming fully coupled thermal-mechanical approach, a strain-rate dependent Taylor-Quinney-Coefficient was introduced to control local adiabatic heating which lead to variable softening effects for different strain rates. Additionally, numerical investigations on the GISSMO damage model were carried out. Influences of the stress state (triaxiality) and strain rate on the failure behavior of HSS&UHSS were characterized and simulated. To demonstrate the capabilities of the used approaches, loading tests on different geometries of specimens e.g. tension, shear tension, notch tension, pierced tension and Nakajima specimens were conducted with optical and infrared measurement of local strain and temperature fields. Especially the adiabatic softening and the change of failure strain at higher strain rates under different stress triaxialities were analyzed.

KEYWORDS: deformation behavior, failure behavior, plasticity model, triaxiality, GISSMO, UHSS, HSS, 22MnB5, HX340LAD, Taylor-Quinney-Coefficient, failure line, adiabatic, thermo-mechanical effects, strain rate

## 2 Material and Damage Modeling

To describe the material behaviors sufficiently enough, a modelling approach based on deformation mechanisms is needed. An appropriate choice leads to use a strain rate dependent plasticity model for describing the deformation behavior and an additional damage model to depict the final failure of the material.

### 2.1 Strain-Rate and Temperature dependent Material Model

It is commonly known that local heating effects occur during high speed loading, which is mostly the case during crash relevant scenarios. This effect is significantly more pronounced for higher loading speeds. The reason of this fact lies in the conversion from the work of plastic deformation to thermal energy, which can be described by the Taylor-Quinney coefficient  $\beta$  [1]. It is obvious that the available time for heat conduction decreases at higher strain rates, which leads to higher temperatures. In that case the heat conduction plays a negligible role and the local deformations run mainly under adiabatic conditions, which means no or remarkably reduced local heat exchange outwards is possible due to the short deformation time. On the other hand in case of lower strain rates the available time for heat conduction increases, which leads to a lower temperature rise, and non-adiabatic local deformation takes place. These mechanisms show the importance of heat conduction during plastic deformation at different strain rates. For complex crash simulations in automotive applications it is not possible to take the heat conduction into account due to the time consuming thermo-mechanical coupled calculation. First approaches to describe these circumstances are based on models of Johnson-Cook type which use a multiplicative combination of the influences of plastic strain hardening  $\sigma_0(\varepsilon_p)$  and strain-rate hardening  $f(\dot{\varepsilon}_p)$  as well as temperature related softening  $g(T)$ . The main idea to describe minor or no adiabatic effects for lower deformation speeds is the reduction of the thermal heating at lower strain rates, which should compensate the not included heat conduction in the model. Out of these

requirements one suggestion of the strain-rate dependent Taylor-Quinney coefficient is given in the following equation (1)

$$\beta = \beta_0 \cdot \left[ \frac{1}{2} + \arctan \left( b_\omega \cdot \ln \frac{\dot{\epsilon}_p}{\dot{\epsilon}_{p,\omega}} \right) \cdot \frac{1}{\pi} \right] \quad (1)$$

The consideration of the strain-rate dependent Taylor-Quinney coefficient (1) in the standard Johnson-Cook Model leads to much more realistic temperature evolutions for lower deformation speeds. For higher strain rates the thermal behavior still shows adiabatic deformation.

### 2.2 Damage Model and Strain-Rate

The used approach for describing failure bases on a scalar damage parameter  $D$ , which is not coupled to the actual stress state of the applied plasticity model. Fracture occurs when the cumulative scalar damage parameter  $D$  reaches the critical value of 1. The damage evolution depends strongly on the failure strain, which is a function of the local stress state (triaxiality) and therefore of the strain-rate too. In Addition, for each tested strain rate the failure line of the model was calibrated separately. This was done by using GISMMO for the UHSS 22MnB5 and the micro-alloyed steel HX340LAD.

### 3 Simulations of Specimen-Tests

During the calibration of the presented “pseudo-thermomechanical” plasticity model a more physically reasonable temperature-softening  $g(T)$  is used, because the commonly known analytical approach of Johnson-Cook does not lead to suitable results (especially for shear dominated stress states), which results from the strong decrease of thermal softening for higher temperatures.

The verifications of the used models demonstrate a good agreement with experiments in the global (force-displacement) measurements for different stress states. The investigated loading speeds reached from quasistatic (nominal strain rate for tension 0.001/s) over medium strain rates (1/s) up to high speeds (nominal strain rate for tension 100/s).

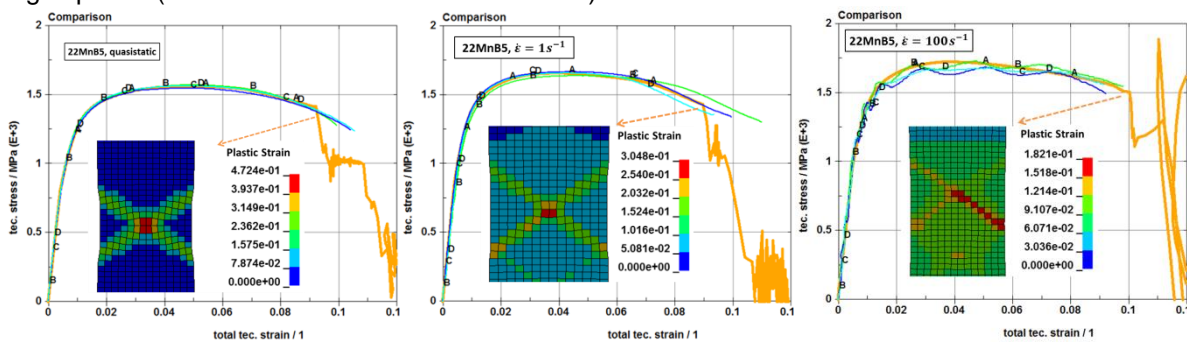


Fig.1: Comparison between simulation (thick orange lines) and experiment (thin colored green, blue and cyan lines) of strain vs. stress curves for the tension tests under three different strain rates for 22MnB5

From the simulations of the tension test one can see clearly a significant less pronounced localization for the high strain rate in comparison to the medium strain rate and the quasistatic load case. In contrast to all tension tests of the UHSS 22MnB5, the other specimens shown a similar localized distribution of the plastic strain field over all observed strain rates, which can be explained by the specimen’s shape that enforces strain localization.

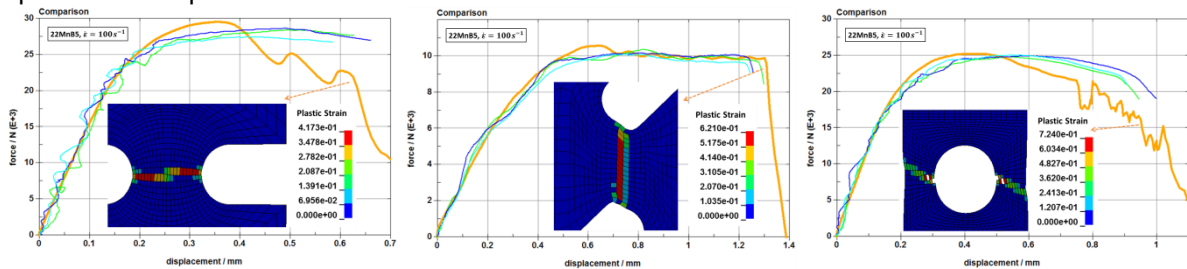


Fig.2: Comparison between simulation (thick orange line) and experiments (thin colored lines) of force-displacement curves and simulated local strain field for strain rate 100/s (22MnB5)

Both materials (less ductile UHSS 22MnB5 and more ductile HX340LAD) shown in the simulation under quasistatic loading an expected minor temperature evolution (<10K) during the strong

localization at the end of the tests, which is related to the influence of the strain-rate dependent Taylor-Quinney coefficient.

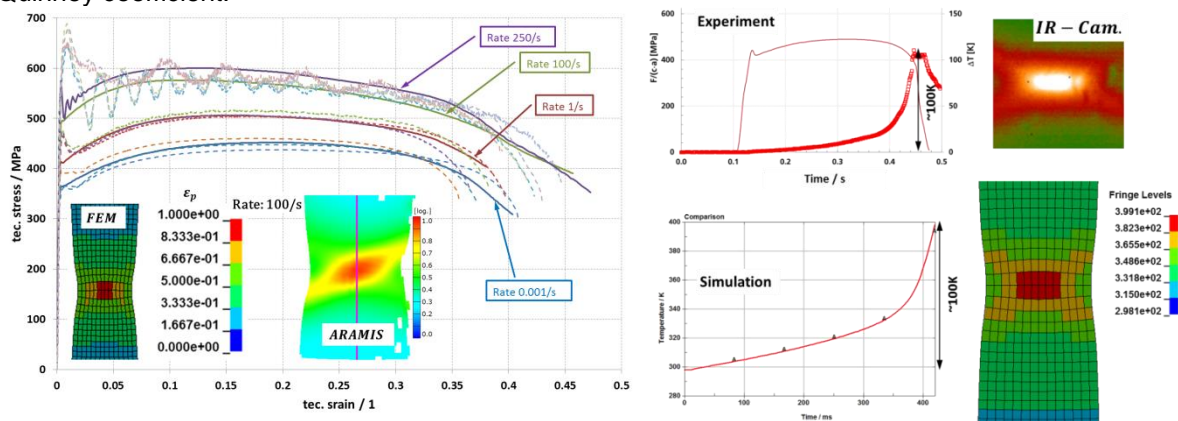


Fig.3: left: Comparison between simulation (solid lines) and experiment (dashed lines) of strain vs. stress curves for the tension tests under four different strain rates and an exemplary local plastic strain field at high strain rate (100/s) for a ductile HX340LAD right: Comparison between simulation (below) and experiment (top) of temperature development and local temperature field for medium strain-rate of 1/s (tension test) HX340LAD

The calibration of the failure model represents a compromise of all different stress states (triaxialities). One problem in the calibration is the interaction of the stress-state evolution between the pure tension- and the holed tension test.

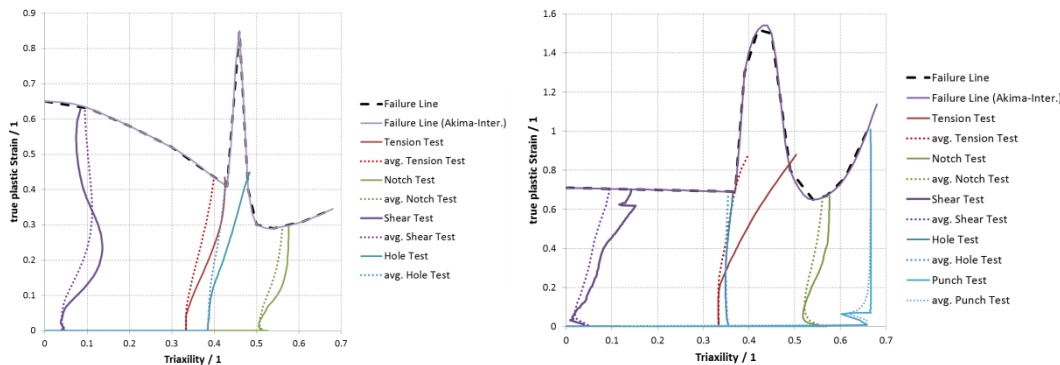


Fig.4: Quasistatic failure behavior for a UHSS 22MnB5 (left) and for comparison a ductile micro-alloyed HX340LAD (right)

Using different failure curves within a strain rate range leads in most load cases (triaxialities) to better agreements between simulations and experiments for the investigated 22MnB5 and HX340LAD. But on the other hand the calibration of the failure model for each strain rate is more time consuming.

#### 4 Summary

The deformation and damage behavior of different steels for automotive application were investigated under multiaxial crash loading through various experiments and numerical simulations. A modified plasticity model was proposed to describe the temperature development for higher and lower strain rates in a sufficient manner without using the time consuming thermo-mechanical coupling, which is important for crash relevant applications. Several examples were presented to show the applicability of the model for different stress states. The comparisons of simulations to experimental investigations show good agreements for different triaxialities. A failure model and a coupling to the plasticity model were presented for the UHSS 22MnB5 and ductile micro-alloyed steel of type HX340LAD. The failure strain shows a significant increasing between triaxialities from 0.5 up to 0.67 for the ductile micro-alloyed steel HX340LAD. For shear dominated dynamic loadings decreasing failure strain with increasing strain rate was observed and verified in simulations. For tension dominated loadings a reduction of plastic failure strains is determined by the simulations, which can be explained by a more pronounced homogeneous plastic strain field for higher strain rates.



**CRASH II**

**FAILURE**





# Development of an Anisotropic Material Model for the Simulation of Extruded Aluminum under Transient Dynamic Loads

Anthony Smith<sup>1</sup>, Paul DuBois<sup>2</sup>, Thomas Borrvall<sup>3</sup>

<sup>1</sup>Honda R&D Americas

<sup>2</sup>LSTC Consultant

<sup>3</sup>DYNAmore Nordic

The movement towards lightweight materials in the construction of automotive bodies is leading to an increase in parts made from extruded aluminum and other materials with a large degree of anisotropic behavior. The need to model these anisotropic properties and predict the behavior of these materials is increasing rapidly. A review of the anisotropic material models available in LS-Dyna including Material types 36, 133, 135, and 243 led to the decision that Material type 36 with option “Hardening Rule 7” (HR7) was the most appropriate choice for application towards analysis of extruded aluminum parts under both static and dynamic loads. Material type 36 (**\*MAT\_3-Parameter\_Barlat**) has a history of use in forming applications and shows promise as a valuable tool for modeling anisotropic behavior in high strain, high velocity simulation applications as well.

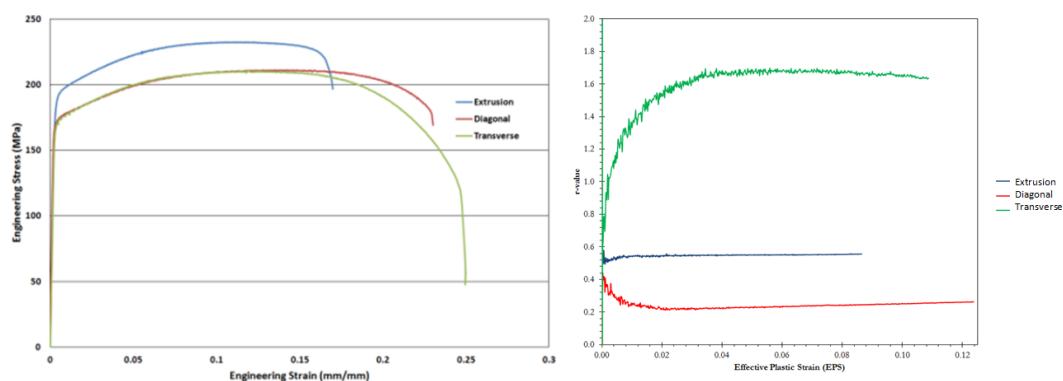


Fig.1: Anisotropic Tensile Test Data (Engineering Stress and R-Values) for 6000 Series Extruded Aluminum.

An investigation into this application of the material model revealed fundamental limitations in the stability of the model, particularly in cases of high anisotropy (with R-values diverging greatly from 1.0). The original implementation of the **\*MAT\_3-Parameter\_Barlat** HR7 material model supports flow stress and R-value inputs for three stress states: uniaxial in the 00° material direction, uniaxial in the 45° material direction, and uniaxial in the 90° material direction. The method behind HR7 is aimed at fitting the input test data rather than fulfilling thermodynamic requirements. The major difficulty and limitations to this approach lie in the interpolation between the known test data points, which is being used to render a yield surface close to convexity and a flow rule close to normality for general stress states. This interpolation is important for robustness and stability. The initial version of this interpolation technique could result in spurious and non-unique responses. Based on this knowledge, the authors updated the material model which should improve both accuracy and stability.

The most important of these updates was the inclusion of four more input parameters to the **\*MAT\_3-Parameter\_Barlat** HR7 formulation. These parameters enable the user to input hardening curves detailing the material stress-strain response in the shear and biaxial loading conditions. They also enable the user to input constant values or load curves defining a novel shear and biaxial “R-Value”

response over a chosen strain range for the material. The R-values in shear and biaxial are defined in a convenient way by the respective expressions:

$$RSHR = \frac{-dEPS11}{dEPS22} \quad (1)$$

$$RBIAX = \frac{dEPS11}{dEPS22} \quad (2)$$

Incorporating these inputs results in a model that can now interpolate between the uniaxial stress state in three material directions as well as the biaxial and shear stress states using additional test data. These additions serve to improve the stability of the model over a greater range of input parameters, and allow for implementation of the model towards materials with higher levels of anisotropic behavior.

Investigations based upon single element and coupon level simulation contibuted to the validation of the robustness of the updated material model. Further work with coupon and component level models will support the effort to understand its predictive capabilities for simulation of transient dynamic loading conditions. The final goal of the project is to predict the anisotropic strength, stiffness and fracture of extruded aluminum during impact loading. The main focus of this presentation is to explain and illustrate the changes to the **\*MAT\_3-Parameter\_Barlat** HR7 formulation to improve the accuracy and robustness of the model.

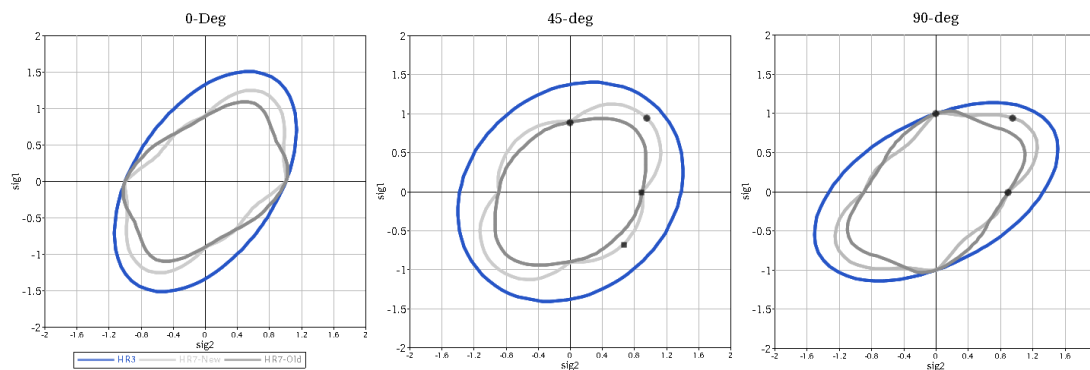


Fig.2: Comparison of Yield Surface Generated by Various Implementations of **\*MAT\_3-Parameter\_Barlat** at Three Material Orientations.

#### Literature

Fleischer, M., Borrvall, T. and Bletzinger, K-U., "Experience from using recently implemented enhancements for Material 36 in LS-DYNA 971 performing a virtual tensile test", 6th European LS-DYNA Users Conference, Gothenburg, 2007.

# The Numerical Failure Prediction by the Damage Model GISSMO in Various Materials of Sheet Metal

Shota Chinzei<sup>1</sup>, Junya Naito<sup>2</sup>

<sup>1,2</sup> KOBE STEEL, LTD., Multi-Material Structural Design and Joining Research Section Mechanical Engineering Research Laboratory Technical Development Group

## 1 Abstract

High-strength steel sheet is widely used for car bodies in response to continuous demands for weight saving and enhancement of vehicle collision safety. In addition, weight reduction is an increasingly pressing requirement for aluminum sheet applications. When applying sheet metals with lower thickness and higher strength to car body fabrication, numerical fracture predictions are an important requirement to ensure collision safety, since the reduction in ductility becomes a key issue. As a failure model, we use a well-examined damage model GISSMO which includes incremental formulation for the description of material instability and localization.

In this study, failure curves for GISSMO were identified by experimental data. Numerical failure prediction using GISSMO was conducted for a quasi-static axial crush test of a HAT member. Based on experimental and numerical results, the validity of the damage model GISSMO for high strength steel and aluminum alloy sheets is then discussed.

## 2 Failure criteria for GISSMO

The fracture strain values at several stress states are required to identify the fracture curve. They are obtained from notched tensile tests (uniaxial and plane strain) [1], shear test [2], and Erichsen test (biaxial tensile). Then, fracture strains are calculated on the assumption of the plane stress condition.

In this study, evaluated several materials were evaluated, namely, PHS (TS 1500MPa grade), UHSS (TS 980MPa grade), aluminum alloy 7000 series and 6000 series. In the present paper, the focus is on the UHSS. "UHSS A-type" is a metal that has higher uniform elongation. "UHSS B-type" is a metal that has better local ductility.

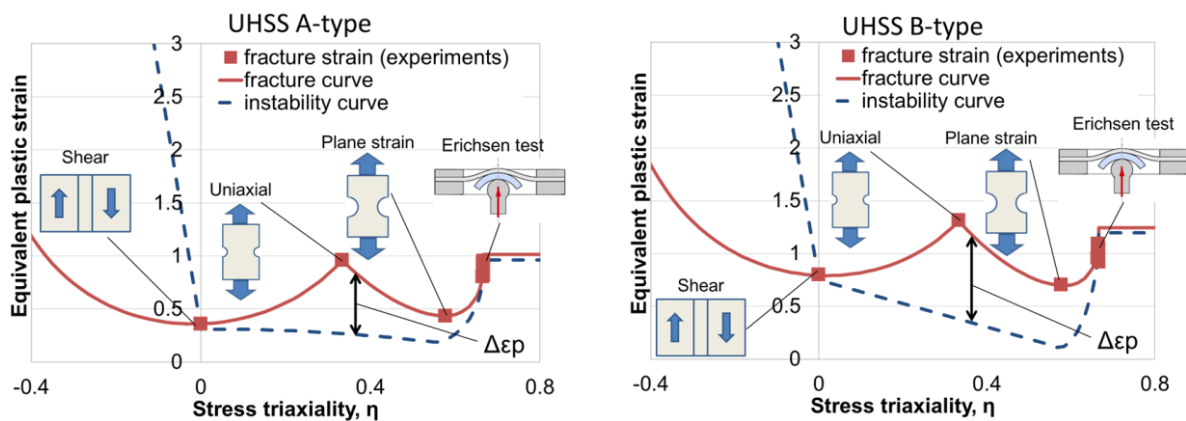


Fig.1: The fitted curve for fracture and instability.

The curve of fracture and instability identified from material tests are shown in Fig.1. In Fig. 1, the difference of equivalent plastic strains between the fracture and instability curves, denoted by  $\Delta\epsilon_p$ , is thought to correspond to the progress of local ductility. From the figure,  $\Delta\epsilon_p$  of the UHSS B-Type is greater than that of UHSS A-Type. This shows that the local ductility of the former is higher than that of the latter, and it corresponds with the experimental facts. The correlation between  $\Delta\epsilon_p$  and the local ductility is also confirmed in other experimental results.

### 3 Numerical failure prediction (Shell model)

Numerical failure prediction using GISSMO with the above failure criteria is performed for the quasi-static 3-point bending test and the axial crush test of a HAT member.

The GISSMO damage model is implemented in card 3 and card 4 of the LS-DYNA keyword **\*MAT\_ADD\_EROSION** and activated by the first flag IDAM=1. In this study, the widely-used **\*MAT\_PIECEWISE\_LINEAR\_PLASTICITY (\*MAT\_024)** was chosen for the material model.

#### 3.1 Quasi-static HAT 3-point bending test

Fig.2 shows the numerical and experimental results for the quasi-static 3-point bending test of a HAT member of UHSS A-Type and UHSS B-Type.



Fig.2: Comparison of numerical and experimental results for 3-point bending test of HAT member

As shown in Fig. 2, there are no cracks in the numerical and experimental results. It is confirmed that numerical prediction can reproduce the same result i.e. that cracking does not occur.

#### 3.2 Quasi-static HAT axial crush test

Fig.3 shows the numerical and experimental results for a quasi-static axial crush test of a HAT member of UHSS A-Type and UHSS B-Type.

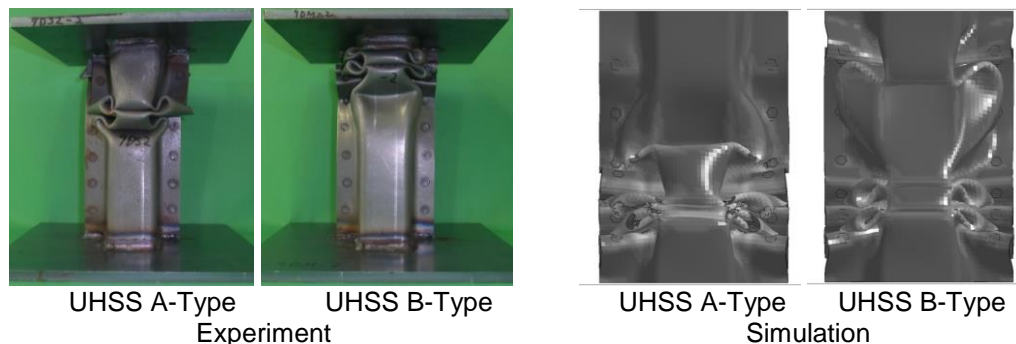


Fig.3: Comparison of numerical and experimental results for axial crush test of HAT member

As shown in Fig. 3, crack locations obtained by the simulation correlate well with the experiment results and it is confirmed that failure prediction can be performed accurately using GISSMO.

## 4 Conclusions

The fracture and instability curves were identified from fracture strains in material tests. Numerical predictions using GISSMO were then performed using those curves. Finally, it was confirmed that numerical predictions are very close to agreement with experimental results.

## 5 Literature

- [1] Till, E. T.; Hackl, B.; Schauer, H.: "Crash simulation of roll formed parts by damage modelling taking into account preforming effects", AIP CONFERENCE PROCEEDINGS, 2011, pp.267-274
- [2] An, Y.G.; Vegter, H.; Heijne, J.: "Development of simple shear test for the measurement of work hardening", Journal of Materials Processing Technology 209, 2009, pp.4248-4254

# An Investigation of Modeling Approaches for Material Instability of Aluminum Sheet Metal using the GISSMO-Model

Georg Falkinger<sup>1</sup>, Peter Simon<sup>2</sup>

<sup>1</sup>LKR Leichtmetallkompetenzzentrum Ranshofen GmbH, Ranshofen, AT

<sup>2</sup>AMAG rolling GmbH, Ranshofen, AT

## 1 Introduction

The use of aluminum sheet for stamped parts in the automotive industry is a continuous trend driven by the pressing need of weight reduction. At the same time the role played by numerical methods for the design of forming processes and components is constantly increasing. Suppliers of aluminium sheet are facing the challenge to (i) optimize the formability of their material and (ii) demonstrate the feasibility of complex geometries to their customers in (iii) as little time as possible. For those three tasks, the standardized, experimentally determined mechanical properties like n- and r-values or the forming limit curve, however, do not always guarantee a reliable assessment. Therefore, in the framework of a joint research project supported by AMAG rolling GmbH, an effort has been made to investigate the suitability of novel alternative methods for the assessment of sheet metal formability.

## 2 Summary

The present contribution shows results from laboratory-scale experiments like tensile tests, Nakajima and Cross-die tests and corresponding FEM simulations for an AA6063-T4 alloy at room temperature. A material model, including the GISSMO damage model, has been calibrated. Specifically the question of the material instability is addressed. It will be shown, that for small to intermediate mesh sizes the criterion according to Hill and for higher mesh-sizes (> 2 mm) the criterion according to Swift, respectively, are resulting in a good correlation to the experimental results. Furthermore, detailed simulations with small solid elements have been performed. The relationship between local physical fracture strains and phenomenological fracture curves used in industrial applications with large shell elements will be discussed.

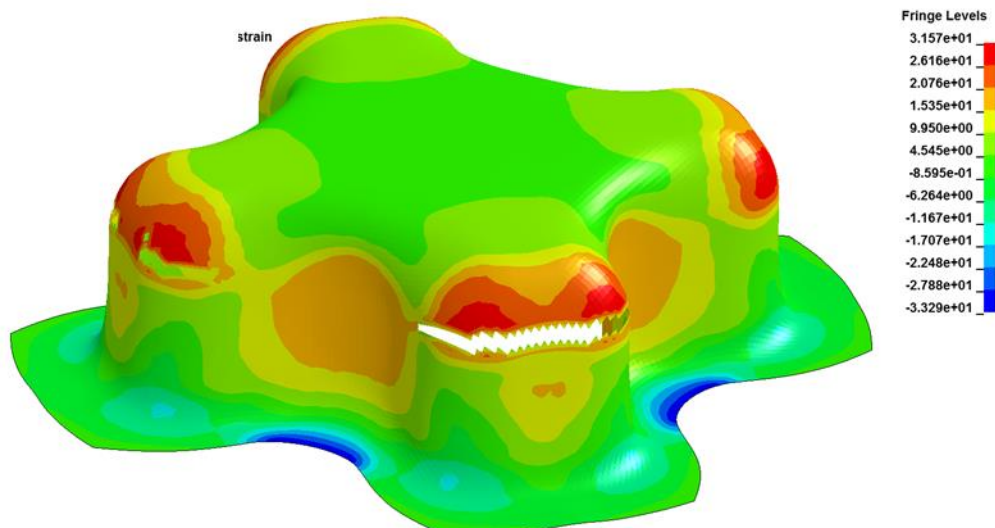


Fig.1: Sheet-Thickness distribution as predicted from FEM-Simulation just after the occurrence of the first macroscopic cracks.



# **CRASH III CONNECTION**





# Modelling of Adhesively Bonded Joints with \*MAT252 and \*MAT\_ADD\_COHESIVE for Practical Applications

F. Burbulla<sup>1</sup>, A. Matzenmiller<sup>2</sup>, U. Kroll<sup>2</sup>

<sup>1</sup>Dr. Ing. h.c. F. Porsche AG, Germany

<sup>2</sup>Institute of Mechanics (IfM), Department of Mechanical Engineering, University of Kassel, Germany

## 1 MAT\_TOUGHENED\_ADHESIVE\_POLYMER (TAPO-Model)

The new material model \*MAT\_TOUGHENED\_ADHESIVE\_POLYMER (\*MAT\_252) has been developed at the Institute of Mechanics of the University of Kassel [1], [2] and become available for the use with solid elements since LS-DYNA R7.1.1. The theoretical framework of the model equations is based on continuum and damage mechanics in order to predict the complex mechanical behaviour of crash optimized high-strength adhesives under combined shear and tensile loading. Therefore, the non-associated l1-J2-plasticity model is extended to consider material softening due to damage, rate-dependency and the constitutive behaviour under compression. Consequently, the mechanical behaviour of structural adhesives is predicted sufficiently well, which is demonstrated by means of various simulations of specimens and components with adhesive joints under quasi-static and crash loading conditions [2].

## 2 MAT\_ADD\_COHESIVE

The cohesive elements ELFORM 19 and 20 in \*SECTION\_SOLID have a major advantage compared to standard solids: They have no influence on the critical time step in explicit analyses, if they are used to model thin adhesive layers [3]. So the modelling of adhesive layers with cohesive elements makes a significant contribution to the increase of the efficiency and the corresponding reduction of computational costs in numerical applications. So far, only approaches based on fracture mechanics (\*MAT\_41-50, 138, 184, 185, 186, 240) have been available in LS-DYNA for cohesive elements. The new interface \*MAT\_ADD\_COHESIVE is available since LS-DYNA R7.1.1 and overcomes this difficulty. The interface allows the application of all classical material models originally developed for solids (\*MAT\_1, 3, 4, 6, 15, 24, 41-50, 81, 82, 89, 96, 98, 103, 104, 105, 106, 107, 115, 120, 123, 124, 141, 168, 173, 187, 188, 193, 224, 225, 252, 255) together with the cohesive elements 19 and 20 without any modification of the previously established set of material parameters [1], [2]. Thus, the numerical efficiency according to the modelling of thin structures with the cohesive elements is accessible to every solid material model.

## 3 Parameter identification and optimization, model verification and validation

The influences of particular model parameters on the model response are elaborated leading to a simple and robust identification procedure. The model parameters for the elastic-plastic behaviour, damage and material failure are directly identified and computationally optimized with the optimization software LS-OPT [1], [2]. Six quasi-static tests of the bluntly-glued steel tube specimen provide the target data for the identification, verification and optimization. The parameters for the rate dependency are determined by means of dynamic tests of the butt jointed steel tube specimen [1], [2]. The responses of the TAPO- and ARUP-model are compared to each other. Comparisons of the simulations with the data of the KS2-, Peel-Shear- and T-Joint test prove the validity of the TAPO-model and the interface \*MAT\_ADD\_COHESIVE in order to predict the mechanical behaviour of the toughness modified structural adhesive investigated [2], [4], [5].

#### 4 Literature

- [1] FOSTA-report P828: Robustheit und Zuverlässigkeit der Berechnungsmethoden von Klebverbindungen mit hochfesten Stahlblechen unter Crashbedingungen. Research association Forschungsvereinigung Stahlanwendung e.V. – FOSTA, Düsseldorf, 2013, [www.stahlforschung.de](http://www.stahlforschung.de).
- [2] Burbulla, F.: Kontinuumsmechanische und bruchmechanische Modelle für Werkstoffverbunde. PhD-thesis, Institute of Mechanics, University of Kassel, 2013
- [3] Matzenmiller, A., Gerlach, S., Fiolka, M.: A critical analysis of interface constitutive models for the simulation of delamination in composites and failure of adhesive bonds. *Journal of Mechanics of Materials and Structures*, Vol. 5, Nr. 2, S. 185-211, 2010.
- [4] FOSTA-report P676: Methodenentwicklung zur Berechnung von höherfesten Stahlklebverbindungen des Fahrzeugbaus unter Crashbelastung. Research association Forschungsvereinigung Stahlanwendung e.V. – FOSTA, Düsseldorf, 2008, [www.stahlforschung.de](http://www.stahlforschung.de).
- [5] Matzenmiller, A., Burbulla, F.: Kontinuumsmechanische Modellierung von Stahlblechklebverbindungen für die FE-Crashanalyse, Contribution to: 7. LS-DYNA Anwenderforum, 30.9-1.10.2008, Bamberg. DYNAmore, Industriestr. 2, 70565 Stuttgart-Vaihingen, 2008

# Practical Failure Criterion of Spot Weld for Crash Simulation

Ji-Ho Lim<sup>1</sup>, Jiwoong Ha<sup>1</sup>, Chang-Young Oh<sup>1</sup>

<sup>1</sup>POSCO, Steel Business Division Steel Solution Marketing Dept. Product Application Center, Korea.

## 1 Abstract

This paper proposed a practical failure criterion of spot welds for combined loading condition for crash simulation. The tests were designed to obtain the failure load of a spot weld under combined loading condition. The seven types of experimental test were conducted to obtain the component of spot weld failure criterion. The failure criterion consists of moment component including normal and shear force. Components of each failure test are obtained from finite element analysis results which are called as hybrid method. The proposed criterion was considered to use Wung [1, 2] model except torsion term. It was found that the criterion of mild steel could be expressed as a function well known in previous researches, however the failure criterion of high strength steel and advanced high strength steel could not be described with it. Here we propose new approach. The newly proposed failure criterion is well applied to hat-specimen simulation result.

## 2 Research Objective

Spot weld fracture is a critical issue in crash simulation. Main object of this paper is to develop the practical spot weld failure model in crash simulation.

## 3 Conventional Spot Weld Failure Model

The coefficients that constitute a force-based failure criterion were determined by a regression analysis from the failure strength data of the spot weld. Lee et al. [3] proposed a test methodology under the combined loading conditions and the spot weld failure model based on experimental results. The failure criterion is expressed as

$$\left(\frac{f_s}{F_S}\right)^n + \left(\frac{f_n}{F_N}\right)^n = 1 \quad (1)$$

Here,  $F_N$  and  $F_S$  are the normal failure load and the shear failure load of a spot weld, respectively. The variable  $n$  is a shape parameter. The coefficients that constitute their failure model are obtained using the least square method to minimize the discrepancy between the experimental data and interpolated data.

In the result of Lee et al. [3], spot weld failure criterions are composed of the normal failure load and the shear failure load. Wung [1] and Wung et al. [2], however, suggested the failure mechanism based on the normal load, shear load, bending and torsion. Wung [1] defined the failure modes of a spot weld by three kinds of mechanism, and proposed the failure criterion based on a failure force. The failure criterion is expressed as

$$\left(\frac{f_s}{F_S}\right)^\alpha + \left(\frac{m_b}{M_b}\right)^\gamma + \left(\frac{f_n}{F_N}\right)^\mu + \left(\frac{m_t}{M_t}\right)^\beta = 1 \quad (2)$$

Here,  $F_N$ ,  $F_S$ ,  $M_b$  and  $M_t$  are the normal failure load, the shear failure load, the failure moment and the failure torsion of a spot weld, respectively. The variables of  $\alpha$ ,  $\beta$ ,  $\gamma$  and  $\mu$  are shape parameters. The coefficients that constitute their failure model are obtained using the least square method to minimize the discrepancy between the experimental data and interpolated data.

#### 4 Newly Proposed Spot Weld Failure Model

It is assumed that influential factors on spot weld failure are normal load, shear load and bending, because torsion can be negligible in the automotive structure. Based on this assumption, the spot weld failure model is expressed as

$$\left(\frac{f_n}{F_N}\right)^\alpha + \left(\frac{f_s}{F_S}\right)^\beta + \left(\frac{m_b}{M_b}\right)^\gamma = 1 \quad (3)$$

Here,  $F_N$ ,  $F_S$  and  $M_b$  are the normal failure load, the shear failure load and the failure moment of a spot weld, respectively. The variables of  $\alpha$ ,  $\beta$  and  $\gamma$  are shape parameters. Based on the hybrid method, newly proposed failure model is constructed by Eq. (3). The coefficients that constitute newly proposed failure model are obtained using the least square method to minimize the discrepancy between the experimental data and interpolated data.

The proposed failure model for spot weld in this paper can predict the spot weld failure accurately. However, a number of failure tests and analysis have to be conducted to construct the failure model. In order to construct the failure model simply, prediction equations were developed for the 6 coefficients of the proposed spot weld failure model. These equations are expressed as

$$F_n, F_s, M_b = f(t, \sigma_{TS}, \phi) \quad (4)$$

$$\alpha, \beta, \gamma = f(t, \sigma_{TS}, \phi) \quad (5)$$

Here,  $t$ ,  $\sigma_{TS}$  and  $\phi$  are thickness, tensile strength and nugget ratio, respectively. 6 coefficients are determined by the function of thickness, tensile strength and nugget ratio.

#### 5 Summary

A number of automotive steel sheets are evaluated and analyzed by various spot-weld tests. The shape of failure criterion to material strength is changed. As the material is stronger, the moment effect to spot weld failure is significant. The failure surface becomes concave and sharp as the material strength increases.

#### 6 Literature

- [1] P. Wung, "A force-based failure criterion for spot weld design", *Experimental Mechanics*, Vol. 41, No. 1, pp. 107–113, 2001.
- [2] P. Wung, T. Walsh, A. Ourchane, W. Stewart and M. Jie, "Failure of spot welds under in-plane static loading", *Experimental Mechanics*, Vol. 41, No. 1, pp. 100–106, 2001.
- [3] Y.L. Lee, T.J. Wehner, M.W. Lu, T.W. Morrisett and E. Pakalnins "Ultimate strength of resistance spot welds subjected to combined tension and shear", *Journal of Testing and Evaluation*, Vol. 26, No. 3, pp. 213–219, 1998.

# Macroscopic Modeling of Flow-Drill Screw Connections

Johan Kolstø Sønstabø<sup>1</sup>, David Morin<sup>1,2</sup>, Magnus Langseth<sup>1,2</sup>

<sup>1</sup>Department of Structural Engineering, Norwegian University of Science and Technology

<sup>2</sup>Structural Impact Laboratory (SIMLab), Centre for Research-based Innovation, Norwegian University of Science and Technology

Flow-drill screws (FDS) are used in the automotive industry to join parts in the load-bearing structure of cars. The process is a simple one-step procedure, which requires access only from one side of the assembly, and a variety of dissimilar materials may be joined. As it is easy to automate, the FDS technology is well suited for the production lines in the automotive industry.

In large-scale finite element simulations (for instance crash simulations) point connections such as FDS connections cannot be modeled with accurate geometry with a reasonable simulation run-time due to limitations in computer power. Hence, simplified models are required to include the connections in such simulations.

The focus of this study was modeling of FDS connections in large-scale shell analyses in LS-DYNA. Five commercial macroscopic connections models available in LS-DYNA were investigated; two element-based models (**\*MAT\_SPOTWELD** and **\*MAT\_240**) and three constraint-based models (**\*CONSTRAINED\_SPR2** and the two versions of **\*CONSTRAINED\_INTERPOLATION\_SPOTWELD**). Cf. [1-3] for detailed discussions of the theory of the models.

All models were calibrated using cross tests in tension, shear and a mixed tension/shear mode. In order to assess the flexibility of the models two sets of experimental data was used. First, a short screw was used to join two sheets of the same rolled alloy. In the second set, a long screw was used to join a rolled alloy to an extrusion. The models were validated using a two-steps approach including benchmark tests (single lap-joint and peeling) and component tests (crash box crushing and T-component tests). Cf. [4] for detailed descriptions of the test set-up.

None of the two element-based models were flexible enough to reproduce the cross test results. The tensile and shear modes were well captured, but the force and initial stiffness in the mixed mode were severely over-estimated for both sets of experimental data. For this reason simulations of the benchmark and component tests were not carried out for the element-based models.

The three investigated constraint-based models gave better results compared to the two element-based models. The tensile and shear modes were well captured, and in the mixed mode the level of the maximum force as well as the ductility were to some extent reproduced. However, the shape of the force-displacement curves was not matched in the mixed mode. In particular the initial stiffness was too high in the simulations of the mixed mode. Best results were obtained using **\*CONSTRAINED\_SPR2**, and in the following some brief results are shown for this model.

The calibration results (cross tests) for both sets of experimental data are shown in Fig. 1. As seen, the tensile and shear modes were relatively well captured, but the model lacks the required flexibility to capture the mixed mode for both data sets. The over-predicted initial stiffness in mixed mode is clearly seen in the left figure. Fig. 2 shows the results from simulations of T-component tests. For both data sets the maximum force was relatively well predicted. The ductility was over-estimated for the short screws, while it was better predicted for the long screws.

This study has shown that of the five models investigated **\*CONSTRAINED\_SPR2** is best suited to represent FDS connections in large-scale shell simulations in LS-DYNA. However, none of the models are flexible enough to capture the physics in the mixed mode. Constraint-based models gave in this study more accurate results than element-based models.

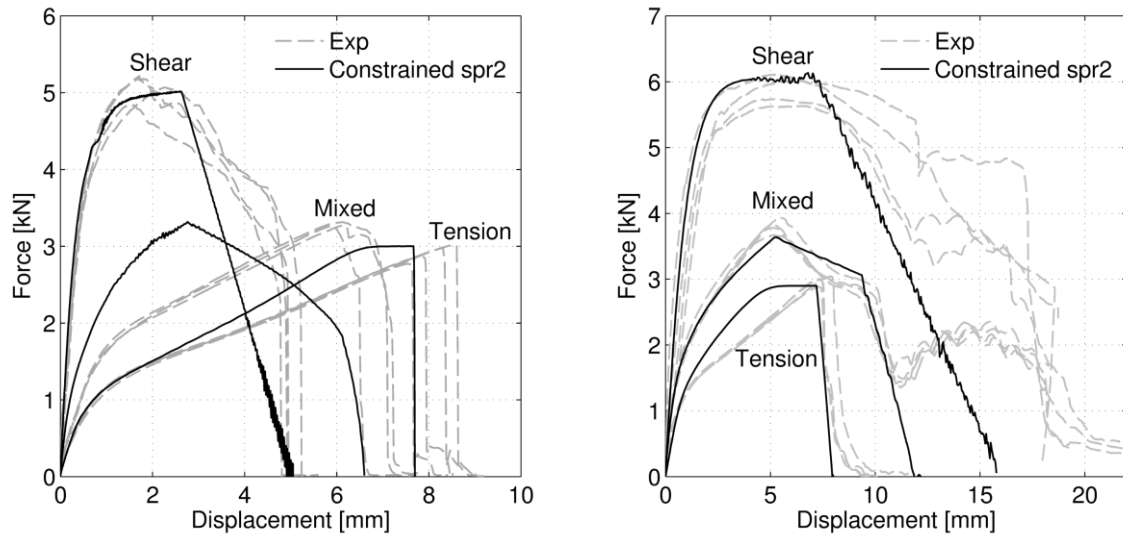


Fig.1: Calibration of *\*CONSTRAINED\_SPR2* to cross test results for short (left) and long (right) screws.

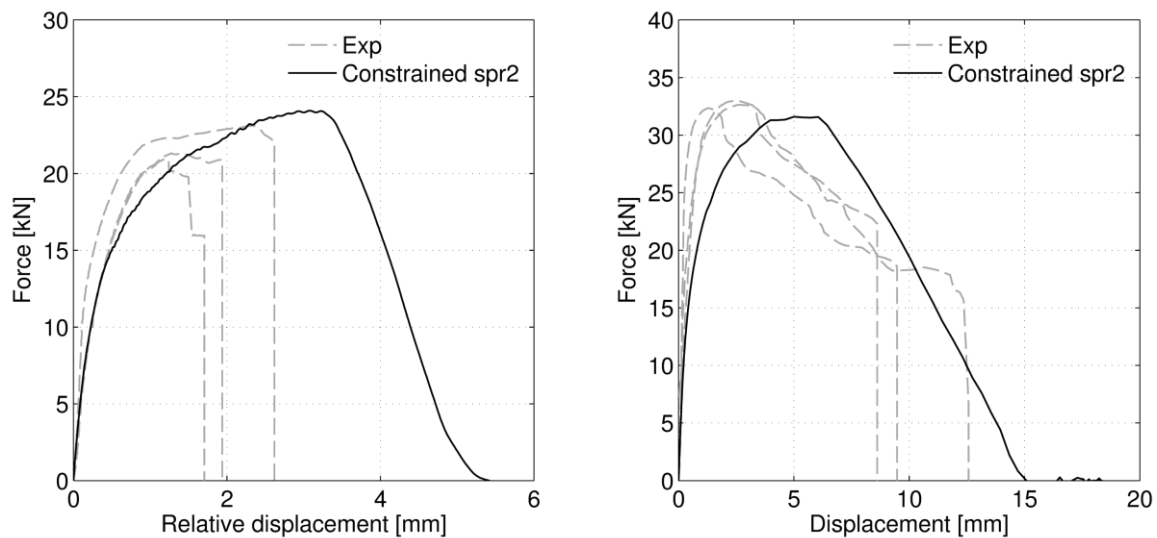


Fig.2: Simulations of T-component tests with *\*CONSTRAINED\_SPR2* for short (left) and long (right) screws.

## Literature

- [1] Sommer, S., Maier, J.: "Failure modeling of a self piercing riveted joint using ls-dyna", 8<sup>th</sup> European LS-DYNA conference, 2011
- [2] Hanssen, A. G., Olovsson, L., Porvaro, R., Langseth, M.: "A large-scale finite element point-connector model for self-piercing rivet connections", *European Journal of Mechanics A/Solids*, 29.4, 2010, 484-495
- [3] Bier, M., Sommer, S.: "Simplified modeling of self-piercing riveted joints for crash simulations with a modified version of *\*CONSTRAINED\_INTERPOLATION\_SPOTWELD*", 9<sup>th</sup> European LS-DYNA conference, 2013
- [4] Sønstabø, J. K., Holmstrøm P. H., Morin, D., Langseth, M.: "Macroscopic strength and failure properties of flow-drill screw connections", *Journal of Materials Processing Technology*, 222, 2015, 1-12

**CRASH IV**  
**CONNECTION/MISCELLANEOUS**





# Modeling of Self-Piercing Riveted Joints for Crash Simulation – State of the Art and Future Topics

Matthias Bier<sup>1</sup>, Silke Sommer<sup>1</sup>

<sup>1</sup> Fraunhofer Institute for Mechanics of Materials IWM, Freiburg, Germany

The requirements for energy efficiency and lightweight construction in automotive engineering rise steadily. Therefore a maximum flexibility of different materials is necessary and new joining techniques are constantly developed. The resulting large number of joints with different properties leads to the need to provide for each type of joint an appropriate modeling method for crash simulation.

In recent years the `*CONSTRAINED_INTERPOLATION_SPOTWELD` was modified to improve the modeling of the behavior of self-piercing riveted joints. The modified version will be available in LS-Dyna soon. This paper gives a short overview about the background and shows the benefits and limitations of the model. Furthermore, future research topics are shown for increasing the model quality. Topics like the influence of deformations in the surrounding sheets and the local loading situation on the rivet behavior will be discussed. For this purpose simulation results of variations of the lap shear specimen are shown and compared with experimental data.

First results of a German research project called “Characterization and modeling of mechanical joints with one-sided accessibility for profile intensive lightweight construction under crash loading” will be presented.

The Industrial Collective Research project (IGF-Nr. 18289 N / FOSTA P1032) of the Research Association for Steel Application (FOSTA), Sohnstrasse 65, 40237 Duesseldorf has been funded by the German Federation of Industrial Research Associations „Otto von Guericke“ e.V. (AiF) within the program for sponsorship of Industrial Collective Research (IGF) of the German Federal Ministry of Economic Affairs and Energy (BMWi) based on an enactment of the German Bundestag.

# Challenges in Tire Modeling for Small Overlap Crashworthiness

Suri Bala

LSTC

# On Automatic Crash Model Translation

Edmondo Di Pasquale<sup>1,2</sup>

<sup>1</sup> SimTech, France

<sup>2</sup> ENSIAME, Université de Valenciennes, France

## 1 Summary

This paper discusses some issues relevant to automatic crash model translation (conversion), based on SimTech experience. We can distinguish three level of conversion: literal translation, consistent translation and effective translation.

The methodology described in the paper is implemented in an ENKIDOU application. We show the conversion of a relatively complex model and the comparison between the results of the original (source) and converted (target) model.

## 2 SimTech approach to model translation

### 2.1 Project approach

Translation between FE models corresponding to different simulation codes arises in several occasions during advanced engineering projects., in project as diverse as stamp/fatigue or stamp/crash coupling [1], bonnet MDO design [2] and composite rail car body design [3][4].

### 2.2 Code development approach

SimTech technology for model translation is implemented in the ModelTranslator tool, based on ENKIDOU technology.

ModelTranslator lets the user import of one or more FE model in different formats, select a target format for a given FE model present in the task, and run the model translation

ENKIDOU data structure is organized in user-defined tasks. For what concerns model translation, the most interesting feature is that to each task can be associated any number of heterogeneous .

ENKIDOU object oriented structure enables the immediate translation of several entities or parts thereof

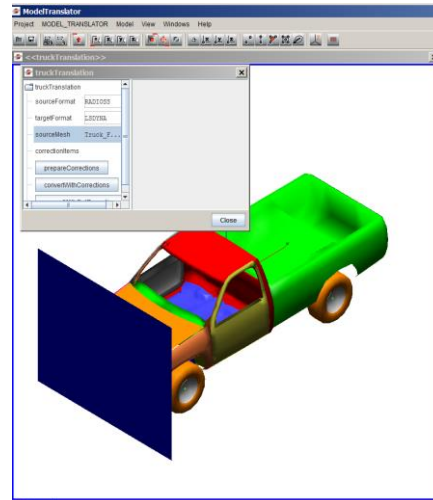


Fig.1: ModelTranslator user interface

## 3 The three levels of model translation

In a model translation we distinguish a source model and a target model. Translating one into another present the same challenges as automatic translation of a written text from a source to a target language.

### 3.1 Literal translation

The first step in the translation is to generate, for each entity of the source model, an equivalent in the target model. What we ask in literal translation, as in the case of the translation of a human language text, is that the resulting target model is syntactically correct, i.e. that it corresponds to the entity description in the user manual.

In this connection, we can have three different types of conversion:: one-to-one, entity split and entity collapse;

### 3.2 Target consistent translation

A target consistent translation is a translation where the target code runs on the translated model, without producing any error message. This leads us to choose between different translations of a given entity, for instance penalty based instead of constrained LSDYNA entities.

### 3.3 Effective translation

A translation is effective when the different entities translated work in the same way during the simulation using the two codes.. Corrections needed to achieve this are user-prompted.. The user has two ways to interact with the translation: dictionaries and entity correction.

## 4 Model translation

The translation is carried out automatically.

Results on RADIOSS and LSDYNA simulation on the crushed beam are compared in terms of overall shape, final impactor stroke and deformation energy.

Energy time history

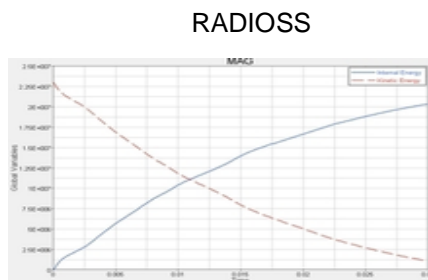


Fig.2: RADIOSS energy time history

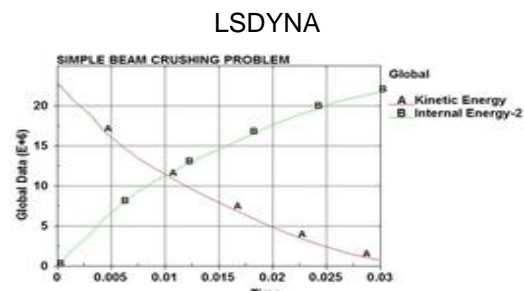


Fig.3: LSDYNA energy time history

We can point out that the pattern of deformation energy, and thus of impactor stroke and axial force, are almost identical.

## 5 Conclusions

Using the ENKIDOU base ModelTranslator, automatic conversion or translation of different crash models is feasible.

We have a theoretical framework and a software structure which can address all the translation problems which can be found in such situations.

Automatic translation can provide (target) models which can be run without any further modification, yielding results which are very close to the original (source) model. However, we should not forget that crash codes are different in their inner working and that, even for simple models, the behavior can be different when we look into the details.

Other translation features are available or under development, such as PAMCRASH to LSDYNA, LSDYNA to RADIOSS, LSDYNA to NASTRAN, ANSYS to NASTRAN.

## 6 References

- [1] Y. Le Roch, J.L. Duval, E. Di Pasquale, " Coupled Sheet Metal Forming And Fatigue Simulation", Proc. IDDRG 98
- [2] Di Pasquale, E., "An innovative approach to bonnet design for pedestrian safety", 9th European LSDYNA Conf., 2013
- [3] Di Pasquale, E. Gielczynski, G., "Multi-Disciplinary Optimization of Railway Systems", Research in Interactive Design, Vol. 3, 2010.
- [4] Di Pasquale, E., Ghys, P., "Structural optimization in the design of a composite rail car body", SIA, Journée d'étude « Optimisation des Composites », February 12, 2014

## 7 Acknowledgments

ENKIDOU and ModelTranslator are the property of SimTech. LSDYNA is the property of LSTC. OPTISTRUC and RADIOSS are the property of ALTAIR Engineering. NASTRAN is the property of MSC Software. ANSYS is the property of ANSYS. Other products are the property of the respective owners.

**CRASH V**  
**SHIPS/PLANES**



# Highly Advanced M&S System for Marine Accident Cause Investigation using FSI Analysis Technique

Sang-Gab Lee, Jae-Seok Lee, Hwan-Soo Lee

Korea Maritime & Ocean University, Marine Safety Technology

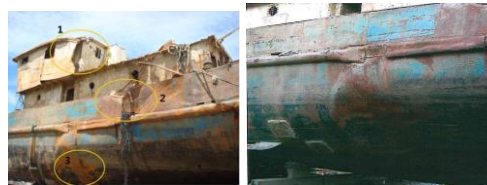
## 1 Abstract

Investigation of marine accident causes usually depends on the judgments of maritime experts, based on the statements of the concerned persons in the case where there is no navigation equipment, such as AIS and VDR. Scientific verification also has a limitation in the case of their conflicting statements. It is necessary to develop a highly advanced Modeling & Simulation (M&S) system for the scientific investigation of marine accident causes and for the systematic reproduction of accident damage procedure. To ensure an accurate and reasonable prediction of marine accident causes, full-scale ship collision, grounding, flooding and sinking simulations would be the best approach using hydrocode, such as LS-DYNA, with its Fluid-Structure Interaction (FSI) analysis technique and propulsion force for ship velocity. The objective of this paper is to present the findings from full-scale ship collision, grounding, flooding and sinking simulations of marine accidents, and to demonstrate the feasibility of the scientific investigation of marine accident causes using a highly advanced M&S system.

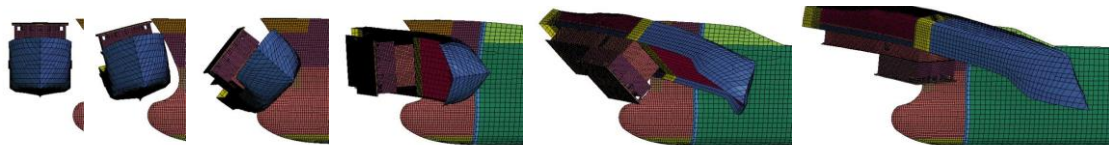
**Keyword Words:** *Highly Advanced Modeling & Simulation(M&S) System, Marine Accident Cause Investigation, Fluid-Structure Interaction(FSI) Analysis Technique, Full-Scale Ship Collision, Grounding, Flooding and Sinking Simulations, LS-DYNA code*

## 2 Highly Advanced M&S Simulation of Marine Accident

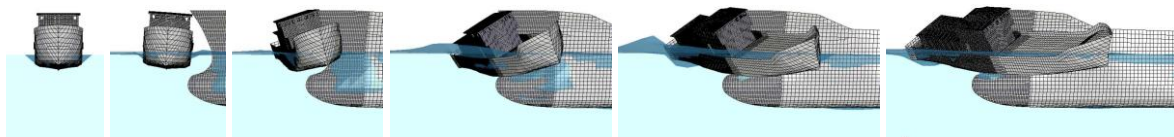
### 2.1 Investigation of collision accident of small fishing ship



*Collision damage configuration of struck ship*

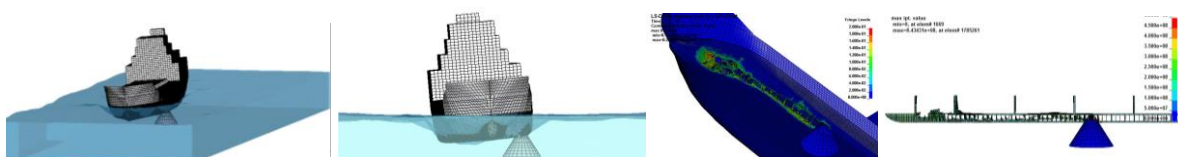


*Collision response behavior of full-scale collision simulation of small fishing ship in void condition*



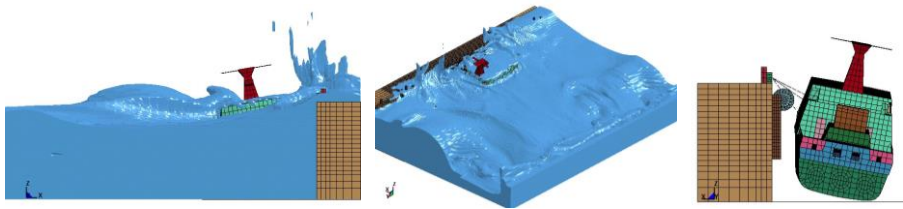
*Close view of response behavior of full-scale collision simulation using FSI analysis technique*

### 2.2 Grounding safety assessment of specialized ship

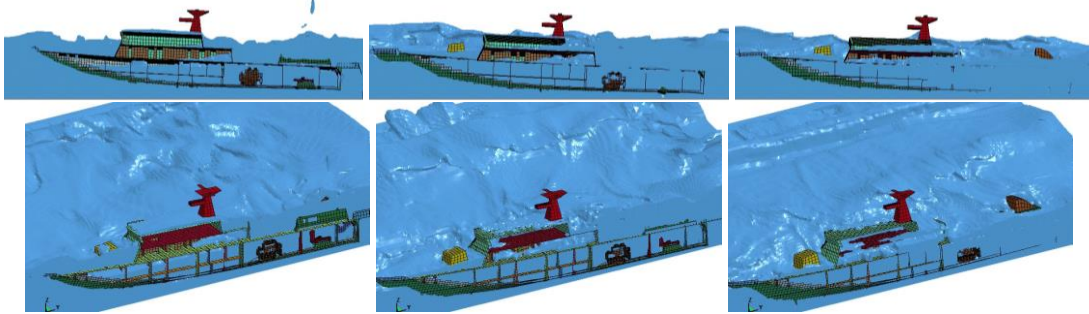


*Grounding response behaviors in free motion condition according to rock position in sea water*

**2.3 Investigation of flooding and sinking accident of ship under breaking wave**



*Breaking wave simulation behavior to mooring ship and quay at final step*

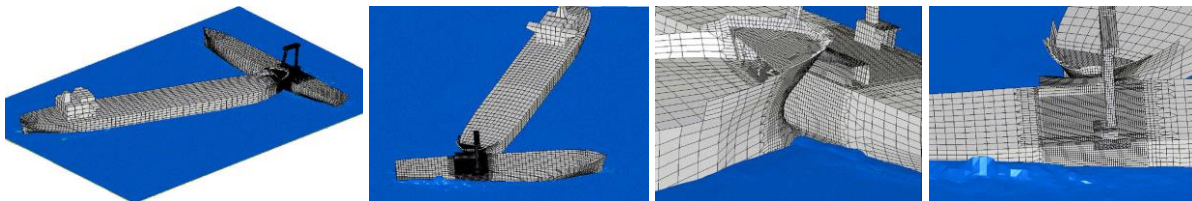


*Inflow of seawater through doors of superstructure and sink down to bottom*

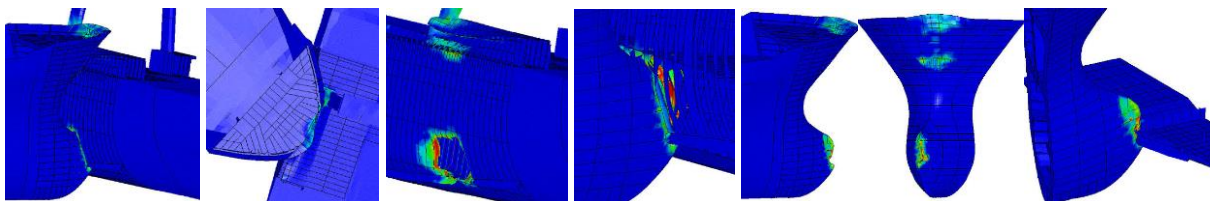
**2.4 Investigation of collision accident between two ships**



*Collision damage configurations and schematic damage drawings of striking ship*



*Full-scale collision behavior configurations using FSI analysis technique*



*Full-scale collision damage configurations using FSI analysis technique*

**3 Summary**

Through full-scale ship collision, grounding, flooding and sinking simulations of marine accidents using FSI analysis technique, the usefulness of highly advanced M&S system could be reconfirmed for the scientific investigation of marine accidents and for the systematic reproduction of accidental damage procedure.



# Use of Forming Limit Curve as a Failure Criterion in Maritime Crash Analysis

Bilim Atli-Veltin, Lex Vredeveltd

TNO, The Netherlands

Recent studies at TNO showed that in collisions of complex structures the deformation is much more complicated compared to that of a simple hull (shell) structure and requires more accurate fracture criterion. In this study, forming limit diagrams (FLD) are used to identify the regions of the impacted structure that are beyond the predefined deformation limit. Ls-Dyna results can easily be post processed using LS Prepost selecting the FLD option. This paper explains why use of FLD in marine crash calculations are more accurate for complex structures compared to the conservative GL criterion use, and provides an example case where a gas tank is impacted by a push barge bow and FLD is used to analyze the damage.

## 1. Conventional method of finding failure strains at crash analysis

A typical way of identification of failure of a structure that is undergoing a significant deformation due to impact is observing the thickness reduction of the impacted surface and pinpointing the moment that the thickness reduction is at the limit of the allowed strain of the given material at given initial thickness. For metals, usually the metal certification documents provide the maximum elongation that the material can undergo under uniaxial deformation. This provided failure strain,  $\varepsilon_f$ , can be translated to the through thickness strain,  $\varepsilon_t$ , by the following relation (Eq. ( 1 )):

$$\varepsilon_t = \frac{\varepsilon_f}{1 + \varepsilon_f} \quad (1)$$

Equation ( 2 ) is known as the GL criterion and assumes that the elements used in finite element model are square.

$$\varepsilon_f(l_e) = \varepsilon_g + \varepsilon_e \frac{t}{l_e} \quad (2)$$

where:

$\varepsilon_g$  = structural uniform strain,  $\varepsilon_e$  = necking strain,  $t$  = element thickness,  $l_e$  = element edge length

## 2. Use of FLC for crash analysis

A typical FLC looks like the dark line shown in Figure 1. In this figure the principal strains are plotted on the x and y axes. When used in an FEM analysis, principal strains of elements are plotted on this diagram. If they stay below the curve, the elements are safe, and if above they are failed.

## 3. Case study: Gas tank impacted by a push barge bow

The procedure for crash analysis involves crash simulations of a cylindrical gas tank with a push barge bow impactor moving at 10 m/s impact velocity, at mid height of the tank. The FE model is shown in Figure 2.

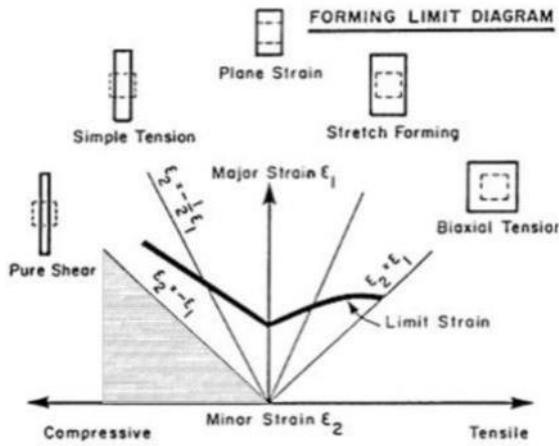


Figure 1 A typical forming limit curve (PVL)

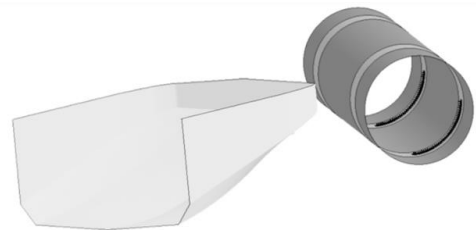


Figure 2 A tank impacted with a push barge bow, constraints highlighted (tank ends removed for better visualisation)

#### 4. Results

Figure 3 shows the gas tank impacted at the tank end and FLD is selected to visualize the deformation. In this particular case, the elements fall below the line, indicating they are in the safe zone.

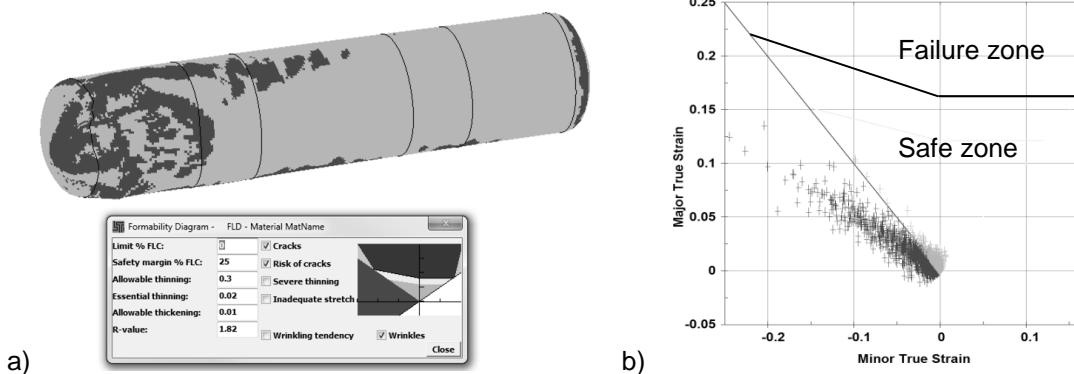


Figure 3 Forming limit diagram is shown on an example case – Tank impacted at the tank end

For the tank ends it is shown that the deformation falls further from the plane strain region (vertical axis), where the allowable strain is typically greater than the plane strain deformation. Therefore, it can be concluded that the conventional method of using GL criterion is conservative for the spherical structures, as shown in the deformation of the tank ends.

#### 5. Conclusions

The conventional method for failure analysis involves reviewing the through thickness strain with respect to the failure strain. Usually the GL criterion, that is based on damaged ship structures failed at plane strain condition, is used where the failure strain is corrected taking into account the size of the elements in the analysis and the thickness of the structure. However, a gage length correction is generally not performed. In the full length paper, a simple gage length correction method is proposed based on the uniaxial stress vs. strain curve.

This paper showed that the use of FLC in crash analysis of complex structures performed in LS Dyna can easily be implemented using LS Prepost, but accuracy depends on the input of a correct curve.

# Non-Structural Mass Modeling in Aircraft Impact Analysis Using Smooth Particle Hydrodynamics

Marin Kostov<sup>1</sup>, Milko Miloshev<sup>1</sup>, Zhivko Nikolov<sup>1</sup>, Ivaylo Klecherov<sup>1</sup>

<sup>1</sup>Risk Engineering Ltd., Sofia, Bulgaria

## Abstract

The non-structural mass in the large commercial airliners includes fuel, cargo, passengers, luggage, seats, lockers, etc. The straightforward approach for modelling of this non-structural mass is to include it as additional mass density to the corresponding structural elements. This approach leads to conservative results in case of impact as the non-structural mass remains attached to the aircraft for the entire duration of the calculation, resulting into an overestimated impact effects. Alternative approach for modelling of non-structural mass is the application of the Smooth Particle Hydrodynamics (SPH) method. For the purposes of the current study two models of the aircraft B777 are created. In the first model the non-structural mass is considered as additional mass density and is referred to as "rigid mass" model. In the second model the entire non-structural mass is modelled with SPH. Impact analyses into a reinforcement containment structure are performed and the damage effects are compared. The damage effects include the area of the perforation of the structure and the displacement at the impact location. The results of the calculations show that the larger perforation area and displacement are obtained from the analysis with "rigid mass" model. This is attributed to the fact that in the case of "rigid mass" model, the impact force is distributed over smaller area. In the case of SPH mass model, the impact force is distributed over larger area due to the dispersion of the SPH particles. The damaged structure is shown in Figure 2 and Figure 3. Furthermore, it is shown that the crushing pattern of the aircraft is different for the two non-structural mass models. The airplane with SPH mass model is destroyed by the pressure of the particles and pieces of the fuselage are torn apart in the course of the impact as seen in Figure 1. The airplane with "rigid mass" model has an accordion-like crushing pattern and no pieces of the fuselage are torn apart. One very important advantage of the use of SPH, which is demonstrated, is the possibility to estimate the spreading of debris and fuel as well as the amount of debris and fuel which penetrate the target structure.

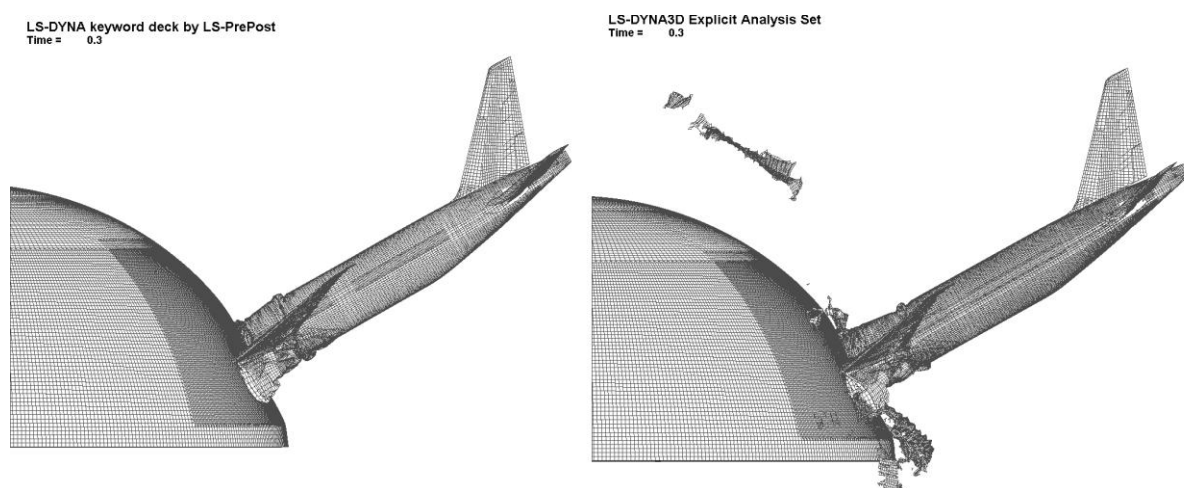


Fig. 1: Impact of the aircraft with „rigid mass“ (left) and SPH model (right, the SPH is not shown)

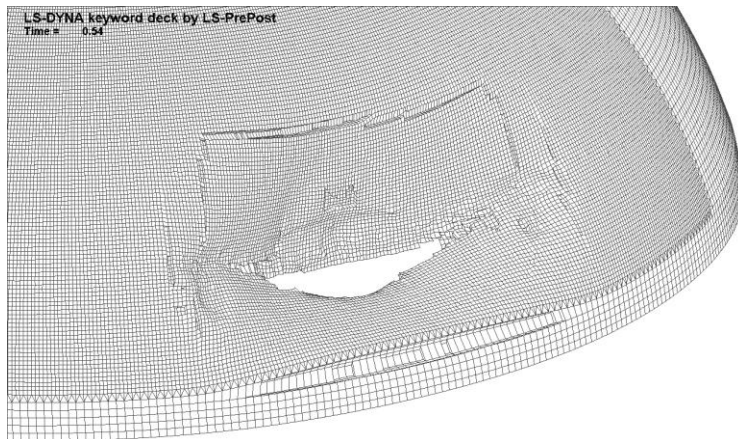


Fig.2: Damage of the dome from the analysis with „rigid mass“ model

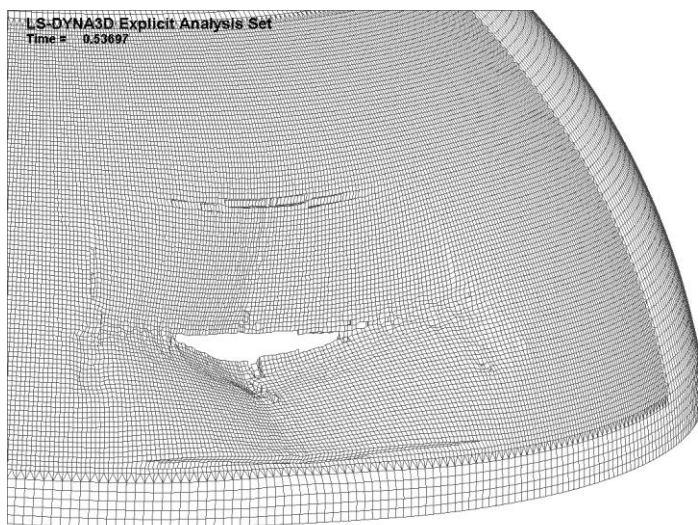


Fig.3: Damage of the dome from the analysis with SPH

## Literature

- [1] Bocchieri, R.T., MacNeil, R.M., Northrup, C.N., Dierdorf, D.S.: „Crash Simulation of Transport Aircraft for Predicting Fuel Release“, Federal Aviation Administration, October 2012
- [2] Kirkpatrick, S.W., Bocchieri, R.T., MacNeil, R.M., Petersen, B.D.: „Modeling Methodologies for Assessment for Aircraft Impact Damage on the World Trade Center Towers“, Proc. of the 9th International LS-Dyna Users Conference, Detroit 2006, 9-53 to 9-67
- [3] Kostov, M., Iliev, A., Andonov, A.: „Load-time function Definition for Large Commercial Aircraft Impact: Parametric Study“, Proc. 22<sup>th</sup> Conference Structural Mechanics in Reactor Technology, San Francisco, USA, 2013, 3 1709-1717
- [4] Lee, K., Jung, J-W., Hong, J-W.: “Advanced aircraft analysis of an F-4 Phantom on a reinforced concrete building”, Nuclear Engineering and Design 273, 2014, 505 to 528
- [5] LS-DYNA Aerospace Working Group: „Modeling Guidelines Document“, Version 12-1, June 2012
- [6] Wilt, T., Chowdhury, A., Cox, P.A.: „Response of Reinforced Concrete Structures to Aircraft Crash Impact“, US NRC, September 2011

# **CRASH VI**

# **MATERIAL**



# Ductile Fracture Prediction with Forming Effects Mapping of Press Hardened Steels

Lay O.Knoerr<sup>1</sup>, Pawel Woelke<sup>2</sup>, Brett Benowitz<sup>2</sup>, Badri Hiriyur<sup>2</sup>, Timo Faath<sup>1</sup>, Sascha Sikora<sup>1</sup>

<sup>1</sup>ThyssenKrupp Steel

<sup>2</sup>Weidlinger Associates Inc.

The escalating usage of Advanced High Strength and Press Hardened Steels to enhance crashworthiness while improving fuel efficiency through light-weighting of vehicles, has become a surmountable challenge to the auto industry. Furthermore, the expanded safety assessment like the IHS-Small Overlap crash test greatly intensify the need for an accurate and reliable fracture prediction model that will take into account the forming effects of the structural components, critical to the inherent load cases. In this study, a press hardened steel component of 1500 MPa ultimate tensile strength and 1.5mm gage thickness, is investigated under experimental and virtual three point bending load conditions. The simulations were conducted with no forming effects, and with thickness variation mapped from optically measured parts. The constitutive numerical model includes a phenomenological plasticity-damage model, formulated within the shell mechanics framework to encompass both the dilatational and plastic deviatoric energy terms. The model calibration was done with only two coupon level tests; uniaxial and plane strain. Excellent correlation of fracture mode and force-stroke curves were seen between experimental and numerical results that considered the thickness mapping of the press hardened component. On the contrary, the model that maintained uniform thickness failed to predict the correct fracture mode and overall response.

# Probabilistic Analysis of Process Chain “Forming to Crash” Regarding Failure Prediction

Burak Özarmut<sup>1</sup>, Helmut Richter<sup>1</sup>, Alexander Brosius<sup>2</sup>

<sup>1</sup>ThyssenKrupp Steel Europe AG, Dortmund, Germany

<sup>2</sup>Institut für Fertigungstechnik, Formgebende Fertigungsverfahren, Technische Universität Dresden, Dresden, Germany

Numerical analysis of forming and crash processes is usually carried out deterministically. However, the variations of the parameters describing materials and processes cause significant deviations in the prediction quality. This observation becomes more important if the failure prediction in process chains like forming to crash is considered. Usually, the material and process parameters are identified by means of an inverse or a direct identification procedure using experimental data. Nevertheless, the identification process itself contains uncertainty, as mean values are usually utilized for this purpose. It is therefore not known whether the process simulated with the identified parameters is robust and how the variation of parameters influences the quality of failure prediction. Stochastic analysis, replacing the parameters with stochastic distributions, can be performed to find out the variation of outputs due to the variation of input parameters. Since the computational cost of such an analysis would be too high to carry out using only FE simulations, it is performed on metamodels generated with relatively few FE simulations. Assuming the generated metamodel is accurate enough, reliable sensitivity information can also be obtained through methods such as Anova and Sobol Indices. The optimization and probabilistic analysis software LS-Opt serves as an efficient tool to conduct such study.

In this paper, parameters of a high strength steel grade, used mainly in the automotive industry, are replaced with distribution functions reflecting the real deviations of material and process parameters. A suitable sampling algorithm for the selected metamodeling technique is then used to generate parameter sets for the FE simulations. In order to keep the computational cost as low as possible, some simplifications and assumptions have been made concerning the hardening and strain rate dependency. The statistics of the desired outputs and the influence of the material and process parameters are computed by means of the metamodel. The results show that the variation of modeling parameters such as fracture curve, hardening, and plasticity, causes higher amount of variation on the failure prediction indicators like displacement up to fracture. Furthermore, it has also been found that the standard deviation of results increases with the increasing element size pointing out the importance of reducing uncertainty in the methods used for defining model parameters if coarser meshes are to be used.



# Development of a Fully-Tabulated, Anisotropic and Asymmetric Material Model for LS-DYNA (\*MAT\_264)

Sean Haight<sup>1</sup>, Dr. Cing-Dao “Steve” Kan<sup>1</sup>, Paul Du Bois<sup>2</sup>

<sup>1</sup> George Mason University – Center for Collision Safety and Analysis (CCSA)

<sup>2</sup> Consulting Engineer, Northville, MI

## 1 Introduction

The purpose of this research is to develop a fully-tabulated, anisotropic, asymmetric and rate dependent material model for solid elements. Physical testing of several metallic materials has shown to have anisotropic (or orthotropic) characteristics. While many material models in LS-DYNA currently have anisotropic modeling options, they are focused on the material forming applications – not crash and impact analysis. Unlike most anisotropic forming material models, this model will have: rate dependency, temperature dependency, tabulated hardening (as opposed to parameterized inputs), associated flow, tensile compressive asymmetry and the ability to maintain stability for large deformations.

## 2 Development

This anisotropic model is an extension of the currently existing Generalized Yield Surface (**MAT\_224\_GYS**) implementation of the Tabulated Johnson Cook material model (**MAT\_224**) [1]. In other words, this model will build upon the currently available features of **MAT\_224** and **MAT\_224\_GYS**. Strain rate and temperature dependencies are utilized as independent tabulated values. Hardening curves for tension, compression and shear will also be tabulated and independent. Isotropic failure will be retained from **MAT\_224** as a function of triaxiality, Lode parameter, strain rate, temperature and element size. Lastly, tabulated hardening for tension and compression will allow the user to specify tensile and compressive yield stress in the 0 degree, 45 degree, 90 degree, and thickness directions (as a function of strain rate).

The first phase of this development was to change the **MAT\_224\_GYS** yield surface (von Mises) to a Hill yield function [2]. This allowed for tabulated inputs for the 0 deg, 45 deg, 90 deg, and thickness tension.

$$\text{MAT\_224\_GYS: } f = \sigma_{vm} [c_1 + c_2 \theta_L + c_3 \theta_L^2]$$

$$\text{MAT\_264: } f = \sigma_{hill} [c_1 + c_2 \theta_L + c_3 \theta_L^2]$$

$$\text{Where } \sigma_{hill}^2 = F(\sigma_{yy} - \sigma_{zz})^2 + G(\sigma_{zz} - \sigma_{xx})^2 + H(\sigma_{xx} - \sigma_{yy})^2 + \dots \\ L\sigma_{yz}^2 + L\sigma_{zy}^2 + M\sigma_{zx}^2 + M\sigma_{xz}^2 + N\sigma_{xy}^2 + N\sigma_{yx}^2$$

The second phase was to generalize the Lode parameter so that 0 deg, 45 deg 90 deg, and thickness compression can also be input by the user. [3][4][5][6]

$$\text{MAT\_264: } f = \sigma_{hill} [c_1 + c_2 \theta_{L-Barlat} + c_3 \theta_{L-Barlat}^2]$$

To verify that the newly developed code is working properly, single element tension and compression simulations were performed. For each material direction (0 deg, 45 deg, 90 deg, and thickness) three material implementations were used: **\*MAT\_224\_GYS**, **\*MAT\_264** (with isotropic hardening) and **\*MAT\_264** (with anisotropic hardening). The results of this simulation show that the isotropic implementation of **\*MAT\_264** is equivalent to **\*MAT\_224\_GYS**. For the anisotropic elements, it was also shown that the true stress in the tension/compression elements is equivalent to the anisotropic tabulated hardening curves.

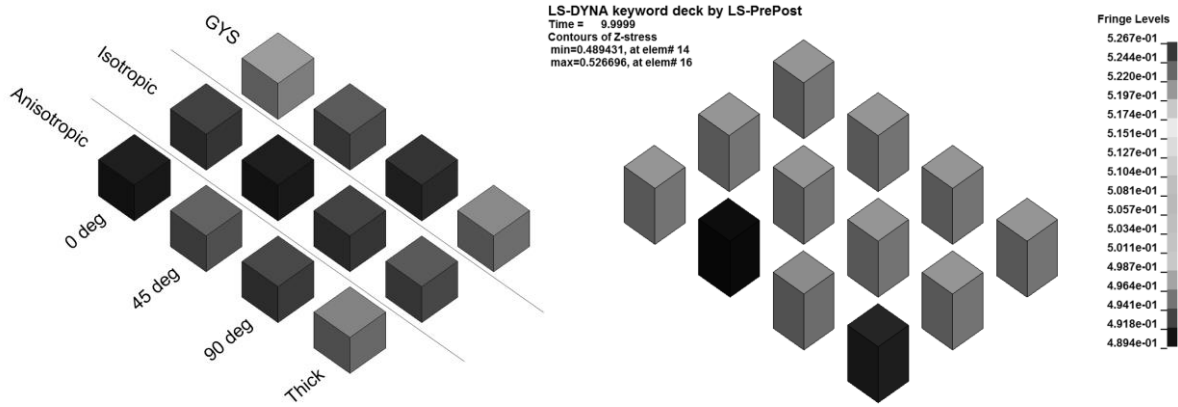


Fig.1: Single element verification simulation setup (left) and stress results (right)

### 3 Results

Physical testing (uniaxial tension and compression) for Al-2024 [7] and Ti-6Al-4V [8] were used to validate the development of this material model. These tests were designed using a typical uniaxial tension specimen. Using a single material model, the authors were able to replicate test results in each specimen direction. The only difference in the material model was the definition of the material direction relative to the rolling direction.

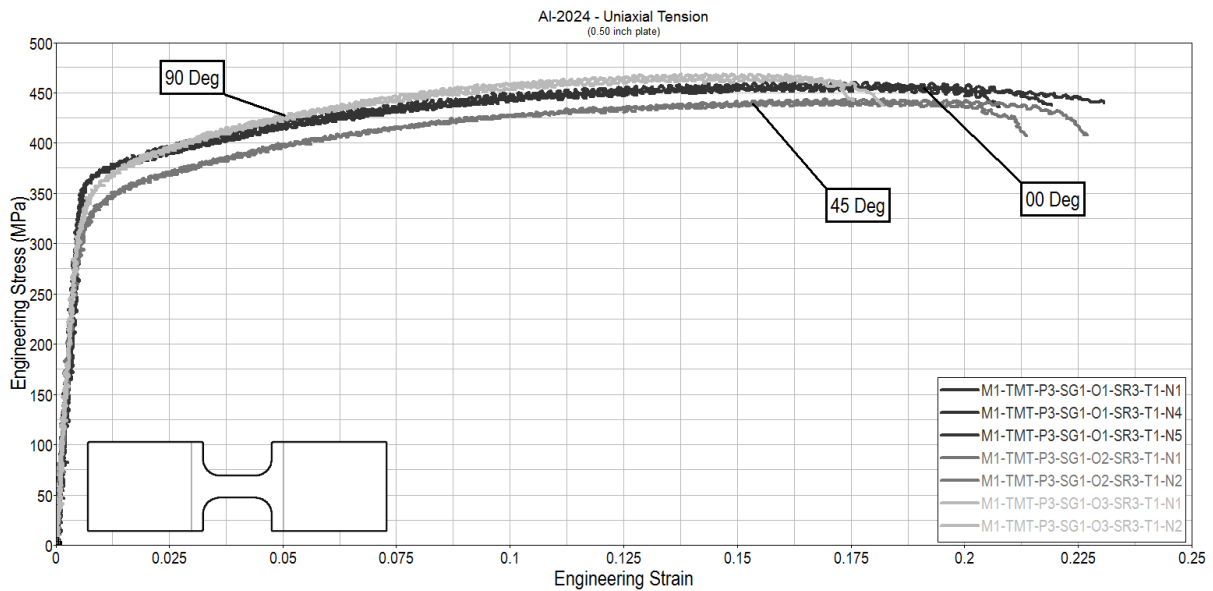


Fig.2: Engineering stress-strain data from anisotropic physical uniaxial testing of Al-2024 specimens

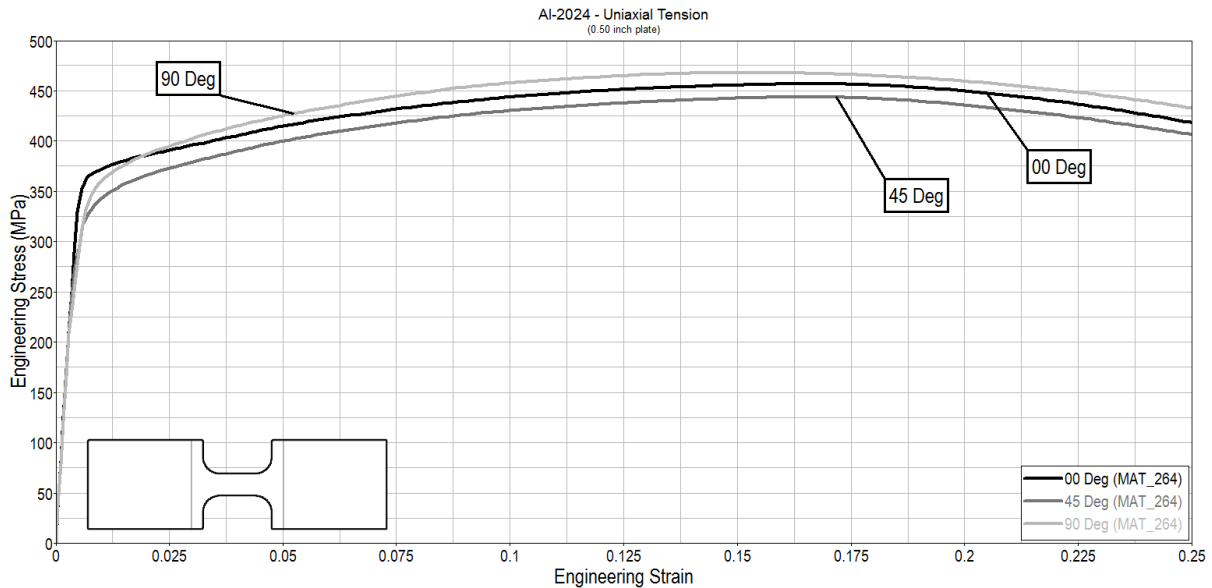


Fig.3: Simulation results using tabulated hardening in MAT\_264 material model

#### 4 Summary

This research introduces a new material model for simulating crash and impact dynamics for metals using solid elements. In addition to strain rate and temperature effects, the effect of material anisotropy is also specified using tabulated hardening curves. Additionally, this model is asymmetric in that it can model elements in tension, compression and shear with different tabulated hardening curves.

Physical testing was used to generate the tabulated hardening curves for each direction of the material. Consequentially, those physical tests were simulated to verify that the model behaves appropriately.

#### 5 Literature

- [1] Sengoz, K.: "Development of A Generalized Isotropic Yield Surface for Pressure Insensitive Metal Plasticity Considering Yield Strength Differential Effect in Tension, Compression and Shear Stress States", Doctoral Dissertation (The George Washington University), 2015
- [2] Hill, R.: "A theory of the yielding and plastic flow of anisotropic metals", 1948
- [3] Cazacu, O., Barlat, F.: "Application of the theory of representation to describe yielding of anisotropic aluminum alloys", International Journal of Engineering Science 41, 2003.
- [4] Cazacu, O., Barlat, F.: "A criterion for description of anisotropy and yield differential effects in pressure-insensitive metals", International Journal of Plasticity 20, 2004.
- [5] Cazacu, O., Barlat, F.: "Generalization of Drucker's Yield Criterion to Orthotropy", Mathematics and Mechanics of Solids 6, 2001.
- [6] Barlat, F.: "Linear transformation-based anisotropic yield functions", International Journal of Plasticity 21, 2005.
- [7] Seidt, J.: "Plastic Deformation and Ductile Fracture of 2024-T351 Aluminum under Various Loading Conditions", Doctoral Dissertation (The Ohio State University), 2010.
- [8] Hammer, J.: "Plastic Deformation and Ductile Fracture of Ti-6Al-4V under Various Loading Conditions", Thesis (The Ohio State University), 2012.

# Comparison of Crash Models for Ductile Plastics

Megan Lobdell<sup>1</sup>, Brian Croop<sup>1</sup>, Hubert Lobo<sup>1</sup>

<sup>1</sup>DatapointLabs, Ithaca NY, USA

## 1 Abstract

There is interest in quantifying the accuracy of different material models being used in LS-DYNA today for the modeling of plastics. In our study, we characterize two ductile, yet different materials, ABS and polypropylene for rate dependent tensile properties and use the data to develop material parameters for the material models commonly used for plastics: MAT\_024 and its variants. We then perform a falling dart impact test which produces a complex multi-axial stress state and simulate this experiment using LS-DYNA. We compare simulation to actual experiment thereby obtaining a measure of fidelity of the simulation to reality. In this way, we can assess the benefits of using a particular material model for plastics simulation.

## 2 Summary

Several material models are commonly used within LS-DYNA to simulate rate dependency in plastics. Because some of these models were not originally designed for plastics, there is concern about the ability of the models to accurately capture the complex polymeric behavior. One approach used to attempt to gain some control over this problem is to validate the models with simulations of well-designed experiments that contain some complexity. This carries the assumption that if a simpler experiment correlates well to simulation, more complex simulations would have comparable accuracy.

Impact tests based on ASTM D3763 [6] were performed using a Dynatup 8250 impact tower to provide a test bench for validating the simulation. A hemispherical tipped dart impactor with a mass of 23kg and radius of 6.35mm was used to impact a circumferentially clamped plate with a radius of 38mm. It was confirmed that there was no slip in the circumferential clamp during the impact, an important criterion for the setup of the simulation. Additionally, the impactor was not lubricated leading to a no-slip assumption in the simulation as the dart penetrated the plastic plate. The velocity during the impact event was not constant but decreased in proportion to the energy absorbed as the impactor penetrated the plastic sheet. The simulation was set up using constant stress Type -1 solid elements, with element sizes around 2mm<sup>3</sup>, as well as an eroding surface-to-surface contact setting between the impactor and the sheet. The static and dynamic coefficients of friction (FS & FD) were set to 1. The impactor was modelled as a rigid ball object with the mass of the entire dart in the tip. For each test case, the simulation model was kept unchanged with the exception of the material model settings. The force v. time data from the simulation and the experiment was compared.

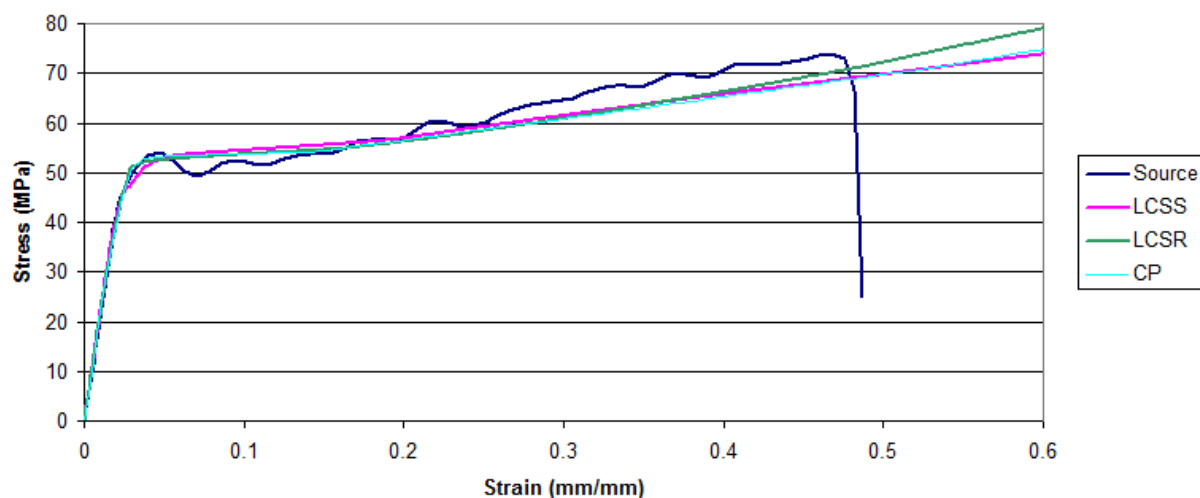


Fig. 1: Closed loop validation of tensile test for ABS – MAT\_024- LCSS, LCSR, CP with  $\nu_p=1$

We first performed a “closed-loop validation” to see if we could simulate the original tensile test used to generate the material model parameters. Fig. 1 shows the validation of the original tensile experiment using a MAT\_024 material model with viscoplasticity  $vp=1$  for each rate-dependency option, LCSS, LCSR, and CP. Simulations were all within 6% of the representative curve at the experimental data's failure strain.

We now used the above material models in the falling dart impact simulations to perform what we call an “open-loop validation” where we sought to validate an experiment that was not the source of data used for developing the material model. As with the tensile validation,  $vp=1$  gave the highest fidelity. Validations of MAT\_024 with CP, LCSS and LCSR options against the experiment are shown in Figure 2. The option with the highest fidelity was found to be LCSS with  $vp=1$ . The variation was quantified by examining the percent error between the peak resultant force and the time where peak force occurs, as well as a visual check for fidelity of the force vs. time curves to the original test data. The percent error of LCSS was 4.1% and -2.6% for force and time respectively. LCSR was the next closest case at an error of 14% force and was almost coincident with CP at 17%.

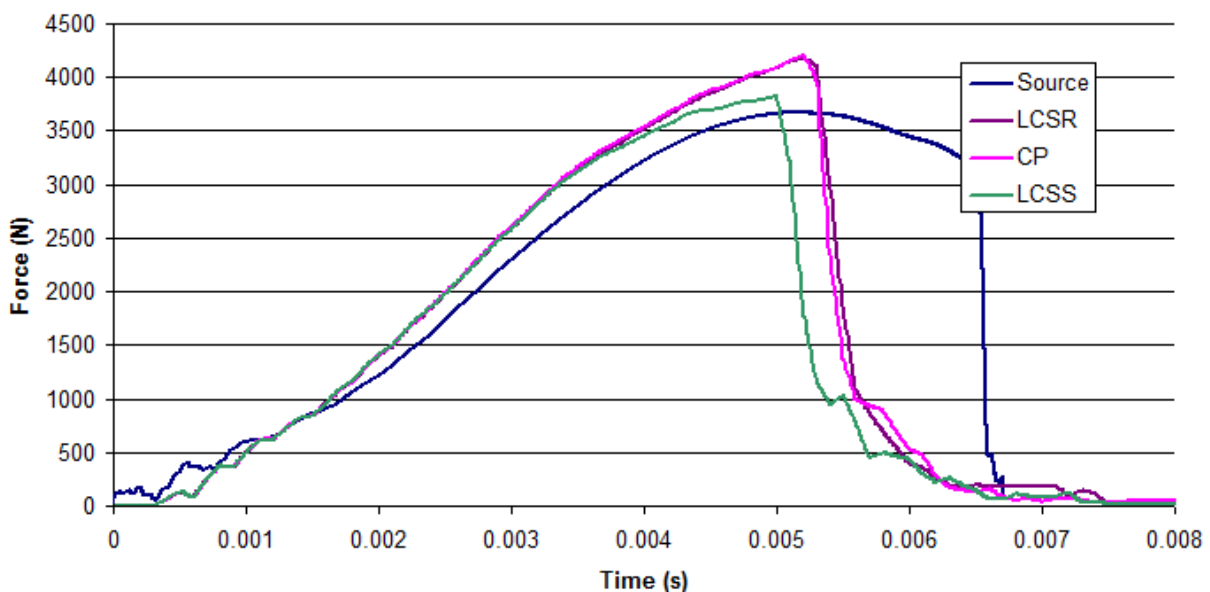


Fig.2: Falling dart (open loop) validation of MAT\_024 for ABS with visco-plasticity  $vp$  set to 1.

The falling dart impact test could serve as a well-structured benchmark experiment for the validation of high strain-rate material models for ductile plastics. The test itself is common and extremely well documented as an international standard for plastics. While containing multi-axial complexity, it possesses boundary conditions that can be well replicated in simulation allowing us to probe the material behaviour without fear of mismatch between simulation and physical experiment. Failure to satisfy this key requirement would seriously mar our ability to make quantitative judgements.

Rate-dependent material models developed using classical high-strain rate tensile test techniques can be used to successfully simulate more complex multi-axial phenomena. The same material model parameters were shown to give good results with shell elements as well as with the solid elements used in the falling dart experiment. There appears to be some need for tuning, such as with the failure strain but this is a known limitation of the MAT\_024 material model.

The commonly used MAT\_024 material model correlates quite well against the falling dart benchmark. It is possible to quantitatively assess the merits of different rate-dependency options and make sound judgements about the impact of different modelling decisions upon the simulation. While all options perform reasonably well, we observe that the Cowper-Symonds option may tend to overpredict, possibly because the equation does not mimic well the rate-dependency of plastics. We also validate the visco-plasticity 1 option as being best suited to plastics.



**PROCESS I**  
**METAL FORMING**





---

# Simulation Aspects for the Application of High Strength Steel Materials in Forming Processes

Dr. Lutz Keßler, Thorsten Beier, Dr. Helmut Richter

ThyssenKrupp Steel Europe AG

High-strength, cold-formable steels offer great potential for meeting cost and safety requirements in the auto industry. In view of strengths of up to 1200 MPa now attainable, some aspects need to be analyzed and evaluated in advance when designing with these materials. In addition to early assessment of crash properties, it is also highly important to design the forming process to match the material potential.

To address the material potential by simulation a complete row of different tasks has to be fulfilled. At first the selection of usefull experiments in combination with robust interpretation methods and the complete effort of transferring the real values into the virtual simulation world. Some aspects of testing and data interpretation will be discussed with respect to high strength steels.

For example, the forming and failure behavior of AHSS steels is not described only by the forming limit curve or thinning. The design of cut edge regions in combination with evaluation methods also has a significant impact on the part and tool design. Different experiments and interpretations allow a better understanding of forming limits and possible work arounds. Some advices are given how to handle cut edge failure in forming simulations an the need for further improvement in this field.

The presentation gives an overview of the process started at TKSE to characterize not only the fracture behavior of newly developed materials and to use the information in customer-relevant FE material models.

# **A Combined Technological Proofing Method for Deep Drawing and Stretch Forming of Sheet Metal Materials**

Dr.-Ing. Roland Hennig

Aleris Rolled Products Germany GmbH - Innovation Center Aachen

# Developments in LS-DYNA for Metal Forming Simulations

X. Zhu & L. Zhang

Livermore Software Technology Corporation

## 1 Introduction

Selected major developments for stamping simulation in LS-DYNA are discussed. These developments are:

- Positioning of unfolded blank in one-step simulation (\*CONTROL\_FORMING\_ONESTEP)
- Tooling mesh automatic fix and physical offset (\*CONTROL\_FORMING\_AUTOCHECK)
- Major improvements in scrap trimming (\*CONTROL\_FORMING\_SCRAP\_FALL)
- Best fitting of two meshes (scanned STL vs. springback mesh)
- 2D and 3D trimming of solids and laminates
- Formability Index (F.I.) extended for \*MAT\_036, \*MAT\_125, \*MAT\_226

## 2 Developments

- Position of unfolded blank in one-step simulation

One-step simulation with keyword \*CONTROL\_FORMING\_ONESTEP has been widely in use in crash and safety for forming stress and strain initialization. It has also being used for initial estimating of blank size in stamping application. One problem stamping users face is the position of the blank after unfolding can be undesirable. Also, the shifted unfolded blank is not easy to align relative to the tooling position. To address this issue, additional entries are now available in keyword \*CONTROL\_FORMING\_ONESTEP\_AUTO\_CONSTRAINT to specify three node IDs (NODE1, NODE2 and NODE3). The unfolded part will be repositioned and re-aligned according to the nodes specified back to the same nodes in the original part. The transformed blank is written in a keyword file "repositioned.k".

- Tooling mesh automatic fix and physical offset

Tooling mesh from imperfect CAD surfaces can be time consuming to fix. Some of the problems are so minute that can be easily missed. These bad meshes create problems during forming simulation runs, costing valuable engineering time that can be spent more productively somewhere else. In addition, if one side of tool mesh needs to be physically offset to create another side of tool mesh, extra manual checks and fixes are needed to ensure that offset tool's meshes are problems-free. Now a new feature in LS-DYNA, with keyword \*CONTROL\_FORMING\_AUTOCHECK, allows users to check for duplicated elements, overlapping elements, skinny/long elements, degenerated elements, disconnected elements, and inconsistent element normal vectors. It will also make each tool's element normal vectors automatically facing the blank. In addition, offset can be applied to the fixed tool to create another tool.

To check and fix the tool mesh, set the variable ICHECK to "1". The variable of IOFFSET can be used to offset the fixed tool. Meshes will be reoriented correctly towards the blank, and the tool offset is determined by an amount of  $0.5 \cdot \text{abs}(\text{MST})$  either on the same or opposite side of the blank, depending on the signs of the MST, where the "MST" is the variable in \*CONTACT\_FORMING.... A new keyword file, "rigid\_offset.inc" file, will be output as fixed, reoriented and offset tooling meshes.

- Major improvements in scrap trimming

The original *constraint release method* of scrap trimming using the keyword \*CONTROL\_FORMING\_SCRAP\_FALL has been in use for quite some times now. This simplified method has the following drawbacks:

1. No scrap trimming – the scrap piece cannot be trimmed directly from a parent piece; an exact scrap piece after trimming must be modeled.

2. Poorly (or coarsely) modeled draw beads in the scrap piece do not fit properly in badly modeled draw beads on the tooling, resulting in initial interferences between the two and therefore affecting the simulation results.
3. For poorly (or coarsely) modeled scrap edges and trim posts, users have to manually modify the scrap trim edges to clear the initial interference with the trim posts.
4. Users must clear all other initial interferences (e.g. between scrap and scrap cutter) manually.

Based on users' feedback, a new method "scrap trimming" (after Revision 91471) has been developed to address the above issues and to, furthermore, reduce the effort involved in preparing the model. The new method involves trimming scrap from an initially large piece of sheet metal, leaving the parent piece as a fixed rigid body. The trim lines are obtained from the trim steel edge node set NDSET and the trim vector VECTID. The variable EFFSET offset the scrap edge away from the trim steel edge, towards the scrap seed node side, useful to remove initial interference between the trimmed scrap (because of poorly modeled trim steel) and coarsely modeled lower trim post. The variable EXTEND is an amount to extend a trim steel's edge based on the NDSET defined, so it can form a continuous trim line together with a neighboring trim steel, whose edge may also be extended, to trim out the scrap piece. The variable NDBEAD can be defined to be excluded from initially imposed constraints after trimming. This node set typically consists of nodes in the scrap draw bead region where due to modeling problems the beads on the scrap initially interfere with the beads on the rigid tooling; it causes scrap to get stuck later in the simulation if left as is. GAP and IPSET can be used to remove initial interference between the scrap and other die components.

- Best fitting of two meshes

In springback prediction and compensation process simulation, there is always a need to assess the accuracy of the springback prediction using physical white-light scanned parts. The keyword \*CONTROL\_FORMING\_BESTFIT is developed for this purpose. Scanned parts are typically given in the STL format, which can be imported into *LS-PrePost* and write out as a keyword mesh file. The converted scanned keyword file can be used as FILENAME as a target mesh in an input. The predicted springback mesh (with \*NODE, \*ELEMENT\_SHELL, \*CONSTRAIN\_ADAPTIVITY cards only) can be included in the input file using **Fehler! Verweisquelle konnte nicht gefunden werden..** The best-fit program uses an iterative, least-squares method to minimize the separation distances between the two parts, eventually transforms the springback mesh of the included file (predicted springback mesh) into the position of the target mesh (scan). The separation distances between the two parts are calculated after the best-fitting, and stored as thickness values in a file bestfit.out, which is essentially a dynain file. Color contours of the separation distances between the two parts can then be plotted via *FCOMP*→*Thickness*. Both positive and negative thickness are calculated and stored as the *Thickness*. Positive distance means the included file is above the target in a larger coordinates, and negative distance is below the target in a smaller coordinates. The fitting accuracy is within 0.1mm. The variable IFAST is a computing performance optimization flag and can be used to speed up the computing time.

- 2D and 3D trimming of solids and laminates

To trim drawn panels of 3-D solid elements, both 2-D (directional) and 3-D (normal to element face) trimming are now available in LS-DYNA. The usage is the same as one would trim those of shell elements. Three keywords need to be included:

```
*CONTROL_FORMING_TRIMMING, or, ELEMENT_TRIM,
*DEFINE_TRIM_CURVE_NEW, (or 3D), and
*DEFINE_TRIM_SEED_POINT_COORDINATES
```

In addition, trimming of laminated materials (core of solid elements sandwiched by top and bottom layers of shells) are also available. A new variable of ITYP under \*CONTROL\_FORMING\_TRIMMING needs to be activated to enable the feature:

```
* CONTROL_FORMING_TRIMMING, or, ELEMENT_TRIM,
$ PSID,,$ITYP
```

where, ITYP=1 triggers a laminated material trim.

- 
- Formability Index (F.I.) extended for \*MAT\_036, \*MAT\_125, \*MAT\_226

Formability Index (F.I.) addresses sheet metal failure under nonlinear strain path. Failure for elements undergoing nonlinear strain paths are different from those with linear strain path, which are handled with the traditional Forming Limit Diagram (FLD). F.I. is based on *critical effective strain method* and is stored in history variable #1 during simulation. Failure occurs when it reaches the value of 1.0. For all these three materials listed above and for \*MAT\_037, history variables (both in contour and in XY format) available to plot include:

- History variable #1: formability index (F.I.)
- History variable #2: strain ration (minor strain/major strain)
- History variable #3: equivalent plastic strain under planner isotropic assumption

To plot these history variables, it is necessary to set NEIPS under \*DATABASE\_EXTENT\_BINARY to "3".

### 3 Summary

Various features related to metal forming have been developed to meet the requirements of our stamping users. Selected developments are discussed. LSTC is committed to working with our stamping users to advance the metal forming simulation technology, and will continue to improve to stay ahead.

### 4 Reference

- [1] LS-DYNA User's Manual (I and II).



**PROCESS II**  
**METAL FORMING**





# Comprehensive Correlation of Seat Track Assembly - From Forming to Assembly Test -

S. Sinne, H. Klose, V. J. Dura Brisa, P. Partheymüller

Brose Fahrzeugteile GmbH & Co. Kommanditgesellschaft, Coburg

## 1 Motivation

The dimensioning of seat structure including its adjusting components is always a challenge between comfort, lightweight and strength. The main interface between seat structure and vehicle is the seat track assembly. It enables the length adjustment and transfers a significant amount of the crash load. The increased demands to lightweight, reduction of development time and cost efficiency require a continuous improvement of simulation models regarding accuracy in predictability.

Objective of the presentation is to illustrate a comprehensive correlation approach of simulation and test in order to achieve a high accuracy in strength assessment for seat track assemblies under crash load.



## 2 Correlation approach

Due to the high number of influencing factors on seat track assembly strength a comprehensive and step-wise correlation approach is applied.

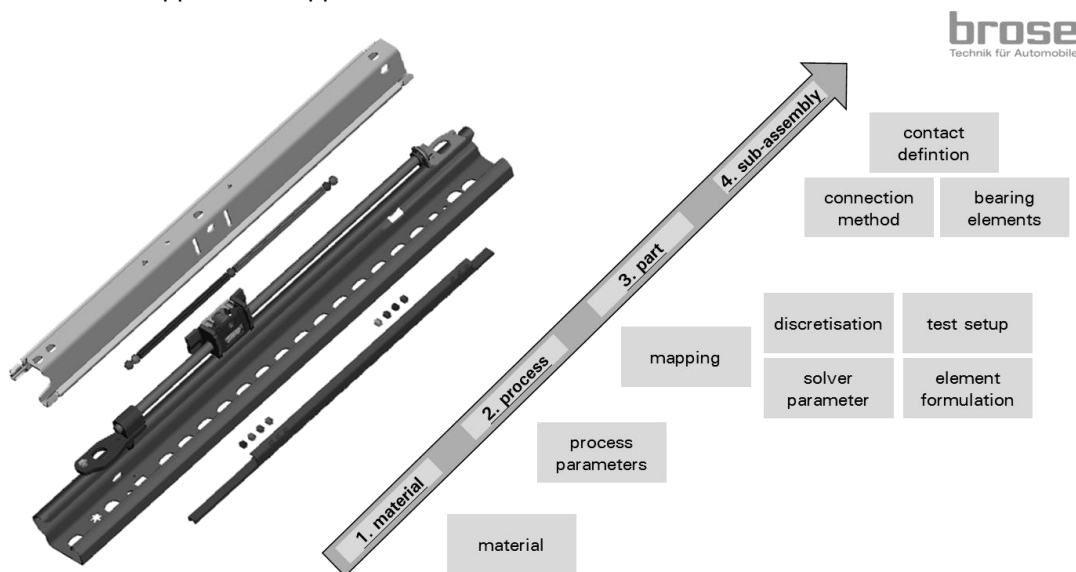


Fig. 1: Influencing factors and overview of correlation approach (greyscale).

1. Characterization of track material is the basis for the simulation of sheet metal forming as well as crash analysis. For this purpose the enhanced material model MGenYld from MATFEM is used.
2. The accuracy of the sheet metal forming (process) is investigated and improved regarding geometry and local cold hardening.
3. On part level, the quality of material model in combination with process history is verified under three-point bending loading for upper and lower track. To assess the accuracy of the simulation model reproducible test results for large deformation under high speed loading are necessary. Thus, a special test rig was developed. An important feature is the continuous measurement of part and test rig deformation using digital image correlation (GOM-PONTOS).
4. On assembly level, load cases equivalent to crash were investigated similar to part level.

### 3 Results

Due to the testing approach highly reproducible result on part and assembly level are achieved, allowing a quantitative assessment of correlation. Starting from a 5 mm and standard MAT24 material improvements in simulation model were investigated.

#### 3.1 Part level – 3-Point-Bending

Material modelling, mesh refinement and forming simulation lead to a significant improvement of accuracy in simulation results compared to reference modelling for upper and lower track.

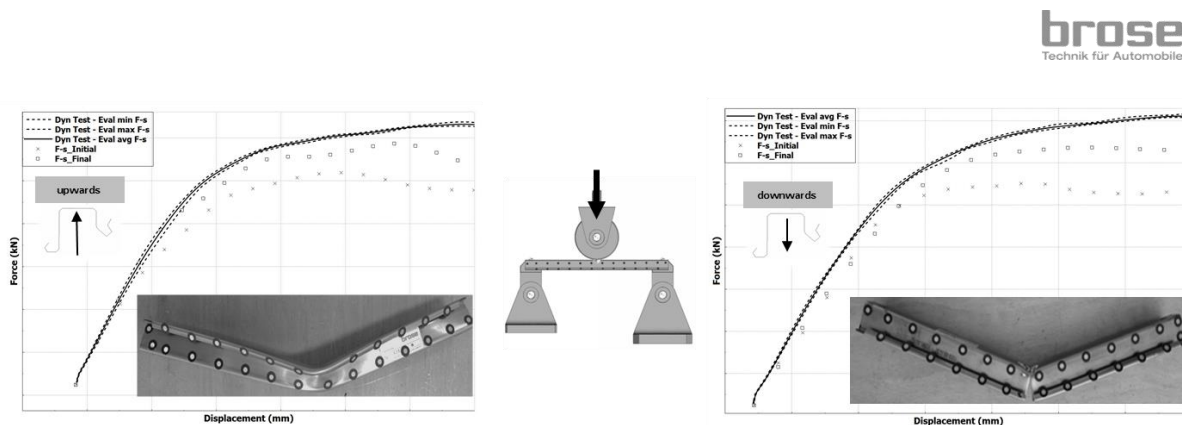


Fig.2: upper track under three point bending

#### 3.2 Assembly level

Based on part level simulation model for tracks, assembly specific modelling techniques for interaction of tracks and internal parts (e.g. bearing) were investigated.

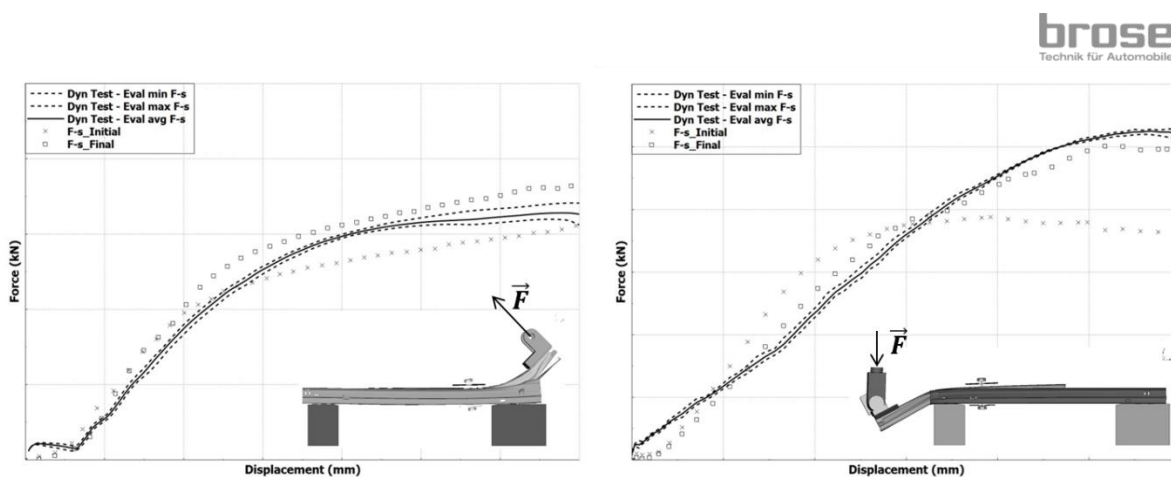


Fig.3: sub-assembly in component test

### 4 Summary and conclusion

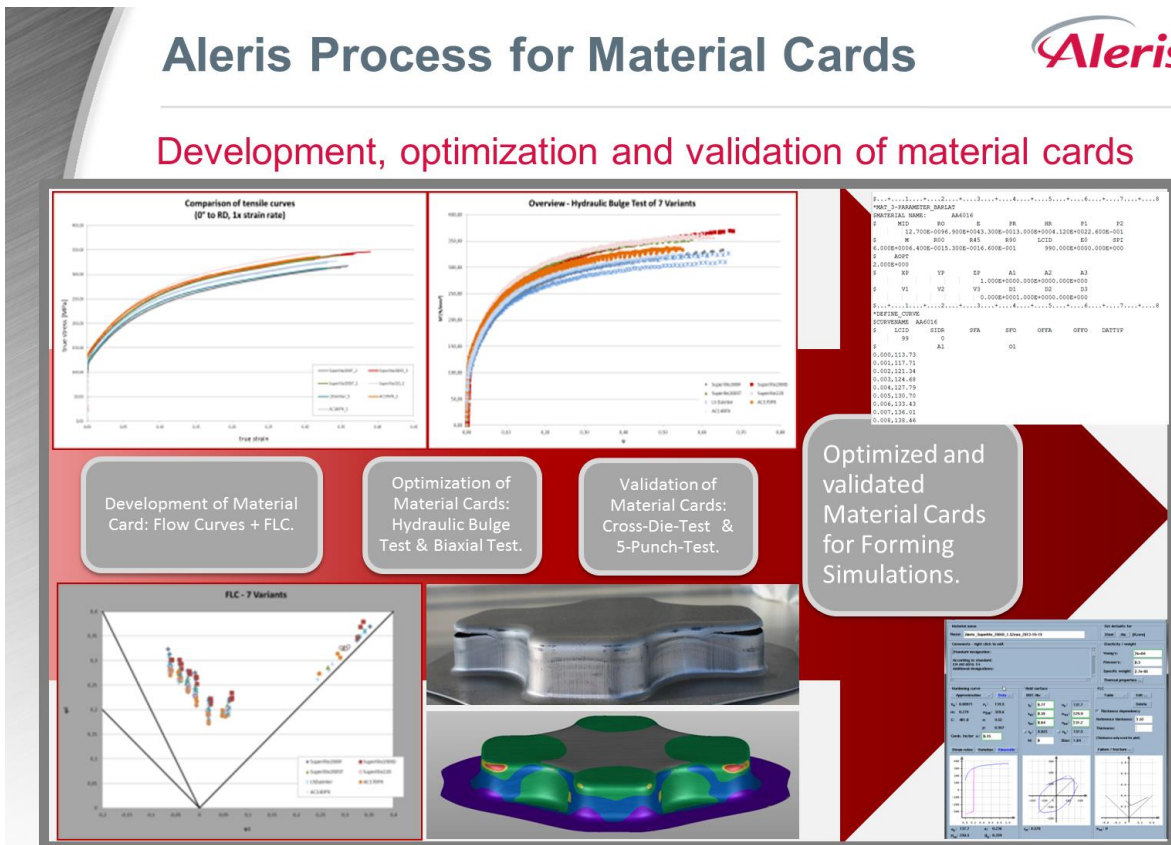
The presentation shows a comprehensive correlation approach allowing a quantitative assessment of correlation for seat track assembly under crash loading. Focus on these investigations was high predictability of strength using industrial available simulation and testing capabilities. The correlation approach is transferable to other part and sub-assemblies.


# Creation and Validation of Material Cards for Aluminum Sheet Metal Materials

Dr.-Ing. Roland Hennig,

Aleris Rolled Products Germany GmbH - Innovation Center Aachen

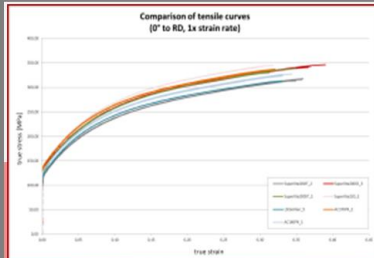
While many simulation programs contain sufficient material cards for most of the steel materials, the aluminum cards often aren't available yet. Therefore many of the aluminum processing suppliers have to create their own cards but aren't willing to change them with other suppliers or customers because of the necessary high effort to get them. This leads to a higher uncertainty of the ability to process aluminum sheet metal materials in the automotive industry especially for small and medium-sized enterprises which aren't able to create their own cards and simulate their forming processes with sufficient reliability and prevents a higher distribution of aluminum sheets in the market in general. Therefore Aleris - one of the leading Aluminum Suppliers in the world - has decided to create their own material cards for all of their sheet materials to help their customers to simulate their forming processes with the Aleris aluminum sheets with ease and reliability. To do so the cards will not only be created but also tested and validated with different known sheet metal testing methods from deep drawing to stretch forming. In this way Aleris will not only improve its serve to their customers in their daily business but also increase the security to process aluminum sheets in general by more reliable forming simulations to meet the demands of an increasing use of aluminum sheets in the automotive industry in future.



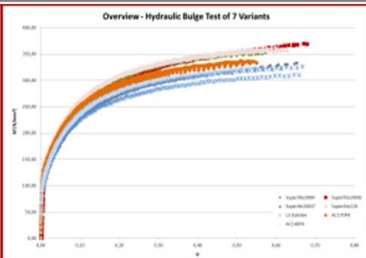
**Aleris Process for Material Cards** 

**Development, optimization and validation of material cards**

**Comparison of tensile curves (D\* to RD, 1x strain rate)**



**Overview - Hydraulic Bulge Test of 7 Variants**



```

*MAT_2PARAMETER_BIASLAW
*****
1  M2  80  0  0  0  0  0  0  0  0  0  0  0  0  0  0  0  0  0  0  0
2  12.700E+004  8.00E+041  2.00E+013  0.00E+004  1.20E+022  4.00E+051
3  0  0  0  0  0  0  0  0  0  0  0  0  0  0  0  0  0  0  0  0
4  0.00E+004  4.00E+055  2.00E+014  4.00E+011  1.00E+000  0.00E+000
5  0.00E+000
6  0.00E+000
7  0.00E+000
8  0.00E+000
9  0.00E+000
10 0.00E+000
11 0.00E+000
12 0.00E+000
13 0.00E+000
14 0.00E+000
15 0.00E+000
16 0.00E+000
17 0.00E+000
18 0.00E+000
19 0.00E+000
20 0.00E+000
21 0.00E+000
22 0.00E+000
23 0.00E+000
24 0.00E+000
25 0.00E+000
26 0.00E+000
27 0.00E+000
28 0.00E+000
29 0.00E+000
30 0.00E+000
31 0.00E+000
32 0.00E+000
33 0.00E+000
34 0.00E+000
35 0.00E+000
36 0.00E+000
37 0.00E+000
38 0.00E+000
39 0.00E+000
40 0.00E+000
41 0.00E+000
42 0.00E+000
43 0.00E+000
44 0.00E+000
45 0.00E+000
46 0.00E+000
47 0.00E+000
48 0.00E+000
49 0.00E+000
50 0.00E+000
51 0.00E+000
52 0.00E+000
53 0.00E+000
54 0.00E+000
55 0.00E+000
56 0.00E+000
57 0.00E+000
58 0.00E+000
59 0.00E+000
60 0.00E+000
61 0.00E+000
62 0.00E+000
63 0.00E+000
64 0.00E+000
65 0.00E+000
66 0.00E+000
67 0.00E+000
68 0.00E+000
69 0.00E+000
70 0.00E+000
71 0.00E+000
72 0.00E+000
73 0.00E+000
74 0.00E+000
75 0.00E+000
76 0.00E+000
77 0.00E+000
78 0.00E+000
79 0.00E+000
80 0.00E+000
81 0.00E+000
82 0.00E+000
83 0.00E+000
84 0.00E+000
85 0.00E+000
86 0.00E+000
87 0.00E+000
88 0.00E+000
89 0.00E+000
90 0.00E+000
91 0.00E+000
92 0.00E+000
93 0.00E+000
94 0.00E+000
95 0.00E+000
96 0.00E+000
97 0.00E+000
98 0.00E+000
99 0.00E+000
100 0.00E+000
101 0.00E+000
102 0.00E+000
103 0.00E+000
104 0.00E+000
105 0.00E+000
106 0.00E+000
107 0.00E+000
108 0.00E+000
109 0.00E+000
110 0.00E+000
111 0.00E+000
112 0.00E+000
113 0.00E+000
114 0.00E+000
115 0.00E+000
116 0.00E+000
117 0.00E+000
118 0.00E+000
119 0.00E+000
120 0.00E+000
121 0.00E+000
122 0.00E+000
123 0.00E+000
124 0.00E+000
125 0.00E+000
126 0.00E+000
127 0.00E+000
128 0.00E+000
129 0.00E+000
130 0.00E+000
131 0.00E+000
132 0.00E+000
133 0.00E+000
134 0.00E+000
135 0.00E+000
136 0.00E+000
137 0.00E+000
138 0.00E+000
139 0.00E+000
140 0.00E+000
141 0.00E+000
142 0.00E+000
143 0.00E+000
144 0.00E+000
145 0.00E+000
146 0.00E+000
147 0.00E+000
148 0.00E+000
149 0.00E+000
150 0.00E+000
151 0.00E+000
152 0.00E+000
153 0.00E+000
154 0.00E+000
155 0.00E+000
156 0.00E+000
157 0.00E+000
158 0.00E+000
159 0.00E+000
160 0.00E+000
161 0.00E+000
162 0.00E+000
163 0.00E+000
164 0.00E+000
165 0.00E+000
166 0.00E+000
167 0.00E+000
168 0.00E+000
169 0.00E+000
170 0.00E+000
171 0.00E+000
172 0.00E+000
173 0.00E+000
174 0.00E+000
175 0.00E+000
176 0.00E+000
177 0.00E+000
178 0.00E+000
179 0.00E+000
180 0.00E+000
181 0.00E+000
182 0.00E+000
183 0.00E+000
184 0.00E+000
185 0.00E+000
186 0.00E+000
187 0.00E+000
188 0.00E+000
189 0.00E+000
190 0.00E+000
191 0.00E+000
192 0.00E+000
193 0.00E+000
194 0.00E+000
195 0.00E+000
196 0.00E+000
197 0.00E+000
198 0.00E+000
199 0.00E+000
200 0.00E+000

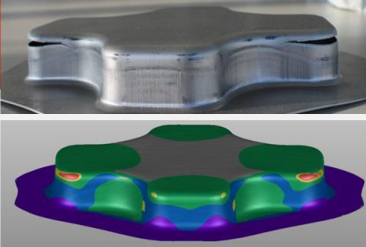
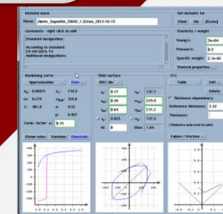
```

Development of Material Card: Flow Curves + FLC.

Optimization of Material Cards: Hydraulic Bulge Test & Biaxial Test.

Validation of Material Cards: Cross-Die-Test & 5-Punch-Test.

**Optimized and validated Material Cards for Forming Simulations.**

# Evaluation of Kinematic Hardening Models for Multiple Stress Reversals under Continuous Cyclic Shearing and Multi-Step Bending

Sebastian Suttner<sup>1</sup>, Martin Rosenschon<sup>1</sup>, Marion Merklein<sup>1</sup>

<sup>1</sup>Friedrich-Alexander-University Erlangen-Nürnberg,  
Institute of Manufacturing Technology LFT, Germany

## 1 Introduction

In complex sheet metal forming processes the material undergoes various strain path changes, for instance, during the passing of a drawbead or a radius. Based on the Bauschinger effect that describes the material's specific decrease of the yield stress after a load reversal, the resultant hardening behavior significantly differs from that of a monotonic loading condition. For a reliable numerical process design, especially in springback analysis, a consideration of the Bauschinger effect is essential.

Within this contribution, the evolution of the material behavior under cyclic loading is investigated with consecutive cyclic shearing of DP-K54/78+Z in a modified ASTM shear test. Moreover, the kinematic hardening models according to Chaboche et al. [1] and Yoshida et al. [2] are identified on the basis of one (1LC) and two load (2LC) path changes. In this context, the influence of the yield criterion and the capability of the different hardening models are analyzed. The applicability of the identified parameters is finally evaluated in a multi-step bending process.

## 2 Experimental and numerical setup

The planar simple shear test based on a built-in tool according to Merklein et al. [3] is predicated on the ASTM standard B831 and used for the characterization of the cyclic material behavior under simple shearing. The results of the cyclic shear tests are used to identify the two kinematic hardening laws for the investigated dual-phase steel. Providing a huge variety of implemented hardening models and yield criteria the FEM-software LS-DYNA® in revision 7 is chosen for the numerical modeling of the material behavior and the applied processes. The identification of the model parameters is done by an inverse procedure using the optimization software LS-OPT® in combination with the FEM-solver LS-DYNA® and an one-element simple shear model.

To produce a springback inherent profile and to approximate the stress-strain history that a sheet metal experiences during the passing of a radius or a drawbead, cyclic bending tests are performed. A validation of the identified hardening models is done by the comparison of the experimental data and the results of an FEM-simulation regarding the force vs. stroke curve and the geometry after springback.

## 3 Results

Using an one-element model, both the isotropic-kinematic hardening law Yoshida-Uemori and the kinematic Chaboche-Rousselier model are able to describe the hardening behavior, e.g. the transient hardening evolution, of the observed dual-phase steel under shear deformation with an equal quality. Based on its complexity and the six parameters that have to be identified, the Yoshida-Uemori model takes nearly the double of identification time at one load change. The parameter sets of the two hardening models identified at one load cycle and two load cycles significantly differ from each other. However, with respect to the cyclic shear stress-strain curves no major difference between the predictions of the models can be seen. Regarding the results of the springback analysis in the cyclic bending test, the error of the predicted force before unloading is reduced to less than 10 %. As a result the calculated geometry after springback stands in good agreement with the real specimen.

As an excerpt, the results of the validation procedure are shown in figure 1 for the hardening model according to Yoshida et al. [2]. In consideration of the force vs. stroke curves, illustrated in figure 1 a), the importance of kinematic hardening laws becomes clear. The pure isotropic hardening law overestimates the bending force especially in the transient areas. Despite the expectations, the parameter set identified at one load cycle (1LC) provides a slightly better prediction of the process forces as well as the springback geometry.

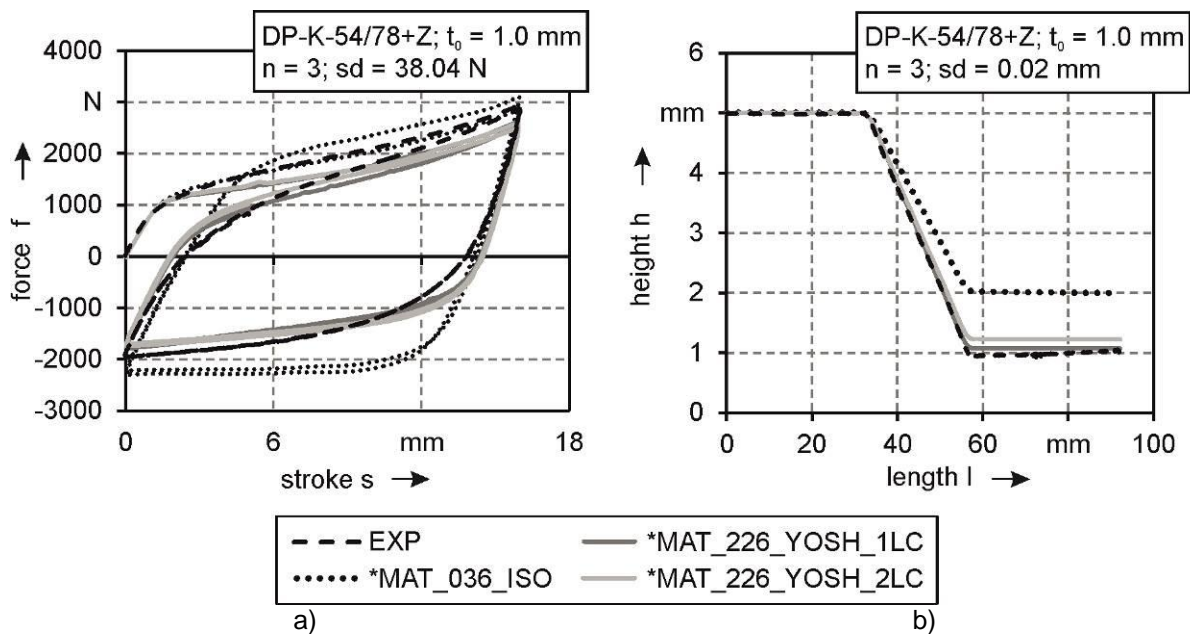


Fig.1: Validation of the Yoshida-Uemori parameters in the cyclic bending test: a) Force vs. stroke curve; b) springback geometry

#### 4 Summary

Planar cyclic shear tests are carried out to characterize the material behavior of DP-K54/78+Z under multiple cyclic loading. Moreover, the results of the shear tests are used to identify and analyze kinematic hardening laws pertaining to the predictability of the springback behavior during a cyclic bending test. It is shown, that an inverse parameter identification with the use of an one element shear model is applicable, whereas no influence of the two observed anisotropic yield criterions Barlat'89 and Yld2000-2d can be detected. In case of the kinematic Chaboche-Rousselier hardening formulation as well as the isotropic-kinematic Yoshida-Uemori model, the identification on only one load cycle is sufficient to predict the . This is also validated by a numerical springback prediction of a cyclic bending test, where both models enhance the numerical prediction quality with respect to a conventional isotropic approach. Contrary to the higher complexity of the isotropic-kinematic Yoshida-Uemori model and its more extensive identification procedure, no significant benefit can be achieved in comparison to the Chaboche-Rousselier model regarding the results of the numerical springback analysis.

#### 5 Acknowledgement

For the support in the research projects EFB 06/112 (AiF 17375 N/2) and ME (2043/11-2) the authors would like to thank the European Research Association for Sheet Metal Working e.V. (EFB) and the German Research Foundation (DFG) as well as the German Federation of Industrial Research Associations „Otto von Guericke“ e.V. (AiF).

#### 6 Literature

- [1] Chaboche, J. L.: A review of some plasticity and viscoplasticity constitutive theories, Int. J. Plasticity 24, 2008, 1642-1693
- [2] Yoshida, F., Uemori, T.: A model of large-strain cyclic plasticity describing the Bauschinger effect and workhardening stagnation, Int. J. Plasticity 18, 2002, 661-686
- [3] Merklein, M., Biasutti, M.: Forward and Reverse Simple Shear Test Experiments for Material Modelling in Forming Simulations, Steel Research International, 2011, 702-707



**PROCESS III**  
**METAL FORMING**





# Parameter Identification for Forming Simulation of High-Strength Steels

Marco Thomisch, Dr. Markus Kley

University Aalen, Germany

In the past most of forming-manufacturing processes were mainly based on trials. For cost effective production, simulation is a reliable tool for getting good predictions before starting with manufacturing. The number of plastic deformation steps during one manufacturing process is mostly more than one. However the load direction of all the deformation steps is in the same way. A few applications are dealing with an alternating direction of the forming loads. These cases are affected by hardening and/or softening effects. Additional to this belonging some special effects like Bauschinger-Effect are relevant as well. Knowing of these effects and their range are mandatory for planning and simulating forming processes.

Based on a research project the University of Aalen is dealing with massive deformation of prismatic beams made of high-strength steels. The deformation of half-finished products consists of more than one deformation step. In this case the load direction of the sequent deformation steps is alternating; in detail the direction of second deformation is in the opposite to the first deformation step. Due to this, hardening effects occur. In deed first investigation shows that yield stress of the second plastic deformation is lower than yield stress of the first plastic deformation with opposite deformation direction. This effect is called Bauschinger-Effect [1]. Classical tensile-pressure-trials are a common method to analyze the Bauschinger-Effect. Unfortunately based on several reasons the tensile-pressure-trials are not very suitable for high-strength steels. On the one hand the availability of half-finished products is limited related to geometrical dimensions. On the other hand the chipping of this material is very restricted based on the high yield stress. Additional to this, milling influences the residual stress situation inside the specimen.

This report shows a new approach for getting the needed material data via trials compared to classical tensile-pressure trials. The test results will be used for optimization of material cards with LS-Opt. After showing the method itself, conclusion with results and outlook will follow.

In general the possibility for getting the needed parameters by curve fitting is possible. For every investigated case, especially bending and tensile/pressure load cases, parameters are identified.

Cross checking of the results is mandatory due to the big differences from one load case transferred to another one.

Related to the results, the optimization for this material will not be valid for the whole behavior. In deed the optimization has to be defined for specific boundary conditions. Especially the bending simulation is more generous than tensile/pressure simulation. This behavior is based on the high elastic zone in bending specimen. In tension/pressure cases, the whole area will plasticize after reaching the yield stress. Therefore inaccurate parameters are acts stronger.

Unfortunately LS-Dyno does not provide any material which do not use the restriction for yield stress described above. Due to this, a better parameter optimization will not be possible.

Additional the transferability from the one basic load situation to another is not possible if the parameters do not fit in total. This is based on different weighting of elastic and plastic mechanism during deformation.

Further parameter optimization of present situation will be done with following restrictions:

- Due to the real specific manufacturing process the plastic deformation is mainly located in the high deformation part (>2% deformation) of the stress-strain curve. That means the section directly after yield stress is not as relevant for the results as in other situations.
- The optimization for bending simulation will be only done with bending optimization.

## Literature

[1] Bauschinger, Johann: "Über die Veränderung der Elastizitätsgrenze und der Festigkeit des Eisens und Stahls durch Strecken und Quetschen, durch Erwärmen und Abkühlen und durch oftmal wiederholte Beanspruchung", Mitteilung aus dem mechanisch-technischen Laboratorium, München, 1886, 62

# ACP Process Integrated 3B Forming Optimization

Akbar Farahani<sup>1</sup>, Ph.D, Divesh Mittal<sup>1</sup>, Jody Shaw<sup>2</sup>

<sup>1</sup>Engineering Technology Associates, Inc.

<sup>2</sup>US Steel

## 1 Introduction

The automotive and steel industry has several initiatives; such as Generation 3 Advanced High Strength Steels (AHSS), the Nonlinear Strain Path Project, and the A/SP AHSS stamping team projects; to expand the forming design space with AHSS to enable increased part complexity, which will allow AHSS to be incorporated into more vehicle components and enable mass reduction. The approach discussed in this presentation will provide a new tool in the effort to expand the forming design space of AHSS.

## 2 Summary

The final design of the Future Steel vehicle (FSV) Project was released in May of 2011. Its development used a new optimization-led design methodology, the Accelerated Concept to Product (ACP) Process<sup>®</sup>, which produced highly non-intuitive designs. Component geometry utilized natural, very organic shapes combined with minimum gauge selections. While these non-intuitive designs have the potential to produce lightweight, low-cost, yet structural efficient products; these types of solutions also create significant manufacturing challenges.

Exploiting the flexibility of AHSS and modern, advanced steel manufacturing technologies, these types of designs are now possible in the real-world production environment. However, due to severe formability challenges, many design iterations are required to create such solutions. As a subset of the ACP Process, formability analysis, using eta/DYNAFORM<sup>®</sup>, has been integrated directly into the optimization based design process.

An Integrated Incremental **3B** (Draw **B**ead, **B**lank Geometry and **B**inder Pressure) Forming **Optimization** approach balances forming parameters such as draw bead force and geometry, blank shape and size and binder pressure. Then, gauge optimization of the product itself is done to create the lightest, most structurally and cost efficient design possible that meets the vehicle performance targets. It achieves this by optimizing the component design for formability while simultaneously validating its in-vehicle crash performance.

This paper will explain the process of "Integrated Incremental 3B forming and Crash Optimization" and will describe the use of its enablers including LS-DYNA, eta/DYNAFORM, HEEDS and ANSA [1-9]. It will describe the methodology as applied to the most challenging FSV components to form.

## 3 Keywords

ACP Process, Optimization, Forming, ACP, WorldAutoSteel, FSV, LS-DYNA, ANSA, DYNAFORM, HEEDS, SFE-Concept

## 4 Literature

- [1] Engineering Technology Associates, Inc. (ETA), (2009). *Methodology Used in Future Steel Vehicle Wins SAE Vehicle Innovation Competition*, [www.theautochannel.com/news/2009/12/18/459143.html](http://www.theautochannel.com/news/2009/12/18/459143.html)
- [2] A. Farahani, R.C. Averill and R. Sidhu, "Design Optimization of Hydroformed Crashworthy Automotive Body Structures," *CAD-FEM Users' Meeting*, Berlin, Potsdam, Germany, November 12-14, 2003.
- [3] A.Farahani, J.Shaw, P.Dolan, H.Sharifi" The Future of Product Design and Development" International Body Automotive Conference (IBAC)" November 2010

- 
- [4] A. Farahani, J. Shaw, "Future Generation Passenger Compartment" Great Designs in Steel (GDIS), May 2007.
  - [5] Auto Steel Partnership, "Future Generation Passenger Compartment", (FGPC) Validation, November 2009.
  - [6] J.M. Madakacherry, D. Eby, M. B. Isaac, A. Farahani, C. Bruggeman and R. C. Averill "A Process of Decoupling and Developing Optimized Body Structure for Safety Performance," "10<sup>th</sup> European LS-DYNA Conference." March 18, 2004.
  - [7] A Farahani, J. Shaw", Highly Optimized Longitudinal Rail Achieving 45% Mass Reduction", Great Designs in Steel (GDIS), May 2009
  - [8] EDAG AG, (2010). *Phase 2 FutureSteelVehicle Steel Technology Assessment and Design Optimization Engineering Report* [www.worldautosteel.org/Projects/Future-Steel-Vehicle/FSVInterimReport.aspx](http://www.worldautosteel.org/Projects/Future-Steel-Vehicle/FSVInterimReport.aspx)
  - [9] A. Farahani, M. Lambtikis, P.Dolan, H. Sharifi, "The Future of Product Design and Development", "8th European LS-DYNA user Conference" May 2011

# Influence of Variations in a Mechanical Framing Station on the Shape Accuracy of S-Rail Assemblies

Klaus Wiegand<sup>1</sup>, Tobias Konrad<sup>1</sup>, Marion Merklein<sup>2</sup>

<sup>1</sup>Daimler AG, Sindelfingen, Germany

<sup>2</sup>Institute of Manufacturing Technology, Erlangen, Germany

In virtual production planning, recent publications have shown the possibility of creating a digital process chain of body parts including the process steps in the press shop and body-in-white shop. The digital process chain is used to get an early impression of the dimensional accuracy of assemblies regarding the single parts that are used. Within the entire process chain, a wide variety of factors influence the dimensional accuracy of (sub)-assemblies. However, not every parameter of the deep drawing and assembly process exerts significant influence on the assembly quality and on process stability. Furthermore, the interaction of certain parameters could lead to an improved result at the end of the process chain.

Therefore, sensitivity and robustness analyzes applying LS-OPT are used to detect factors influencing the shape accuracy of single parts and assemblies. This contribution covers the shape deviation behavior of single parts in the press shop and their state after parameter variations in a virtual framing station. The aluminum alloy AA6014 and the mild steel alloy CR3 with a sheet thickness of 1.0 mm are investigated.

Parameter variations of the clinching process are presented in this paper by joining an S-rail specimen. The S-rail geometry shows a visible und measurable shape deviation behavior.

Finite element tools, such as LS-DYNA and Abaqus, are applied to model an S-rail assembly process. Following a feasibility simulation regarding cracks and wrinkles, the simulation process is used to detect the significance of factors in the digital process chain with respect to the dimensional accuracy of assembled components.

Besides this aspect, the finite element simulation is subsequently used to optimize the assembly process of S-rails in the framing station.

# Structural Analysis of an Automotive Forming Tool for Large Presses using LS-DYNA

K. Swidergal<sup>1</sup>, C. Lubeseder<sup>2</sup>, I. von Wurmb<sup>2</sup>, A. Lipp<sup>2</sup>, J. Meinhardt<sup>2</sup>, M. Wagner<sup>1</sup>, S. Marburg<sup>3</sup>

<sup>1</sup>Ostbayerische Technische Hochschule Regensburg, Mechanical Engineering Department, Laboratory for Finite Element Analysis and Structural Dynamics, Germany

<sup>2</sup>BMW Group, Construction methods and Standards Department, Germany

<sup>3</sup>Universität der Bundeswehr München, LRT4 – Institute of Mechanics, Germany

## 1 Abstract

To improve efficiency in automotive press shops, press systems with increasingly high stroke rates are being implemented, raising thereby the structural dynamic load on the press and especially on the forming tool. In this paper, the detailed knowledge about the tool's deformation, which is essential for an accurate and robust design of forming tools, is gained by conducting a structural dynamic finite element method (FEM) simulation of a selected automotive tool. The focus in the presented model is put on one of the tool's components, namely the forming slide. The transient simulation is preceded by a dynamic relaxation phase where the gravity load is applied and the gas springs are pre-stressed. The model is built with ANSA and solved with LS-DYNA explicit. For validation of the simulation results, the kinematic responses of the slide are compared with the measurements obtained in an experiment.

## 2 Introduction

Due to high investment costs of an automotive forming tool for large presses, the tool designers are trying to integrate as much forming operations in one tool as possible, reducing therefore their overall number. As a side effect, the modern tools are getting more and more complex. Moreover, due to the press systems with increasingly high stroke rates and a growing usage of high strength steels the structural dynamic loading on those tools increases [1]. Therefore, to gain a detailed knowledge of deformations and thus enable an accurate and robust design of complex forming tools numerical simulation can be advantageously applied. This has already been shown in [2], where a coupled multibody finite element simulation (MBS-FEM) approach for analyzing the vibration of the blankholder was presented. In this work, a structural FEM analysis of a forming slide in a selected tool is conducted.

## 3 Developing the LS-DYNA model

The FE model of the forming tool, shown in Figure 1, is built within the ANSA environment.

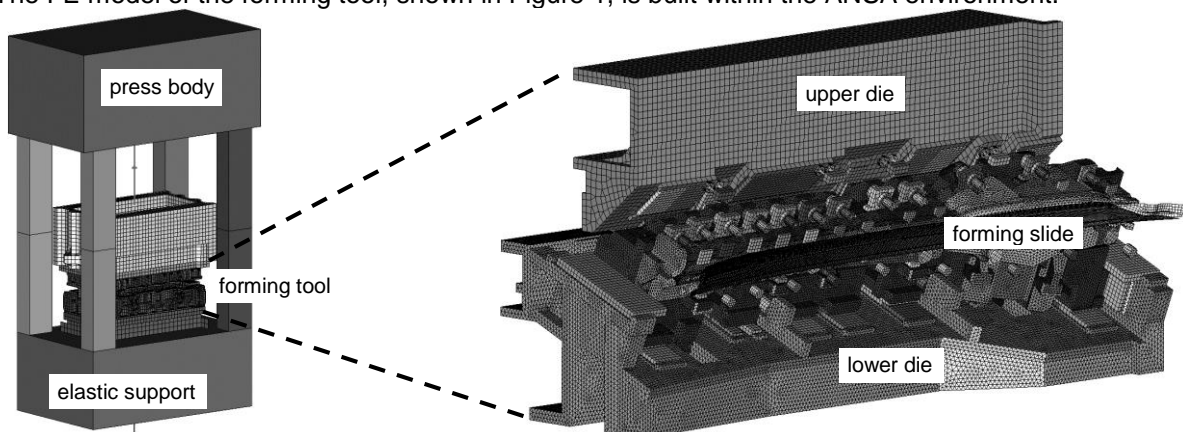


Fig. 1: LS-DYNA model of simplified press with the forming slide assembly.

Due to the large number of geometrical parts, the model is organized into several subassemblies like the press or the forming slide assembly. The defeatured CAD geometry is discretized with linear hexahedral and tetrahedral elements. For representing the strings and damper, discrete elements are used. Relevant parts like cast iron structures, punches or sliding pads are considered to be elastic and

modelled with a `*MAT_PIECEWISE_PLASTICITY` material model. For rubber components like elastomer dampers, a `*MAT_SIMPLIFIED_RUBBER` material model is taken, which is a tabulated version of the Ogden hyperelastic material model. The necessary uniaxial stress-strain curves for several discrete strain rates have been obtained experimentally, see [3], and provided in a table definition. Several constraining techniques, such as `*CONSTRAINED_RIGID_BODY_NODES` or `*CONTACT_TIED_NODES_TO_SURFACE` are utilized to connect assembly components. The prescribed motion of the press slide is realized with the `*CONSTRAINED_JOINT_TRANSLATIONAL_MOTOR` keyword with an acceleration slide curve defined. Applying the gravity load and pre-stressing the gas springs is done in the dynamic relaxation phase. The complete model is solved with LS-DYNA explicit.

#### 4 Results and discussion

For the validation, the numerically obtained velocity response of the forming slide assembly was compared to the signal gained in experiment, which was carried out under operational loading. Both velocity responses are shown in Figure 2.

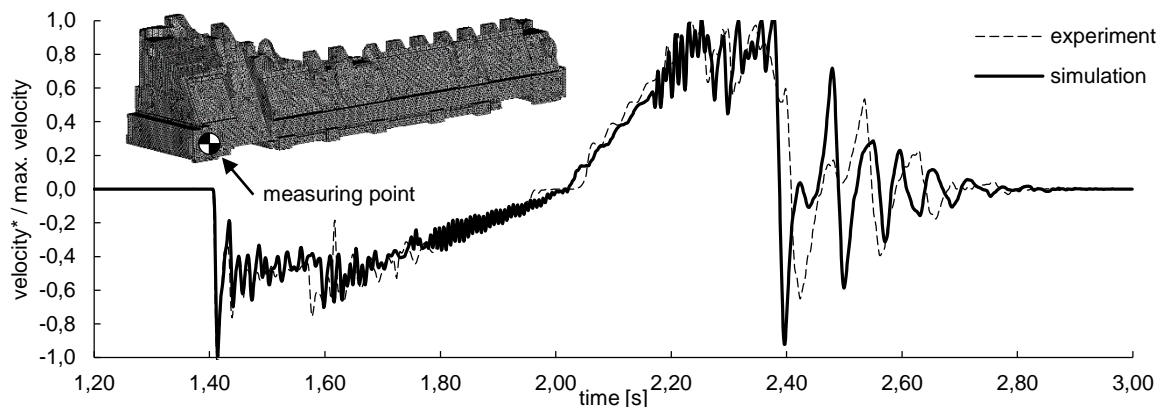


Fig.2: Translational velocity of the forming slide (\*lowpass, cutoff freq.: 100Hz) during its stroke.

It can be seen, that the simulation results are in relatively good agreement with the measurements. During the travel of the forming slide, both velocity curves possess similar characteristic and their values lie within the same range. However, when the forming slide returns and hits the elastomer stoppers at time  $t \sim 2.4$ s, it vibrates differently. The oscillations in the simulation begin about 10ms later, which can be explained with a different length of the elastomer stoppers used in the simulation and experiment. Due to the Mullin's effect, the stoppers in the real tool have a reduced height, whereas in the FE model initial unchanged length is used.

#### 5 Conclusion and outlook

In this work, a structural finite element analysis of the forming slide component in LS-DYNA was successfully conducted. Based on an experimental validation, the simulated resulting dynamic loading on the forming slide showed good agreement with measurements. In addition, the regions of critical stresses in the forming slide's body could be identified. Therefore, the structural dynamic loading on the forming tool and indirectly on the press can now be predicted, enabling fatigue life calculation.

#### 6 Literature

- [1] Osakada, K.; Mori, K.; Altan, T.; Groche, P.: "Mechanical Servo Press Technology for Metal Forming", CIRP Annals - Manufacturing Technology, vol. 60, 2011, pp. 651-672
- [2] Swidergal, K.; Lubeseder, C.; von Wurmb, I.; Lipp, A.; Meinhardt, J.; Wagner, M.; Marburg, S.: "Experimental and numerical investigation of blankholder's vibration in a forming tool: A coupled MBS-FEM approach", Production Engineering, (in review process)
- [3] Swidergal, K.; Thumann, P.; Lubeseder, C.; von Wurmb, I.; Meinhardt, J.; Wagner, M.; Marburg, S.: Modeling and simulation of carbon black filled elastomer damper using LS-DYNA, 13. LS-DYNA Forum, Bamberg, Germany, 6-8 October 2014

**PROCESS IV**  
**COMPOSITES**





# Simulation of Forming of Paperboard Packaging using LS-DYNA

Mikael Schill<sup>1</sup>, Johan Tryding<sup>2</sup>, Jesper Karlsson<sup>3</sup>

<sup>1</sup> DYNAmore Nordic, Linköping, Sweden

<sup>2</sup> Tetra Pak, Lund, Sweden

<sup>3</sup> DYNAmore Nordic, Gothenburg, Sweden

Paperboard is widely used as a package material for food and beverage. The ability to simulate the forming of the packages is of great interest, due to the variety in shapes and paperboard material structure combined with production speed. The main task when producing a paperboard package is that the structural integrity of the container is not compromised through e.g. in-plane surface cracks of the paperboard. This may lead to leakage which will jeopardize the integrity of the container.

As a material, paperboard is highly anisotropic due to the composition and alignment of fibers. Also, the stacking of fibers into planes introduces a vast difference in out of plane and in plane properties. To accommodate for this, a material model denoted \*MAT\_PAPER has been implemented into LS-DYNA based on the work done by Xia [1] and Nygård's [2]

The forming of a paperboard package includes a creasing stage where the material is delaminated locally to achieve a nice fold pattern without causing in-plane surface cracks. The paperboard is then folded and subsequently filled. This paper will present the current status of \*MAT\_PAPER in LS-DYNA. Also, a brief overview of the modeling techniques used for modeling of paperboard will be described as well as results from in plane bending and creasing simulations compared with experiments, see Fig. 1.

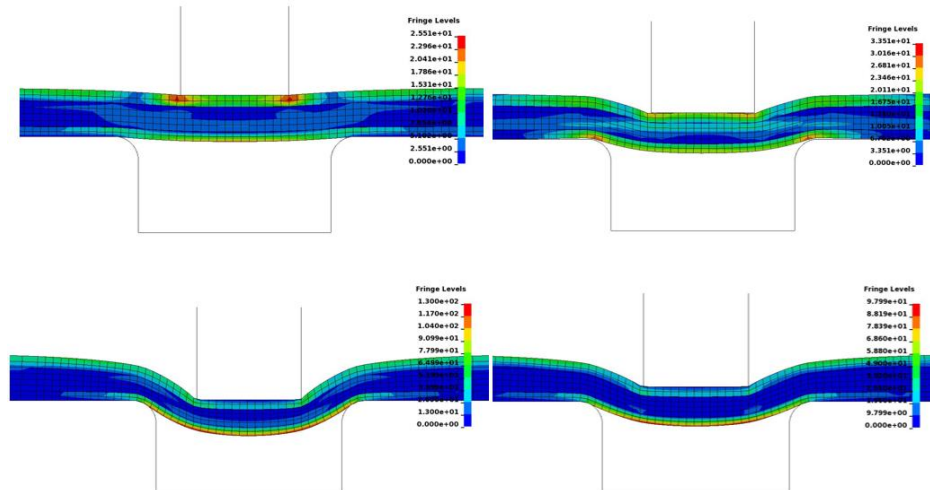


Fig. 1: Creasing simulation using \*MAT\_PAPER and cohesive elements for delamination

## 1 Literature

- [1] Xia, Q., Bouyce, M., Parks, D., 2002. A constitutive model for the anisotropic elastic plastic deformation of paper and paperboard. *Int. J. of Solids and Structures* 39, 4052-4071.
- [2] Nygård's, M, Just, M., Tryding, J., 2009. Experimental and numerical studies of creasing of paperboard. *Int. J. of Solids and Structures* 46, 2493-2505

# Forming Simulation of Textile Composites using LS-DYNA

Masato Nishi, Tei Hirashima

JSOL Corporation

## 1 Introduction

The primary focus of this paper is on FE modeling and simulations performed, using LS-DYNA, to capture the material behaviors during textile reinforcement preform and thermoplastic resin pre-impregnated sheet (pre-preg) forming manufacturing. Although the out-of-plane bending stiffness of textile reinforcement is often ignored as it is very low compared to in-plane stiffness, more accurate simulation, especially the prediction of wrinkles, is achievable by considering out-of-plane bending stiffness in forming simulation. We propose a hybrid model which consists of a membrane and shells that can describe out-of-plane bending stiffness which is independent from in-plane behavior. In order to extend the textile reinforcement model to a thermoplastic pre-preg model for thermoforming simulation, temperature dependent stress contribution of thermoplastic is added to the textile reinforcement by applying Reuss model which can take the volume fraction of fiber ( $V_f$ ) into account.

## 2 Preform simulations of dry textile reinforcement for RTM process

Here we propose the shell and membrane hybrid model in order to consider the bending stiffness that is independently free from any in-plane properties. In-plane properties are described by the membrane element and the bending stiffness is represented by a set of shell elements as shown in Fig.1.

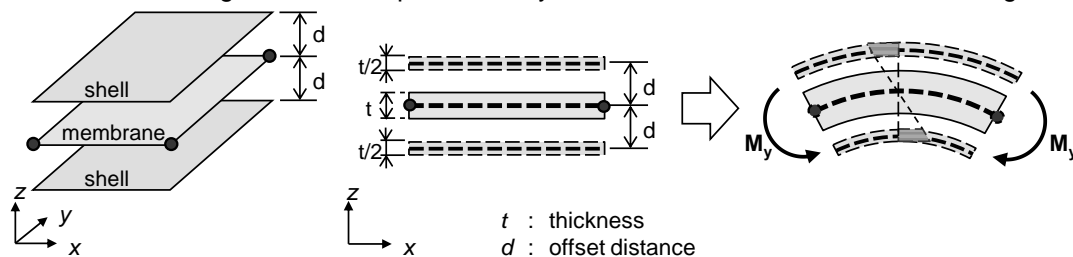


Fig.1: Shell and membrane hybrid model considering in-plane and out-of-plane properties.

Fig.2 shows the deformed shapes of the meso-scale model. The model which consists of only membrane elements is also calculated to investigate the effect of the bending stiffness. In this model, only in-plane property is considered. The proposed model considers out-of-plane bending stiffness as well as in-plane properties. Many small wrinkles are observed in the model which considers only in-plane properties. The shapes of wrinkles in the proposed model are similar to the ones in the meso-scale model. Here the simulations demonstrate that the bending stiffness plays a very important role in the shapes of wrinkles.

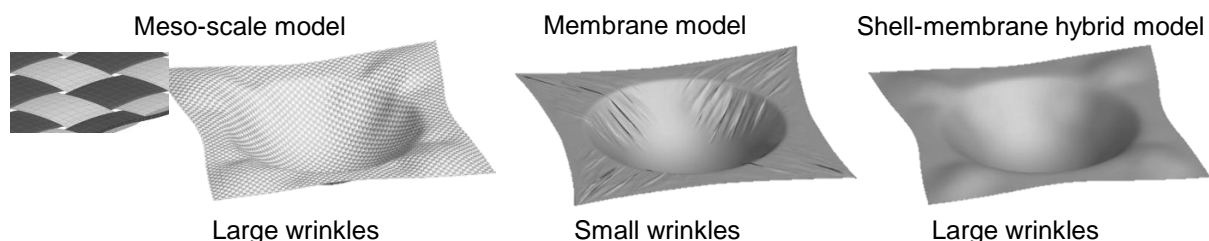


Fig.2: FE model without blank-holder and comparison of wrinkles.

## 3 Thermoforming simulation of thermoplastic pre-preg

In order to add the effect of thermoplastic resin to the textile reinforcement model, additional membrane elements are placed around the textile membrane. In-plane stress response of the pre-

preg is represented in a parallel system of textile reinforcement and thermoplastic resin where those stresses are separately calculated by introducing Reuss model. S-rail forming experiments with  $[(0/90)_4]$  and  $[(45/-45)_4]$  lay-ups were performed with a non-heated metal tool at room temperature in order to assess the capability of the proposed FE model. Simulations are also performed by two different approaches to investigate the effect of the change in the temperature during the forming. One is non-isothermal simulation which can consider the change in the temperature during forming. The other is isothermal simulation under the assumption of a constant temperature during the forming process. Fig. 3 shows the comparisons of the outlines between the experiments and each simulation. The outlines simulated by the non-isothermal simulations show good agreement with the experimental measurements for both lay-ups. On the other hand, the outlines simulated by the isothermal simulations are different from the experimental measurements. These simulation results demonstrated that formability is significantly changing throughout the non-isothermal forming.

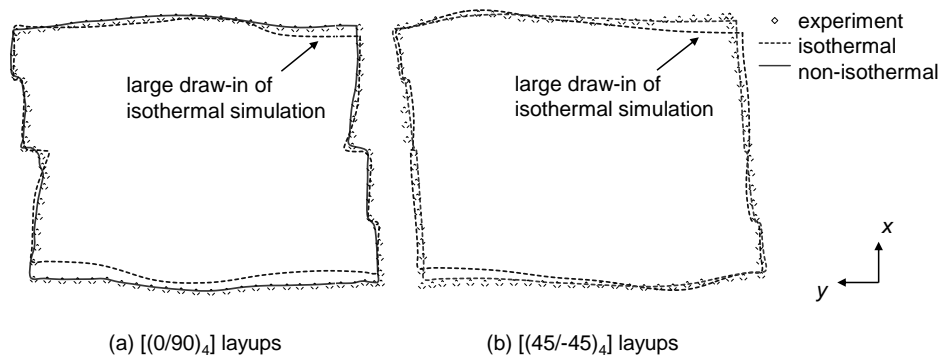


Fig.3: Comparison of final outlines between experiments and simulations.

#### 4 Summary and outlook

An FE model for the forming of textile reinforcement was proposed in this study. The proposed model overcame the bending stiffness by placing shell elements on both sides of a membrane element. The results of sensitivity studies showed that an accurately described bending stiffness was very important for evaluating wrinkles. Furthermore, we extended the textile reinforcement model to a thermoplastic pre-preg model for non-isothermal forming simulation. S-rail thermoforming simulations are performed and compared to experimental results. Simulated outline and shear angle are in good agreement with experimental results.

Now, JSOL Corporation is developing a software tool for the forming simulation of dry textile reinforcement, textile pre-preg and UD pre-preg. This software tool enables users to optimize process condition, and minimize lead times and design costs.

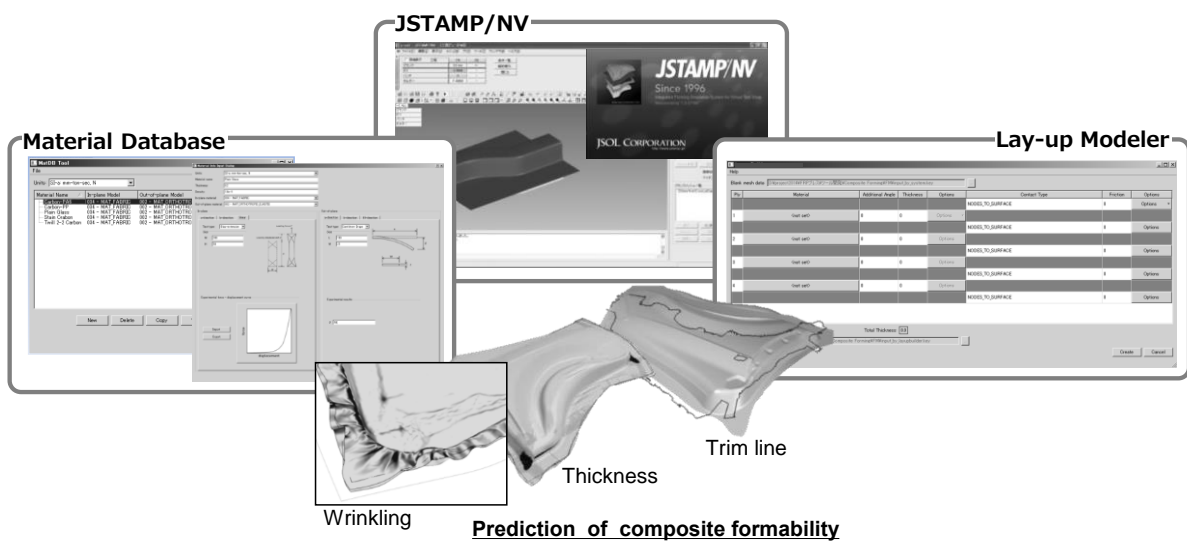


Fig.4: Software tools for composite forming simulation linking with JSTAMP/NV.

# A Graphical User Interface for Simulating Resin-Transfer-Molding Combining LS-DYNA and OpenFOAM

M. Wagner<sup>1</sup>, M. Martins-Wagner<sup>1</sup>, A. Haufe<sup>2</sup>, C. Liebold<sup>2</sup>

<sup>1</sup>Ostbayerische Technische Hochschule Regensburg  
Laboratory for Finite Element Analysis and Structural Dynamics  
Regensburg, Germany

<sup>2</sup>Dynamore GmbH  
Stuttgart-Vaihingen, Germany

The paper describes parts of the joint research project Swim-RTM including several industrial and academic partners. Its goal is to combine LS-DYNA and the open-source CFD solver OpenFOAM® to simulate the production process of continuous fiber-reinforced plastics, particularly the resin-transfer-molding (RTM) process, in which the layers of dry fabric (unidirectional or woven) are formed in the mold (draping) and then filled with liquid resin with high pressure at injection points. Through a combined analysis of both the structural mechanical and the fluid dynamical phases, a better prediction and thereby optimization of the textile components properties as well as injection points can be achieved, improving the manufacturing process.

The draping simulation of the fabric layers is carried out with LS-DYNA, while the injection simulation of the matrix material is performed in full 3D with OpenFOAM®. A key question that has to be answered in this research project is how local porosities and tensorial permeabilities for the fluid simulation can be derived from the structural computation in the draping step.

The purpose of the presented subproject is to develop a graphical user interface (GUI) to enable the simulation of the entire RTM process of long-fiber-reinforced components including the transfer of simulation results from the draping to the injection phase and backwards (see Fig. 1). The complete simulation task is relatively complex and involves several software packages, meaning a high effort for the user to get familiarized with. To circumvent this, the GUI aims at requiring from the user only the minimum necessary input data, creating and running the simulation and mapping tasks in the background, and showing graphically all demanded intermediate and final results.

For the draping step several current fabric materials such as \*MAT\_34, \*MAT\_234, \*MAT\_235, \*MAT\_249 are available. Several modelling techniques for the composite setup are also conceivable, including a workflow similar to metal forming applications. In the injection step the fabric is modelled as a porous medium and different transport models and liquid resin types are at hand.

For the data transfer between the draping and injection models, i.e. the mapping of data between shell and volume meshes within the developed GUI, first the OpenFOAM® volume mesh is converted to LS-DYNA format and the necessary passing parameters are extracted from the output files, then a mapping algorithm from DYNAmore GmbH is invoked, and finally the OpenFOAM® command files are created. After the injection simulation is started and successfully terminated, information, such as the distribution of air inclusions or the shear force distribution to analyze the reorientation of component fibers, are available and can be transferred back to the LS-DYNA shell mesh for further computations, for instance a crash simulation. A backward data mapping between the volume and shell meshes can then be performed inside the GUI.

An example of the GUI application for the simulation of the resin transfer molding of an L-shaped component is presented.

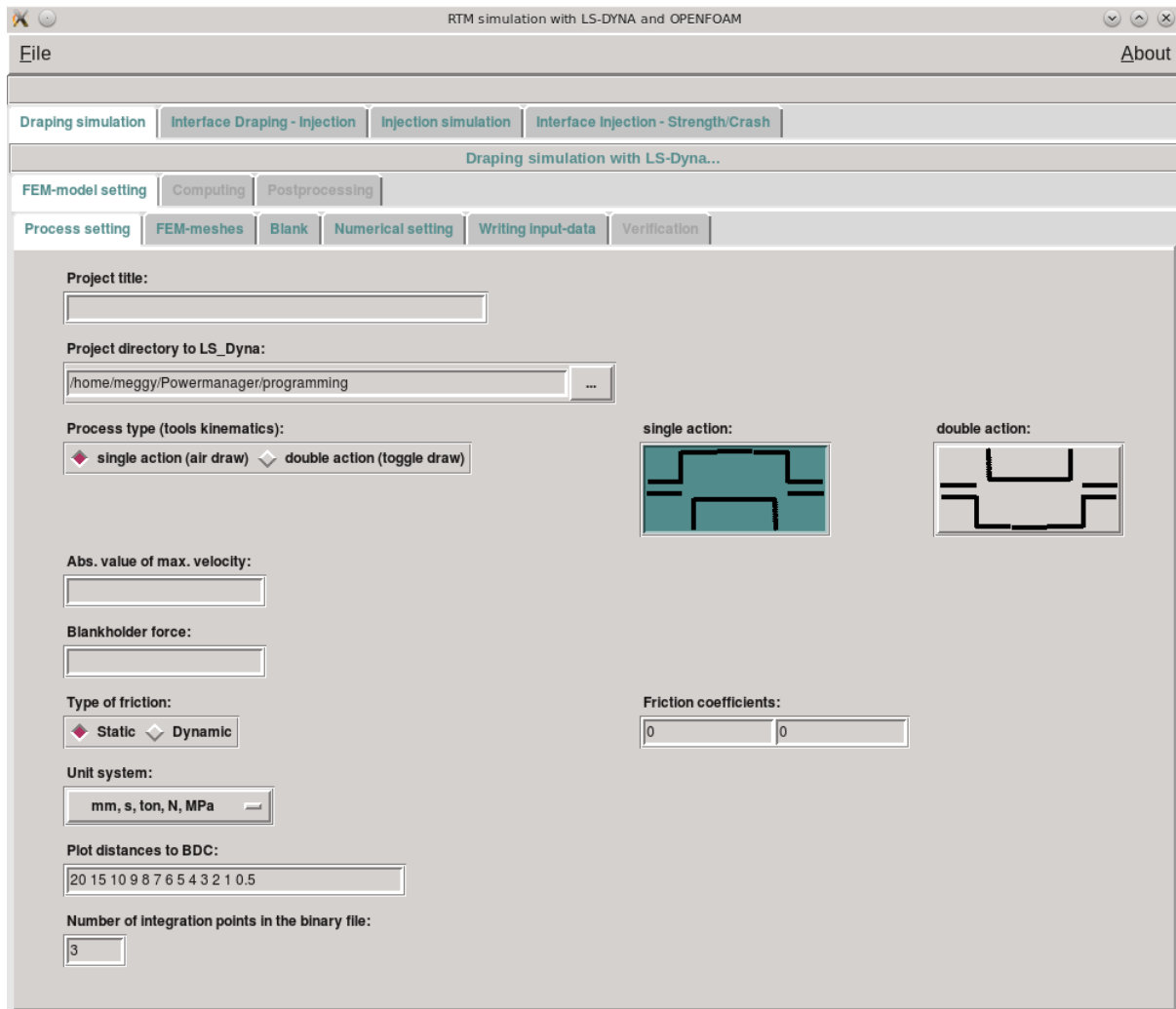


Fig. 1. Start page of the GUI for RTM processes with LS-DYNA and OpenFOAM®.

Support of this research project under grant KF2133705SS2 by the Federal Ministry for Economic Affairs and Energy is gratefully acknowledged

# Modeling Non-Isothermal Thermoforming of Fabric-Reinforced Thermoplastic Composites

Dominic Schommer, Miro Duhovic, Joachim Hausmann

Institut für Verbundwerkstoffe GmbH, Germany

The correct modeling of the sheet forming of fabric reinforced thermoplastic composites, so called organosheets, is still a challenge. In the past it was possible to predict accurately and efficiently the fiber orientation during the draping of dry reinforcement or constant temperature organosheet (reinforcement and molten polymer) using the explicit FEM-Software LS-DYNA®. The developed model was only able to simulate the right material behavior for a purely isothermal process. However, the draping of an organosheet is in reality a non-isothermal process that takes place at elevated temperatures. During thermoforming, the sheet cools down by contact with the forming tools and changes its temperature dependent mechanical behavior. With several enhancements, it is now possible to implement the temperature dependent shear and bending stiffness of the thermoplastic material into the model. This allows the modeling of a non-isothermal forming process. The method is based on a "hybrid unit-cell" model which uses a combination of shell and beam elements. The bending stiffness of the composite is represented by the beam elements. The bending behavior is characterized using a three-point bending test, performed inside a heating chamber in the range of the forming temperature of the thermoplastic resin. The shell elements represent the shear behavior of the fabric reinforcement which is influenced by the temperature dependent stiffness of the resin. Using a horizontal picture frame test, it is possible to characterize the shear behavior of the composite for different sheet temperatures. With the new extended modeling approach, it is possible to predict fiber orientation and occurring defects, such as wrinkling, even more accurately. The verification of the developed modeling approach is carried out through the simulation of material characterization tests (shear and bending behavior) for a commonly used commercially available material TEPEX® dylalite 102. The material model parameters derived from the verification models are used to simulate the forming behavior of a novel automotive crash element geometry.

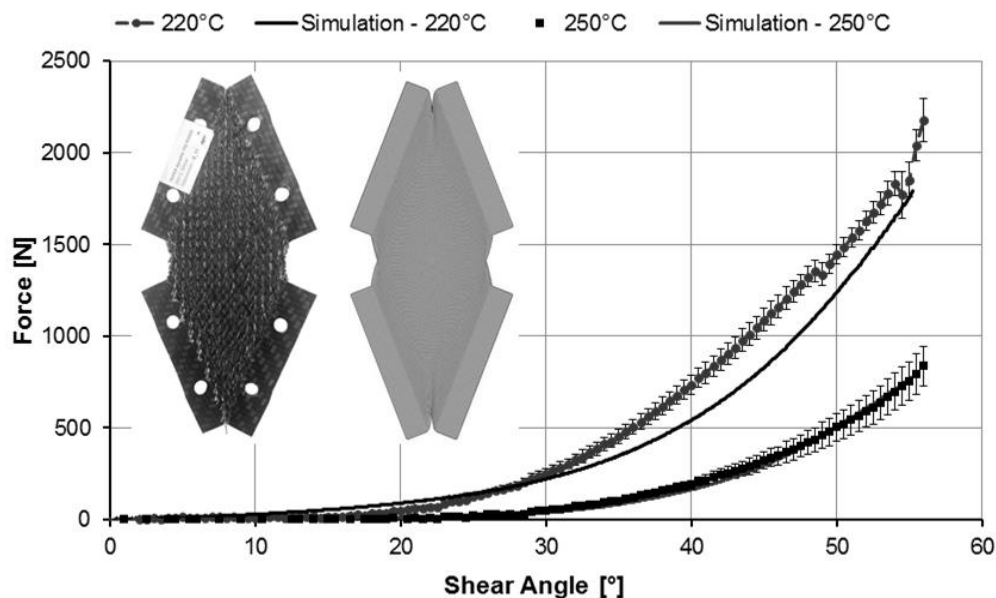


Fig. 1: Comparison between experiment and simulation of the picture frame test using the example of TEPEX® dylalite 102 RG600.

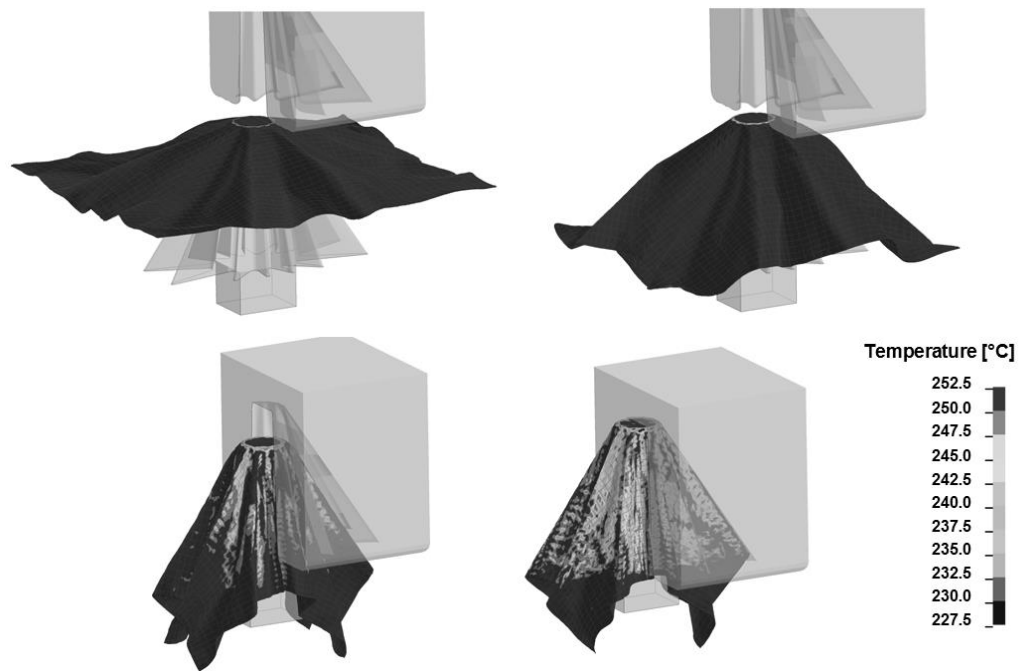


Fig.2: Temperature contours of non-isothermal thermoforming process of a crash absorber performed in LS-DYNA®.

## Literature

- [1] Duhovic, M.; Mitschang, P.; Bhattacharyya, D.: Modelling approach for the prediction of stitch influence of woven fabric draping. Composites. Part A, applied science and manufacturing. Volume 42A, Issue 8, 2011, S.968-978.
- [2] Sidhu, R.M.J.S.; Averill, R.C.; Riaz M., Pourboghrat, F.: Finite element analysis of textile composite preform stamping. Composites Structures, 52, 2001, S.483-497
- [3] Liang, B.; Hamila, N.; Peillon, M.; Boisse, P.: Analysis of thermoplastic prepreg bending stiffness during manufacturing and of its influence on wrinkling simulations. Composites: Part A, applied science and manufacturing.. Volume 67, 2014, S.111-122.
- [4] Norm DIN EN ISO 14125, May 2011
- [5] k.A.: Thermoplastischer offaxisstabiler Crashabsorber. Crash-Muffin aus Faser-Kunststoff-Verbunden, [www.kunststoffe.de/produkte/uebersicht/beitrag/thermoplastische-crash-muffins-crashabsorber-aus-faser-kunststoff-verbunden-fkv-945632.html](http://www.kunststoffe.de/produkte/uebersicht/beitrag/thermoplastische-crash-muffins-crashabsorber-aus-faser-kunststoff-verbunden-fkv-945632.html), 17.04.2015.





**PROCESS V**  
**MISCELLANEOUS**



# RollerPaG a tool for the automatic path generation for roller hemming simulation using LS-DYNA

Omar Ghouati<sup>1</sup>, Bruno Boll<sup>2</sup>

<sup>1</sup>Ford Research & Advanced Engineering, Aachen, Germany

<sup>2</sup>DYNAmore GmbH, Stuttgart, Germany

## 1 Introduction

Compared to tool or table-top hemming, the roller hemming is unique by its specific kinematic. A robot guides a roller along the flange to perform the hemming, with more than one robot used for an assembly in order to speed up the process. Main advantages of the roller hemming are low investment for a new product and short lead time to design and manufacture product specific equipment. Application of roller hemming was up to now restricted to low and middle volume production, though new developments made it more suitable for higher production volumes as well.

Because of its special kinematic, the setup of the roller hemming simulation can be rather cumbersome and very time consuming. It is indeed necessary to describe the movement of the rollers along the flange in an accurate way. This paper describes a concept to set up simulation models of roller hemming processes with a high degree of automation. As an essential part of this concept, program *RollerPAG* is used for the automatic generation of the LS-DYNA input decks including Master Input Deck and the Load Curves which control the rollers motion and orientation during the simulation.

## 2 Basic Concept

The motivation for the development of program *RollerPAG* was to provide a tool for an easy as possible setup of an FE model for the simulation of roller hemming processes. The parts involved in roller hemming usually consist of an *inner* and *outer* part, a *hemmed*, *blank holders* and, optionally, *guide pins*. The user has to provide a description of these parts in terms of an FE mesh and material and section data. What the user also has to provide are curves describing the path for the rollers to travel along. For each path, two parallel curves, used to control the motion and orientation of the roller and discretized by beam elements, have to be provided. Everything else is generated automatically by program *RollerPAG*. The basic concept consists of *Discretized Path Curves Concept*, *Roller Repository Concept* and *Roller Approach Concept*.

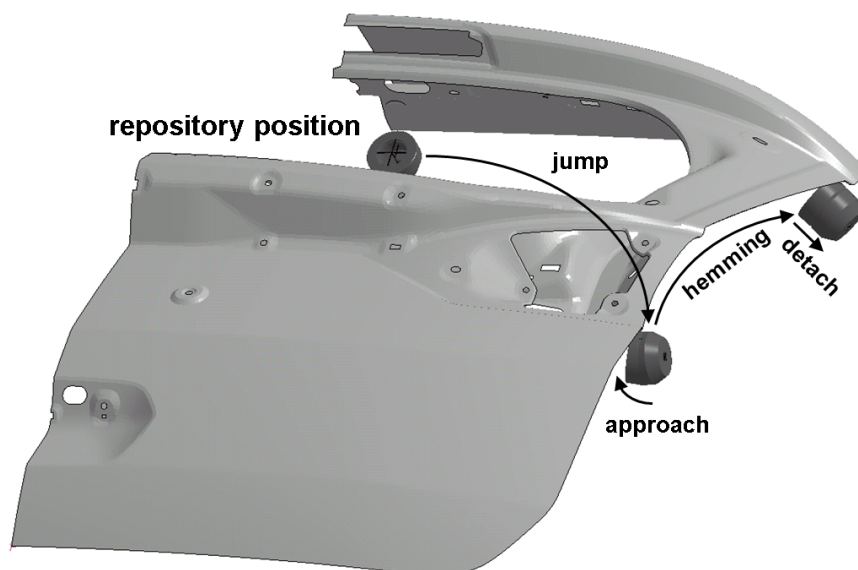


Fig. 1: Illustration of the roller movement steps

# Simulation of the Manufacturing Process of Self-Piercing Rivets with LS-DYNA with Focus on Failure Prediction for Sheets and Rivet

Michael Buckley<sup>1</sup>, Helmut Gese<sup>2</sup>, Matthias Reissner<sup>2</sup>, Gernot Oberhofer<sup>2</sup>

<sup>1</sup>Jaguar Land Rover Limited, Gaydon (GB)

<sup>2</sup>MATFEM Partnerschaft Dr. Gese & Oberhofer, Munich (D)

## 1 Introduction

There are many two-sheet and three-sheet material combinations in a body-in-white which can be joined via self-piercing rivets (SPR). A physical trial-and-error approach to ensure the feasibility of all combinations would be very time consuming and expensive. In addition the physical manufacturing test will not deliver the amount of accumulated damage in the sheets which is relevant for the strength of the SPR in a successive crashworthiness load case. An appropriate virtual simulation of the manufacturing process can be used to assess manufacturability and to evaluate the accumulated damage.

## 2 Simulation Approach

The use of 2d-rotational symmetric elements with r-adaptivity is the most effective way to simulate the riveting process. R-adaptivity is supported in the SMP version of LS-DYNA. The functionality of r-adaptivity in LS-DYNA includes a geometric criterion for the splitting of the upper sheet during the riveting process. The geometric criterion is defined by a residual thickness of the upper sheet controlling when elements are deleted for final sheet fracture. This approach might give acceptable results for very ductile sheet qualities (e.g. mild and high strength steels). However for aluminium sheets and AHSS grades the upper sheet may be split earlier due to limited ductility. Also there is a risk for fracture in the lower sheet which has to be estimated with an appropriate fracture model. In the case of riveting AHSS grades there is also a chance of a rivet fracture [1].

The focus of the development work in this paper was an improved prediction of material failure in this simulation environment. The user material MF GenYld+CrachFEM of MATFEM was used for this purpose. The available functionality of module CrachFEM for the prediction of material failure is summarized in [2]. The riveting of two aluminium sheets was used as an example (case 1 with alloy type ENAW6xxx-T4 and identical thickness, case 2 with alloy type ENAW5xxx and different thicknesses of upper and lower sheet).

## 3 Optimization of Numerical Parameters for R-adaptivity

In a first attempt the numerical parameters for r-adaptivity of 2d-rotational symmetric elements were optimized to ensure correct results (e.g. fulfill volume constancy of the sheets). For this study the basic material model `*Mat_024` without physically based failure criteria was used. First simulations with mesh size 0.1 mm in both sheets (sheet thickness 1.5 mm) and rivet and a small time step between adaptive meshing yielded unrealistic deformations in the sheets and rivet. Volume constancy of the sheet material was significantly violated. In some cases the simulations stopped due to high element distortion. The parameter study yielded the following outcome:

- shorter remesh time intervals show a positive effect on numerical stability of simulation
- shorter remesh time intervals show a negative effect on the volume constancy
- remeshing of the rivet (in addition to remeshing of the blanks) shows a negative effect on numerical stability of simulation
- Finer mesh sizes (0.05 mm instead of 0.1 mm) improve volume constancy
- different mesh sizes seem to require different remeshing time intervals
- A limiting equivalent plastic strain for element elimination is needed (suggested value 3.0) to avoid severe element distortion after fracture of the upper sheet

## 4 Application of Material Model MF GenYld+CrachFEM for Failure Prediction

In a second step the user material model MF GenYld+CrachFEM with failure criteria for ductile normal fracture (DNF) and ductile shear fracture (DSF) was introduced to allow for a damage accumulation in the sheet materials and the rivet material. Besides an improved prediction of the sheet failure of the upper sheet, the failure criteria also allow the user to estimate the margin of safety for a possible fracture of the rivet and of the lower sheet. The accumulated damage in sheets and rivet might be used later on for simulations of virtual mechanical tests on the riveted structure (e.g. to derive strength values for crashworthiness simulation).

Material model MF GenYld+CrachFEM is based on a tensorial description of damage [2]. This tensorial description provides more realistic fracture predictions in the case of nonlinear strain paths compared to a scalar description of damage. However the damage tensor must be expressed in a material coordinate system. An orthotropic mapping would be needed, if this tensorial description is used throughout an adaptive meshing process. This orthotropic mapping is supported in LS-DYNA for an adaptive meshing with shells (h-adaptivity) in deep drawing simulation, but is still not available for the r-adaptivity with 2d-rotational symmetric elements. Therefore the damage model in CrachFEM was reduced from a tensorial description to a simplified scalar description for the SPR application. For the process of riveting the assumption of linear strain paths might be still acceptable. However the use of the tensorial model would be favorable, if the process chain of riveting and crash load is to be simulated.

Predictions of force-deflection and cross section geometry after riveting were already in good agreement to the experiments with the standard material model `*Mat_024` and optimized numerical parameters for r-adaptivity. By the use of material model MF GenYld+CrachFEM the fracture of the upper sheet is predicted based on the ductility of the sheet material and no longer due to a simplified geometrical criterion. As a consequence the time of splitting and direction of splitting can be different. In addition a failure risk is predicted for both sheets and rivet material. As soon as element elimination is initiated in one of the sheets the crack propagation process is mesh size dependent (typically one element represents the crack tip zone). For the given mesh size of 0.05 mm the residual strength of the crack seems to be unrealistically low. The crack propagates too quickly. MF GenYld+CrachFEM offers the possibility to scale the fracture limit curves as a function of mesh size for crack propagation problems. However scaled curves will not give a correct value for the failure risk in regions of stable deformation. Therefore the fracture model should be combined with `*Mat_nonlocal` in the future to ensure a correct prediction of failure risk and crack propagation.

## 5 Summary and Discussion

The use of 2D-rotational symmetric elements with r-adaptivity is an effective way to simulate riveting processes in LS-DYNA. However the user should optimize discretization and numerical parameters to ensure robust results (e.g. avoid violation of volume constancy). The use of physically based fracture criteria is a step forward in the numerical assessment of the manufacturing process of self-piercing rivets. However crack propagation still suffers from mesh size dependency. A combination of the fracture model with `*Mat_nonlocal` might solve the problem in future.

## 6 Literature

- [1] Eckstein, J.: Numerische und experimentelle Erweiterung der Verfahrensgrenzen beim Halbhohlstanznieten hochfester Bleche; Dr.-Ing. Dissertation, Institut für Materialprüfung, Werkstoffkunde und Festigkeitslehre (IMWF), Universität Stuttgart und Materialprüfungsanstalt (MPA) Universität Stuttgart, 2009
- [2] Gese, H., Dell, H., Oberhofer, G., Oehm, M. and Heath, A.: CrachFEM – A Comprehensive Approach for the Prediction of Sheet Failure in Multi-Step Forming and Subsequent Forming and Crash Simulations, Proceedings of the forming Technology Forum 2013, September 19 – 20, 2013, utg, TUM, Germany

# Towards Location Specific Statistical Fracture Prediction in High Pressure Die Castings

R. Watson<sup>1</sup>, W.D.Griffiths<sup>1</sup>, T. Zeguer<sup>2</sup>, S. Ruffle<sup>3</sup>

<sup>1</sup>Univeristy of Birmingham

<sup>2</sup>Jaguar Land Rover Automotive PLC.

<sup>3</sup>JVM Castings Ltd.

## 1 Introduction

High Pressure Die Castings are widely used in the automotive industry, because they may be designed with relatively complex geometries, and produced in high volumes at low cost. However, they are often designed based on a conservative strength estimate, because the factors which influence their strength are difficult to account for. One of these factors is the unique distribution of entrainment defects within each casting.

The aim of this work is to summarise and demonstrate some recent developments that allow the effect of entrainment defects in cast aluminium parts to be better modelled. When this new understanding is formulated into a set of linked mathematical models, it can be applied to generate a map of the statistical strength distribution in a cast part, which is based on the distribution of entrainment defects that is predicted by a simulation of the casting process. This damage mapping model was calibrated to the failure statistics of 3 sets of test bars, each from 2 variants of a casting process. The model was then used to try to predict the strength distribution in those test bars, allowing the mapping methodology to be evaluated as a closed loop.

## 2 Background to Entrainment Defects

Since the first edition of Campbell's "*Castings*"[1], awareness has been growing within the aluminium industry of defects known as oxide bi-films. A bi-film defect forms a discontinuity in the metal, which may nucleate other forms of defect [2] as the casting solidifies, or simply form a site for crack initiation. Oxide bi-films are formed by the action of fluid surface turbulence mixing air with liquid metal, so it might be supposed that High-Pressure Die Castings would be extremely vulnerable to this kind of defect. However, during the fractography of High Pressure Die Cast samples, the author has observed very few defects typical of oxide bi-films. Instead, related defects were observed, which more closely resemble bubbles.

## 3 Method

### 3.1 Casting Simulation

Two variations on the casting process of a commercial High Pressure Die Cast part were simulated using the FLOW-3D, a commercial CFD package. An additional model to quantify the formation of entrainment defects was implemented as a user subroutine. This algorithm, called the Surface Area Entrainment Code, was described in a previous work by Watson et. al. [3], and uses a Lagrangian particle model for defect tracking. The algorithm has improved robustness over previous models, particularly for high velocity or non-intuitive flow patterns.

### 3.2 Statistical Mapping

New logical insights indicate that it may be valid, to some extent, to infer case to case variation at a specific location, from the geometric variation around that location in a single case. Building on this hypothesis, a random walk type algorithm was developed, which repeatedly samples the defect concentration in the vicinity of a starting location, and then fits a 3-parameter Fréchet distribution to those samples.

A simple program was used to calculate the centroids of selected elements from an LS-DYNA model of a tensile test bar, and transform these into the co-ordinate system of the casting simulation. This data was read into an in-house program to produce a statistics describing the probable damage distribution for each element in the test bar gauge lengths, using the above random walk algorithm.

A combination of response surface, numerical and analytical optimisation was used to find a set of mapping parameters which best fit the modelled damage statistics of the test bars to the equivalent failure statistics derived from tensile testing.

### 3.3 Damage Mapping and Verification

Once the optimum mapping parameters were found, these were used as inputs to a PRIMER script, which assigns a strength distribution to a set of \*PARTs within an LS-DYNA model.

Variation in strength is modelled by first sampling the statistical damage distribution corresponding to each element, and so calculating the strength value for each element. However, instead of assigning an individual strength value to each element, a binning algorithm is used to group elements with similar strengths together into a number of "bins"; in this exercise 50 bins were used for each test bar. New \*PART ids are then created corresponding to each bin, based on a master \*PART. A unique material id is also created for each new \*PART, so that its strength can be set to the average strength of the elements in each bin using the \*MAT\_ADD\_EROSION keyword. The elements grouped into each bin are then assigned the \*PART id corresponding to each bin.

Additionally, the script outputs a summary of the binning results, which was used to evaluate how effectively the algorithm reproduced the intended strength statistics.

LS-DYNA simulations of tensile tests were performed using the mapped test bars to complete the verification of the mapping method, and to qualitatively assess the features of the resulting fracture.

## 4 Results

The results showed that the statistical distribution of strength mapped into the test bar models was closely equivalent to the strength distribution derived from tensile testing, for all three test bar locations, in both casting process variants.

Additionally, the damage model used gives more realistic estimates for the strength of material that is *not* involved in fracture, compared to a simple extrapolation from tensile test data.

Compared with a tensile test simulation that assumes uniform material properties, the simulated fracture path of the stochastically mapped test bars more closely resembled experimentally observed fractures.

## 5 Summary

High pressure die casting is an economical means of producing a high volume of aluminium parts, with a design freedom that can enable lighter structures to be envisioned, compared with wrought assemblies. However, cast aluminium parts have been shown to be vulnerable to damage by defects caused by the entrainment of air during the casting process.

A recently developed entrainment prediction algorithm, which is believed to more quantitatively predict the distribution of entrainment defects within a casting, was used to predict the distribution of these defects for two variants of the casting process for a commercial part. Using a novel fuzzy statistical correlation method, the predicted distribution of entrainment damage was correlated with the statistical distribution of entrainment damage, as determined by tensile testing.

This work demonstrates a verification of the mapping methodology, in which the correlated strength distribution was mapped into LS-DYNA models of the test bars used for correlation. The results showed that the fuzzy statistical entrainment damage model can be tightly fitted to tensile test data, and that this fidelity can be reproduced in LS-DYNA simulations using the methods described, however further work is required to demonstrate the method's predictive capability.

## 6 Literature

- [1] Campbell, J: "Castings", issue 1, 1991
- [2] Campbell, J: "Complete Casting Handbook", issue 1, 2011
- [3] Watson, R; Zeguer, T; Ruffle, S; Griffiths, W.D: "Application of a Novel Entrainment Defect Model to a High Pressure Die Casting", Advanced Materials Research, THERMEC 2013 Supplement, pp. 801-806





**PROCESS VI**  
**DEEP DRAWING**



# Numerical Analysis of Multistep Ironing of Thin-Wall Aluminium Drawpiece

Artur Rękas<sup>1</sup>, Tomasz Latos<sup>1</sup>, Łukasz Brodawka<sup>2</sup>, Maciej Kociołek<sup>2</sup>, Michał Siedlik<sup>2</sup>, Robert Budzyn<sup>2</sup>, Andrzej Furman<sup>2</sup>

<sup>1</sup>AGH University of Science and Technology, <sup>2</sup>Can-Pack S.A.

## 1 Introduction

This paper focuses on the results of numerical simulation of gradually ironed side wall of a beverage can body. The analysis was made taking into account deformation that occurred in two previous stages: cup forming and cup redrawing. The ironing operation was divided into 3 separate stages which corresponds to the actual production process. In each stage, input material is a product obtained from the previous step. In order to verify obtained numerical results, simulated can body thicknesses were compared with the thickness of an actual product.

## 2 Ironing Process

The mechanism of a horizontal press is equipped with a punch (Punch Sleeve) and a special die (Punch Nose) which are mounted on the end of a ram. The Ram forces a cup to go through a redrawing ring followed by a set of rings which gradually decrease thickness of the wall and extend the height of the component.

## 3 Finite element simulation

The input drawpiece for the numerical simulation is geometry received in the previous two forming stages (Drawing on a Copper Press and Redrawing on a Horizontal Press) with full history of stress and strain. The thickness of the batch material was 0.250mm.

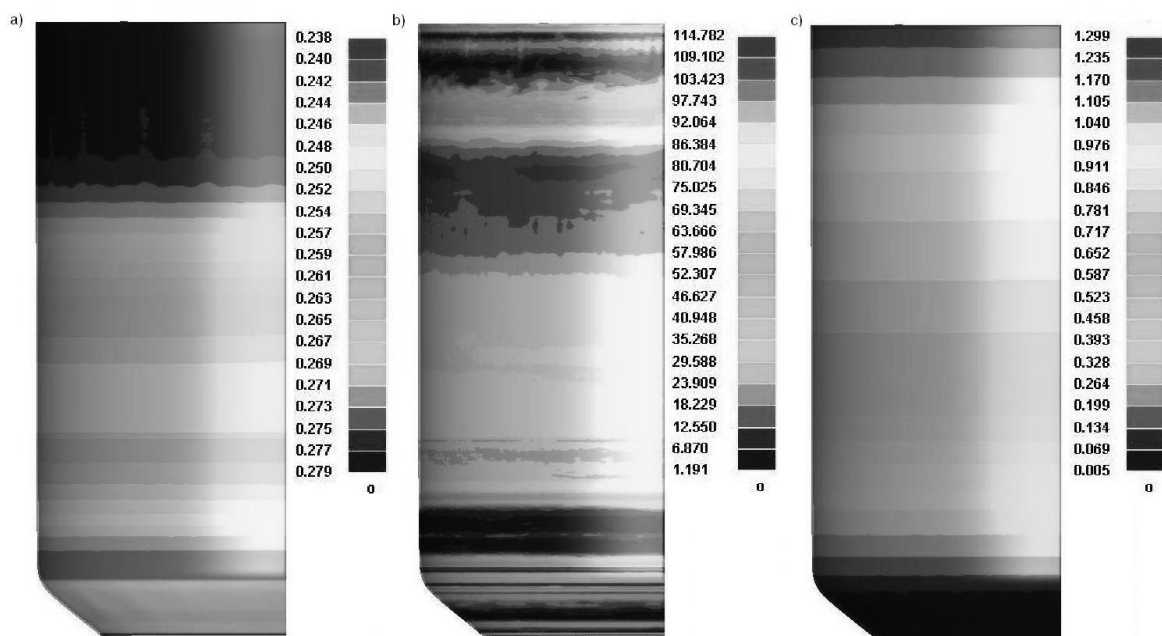


Fig.1: The input drawpiece determined to the ironing process: the average height 80.75mm, a) thickness distribution, b) max Von Mises stress, c) total strain

The part that was the subject of the research was divided into three separate stages in which 4 tools were used: one punch and three ironing dies. In each step material was ironed through one die. Small size of the blank and tools finite element mesh was applied to maintain high accuracy of the thickness

distribution results. All boundary conditions and process parameters were determined using the Autosetup module in Dynaform 5.9.1 Software.

## 4 Results

Results obtained after each of the ironing steps contain thickness distribution and total deformation. The main concern is focused on the final can body after the 3rd ironing.

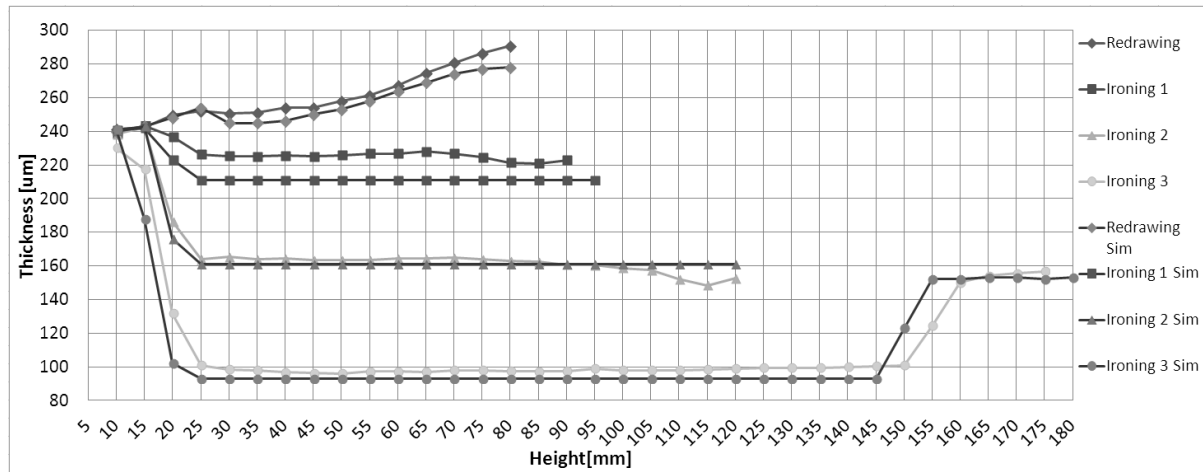


Fig.2: Thickness distribution as a function of can body height, after redrawing process and after each sidewall ironing compared with the results of numerical analysis (Sim)

## 5 Conclusion

Numerical thickness distribution along the can height is very comparable with produced can which indicates that simulation was carried out properly. In order to proper definition of the ironing simulation use of solid elements is preferable. Contact type **forming\_one\_way\_surface\_to\_surface** gives promising results but only with constrained method (SOFT=4). The simulation results show a perfectly homogeneous side wall which is a result of perfectly aligned tools, their ideal working surface and the use of isotropic material instead of anisotropic one. Properly set numerical simulation is able to provide input data (geometry, stress and strain history) for subsequent can body forming processes, i.e. trimming, dome forming or thick wall necking.

## 6 Literature

- [1] Jordan-Cordera, A., Miranda-Valenzuela, J.C.: "Simulation and Analysis of the Beverage Can Necking Process Using LS-DYNA", 8th International LS-DYNA Users Conference (2004), Session 9 - Metal Forming Technology.
- [2] Dick R.E., Yoon J.W.: "Effect of Material Characteristics on Wrinkling During Dome Forming of a Beverage Can using LS-DYNA", 10th International LS-DYNA Users Conference (2008), Session 17 – Metal Forming.
- [3] Dick R.E.: "Improvements to the beverage can redraw process using LSDYNA", 7th International LS-DYNA Users Conference (2002), Session 15 – Metal Forming Technology.
- [4] Danckert j.: "LS-DYNA used to analyze the manufacturing of thin walled cans", 6th European LS-DYNA Users' Conference (2007),
- [5] Kang K.: "Impact of die wear and punch surface textures on aluminium can Wall", An International Journal on the Science and Technology of Friction, Lubrication and Wear, Wear 266 (2009) 1044–1049.
- [6] Wootton E., "Case Study on Can Making" Training in Aluminium Application Technologies, European Aluminium Association, Information on <http://www.alueurope.eu/talat/lectures/3710.pdf>
- [7] Rekas A., Latos T., Budzyn R., Furman A., Siedlik M.: "The Analysis of Mechanical Properties of 3XXX series Aluminium Sheets Used for Beverage Can Production", Key Engineering Materials, Vol 641, Apr. 2015, pp. 246-256

# Numerical Analysis of Relationship between Height and Geometry of Bottom of a Beverage Can and its Resistance to Increase in Internal Pressure

Artur Rękas<sup>1</sup>, Tomasz Latos<sup>1</sup>, Łukasz Brodawka<sup>2</sup>, Maciej Kociołek<sup>2</sup>, Michał Siedlik<sup>2</sup>,  
Robert Budzyn<sup>2</sup>, Marcin Fijałkowski<sup>2</sup>

<sup>1</sup>AGH University of Science and Technology

<sup>2</sup>Can-Pack S.A.

## 1 Introduction

This work presents results obtained from numerical analysis of dome reversal pressure test with use of finite element mesh. Dome reversal pressure test is one of crucial quality tests required of such products as beverage cans. The material used in the analysis was 3104 aluminum work hardened to H19 temper. The comparison was conducted on 2 thicknesses of input stripes: 0.250 and 0.241. The module used in the analysis included a full history of deformation that resulted from preceding simulations of drawing and redrawing. In this study, it is focused on the numerical analysis the influence of height and geometry on the bottom of beverage cans for bottom reversal pressure test.

## 2 Dome Forming - Finite Element Analysis

Raw material for the pressure testing, as already mentioned, is formed redraw cup with the bottom and an additional reforming operation. To prepare such a bottom before they had to be properly modeled. It was used the basic operations of drawing a cup from a flat sheet, redrawing and forming the bottom. Additional reforming operation is achieved by performing roll doing rotary motion and forming the reversal wall. In numerical analysis it was obtained the dome profiles shown below.

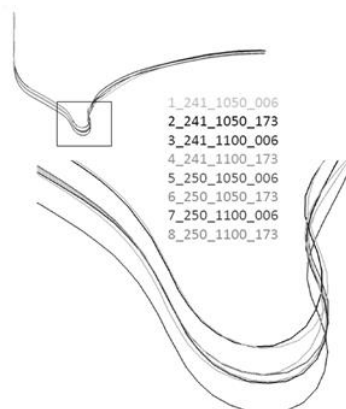


Fig.1: Geometry of dome profiles

## 3 Dome Reversal Pressure – Finite Element Analysis

Formed dome from the eta/Dynaform analysis containing the full story stresses and deformations and change the material properties were then used for analysis in the pressure test. These analyzes were performed in a special module prepared for testing in an LS-DYNA. Pressure test involves loading an empty cans, dispensed pressure inside it. The test is considered completed when dome is reversed of the can outside.

## 4 Results

As a result of numerical analysis it was given the dome of the shapes (Fig. 1) and results of the dome reversal results test as in the following graph.

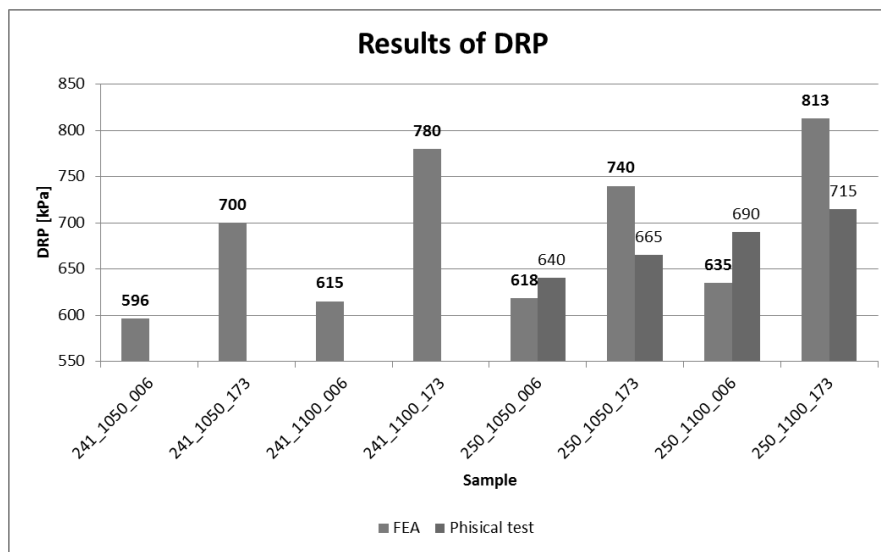


Fig.2: Results of FEA and physical test of DRP

## 5 Conclusions

The results of numerical analysis in the confrontation with the real tests give promising results. The next step in the analysis of numerical modeling of the pressure test is a model for the optimization convergence results from physical testing and time optimization calculations. However, in the case of bottoms, further action will focus on a wider range of depth and analyzed the subsequent attempts to analyze the changing parameters such as forming speed of punch and coefficient of friction.

## 6 References

- [1] Dick R.E.: "Improvements to the beverage can redraw process using LSDYNA", 7th International LS-DYNA Users Conference (2002), Session 15 – Metal Forming Technology.
- [2] Danckert J.: "LS-DYNA used to analyze the manufacturing of thin walled cans", 6th European LS-DYNA Users' Conference (2007).
- [3] Dick R.E., Yoon J.W.: "Effect of Material Characteristics on Wrinkling During Dome Forming of a Beverage Can using LS-DYNA", 10th International LS-DYNA Users Conference (2008), Session 17 – Metal Forming.
- [4] Jordan-Cordera A., Miranda-Valenzuela J.C: " Simulation and Analysis of Beverage Can Necking Process Using LS-DYNA", 8th International LS-DYNA Users Conference (2004), Session 9 – Metal Forming Technology.
- [5] Bielenberg R.W., Magner S.H., Reid J.H.: "Sidewall Indentation and Buckling of Deformed Aluminum Beverage Cans", 6th International LS-DYNA Users Conference (2000), Session 10 – Impact 2.
- [6] Conn B.A., Anugonda P., Reid J.D.: "Piercing of Aluminum Beverage Cans", 6th International LS-DYNA Users Conference (2000), Session 10 – Impact 2.
- [7] Utsunomiya H., Nishimura H.: "Effect of base profile of a DI beverage can and material properties on the dome reversal pressure", Journal of materials processing technology, Vol 97 (2000), pp. 54-60.
- [8] Rękas A., Latos T., Budzyn R., Fijałkowski M., Brodawka Ł.: "The analysis of influence of sheet properties on the ironing process of thin-walled cylindrical shell products from aluminum alloys", Key Engineering Materials, Vol 641, April 2015, pp. 232-245.

# Optimisation of the Blank Holder Stiffness in Deep Drawing Processes by using FEA

Ranko Radonjic<sup>1a</sup>, Mathias Liewald<sup>1b</sup>, Fei Han<sup>1c</sup>

<sup>1</sup>University of Stuttgart, Institute for Metal Forming Technology

Current requirements for vehicle safety and weight reduction in automotive industry lead to the increased use of high strength steels (HSS). Usually, these materials are used for manufacturing of car body components which are placed in many areas within the car body structure. They have a lower drawability, while spring back amount after deep drawing process is tremendously higher compared to mild steels. Also they have a bigger tendency to wrinkle due to lack of adequate capacity of blank holder and often a reduction in sheet metal thickness.

When deep drawing sheet metal components having complex geometries, varying thicknesses of materials occur in the flange area. Extreme thickening of the part flange will cause pressure peaks and therefore increased restraining forces being applied onto the contact surface between blank holder and part occur. This undesired effect during deep drawing will reduce process window and process robustness as well.

In this paper, a new approach is presented to optimise the blank holder stiffness in deep drawing process. In this case the blank holder consists of one cover plate which is supported by numerous appropriate elastic elements made of cast iron. Stiffness of the blank holder as well as pressure distribution during deep drawing was optimised by varying elasticity and order of the supporting elements in real trials. For this purpose simulation and experimental investigation of car fender geometry were performed.

First, the deep drawing simulation was carried out using a rigid tool (punch, die and blank holder). Simulation results showed that the first wrinkle is initiated in a very early stage of the deep drawing process (at the drawing depth of 17 mm). By further optimising of the blank holder force it was possible to decrease the wrinkle height. The achievable part height without occurring cracks was 60 mm in this case.

Afterwards, the finite element simulation with an elastic blank holder was carried out considering the requirements for part surface quality (wrinkles, cracks, etc.). In this case blank holder plate and corresponding supporting elements were meshed with solid elements and considered as elastic bodies in FEA. One elastic material model \*MAT\_ELASTIC was assigned to the mentioned tool parts. Deep drawing was simulated systematically with different FE-Models using LS-Dyna software code. Obtained simulation results showed that the blank holder stiffness has an influence on material draw-in as well as on stress-strain distribution in the part during the deep drawing process. Compressive stresses which occurred in critical areas of the part regarding the development of wrinkles were analysed considering new wrinkling criterion which is developed at the Institute for Metal Forming Technology (IFU) Stuttgart. For optimised blank holder stiffness, the compressive stress achieves its maximum values at the drawing depth of 44 mm. After achieving maximal value, it changes its value cyclically, but does not diminish entirely. Due to this result it is assumed that the wrinkling was initiated (at the drawing depth of 44 mm), but it was not formed in regard to unstable changes of compressive stress. Also, achievable drawing depth without having development of cracks considering a satisfying part shape quality was 70 mm in this case.

In order to experimentally determine wrinkle height after deep drawing process, part shape deviations were measured by 3D scanner, and they were compared with the reference geometry. Simulation results were compared to measurements obtained during the experiment, and they were in good accordance with each other. Simulation and experimental results showed that the wrinkles of second order as well as crack tendency in deep drawing process can be significantly reduced with optimised blank holder stiffness for die assembly. Due to that, the process window for such deep drawing process was enlarged. When using load optimised blank holder the wrinkle initiation process will start later. This phenomenon will result in improving the part shape quality.





## **PROCESS VII**

### **WELDING**



# SimWeld and DynaWeld

## Software Tools to Setup Simulation Models for the Analysis of Welded Structures with LS-DYNA

Tobias Loose<sup>1</sup>, Oleg Mokrov<sup>2</sup>

<sup>1</sup>Ingenieurbüro Tobias Loose, Germany

<sup>2</sup>Institut für Schweißtechnik und Fügetechnik der RWTH Aachen (ISF), Germany

### 1 Motivation

The analysis of residual stresses or distortion of welded structures requires a welding structure analysis. This kind of analysis incorporates some specifics compared to other FEM-simulations. Apart from the definition of geometry (mesh) and clamps, the welding structure analysis requires the definition of heat sources, trajectories and time schedules. The heat source applies the heat in the model according to the welding process. An equivalent heat source is used which needs to be calibrated for tests or predictively calculated from a welding process analysis. The trajectories describe the path of the moving welding heat source in the simulation model. most welding heat sources are not rotational symmetric. Their trajectories require a path to define the local origin of the heat sources and a reference line to define the orientation of the heat source. Welding is a transient process where the time schedule of the actions - welding time, intermediate time - have an impact on the result. The process plan defines the welding time schedule and has to be considered in the simulation model.

The setup of simple models with single welds is easy and can be performed by writing the input deck with text editors. More interesting are assemblies with many weld seams. The setup of these models requires auxiliary tools (setup 2x im satz=>redundant) in order to decrease the work time and to minimize the risk of errors in the input deck.

### 2 SimWeld

SimWeld, a software for the simulation of gas metal arc welding has been developed continuously in research and industry projects since over 25 years. SimWeld is highly specified to its application, thus the simulation time of less than 1 minute is extremely short. The welding engineer can predict the weld pool geometry and its quality according to the process parameters and machine settings. The predictive calculation of the heat input can be performed with every SimWeld (Fig.1) simulation and can be used for the welding structure analysis.

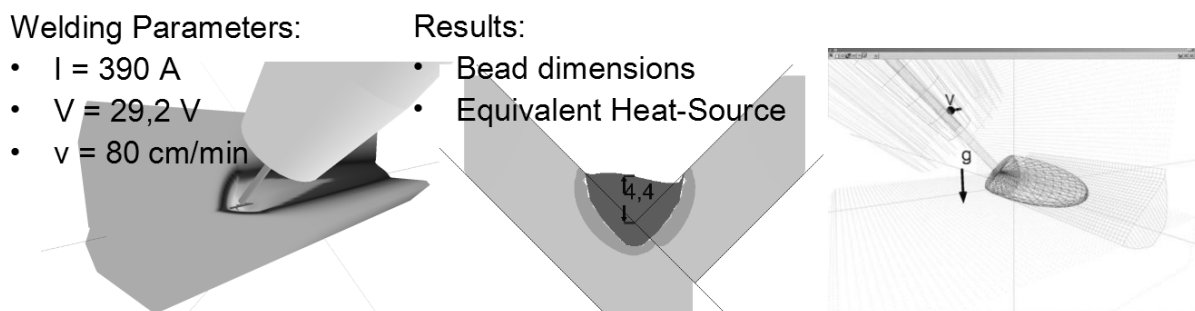


Fig.1: SimWeld Simulation

An interface exports the parameter of the equivalent heat source either in general format or in LS-DYNA Keyword format. Thus SimWeld resolves the issue of a calibrated heat input for the welding structure analysis. This benefit has a big impact on the design state. Apart from the manufacturing, SimWeld enables the design engineer to calculate realistic conditions for the weld and use these data in numerical analyses.

### 3 DynaWeld

The DynaWeld project was established at the engineering office Tobias Loose in 2015. DynaWeld concentrates software modules for an efficient setup of input decks for the LS-DYNA solver and associated auxiliary tools. DynaWeld is intended for welding and heat treatment processes. The philosophy is to provide a general tool as well as special versions adapted to the customers' needs.

The Process Plan collects all relevant information and data for the simulation. In case of a welding structure analysis the main information consist of the welding tasks, its time schedule and their heat source parameter. Additionally, the part definition with material assignment, boundary condition(s), contact and general parameter are defined (Fig.2 left).

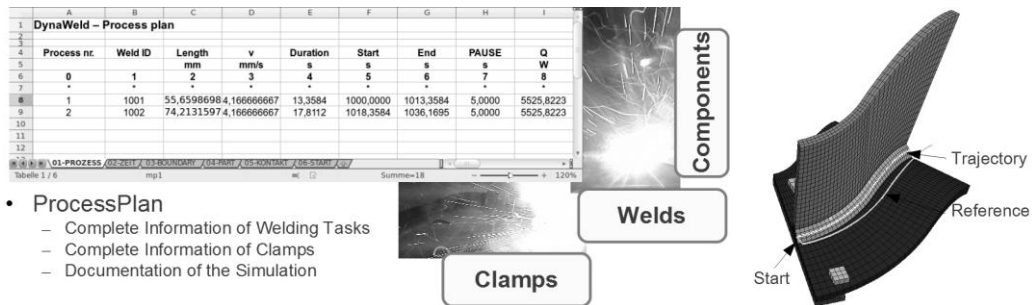


Fig.2: Left: Process Plan

Right: Curved Weld Trajectories

Special functions provide the treatment of the trajectories for the welds in a manner that only initial sets of nodes have to be defined previously in LSPrePost or any meshing software. Thus DyaWeld enabelns a quick and easy definition of curved trajectories as shown in Fig 3 right.

Finally, the DynaWeld welding input-writer reads the welding process plan and generates the LS-DYNA input for a welding structure analysis (Fig. 4).

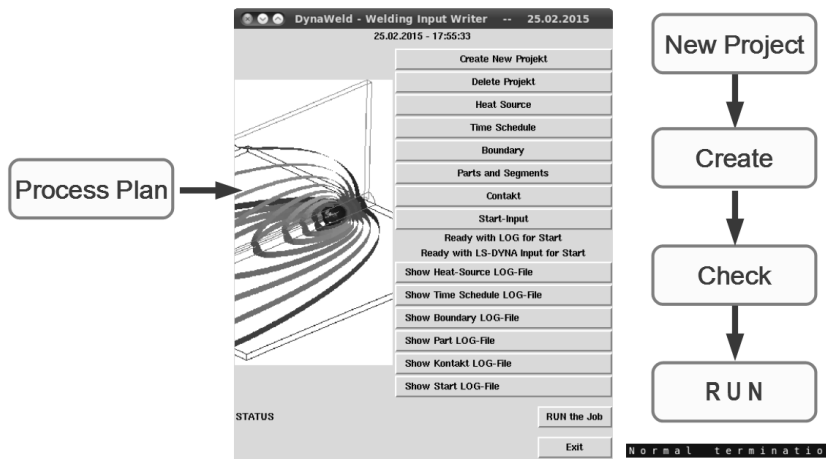


Fig.3: DynaWeld Input Writer

SimWeld and DynaWeld do not require a change of existing pre- or postprocessor but can be supplemented to any existing software in the simulation or design departments.

This paper demonstrates the workflow of an efficient setup of welding structure analysis with LS-DYNA using SimWeld and DynaWeld, especially for assemblies with a large number of weld seams.

# A Finite Element Investigation into the Continuous Induction Welding of Dissimilar Material Joints

Miro Duhovic<sup>1</sup>, Joachim Hausmann<sup>1</sup>, Pierre L'Eplattenier<sup>2</sup>, Inaki Caldichoury<sup>2</sup>

<sup>1</sup>Institut für Verbundwerkstoffe GmbH, Germany

<sup>2</sup>Livermore Software Technology Corporation, USA

Continuous induction welding is an advanced material processing method with a very high potential of providing a flexible, fast and energy efficient means of joining together thermoplastic composites to themselves and metals and alloys. However, selection of the processing parameters and optimization of the process is very difficult as it involves the interaction of up to four different types of physics. In addition, many different material combinations including materials with low or high electrical conductivity, thermal conductivity and heat capacity, make the intuitive selection of processing parameters impossible. In this work, a simulation test-bed, setup for the continuous induction welding of two material partners and their corresponding physics interactions is used to investigate the induction welding possibilities for several combinations of hybrid material joints. The materials include 2mm thick plates of structural grade aluminium (Al) and steel (St) along with polyamide 6 (PA 6) thermoplastic prepregs containing either glass (GF/PA 6) or carbon fiber (CF/PA 6) reinforcements. In total, six different material combinations are considered (Al-GF/PA 6, Al-CF/PA 6, St-GF/PA 6, St-CF/PA 6, CF/PA 6-GF/PA 6 and CF/PA 6-CF/PA 6) along with their appropriate weld orientation (i.e. on which side of the material stack the coil should face). A target welding temperature of 250°C is taken for all material combinations as each combination contains the common PA 6 polymer based partner. Surface temperature plots of the developed temperature profile at the coil side surface and welding interface are generated and examined using node selections across the width of the lap-joint at a location where steady state heating has been achieved. Finally, the setup for an ON/OFF switch and proportional-integral-derivative (PID) type process controller is described and initially tested.

All of the necessary features and physics of the continuous induction welding process have been captured in the developed simulation test-bed as shown in Figure 1.

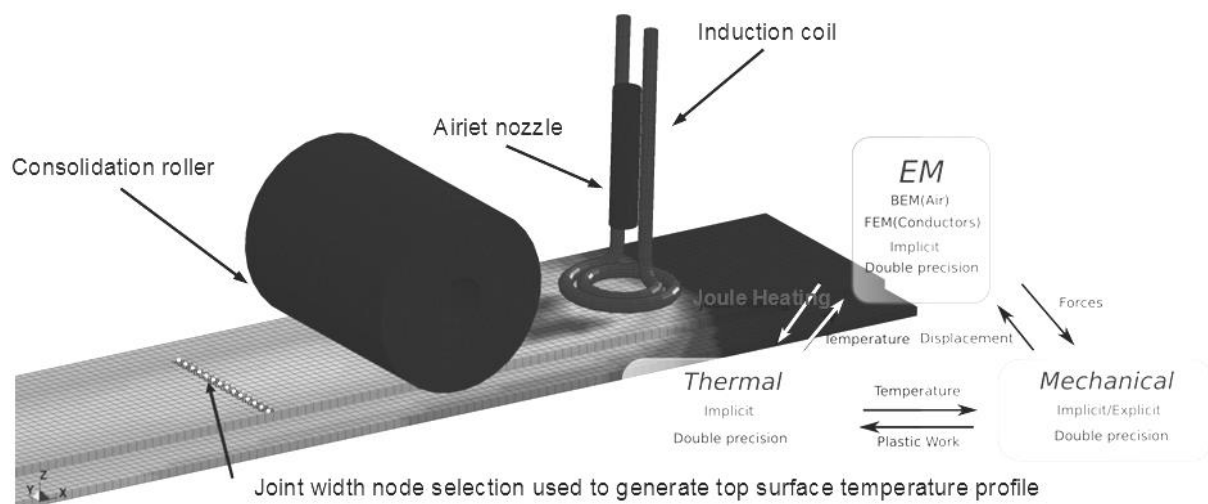


Fig.1: Simulation test-bed setup for the continuous induction welding of two material partners and their corresponding physics interactions developed at the Institut für Verbundwerkstoffe, GmbH together with LSTC.

The simulation test-bed sets the stage for more complex finite element investigations using moving coil cases where the steady state induction heating temperature patterns become different to that of the static case and are far more difficult to predict and measure. Using this process simulation tool, the effects of the consolidation roller as well as an impinging air jet on the temperature developed on the top surface of the laminate stack, and more importantly the joint interface, can be investigated in full

detail. Simulations can be carried out to gain a better understanding of the process and how to go about optimizing it for dissimilar material combinations.

Some initial results of the test-bed used to simulate the dissimilar material joints firstly without any control system and then using a PID implementation are presented here. All simulations have been performed using a welding speed of 3 mm/sec and have a coupling distance to the coil side plate (even when this is not electrically conductive, e.g. GF/ PA 6) of 2mm.

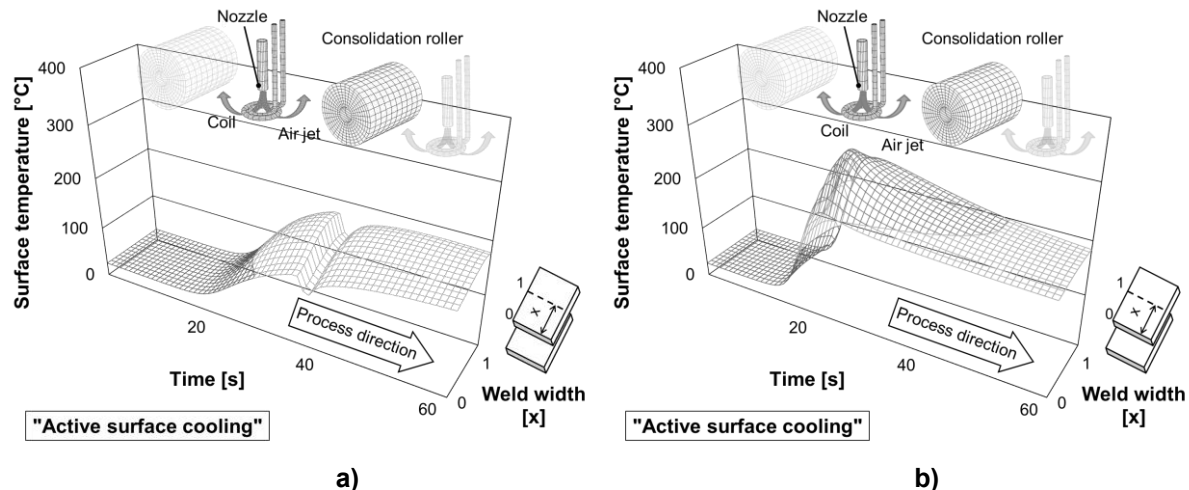


Fig.2: Surface temperature plots GF/ST (270A) for a welding speed 3 mm/sec, fixed coil coupling distance 2 mm and coil to roller offset distance 60 mm; a) top surface and b) joint interface with coil side surface air-jet cooling.

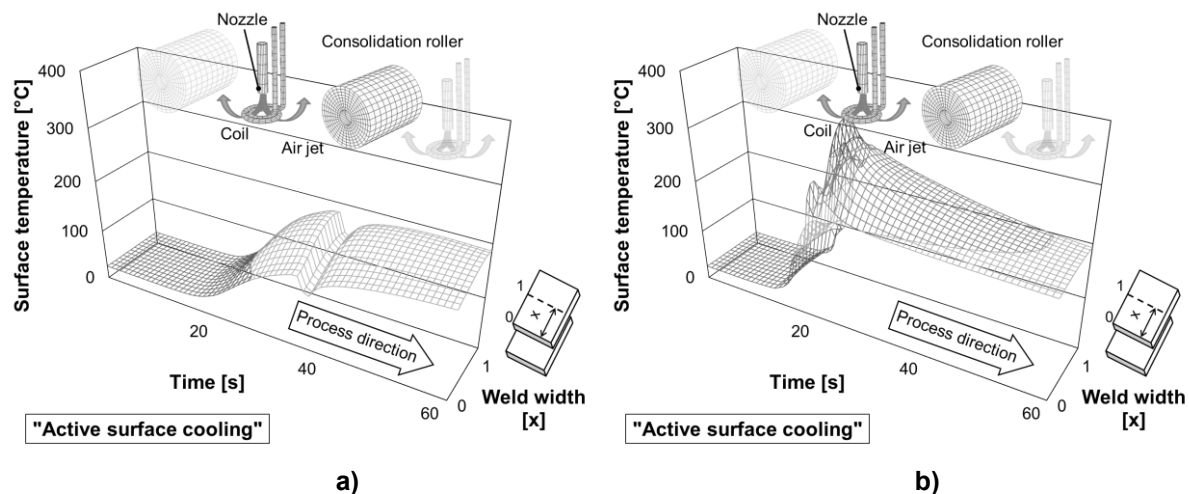


Fig.3: Surface temperature plots GF/ST (PID Control with 300°C as set point) for a welding speed 3 mm/sec, fixed coil coupling distance 2 mm and coil to roller offset distance 60 mm; a) top surface and b) joint interface with coil side surface air-jet cooling.

Figures 2 and 3 both show the case of a non-conductive thermoplastic organosheet material induction welded to steel (GF/ST). An air jet cools the top surface of the organosheet. With no control system and a fixed coil current of 270A, a relatively uniform temperature distribution compared to the case where PID control is used can be seen. In this case, the PID controller seems to fluctuate between the "umin" and "umax" parameters defined in the controller function in order to achieve the desired maximum temperature set point of 300°C. Further work in tuning the PID controller parameters for the test-bed model is required with the aim of obtaining a smooth rise to the desired set point temperature by manipulating the coil current.

# Simulating the Induction Spot Welding of Hybrid Material Joints

Mirja Didi, David Wind, Miro Duhovic, Joachim Hausmann

Institut für Verbundwerkstoffe GmbH, Germany

Spot welding is a very common process used to join sheet metal components in the automotive industry mass production environment. Recently, thermoplastic composites as lightweight alternatives to metals have begun to make their way into production. The induction spot welding of hybrid materials, in particular aluminum or steel to thermoplastic based composite materials, is one promising method to create the required connections between these dissimilar materials and maintain productivity. As opposed to continuous welding, the spot welding of two materials with different thermal properties can help prevent heat distortion and internal stresses in parts. To improve on the design of the process a deep understanding of the interacting physics of an induction spot welding head is required. A hybrid material spot welding head consists of a stamp, an integrated induction coil and cooling channels. During the process the metal (aluminum) joining partner on the top surface and the fiber reinforced thermoplastic (CF-PA66) on the bottom are fusion bonded to one another via induction heating and pressure. The novel idea of locally concentrating pressure in the fusion zone through a preformed dimple in the metallic joining partner, in order to prevent deconsolidation during induction heating in the thermoplastic adherend, led to noticeably improved joints.

In order to gain a better understanding of this method, the effects of different dimple geometries in the aluminum sheet were reviewed in a simulation utilizing the LS-DYNA® EM Solver. The model considers the mechanical deformation of both metal and composite, the initial micro stresses in the aluminum adherend, thermal convection and radiation, in addition to the electrical conductivity and contact of both joining partners. The model is then used to investigate the temperature, pressure and stresses at the location of the spot weld in order to assess whether an adequate bond has been achieved.

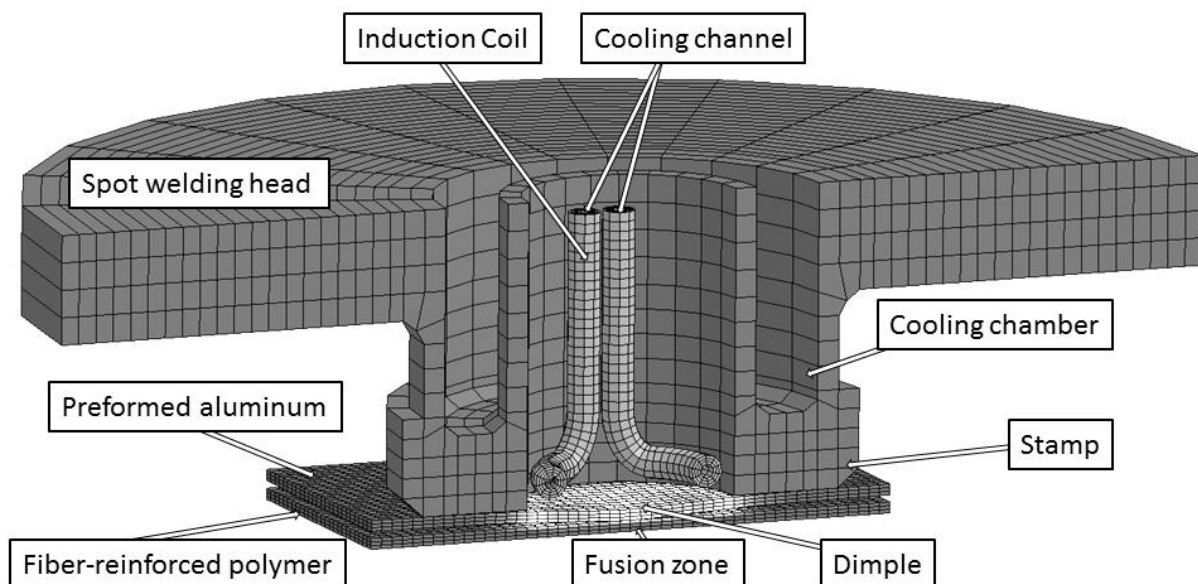


Fig.1: Section view of simulation test-bed setup for the induction spot welding method of two dissimilar material partners and their corresponding physics interactions.

An important aspect of the process is to be able to predict and visualize the temperature distribution within the defined welding area. Figure 2 shows the temperature development after A=5, B=20 and C=70 seconds heating time and demonstrates that the developed welding head can provide a homogeneous melting temperature over the desired spot weld area.

### Temperature distribution in the weld interface at times A, B & C

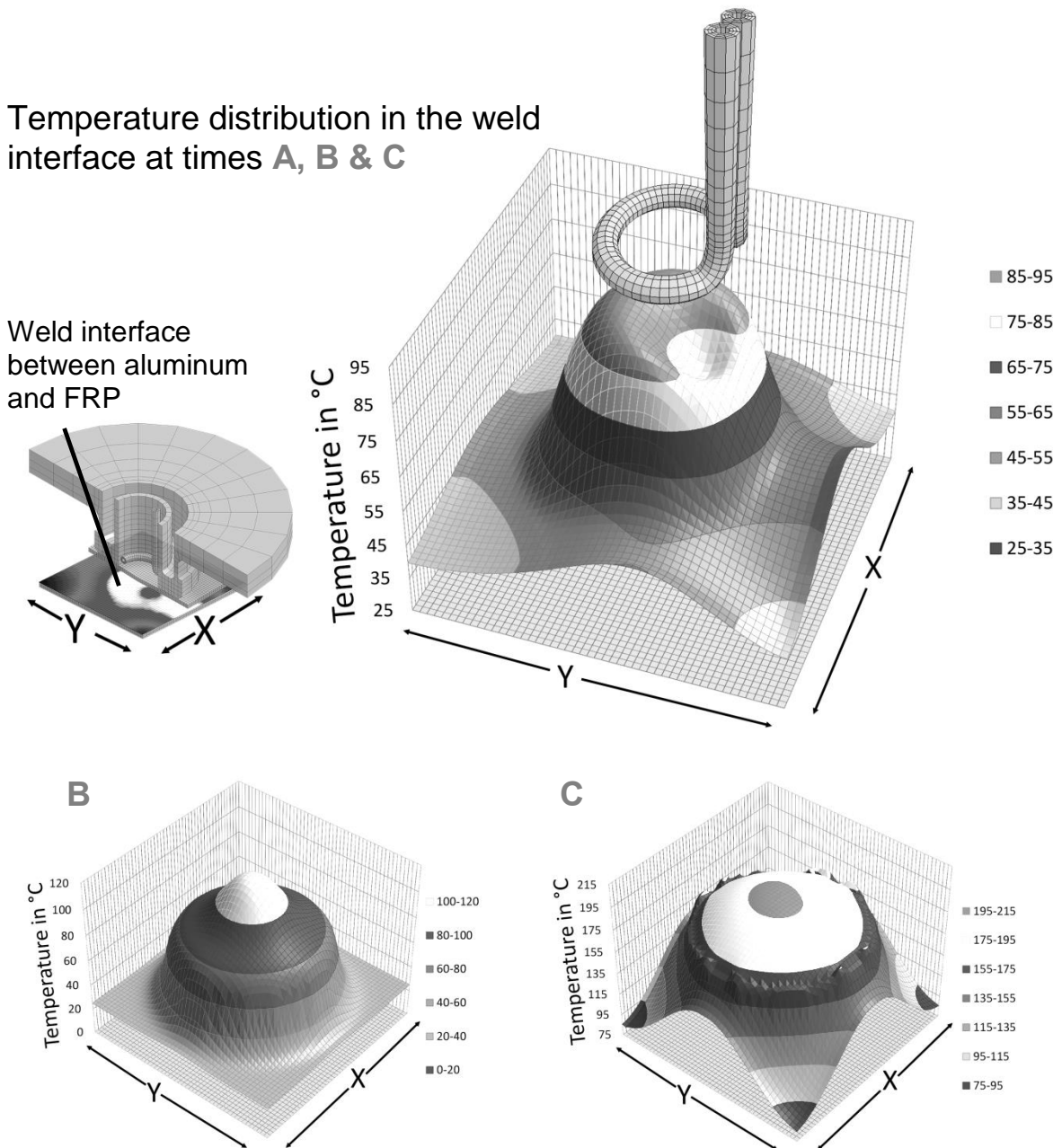


Fig.2: Thermal contour plots at process stages A (5sec), B (20sec) and C (70sec) for the case of a 1 mm thick aluminum plate and 1 mm deep dimple geometry.

Due to the general complexity of the induction spot welding process and its myriad of parameters, the employment of an advanced multi-physics finite element model to further assist the experimental investigations, was necessary. The LS-DYNA® R8 solver has proven to be capable of such complex coupled multi physics simulations enabling the evaluation of different plate and dimple geometries on the induction spot welding of AlMg3 to CF/PA66. It has been shown via simulation, that dimples in the aluminum plate provide significant advantages in terms of heating in addition to assisting the consolidation during the spot welding procedure. The numerical simulations have delivered crucial insights into the complex procedures which would otherwise, in an experimental only setup, require heavy costs and time consuming efforts.



## **PROCESS VIII**

### **WELDING**



# Numerical Simulation of Impact Welding Processes with LS-DYNA

Peter Groche<sup>1</sup>, Christian Pabst<sup>1</sup>

<sup>1</sup>Institute for Production Engineering and Forming Machines, Technische Universität Darmstadt

## 1 Abstract

Impact welding enables metallurgical bonding even between dissimilar metals. The bond is formed during a high speed impact between the two workpieces to be joined under accurately defined conditions. In the application, the accelerating force is provided by an explosive (explosion welding, EXW) or by an electromagnetic field (electromagnetic pulse welding, EMPW). One workpiece is usually accelerated within a few millimeters up to 200 m/s and above. The impact and consequently the bond formation takes place in only a few microseconds which makes it hard to observe. The numerical simulation with LS-DYNA is used to gain detailed insights into the process. Three phenomena, which are thought to have a significant effect on the bond formation, are currently investigated numerically: The supersonic displacement of the surrounding gaseous medium, the strains and strain rates at the bonding zone and the macroscopic flow of material. The results of the numerical simulations are compared to experimental and metallographic investigations.

## 2 Impact welding: theory of the bond formation

Impact welding is thought to be a cold joining process which does not produce any heat in the parts to be joined [1]. However, studies from the recent years have shown that the joint area always exhibits a very thin interlayer. In case of similar metals it consists of ultra fine grains [2], in case of dissimilar metals intermetallic phases can be found [2,3,4]. The thickness of this interlayer is very small, thus its negative influence on the joint strength is usually negligible. Based on these findings, the authors have developed a new hypothesis. It implies that the interlayer is caused by a quick melting and solidification process [5]. During the impact and during the closing of the gap between the workpieces, the surrounding gas is ejected from the gap at supersonic speeds. The fast compression could lead to a rapid increase in temperature which could be sufficient to melt a thin superficial layer of the workpieces, creating a thin fusion weld. An analytical estimation of the temperatures for different gases in [6] shows that the temperature reaches from about 900 K to several thousand Kelvin.

## 3 Electromagnetic pulse welding: experiments and numerical simulation

The welding trials are carried out using a standard sheet metal welding tool coil and a pulse generator from PSTproducts. The pulse generator has a maximum energy of 32 kJ at a charging voltage of 16 kV. The oscillating circuit consisting of coil and pulse generator (i.e. cables and capacitors) has a natural frequency of 20 kHz. The current versus time measured in the experiment is used one-to-one for the simulation. The peak current of the first half wave is 300 kA. A simple standard sheet metal welding geometry is used for the experiments, which is shown in figure 1. The sheets are made of EN AW1050A and have a thickness of 2 mm. They have a size of 50 x 50 mm and the initial distance between them is 2 mm. The coil is separated from the target sheet by a thin insulating layer (0.7 mm). The target sheet is supported by a block of steel to prevent it from moving by the impulse from the impact. The photograph of a welded specimen is depicted in figure 1 as well.

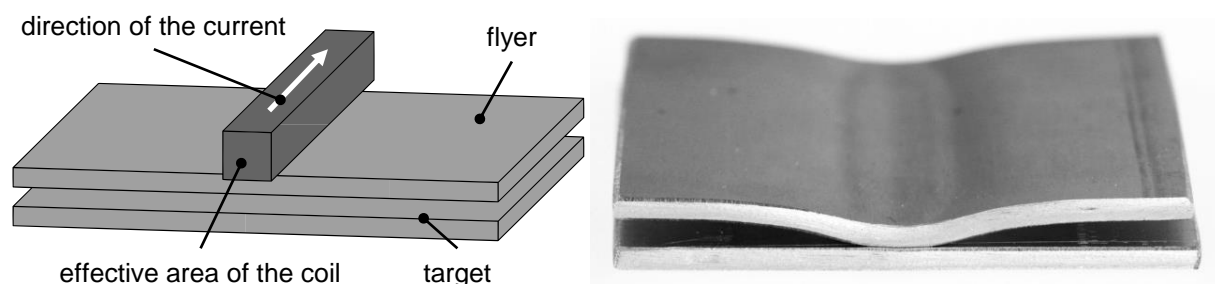


Fig. 1: A simple setup for electromagnetic pulse welding (left) and photo of a joined specimen (right).

It can be seen that only the central part below the coil has been moved. Due to the high acceleration, the mass alone is sufficient to keep the surrounding material in place.

No detailed high speed images exist from the impact so far to verify the simulation. Thus the only currently feasible method to compare simulation and experiment is the geometry after the impact. The comparison depicted in figure 2 shows that the numerical result is at first glance in satisfactory accordance with the experimental deformation. However, major deviations can be identified which lead to the conclusion that the numerical material model seems to be too soft. One possible reason is that the effect of strain rate hardening is not taken sufficiently into account. Similar phenomena have been observed in [7]. The given parameters for the Johnson-Cook model, which is utilized for the numerical simulations of this publication, are only valid for strain rates up to  $10^3$  1/s. However, during the acceleration, the flyer sheet experiences strain rates of more than  $5 \cdot 10^4$  1/s.



Fig.2: Comparison between the cross-sections of the numerical result (grey) and the experimental result (black).

For a rough estimate, parameter C is increased from 0.0125 (taken from [7]) to 0.05. Figure 3 shows the result. Using the intersection of the two cross sections as quality criterion, the accuracy of the numerical simulation increased by more than 75%. Thus it can be concluded that the strain rate sensitivity is an important issue for material modelling in impact welding.



Fig.3: Comparison between the cross-sections of the numerical result with increased strain rate sensitivity (grey) and the experimental result (black).

#### 4 Summary

Impact welding is a very promising process, especially if dissimilar metals have to be joined metallurgically. Explosion welding and electromagnetic pulse welding are already in use, but the principles of the joint formation are not completely understood. Welding experiments and numerical simulations can help identifying the macroscopic mechanisms (flow of material) and the microscopic mechanisms (local melting due to compressed and heated gases).

#### 5 Literature

- [1] Shribman, V.: "Magnetic Pulse Welding for Dissimilar and Similar Materials", 3<sup>rd</sup> International Conference on High Speed Forming, 2008
- [3] Geyer, M.; Böhm, S.: "Influence of contact surface on weldability with electromagnetic pulses", IIW Denver Annual Assembly, 2012
- [2] Stern, A.; Shribman, V.; Ben-Artzy, A.; Aizenshtein, M.: "Interface Phenomena and Bonding Mechanism in Magnetic Pulse Welding", Journal of Materials Engineering and Performance 23, 2014, pp. 3449-3458
- [4] Song, J.; Kostka, A.; Veehmayer, M.; Raabe, D.: "Hierarchical microstructure of explosive joints: Example of titanium to steel cladding", Materials Science and Engineering A 528, 2011, pp. 2641-2647
- [5] Pabst, C.; Groche, P.: "Electromagnetic Pulse Welding: Process Insights by High Speed Imaging and Numerical Simulation", 6<sup>th</sup> International Conference on High Speed Forming, 2014
- [6] Koschlig, M.; Veehmayer, M.; Raabe, D.: "Production of Steel-Light Metal Compounds with Explosive Metal Cladding", 3<sup>rd</sup> International Conference on High Speed Forming, 2008
- [7] Li, J.; Gao, H.; Cheng, G.J.: "Forming Limit and Fracture Mode of Microscale Laser Dynamic Forming", Journal of Manufacturing Science and Engineering 12, 2010

# Evaluation of Electromagnetism Capabilities of LS-DYNA: Alternative Heating Processes

Edith Grippon<sup>1</sup>, Timothy Senart, Vincent Lapoujade<sup>1</sup>,

<sup>1</sup>DynaS+, France

## 1 Abstract

The main subject presented in the paper is a way to reduce the heating time and to offer more flexibility when increasing the temperature of the automotive steel blanks, based on Joule effect heating. Two techniques will be explained, inductive and resistive heating, focusing on numerical aspect in order to help manufacturers to reduce the time of setting up such processes. Models using Lagrangian, Thermal and EM solvers will be presented with a comparison to experimental data.

## 2 Introduction

Whatever the intended applications, hot forming processes require preheating. The controlled deformability of hot steel allows to establish complex part geometries without adding reinforcement, welding or assembly point. However, two issues arise from this type of methodology: the significant heating time and the wear of the shaping tools.

To reduce the energy resources necessary for the heaters and implementation time, large steel companies are investigating alternative heating techniques. One of them, proposed by ArcelorMittal Global R&D Montataire, is the use of electrical power to create a magnetic field that will heat conductive parts by induced current. The optimization of this method requires numerical and experimental studies. Indeed, the integration of digital simulation upstream of the design process helps limits the loss of raw material and energy. It is a very useful way of analyzing and understanding the heating and deformation mechanisms of the steel sheets during the various operations.

## 3 Inductive heating

### 3.1 Presentation of the case study

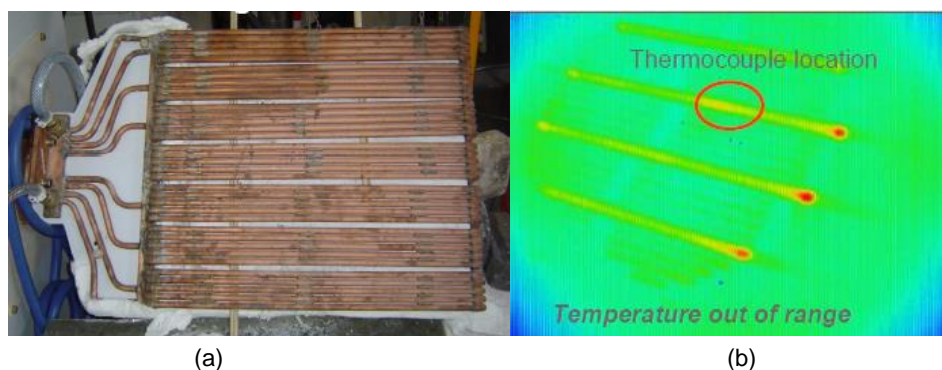


Fig. 1: (a) experimental system for inductive heating and (b) highlighting heating location

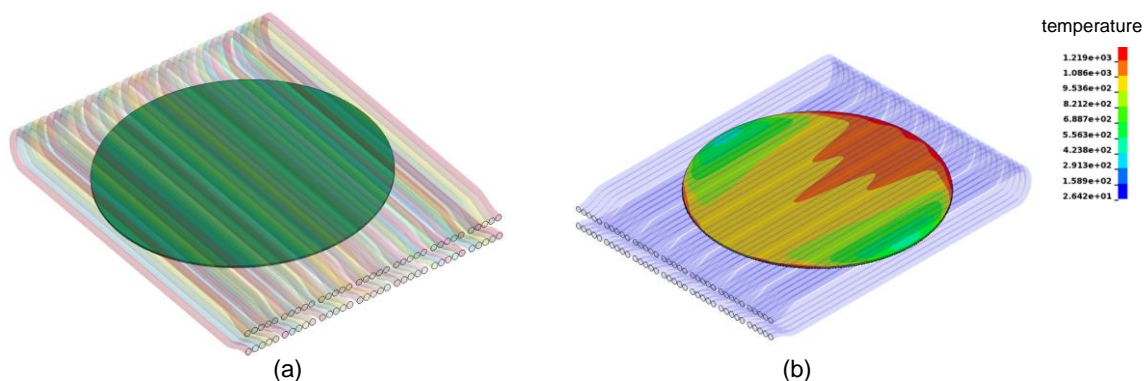


Fig. 2: (a) modeling of the experimental device for inductive heating and (b) temperature profile for the final model

## 4 Resistive heating

### 4.1 Presentation of the case study

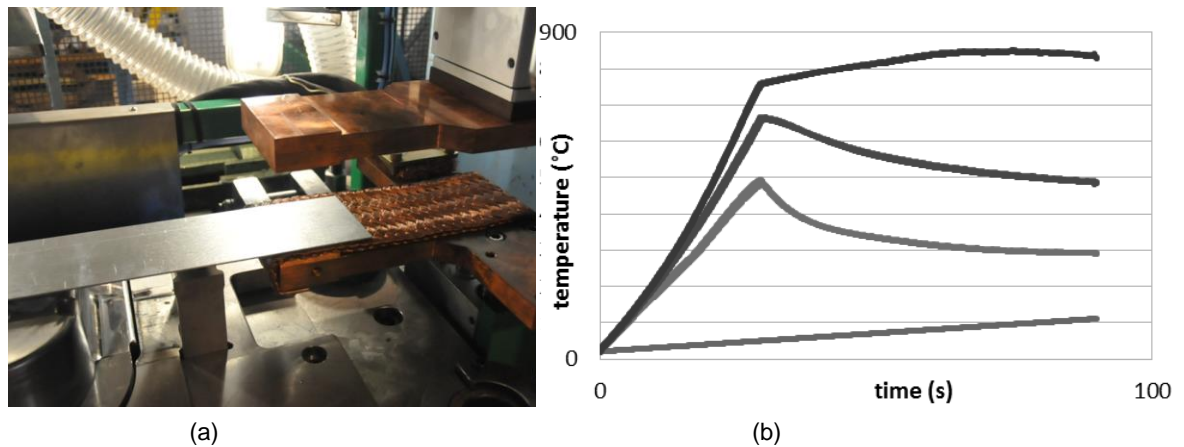


Fig 3: (a) experimental device of resistive heating on thin steel plates, (b) temperature profile function of the distance to the electrode

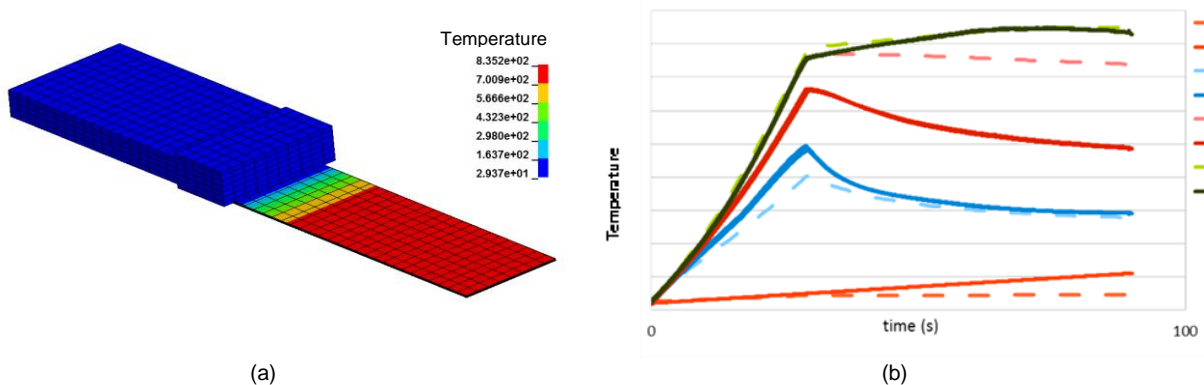


Fig. 4: (a) modeling of the experimental device of resistive heating, (b) comparison between experimental and numerical results

## 5 Conclusion

Two alternative heating techniques were studied in this paper : the inductive heating which heats a steel plate by induced heating, without contact and the resistive heating that, thanks to two electrodes in contact, is used to apply a potential difference and heat the part by Joule effect. These studies show that the LS-DYNA software is able to simulate the inductive and resistive heating phenomena with an acceptable computation time in an industrial context and good accuracy.

Changes in temperature in a steel plate massively heated by induction seem physical. However, new experimental tests should be established for further correlation and validation of the model.

The resistive model is well correlated temperature profiles away from the boundary conditions. The current level of modeling is sufficient to represent the overall behavior of the part, but depending on the level of requirements requested by the manufacturer, the model can be improved. Several ways of improving were identified as the set-up of electrical and thermal contacts, mesh refinement and adjusting convection and radiation coefficients to the experimental conditions.

## 6 Acknowledgment

Dr. Romain CANIVENC of ArcelorMittal Global R&D Montataire is acknowledged for providing experimental results. Dr. Arthur SHAPIRO, Dr. Pierre L'EPLATTENIER, M. Iñaki ÇALDICHOURY and Mrs. Julie ANTON of LSTC are acknowledged for their helpful comments and suggestions.

# Cohesive Contact Modeling in Thermoforming Simulations of Metal-CRFP-Metal Sandwich Sheets

Özgür Cebeci<sup>1</sup>, Malte von Scheven<sup>2</sup>, Andreas Zeiser<sup>1</sup>

<sup>1</sup> inpro Innovationsgesellschaft für fortgeschrittene Produktionssystem in der Fahrzeugindustrie mbH, Berlin, Deutschland

<sup>2</sup> Institut für Baustatik und Baudynamik, Universität Stuttgart, Stuttgart, Deutschland

## 1 Introduction

A novel carbon fiber reinforced metal laminate based on thermoplastic polymer is investigated in the project LEIKA. For the safeguarding of the production of the parts made of this material, coupled thermo-mechanical simulations have to be carried out. Experiments show a large relative sliding, separation and re-sticking behavior between layers during the forming of the heated sheets. Hence, each layer of the laminate needs to be modeled as an individual shell in order to represent the different forming behavior.

In this work, we concentrate on the complex interlayer contact behavior. For the modeling of the cohesive interlayer behavior the main idea is to apply traction separation laws in the normal direction and use friction laws regarding to the tangential force components. The only available built-in contact model in LS-DYNA which allows tangential movement and constrains the normal separation is `*Contact_Surface_to_Surface_Tiebreak` with the separation option 4. It applies a linearly increasing reaction force in the normal direction with an instantaneous failure. Also no re-sticking capability is available.

Since the built-in contact models in LS-DYNA are not capable of modeling all the relevant physical aspects, an improved user defined contact model has been developed and implemented using the LS-DYNA user defined friction routine. The main goal of the developments is to provide a smooth traction separation behavior with damage and re-sticking properties.

## 2 Modeling and Implementation

The development of the model is based on the RCCM model [1] which uses a bi-functional traction separation law with damage, which is able to reproduce the characteristic behavior of soft adhesive bonds [2]. The model has been extended to include re-sticking and a pressure dependent re-healing. Hence if a pressure is applied long enough, a previously separated interface may completely re-heal in contact. For the tangential behavior standard built-in temperature dependent Coulomb friction definition in LS-DYNA is used.

The model has been implemented in LS-DYNA using the user-defined friction routine. Although this routine is designed for implementing alternative friction laws, the manipulation of all components of the slave node contact force is possible. For modeling the cohesive contact, the contact zone has to be extended in order to utilize the user-defined friction routine for the separation zone as well. Therefore implementations are carried out using the scaled contact zone approach. As a consequence the force components have to be corrected to represent actual contact forces. Finally, the separation behavior is modeled temperature dependent.

## 3 Numerical applications

The developed contact model has been verified in a systematic way with different models. To begin with, different contact states and the functionalities have been demonstrated with a fundamental shell model. It consists of two shell parts subjected to approach de-approach movement towards each other. Furthermore, in order to see the deformation impact of the contact forces, a deformable hyperelastic model with 8 node solid elements has been tested (see Figure 1).

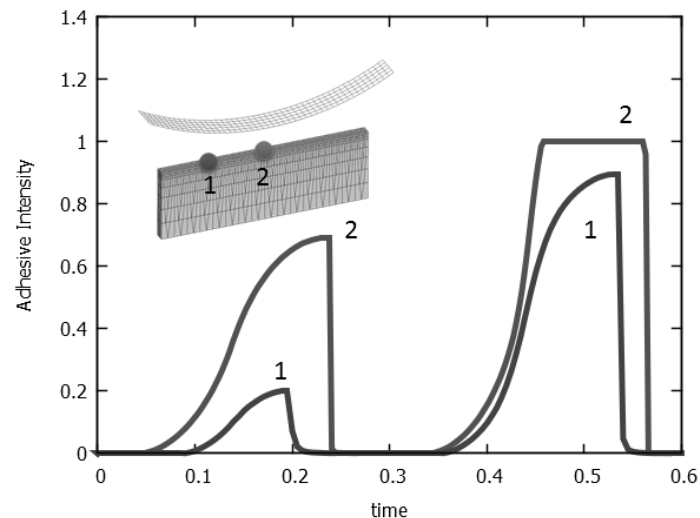


**Figure 1 Adhesive intensity at two locations (position 1 and 2) in deformable test model showing a re-healing with pressure and a re-sticking after separation**

Finally the developed model has been applied to the deep drawing simulation of real test parts made of the metal-CFRP laminate. Simulation results show a qualitatively good agreement with experiments provided by IUL at University of Dortmund (see Figure 2).

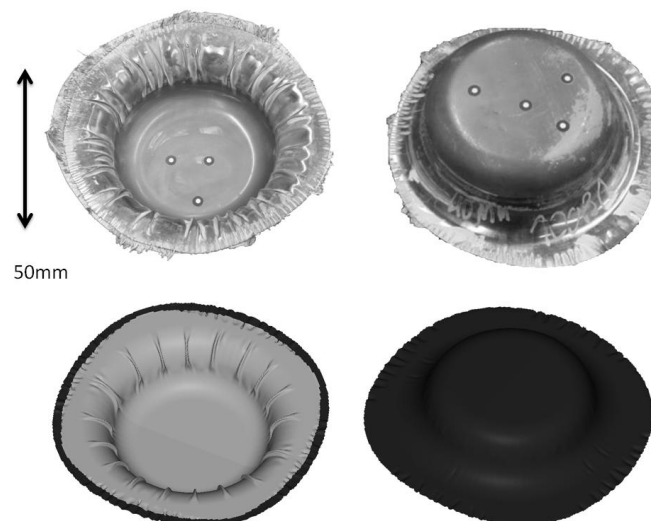


**Figure 2 Comparison of the simulation and the experimental results [3]**

### Acknowledgement

This research and development project is funded by the German Federal Ministry of Education and Research (BMBF) within the Framework Concept "Research for Tomorrow's Production" (fund number 02PJ2775) and managed by the Project Management Agency Forschungszentrum Karlsruhe (PTKA). We would like to thank Dr. T. Erhart (DYNAmore GmbH) for his support.

### References

- [1] Raous M., Cangemi L., Cocu M., "A Consistent Model Coupling Adhesion, Friction, and Unilateral Contact", *Computational Methods Applied Mechanics and Engineering*, 177, 1999, 383-399
- [2] Creton C., Hooker J., "Bulk and Interfacial Contributions to the Debonding Mechanisms of Soft Adhesives: Extension to Large Strains", *Langmuir*, 17, 2001, 4948-4954
- [3] Tekkaya A. E., Hahn M., Hiegemann L., Weddeling C., Ben Khalifa N., "Umformen faserverstärkter thermoplastischer Kunststoff-Halbzeuge mit metallischen Deckblechen für den Leichtbau", *Proceedings of 35. EFB-Kolloquium Blechbearbeitung 2015*, 24./25. March 2015, Bad Boll, 185-199



**PROCESS IX**  
**CUTTING/MODEL REDUCTION**



# The Influence of Johnson-Cook Parameters on SPH Modeling of Orthogonal Cutting of AISI 316L

Alaa A. Olleak<sup>1</sup>, Mohamed N.A. Nasr<sup>2</sup>, Hassan A. El-Hofy<sup>1</sup>

<sup>1</sup> Department of Industrial Engineering and Systems Management, Egypt-Japan University of Science and Technology, Alexandria, Egypt

<sup>2</sup> Department of Mechanical Engineering, Faculty of Engineering, Alexandria University, Alexandria, Egypt

## 1 Abstract

Over the past few decades, there has been a growing interest in modelling of machining processes. In this regard, smoothed particle hydrodynamics (SPH) is one of the latest methods used for that purpose. SPH is a powerful technique that can be used in handling problems of large deformation that are difficult to be tackled using traditional finite element methods. The current work aims to present and evaluate the use of SPH in modelling the machining process. A coupled thermo-mechanical analysis of a 3D model is performed using LS-DYNA to predict the cutting forces and residual stresses (R.S.) during orthogonal cutting of AISI 316L, at different sets of machining conditions. The Johnson-Cook material constitutive model is used to simulate the material behavior. The simulation results are validated by a previously published experimental work and compared to finite element (F.E.) model.

## 2 Machining Model

The current study aims to re-evaluate the use of SPH technique in modelling of machining and extend its use to R.S. prediction. A thermo-mechanical analysis of orthogonal cutting of AISI 316L using SPH technique is proposed. The results are validated by a previously published experimental results, and compared to F.E. simulations results. The Johnson-Cook material constitutive model is used since it is well suited for simulating materials subjected to large strains, high strain rates, and high temperatures. Five Johnson-Cook parameters measured by different means were selected to be used in this study with the aim of studying the influence of them on the SPH model results.

A tool of rake angle  $0^\circ$ , clearance angle  $11^\circ$ , and edge radius of  $30\ \mu\text{m}$  is used for dry cutting of AISI 316L round bars. The cutting speeds are 100-200 m/min, the uncut chip thickness is 0.1-0.2 mm, and the width is 6 mm.

A 3D SPH model is developed in order to predict both cutting forces and R.S. in the machined surface of the workpiece. The tool is assumed rigid and fixed in all directions except the cutting direction. The cutting distance is set to 10 mm to achieve the steady state condition, the width to 0.05 mm to reduce the computational time, and the height to 1 mm, Fig. 1.

The simple Coulomb's law was considered on the whole contact zone. Even though this is a simplistic approach, it has been widely used in metal cutting simulations. In order to investigate the effect of friction coefficient ( $\mu$ ) on the process, different values ranging from 0.2 to 0.8 were used.

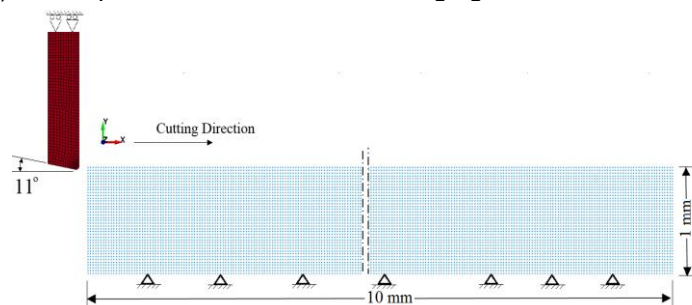


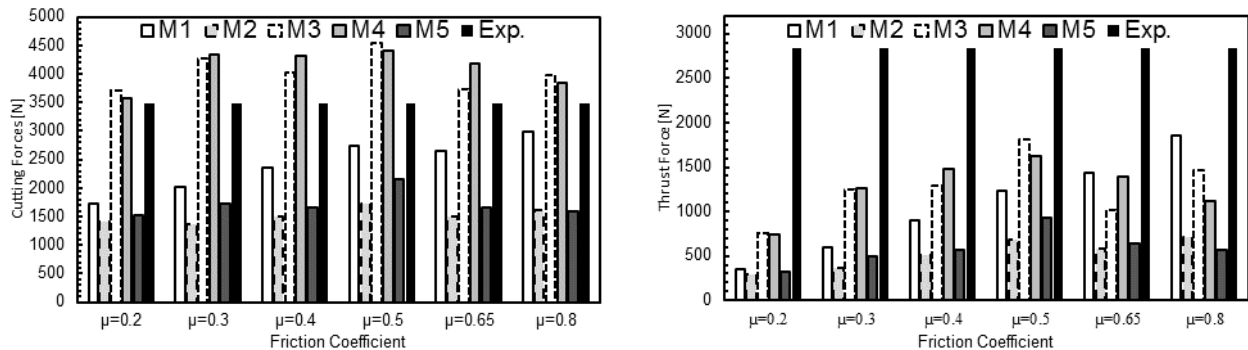
Fig. 1: SPH cutting model

## 3 Results

### 3.1 Cutting forces

It can be noticed that sets M2 and M5 are highly underestimating the forces. This high underestimation can be a result of their low strain hardening constants compared to the other sets of

material parameters. From Fig. 2, It is obvious that the least difference between the predicted and measured cutting forces can be achieved at friction coefficient of 0.2 for M3 and M4 (2% and 6% respectively), and 0.8 for M1. However, for thrust forces, the least difference can be achieved at friction coefficient of 0.8 for sets M1, M3, and M4. After excluding the results of M2 and M5, the average difference between the predicted forces and the measured forces at  $\mu=0.8$  is 13% for the cutting forces, and 48% for the thrust forces. The best prediction is given by M1 parameters.



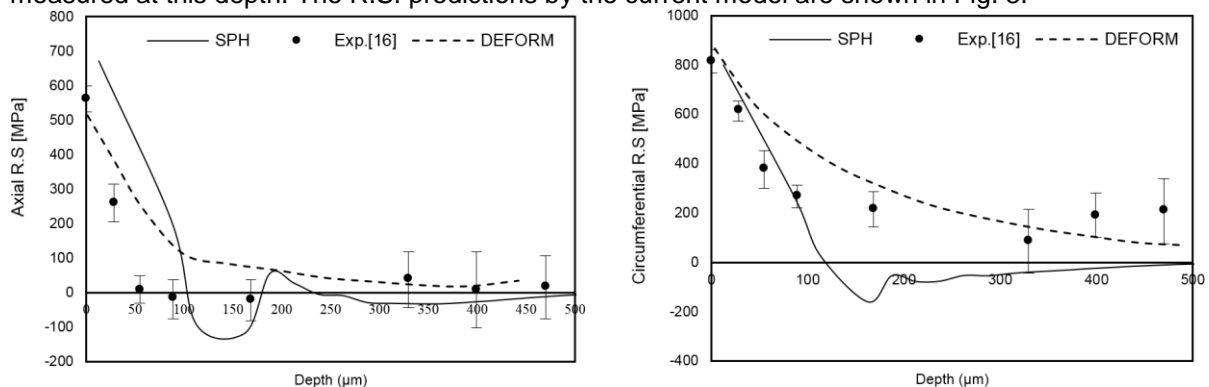
(a) Cutting force

(b) Thrust force

Fig. 2: Comparison between predicted and measured forces for different sets of Johnson-Cook parameters and friction coefficient

### 3.2 Residual Stresses

The best prediction is given by M1 parameters at friction coefficient of 0.8; therefore, these conditions are used in predicting the R.S. for cutting speed 200 m/min and uncut chip thickness of 0.1 mm. The average R.S. are taken at the middle of the workpiece for 160 particles at every depth (total of 3,200 particles). The minimum depth below the machined surface is 12.5  $\mu\text{m}$  and the R.S. at the surface is measured at this depth. The R.S. predictions by the current model are shown in Fig. 3.



(a) Axial R.S.

(b) Circumferential R.S.

Fig. 3: Comparison between experimentally and numerically obtained residual stresses.

## 4 Conclusions

- A numerical analysis of cutting forces and residual stresses induced by orthogonal cutting of AISI 316L was performed using SPH method. The predicted results of SPH simulations show good correlation with the experimental results for M3 and M4. Therefore, in order to have accurate results, the choice of the Johnson-Cook constants is of crucial importance. Johnson-Cook constants identified experimentally from Split Hopkinson's Bar tests should be used while using SPH.
- The SPH method was underestimating the feed forces at high friction coefficients. Therefore, it is recommended to use the SPH method for applications in which the ratio between the thrust and cutting forces is low.

# SPH Modelling of Cutting Forces while Turning of Ti6Al4V Alloy

Alaa A. Olleak, Hassan A. El-Hofy

Department of Industrial Engineering and Systems Management, Egypt-Japan University of Science and Technology, Alexandria, Egypt

## 1 Introduction

A growing interest in modelling and simulation of machining processes has been witnessed in the past few decades. The common approaches that have been used for that purpose are Lagrangian, Eulerian and Arbitrary Lagrangian-Eulerian (A.L.E.).

However, using these approaches in such models require special techniques in order to avoid their shortcomings. One of these shortcomings is the need to adopting a damage model that artificially initiates the crack, and as a result, the accuracy will be affected.

In this regard, the mesh-free methods could overcome the struggles of finite element techniques by avoiding the mesh distortion problems, and the need to remeshing and defining a damage model. Consequently, these methods can be employed in large deformation problems. One of these methods is the Smoothed particles hydrodynamics (SPH), which is one of the latest and developing methods used for that purpose. The SPH method does not require any damage model and remeshing technique to be adopted for the simulation.

The previous research studies in which SPH is employed to represent the workpiece in machining modelling were limited to 2D orthogonal cutting simulation. Furthermore, most of them validated the force in the cutting direction only. Therefore, it is necessary to extend the use of SPH method in 3D cutting simulations in order to evaluate the ability of SPH method to predict all components of forces.

## 2 Machining Model

The current work aims to present and evaluate the use of SPH in 3D advanced models. A coupled thermo-mechanical analysis of the 3D model is performed using LS-DYNA to predict the cutting forces during face turning of Ti6Al4V alloy. A rigid tool with rake angle  $\gamma = -5^\circ$ , relief angle  $\alpha = 11^\circ$ , nose radius  $r_\epsilon = 0.8$  mm, and edge radius  $r_\beta = 25$   $\mu\text{m}$  is used to cut the workpiece at cutting speeds of 55 and 90 m/min, and at uncut chip thickness of 0.1mm, and depth of cut of 2.2mm.

The workpiece was represented by a traditional finite element in the region in which low deformation occurs, and SPH particles in the region where high deformation occurs. The spacing between the SPH particles is set to 50  $\mu\text{m}$  in x and y directions, and to 25  $\mu\text{m}$  in z direction.

For material modelling, the Johnson-Cook material constitutive model is used since it is well suited to simulate materials subjected to large strain, high strain rates, and high temperature. The parameters used for Johnson-Cook constitutive model are  $A = 870$  MPa,  $B = 990$  MPa,  $C = 0.008$ ,  $n = 1.01$ ,  $m = 1.4$ ,  $T_M = 1680$   $^\circ\text{C}$ ,  $T_R = 25$   $^\circ\text{C}$ , and the reference strain rate  $= 1$   $\text{s}^{-1}$ . In order to optimize the model, the both linear polynomial and Gruneisen equations of state are adopted in order to accurately simulate the material behavior and investigate their effects on the results.

For friction modelling, the simple Coulomb's law was considered on the whole contact zone even though its simplicity. However, it has been widely used in metal cutting simulations. Different friction coefficient values were used in order to predict the cutting forces over wide range of frictional conditions.

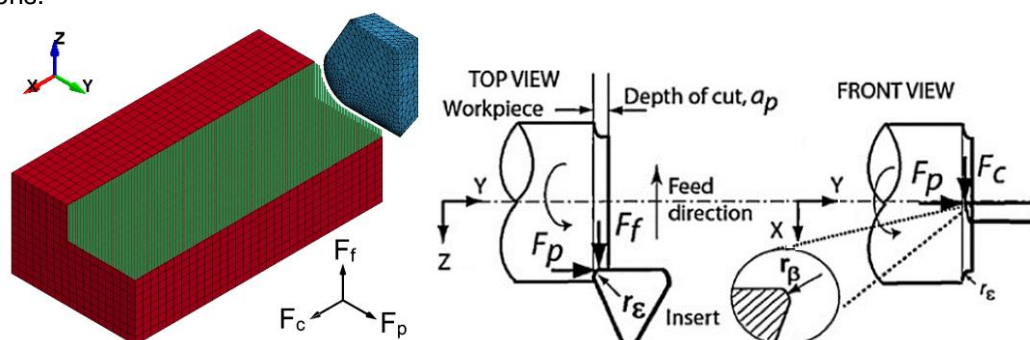


Fig. 1: Configuration of Face turning model

### 3 Results

The results considered in the figure are the results with the least difference between the predicted and measured values. At cutting speed of 55 m/min, a difference of 7%, 1%, and 9% for  $F_c$ ,  $F_p$ , and  $F_f$  respectively is achieved at friction coefficient  $\mu=0.35$  for linear polynomial E.O.S., and 1%, 1%, and 15% at friction coefficient  $\mu=0.5$  for Gruneisen E.O.S.. At cutting speed 90 m/min and friction coefficient  $\mu=0.7$ , a difference of 0%, 6%, and 9% for  $F_c$ ,  $F_p$ , and  $F_f$  respectively is achieved for Linear polynomial E.O.S., and of 4%, 4%, and 7% for Gruneisen E.O.S.. The chip formation of the analysis is shown in Fig. 2.

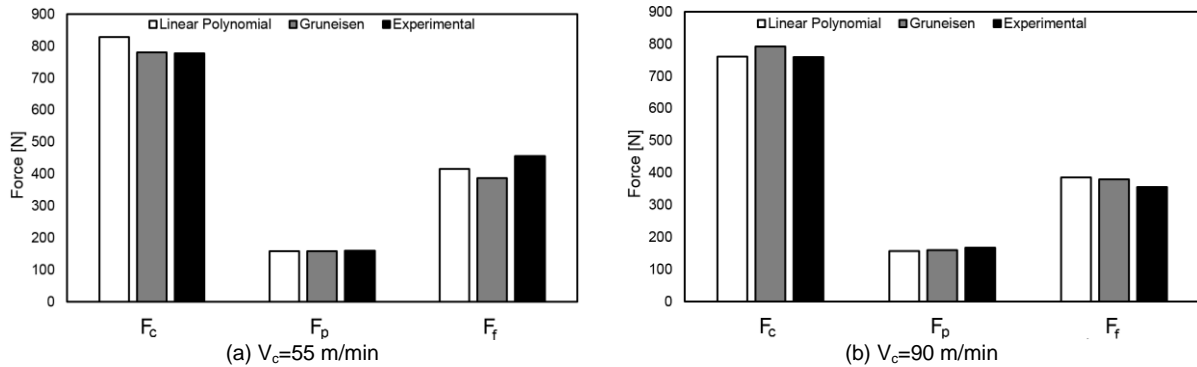


Fig. 2: Comparison between simulation and experimental results

### 3 Conclusions

- A 3D SPH/F.E. model was developed in order to predict the cutting forces while face turning of Ti6Al4V rods. The simulation results for the three components of forces find an excellent agreement with the published experimental results.
- The study proved that the equation of state type, whether it was Linear Polynomial or Gruneisen E.O.S., is insignificant on the results for the proposed model. However, the predictions of Gruneisen E.O.S. are slightly higher than the Linear Polynomial E.O.S. predictions.
- The coefficient of friction values is of significant effect on the results. Therefore, it should be accurately determined. Furthermore, a further investigation on the frictional behavior for contacts including SPH parts at high friction coefficients has to be conducted.
- The SPH method proved itself as an efficient tool to be used in machining modelling.

# Simulation of the Circular Sawing Process

Hector Vazquez Martinez<sup>1,2</sup>

Fraunhofer Institut für Produktionstechnik und Automatisierung IPA<sup>1,2</sup>

## 1 Abstract

Machining processes are characterized by high dynamic and states of deformation. With the use of simulation technology different machining processes have been analyzed and have shown reliable results. However, the simulation of sawing process has been carried out in very few cases. In order to analyze deeper the saw processes and identify process optimization potentials, the present work contains the results of finite-element (FE) simulations of circular saw processes designed in LS-Dyna. The effects of the variation of the cutting speed and tooth feed on the process forces, temperature development and the chip formation, are shown by the results of these simulations.

## 2 The circular saw process and its simulation

In circular saw processes material is separated by the action of several cutting teeth in the tool. Circular saws are characterized by a high number of geometric defined cutting teeth in comparison to any other machining tool. Either with a circular or a linear cutting kinematic, sawing processes are used for the cutting of sheets and profile tubes, the perforation of sheets, or for the machining of grooves and slots on components.

Figure 2.1 shows standard geometrical parameters which characterize sawing blades. In accordance to the material to be sawed, the form and separation of the cutting teeth must be selected. Next to the geometrical characteristics of the cutting tools, the process parameters play a very important role for the quality of the machining process as well. The process parameters determine the thermal and mechanical conditions of the process, which finally affect the surface quality after the process and the integrity of the cutting tool.

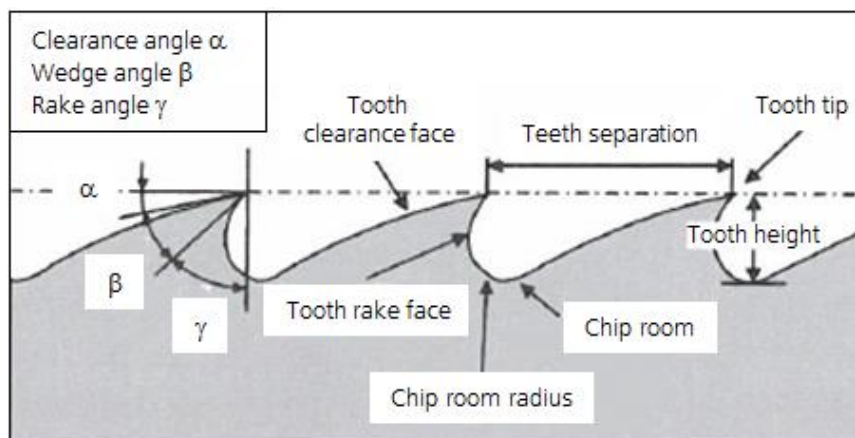


Fig. 2.1: Geometrical parameters in the cutting teeth of saw blades [1]

Although circular saw processes are high-productive machining processes and longer service performance of the sawing blades can be expected through the action of the higher number of teeth, very few circular saw processes have been simulated.

### 3 Construction of the models

In figure 3.1 a FE-model for the circular sawing is presented. The effects of the variation of process parameters cutting speed  $v_c$ , and tooth feed  $f_z$  have been analyzed in LS-Dyna. The table 1 contains the implemented materials and parameters in the FE-model in LS-Dyna.

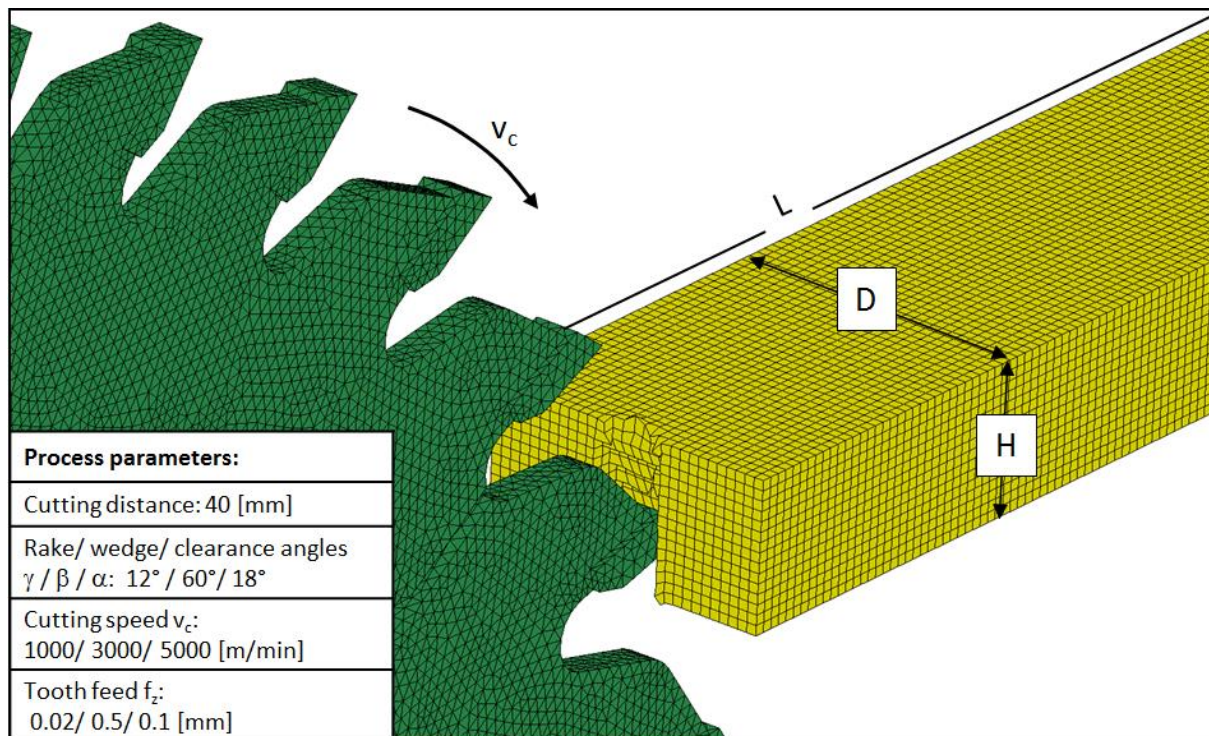


Fig. 3.1: Model design of the circular saw process in LS-Dyna

Table 1: Parameters of models

Tool properties (Circular saw)	FE-Model properties (Tool)	Work piece properties	FE-Model properties (Work piece)
Tool dimensions (DxW): 200x3.2 [mm]	Number of Elements: 70000	Work piece dimensions (HxLxW): 10x100x20 [mm]	Number of Elements: 60000
Tool material: <b>Tungsten carbid (WC)</b>	Material model: <b>Rigid</b>	Work piece material: <b>Al 6061</b>	Material models: <b>Johnson Cook + Thermal isotropic</b>
Number of teeth: 36	Element type: <b>Shell</b>		Element type: <b>Solid</b>
	<b>Interface conditions:</b>	Contact: <b>Eroding Surface to Surface</b>	Sliding friction coefficient: $\mu = 0.1$

### 4 Literature

- [1] Leitfaden von Sandvik Steel: Das Handbuch. Herstellung, Einsatz und Pflege von Holzsägeblättern. Sandviken, 1999.
- [2] Träger, J.; Shneider, M.: „Grundlagen der Holzbearbeitung - Kreissägeverfahren“. Institut für Werkzeugmaschine (IfW) der Universität Stuttgart, 2012.



# Model Reduction Techniques for LS-DYNA ALE and Crash Applications

Kambiz Kayvantash<sup>1</sup>, Amadou-Tidiane Thiam<sup>1</sup>, David Ryckelynck<sup>2</sup>, Samir Ben Chaabane<sup>3</sup>,  
Josselyn Touzeau<sup>3</sup>, Philippe Ravier<sup>3</sup>

<sup>1</sup>CADLM SARL

<sup>2</sup>Mines Paris Tech

<sup>3</sup>SILKAN SA

## 1 Model Reduction

Model Reduction Techniques (MRT) are algebraic approximation solutions allowing for fast (real-time) interpolations (reconstruction) or extrapolations (prediction), based on previously existing DOE-type results, obtained either from FE computations or directly from constructions of reduced FE solutions. In a sense reduced models are subsets or decomposed domains of the solutions allowing for reconstruction of all spatial or temporal domain response.

## 2 Stat of the art

Apart from a few matrix algebra manipulations, the algorithms are straight forward and may be applied with more or less efficiency to LS-DYNA or any other explicit finite element models. We shall briefly present two applications for crash (Lagrangian) and for missile impact simulation requiring (ALE) solutions. Other applications such as safety or multi-physics are also typical candidates since they require a complete and simultaneous simulation of all model components. Notice that these applications are often very time consuming (such as crash barriers or airbag ALE or CFD simulations) irrespective of the objectives of simulation. Additionally the interest in the modelling of such computationally expensive components (missile, barrier, airbag) is secondary and the real objective (criteria) of the simulations are often structural (damaged parts) or human biomechanical response. Additionally while the inclusion of these models in a full model may be considered affordable, their applications for either direct or surrogate based optimization or parametric studies becomes computationally expensive and often prohibitive.

### 2.1 The POD method

In the following we shall present the basic steps of the POD method, which is a decomposition technique, allowing for real-time (on-board) solutions used in optimization or simulator technologies. The two solutions presented are generic and may be readily applied for other multi-physics applications such as coupled fluid/thermal-structure interactions. The engineering consequence of this decomposition is an encapsulation of the reduced model as two independent, uncoupled responses in space and in time of the original function which may be used in a full model as easily as a material law, a contact force or a loading-time function, etc.

## 3 Applications

We shall present a simple crash type application allowing for the reconstruction of complete time-histories of a typical crash scene using only a few runs obtained via an Optimal Latin Hypercube design procedure. The "POD snapshots" method is used. The reconstructed responses may then be used for further predictions, allowing for parametric studies or real-time simulations to be performed with little computational effort. A second ALE type application where the "POD SVD" method is used and will be presented during the oral presentation (omitted here for page limit considerations) and may be obtained by contacting the first author

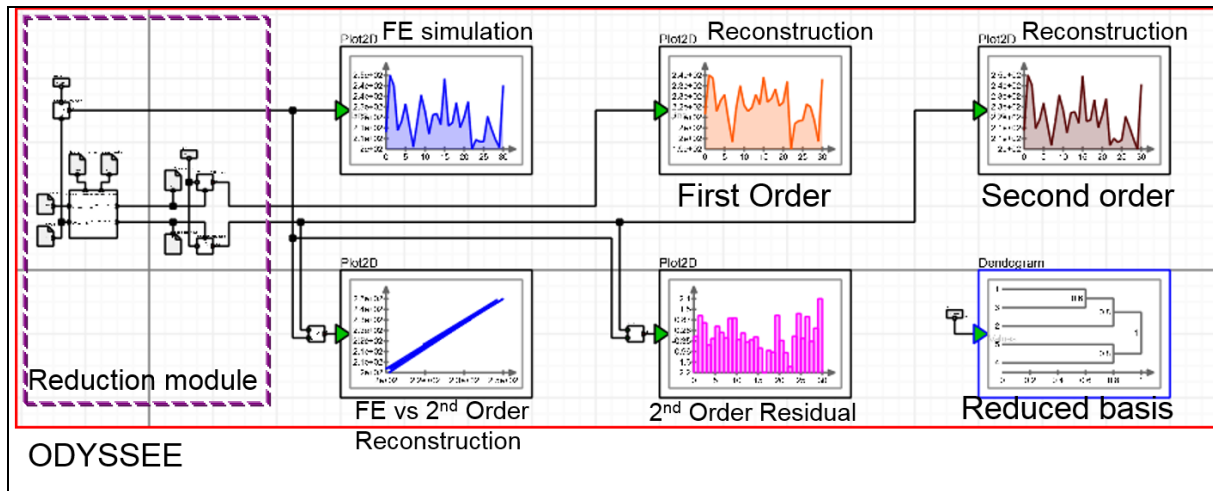


Fig. 1: ODYSSEE Reduced Modelling Application for a 1<sup>st</sup> and 2<sup>nd</sup> order reconstruction of the respons

# **MATERIALS I**

## **PLASTICS**



# Failure of Thermoplastics - Part 1 Characterization, Testing

A. Fertschej, P. Reithofer, M. Rollant

4a engineering GmbH, Austria

## 1 Characterizing plastics using 4a impetus

In recent years the light weight construction has become more and more important due to the rising demand of energy savings. Coming along with that reason plastics substitute other materials and they are also carrying the applied loads. Therefore it is necessary to consider the deformation behavior (plasticity) as well as damage and failure in the material model.

The tensile test is a standard testing method for many different materials to determine elasticity, plasticity and failure. Compression and shear tests have a rather scientific character, they can be used to determine elastic and plastic properties, but failure never occurs in the favored triaxiality. Due to DIC all these tests are time consuming and in the case of dynamic testing also cost intensive. To characterize the dynamic deformation behavior dynamic bending tests on 4a impetus are a cost-efficient alternative. The bending case is also the most frequently occurring load case in reality. As a result of the processing plastics have different mechanical properties at the outer surface compared to the inner core. So the bending properties (stiffness, failure behavior ...) are accordingly higher and near to reality because of the higher loading of the outer fiber compared to the tension properties.

## 2 Characterizing failure

To characterize failure further test methods for 4a impetus were developed in the last years. They are easy and fast to perform and available for 4a impetus (figure 1). Using the test methods shown in figure 2 failure at different triaxialities can be specifically investigated.

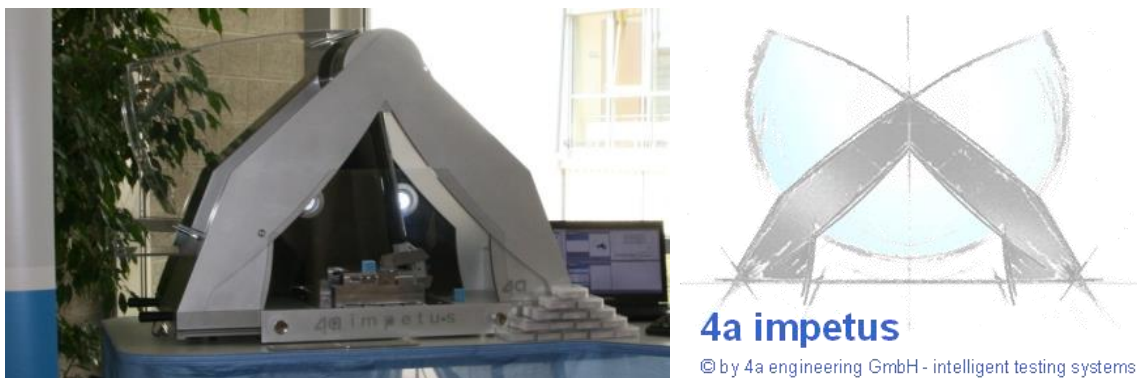


Fig.1: Testing system 4a impetus

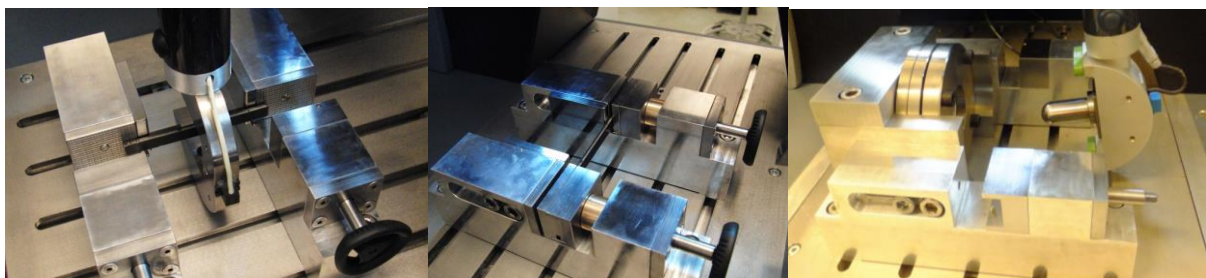


Fig.2: Dynamic bending test (left); dynamic clamped bending test (middle); dynamic puncture test (right)

The bending test is the standard test method in 4a impetus; the strain rate dependency can be determined quite well. Testing brittle materials (e.g. talc reinforced PP, see figure 3) failure can be achieved in the bending tests.

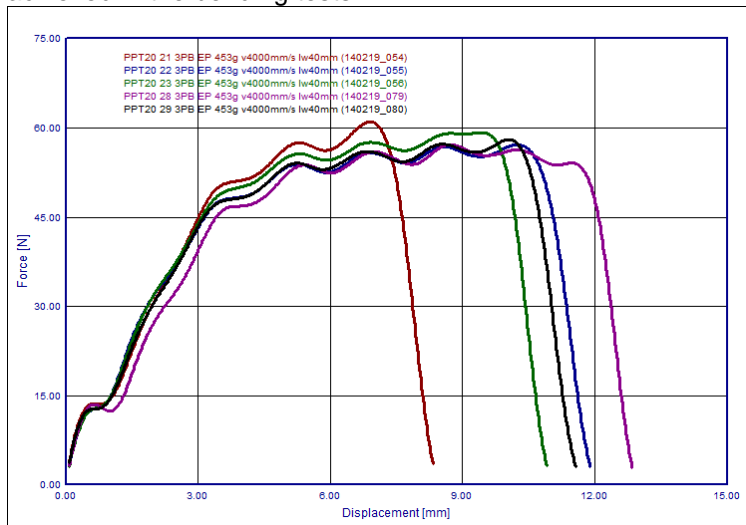


Fig.3: Force-displacement curves for 3-point-bending at a speed of 4 mps; material: PP T20

The clamped bending test has a significant area where tension dominates, so the tension/compression asymmetry of the material can be determined. The puncture test provides information on the mechanical behavior under biaxial tensile load. Having ductile plastics these two test methods have to be performed on 4a impetus to characterize the test specimens concerning failure at dynamic loading. As an alternative measurement results from other testing machines can be imported into the 4a impetus software, evaluated and used for the process of creating material cards. As an example static and dynamic tensile tests including optical strain measurement can be used for the material mapping process.

In addition to the influence of the strain rate and triaxiality to the failure also imperfections in the parts are essential. These lead to different failure times and can be integrated in the simulation using appropriate probability considerations. As the test specimen geometry is simple and the tests are easy to perform the higher amount of tests needed for statistical reasons can be considered cost efficiently. Attention regarding the failure time has to be paid for the preparation of the raw data (filtering and evaluation), so that failure time and behavior are not falsified (see figure 4).

Using the aforementioned tests the base for a material modeling near to reality is created. This aspect is shown more detailed in the second part (Failure of Thermoplastics - Part 2 - Material Modeling and Simulation).

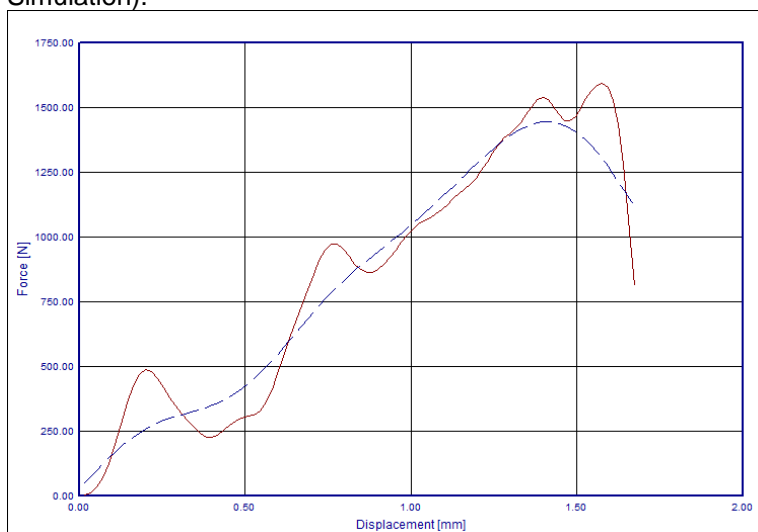


Fig.4: Force-displacement curves for a puncture test at a speed of 4 mps; solid line (red): unfiltered curve, dashed line (blue): filtered curve

# Failure of Thermoplastics - Part 2

## Material Modeling and Simulation

A. Fertschej, P. Reithofer, M. Rollant

4a engineering GmbH, Austria

### 1 Complex material models

Complex material models compared to the standard \*MAT24 are much more used nowadays. The reasons are the increasing usage of plastics in automotive parts that have high security relevance and the demand for virtual modeling including damage and failure. These complex material models allow a more detailed reproduction of reality, e.g. the tension/compression dependency. Implementing damage and failure is a time-consuming step and depends on the real material behavior but as well as on the testing method and on specific settings for the solver.

LS-Dyna offers many material models for plastics that have an implemented damage/failure modeling. This modeling goes from

- simple failure models (e.g. plastic strain, \*MAT24)
- over comprehensive damage/failure models (e.g. plastic failure strain with damage, \*MAT81)
- up to highly complex damage/failure models (e.g. failure in dependence of strain rate and triaxiality, \*MAT\_ADD\_EROSION, see figure 1)

With the exception of \*MAT187 which was developed especially for plastics, all these material resp. damage models were derived from the metals section. Anyway these models allow a good and technical suitable approximation to the reality of plastics. Just visco-elasticity and temperature dependency are neglected due to missing material models. Damage and failure can be included generally (piecewise linear). Of course approaches describing the basic behavior of unreinforced plastics are still missing.

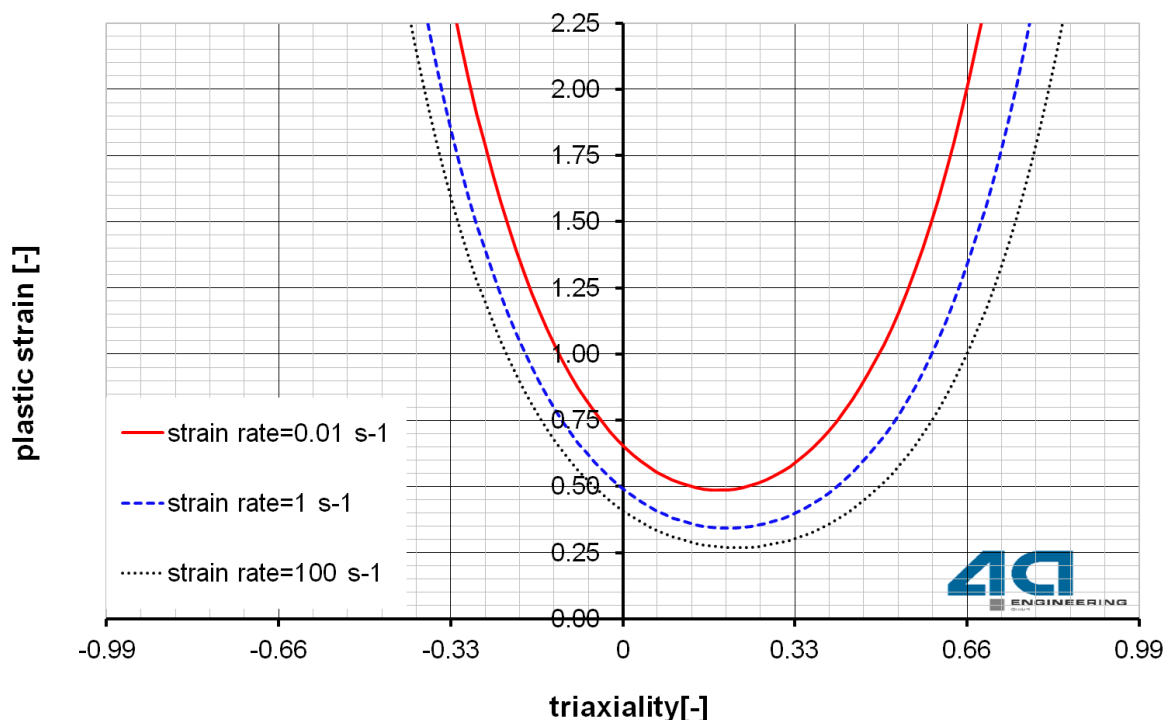


Fig.1: Example of failure curves in dependence of triaxiality and strain rate

## 2 Modeling failure

When simulating crash, failure (place and time) is essential for the development of the further load path and energy consumption. Because of increasing lightweight constructions plastics are carrying more and more the applied loads; therefore a comprehensive virtual modeling becomes more important. This situation is considered in the software of 4a impetus by implementing some possibilities for modeling failure. So damage/failure in dependence of the load (triaxiality and strain rate) can be defined. Figure 2 shows exemplary a comparison of various failure models resp. failure settings of LS-Dyna, calculated in a one-element-test in 4a impetus.

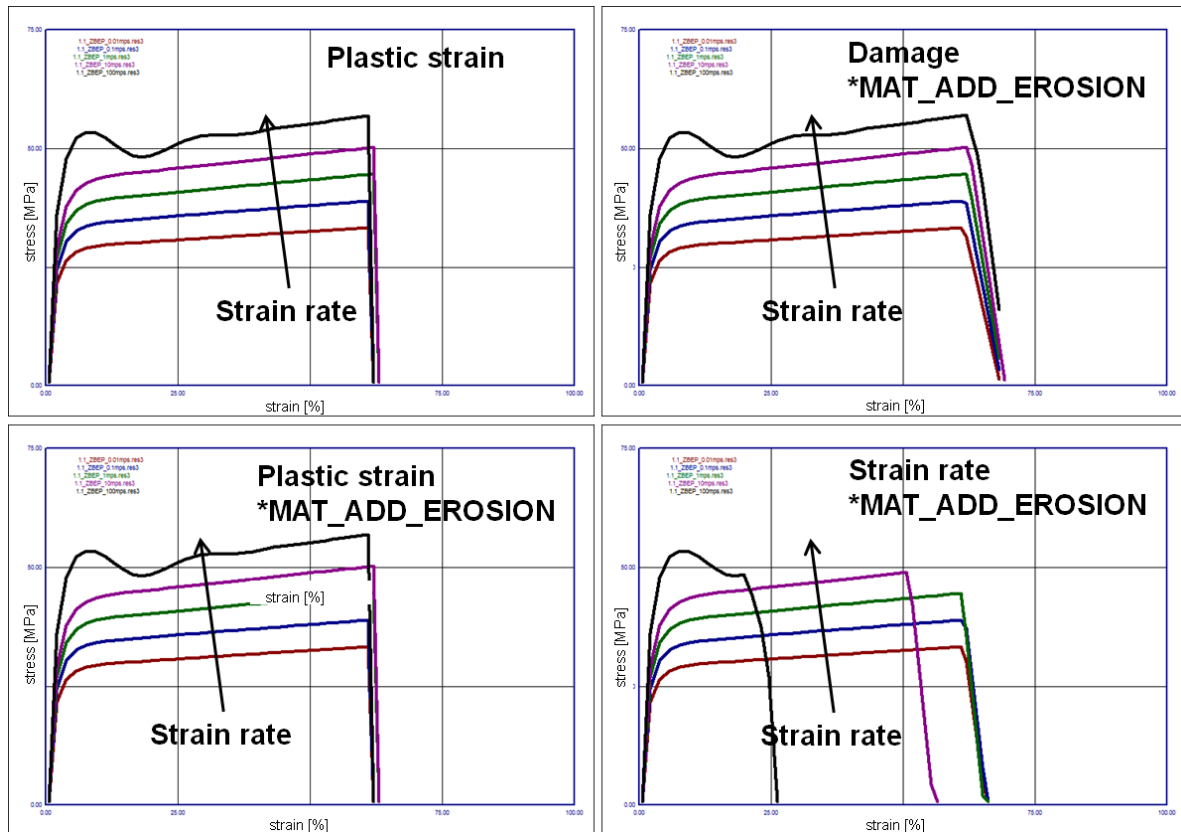


Fig.2: Results in stress/strain for using various failure models resp. settings

Doing the material characterization using the 4a impetus process

- from elasticity,
- over visco-plasticity
- ending in the failure and damage modeling,

the material behavior of plastics for the usage in crashworthiness applications can be described adequate. Figure 3 shows the final validation of a complex material model with damage and failure for a part that was tested by a dynamic puncture test.

## 3 Implementation in 4a impetus

An essential role in the simulation is the used idealization (shell vs. solid), element type and element size which have a significant influence on the calculation results. Fig 4 shows exemplary the influence of the element size on failure for various test velocities using \*MAT24 with plastic strain as failure model; test setup was 3-point-bending. Such calculations can be done in 4a impetus just by changing the parameter (here: the element size) in the software interface.

As the complexity of the adaption of the material cards rises, the future topic is the automation of the simulation process. Statistical methods have to be included to ensure the robustness in the usage of



such complex material models. Both topics were considered in the past as well as they will be considered in the future in the testing system and the software 4a impetus.

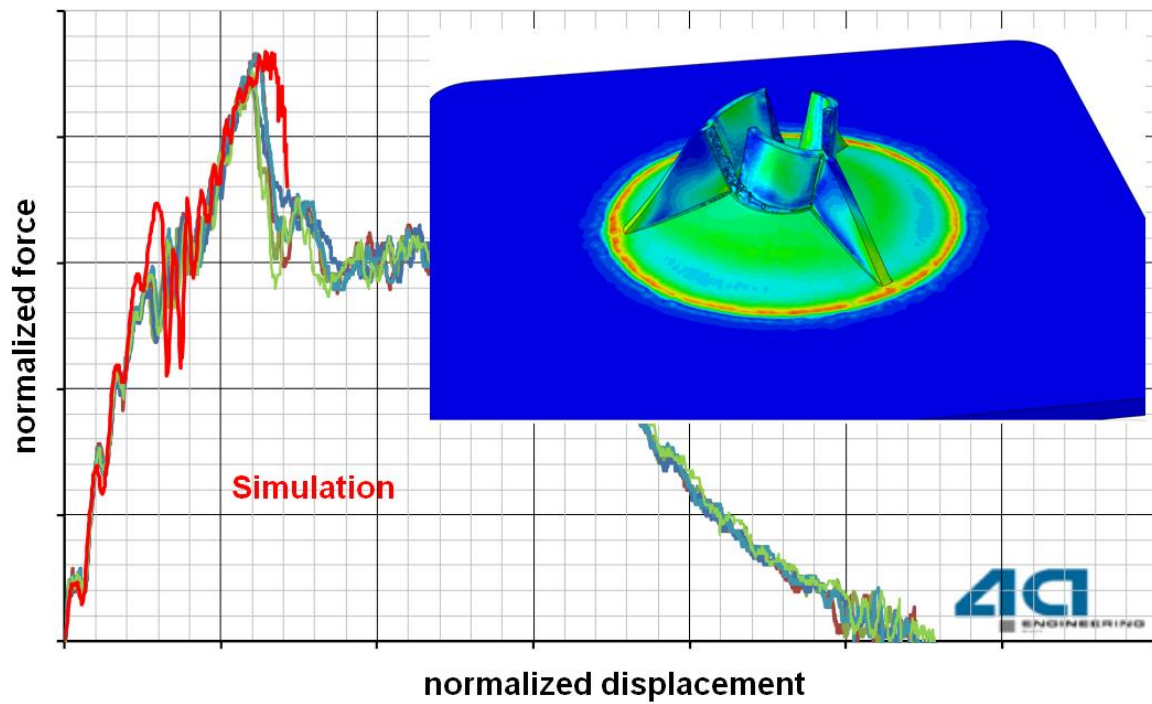


Fig.3: Comparison of test results to calculation results for a part characterized by a complex material model (test setup: dynamic puncture test)

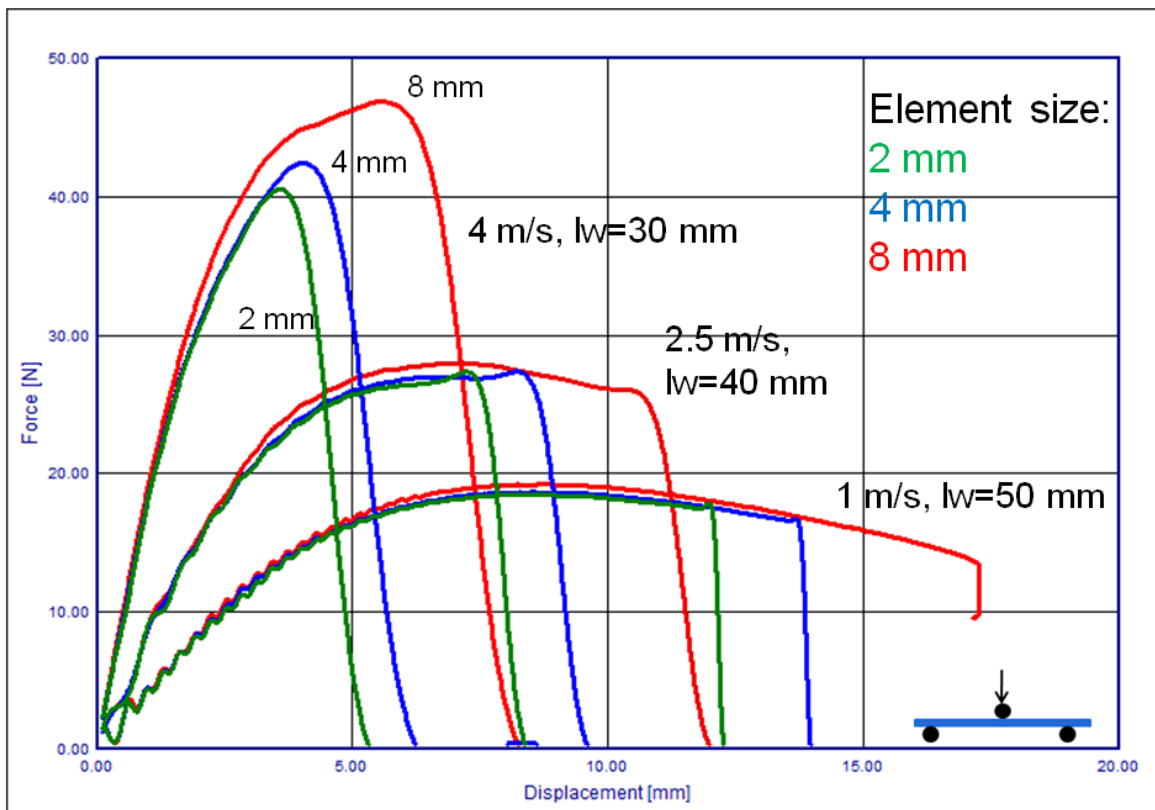


Fig.4: Influence of the element size on failure for various test velocities in 3-point-bending (\*MAT24, plastic strain as failure model; shell elements with 5 integration points)

# Macroscopic Modeling of Flow-Drill Screw Connections

Johan Kolstø Sønstabø<sup>1</sup>, David Morin<sup>1,2</sup>, Magnus Langseth<sup>1,2</sup>

<sup>1</sup>Department of Structural Engineering, Norwegian University of Science and Technology

<sup>2</sup>Structural Impact Laboratory (SIMLab), Centre for Research-based Innovation, Norwegian University of Science and Technology

Flow-drill screws (FDS) are used in the automotive industry to join parts in the load-bearing structure of cars. The process is a simple one-step procedure, which requires access only from one side of the assembly, and a variety of dissimilar materials may be joined. As it is easy to automate, the FDS technology is well suited for the production lines in the automotive industry.

In large-scale finite element simulations (for instance crash simulations) point connections such as FDS connections cannot be modeled with accurate geometry with a reasonable simulation run-time due to limitations in computer power. Hence, simplified models are required to include the connections in such simulations.

The focus of this study was modeling of FDS connections in large-scale shell analyses in LS-DYNA. Five commercial macroscopic connections models available in LS-DYNA were investigated; two element-based models (**\*MAT\_SPOTWELD** and **\*MAT\_240**) and three constraint-based models (**\*CONSTRAINED\_SPR2** and the two versions of **\*CONSTRAINED\_INTERPOLATION\_SPOTWELD**). Cf. [1-3] for detailed discussions of the theory of the models.

All models were calibrated using cross tests in tension, shear and a mixed tension/shear mode. In order to assess the flexibility of the models two sets of experimental data was used. First, a short screw was used to join two sheets of the same rolled alloy. In the second set, a long screw was used to join a rolled alloy to an extrusion. The models were validated using a two-steps approach including benchmark tests (single lap-joint and peeling) and component tests (crash box crushing and T-component tests). Cf. [4] for detailed descriptions of the test set-up.

None of the two element-based models were flexible enough to reproduce the cross test results. The tensile and shear modes were well captured, but the force and initial stiffness in the mixed mode were severely over-estimated for both sets of experimental data. For this reason simulations of the benchmark and component tests were not carried out for the element-based models.

The three investigated constraint-based models gave better results compared to the two element-based models. The tensile and shear modes were well captured, and in the mixed mode the level of the maximum force as well as the ductility were to some extent reproduced. However, the shape of the force-displacement curves was not matched in the mixed mode. In particular the initial stiffness was too high in the simulations of the mixed mode. Best results were obtained using **\*CONSTRAINED\_SPR2**, and in the following some brief results are shown for this model.

The calibration results (cross tests) for both sets of experimental data are shown in Fig. 1. As seen, the tensile and shear modes were relatively well captured, but the model lacks the required flexibility to capture the mixed mode for both data sets. The over-predicted initial stiffness in mixed mode is clearly seen in the left figure. Fig. 2 shows the results from simulations of T-component tests. For both data sets the maximum force was relatively well predicted. The ductility was over-estimated for the short screws, while it was better predicted for the long screws.

This study has shown that of the five models investigated **\*CONSTRAINED\_SPR2** is best suited to represent FDS connections in large-scale shell simulations in LS-DYNA. However, none of the models are flexible enough to capture the physics in the mixed mode. Constraint-based models gave in this study more accurate results than element-based models.

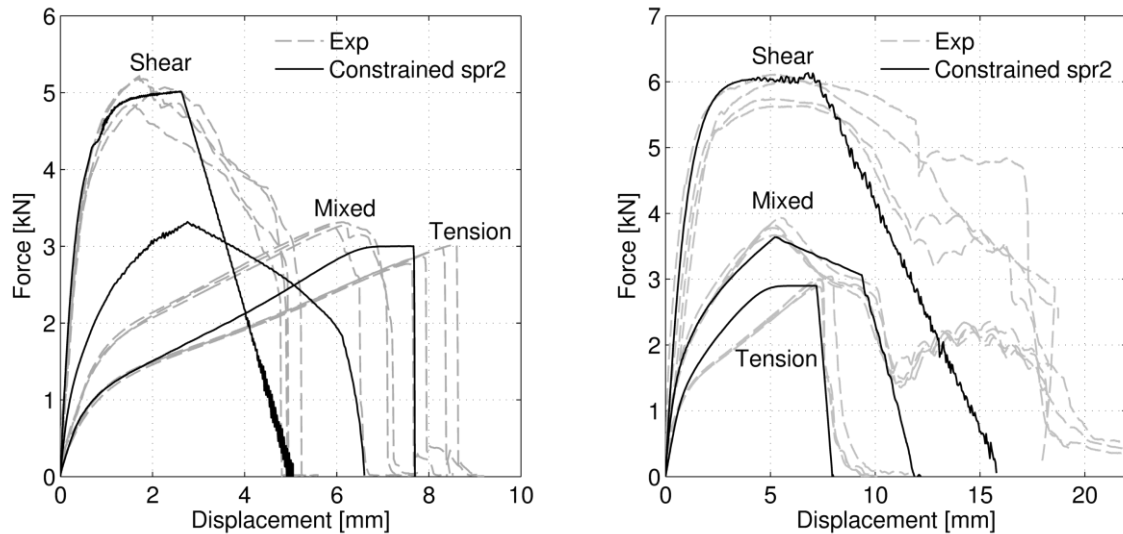


Fig.1: Calibration of *\*CONSTRAINED\_SPR2* to cross test results for short (left) and long (right) screws.

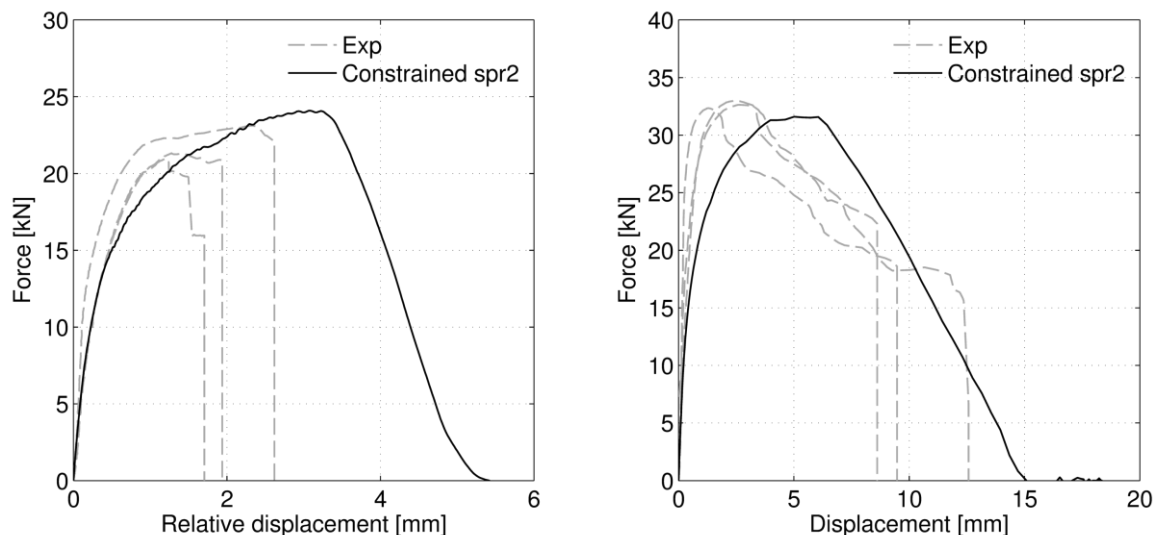


Fig.2: Simulations of T-component tests with *\*CONSTRAINED\_SPR2* for short (left) and long (right) screws.

## Literature

- [1] Sommer, S., Maier, J.: "Failure modeling of a self piercing riveted joint using ls-dyna", 8<sup>th</sup> European LS-DYNA conference, 2011
- [2] Hanssen, A. G., Olovsson, L., Porvaro, R., Langseth, M.: "A large-scale finite element point-connector model for self-piercing rivet connections", *European Journal of Mechanics A/Solids*, 29.4, 2010, 484-495
- [3] Bier, M., Sommer, S.: "Simplified modeling of self-piercing riveted joints for crash simulations with a modified version of *\*CONSTRAINED\_INTERPOLATION\_SPOTWELD*", 9<sup>th</sup> European LS-DYNA conference, 2013
- [4] Sønstabø, J. K., Holmstrøm P. H., Morin, D., Langseth, M.: "Macroscopic strength and failure properties of flow-drill screw connections", *Journal of Materials Processing Technology*, 222, 2015, 1-12



**MATERIALS II**  
**ENDLESS FIBER**



# Textile and Composite Modelling on a Near Micro-Scale: Possibilities and Benefits

Oliver Döbrich<sup>1</sup>, Thomas Gereke<sup>1</sup>, Chokri Cherif<sup>1</sup>

<sup>1</sup>Institute of Textile Machinery and High Performance Material Technology,  
Technische Universität Dresden, Germany

Textile materials are increasingly used in civil engineering for the purpose of reinforcing high performance composites, acting as membranes or fulfil technical tasks like filter contaminated media. Therefore, the demand for accurate numerical models which are able to predict the textile mechanics and the forming behaviour of dry and consolidated textiles is increasing and the requirements on the models accuracy and fineness rises. Many numerical models have been introduced in the literature for the different levels of objectivity. These levels are shown in Figure 1. For macro-scaled models, complex material models have been carried out to account for the various deformation mechanisms and the anisotropic mechanic of textile fabrics. For meso- or micro-scaled models, the quality of the geometrical model is mainly influencing the simulation results. The quality of a numerical simulation in general strongly depends on the models accuracy. Therefore, providing an accurate model is the key factor for a successful simulation. For textile micro-scale modelling, the digital-element approach was introduced to account for the typical behaviour of technical multifilament yarns [1].

In this paper, methods for the unit-cell generation of textile models as well as composite models are presented for a near micro-scale resolution. The application of the digital-element approach with LS-DYNA® is explained. Possibilities and benefits of structural analysis on the micro-scale as well as challenges in using digital-elements are shown and discussed. Convergence examinations on the models fineness are carried out and the results of optical validations are shown. The method of Lagrange-coupling, which is implemented in LS-DYNA, is used to model a textile reinforced composite. The use of the keyword: \*CONSTRAINED\_LAGRANGE\_IN\_SOLID, is discussed and results of the micro-scale composite analysis with LS-DYNA are given.

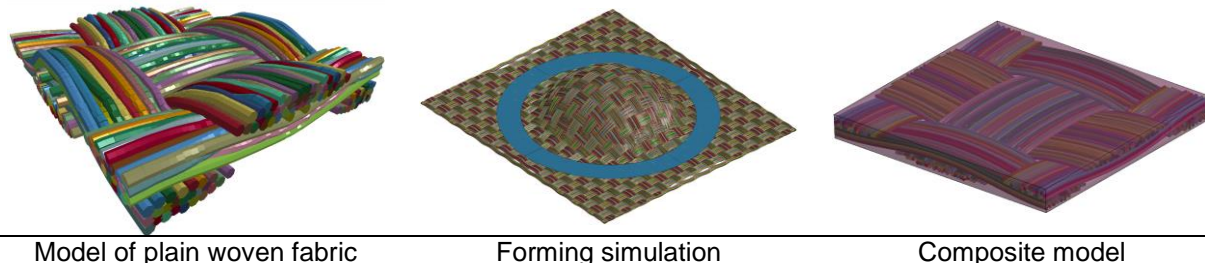


Fig. 1: Examples of textile and composite models in a near micro-scale resolution

## References:

- [1] Wang, Y.; Sun, X.: Digital-element simulation of textile processes, Compos. Sci. Technol., 61(2001)2, pp. 311-319, ISSN 0266-3538

# Micro-Meso Draping Modeling of Non-Crimp Fabrics

Oleksandr Vorobiov<sup>1</sup>, Dr. Th. Bischoff<sup>1</sup>, Dr. A. Tulke<sup>1</sup>

<sup>1</sup>FTA Forschungsgesellschaft für Textiltechnik mbH

Composite materials with textile reinforcements are showing rapid growth of integration in aerospace, automotive, sport and other industrial sectors. Especially non-crimp fabrics (NCF) are widely spread because of their high drapeability and good in-plane mechanical properties in main fibre directions. For prediction of mechanical response of composite parts in particular with high curvature it is important to consider the local orientations and gaps in textile structures obtained after draping. Draping simulations are performed on meso-scale structure for this reason. This requires both the geometrical and mechanical properties of the textile components.

For determination of the glass roving mechanical properties the microscale simulations were performed for three load cases: transverse compaction, torsion and shear. These results were directly transferred in developed user material model for corresponding filament misalignment rate and compared with the experiment. Results are showing very good agreement both for compression force and for width change (Figure 1).

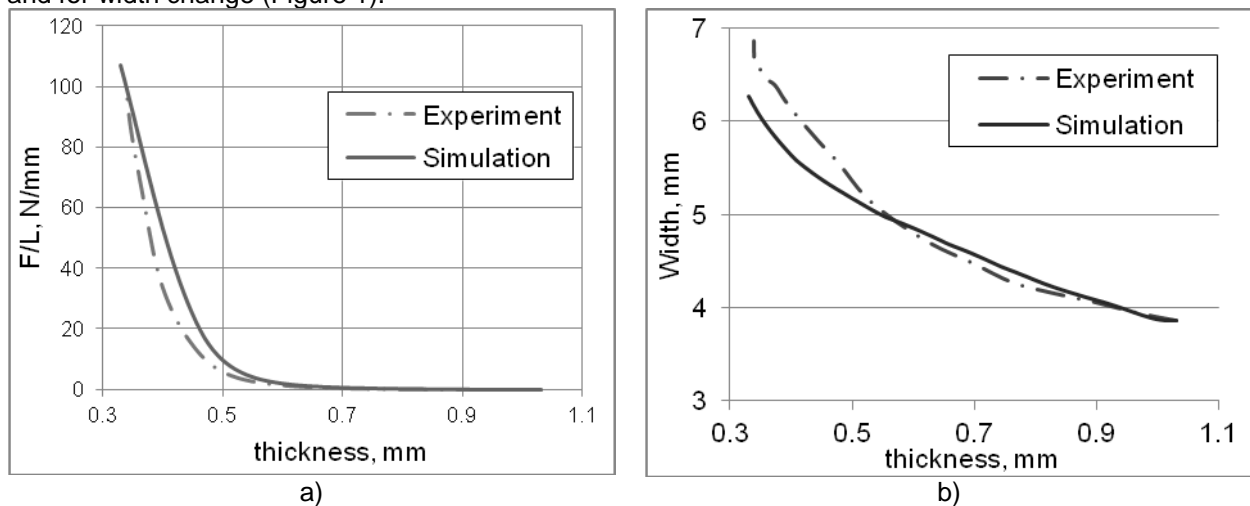


Fig.1: Comparison of the experimental and simulation results for roving compaction: a) compaction force per unit length and b) roving width versus roving thickness.

The representative volume elements (RVE) of the leno-woven NCF with different levels of the refinement were developed using the combination of the developed material model with the transverse thermal expansion as shown in the Figure 2 and 3. This allows to consider the local fibre volume fraction (FVFr) of the elements.

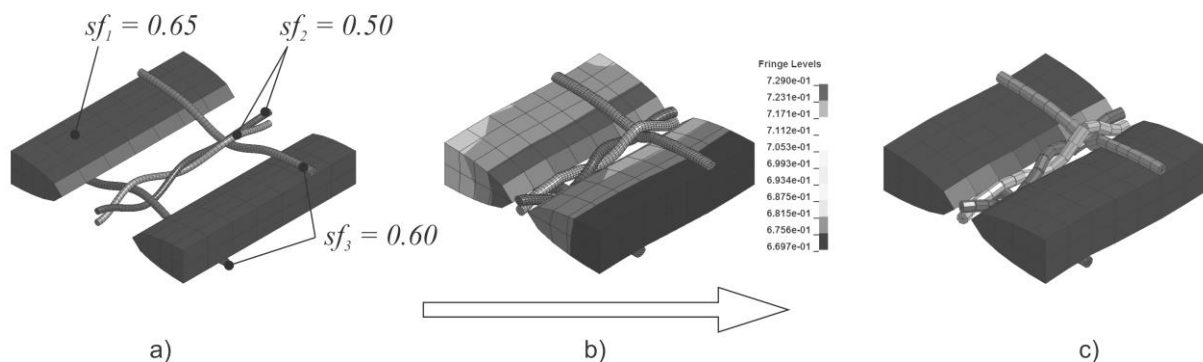


Fig.2: RVE of the leno-woven NCF for draping simulation: a) initial conditions, b) after thermal expansion simulation with calculated local FVFr and c) auxiliary yarns are represented as beams.



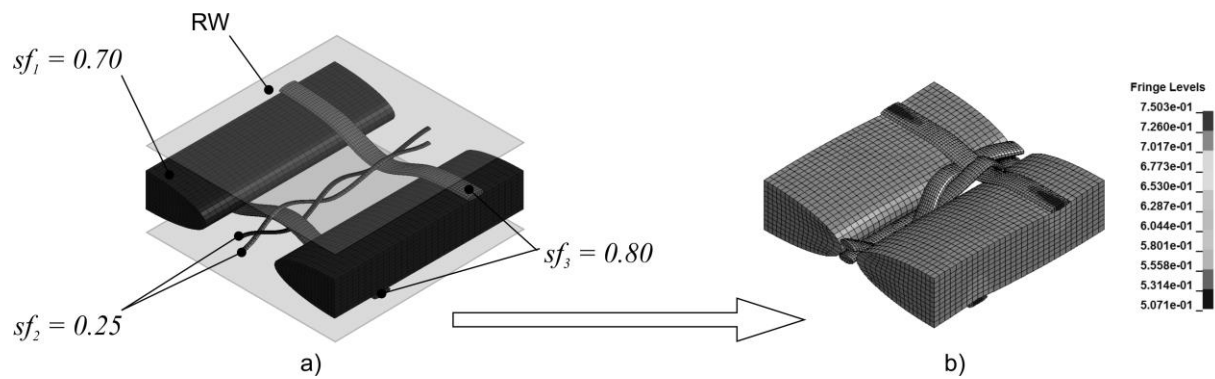


Fig.3: RVE of the leno-woven NCF for calculation of the mechanical properties: a) initial conditions, b) after thermal expansion simulation with calculated local FVFs.

Generated RVEs were used for draping simulations and estimation of the mechanical properties in composite structure.

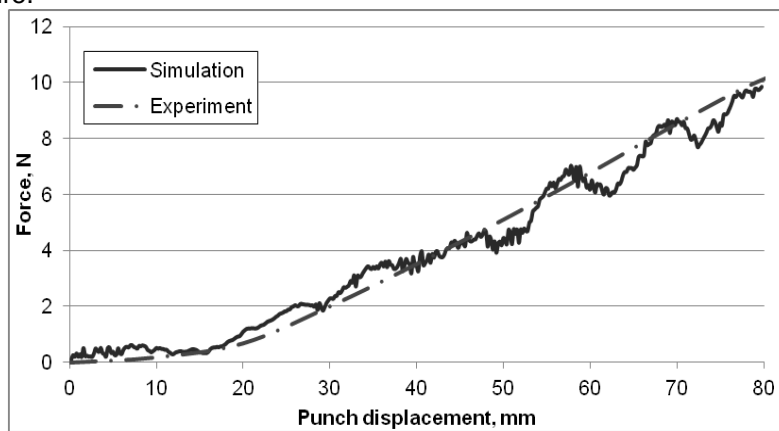


Fig.4: Punch force versus punch displacement obtained from simulation and experiment.

The forming force obtained from simulation converges very well with measured experimentally (Figure 4). Also the local orientations of the textile are showing good agreement.

Error in estimation of the composite mechanical properties using implemented in LS-Dyna mesh superposition technique lies below 4% for leno-woven NCF.

# Numerical Investigation of Carbon Braided Composites at the Mesoscale: using Computer Tomography as a Validation Tool

Mathieu Vinot<sup>1</sup>, Martin Holzapfel<sup>1</sup>, Raouf Jemmal<sup>1</sup>

<sup>1</sup> Institute of Structures and Design, German Aerospace Center, Stuttgart

## 1 Motivation

So far analytical and, to a lesser extent, numerical approaches have been limited in their capabilities to predict the properties of braided composites due to the high complexity of the rovings' interlacing. While many analytical theories have been developed to estimate the stiffness of braided composites, only few models tried to describe the behaviour up to the global failure. As part of the research campus ARENA2036 [1], which groups together partners from the industry and research facilities, the DigitPro (Digital Prototype) project aims to develop a closed process chain for the manufacturing of braided composite parts including, amongst others, braiding, draping and infiltration simulations as well as virtual material tests (*Figure 1*). The objective of the present study is to develop a prediction tool for the material characterisation of braided composites and to validate the methodology with experimental tests on a 60°-biaxial braid.

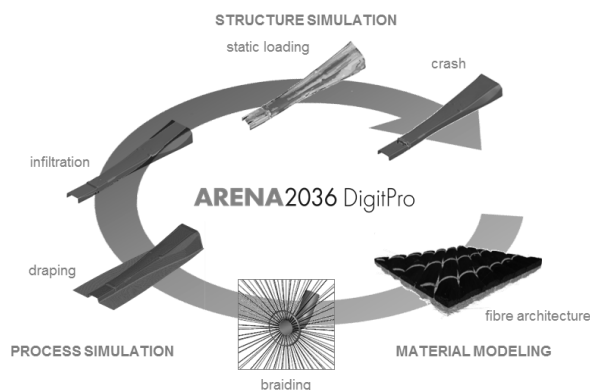


Figure 1: Process chain for braided textiles in DigitPro

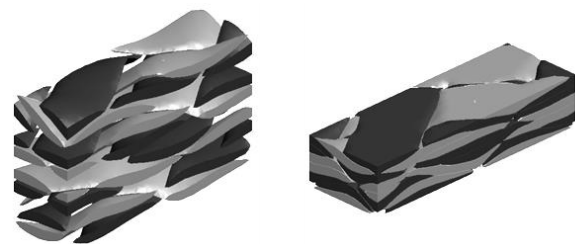


Figure 2: Dry fibres FE-model before (left) and after (right) the compaction

## 2 Simulation

The numerical material characterisation requires the generation of an idealised geometrical model (Representative Volume Element, RVE) using the open-source software TexGen [2]. In order to increase the fibre content, the dry fibre's compaction is simulated using the Finite Element Method in LS-DYNA (*Figure 2*) based on the work of G. Grail [3]. After the creation of the matrix mesh periodic boundary conditions are applied using the command `*CONSTRAINED_MULTIPLE_GLOBAL`. Simulations under tension, compression and shear loads are performed to predict the mechanical properties. The material models `*MAT124` and `*MAT261` are used for the matrix and the rovings respectively. `*MAT261` takes into account several failure mechanisms in composites (matrix and fibre failure under tensile, compressive and shear loads) and implements a non-linear response in the shear direction. The material properties of the rovings are estimated based on the theory of Chamis [4] and material datasheets.

## 3 Testing

In order to validate the numerical simulation chain, in-situ CT-scans are performed on a 60°-biaxial carbon braid. To this end, a mechanism was developed at the DLR, which makes it possible to investigate the geometry of the rovings and their deformation under load and avoids perturbations due to the fixture mechanism [5]. The coupon is loaded in steps of 1 kN up to global failure. The quasi-static response is obtained from a separate tensile test performed at a speed of 1 mm/min.

The roving's interlacing resulting from the compaction simulation is in good agreement with the structure captured with the CT-scans. Features like matrix-rich zones were successfully simulated. 2D views of the scan and of the simulation are given in *Figure 3* and *Figure 4*. The numerical compaction increases the overall fibre content from 35% to 54% while the experimental value lies at 61%.

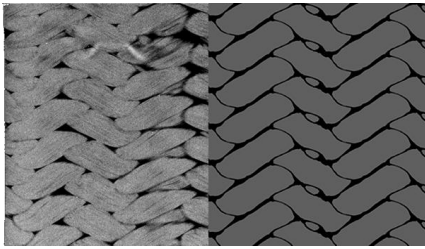


*Figure 3: Comparison of the in-situ (left) and simulated (right) 60°-biaxial braid*

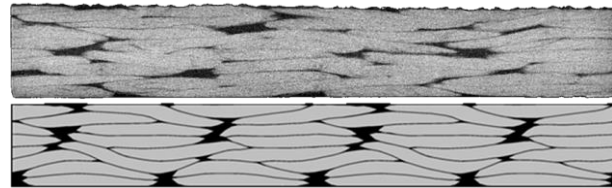


*Figure 4: Comparison of the in-situ (top) and simulated (bottom) 60°-biaxial braid*

Figure 5 shows the numerical response of the simulated 60°-biaxial braid in comparison with the experimental results. Considering the scatter in the experimental results and the uncertainty of the roving's calculated properties, the simulated mechanical properties and the experiment are in good agreement (Table 1). The use of the material **\*MAT261** allows for an accurate simulation of the braid's failure and post-failure behaviour.

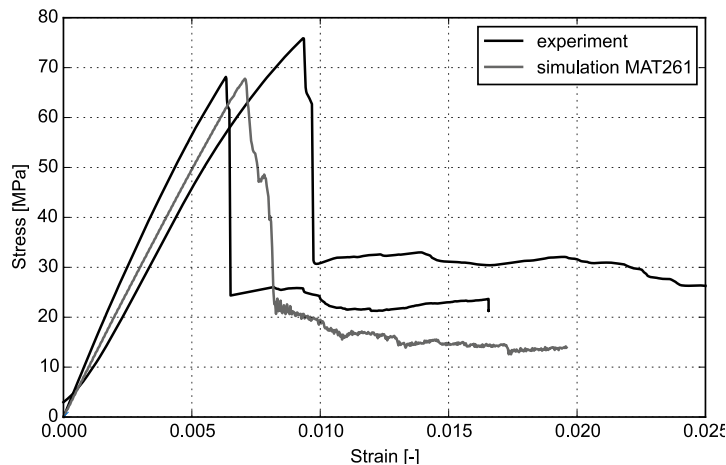


*Figure 5: Simulated quasi-static response of a 60°-biaxial braid under tension compared to the experiment*

	exp.	sim.
$E_{11}$ [GPa]	10.5	10 (-5%)
$\sigma_{11}$ [MPa]	72	67.8 (-6%)
$\epsilon_{11}$ [%]	0.77	0.71 (-8%)

*Table 1: Comparison of the mechanical properties of a 60°-biaxial braid*

## 4 Summary and outlook

It has been shown that simulating the compaction of the dry rovings results in an accurate representation of the rovings' interlacing in the braided textile. The numerical model of a 60°-biaxial braid appears to be in good agreement with the rovings' structure captured in the CT scans. Moreover, the material model **\*MAT261** turns out to be the best solution for modelling orthotropic carbon rovings. The determination of roving properties must, however, be improved and further validation and testing is required. A multiscale strategy will be developed as part of the next project steps in order to transfer the braid's properties to a macroscopic scale for crash simulation.

## 5 Literature

- [1] <http://www.arena2036.de/de/>, 2. April 2015.
- [2] H. Lin, L. P. Brown and A. C. Long, Modelling and Simulating Textile Structures using TexGen, *Advances in Textile Engineering*, Vol. 331, 44-47, 2011.
- [3] G. Grail, *Approche multimodèle pour la conception de structures composites à renfort tissé*, 2013.
- [4] C. C. Chamis, *Mechanics of Composite Materials: Past, Present, and Future*, 1984.
- [5] R. Jemmali, *Quantitative Bewertung von Verbundwerkstoffen auf der Basis von tomographischen Bildern*, 2014.

# Modeling of Thick UD Composites for Type IV Pressure Vessels

Ralf Matheis<sup>1</sup>, Helmi Murnisya<sup>1</sup>, Thomas Johansson<sup>2</sup>

<sup>1</sup>Forschungsgesellschaft Krafftahwesen mbH Aachen

<sup>2</sup>DYNAmore Nordic AB

## 1 Introduction

The project MATISSE funded by European Commission's 7<sup>th</sup> Framework Programme aims to make a significant step forward in the capability to model, predict and optimise the crash behaviour of mass produced fibre reinforced polymers (FRP). One of the project's main research goals is a general virtual testing methodology (VTM) for the development of storage systems for compressed natural gas (CNG) made of wound carbon FRP as well as glass FRP with polymeric liners and metallic bosses.

## 2 Modelling approach

As part of the VTM a modelling approach for the dynamic loading behaviour of a reference tank structure was developed. Each sub-component of the tank was modelled appropriately. For the aluminium bosses a rigid model in combination with solid elements was chosen; the polymeric inner liner was modelled elastically with a shell mesh. The modelling of wound FRP layers was considered to be the essential part of the tank model. Thus, special focus was set on the corresponding approach. For these structures the LS-DYNA material model **\*MAT\_LAMINATED\_FRACTURE\_DAIMLER\_CAMANHO** (**\*MAT\_262**) was chosen. This orthotropic continuum damage model for laminated fibre reinforced composites is based on the work of Maimí, Camanho, Mayugo and Dávila [1]. It is a constitutive model whose failure criteria are derived from physical findings and it considers simplified non-linear in-plane shear behaviour [2]. It uses maximum stress criteria in a plane stress assumption and a constant fibre misalignment instead of fibre kinking. The failure surfaces are not controlled by the model but assumed to be constant. It is implemented for solid, shell and thick shell elements [3]. Furthermore, in order to accurately model the winding structure and to consider delamination as well, a so-called combined stacked and layered thick shell (t-shell) approach was applied. This comprises t-shell elements as well as solid decohesive elements with a special decohesive material model.

## 3 Material validation approach

Because of a lack of availability of significant test specimens or respectively test procedures to estimate the material values for the FRP structure a so-called reverse FEM approach was applied in order to validate the material models for the wound CFRP and GFRP materials. This comprised the testing and simulation of tubes with representative winding structures to validate a number of calculated, researched and assumed material values. Furthermore, a set of test procedures was carried out on the virtual level in order to monitor the plausibility of the material behaviour. Additionally the material model for the liner was validated on the basis of a three point bending test (3PB). For the validation of the decohesive model no test results were available and consequently the validation of the model was done theoretically. Therefore, force deflection curves of the simulation of two test procedures considering the delamination mode I (opening delamination) and mode II (shear forward delamination) and curves calculated using fundamental mechanic assumptions were compared. All sub-component models were combined in a full tank model (see Fig.1).



Fig.1: Full tank model (sectional view)

#### 4 Tank validation approach

Furthermore, several tests on the tank level were conducted that are based on the tank's operating conditions and on potential impact conditions derived from full vehicle crash scenarios.

In order to validate the full tank model, evaluations and comparisons of the conducted tests and their virtual counterparts are currently ongoing. Special focus is set on the accurate evaluation of material damage of the wound layers.

In a final step a simplification of the complex model is currently carried out, allowing an application in a full vehicle simulation with reasonable simulation costs. For this reason an iterative simplification procedure is applied.

#### 5 ACKNOWLEDGEMENT

All the presented work was carried out within the project MATISSE funded by European Commission's 7<sup>th</sup> Framework Programme.

The authors would like to acknowledge the MATISSE partners Xperion Energy & Environment GmbH and Centro Ricerche Fiat S.C.p.A. for the collaboration since the very beginning of the project.

#### 6 Literature

- [1] Maimi, P., Camanho, P., Mayugo, J., Davila, C.; "A continuum damage model for composite laminates: Part II – Computational implementation and validation"; *Mechanics of Materials*; Iss.: 39; 2007; pp. 909-919
- [2] N.N.; "LS-DYNA Keyword User's Manual - Volume II Material Models"; Revision 3372 (Draft); Livermore Software Technology Corporation; 2013
- [3] Hartmann, S.; "Neue Materialmodelle für Composites in LS-DYNA; Infotag: Composite Berechnung mit LS-DYNA"; 2013



**MATERIALS III**  
**SHORT/LONG FIBER**





# Digmat Material Model for Short Fiber Reinforced Plastics at Volvo Car Corporation

Mats Landervik<sup>1</sup>, Johan Jergeus<sup>2</sup>

<sup>1</sup>Dynamore Nordic AB

<sup>2</sup>Volvo Car Corporation

The paper concerns a study of the potential of using the Digmat material model [1] for modeling injection molded reinforced plastics at Volvo Car Corporation. The material model is based on micromechanics and it comprises models for the fiber- and matrix materials, the microstructure and the homogenization of the microscopic response. For the present applications however, the so-called Hybrid solution method is employed. It means that the microscale models are replaced by a macroscale model with its parameters determined from the microscale parameters in a preprocessing step. The result is a macroscopic model dependent on the local distribution of fiber orientations. The model is here applied to injection molded reinforced plastics components and Moldflow is used to simulate the production process and provide predictions of the fiber orientation throughout the part.

Digmat has interfaces to the major CAE codes and in the present work, LS-DYNA and Abaqus have been used. The present study includes strength, crash, thermal creep and fatigue analyses. However, only strength and crash analyses are covered in the paper since by the time of writing, thermal creep simulations have not been finished and fatigue is an ongoing thesis project [2]. The aim has been to explore the potential of the model terms of predictability, computational cost, material test and process data requirements. Easy access of material parameters is highly desirable since the time from material specification to CAE input is critical in a CAE-driven product development process.

A brief description of the applied models as well as the calibration procedure is included in the paper. For application of the material model, a pre-production version of a front end carrier (FEC) for the new Volvo XC90 model was chosen to be studied. It is made from Lanxess Durethan BKV 30 (PA6 reinforced with 30% glass fiber). Simulation of two quasistatic loadcases and two dynamic loadcases with a Digmat model has been done yielding a good correlation with experimental results. There is potential to improve the confidence in the material parameters and possibly its predictions with a more complete set of test data and also measurement of the orientation in the material test specimens. Furthermore, there is a need to enhance the failure model to account for different failure levels in tension and compression which would be accompanied by the need of additional test data.

For strength analysis, the improvement of the accuracy of the predictions of stiffness and failure load is substantial compared to an isotropic Abaqus model with a maximum allowed strain as design guideline. There is also a decrease in simulation time when using the Digmat model in the particular case since the increased convergence rate overcomes the increased time per iteration. However, there is demand for additional material and process data for an anisotropic Digmat simulation compared to standard isotropic materials. Additionally, anisotropic simulations in general require predictions of fiber orientations. For crash analysis, a direct comparison of Digmat to CrachFEM [3] was not possible since the available CrachFEM model is isotropic and represents a material different from the one in the component. Running the anisotropic Digmat model for only one component in a full scale pedestrian impact loadcase yields an increase of simulation cost of about 7% compared to keeping the original isotropic CrachFEM model.

## Literature

- [1] DIGIMAT: [www.e-xstream.com](http://www.e-xstream.com)
- [2] Lindhult, J-A, Ljungberg, M: Fatigue Analysis of Anisotropic Short Fibre Reinforced Polymer by Use of Digmat and nCode DesignLife (*In preparation*), Chalmers University of Technology, 2015
- [3] CrachFEM: [www.matfem.de](http://www.matfem.de)

# Simplified Integrative Simulation of Short Fibre Reinforced Polymers under Varying Thermal Conditions

Christian Witzgall<sup>1</sup>, Sandro Wartzack<sup>1</sup>

<sup>1</sup>Chair of Engineering Design KTmfk  
University of Erlangen-Nuremberg FAU, Germany

## 1 Introduction

Short fibre reinforced polymers (SFRPs) are increasingly applied in part design within the modern automotive industry due to their low density and outstanding mechanical properties. Additionally, injection moulding is an economic process to produce parts in large quantities. However, the distribution and orientation of fibres within the components are heavily dependent on the moulding process and the material behaviour is characterised by numerous effects like non-linearity, plasticity and strain-rate as well as temperature dependency. Therefore, it can be considered challenging to predict the mechanical behaviour of parts made of SFRPs by simulation. Meaningful results can only be achieved by coupling an injection moulding and a structural simulation – the so called integrative simulation. To make these integrative simulation methods accessible in early design stages, when a quick estimation of the structural behaviour is required, Gruber and Wartzack developed a simplified approach, called Integrative Simulation 4 Early Design Steps (IS4ED). It considers the material's anisotropy by using the fibre orientation data gained from the injection moulding simulation. By reducing the complexity of the orientation condition and the material representation, a simulation approach suitable for early design stages was created. [1]

However, within the IS4ED-approach the influence of high or low temperatures on material behaviour is not considered. As thermoplastic matrix materials are sensitive to changes in temperature, IS4ED has to be enhanced. The decreases of stiffness and maximum stress levels as well as the increase of maximum strain at elevated temperatures have to be added to the approach. Within automotive applications, structural parts may be exposed to a temperature range from -40 °C up to 100 °C [2]. At these temperatures, the fibre-supporting properties of the thermoplastic matrix material decline, which especially affects compressive loading. Still, occupant safety has to be maintained even at extreme conditions. As it seems likely that anisotropy influences the temperature-dependency, relevant changes to the part can only be taken within the early design stages. Therefore, the basic concept of IS4ED still remains the same.

## 2 Characterisation results

Fig.1: displays the results of tensile tests with varying testing conditions. Plot (a) and (c) display a set of tests performed at the lowest testing speed, 0.01 m/s and at seven temperatures (-20, 0, 23, 40, 60, 80 and 100 °C). Plot (b) and (d) show tests performed at room temperature (23 °C) with four different testing speeds (0.01, 0.5, 2 and 4 m/s) and accordingly, strain rates. The tests for (a) and (b) were performed with orthogonal fibre orientation, (c) and (d) with parallel fibre orientation respectively.

Although plots (b) and (d) are taken from tests with the same nominal velocity, it is conspicuous that the strain rates for all tests with orthogonal fibre orientation are higher than with parallel fibre orientation. Two reasons can be named for that: firstly, the actual piston speed is not constant during the test. Instead, its speed is slightly lower for specimen with parallel fibre orientation as, due to the higher specimen stiffness, the piston is decelerated stronger. Secondly, even with identical piston speed and displacement, the lower stiffness of orthogonally oriented specimen leads to higher strains and thus, higher strain rates. This can be confirmed by virtual tensile tests [3].

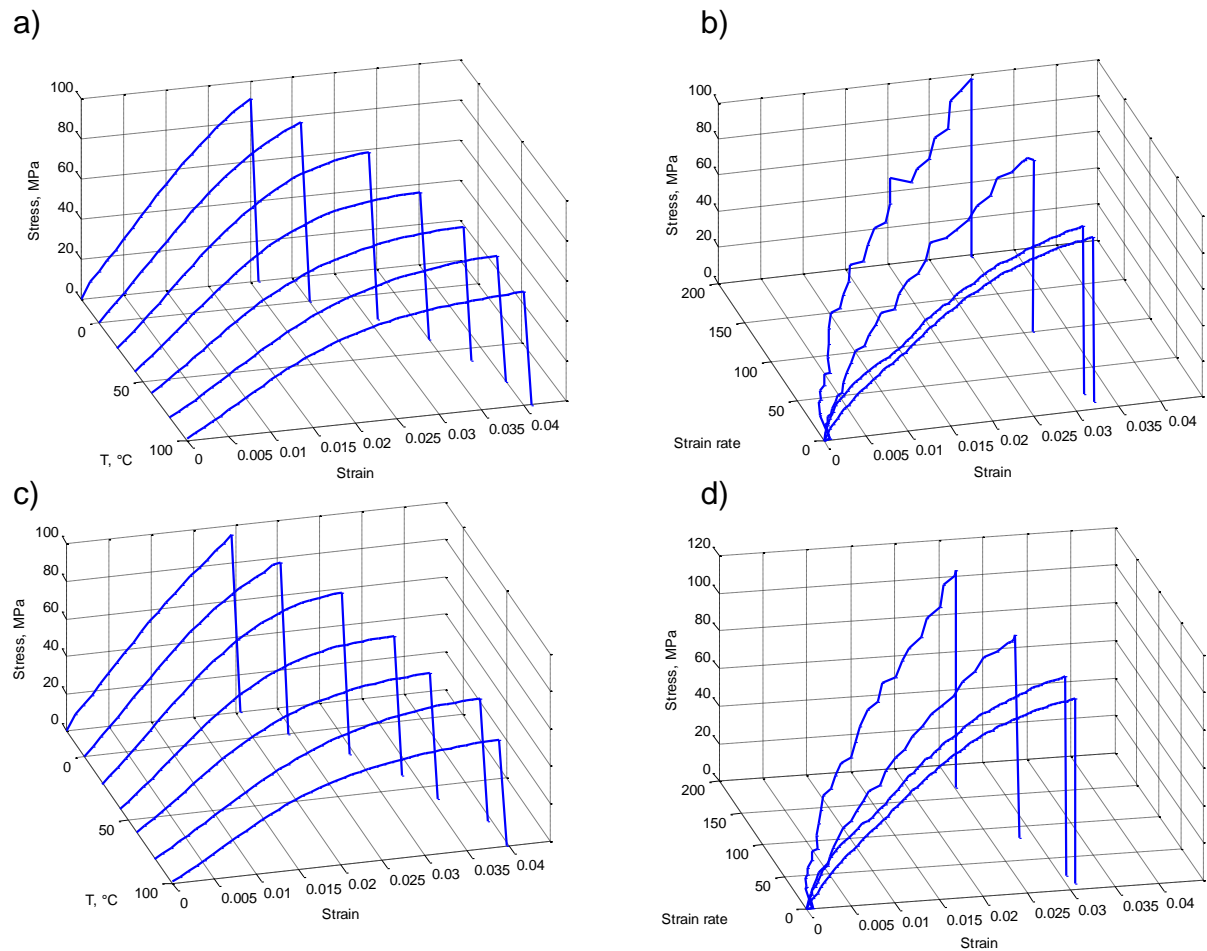


Fig.1: Stress-strain curves over temperature and strain rate

### 3 Literature

- [1] Gruber, G.; Wartzack, S.: "Evaluierung der orientierungsbezogenen Leichtbaugüte", Lightweight Design, No. 5/2013, pp. 18-23.
- [2] Dehn, A.: "Experimentelle Untersuchung und numerische Simulation des Crashverhaltens gewebeverstärkter Thermoplaste unter Temperatureinfluss". PhD-Thesis, TU Kaiserslautern, 2001.
- [3] Gruber, G.: "Ein Beitrag zur rechnerunterstützten Auslegung crashrelevanter kurzfaserverstärkter Kunststoffbauteile in der frühen Entwurfsphase", PhD-Thesis, University of Erlangen-Nuremberg, 2014.

# Recent Enhancements on Short-Fiber Reinforced Plastics Modeling in LS-DYNA

Christian Liebold<sup>1</sup>, Andrea Erhart<sup>1</sup>

<sup>1</sup>DYNAmore GmbH, Stuttgart, Germany

## 1 Motivation

A constitutive model for the simulation of the behavior of short-fiber reinforced plastics is currently being realized in LS-DYNA associated with an appropriate data mapper for LS-DYNA. Homogenized anisotropic and if needed locally varying effective elastic properties of SFRP can thus be determined and provided for structural analysis of SFRP components.

As a preprocessing step a simulation of the molding process could be performed. The resulting fiber orientation and fiber content information of the molding simulation model can be transferred to the structural analysis model through a data-mapper. This data mapper exports the appropriate information as `*INITIAL_STRESS_SOLID` card for each integration point of the structural analysis model. Using this information, locally homogenized anisotropic elastic material properties are computed and provided or directly used for a structural analysis.

## 2 Data Mapping

In order to properly consider the anisotropy within the finite element analysis, the results from previously run infiltration simulations have to be mapped onto the crushing mesh. Standard output data of such simulations are either the 2<sup>nd</sup> order fiber orientation tensor or the two main axis (eigenvectors) of this orientation tensor with the according eigenvalues. During the mapping, it has to be considered that the number of integration points and the discretization between the source mesh being used for the infiltration simulation usually differs from the one being used for the finite element analysis and therefore, data have to be homogenized. Figure 1 shows a box with an initialized main fiber orientation using `*ELEMENT_SHELL_COMPOSITE`. The example is taken from [14].

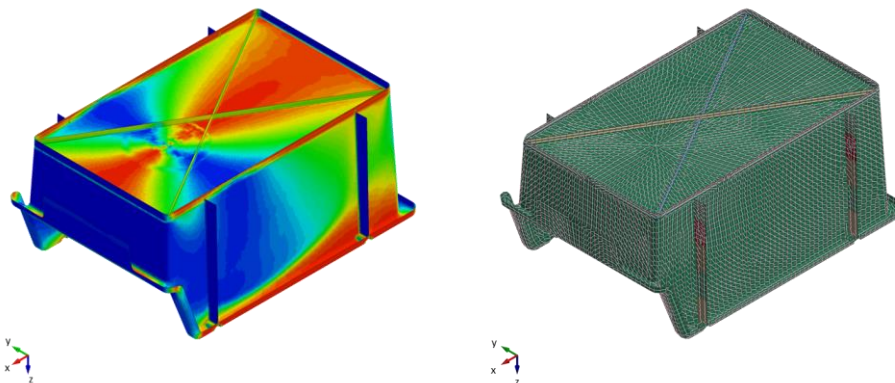


**Figure 1:** mapping of fiber orientation tensor's main axis from an infiltration mesh onto a crushing mesh.

## 3 Constitutive Formulation

Nice overviews over analytical homogenization techniques of heterogeneous materials are given in Mura [10] or the PhD-thesis of Lusti [6], Mlekusch [7], Radtke [12].

For non-aligned short fiber reinforced composites, the homogenization procedure to determine the equivalent elastic properties can be realized as a two-step process, see for example Dray et al. [2]:

First, the homogenized properties of an aligned fiber-reinforced composite with appropriate fiber geometry, content and fiber and matrix elastic properties have to be estimated. This can be done

analytically based on Eshelbys equivalent inclusion method [4] and Mori & Tanakas double inhomogeneity model [9]. Based on these publications various analytical homogenization models have been established (see for example Dvorak [3]).

For the case of transversal isotropic composites with higher fiber content Tandon & Weng [13] derived equations for the equivalent elastic properties. Another frequently used approach is the semi-empirical approximation of Halpin & Tsai (see Halpin et al. [5]).

As a second step, an orientation averaging is performed, i.e. the fact, that we are not dealing with an aligned composite, but with short fibers, with locally varying orientation distribution is taken into account. Following the publication of Advani & Tucker [1], this orientation averaging can be conducted using the fiber orientation tensors 2<sup>nd</sup> and 4<sup>th</sup> order. To this end a closure approximation of the usually unknown orientation tensor 4<sup>th</sup> order, based on the given 2<sup>nd</sup> order orientation tensor is needed. Various assumptions for determining closure approximations are given in the literature and a comparison of the accuracy of different closure approximations is for example given in Dray et al. [2].

#### 4 Literature

- [1] Advani, S. G., Tucker, C. L., Journal of Rheology, The Use of Tensors to Describe and Predict Fiber Orientation in Short Fiber Composites, 31 (8), 1987, 751-784.
- [2] Dray, D., Gilormini, P., Regnier, G., Composites Science and Technology, Elsevier, Comparison of several closure approximations for evaluating the thermoelastic properties of an injection molded short-fiber composite, 2007, 1601-1610.
- [3] Dvorak, G., Micromechanics of Composite Materials, Springer Heidelberg, 2013.
- [4] Eshelby J. D., Proc. R. Soc. Lond., The determination of the elastic field of an ellipsoidal inclusion, and related problems. A241, 1957, 376-396.
- [5] Halpin, J. C., Kardos, J. L., Polym. Eng. Sci., The Halpin-Tsai Equations: A Review, 16, 1978, 344-352.
- [6] Lusti, H. R., Property Predictions for Short Fiber and Platelet Filled Materials by Finite Element Calculations, PhD-thesis, Swiss Federal Institute of Technology - ETH Zürich, 2003.
- [7] Mlekusch, B., Kurzfaserverstärkte Thermoplaste Charakterisierung und Messung der Faserorientierung, thermoelastische Eigenschaften sowie Schwinden und Verzug, PhD-thesis, Institut für Konstruieren mit Kunst- und Verbundstoffen - Montanuniversität Leoben, 1997.
- [8] Mlekusch B., Comp. Sci. Technol., Thermoelastic properties of short-fibre-reinforced thermoplastics, 59, 1999, 911-923.
- [9] Mori, T., Tanaka, K., Acta Metallurgica, Average Stress in Matrix and Average elastic Energy of Materials with misfitting Inclusions, 21, 1973, 571-574.
- [10] Mura, T. Micromechanics of defects in solids, Martinus Nijhoff Publishers, Boston, 1987.
- [11] Pierard, Friebel, Doghri, I., Composites Science and Technology, Mean-field homogenization of multi-phase thermo-elastic composites: a general framework and its validation, 64, 2004, 1587–1603.
- [12] Radtke, A., Steifigkeitsberechnung von diskontinuierlich faserverstärkten Thermoplasten auf der Basis von Faserorientierungs- und Faserlängenverteilungen, PhD-thesis, Institut für Kunststoffprüfung und Kunststoffkunde, Universität Stuttgart, 2009.
- [13] Tandon G. P., Weng G. J., Comp. Sci. Technol., Average stress in the matrix and effective moduli of randomly oriented composites, 27, 1986, 111-132.
- [14] Jennrich, R., Roth, M., Kolling, S., Liebold, C., Weber, G., Experimental and Numerical Analysis of a Glass Fiber Reinforced Plastic, 13. LS-DYNA Forum, Bamberg, 2014.

# Short and Long Fiber Reinforced Thermoplastics – Material Models in LS-DYNA

S. Hartmann<sup>1</sup>, T. Erhart<sup>1</sup>, A. Haufe<sup>1</sup>, P. Reithofer<sup>2</sup>, B. Jilka<sup>2</sup>

<sup>1</sup>DYNAmore GmbH  
<sup>2</sup>4a engineering GmbH

In the last years the demand on weight reduction in the automotive industry has led to a strong interest for various composite applications. Due to the complexity of those usually highly anisotropic materials virtual product development is one of the key factors to understand the load carrying behavior of such parts. Furthermore enhanced CAE tools and models are necessary to ensure an efficient and robust product development.

Especially fiber size and geometry have a significant influence on the part performance. Orthotropic properties increase with increasing fiber content while at the same time the effect of strain rate diminishes due to the lesser content of matrix material (fig. 1).

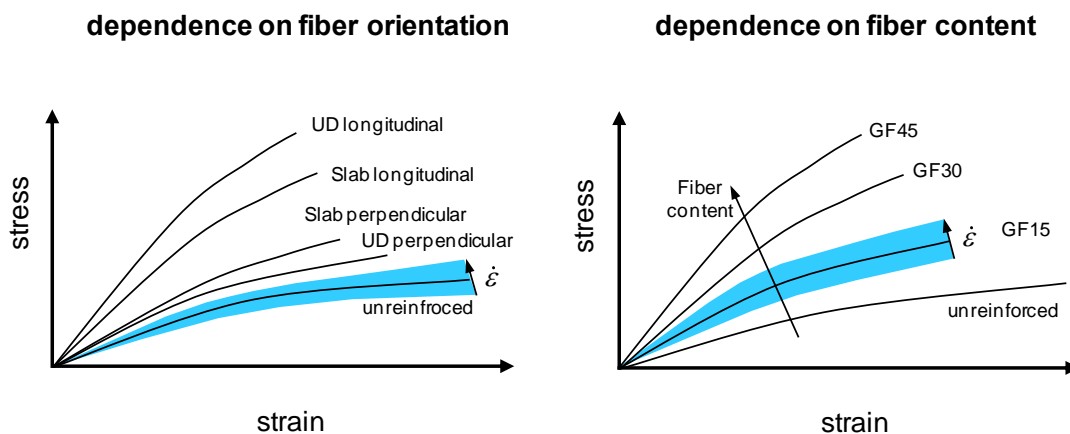


Fig. 1: Influence of fiber orientation, content and strain rate on the stress-strain-behavior

LS-DYNA offers a great number of constitutive models for anisotropic materials. These models are able to consider anisotropic influences to some extent (e.g. \*MAT\_002, \*MAT\_022, \*MAT\_054/055, MAT\_058, \*MAT\_103, \*MAT\_108, \*MAT\_157, ...). The aforementioned currently available constitutive models may not be able to fulfil all of the many effects and requirements to describe the real material behavior, however most of these models are well suited to resemble the main anisotropic influence of the fiber reinforcement.

In the present contribution the principal behavior of different constitutive models and their individual advantages and disadvantages is discussed by one-element tests (see fig 2 for uniaxial loading in tension). Based on dynamic 3-point-bending test results, conducted on the 4a impetus pendulum, samples loaded in different directions were investigated. The influence of the fiber orientation distribution across the thickness is shown and discussed.

Furthermore 4a has developed a user material in LS Dyna, based on micro-mechanics. Results and a comparison to classical material models are presented.

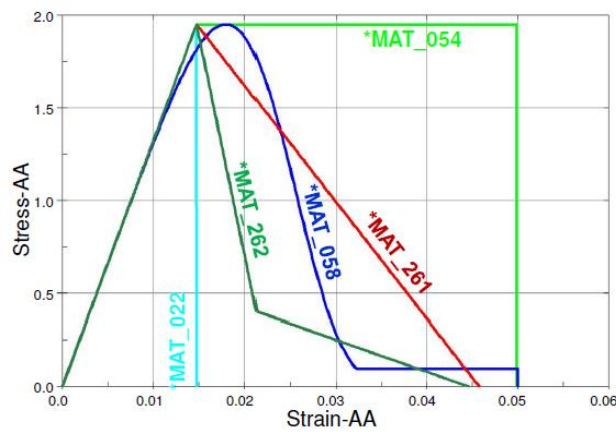


Fig.2: Some anisotropic material models and their stress-strain-behavior in 1-element-tests

Newly implemented features in LS-DYNA, 4a micromec and 4a fibermap that are able to consider the effects of process induced fiber orientation (e.g. due to injection moulding during production) are shown. A discussion focusing on the benefits of their application within the simulation process chain (fig. 3) is added. Finally an overview of current developments and an outlook to future work is given.

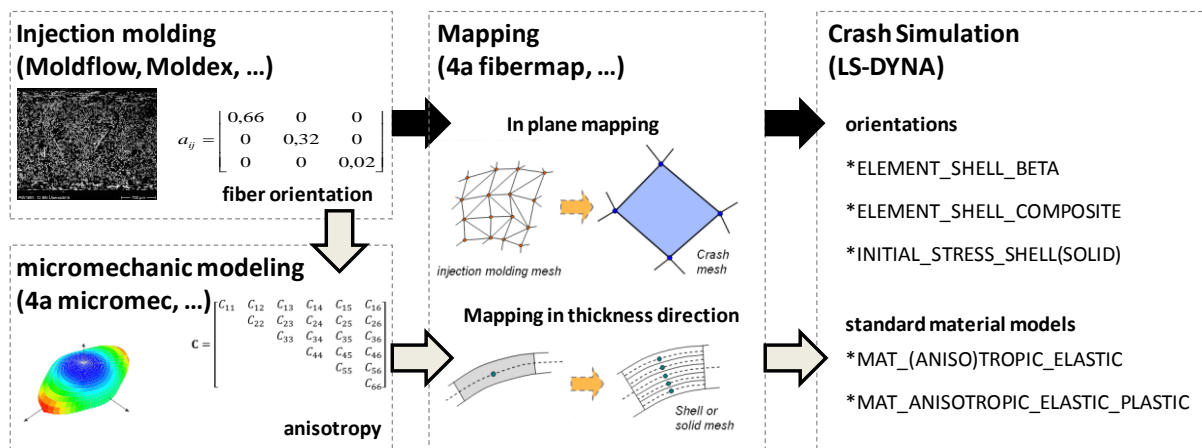


Fig.3: Available simulation process chain for injection molded parts





**MATERIALS IV**  
**ADHESIVES/FAILURE**



# Strain-Rate Dependant Damage Material Model of Layered Fabric Composites with Delamination Prediction for Impact Simulations

Sylvain Treutenaere<sup>1</sup>, Franck Lauro<sup>1</sup>, Bruno Bennani<sup>1</sup>, Tsukatada Matsumoto<sup>2</sup>, Ernesto Mottola<sup>2</sup>

<sup>1</sup>University of Valenciennes and Hainaut Cambrésis, France

<sup>2</sup>TOYOTA MOTOR EUROPE, Belgium

## 1 Introduction

The use of carbon fabric reinforced polymers (CFRP) in the automotive industry increased very significantly due to their high specific stiffness and strength, their great energy absorption as well as the reduced manufacturing cost.

The behaviour understanding and modelling of these materials become essential for their implementation into the design loop, needed for the deployment on mass-produced vehicles. In order to ensure the protection of pedestrians and drivers/passengers in case of collision with a CFRP panel, a model dedicated to the finite element analysis (FEA) of impacts is needed.

The nonlinear material behaviour which leads to differences in the impact response of composites is attributed to fibre failure, intra- and interlaminar matrix cracking, fibre-matrix debonding and strain rate sensitivity of the matrix. Additionally, the textile composite materials are capable of large shearing prior to the ultimate failure due to the sliding and reorientation of yarns. The modelling of all these phenomena is essential to describe the impact behaviour of layered fabric composites.

## 2 Intralaminar matrix damage model

The intralaminar matrix damage model relies on a close version of the Onera Damage Model proposed by Marcin [1]. Marcin adapted and extended the micromechanics based Continuum Damage Mechanic model proposed by Chaboche [2] to the fabric reinforced materials for implicit simulations.

The spectral viscoelastic model used in the Onera Damage Model is replaced by a generalized Maxwell model. It has been successfully extended and used in finite strain for anisotropic materials [3]. This present damageable viscoelastic model is then expressed in the finite strain framework. A Total Lagrangian Formulation is used to respect the material objectivity (frame indifference) and the anisotropy of the material during the large shear deformations. This model is then coupled to the Co-rotational updated Lagrangian Formulation used in LS-Dyna through a push forward operation.

## 3 Strain recomputation for laminate and delamination

The consideration of the interlaminar damage in finite element analysis is nowadays a challenge. The classical framework is to use cohesive elements associated to specific cohesive laws in the ply interface layers. However this method is time-consuming and does not allow the formulation of the dependence between the intralaminar and the interlaminar damages. Moreover, the number of elements through the thickness of the layered material has to be expanded to approach the real transverse strain distribution. Another solution is to recompute the strain distribution by using a higher-order zigzag formulation. Kim and Cho [4] have proposed a formulation with five degrees of freedom and which takes into account interfacial imperfections. By ensuring an energy balancing between this formulation and the formulation used by the shell elements, it is possible to recover a realistic displacement field through the thickness of the layered materials [5].

Thanks to the intralaminar model and since the transverse shear stress is continue through the thickness, the stress values at interfaces are able to be computed. This allows updating the compliance of the interface layers modelled as springs. The delamination area and their effects are thus considered in real-time during the simulation.

This theory has been implemented in a user material subroutine in LS-Dyna.

Thus, it is possible with this method to precisely simulate impacts on composite plates, by keeping only one classical shell element (formulation `type 2` for example) through the thickness of the plate. The transverse shear stiffness as well as the delamination is therefore well predicted without massive addition of elements.

## 4 Applications

Through both examples (Fig.1 and Fig.2), the accuracy of the model is shown.

The first one highlights the intralaminar matrix damage ability to predict the in-plane shear behaviour of textile preforms with large rotations of the yarns.

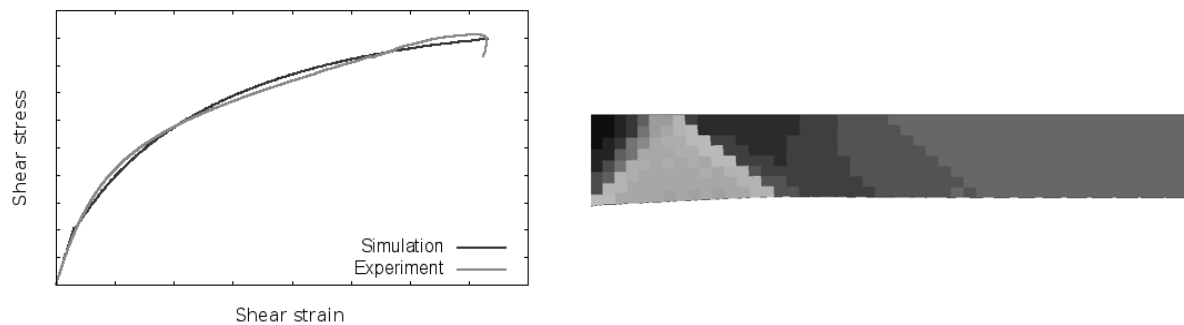


Fig.1: Experimental/numerical comparison of a monotonic tensile shear test ( $\pm 45^\circ$ ) on a Non-Crimp Fabric coupon and visualisation of the damage parameter (black is maximum) on a quartile of coupon.

The second one is a visualisation of the transverse shear stress through the thickness of a layered unbalanced textile composite under 3-point bending.

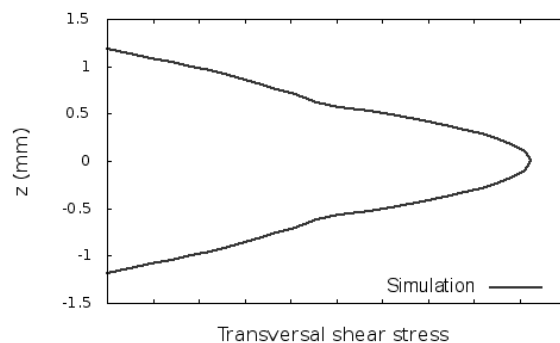


Fig.2: Transverse shear stress of a layered  $[45^\circ, 0^\circ]_s$  unbalanced textile composite during 3-point bending obtained by application of the EFSDT in the user material model.

## 5 Acknowledgment

The present research work has been supported by International Campus on Safety and Intermodality in Transportation, the Region Nord Pas de Calais, the European Community, the Délégation Régionale à la Recherche et à la Technologie, the Ministère de l'Enseignement Supérieur et de la Recherche, the Centre National de la Recherche Scientifique and TOYOTA MOTOR EUROPE: the authors gratefully acknowledge the support of these institutions.

## 6 Literature

- [1] MARCIN, Lionel. Modélisation du comportement, de l'endommagement et de la rupture de matériaux composites à renforts tissés pour le dimensionnement robuste de structures. 2010. Thèse de doctorat. Université Bordeaux 1.
- [2] CHABOCHE, J.-L. et MAIRE, J.-F. A new micromechanics based CDM model and its application to CMC's. *Aerospace Science and Technology*, 2002, vol. 6, no 2, p. 131-145.
- [3] KALISKE, M. A formulation of elasticity and viscoelasticity for fibre reinforced material at small and finite strains. *Computer Methods in Applied Mechanics and Engineering*, 2000, vol. 185, no 2, p. 225-243.
- [4] KIM, Jun-Sik et CHO, Maenghyo. Efficient higher-order shell theory for laminated composites with multiple delaminations. *AIAA journal*, 2003, vol. 41, no 5, p. 941-950.
- [5] KIM, Jun-Sik, OH, Jinho, et CHO, Maenghyo. Efficient analysis of laminated composite and sandwich plates with interfacial imperfections. *Composites Part B: Engineering*, 2011, vol. 42, no 5, p. 1066-1075.

# Predicting Mechanical Behavior of Reinforced Plastic and Composite Parts

Sylvain CALMELS - e-Xstream Engineering

## 1 Introduction

All the main industries worldwide are progressively adopting the usage of reinforced plastic and composite material for their product and have to face one major difficulty when it comes to design them: predicting the mechanical behavior of multi-phases and heterogeneous materials. On the structural side, each of these materials show a specific heterogeneous and anisotropic behavior in terms of stiffness, failure or electrical behavior as well as strain rate or thermal dependency fully driven by the microstructural organization of the reinforcements in the matrix. On the other side, the manufacturing process drives the final fibers orientation and distribution throughout the part. This means the design teams need a material and structural engineering technology able to create the link between the manufacturing process and the structural behavior of the components. Such technology is based on a micromechanical material modeling strategy based on the combination of the constituents' behaviors and the local microstructure definition. This extended abstract address briefly how this technology can be used to obtain accurate prediction of reinforced plastic and composite parts for any performance. A brief example is shown here. Other application examples will be shown during the presentation.

- **Heterogeneous and anisotropic local behavior**

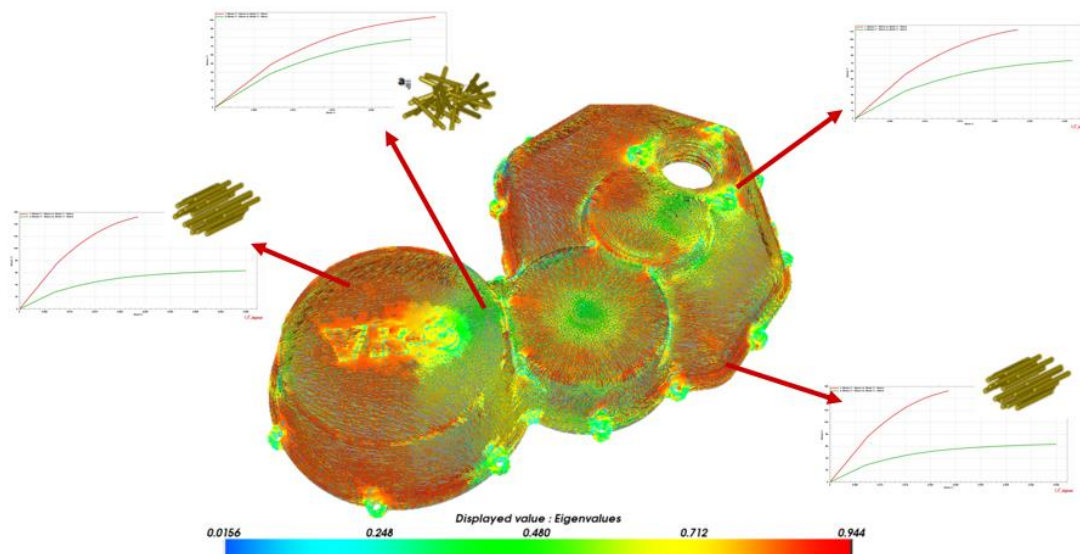


Fig. 1

The local mechanical behavior is driven by the result of the manufacturing process: the fiber orientation distribution

## 2 The multi-scale material modeling strategy

Reinforced plastics and composites consist of a material matrix with embedded inclusions. The constituents commonly used are short, long or continuous fibers, mainly glass or carbon, combined with thermoplastic or thermoset matrices. Parts made of these materials can be manufactured using different processes: injection molding, compression molding, RTM and so on. Their specific performance depends a lot on the local microstructure in the part. Fiber orientations are heavily

influenced by the processing step which drives the final distribution of material properties over the part. This is where the complexity of composite design sets in. The manufacturing step, the local microstructure, material properties and final performance of the part depend on each other. To be really able to take advantage of tailored properties and hit the goal of finding the optimal overall design, it is mandatory to take all influences into account.

The multi-scale material modeling approach starts with an in-depth investigation of multi-phases materials on the microscopic level. Based on the lessons learned, homogenization technology delivers a micromechanical model that can take into account the impact of the fiber orientation on the requested material performance, e.g. stiffness and failure. In structural analyses, be it on dumbbell, part or system level, this material model is coupled to results from processing simulations.

- **Mean Field Homogenization**

- **Phases**

- Material 1 [matrix]
- Material 2 [fibers]

- **Microstructure**

- Matrix
- Inclusions
  - Shape
  - Orientation

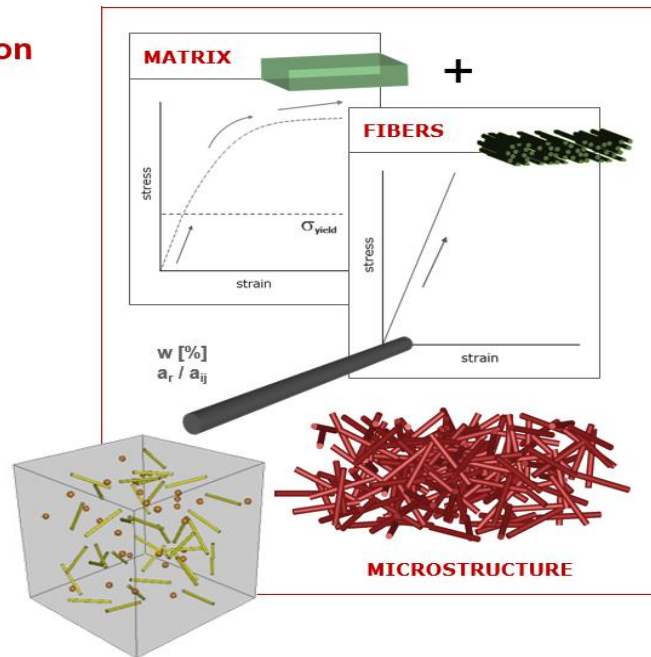
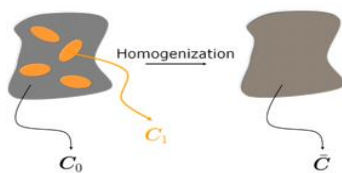


Fig. 2

The multi-scale material modeling strategy is based on the Mori-Tanaka homogenization method applied on material models built on the matrix and reinforcement materials combined with the microstructure definition of the given reinforced plastic or composite.

### 3 Micromechanical material models coupled to LS-Dyna explicit solver

To complete the answer for design teams, a complete easy to use workflow must be available for the end user which allow to assign the multi-scale material model to the concerned part and to map onto its structural mesh the fiber orientation definition resulting from the process simulation or measurement previously performed on a different mesh.

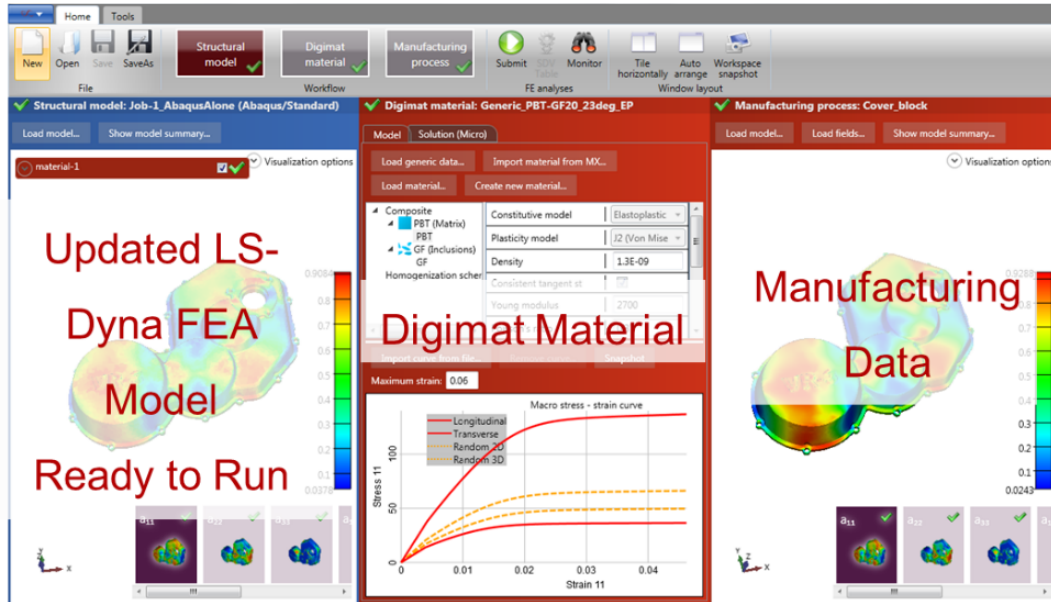
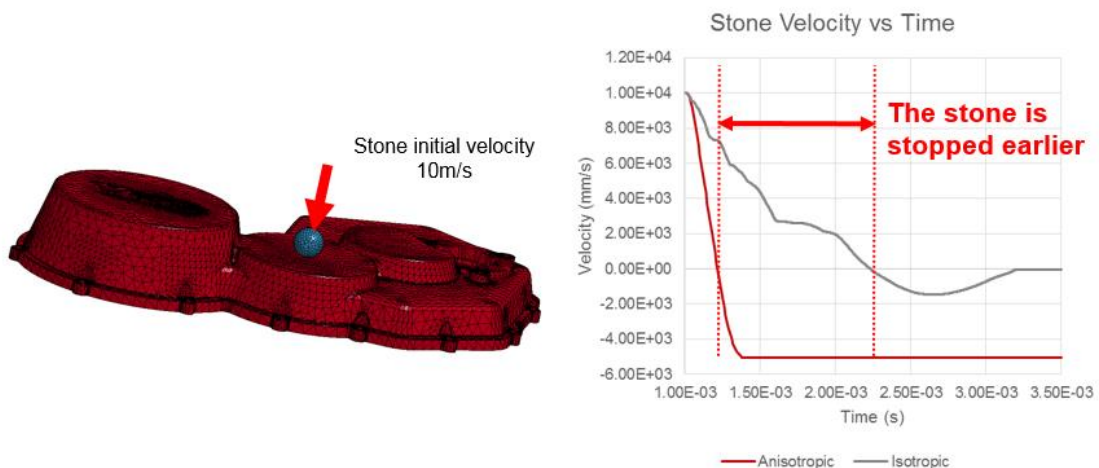


Fig. 3

An efficient and quick tool dedicated to design engineer to set up LS-DYNA FE models with micromechanical material models and taking into account the manufacturing effect on the fiber orientation distribution for an accurate behavior prediction

The results of the FEA taking into account the heterogeneity and then the variable local anisotropic behavior of the material induced by the effect of the manufacturing process throughout the part will show highly different response of the structure compared to an isotropic approach quickly unable to be accurate enough with such material.

- **Taken into account the effect of the manufacturing process influences the predicted behavior of the component**



# Implementation of Peridynamic Theory to LS-DYNA for Prediction of Crack Propagation in a Composite Lamina

Tezcan Kahraman<sup>1,2</sup>, Uğur Yolum<sup>2</sup>, M. Ali Guler<sup>2</sup>

<sup>1</sup>MAN Turkey A.Ş , Turkey

<sup>2</sup> Tobb University of Economics and Technology, Department of Mechanical Engineering, Turkey

## 1 Introduction

Failure mechanisms of composites are more complicated than metallic structures. Main failure modes can be divided into two subcategories as interlaminar failures (delamination) and intralaminar failures (matrix and fiber breakage). Final failure of a composite part occurs as interactions of those failure modes. Thus failure prediction of composite structures are rather complicated than metallic structures. This topic has been studied by researchers for many years and there have been various numerical methods to estimate failure load and failure type of composites. However, none of these techniques are confident enough. Thus in design phase, substantiation of load carrying capacity of the structures are done with experiments.

Peridynamic theory which is a nonlocal theory of continuum mechanics is first proposed by Silling [1]. In classical continuum mechanics, spatial derivatives of stress field are needed to evaluate the equation of motion. In classical continuum mechanics equation of motion is not valid at the points of discontinuity such as cracks and voids and results in infinite stresses. In Peridynamic equation of motion, instead of spatial derivatives, integrals of interaction force densities between material points are needed which can be evaluated at singularities.

## 2 Peridynamic Modeling of a Composite Lamina

In Peridynamics, pairwise interaction forces between material points are represented with Peridynamic bonds. Peridynamic model of lamina consist two types of bonds. Matrix bonds are oriented in all directions and they represent mechanical properties of the resin material. Fiber bonds which represent mechanical properties of fibers are oriented only in the fiber direction.

Peridynamic model of a lamina can be generated with mass elements and truss elements using LS-DYNA software. Mass elements represent material points whereas truss elements represent interaction forces between material points [6].

Within the scope of this paper, fiber reinforced lamina with a circular cutout under in-plane loading was considered as test subject. To understand how the fiber orientation angle effect deformation distribution and crack propagation under certain loading conditions, lamina was modeled with several fiber orientation angles. Both conventional FEA and Peridynamic Theory implemented FEA(PTIFEA) were conducted. Fig. 1. shows the comparison between FEA and PTIFEA for  $U_x$  and  $U_y$  displacements for  $0^\circ$  orientation. As it can be seen from Fig. 1, the comparisons are in agreement.

In addition, crack initiation and propagation was clearly captured for different fiber orientation angles. As illustrated in Fig. 2., crack propagates in fiber direction for fiber angle  $\theta=0$ . This kind of failure mode is also known as splitting fiber mode [2].



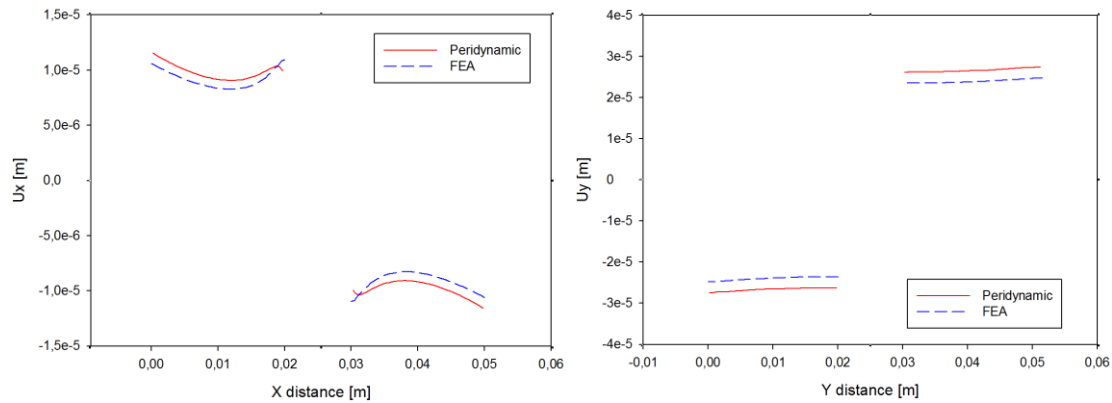


Fig. 1: a)  $U_x$  and b)  $U_y$  displacement graphs for lamina with  $0^\circ$  fiber orientation

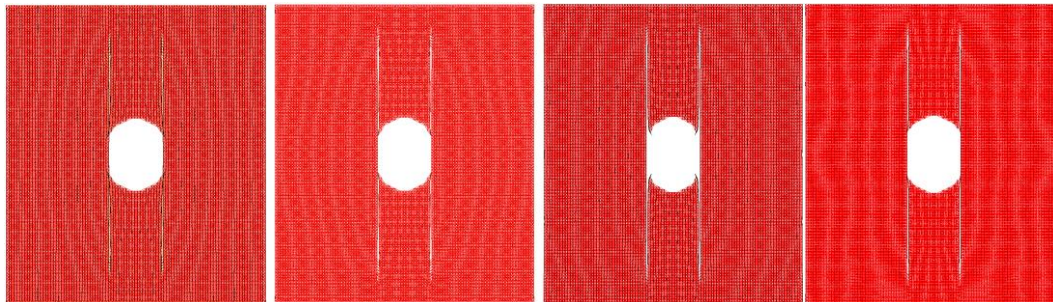


Fig. 2: Crack propagation for the composite lamina with  $0^\circ$  fiber orientation

### 3 Summary

Finite Element Implementation of Peridynamic Theory into LS-DYNA software is achieved in this study. Peridynamic Theory is a nonlocal theory of continuum mechanics which is suitable for modeling of crack initiation and propagation. This theory is implemented in LS-DYNA using mass and truss elements. Peridynamic model of a lamina with a circular cutout under velocity boundary condition is modeled and validated by comparing with the results from conventional FEA approach. PTIFEA results are in agreement with the ones in literature.

### 4 Literature

- [1] Silling S. A., "Reformulation of elasticity theory for discontinuities and long-range forces," *Journal of the Mechanics and Physics of Solids*, vol. 48, no. 1., 2000, pp. 175–209,.
- [2] Oterkus E., "Peridynamic Theory for Modeling Three-Dimensional Damage Growth in Metallic and Composite Structures," *Sci. York*, vol. 9, no. 3, , 2008, pp. 1–108.
- [3] Madenci E., Oterkus E., *Peridynamic theory and its applications*. 2014.
- [4] Oterkus E., Madenci E., "Peridynamic analysis of fiber-reinforced composite materials," *Journal of Mechanics of Materials and Structures*, vol. 7, no. 1., 2012, pp. 45–84,.
- [5] Oterkus E., Barut A., and Madenci A., "Peridynamics Based on Principle of Virtual Work," in *53rd AIAA/ASME/ASCE/AHS/ASC Structures, Structural Dynamics and Materials Conference*, 2012, no. April, pp. 1–25.
- [6] Macek R. W., Silling S. A., "Peridynamics via finite element analysis," *Finite Elem. Anal. Des.*, vol. 43, no. 15, 2007, pp. 1169–1178,.
- [7] Livermore Software Technology Corporation, *LS-DYNA Keyword User's Manual, vol. 1*, vol. 1, no. May. 2007.



## **MATERIALS V**

## **COMPOSITES**



# Damage in Rubber-Toughened Polymers – Modeling and Experiments

M. Helbig<sup>1</sup>, Th. Seelig<sup>2</sup>

<sup>1</sup>DYNAmore GmbH, Stuttgart Germany

<sup>2</sup>Institute of Mechanics, Karlsruhe Institute of Technology

## 1 Introduction

The enhanced ductility and fracture toughness of rubber-toughened polymers such as Acrylonitrile-Butadiene-Styrene (ABS) relies on microscopic deformation and damage mechanisms, which are void growth, shear yielding and crazing, e.g. [1,2].

In the present work a constitutive model is suggested which explicitly accounts for microstructural parameters and assumes distributed crazing to be the only inelastic deformation mechanism. The model was implemented in LS-Dyna as user-material.

The deformation and fracture behavior of a commercial ABS was determined by tensile tests under different conditions. Digital image correlation (DIC) was used to analyze the strain from the optical displacement measurement.

## 2 Homogenized model for distributed crazing in rubber-toughened materials

Crazes are localized zones of fibrillated polymer material, which form in the direction normal to the maximum principal stress and are able to transfer stress. Under continued loading their growth proceeds until a critical craze thickness is reached. Then rupture of the fibrils takes place and the craze turns into a micro-crack.

Crazing is found uniformly distributed over large regions of the material allowing for macroscopic description in a homogenized manner. The rubber particles typically cavitate prior to the occurrence of crazing and are considered simply as voids in the present study.

The kinematics of inelastic deformation is described by the overall separation vector  $\delta$ , the craze orientation (unit normal vector)  $\mathbf{n}$  and the average spacing  $b$  between the craze zones.

Key microstructural parameters in rubber-toughened polymers are the size  $r$  and the volume fraction  $f$  of the rubber particles. In addition, since inelastic deformation and failure take place by crazing, the ultimate craze opening  $\delta_{crit}$  at craze breakdown plays a pivotal role and introduces a characteristic length which has to be related to the initial craze spacing  $b_0$  being a function of  $r$  and  $f$ . We establish the connection between these microstructural characteristics by means of simple micromechanical considerations based on the unit cell model sketched in Fig. 1. Simple scaling relations are used to determine the initial spacing  $b_0$  between crazes and the effective normal and shear stress  $\tilde{\sigma}_n, \tilde{\sigma}_\tau$  acting on the craze area [4].

The overall elastic stiffness is considered by a two-step homogenization. According to the Mori-Tanaka model the void volume fraction  $f$  of the rubber particles is considered e.g. [3]. Additionally the evolution of damage  $D$  due to distributed crazing is considered at effective the 4<sup>th</sup> order effective elasticity tensor  $\mathbf{E}^*(f, D)$ .

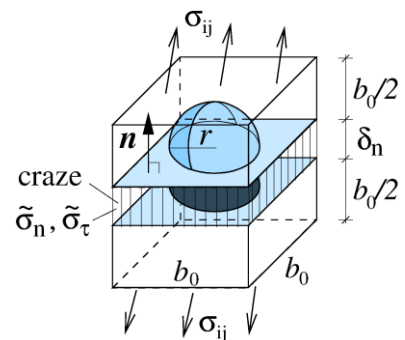


Fig. 1: Unit cell of microstructure with single craze in equator region of rubber particle

### 3 Model calibration of evaluation

In order to analyze in how far the model is capable to capture the deformation behavior of some real ABS material, tensile tests have been performed on a commercial, off-the-shelf ABS grade without any information of its microstructure. The tensile experiments were carried out on a servo-hydraulic testing machine at room temperature and at different constant values of the nominal strain rate. The in-plane strain field was analyzed using 2D digital image correlation (DIC). Fig. 2a shows stress-strain curves to compare the adjusted model and experiments under uniaxial tensile loading. Uniaxial cyclic tensile tests show hysteresis and a decreasing unloading-reloading slope with increasing inelastic deformation (Fig. 2b). The model response under repeated unloading and reloading is depicted by the solid curve in Fig. 2b.

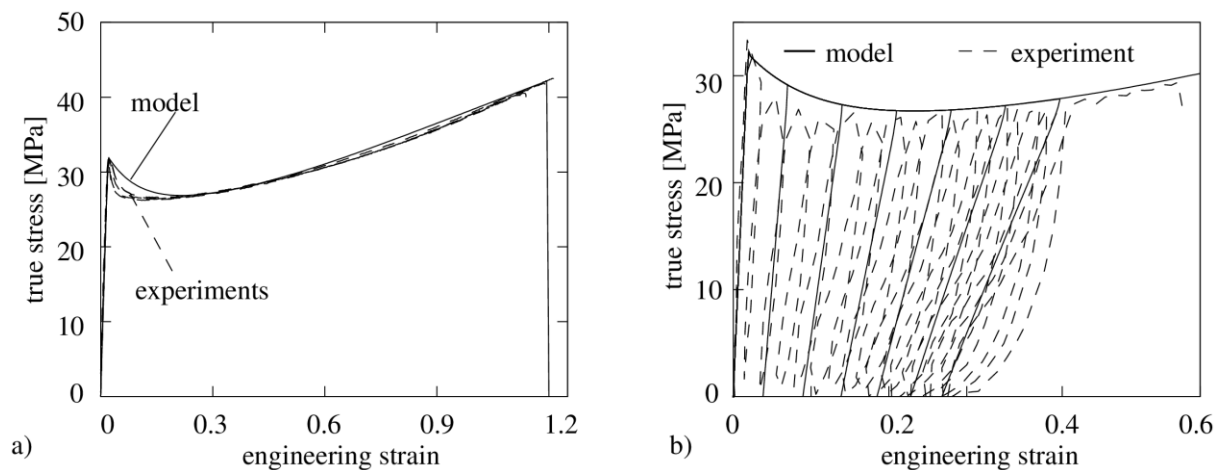


Fig. 2: a) uniaxial true stress vs. engineering strain response of commercial ABS and calibrated model, b) effect of unloading after different levels of straining

### 4 Summary

A micromechanical material model for distributed crazing in rubber toughened amorphous thermoplastics is introduced, which takes the most important microstructural parameters into account. The model was adjusted to experiments on a commercial ABS.

### 5 Literature

- [1] C. R. Bernal, P. M. Frontini, M. Sforza, and M. A. Bibbó, J. Appl. Pol. Sci. 58, 1-10 (1995).
- [2] A. Steenbrink, PhD thesis, TU Delft, 1998.
- [3] D. Gross and Th. Seelig, Fracture mechanics – with an introduction into micromechanics, Springer, 2011
- [4] M. Helbig, E. Van der Giessen, A.H. Clausen and Th. Seelig, Continuum-micromechanical modeling of distributed crazing in rubber-toughened polymers, Submitted, 2015

# Calculation and Validation of Material Tests with Specimens Made out of Filled Elastomers

Philipp Thumann<sup>1</sup>, Krzysztof Swidergal<sup>1</sup>, Marcus Wagner<sup>1</sup>

<sup>1</sup> Ostbayerische Technische Hochschule Regensburg  
Department of Mechanical Engineering  
Laboratory for FEM (Finite-Element-Method)

In deep-drawing dies for steel sheet parts of car bodies huge masses are moved. To prevent vibrations, which occur by sudden acceleration or stopping of those masses, elastomeric tubular dampers are used. The dampers are made out of carbon filled elastomers. A good knowledge about the material behaviour of metals is available. But for the numerical investigation of complete deep-drawing dies the elastomeric dampers must be taken into account, too. To characterize the material behaviour of the elastomers tensile tests and pressure tests were carried out. The received material data from the tests were read into LS-DYNA [1]. Simulation models of the tensile test and the pressure test were created for LS-DYNA according to the real dimensions and boundary conditions. For validation purposes, calculations of loading cycles were done to enable a comparison between test data and simulation results. For the calculations the implemented material model **\*MAT\_SIMPLIFIED\_RUBBER\_WITH\_DAMAGE (\*MAT\_183)** was used. The comparison shows a good fitting between the test data and the calculation results with respect to the mechanical material behaviour by using this material model in single loading cases. The settings from the simulations of material tests were transferred to simulations of a tubular damper, which is used in deep-drawing dies.

## 1 Modelling, simulation and validation of material tests

To get material data through tensile and pressure tests special specimens were used. For a comparison between test data and simulation results it is necessary to create identical specimens in the simulations. The specimens have to be discretized with elements with a suitable sizes. Therefore, an analysis concerning the element size were carried out. The elements were minimized step by step until no changes in the simulation results were registered. In Fig.1 the discretized tensile and pressure specimens with the chosen boundary conditions are shown. The boundary conditions are defined according to the conditions in the real testing machines. For the description of the material behaviour the material model **\*MAT\_183** is used. This card allows to read in rate depended material characterization data, which are available in pressure loading cases. Fig.1 also shows the two simulation results compared to the test data. The good fitting is clearly visible.

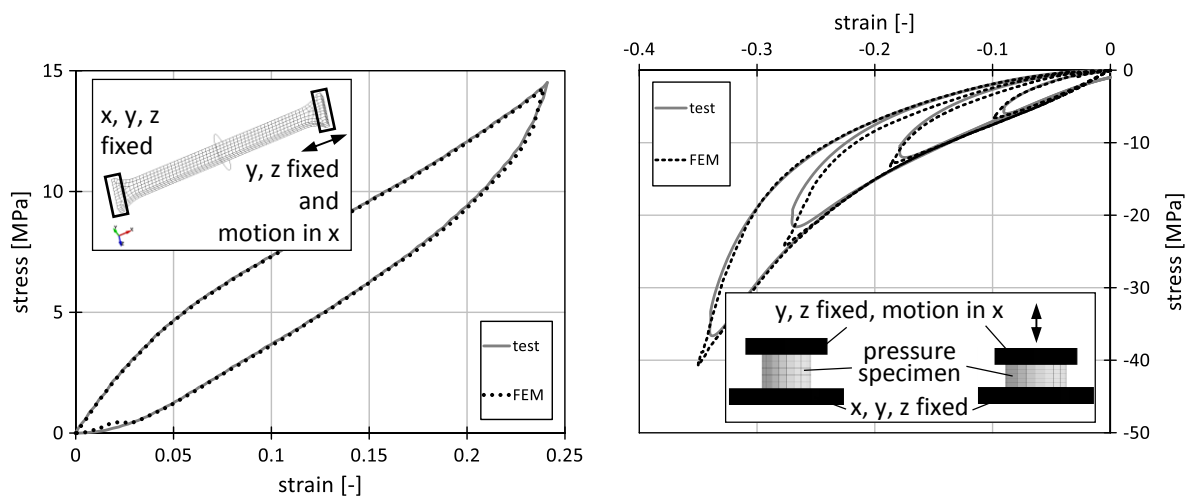


Fig. 1: Left side: Discretized tensile specimen with the boundary conditions and comparison between test data (test) and simulation results (FEM).

Right side: Discretized pressure specimen and additional components with boundary conditions and comparison between test data (test) and simulation results (FEM).

Furthermore, a parameter analysis was done in respect to the following items:

- Strain rate dependency → good fitting, see Fig.2 and [2].
- Irreversible deformation (damage) → good fitting, see [2].
- Hysteresis → good fitting, see Fig.1 and [2].
- Repeated loading → not possible to simulate, see [2].

## 2 Modelling and simulation of a tubular damper

In Fig.2 in the left diagram a tubular damper is shown. The picture in the right hand diagram illustrates the implemented parts in the simulation. The modelling of a damper is similar to the modelling of a pressure test. Also the general settings, such as element formulation, parameters in \*MAT\_183, etc. are transferred from the simulation of the pressure tests.

In the diagram in Fig.2 on the left side material test data are compared to the simulation results. As can be seen the characteristics of the curve progressions are similar. In the diagram on the right side there are shown the simulation results with different velocities  $v$  of the moveable part. Hence, also the strain rate is varying. Clearly visible is the higher stiffness at higher strain rate due to higher velocity  $v$ .

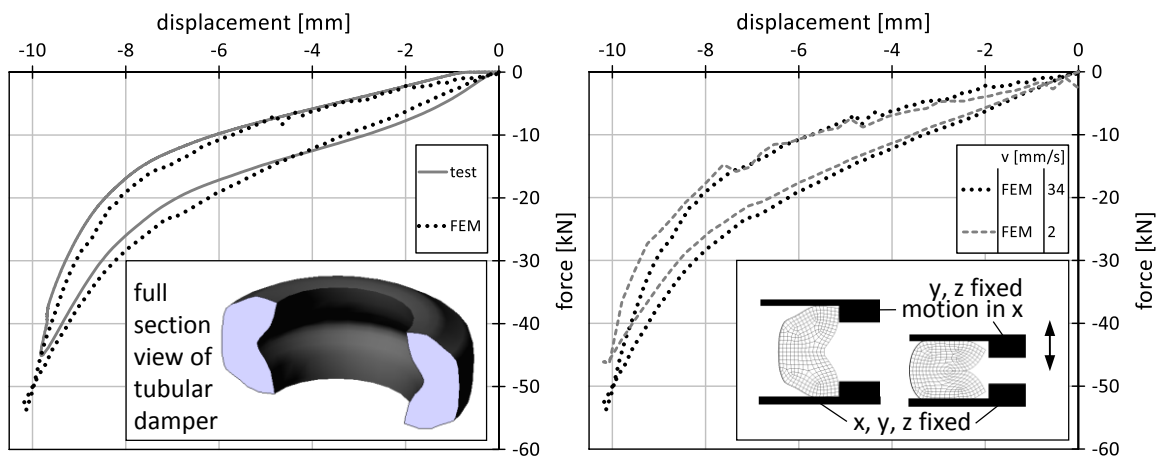


Fig.2: Left side: Full section view of tubular damper and comparison between test data (test) and simulation results (FEM).

Right side: Discretized damper and additional components with boundary conditions and simulation results by varying loading velocity.

## 3 Conclusions

The curve progression in the stress-strain diagram from the simulation of the tensile and pressure test are nearly identically to the material test data. Furthermore, it is possible to consider the strain rate dependency with \*MAT\_183 if material characteristic data are available. Also a material damage (irreversible deformation) and hysteresis behaviour can be considered. One disadvantage of \*MAT\_183 is the numerical instability in repeated loading cases (reloading after unloading) [3]. In repeated loading cases the reloading follows the unloading path [3]. That describes a non-physical behaviour and has a disadvantageous effect for simulations of rubber parts in deep-drawing dies.

## 4 Future works

The friction between damper and further components (support, hydraulic jack) should be considered. Hence, e.g. solid elements instead of rigid walls have to be used for the additional parts. Alternatively to \*MAT\_183 the material model \*MAT\_181 can be used to consider repeated loading cycles [3]. Furthermore, a study concerning damage (irreversible deformation) can be carried out. Also an additional material test with a damper should be made. The damper's shape has to be measured before and after the test. Simulations with the corresponding damper shapes have to be carried out. Finally the test data and the simulation results can be compared.

## 5 References

- [1] LSTC Inc. *LS-DYNA (a general-purpose finite element program)*. LSTC Inc.
- [2] Thumann, P., Swidergal, K., Wagner, M., Calculation and validation of material tests with specimens made out of filled elastomers, 10<sup>th</sup> European LS-DYNA Conference, 2015.
- [3] Du Bois, P. A., personal communication, 2015.



# **OCCUPANT SAFETY I**

## **AIRBAGS**



---

# Numerical Simulation of the Laser Scoring Line Behavior in Airbag Deployment

M.Nutini<sup>1</sup>, S.Bianco<sup>2</sup>, D.Brancadoro<sup>2</sup>, A.Luera<sup>2</sup>, D.Marino<sup>2</sup>, M.Olivero<sup>3</sup>, M.Vitali<sup>1</sup>

<sup>1</sup>Basell Poliolefine Italia, a Company of LyondellBasell Industries

<sup>2</sup>FCA (Fiat Chrysler Automobiles)

<sup>3</sup>CRF (Fiat Research Centre)

The airbag door system is one of the most delicate aspects in the design phase of a car instrument panel: seamless systems are increasingly used, which combine styling criteria with good functional performances. These systems typically include a tear seam, which may be obtained through laser scoring, to pre-determine the location of the opening during airbag deployment.

The design of the scoring line is currently validated through experimental tests on real life exemplars, submitted to airbag deployment, resulting in high development times and relevant costs. This is the main reason which suggests proposing numerical simulation in the design phase, not to substitute actual part homologation by testing but in order to limit the scope and complexity of the experimental campaign, thus reducing the development costs and the time to market.

So far, modeling the scoring line has been difficult due to limitations in the testing methods and simulation codes available to the industry. The methodology proposed in this paper takes advantage from the availability of a material law as LS-Dyna SAMP-1, with polymer-dedicated plasticity, damage model and strain-rate dependent failure criteria, which is supported by local strain measurement used for material characterization.

The method, here described in detail, is validated on a benchmark test, consisting in the real and virtual testing on a variety of scoring profiles obtained on a polypropylene box submitted to high speed impact test.

# CAE Analysis of Passenger Airbag Bursting through Instrumental Panel Based on Corpuscular Particle Method

Feng Yang, Matthew Beadle

Jaguar Land Rover

The safety regulation requires that passenger airbag (PAB) to deploy into working position in time without causing any fragmentation of its surrounding structure. Due to the significant load of airbag deployment and its complex unfolding process, it is always a challenge to design a PAB system which enables airbag safely bursting through the instrumental panel.

A CAE based approach has been developed at Jaguar Land Rover (JLR) to lead the passenger airbag system design. The core of the CAE approach is to model the airbag bursting load condition representatively. Hence the corpuscular particle method (CPM) has been applied in passenger airbag model building. Compared to control volume (CV) airbag model, CPM model can provide vital information of early gas dynamics and local pressure distribution (Fig.1 ) of PAB deployment, which are the key to understand the loading condition before PAB door splitting.

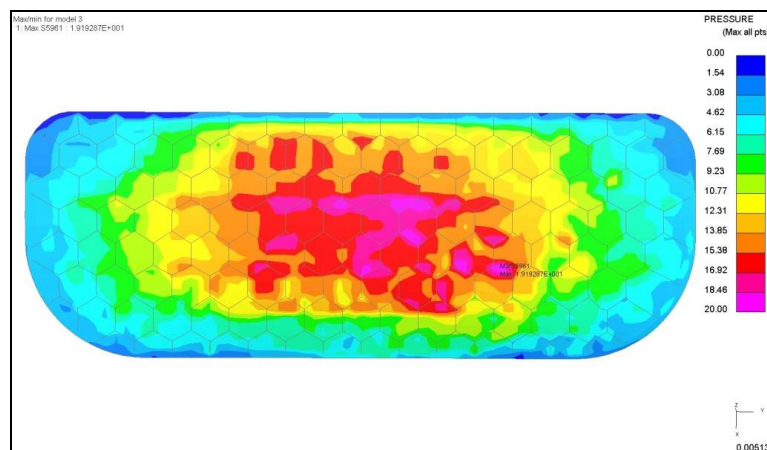


Fig.1: CPM pressure distribution on airbag door

The CAE simulation using CPM model successfully predicted initial PAB bursting load. It reproduced the process of airbag door initiation, propagation and opening. The CPM airbag model loaded representatively to its surrounding structures (Fig. 2). As a result, CAE PAB door splitting kinematics achieved good correlation to the test result. More importantly, the CAE analysis highlighted the stress concentration area of the key component such as topper pad (Fig. 3), it also identified the potential failure modes. Based on the CAE results, further design optimisation and verification had been conducted. The potential failure mode was corrected at the design stage.

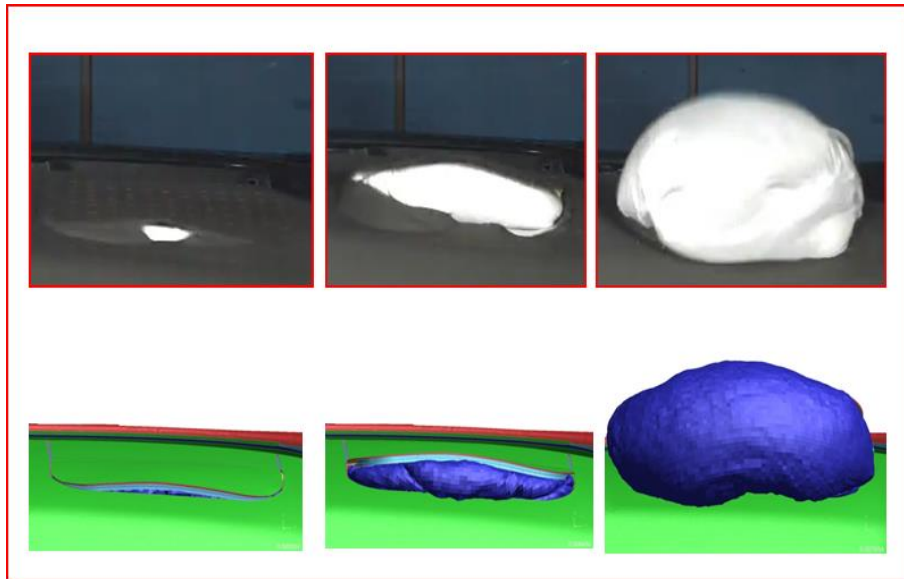


Fig.2: The correlation of airbag door opening

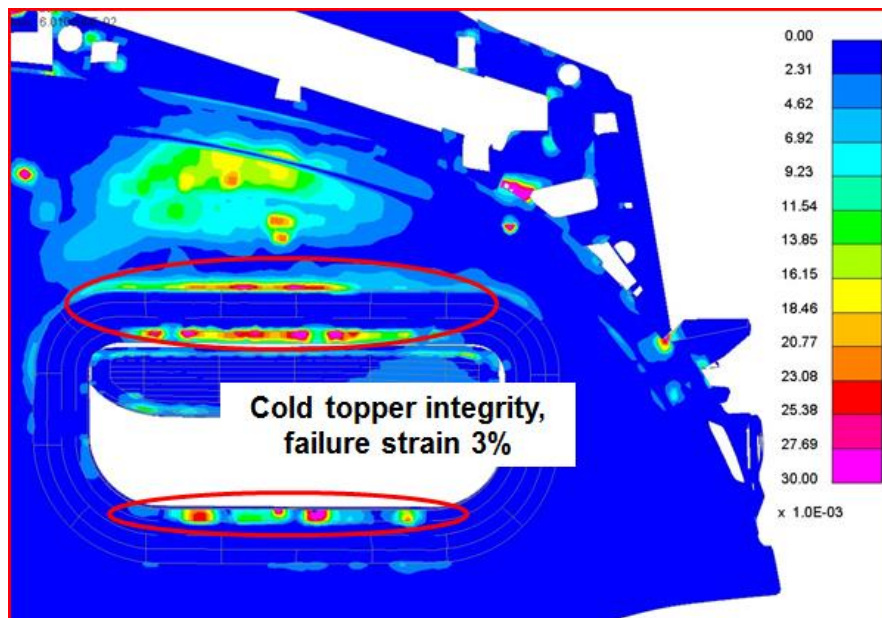


Fig.3: Simulation results of the plastic strain of the topper pad

Overall, CPM based approach provides a pragmatic method to simulate passenger airbag deployment, which leads to a robust design for passenger airbag system. The JLR CAE approach based on CPM has been successfully applied to several real projects, It has accomplished “right at first time” for passenger airbag system design.

# Using JFOLD & LS-DYNA to Study the Effects of Folding on Airbag Deployment

Richard Taylor<sup>1</sup>, Shinya Hayashi<sup>2</sup>

<sup>1</sup>Ove Arup & Partners International Ltd.

<sup>2</sup>JSOL Corporation

## 1 Abstract

Today's engineers and designers need accurately folded airbags in their deployment simulations. Minor changes in the way the real airbag is folded can cause different deployment behaviour, which can lead to trim fracture, hang-ups and unintended injury. There is a growing demand for robust, accurate analysis to study and mitigate these problems, and this requires a good prediction of gas dynamics through an accurately folded airbag. The corpuscular particle method (CPM) is being continuously improved to simulate the gas flow, but creating an accurate model of a folded airbag is still a challenge.

JFOLD is a software tool developed to meet the growing demand for fast and easy simulation based airbag folding. Running inside the pre-processor Oasys PRIMER<sup>®</sup>, JFOLD helps the user to quickly set up folding simulations that run in LS-DYNA<sup>®</sup>. Once the initial folding process is complete, the user can easily generate many different fold patterns by only making small adjustments to the set up.

This paper introduces some examples of using JFOLD Ver.2.1 to create different fold patterns and compares deployment characteristics using the corpuscular particle method in LS-DYNA.

## 2 How it works

JFOLD manages the folding processes in a series of "steps". Each step requires one LS-DYNA analysis to deform the model like a real fold, stitch panels or relax fabric. The airbag model is passed from step to step, using the deformed shape from the previous analysis. Folding steps can be modified, copied and branched off at any stage to investigate different folding patterns. "Tools" are used to deform the airbag and these can be copied across steps, imported from the built-in library or the user's own.

## 3 Example: Side Airbag Folding and Deployment Study

### 3.1 Study Objectives:

1. Demonstrate JFOLD using a simple but realistic airbag and common folding techniques
2. Compare the deployment performance of each folded design using CPM in LS-DYNA

JFOLD data and models created in this study will be made freely available to JFOLD customers.

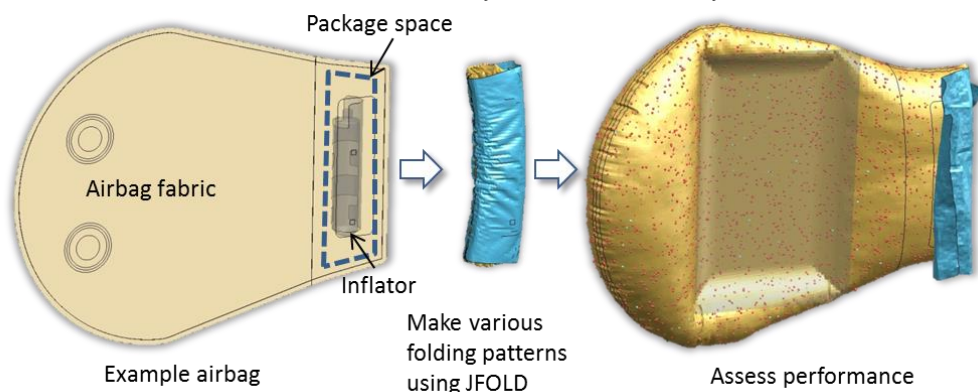


Fig.1: Side airbag example model for study

### 3.2 Folding Techniques

The example model was folded using several different techniques which are discussed in detail.

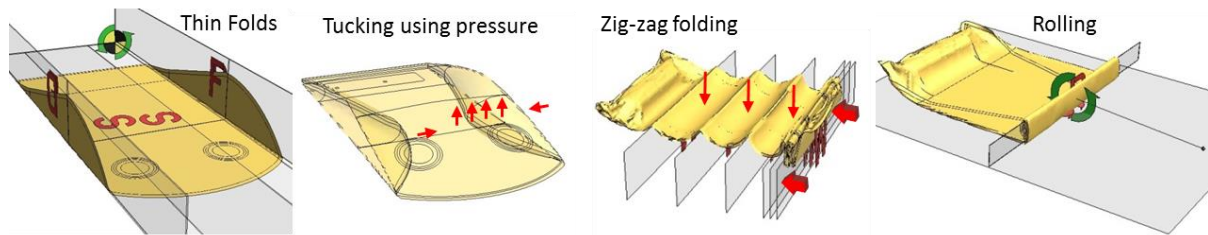


Fig.2: Techniques for simulation based folding using JFOLD

### 3.3 Deployment Results

Two loadcases were analysed for each of the six models: impactor (left pic) and OOP (right pics). The rolled designs performed better in the impactor cases but became stuck against the reverse impactor so were more aggressive than the zig-zag designs in the OOP loadcase.

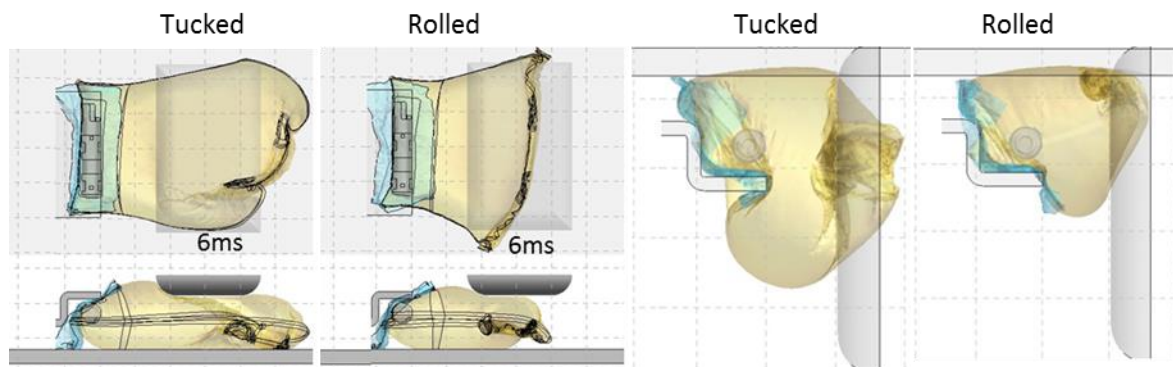


Fig.3: Left: moving impactor results, Right: OOP reverse impactor results

## 4 Summary and Conclusions

In this paper JFOLD Ver. 2.1 and LS-DYNA were used to study the deployment behaviour of a simple side airbag with six different folding patterns.

Various JFOLD tools and techniques were used to quickly generate the models. The conclusion is that JFOLD is a proven enabler for fast and realistic simulation based folding.

User feedback, requests and continuous research into quicker and easier folding techniques drives the development of the software. The next version Ver. 3.0 will have even more capabilities.

## 5 JFOLD Information

JFOLD Ver.2.1 is a JavaScript based software tool that runs inside Oasys PRIMER v12. JFOLD requires an additional license in addition to those needed for Oasys PRIMER and LS-DYNA. For the latest Ver.2.1 release English and Japanese language installations are available. The product includes an extensive built-in help manual and also a self-learning based tutorial with example model. A variety of folding example models will be available from JSOL Corporation for JFOLD customers. For more details please see your local JFOLD distributor.





# **OCCUPANT SAFETY II**

## **DUMMIES**



# Optimal Forces for the Deceleration of the ES-2 Dummy

Jörg Fehr<sup>1</sup>, Johannes Köhler<sup>1</sup>, Christian Kleinbach<sup>1</sup>

<sup>1</sup>Institute of Engineering and Computational Mechanics, University of Stuttgart

## 1 Introduction

The purpose of this project is to improve the development process of vehicle safety systems by introducing a new analytic approach. Today the development of vehicle safety systems, especially the airbag design process, requires many iteration loops via simulations and experiments. In this process parameters are changed and after each change a new simulation is conducted and the injury values are evaluated. We have a different, two folded approach. First we calculate the optimal forces to decelerate a dummy or human body. In a second step these optimal forces can be used to design vehicle safety systems. This may still require some small parameter variations through iteration loops, but should advance the performance and decrease the development time.

## 2 Method

This project focuses on side impacts. To calculate the optimal forces a generic side impact setup is designed, see figure 1 and figure 2. The ES-2 dummy is positioned on a Heidelberg-type seat and has an initial lateral velocity of 12 m/s. Steel plates are positioned next to characteristic body regions of the dummy in order to decelerate the dummy. This setup is based on the experimental setup of Cavanaugh[1]. In the simulation experiment a controller calculates the optimal force for each plate to decelerate the dummy as swift as possible without exceeding the critical injury values. To design such a controller a modellidentification is necessary. As critical injury values, we use the injury values that are used to achieve a five star rating in the EURO NCAP. The simulation yields the optimal forces to decelerate the dummy without exceeding the critical injury values. To implement the controller, the user loading subroutine is used. Based on the current injury vales, this function calculates the current forces necessary to decelerate the dummy. The model is simulated on the High Performance Computing Center(HPC) cluster of SimTech. For the evaluation of the results the binout data is imported via a Matalb Converter to Matlab and automatically the energy applied to the most relevant regions is calculated.

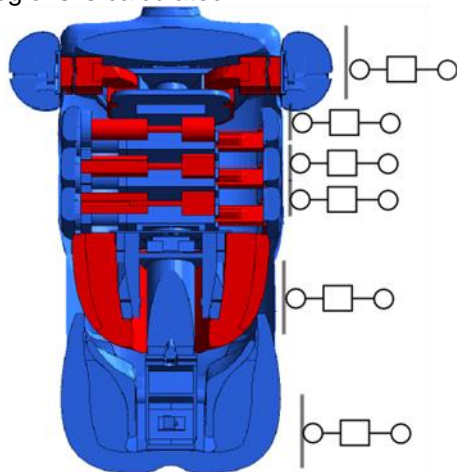


Fig.1: Generic side impact setup designed for evaluation of models of the human body

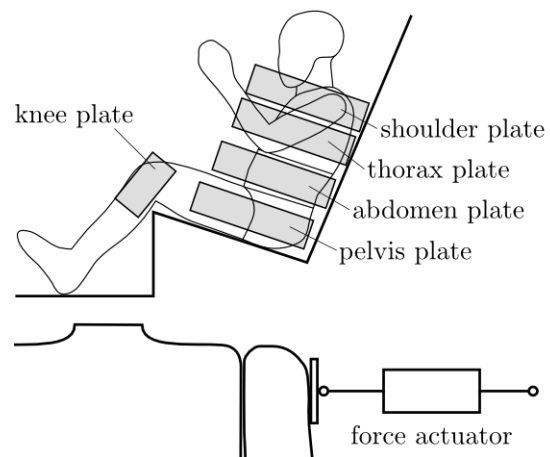


Fig.2: Controller approach for an optimal deceleration of a passenger considering the injury risks to be met.

### 3 Summary

The following section summarizes the results of this approach. The performance of the controllers is shown at the example of the ribdeflection, see figure 3. Here the actual ribdeflection is always close to the target trajectory. The controller quickly reaches the maximal ribdeflection without exceeding the critical injury value of 22 mm. By using similar controllers for the other body parts of the ES-2 Dummy the whole ES-2 Dummy is decelerated. This deceleration of the ES-2 Dummy, with an initial velocity of 12 m/s, takes 56 ms and a distance 408 mm. The resulting optimal energy distribution is shown in figure 4. The biggest portion of the energy is transmitted through the pelvis. The shoulder and thorax roughly dissipate an equal part of the energy and the abdomen dissipates the smallest amount of energy.

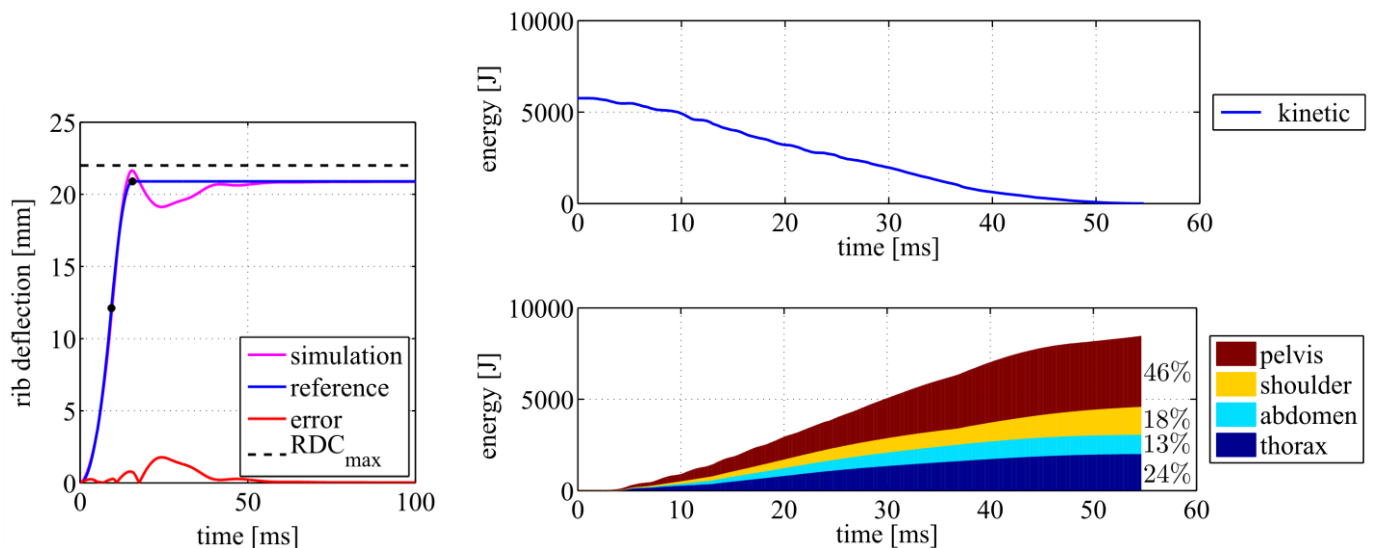


Fig.3: Ribdeflection approaches desired maximum value without exceeding critical value  $RDC_{max}$  of 22 mm

Fig.4: Optimal distribution of the energy absorption.

### 4 Literature

- [1] Cavanaugh, J.M.; Waliko, T.J.; Malhotra, A.; Zhu, Y.; King, A.I.: "Biomechanical Response and Injury Tolerance of the Thorax in Twelve Sled Side Impacts". SAE Technical Paper, 1990.

# Assessment of Motorcycle Helmet Chin Bar Design Criteria with Respect to Basilar Skull Fracture using FEM

Siamak Farajzadeh Khosroshahi<sup>1</sup>, Mazdak Ghajari<sup>2</sup>, Ugo Galvanetto<sup>1</sup>

<sup>1</sup>Department of Industrial Engineering, University of Padova, Padova, Italy

<sup>2</sup>Department of Aeronautics, Imperial College, London, UK

## 1 Abstract

Statistical studies showed that the chin bar of full-face helmets is the region with the highest number of impacts. In an Australian research, fifty percent of severe impacts took place to the front of the helmet and forty percent of these resulted in Basilar Skull Fracture (BSF). There are two standards, which include criteria for assessing the performance of the helmet's chin bar, Snell M2015 and ECE 22.05. These standards have developed some methods for testing the chin bar in order to protect the head from facial impact during motorcycle accidents, but they do not seem to consider head and neck injuries. The present work has utilized the finite element method to assess the Snell M2015 and ECE 22.05 criteria for chin bar design with respect to the injuries at the base of the skull. In the first step, the fem model has been mounted on a headform to simulate the chin bar test for both standards. In the next step, the Hybrid III dummy model has been coupled to the helmet to simulate the response of the whole body, in particular at head and neck connection, to the facial impact. Finally, the results obtained from the dummy model simulations have been utilized to assess if the standards could provide reasonable criteria for BSF. The simulations are performed with LS-Dyna and the focus of the assessment is about the injuries at the intersection between skull and spine.

## 2 Introduction

An Australian governmental project, which studied helmets against BSF, proposed further investigation based on simulation in order to identify the effect of the helmet's chin bar stiffness on BSF [1]. So in this work the effect of stiffness of helmet's chin bar design criteria has been assessed with respect to induced neck force, which is an indication for BSF [2, 3].

## 3 Helmet Chin Bar Tests Methods

There are two standards which prescribe some experimental tests for validating the chin bar of full-face helmets. These standards have been used in order to verify the models used in this work.

## 4 Basilar Skull Fracture (BSF)

Any fracture, which occurs exactly at the skull base or originate remotely from base of skull and propagates to the bones at the base of the skull, could be called Basilar Skull Fracture [1].

An experimental survey introduced the induced axial tensile load on Foramen Magnum because of mandibular impact, as an indicator of BSF [2, 3] so in the present work, the upper neck tensile load has been also considered as an indicator of BSK.

## 5 Finite Element Simulation

A commercial helmet was numerically modified by changing the thickness of the chin bar in order to show the effect of chin bar stiffness on the induced force at the upper neck section.

In the present work LSTC/NCAC Hybrid III 50<sup>th</sup> percentile male dummy model (LSTC.NCAC\_H3\_50TH.130528\_BETA), used in order to represent the human body behaviour during the chin bar impact.

## 6 Methodology

The standard tests were carried out numerically for all models in order to check that all of them were still acceptable according to the same standards.

The obtained helmet models were coupled with the dummy model, as it is illustrated in Figure 1. The impact of the helmeted dummy to a flat anvil on the helmet's chin bar, were simulated for different helmet models, in order to compare induced load at the upper neck section.

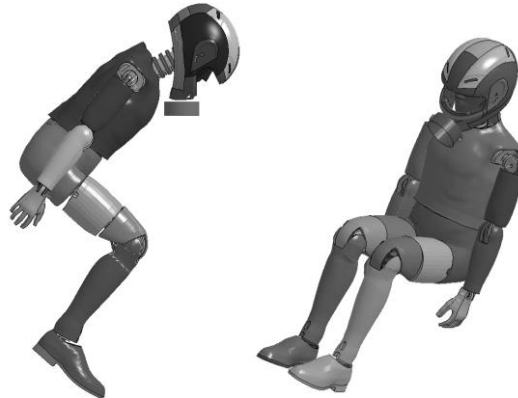


Fig.1: *Helmeted Dummy model impacting a flat anvil*

## 7 Results and Discussion

With considering the model number "I" as the reference, Figure 2 illustrates the variation of neck force and acceleration for different models.

Figure 2 describes that, changing the acceleration, which was due to change of chin bar stiffness, led to slight changes in the neck force.

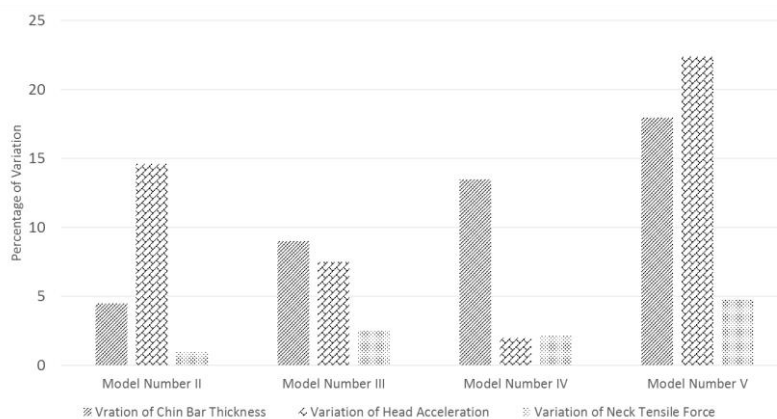


Fig.2: *Variation of Acceleration and Neck Force for Different Chin Bar Stiffness*

## 8 Conclusion

Simulations did not provide a clear trend of variation of the tensile neck force with the stiffness of the chin bar. Therefore, further investigations are required in order to verify the reliability of available chin bar design criteria for providing protection against BSF.

## 9 Acknowledgment

This work performed as a part of the research training network MOTORIST funded by a Marie Curie fellowship of the 7th framework programme of the EU under contract number FP7-PEOPLE-2013-ITN-608092. The authors would like to thank Dainese S.p.A. for providing the helmet's CAD model.

## 10 Literature

- [1] Gibson, K.T.: Helmet Protection against Basilar Skull Fracture, Australian Transport Safety Bureau Research and Analysis Report, Research Grant Report 2007-3, 2007
- [2] McElhaney, J.H., Hopper, R.B., Roger J.R., Nightingale, W.: Mechanisms of Basilar Skull Fracture, Journal of Neurotrauma, Volume 12, 1995, 669-678
- [3] Hopper, R.B., McElhaney, J.H., Myers, B.S.: Mandibular and Basilar Skull Fracture Tolerance, SAE Technical Paper 942213, 1994

# CAE Validation Study of a Side Window Impact using Plexiglas Materials

Damaso Lopez Ruiz<sup>1</sup>, Andreas Rühl<sup>2</sup>, Stefan Kolling<sup>2</sup>, Eckart Ruban<sup>3</sup>, Bernd Kiesewetter<sup>3</sup>, Steffen Ulzheimer<sup>3</sup>

<sup>1</sup>TECOSIM Technische Simulation GmbH

<sup>2</sup>Institute of Mechanics and Materials, THM Giessen

<sup>3</sup>Evonik Industries AG

An experimental and numerical study regarding the head impact on a side rear window was performed. Based on several years of material development and manufacturability (Evonik Industries AG), the expert knowhow in material testing and LS-DYNA material implementation (Giessen Institute of Mechanics and Materials) and the CAE user experience (TECOSIM Technische Simulation GmbH) and in closer cooperation between all parties, it was decided to start a development study. The outcome of the study should show the behavior of different PLEXIGLAS® (PMMA) windows using different PLEXIGLAS® grades and possible feasible combinations.

The study was based on a custom made predefined head impact to a fixed side window of a reduced TEC|BENCH™ FE-Model\*. Since the side window typically is defined as a small area a child head had been selected as impactor. The impact direction was predefined as perpendicular to the central impact point of the window geometry. The hardware testing was conducted by ACTS GmbH & Co KG at 10 m/s.

This paper shows the correlation between simulation and hardware tests and also the potential of the PLEXIGLAS® materials to ensure crash impact performance for the automotive, aviation and building industries. All simulations were performed using LS-DYNA V971 R7.0.0 as solver and HyperWorks as pre- and postprocessor.

This study could be used as a starting reference point to material substitution of glass for weight reduction, for easy forming of complex geometries and to increase safety protection.

\*TEC|BENCH™ FE-Model is the property of TECOSIM Technische Simulation GmbH.

# Agile Dummy Model Development Illustrated by Refinement Activities of the WorldSID Shoulder Model.

Sebastian Stahlschmidt<sup>1</sup>, Uli Franz<sup>1</sup>, Richard Brown<sup>2</sup>, Gareth Stokes<sup>2</sup>

<sup>1</sup>DYNAmore GmbH  
<sup>2</sup>Jaguar Land Rover Limited

## 1 Introduction

The Agile Software Development is a method that promotes adaptive planning, evolutionary development, early delivery, continuous improvement, and encourages rapid and flexible response to changes. This method is established in the development of software and influences also many other development processes. The employees at DYNAmore are developing dummy models together with a consortium of car companies since decades. The models are used world wide by almost all automotive companies that run LS-DYNA to design their restraint systems.

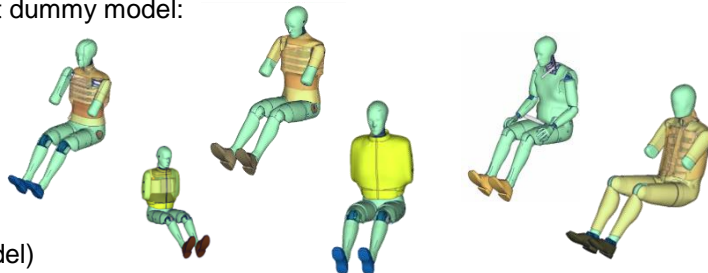
The process of creating the models has been refined several times. The paper describes the applied methods for one of the latest dummy model developments, the WorldSID 50% dummy model. Although the model quality is already high, there is still a frequent exchange between the developers and customers to refine the model for specific load cases. The input and interaction with users is highlighted by the adaptations made for the shoulder area and other detailed investigations.

Finally, the paper compares the applied methods with the methods published for Agile Software Development and concludes with ideas to further optimize the processes to develop dummy models.

## 2 Dummy Modeling process at DYNAmore

The dummy modeling process which is described in this section is applied in several FAT and PDB projects. The main members of the Groups are several Suppliers of Germany and the big five OEM's of the German automotive industry AUDI AG, BMW AG, Daimler AG, Dr. Ing. h.c. F. Porsche AG and Volkswagen AG. The models which are developed in these working groups are mainly side impact dummy models and one rear impact dummy model:

- EUROSID
- ES-2
- ES-2re
- WorldSID 50%
- USSID
- SIDHIII
- BioRID II (rear impact model)



All these Models are frequently used world-wide and updated continuously to new validation tests and the requirements of the users world wide.

## 3 Validation process at DYNAmore

The validation process is a sequence of loops through the above explained tests. It starts with a detailed mesh and a mass validation. In the next step the material tests are defined and the results are used to generate material cards. This leads to a first model, which can be used in a vehicle simulation to learn about the load levels and load characteristics.

The model is then used to define appropriate boundary and initial conditions for a set of component and sled tests. With the test results the model can be enhanced. The new enhanced model can then be used again in vehicle simulations and the loop starts again. During each loop new test are defined and performed based on the gained knowledge where the model has to be enhanced.



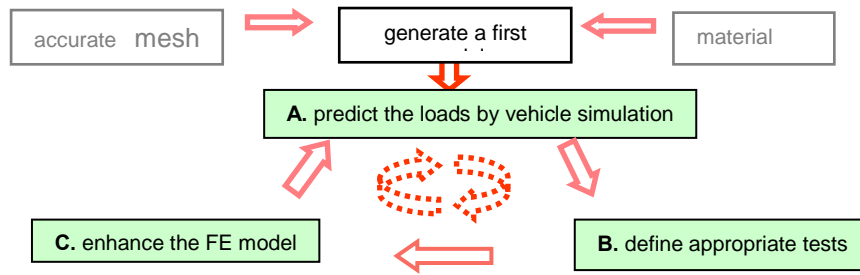


Fig. 1: Validation process of FAT and PDB dummy models.

The circle between the sampling Points A, B and C seems to give a never ending process to enhance the model. At the beginning of a Dummy development all three Points are located mainly at the dummy developer until a validation state is reached which can also be used for pre testing or in production of customers. Mainly the first customers are the members of the working group. Then also the experience of the customers are counted to Point A and at the end all findings of all users can be used to enhance the model.

#### 4 Agile development

In February 2001 software developers met in Utah to discuss lightweight development methods for software. They summarized their ideas about a process to develop software in an iterative way in the Agile Manifesto [1]:

“We are uncovering better ways of developing software by doing it and helping others do it. Through this work we have come to value:

- Individuals and interactions over processes and tools working software over comprehensive documentation
- Customer collaboration over contract negotiation
- Responding to change over following a plan

That is, while there is value in the items on the right, we value the items on the left more.”

Based on the Manifesto several guidelines and methodologies have been developed lately. Maybe Scrum is the one of the most frequently used method which describes in detail the roles of the different players, the events and the artefacts to develop complex products.

#### 5 Summary

The paper describes the development of the dummy models as it is practiced since more than 20 years. During this time many dummy models have been released. Since the results of each project were obviously very successful the same stakeholders launched several subsequent development projects. Some projects targeted to develop new models and others aimed to enhance the quality of an existing model. One of the enhancing projects on the performance of the WS50% model has been presented in this paper in more detail.

The methods applied within the FAT/PDB framework to develop the dummy models have very much in common with the ideas of the Agile Manifesto. Almost all aspects presented in the Manifesto can be observed in the development process as practiced by the developers, the FAT/PDB and the other customers of the models. That the ideas match so well is remarkable because the authors were not familiar with the ideas presented for the development of software.

After publishing the Manifesto the ideas have been formalized and detailed significantly. As results management methods like Scrum are now available to develop software and other products. Within the FAT/PDB the refinement and formalization of the methods did not take place and more informal ways of handling the ideas of the Manifesto are still practiced.

# **OCCUPANT SAFETY III**

## **DUMMIES**

# LS-DYNA Model Development of the THOR-M Crash Test Dummy

Ismail Maatouki\*, Zaifei Zhou\*\*, Paul Lemmen\*

\*Humanetics Europe GmbH, Heidelberg, Germany

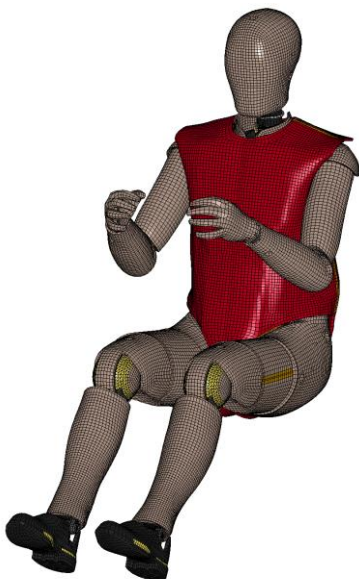
\*\*Humanetics Innovative Solutions, Inc. Plymouth, USA

Developments on the THOR dummy over the past years resulted in the THOR-M version which is foreseen for introduction into regulatory and Consumer tests in the 2020 timeframe. NHTSA considers to use the THOR-M dummy in an angled impact test while Euro NCAP includes plans for the development of a frontal barrier test with THOR-M in their roadmap for 2020.

To support the development of restraint systems for both test configurations Humanetics is developing a Finite Element model of the THOR-M dummy. This paper presents activities which results in the version 1.0 model as well as an outlook to future model releases.

Geometry information was obtained from 2-D drawings and CAD models of individual parts. Like for a physical dummy the individual parts were assembled into a full model by means of quasi static simulations. The geometry of the resulting THOR-M model was then checked against laser scans of available ATD's and refined where needed. Detailed mass and inertial properties are obtained from CAD models and mass measurements of physical parts. The model connectivity and structural integrity are verified against the hardware. The model represents the latest features in the hardware like the SD3 shoulder and the latest foot design.

The THOR-M dummy is more biofidelic than existing dummies like HIII and ES. Combined with potentially higher and more complex, out of plane, loadings resulting from angled impact and frontal barrier test procedures it is to be expected that larger deformations occur in the THOR-M. This makes the development of the THOR-M material models more challenging. The possible loading and deformation patterns of relevant materials, as can be expected in future testing, have been identified and analyzed from available full scale test results. Material tests (a total number of 210 tests for about 35 materials) were defined and performed to collect the essential information needed to describe the characteristics of the materials for applicable deformation modes and its severities. The coupon tests have been simulated to verify the material cards. Furthermore the performance of the material models is being verified in additional material, component, sub-assembly and full dummy tests which undergo more complex deformation patterns. The material modelling approach proves to show excellent stability in an extensive robustness test program and in the first user applications.



The THOR-M model is validated against a first set of validation load cases which shows promising initial correlation. Further validation tests will be executed in this project to prove overall correlation to nominal hardware response in complex but relevant load cases. The THOR-M model represents all available hardware instrumentation.

# LS-DYNA Model Development of the Harmonized Hybrid III 05F Crash Test Dummy to Meet the Euro NCAP Testing Protocol Requirements

Robert Kant\*, Paul Lemmen\*, Chirag Shah\*\*

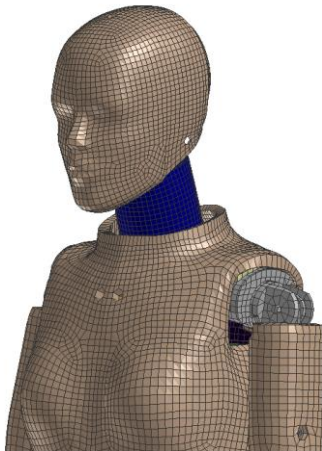
\*Humanetics Europe GmbH, Heidelberg, Germany

\*\*Humanetics Innovative Solutions, Inc. Plymouth, USA

Starting per January 2015 Euro NCAP requires use of the HIII-5<sup>th</sup> percentile small female for its full width frontal barrier test procedures. The dummy should be according to the latest agreed FTSS / Denton brand harmonization and thereby eliminates brand variability effects.

The dummy configuration includes a neoprene neck shield, the SAE harmonized jacket (SAE J2921) and the Denton lower leg cavities. In addition, the thorax pendulum certification should be done for both 3.0 (SAE J2878) and 6.7 m/s, and use of polynomial scale factor for the calibration of the chest deflection sensor (SAE J2517) is required. The HIII 05F dummy is employed at two locations during the aforementioned test protocol: 1) the front passenger seat and 2) the rear passenger seat opposite to the driver. In addition OEMs may hand over data for the front passenger seat.

An LS-Dyna model for this Euro NCAP compliant HIII 05F has been developed. The model is optimized to predict the nominal response of the Harmonized HIII 05F dummies in the market. New tests were performed to validate the model.



To allow users to explore possible influence of chest variability the model features settings that result in response characteristics representing either stiffer or softer behavior. It is well known that chest stiffness, even within the range of certification corridors, can cause significant variation in the final Euro NCAP tests. As such, the model allows to make an estimate of the probability that Euro NCAP targets for chest deflection will be reached once the independent Euro NCAP test is performed.

# H-Point Machine and Head Restraint Measurement Device Positioning Tools – Extended Capabilities

Brian Walker, Liliana Cowlam, Jamie Dennis - Arup

Simon Albery, Nicolas Leblanc - Futuris

The H-point of a seat is an important parameter for in the design process of a vehicle, and in particular the design of a seat. This can be estimated empirically, but this method is usually not sufficient to accurately determine how the manikin's position is affected by subtle yet complex interactions within the seat and its trim. To aid this process, Arup have developed a positioning tool kit for use in conjunction with the Oasys PRIMER software [1]. The positioning tool kit calculates the H-Points of the automotive seats, as well as the backset measurement, thus providing the scores of the head restraint.

The HPM Positioning Tool is a JavaScript tool for prediction of the H-Point of a seat, based on the SAE J826 regulation [2], used in conjunction with Oasys PRIMER and LS-DYNA® [3]. All pre-simulation positioning of the HPM is completed automatically within Oasys PRIMER, and the output is a ready-to-run LS-DYNA model. Once LS-DYNA has calculated the settling of the manikin using the seat properties, Oasys PRIMER is used for interpretation of the results to report the H-point coordinates and back angle of the HPM.

The HPM Positioning tool follows the SAE J826, which requires the location of the accelerator pedal. The accelerator pedal info is not always available in the early stages of the seat design, and only the location of the ball of foot (BOF) of the right foot might be known. For this case, based on customer requests, the tool has been extended to allow the value of the BOF to be entered instead. Another potential use of this new option is predicting the H-point of a front passenger seat, in which case the BOF is positioned on the floor.

HRMD Positioning Tool is a JavaScript tool for prediction and assessment of seat and head restraint geometries according to the following procedures:

- IIHS
- NHTSA
- EuroNCAP
- C-NCAP

The HRMD Positioning Tool has now been extended to follow the new EuroNCAP Rear Whiplash Test Protocol.

The HPM and HRMD Positioning Tools have been validated through comparison to physical measurements and tests based on Futuris seat data. The tools show good correlation to physical HRMD drops conducted by Thatcham on a seat package. The prediction was shown to consistently lie in within the scatter of the available test data.

[1] Oasys® PRIMER11.0 User Manual. Ove Arup& Partners Ltd: Solihull, UK, 2013.

[2] SAE International: "J826 NOV2008 Devices for Use in Defining and Measuring Vehicle Seating accommodation", Revised 2008-11.

[3] LS-DYNA® Keyword User's Manual, Version 971. Livermore Software Technology Corporation (LSTC): Livermore, CA 94551-5110, USA, May 2007

# Investigation of Seat Modelling for Sled Analysis and Seat Comfort Analysis with J-SEATdesigner

Noriyo ICHINOSE<sup>1</sup>, Hideki YAGI<sup>1</sup>

<sup>1</sup> JSOL Corporation, Nagoya, Japan

## 1 Abstract

We have been developing new integrated seat design system named J-SEATdesigner. The concept of J-SEATdesigner is to provide big benefit for the seat design related engineer to resolve their issues. In July 2014, we released first version which is dedicated on automation for sled model assembling process. Toward the next release, we have been developing new tools on J-SEATdesigner to make more detailed and complex seat model easily and efficiently.

In this paper, our investigation for detailed seat modelling and introduction of new seat modelling tools on J-SEATdesigner will be shown. Regarding the seat modelling investigation, the seat covering processes simulation from two dimensional fabric cutting pattern has been evaluated and we will propose efficient approach for seat covering process. As new tool application on J-SEATdesigner, effect of residual stress in seat model on sled analysis and seat comfort analysis with human FE model (THUMS) will be discussed.

## 2 Introduction of J-SEATdesigner

### 2.1 System concept

The main objective of J-SEATdesigner is to provide high accuracy results of seat related simulations for all engineers without special effort and knowledge. This means that the engineer who has no information about crash regulations can run sled simulation and have high accuracy results for JNCAP, Euro-NCAP, US-NCAP, etc.

J-SEATdesigner consists of four systems as below:

- Graphical user interface
- Database management system for models and related information
- Automatic assembly system
- Seat modelling system

### 2.2 Simulation base THUMS positioning

J-SEATdesigner has THUMS positioning panel which helps you to make input deck for THUMS positioning simulation. This panel provide two different user input for positioning. First input is specifying angles for each joint and second input is to specify distance vector to your target point. This positioning procedure is also implemented in automatic assembling process of J-SEATdesigner. Thus user can use THUMS like usual FE dummy model. Fig.1 shows positioning simulation results for THUMS sled test. Each joint angle is calculated by distance from initial points of hand and foot to their target point.

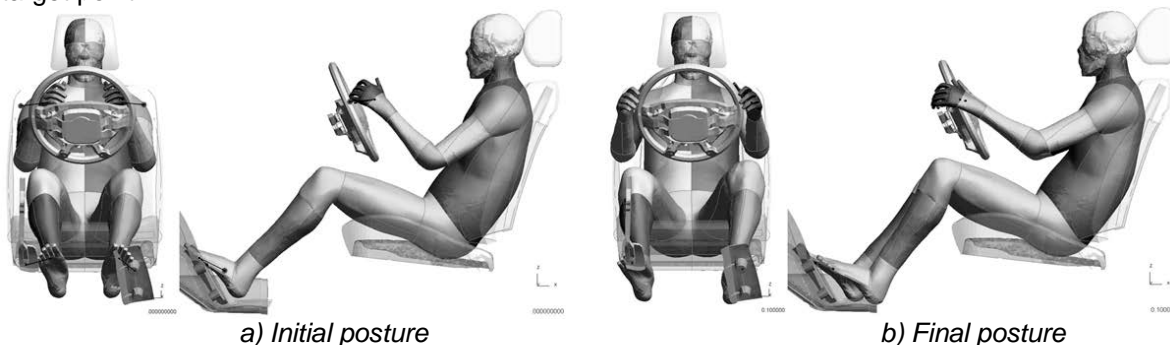


Fig. 1: THUMS positioning results based on pre-calculated joint angles

### 3 Effect of residual stress on comfort analysis

#### 3.1 Covering simulation for seat structure

Covering simulation for seat structure has been done. As material properties of seat cover fabric, we assumed real leather. The deformation during covering simulation is shown in Fig.2. Because the seat cover is not put on the seat foam yet, a lot of wrinkles on the cover are observed after sewing step. After applying proper tension in covering step, almost all wrinkles are removed in final geometry. Fig.3 shows maximum principal stress and maximum principal strain with real leather.

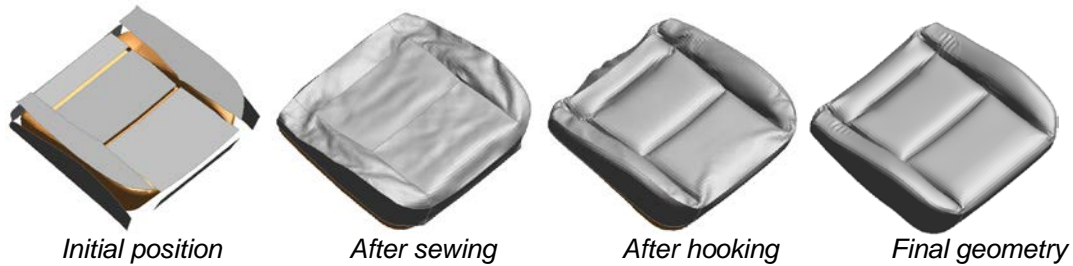


Fig.2: Covering simulation result (Real leather)

#### 3.2 Comfort analysis with rigid dummy

To discuss effect of residual stress in seat foam and seat fabric on the comfort, two simulations have been done with the residual stress and without the residual stress. The rigidified dummy was moved by displacement. Fig.3 shows contact pressure distribution on seat cushion surface. In case of considering residual stress, lower pressure at hip area can be observed. These results indicate that the applied pressure will be reduced with considering residual stress in the foam and the fabric.

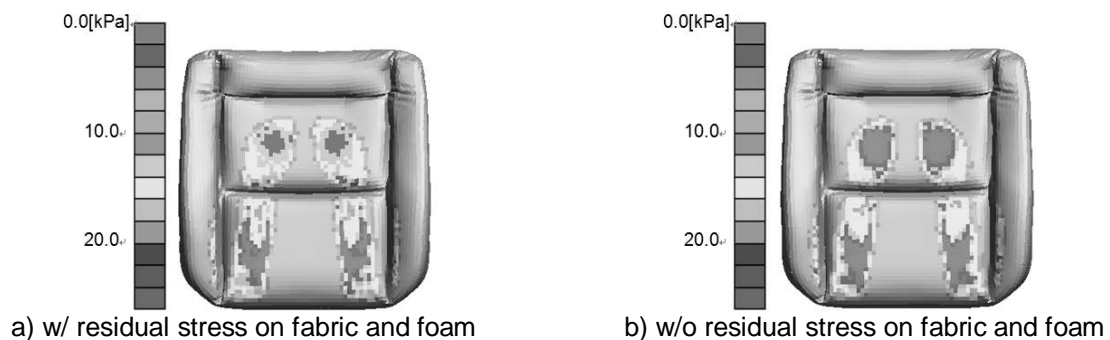


Fig.3: Contact pressure on cushion surface

### 4 Conclusion

In this paper we show the J-SEATdesigner concept and some useful features for seat simulation in LS-DYNA and our investigation for seat covering process simulation. This investigation is implementing in next version of J-SEATdesigner that will be released at the end of this year. J-SEATdesigner is not a simple pre-processor but an integrated system to assemble models efficiently and avoid time loss coming from miss-communication between each engineer. In addition, J-SEATdesigner is designed based on over 20 years' experience in automotive crash simulation. By using J-SEATdesigner, all users can obtain our know-how for automotive crash simulation without any effort and spending time. We hope that J-SEATdesigner helps engineers who need seat related simulation to have useful simulation result in LS-DYNA.





## HUMAN MODELS



# The Effects of Active Muscle Contraction into Pedestrian Kinematics and Injury during Vehicle-Pedestrian Collision

I Putu Alit Putra<sup>1</sup>, Julaluk Carmai<sup>1</sup>, Saiprasit Koetnियom<sup>1</sup>, Bernd Markert<sup>2,3</sup>

<sup>1</sup>Automotive Safety and Assessment Engineering, The Sirindhorn International Thai-German Graduate School of Engineering, King Mongkut's University of Technology North Bangkok, Thailand

<sup>2</sup>Institute of General Mechanics (IAM), RWTH Aachen University, Germany

<sup>3</sup>Faculty of Engineering and Science, University of Agder, Norway

## 1 Introduction

The objective of this study is to develop a finite element model of active human skeletal muscle, which can mimic the contraction behavior of the skeletal muscle in order to get better biofidelic properties of human FE Model. The active 3D muscle model will be combined together with THUMS model from Toyota in order to develop a pedestrian finite element model with 3D active and passive muscles properties. The simulation of pedestrian-vehicle collisions is also conducted in order to analyze the effects of skeletal muscle contraction to the pedestrian injury.

## 2 Hill's 3 element model

The Hill's three element model of muscle is originated from the Hill's work [1]. Hill's model is the basis for most of currently used muscle models and his model is composed of three elements : The Contractile Element (CE), The Series Elastic Element (SEE) and The Parallel Element (PE), as depicted in Figure 1.

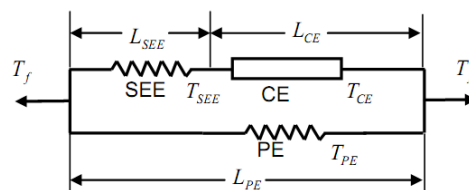


Fig.1: Hill's three-element muscle model

## 3 Material Modelling in LS DYNA

The muscle model was developed by combination of 1D elements and 3D solid tetrahedral elements. In order to simulate the passive behaviour of the muscle, the solid tetrahedral elements were modeled by using Ogden material model (LS Dyna Material model number MAT\_181-SIMPLIFIED\_RUBBER/FOAM) and the 1D elements were used to simulate the active behaviour of the muscle. Material number 156 based on Hill's Muscle (MAT\_156\_MUSCLE) model was applied in the 1D truss elements. Modeling the muscle by the combination of 3D element and 1D element have been published also by Iwamoto et al [2] and Hedenstierna et al [3].

## 4 Results

### 4.1 Simple Biceps simulation

#### 4.1.1 Simple Biceps Isometric Simulation and Kinematics

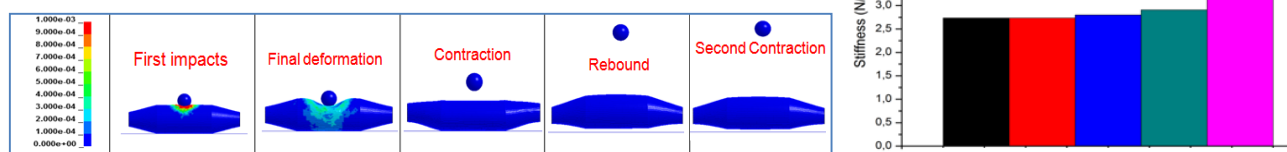


Fig.2: Simple biceps isometric simulation (contour : Von Misses Stress) and stiffness variation result based on activation

#### 4.1.2 Shortening and lengthening simulation

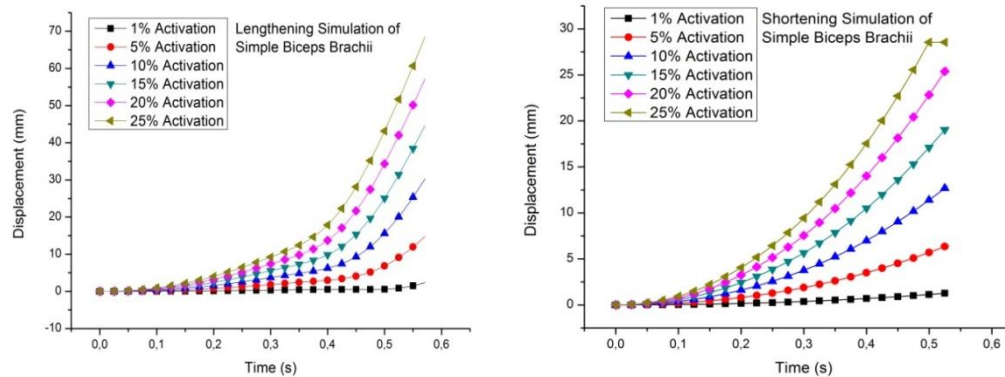


Fig.3: Displacement vs time graph of the shortening and lengthening behaviour of Biceps Brachii in different value of activation

#### 4.2 Vehicle-Pedestrian leg simulation result

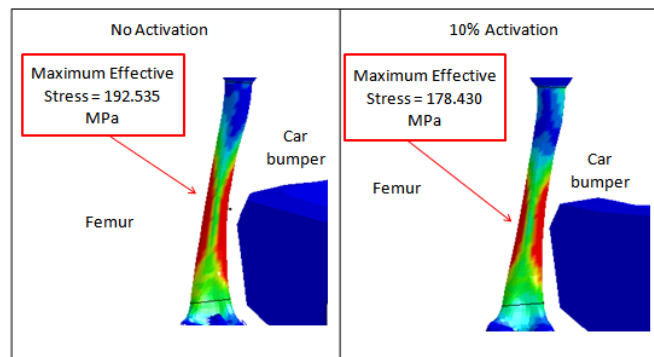


Fig.4: Comparison of effective stress in Femur

### 5 Summary

It has successfully developed a 3D Finite Element Model of Active muscles with real 3D geometries. These muscles were developed by the combination of solid 3D tetrahedral elements with line 1D beam elements. In order to mimic the passive properties of the skeletal muscle, an Ogden material model was implemented for solid tetrahedral elements. To simulate the active behavior of these muscles, a Hill-type muscle model for the line beam elements was implemented. Based on the simulation that were conducted, these muscles model can mimic the contraction behaviour of the human muscles. It has also proven that these muscles can has different stiffness value by changing its activation level. These muscles were also successfully inserted into THUMS Pedestrian Model. Then, from the vehicle- pedestrian leg simulation can be concluded that the active muscles contraction can reduce the injury of the pedestrian, in this case, the effective stress in the femur were decreasing when the muscles contracted. This present study is still in the beginning study regarding active muscle contraction effects in the pedestrian during the pedestrian-vehicle crash. For the next study, there must be an experiment and measurement regarding the activation level of the pedestrian when its in standing and walking position and also when its in danger situation (when the vehicle seems will hit the pedestrian) . This can be done probably by the combination of EMG measurement and 3D virtual-reality video simulation.

### 6 References

- [1] Hill, A.V. The heat of shortening and the dynamic constants of muscle. Proceedings of the Royal Society of London. Series B, Biological Sciences 126(843), 1938,136-195
- [2] Masami Iwamoto, Yuko Nakahira. A Preliminary Study to Investigate Muscular Effects for Pedestrian Kinematics and Injuries Using Active THUMS. IRC-14-53 IRCOBI Conference 2014
- [3] S. Hedenstierna, P. Halldin, and K. Brolin. Evaluation of a combination of continuum and truss finite elements in a model of passive and active muscle tissue. Computer Methods in Biomechanics and Biomedical Engineering, 11(6), 2008, 627-639.

# Stability and Sensitivity of THUMS Pedestrian Model and its Trauma Response to a Real Life Accident

Lianjie Wen<sup>1</sup>, Christophe Bastien<sup>1</sup>, Michael Blundell<sup>1</sup>, Clive Neal-Sturgess<sup>1</sup>, Kambiz Kayvantash<sup>2</sup>

<sup>1</sup> Coventry University  
Faculty of engineering and Computing, UK

<sup>2</sup> CADLM, France

## 1 Introduction

With dramatically rapid development of computing and modelling technology, occupant and pedestrian safety models went through the development of crash test dummies and multi-body mathematical dynamic modelling to finite element pedestrian human model (THUMS 4.0). THUMS 4.0 is a state of art human model which includes a skeleton structure, as well as internal organs and soft tissues, which makes it a suitable candidate to analyze accident trauma. The THUMS model has been correlated at the limbs level [1], as well as successfully validated against rigid impactor tests, in frontal [1][2], lateral and oblique [3]. Nevertheless, the responses capture during these tests were overall force-displacement characteristics, not at the trauma and injury level [1][3], consequently more research is needed to investigate whether human models are accurate enough and adequate to capture trauma injury levels. The THUMS human model is based on finite element analysis and the injury threshold levels are captured using a plastic strain tensor and only a kinematics computation was undertaken as a mean of validating the model [1]. Little to no research has documented trauma correlation to real-life accidents, but only the kinematics [4] using accident data from the APROSYS database [5]. The APROSYS relates to pedestrian and cyclists fatalities and is limited in the detail photographic evidence on the damage vehicle and the deceased [5], as well as a computation of the thrown away distances and objective measurements of the accident scene. Consequently, Coventry University has approached West Midlands Police in order to access best in class accident data, used in criminal courts, in order to investigate the accuracy and adequateness of the THUMS human model. This paper investigates the stability of the THUMS pedestrian model in different impact scenarios, as well as performing an initial injury response comparison against a real-life pedestrian collision and will focus on the ability for the THUMS model to relate to the pedestrian injury and trauma autopsy results.

## 2 Results

### 2.1 Stability and sensitivity at 30km/h

The study has showed that the THUMS pedestrian model was very stable at European city speeds (30km/h) and that its response in various postures was numerically stable.

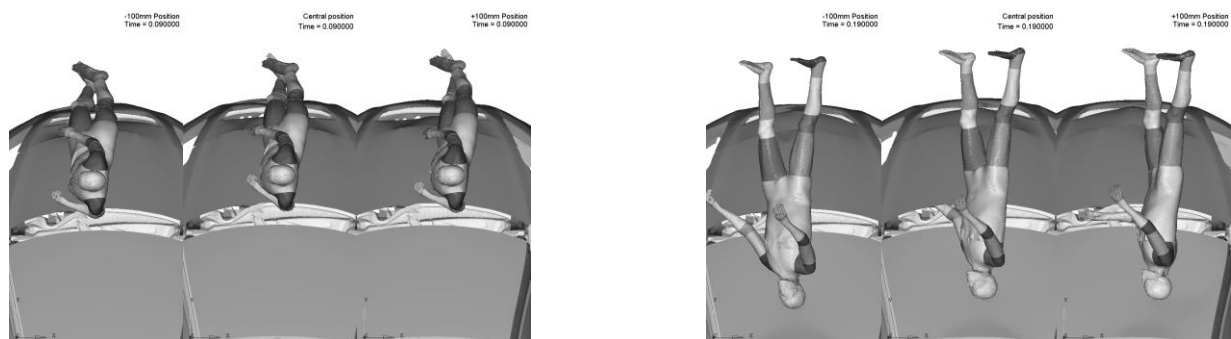


Fig. 1: Sensitivity study – pedestrian kinematics (focus on early human body rotation). (-100mm Left, centre and +100mm Right)

A kinematics sensitivity analysis was undertaken by changing the pedestrian position  $\pm 100\text{mm}$  from the center line and concluded that the head cross vehicle excursion was small; however the body rotation was noticeable (Fig.1:). Further analysis of the contact forces between the pedestrian and the bumper system has highlighted some different force level in the first 0.03s which initiate body rotation which is visible from time 0.09s.

## 2.2 Accident correlation to autopsy (16m/s to 19m/s)

A Pedestrian accident, involving a 183cm, 61kg Caucasian male, was reconstructed and the trauma analyzed, as depicted in Fig.2:

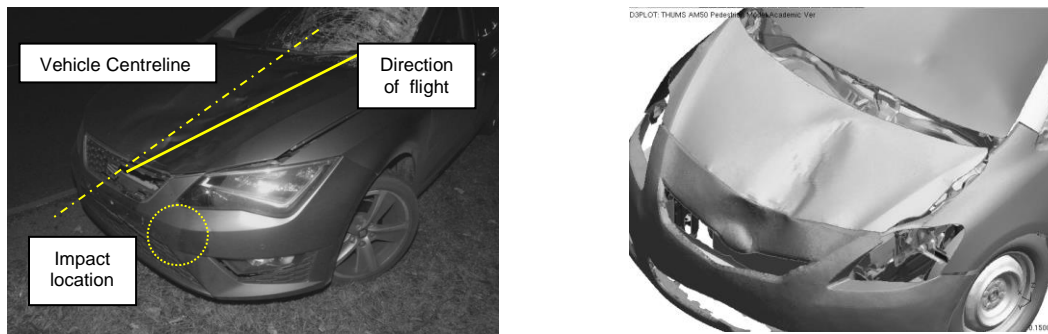


Fig.2: Vehicle damage at the accident scene and related computer model

The study has shown that the computed pedestrian head end positions are different, because no failure criteria in the windscreen have been set in the standard Toyota Yaris computer model [6]. As the computer model's windscreen does not numerically fail on impact, it causes artificial forces in the head which is then compressing the vertebrae. Consequently, the THUMS trauma outcome and the autopsy results diverge in the neck area. Overall, the THUMS model was able to compute trauma values to internal organs (liver, kidney and spleen) successfully matching the area referenced in the autopsy, especially at 19m/s. Heart damage was not correctly captured for either speed. The THUMS predictions were also promising in the ribs area, where comparable damage was observed at 19m/s in a comparable area. The clavicle damage was observed in the autopsy, but only well captured by the 16m/s impact, while marginal fracture was predicted for a 19m/s pedestrian impact.

There was a level of interpretation in the leg positions and the likelihood of which leg would have bared the initial body weight just before the impact. Nevertheless the trauma of the right leg accident outcome matched the autopsy results for 19m/s. it is suggested that more left leg position variations need to be investigated to capture a wider range of kinematics and trauma outcomes to ascertain the initial pedestrian stance prior to impact.

## 3 Conclusions

The THUMS model has been tested against a 30km/h pedestrian impact scenario against a typical sedan vehicle, including different postures. The THUMS model proved to be stable at this speed. It has been observed that the kinematics of a pedestrian human model is sensitive at the early impact stage in the bumper area, as localized impact pattern responses dictate the body rotation during the accident. The paper has shown that the knee area is numerically sensitive and would require some improvements to allow the model to compute with much higher impact speeds (57 to 70km/h). After local modification of the knee ligament material definition, the THUMS model has shown to be very stable and provide some useful trauma information, which in some area related to the autopsy report provided by West Midlands Police. It has been observed that the modelling of windscreen shattering is necessary, as artificial head and neck loads were computed but not present in the autopsy report.

The study has shown that the THUMS is capable of providing trauma injuries comparable to an autopsy.

#### 4 Literature

- [1] THUMS, Total Human Model for Safety, AM50 Pedestrian Model. Academic Version 4.0\_20111003, October 2011, Toyota Motor Corporation
- [2] Charles K. Kroell, D. C. S. A. M. N., 1974. Impact Tolerance and Response of the Human Thorax II.
- [3] Joshua M. Shaw, R. G. H. J. D. M. B. R. D. J. H. B., 2006. Oblique and Lateral Impact Response of the PMHS Thorax. *Stapp Car Crash Journal*, pp. 147-167.
- [4] AsPeCSS, EU funded project. <http://www.aspecss-project.eu/>
- [5] APROSYS, EU funded project. [http://cordis.europa.eu/result/rcn/47920\\_en.html](http://cordis.europa.eu/result/rcn/47920_en.html)
- [6] NCAC vehicle database, <http://www.ncac.gwu.edu/vml/models.html>

# The CASIMIR model for Simulation in Seating Comfort Applications – A Status Update for LS-DYNA

Nikolay Lazarov<sup>1</sup>, Dirk Fressmann<sup>1</sup>, Alexander Siefert<sup>2</sup>

<sup>1</sup>DYNAmore GmbH

<sup>2</sup>Wölfel Beratende Ingenieure GmbH + Co. KG

For those who spend a lot of time driving, issues of comfort can become issues of health and safety. Therefore seating comfort is an important point in seat development. Currently, the OEM and Tier-1 are mainly using experimental setups with test drivers for the evaluation of seating comfort. An enhanced seat development is possible by a virtual analysis using software tools like Wölfel Group's CASIMIR/Automotive (see Figure 1). The virtual analysis shows the advantages that non-measurable quantities can be evaluated, the results are reproducible, the assessment is objective and the application is feasible within the early development phase, leading to reduced time and cost expenditure.



Fig.1: Wölfel Group's FE-human-body model CASIMIR with (left) and without (right) seat model.

With a coupled Finite-Element model (Seat and occupant model CASIMIR) the simulation tool CASIMIR/Automotive enables the user to assess the seating comfort. By using digital prototypes comfort relevant aspects and innovative concepts can be investigated within the early development phase.

Main component is the anthropometric occupant model CASIMIR. The development started about 20 years ago at the Technical University Darmstadt and was focused on the internal loads of the lumbar spine with respect to vibrations. Meanwhile a great variety of human models exist. While for Europe only average percentiles as m50 are modeled for North America individual setups as an averaged size women with wide hips are generated. In addition to the human body models also the SAE dummy J826 can be applied providing additional information as the H-point which is relevant for safety issues. The nonlinear properties of the upholstery and the human body with its posture dependence are crucial for a realistic simulation of seating comfort. Accordingly, CASIMIR/Automotive supports the user here by its main components. For identifying and implementing nonlinear upholstery properties, the Material Manager includes all functionalities, starting with material test data up to the integration into an existing Finite-Element-model.

For representing realistic scenarios the posture of the occupant models and their position with respect to the seat can easily be changed by the Posture and the Position Manager. Currently an interface to the ergonomic tool RAMSIS is under development, enabling that information from the packaging can be taken into account in the future.

In general, the simulation uses default load cases as e.g. gravity, but can also be individualized. By applying CASIMIR/Automotive the following quantities can be computed for the investigated design: Static seat pressure distribution of cushion & backrest, Meat-to-Metal, Hip joint position as input data for packaging tools, H-Point following SAE-J826 standard, Backset-Value following FMVSS 208 standard.



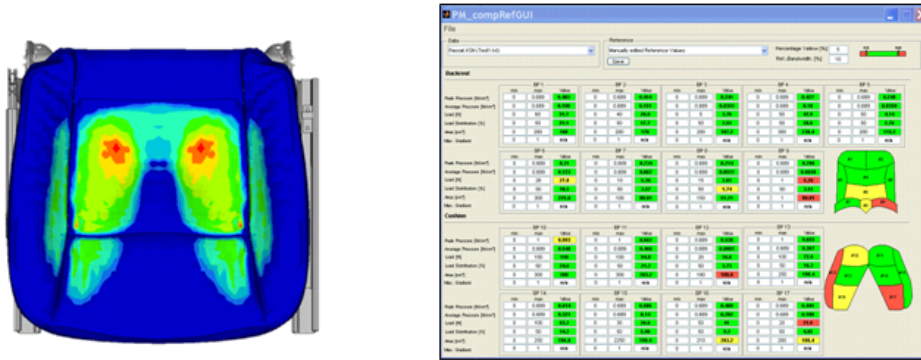


Fig.2: Result of seat pressure distribution (left) and post-processing using Bodymap procedure (right) using the original ABAQUS-model.

Besides the standard viewer tools CASIMIR/Post can be used for the evaluation. Objective assessment methods such as the Body-Map procedure are implemented (Figure 2). Thereby multi-axial result values are reduced to scalar quantities enabling a straight forward seat development by comparing design variants. Additionally, CASIMIR/Post can be applied for measurement data, to link the virtual with the experimental processes.

CASIMIR was initially developed for ABAQUS. Due to increasing user community the tool is currently converted to LS-DYNA. Accordingly companies using LS-DYNA for crash can use their existing knowledge for seating comfort simulations. Nevertheless it must be mentioned that the conversion is made stepwise, i.e. the complexity of the seat modeling is increased steadily.

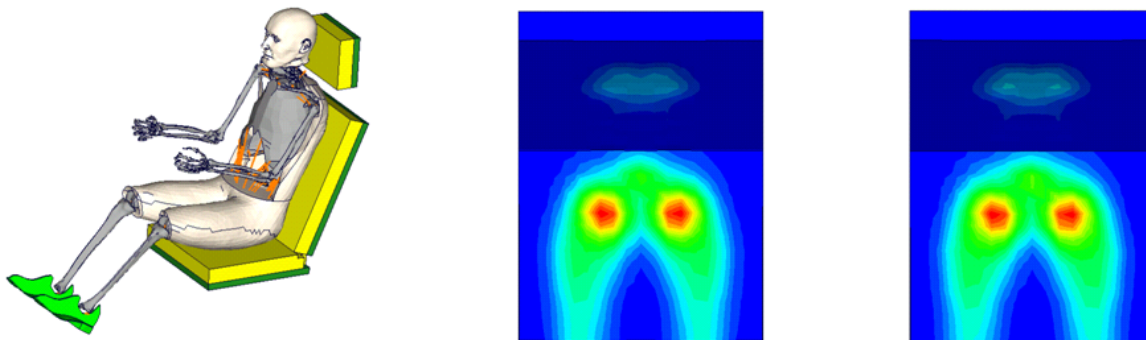


Fig.3: CASIMIR-model for LS-DYNA using a simplified seat model (left) and distribution of the von Mises Stress after seating procedure with LS-DYNA (center) and ABAQUS (right).

First LS-DYNA simulations with the simple seat model (Figure 3, left) showed a good correlation to results with ABAQUS regarding seat stress distribution (Figure 3, center and right) and eigenmodes in seated position. When comparing, both elastic and inelastic behavior of the seat foam respectively CASIMIR flesh were taken into account.

In the presentation the main features of the modeling and the current state of the conversion to LS-DYNA will be shown.

- [1] Siefert, A., Pankoke, S., and Hofmann, J., "CASIMIR/Automotive: A Software for the virtual Assessment of Static and Dynamic Seating Comfort," SAE Technical Paper 2009-01-2311, 2009, doi:10.4271/2009-01-2311
- [2] Siefert, A.; Pankoke, S.; Wölfel, H.-P.: „ Virtual optimisation of car passenger seats: Simulation of static and dynamic effects on drivers' seating comfort Virtual optimisation of car passenger seats: Simulation of static and dynamic effects on drivers' seating comfort ", International Journal of Industrial Ergonomics, Vol. 38 410-424, 2008



**SIMULATION I**  
**MULTIPHYSICS**



# Simulation of the Electromagnetic Flux Compression using LS-DYNA® Multi-Physics Capability

Kunio Takekoshi

Terrabyte Co., Ltd, Japan

## 1 Introduction

Since the release of version R.7.0, LS-DYNA can simulate electromagnetism behavior. In combination with the electromagnetism solver and established/sophisticated structural and thermal solvers, LS-DYNA can simulate the electro-magnetic forming process using one FEM model within one code without any extra licenses.

In this study, simulation results for the electro-magnetic compression method are presented. The method employs the electro-magnetic forming technique and has been experimentally investigated by a lot of researchers for a long time since 1960s. Thus the simulation of the electro-magnetic flux compression can be a good benchmark test for LS-DYNA multi-physics capability.

## 2 The Electro-Magnetic Flux Compression

The electro-magnetic flux compression is mainly used to investigate electronic property of materials such as Carbon Nano Tubes and is also used to prove theories developed in the condensed matter physics and the statistical physics. This is because the spin and the orbital motion of electrons are affected and precisely controlled by magnetic flux density.

A schematic illustration of the electro-magnetic flux compression system is shown in Fig.1. This is based on the system which has been developed by the International Megagauss Science Laboratory, the ISSP, University of Tokyo [1]. There are 4 components, a liner coil, a primary coil, a support coil, and a Helmholtz coil in the system. The liner and primary coils are made of bulk copper (or can be represented as a single turn copper coil). The support coil is made of bulk steel (a single turn steel coil). The Helmholtz coil is composed of two coils (242 turns for each coil) using copper wire.

A specimen of interest is placed at the center of the liner coil during experiment with pickup coils to measure magnetic field, and its temperature is usually controlled using a cryostat. The specimen placed at the system developed by the ISSP-group is subjected to ultra-high magnetic flux density nearly 730 T [1].

The experimental procedure is described in the full paper.

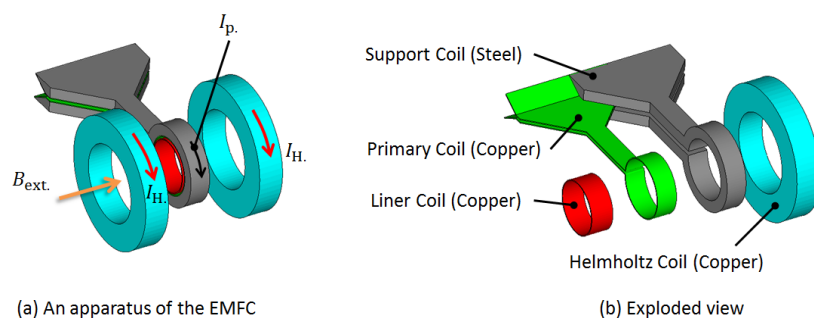


Fig.1: The electro-magnetic flux compression (EMFC) system developed by the ISSP [1].

## 3 Results

The electro-magnetic flux compression analysis is carried out using the development version of MPP-DYNA (SVN Revision 95378) to invoke proposed features in `*EM_SOLVER_BEM` and `*EM_SOLVER_FEM`.

Time evolutions of the deformation of the liner coil are shown in Fig. 2. Although the elapsed time in the simulation result differs from that in a typical experimental result [2], the imploding of the liner is successfully predicted.

Diameter of the liner coil as a function of magnetic flux density is shown in Fig. 3. It is found that both of the simulation and the experiment data shows the same trend less than 100 T, but more than 100 T region, the diameter for the simulation result is underestimated as compared with the experimental result. In other words, the maximum magnetic flux density at the center of the coil evaluated in the simulation is one third of that evaluated in the experiment. It is also found that the minimum diameter of the liner coil observed in the simulation is roughly the same as that in the experimental result shown in Fig. 3 (Right)

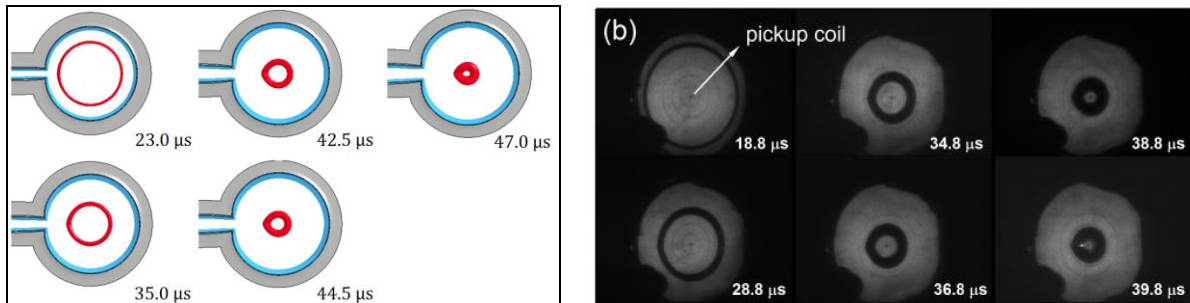


Fig.2: (Left) Evolution of liner coil predicted by the electro-magnetic flux compression simulation. (Right) A typical shadowgraph of the imploding liner [2, 3].

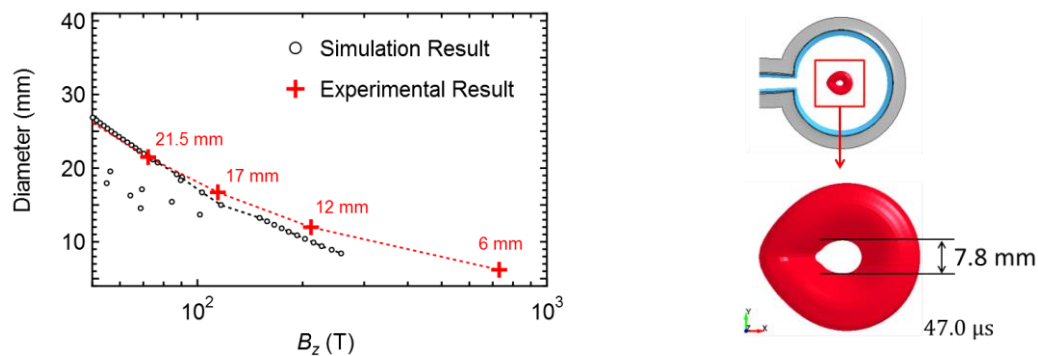


Fig.3: (Left) Diameter of the liner coil as a function of magnetic flux density at the center of the liner coil. The experimental result shown by cross-mark was obtained from reference [1]. (Right) Diameter of the liner coil obtained by the simulation at 47.0 microseconds.

#### 4 Summary

The Electro-magnetic flux compression using LS-DYNA multi-physics capability is presented. The deformation of the liner coil shown in this study is qualitatively the same as the typical experimental result reported in previous papers. Therefore LS-DYNA can be helpful tool in predicting deformations of electrical conductive parts subjected to the elect-magnetic forming. However, the generated magnetic flux density simulated by LS-DYNA is about one third of the value measured by experiments. More sophisticated methods and knowledge about the electromagnetic forming simulation are required to address the discrepancy of the compressed magnetic field between typical experimental results and simulation results.

#### 5 Literature

- [1] Takeyama, S. and Kojima, E., "A copper lined magnet coil with maximum field of 700 T for electromagnetic flux compression", J. Phys. D: Appl. Phys., 44 (2011), 425003
- [2] Nakamura, D., Sawabe, H., Matsuda, Y. M., and Takeyama, S., "Dynamical Process of Liner Implosion in the Electromagnetic Flux Compression for Ultra-high Magnetic Fields," arXiv, 2013, p. 1309.1038
- [3] Photos are presented from the International Megagauss Science Laboratory, the ISSP, Univ. of Tokyo by their courtesy.

# Numerical Methodology for Thermal-mechanical Analysis of Fire Doors

Alessandro Bozzolo<sup>1</sup>, Carolina Ferrando<sup>1</sup>, Angelo Tonelli<sup>2</sup>, Enrico Cabella<sup>2</sup>

<sup>1</sup>D'Appolonia S.p.A. – RINA Group

<sup>2</sup> RINA Group

## 1 Summary

The certification process of a fire door implies that the structure is subjected to a standard fire test, to evaluate its resistance to thermal load. In particular, the door must fulfil specific requirements, such as, that the gaps among the door labyrinths and frame are able to stop flame propagation and that the mean and maximum temperature on the unexposed surface does not exceed defined values.

The present paper describes the numerical methodology used to assess the fire performance of large fire doors (single-leaf and double-leaf sliding doors) commonly used for civil/industrial applications, having length and height of the order of 15-25m and 7-8m respectively. These fire doors cannot be tested at laboratory scale, due to their size, and the only way to verify their structural integrity when subjected to fire is via numerical simulations. The developed methodology aims at verifying thermo-structural response of fire doors when subjected to fire conditions for 60/90/120 minutes, starting from results of laboratories tests on specimen fire doors. The aforementioned methodology, based on the use of the Finite Element Method (FEM), foresees, first, the implementation of a coupled thermal-structural analysis on the 3D FE model of the specimen fire door, to predict the evolution of the distribution of temperature and deformations, to be validated with the values obtained from a set of instruments during the experimental tests. Then, the second step is the thermal-structural analysis on the FE model of the full scale fire door using the same materials and simulations' parameters used for the specimen fire door's model.

The experience carried out for different configurations of door for various applications confirms the procedure is valid and reliable.

**Key words:** Fire resistance; fire modelling; finite element; furnace test.

## 2 Acknowledgments

The publication of data and information included in the present paper have been kindly authorized and made available by MEVERIN, designer and manufacturer of certified fireproof closures and fixed and movable elements for fire compartmentation.

## 3 Objectives

The present study describes the numerical methodology used to assess the fire performance of large fire doors (single-leaf and double-leaf sliding doors) commonly used for civil/industrial applications, having respectively length and height of 15-25m and 7-8m respectively. These fire doors cannot be tested at laboratory scale, due to their large sizes, and the only way to verify their structural integrity, when subjected to fire, is via numerical simulations, using as reference results of standards laboratories tests on specimen fire doors.

The developed numerical methodology aims at verifying thermo-structural response of fire doors when subjected to fire conditions for 60/90/120 minutes, starting from results of laboratories tests on specimen fire doors. The aforementioned methodology, based on the use of the Finite Element Method (FEM), foresees, first, the implementation of a coupled thermal-structural analysis on the FE model of the specimen fire door, to predict the evolution of the distribution of temperature and deformations, to be validated with the values obtained from a set of thermocouples during the experimental tests. Then, the second step is the thermal-structural analysis on the FE model of the full scale fire door using the same materials and simulations' parameters used for the specimen fire door's model.

#### 4 Methodological approach

The numerical analyses were performed using the LS-DYNA software. The implicit solver was used for performing the numerical calculations.

The thermal and mechanical analyses were coupled in the same computational run, thus allowing considerable savings in modeling and computing time. The temperature distribution in the structure was obtained by a transient thermal analysis and used to generate the thermal loads in the mechanical analysis [3].

The methodology adopted for performing the thermo-structural analysis of the enlarged fire doors is articulated in three steps as follows:

- Standard fire test performed on the “specimen barrier” (see Figure 1), to obtain reference experimental temperatures and displacements;



Fig.1: Standard fire test for one specimen barrier including a pass door– Exposed side (left side) and unexposed side (right side) after fire resistance test

- Finite Element (FE) analysis, able to accurately replicate the experimental test on the specimen barrier, by setting up the FE material model parameters. The following Figure shows, as example, a FE model of a specimen barrier (sliding door), having a wall opening dimension of 2600 x 2800 mm; as shown in the picture, the FE model includes a pass door;

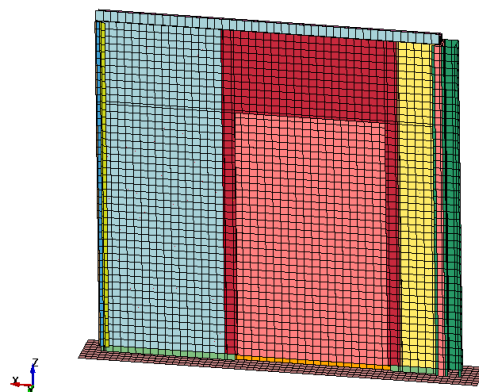


Fig.2: Example of Finite Element model of a specimen barrier having an opening wall dimension of 2600 x 2800 mm

- Coupled thermal-structural analysis on the enlarged fire door (wall opening dimension of 15000 x 8000 mm, carried out by using the previously calibrated model;





Fig.3: Example of Finite Element model of an enlarged fire door (wall opening dimension: 15000 x 8000 mm)

- Results analysis: the calculated displacements and temperatures distribution on the FE enlarged fire door model are analysed, to evaluate its structural integrity; more in detail, it must be verified that the gaps among the door labyrinths and frame are able to stop flame propagation and that the mean and maximum temperature on the unexposed surface does not exceed defined values.

## 5 Conclusions

This work has described the numerical approach that has been developed by RINA Group to assess the fire performance of large fire doors (single-leaf and double-leaf sliding doors), commonly used for civil/industrial applications. These fire doors cannot be tested at laboratory scale, due to their large size (length and height of the order of 15-25m and 7-8m respectively), and the only way to verify their structural integrity when subjected to fire is via numerical simulations.

The methodology, starting from experimental standard fire tests carried out on specimen barrier of reduced sizes, is articulated in several steps: first, the generation of FE models for the 'specimen' fire doors, properly calibrated on the basis of the available experimental results; second, the development of enlarged FE models, where the same loads, boundaries conditions, materials properties of the specimen barrier are applied; third, the development of coupled thermal structural simulations of enlarged doors, reproducing the standard fire test of different time duration (60/90/120 minutes, on the basis of the resistance class to achieve), according to the standard UNI EN 1634-1 [1].

The FE models described in this paper included the necessary complexity of the fire doors and test setup along with the temperature dependency of the constituent materials. The challenges of validating FE numerical models with the data available from the standard fire test have been also described.

The FE models were shown able to capture key thermal and structural responses, thereby giving confidence in its ability to reproduce the real behavior of 'specimen' barriers and enlarged fire doors, when subjected to fire.

## 6 Literature

- [1] EN 1634-1, Fire resistance and smoke control tests for door and shutter assemblies, openable windows and elements of building hardware 2014
- [2] M. Tabaddor, P. D. Gandhi, G. Jones, 'Thermo-mechanical Analysis of Fire Doors Subjected to a Fire Endurance Test', Journal of Fire Protection Engineering 2009 19: 51, DOI: 10.1177/1042391508098899
- [3] A. B. Shapiro, 'Heat transfer in LS-DYNA', Livermore Software Technology Corporation, 4<sup>th</sup> European LS-DYNA Users Conference – Implicit/New Development
- [4] Eurocode 3 'Design of Steel Structures - Part 1-2: General Rules - Structural Fire Design' European Prestandards ENV 1993-1-2
- [5] MEVERIN, Engineering Fire Doors and Wall; web site: <http://www.meverin.com>
- [6] S. Lundberg, 'Material Aspect of Fire Design', TALAT Lectures 2502, Date of Issue: 1994
- [7] P. Boscarol, F. De Bona, A. Gasparetto, S. A. H. Kiaeian Moosavi, L. Moro, 'Thermal Analysis of Fire Doors for Naval Applications', Proceedings of the PRADS2013, pp. 451~456 20-25 October, 2013 CECO, Changwon City, Korea

# A Contribution to CESE Method Validation in LS-DYNA

Edith GRIPPON<sup>1</sup>, Nicolas VAN DORSSELAER<sup>1</sup>, Vincent LAPOUJADE<sup>1</sup>

<sup>1</sup>DynaS+, France

## 1 Introduction

In fluid mechanics, a compressible flow is said when the density varies during a pressure change. Empirically, it is considered that when  $\text{Mach} > 0.3$  the flow is compressible. In this case, shock waves, contact discontinuities and relaxation can be created when an obstacle is encountered.

Since LS-DYNA R7, a new CESE method is available. Several finite element studies were performed by DynaS+ to evaluate the precision of this method in pure CFD studies and to confirm good abilities in Fluid Structure Interaction studies [1].

Pure fluid cases were tested on strong shocks and expansion studies. Results were compared to experimental data extracted from reference papers. The very good precision obtained with the CESE solver and its ability to represent very dynamic phenomenon will be shown. Fluid Structure Interaction in 2D was tested with a deformable plate. Results (also compared with experimental data extracted from a reference paper) will be presented and will highlight that the Coupling method in 2D is as efficient as in 3D.

## 2 Validation cases

Several validation cases for the CESE numerical scheme can be found on the LSTC website [2]. So far, this method has been used to solve many different types of flow problems, such as detonation waves, shock/acoustic wave interaction, cavitating flows, and chemical reaction flows.

The solver CESE has proven itself on cases of shock, expansion, interaction shock/shock, expansion/shock and expansion/expansion. The purpose of the tests presented in this paper is to compare the CESE solver in terms of performance with dedicated specialist solvers of the domain.

### 2.1 1D Problem

The two cases presented in this paper are classic 1-D models, corresponding to variant of shock tube [3]. For both, the main purpose is to verify the ability of the CESE solver to effectively solve fluid dynamics problems with strong or/and interaction between discontinuities due to the compressive behavior of the flow [4]. These 1D models correspond to simple data set for which the computation time (less than 1 minute) allow for extensive testing. Most of the time the 1D case has an analytical solution, which allows comparison with real and physical data depending on any parameter.

#### 2.1.1 Pressure Jump 5 orders of magnitude

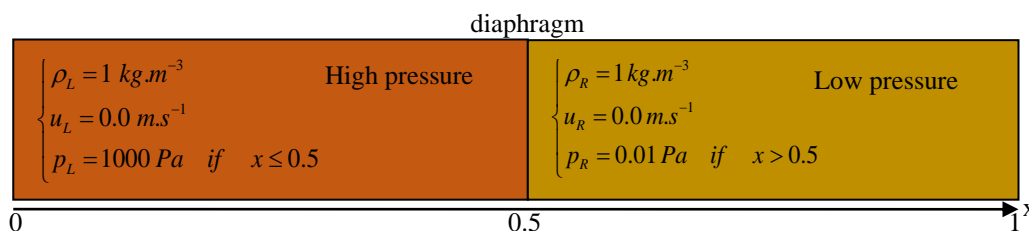


Figure 2: Initial state in the shock tube

#### 2.1.2 Interaction between two shock waves

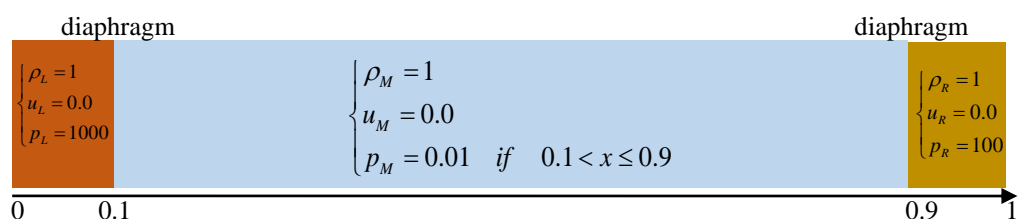


Figure 2: Initial state in the shock tube with 2 diaphragms

## 2.2 2D Problem

The default for CESE solver in LS-DYNA is 3D. But an option for 2D problem calculations is given using a mesh that has only a single layer of elements and no boundary conditions in the z-direction. In some cases, 2D problem calculations save a lot of CPU time.

### 2.2.1 Oblique shock

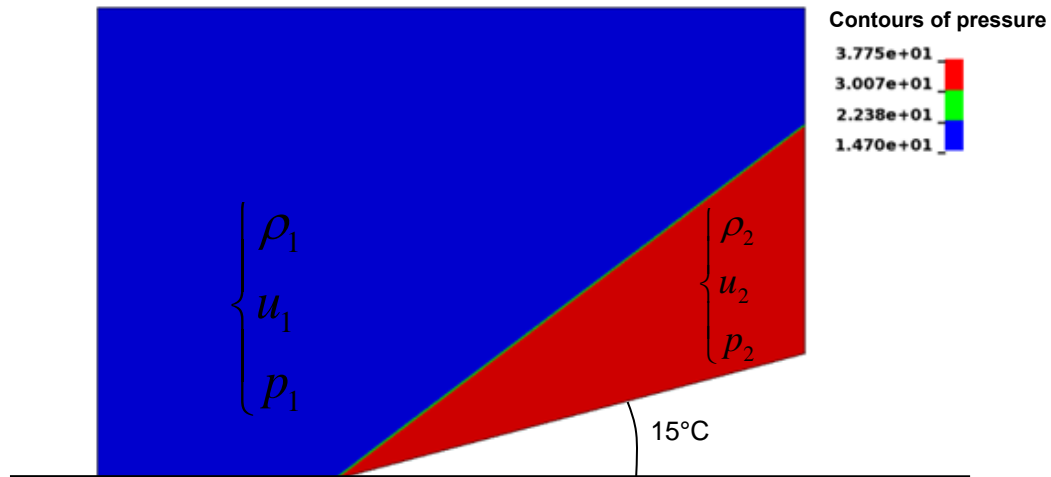


Figure 3: model geometry and contours of pressure, diffraction of a shock wave around a 15° corner

## 3 An introduction to Fluid-Structure Interaction Oblique shock

Because of the lack of fluid-structure interaction FSI validated cases of the CESE solver, different tests were made. The reference study of the behavior of a cantilever panel submitted to a shock tube flow is presented with comparison of numerical and experimental data [5], [6]. The purpose is to confront the CESE solver to an unsteady FSI problem.

### 3.1 Shock wave impacts on deforming panel

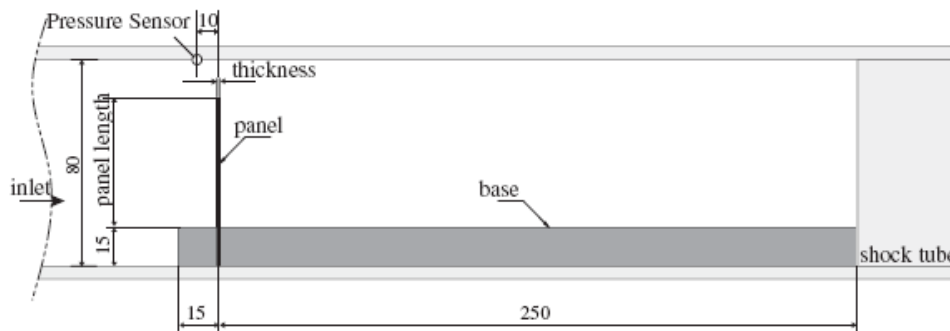


Figure 12: FSI set-up (all dimensions are in millimeters)

## 4 Conclusion

The comparison between the different models (analytical, numerical) and experiments has shown the good accuracy of CESE solver. The 1D cases have validated the capture of the different discontinuities related to a compressible flow: shock, expansion, and contact discontinuities. When discontinuities are not very close, the results are very reliable. Moreover, interaction between shock waves and a complex phenomenon demonstrates the robustness of the CESE solver. The 2D cases involving shock waves and expansions have revealed high accuracy of the calculation code.

Finally, the coupling between the mechanical solver and the CESE solver allows fluid-structure interaction studies. The results obtained by the LS-DYNA code correlate well with the experimental data in reasonable computation time (strong coupling highly parallelized).

## 5 Acknowledgment

M. Iñaki ÇALDICHOURY and Dr. Zeng-Chan ZHANG of LSTC are acknowledged for their helpful comments and suggestions.

## 6 Literature

- [1] Zeng Chan Zhang, Kyoung Su Im, İñaki Çaldichoury, Compressible CFD (CESE) module presentation, 9th European LS-DYNA Conference, Manchester, 2013
- [2] [http://www.lstc.com/applications/cese\\_cfd/test\\_cases/supersonic](http://www.lstc.com/applications/cese_cfd/test_cases/supersonic)
- [3] G. Sod, A survey of several finite difference methods for systems of nonlinear hyperbolic conservation laws, J. Comput. Phys., 1978
- [4] Inaki Caldichoury, Zeng Chan Zhang, 1-D Shock Tube Problem, STC-QA-LS-DYNA-CESE-VER-1.1-, 2012
- [5] Jourdan G., Houas L., Schwaederlé L., Layes G., Carey R., Diaz F.: A new variable inclination shock tube for multiple investigations, Shock Waves, 2003
- [6] J. Giordano, G. Jourdan, Y. Burtschell, M. Medale, D.E. Zeitoun, L. Houas, Shock wave impacts on deforming panel, an application of fluid-structure interaction, Digital Object Identifier (DOI) 10.1007/s00193-005-0246-9, shock wave, 2005



**SIMULATION II**  
**IMPACT/CRACKS**





# Hail Impact Problem in Aeronautical Field

Alessia Prato<sup>1</sup>, Marco Anghileri<sup>1</sup>, Luigi M.L. Castelletti<sup>1</sup>

<sup>1</sup> Politecnico di Milano, Dipartimento di Scienze e Tecnologie Aerospaziali, Milan, Italy

Among soft body impacts, hail impact can be considered as one of the most dangerous, especially in aeronautical field. Even in the last month, some accidents occur because of hail impact. An example, in September 2014, an Airbus A330 from Madrid to Buenos Aires has been forced to land at the Ezeiza airport, near Buenos Aires, due to a hailstorm.

The impact of hailstones against structures can have barely visible consequences, such as damage inside materials, especially in composite ones, or heavy consequences, from evident damage of the aircraft to fatal consequences for the passengers.

For all these reasons, a huge champagne of investigation on these phenomena has been done in the last years, especially from aircraft companies and research centers. Even if experimental tests are required to investigate the behavior of structural components subjected to hail impact, the use of numerical simulations becomes more and more important, especially for the predictive possibility of investigation of complex impact scenario.

Explicit finite element codes allow modeling the hailstone using different approach. The historically most used is the Lagrangian (LAG) approach but the high distortion of elements caused numerical instabilities till the bad termination of the analysis. The Smoothed Particle Hydrodynamics (SPH) technique is also used but it presents some limits. To overcome these problems, some explicit codes have recently implemented a new technique that allow to switch from LAG to SPH approach as the distortion of the lagrangian elements increase or as a failure criteria is imposed to the finite elements (FE).

Few research works have been performed using this method and applied it to the study of different material such as aluminum (Plassard et al. in [1]) or soil behavior. Some numerical models have been performed not only using LS-DYNA (Beal et al. in [2]) but also using other explicit finite element codes. In this paper, an investigation of the hail impact phenomena under a numerical point of view is presented. After a short description of different hail models, a comparison among them has been done. Two different case studies are also proposed: an investigation of the effect of different target materials and a single/multiple hail impact against a complex structure (Fig.1). As a result of this investigation, some general considerations on the argument are here presented.

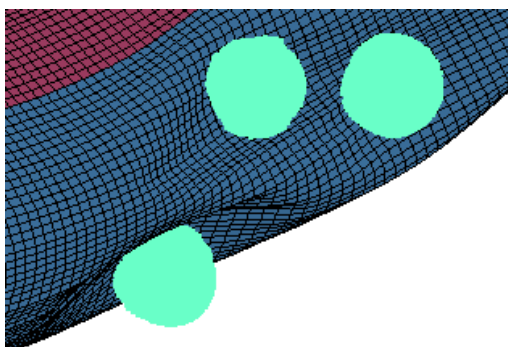


*Fig. 1: Multiple hail impact: contact force.*

**References**

- [1] Plassard F., Mespoulet J., Hereil P., "Hypervelocity impact of aluminium sphere against aluminium plate: experiment and LS-DYNA correlation", 8th European LS-DYNA conference, Strasbourg, 2011
- [2] Beal T., Van Dorsselaer N., Lapoujade V., "A contribution to validation of SPH new features", 9th European LS-DYNA conference, Manchester, 2013
- [3] Kim H., Kedward K.T., "Modeling hail ice impacts and predicting impact damage initiation in composite structures", AIAA Journal, Vol. 38, 2000
- [4] Sánchez, J.P., Pedroche D. A., Varas D., López-Puente J., Zaera R., "Numerical modeling of ice behavior under high velocity impacts", International Journal of Solids and Structures, Vol. 49, 2012, p. 1919-1927
- [5] Livermore Software Technology Corporation, LS-DYNA Keyword User's Manual Vol 2, Version 971 R6.1.0, August 2012

# Simulation of Bird Strike on Airplane Wings by using SPH Methodology

Tugce Kiper Elibol\*, Ibrahim Uslan\*\*, Mehmet A. Guler\*\*\*, Murat Buyuk\*\*\*\*

\*TAI - Turkish Aerospace Industries, Inc., Turkey

\*\* Department of Mechanical Engineering, Gazi University, Turkey

\*\*\* Department of Mechanical Engineering, TOBB University of Economics and Technology, Turkey

\*\*\*\*TSE - Turkish Standards Institution, Turkey

According to the FAA report, 142603 bird strikes were reported for a period of 24 years, between 1990 – 2013. Bird strike with aerospace structures not only threaten the flight security but also cause financial loss and puts life in danger. The statistics show that most of the bird strikes are happening with the nose and the leading edge of the wings. Also, a substantial amount of bird strikes are absorbed by the jet engines and causes damage on blades and engine body. Crash proof designs are required to overcome the possibility of catastrophic failure of the airplane.

Using computational methods for bird strike analysis during the product development phase has considerable importance in terms of cost saving. Clearly, utilization of simulation techniques can dramatically reduce the number of reference tests, where full scale tests are often considered for bird strike. Therefore, development of validated numerical models are required that can replace preliminary tests and accelerate the design cycle.

In this study, several different numerical options are studied for an impact case against a primitive structure to verify the simulation parameters for a bird strike analysis. Then, a representative bird model is generated with the verified parameters. Finally, it collided against the leading edge of a training aircraft wing, where each structural member of the wing was explicitly modelled.

A nonlinear explicit dynamics finite element code, LS-DYNA was used for the bird impact simulations. SPH methodology was used to model the behavior of the bird. Dynamic behavior of the wing superstructure was observed and will be used for further design optimization purposes.



**SIMULATION III**  
**BLAST/PENETRATION**



# An Advanced Identification Procedure for Material Model Parameters based on Image Analysis

Lorenzo Peroni, Martina Scapin, Claudio Fichera

Department of Mechanical and Aerospace Engineering, Politecnico di Torino

## 1 Introduction

Nowadays, Finite Element (FE) simulations are a valid and widespread tool used in the design phase in several fields as well as in the understanding of complex phenomenon allowing, in some cases, the limitation of full-scale experimental tests, which could be dangerous and expensive. The reliability of the numerical results are strongly dependent from the chosen constitutive model and its parameters, which have to be properly determined. The tensile test is often considered for the material model identification. In case of ductile metals and alloys, for which large strains can be reached before fracture, the data analysis at the basis of identification process has to be carefully treated: after the maximum of the engineering stress is reached, the presence of geometrical instability and the localization of necking produce a complex triaxial state. Commonly, in the scientific literature different approaches are used to compute the equivalent stress-strain relation: analytical methods, iterative numerical inverse procedures based on FE simulation and Virtual Field Methods (VFM). The analytical methods implies the definition of mathematical relations for the estimation of the equivalent stress starting from the nominal stress and the geometry of the necking region (e.g. [1]). Some authors proposed to use full-field measurements combined with Virtual Field Methods (e.g. [2]). The majority of the approaches are based on iterative numerical inverse methods based on FE simulations, in which the target function is the minimization of the difference between experimental and computed quantities (e.g. [3]). One limitation of this technique is that the model identification is obtained by fitting the macroscopic quantities (such as force and stroke) while there are not any constraints on the specimen deformation.

## 2 Advanced numerical inverse method

In this work, an advanced FE-based numerical inverse procedure is proposed, with the idea of taking under control also the specimen deformation. The method is based on the digital image analysis of the recorded sequence of the specimen deformation, used to constrain the specimen deformation. The authors propose to define a second part in the FE model (the "Reference Shape", RS), which is able to impose the correct (experimental) deformation to the external profile by interacting with the model of the specimen.

The methodology is applied to the simulation of a tensile test performed on a cylindrical dog-bone specimen, modeled with 2D axis-symmetric elements (Fig. 1). The RS part is modelled with elastic elements and displacement time histories are imposed to its nodes. A contact algorithm is defined between the two parts. The built FE model allows to perform the numerical inverse optimization with two objectives: the minimization of the error between the experimental and the computed force-stroke curves and the minimization of the contact force, which represents an appropriate quantity for the evaluation of the goodness of the deformation.

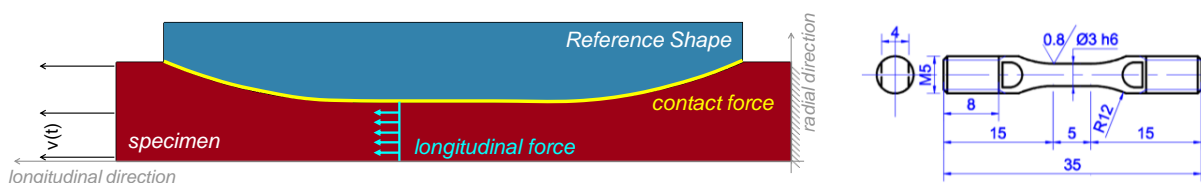


Fig. 1: a) Advanced FE model used in the numerical inverse optimization; b) sketch of the specimen.

The above described procedure is applied to the Johnson-Cook model identification for T91 steel and HDHC pure copper. For each material, also the standard approach (without shape control) is applied.

In Fig. 2, the deformed profiles of specimen and RS are reported at different time steps for T91 steel as obtained from the optimization with shape control. In Fig. 3.a, the experimental mechanical response in terms of force-stroke curve is shown and compared to those obtained from the two optimization processes. The material responses are very close and they well represent the experimental curve. A quantitative evaluation of the differences in the deformation is performed by calculating the RMSE between the coordinates of the nodes of specimen and RS during the deformation (see Fig. 3.b). Before necking, the specimen deformation obtained without shape control is close to that obtained with shape control, but, when the necking becomes significant, the error computed from the case without shape control grows up.

The results show that the advanced optimization procedure leads to an optimum which fulfils both the objectives and allows to increase the reliability of the optimized strength material model. Moreover it is a suitable tool to validate the goodness of the standard optimization results.

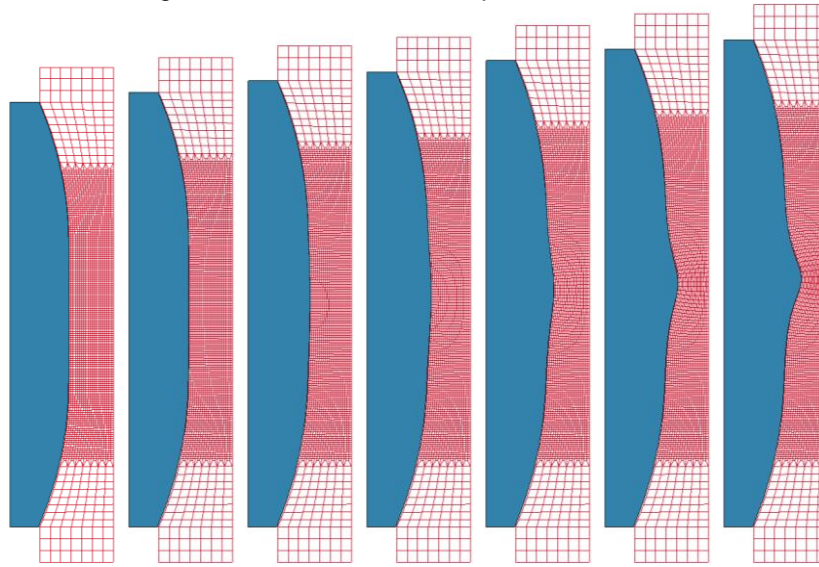


Fig.2: Sequence of the specimen deformation for the optimization with shape control (T91 steel).

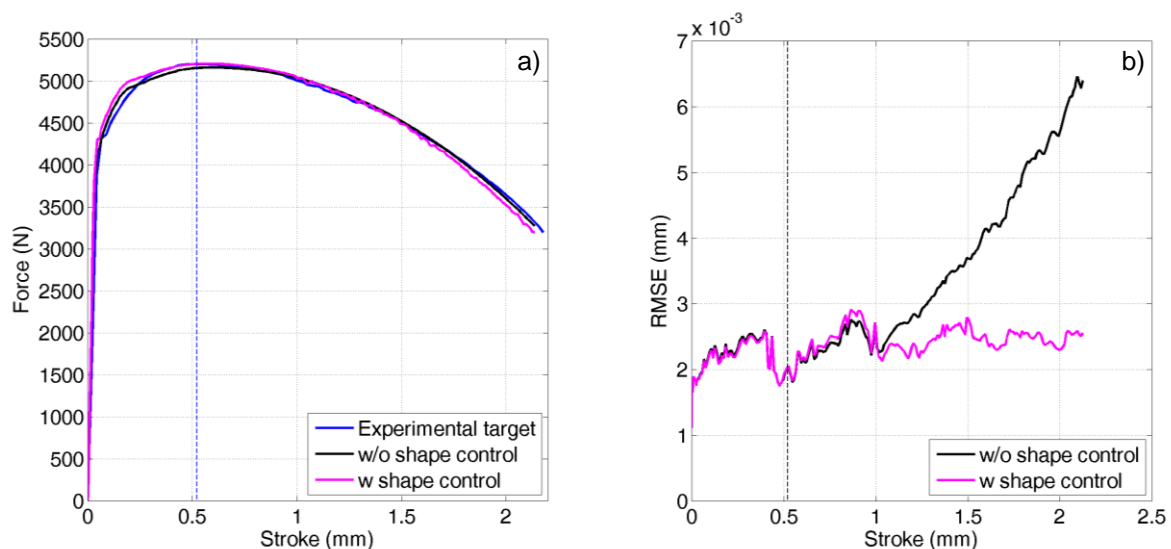


Fig.3: a) Comparison in terms of force-stroke curve; b) RMSE of the node coordinates (the dashed line represents the stroke at which the necking starts).

### 3 Literature

- [1] P. W. Bridgman, McGraw-Hill, New York, 1952, 9-37
- [2] Grédiac M., Pierron F.: "International Journal of Plasticity", 22, 2006, 602-627
- [3] Scapin M., Peroni L., Fichera C., Cambriani A.: "Journal of Materials Engineering and Performance", 23, 2014, 3007-3017



# Model Based Design of Pressure Profiles for Pyrotechnic Actuator using SPH Method & LS-OPT Solution

Etay Kantor, Yoav Lev

Rafael Ltd., Israel

Pyrotechnic Pistons are communally used as fast reacting actuators in many fields and applications, such as seat belt pretensioners, wire and cable cutters and power disconnect devices. The design of such devices is subjected to many unknowns and the design methodology sometimes consists of many experiments in a trial & error process. This paper presents the design process of such a device. In this work a MBD process was applied using LS-DYNA model and LS-OPT optimized solution for reaching upper and lower bounds for the pressure profiles of a pyrotechnic device. The numerical solution decreases the number of required experiments in the design process and cuts its costs.

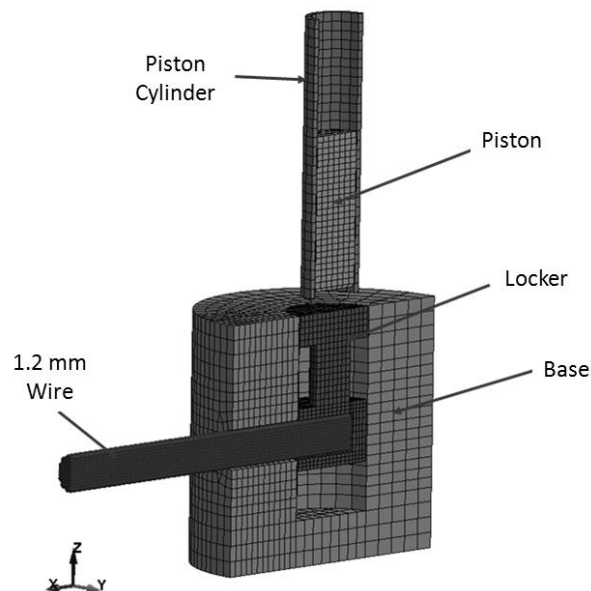


*Fig.1:* The FE model

The designed device is a micro wire cutter, the piston is subjected to pyrotechnic pressure and cuts a 1.2mm wire. Figure 1 presents the LS-DYNA FE model. The wire is modeled with LS-DYNA's SPH mesh- less method in order to achieve better representation of the failure and better contact behavior between the wire and the base's sharp edge.

The applied pressure is then used to simulate the cutting of the wire as can be seen in Figure 2.

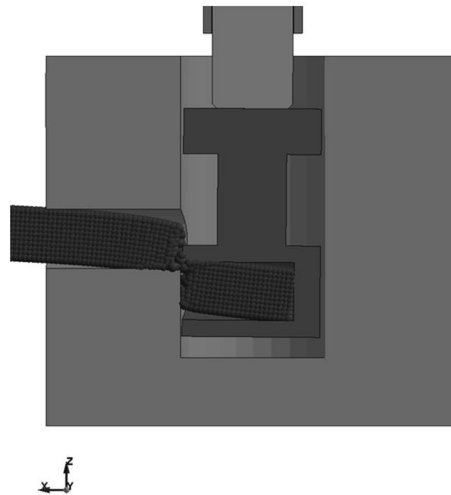


Fig.2: The cutting moment of the wire

The analytic parameters are the design variables used in the LS-OPT tasks, which are solved for two cases-

- a. In order to find the maximum pressure allowed without deforming the bottom of the stopper base.
- b. In order to find the minimum pressure that still cuts the wire.

The use of this numeric method greatly decreases the number of required experiments and lets us understand the device's sensitivity to the examined parameters very early in the design stage.

# LS-DYNA Air Blast Techniques: Comparisons with Experiments for Close-in Charges

Len Schwer<sup>1</sup>, Hailong Teng<sup>2</sup>, Mhamed Souli<sup>3</sup>

<sup>1</sup>Schwer Engineering & Consulting Services

<sup>2</sup>Livermore Software Technology Corporation

<sup>3</sup>University of Lillie

## 1 Introduction

Numerical simulations used to predict events are always challenging. Among the challenges is establishing some basis for confidence in the results when no experimental results exist, i.e. a prediction. While there is no assurance that all the necessary physics have been included in the model, e.g. thermal effects, until the experimental results are available for comparison, there are procedures the user can adopt in model development that will build confidence in the modeling.

The first of these confidence building procedures is mesh refinement. In refining the mesh, or key parts of the mesh, the user should see the results of interest converge. The results may not converge to the eventual experimental result, due to possible missing physics, but a convergent model is an indication of a well posed model. Conversely, if the mesh refinement does not produce a converged result this is an indication of an ill posed model.

While some (all too few) users understand the value of mesh refinement, even fewer users appreciate the confidence provided by solving the problem at hand using different solution strategies. Too many users apply the method they know even if alternative, and possibly better, solution techniques exist. LS-DYNA offers a menu of solution strategies and the knowledgeable user takes advantage of multiple solution strategies when predictions are required.

In this manuscript four solution strategies for air blast loading of structures are presented. The techniques are: Load Blast Enhance (LBE), Multi-Material Arbitrary Lagrange Eulerian (MM-ALE), Particle Blast (PB) and Smooth Particle Hydrodynamics (SPH). The first is an engineering model requiring minimal input and with minimal CPU requirements. The latter three are so called 'first principal' models requiring fairly extensive user input, e.g. equations of state of the explosive and air. The computing resources required for these three techniques are substantial.

**\*KEYWORDS** `LOAD_BLAST_ENHANCED`, `PARTICEL_BLAST`, `Multi-Material ALE`, `Smooth particle Hydrodynamics`, `near-field`, `near-contact`, `explosive charges`

## 2 Summary

This section provides a summary of the experimental results and the corresponding simulations. The reader is reminded that the goal of this effort is not to 'tune' a given solution technique to the experimental results, but rather to illustrate how a suite of solution techniques can be used to establish some confidence in a simulation when no experimental result is available, i.e. a predictive simulation.

### 2.1 Hargather and Settles – Near Field Explosions

Figure 1 is a bar chart summary comparison of the Hargather & Settles near field explosions experimental results – average of three tests with nearly identical scaled ranges – and the corresponding simulation results for the four solution techniques. The experimental results are shown with 'error bars' of one standard deviation computed for the three similar scaled range tests, as indicated on the abscissa.

The `PARTICLE_BLAST` results agree quite well with the average experimental measurements, especially when the standard deviations of the data are considered. The largest relative error, a 9%

under prediction, occurs at the intermediate scaled range of  $Z = 0.69m / kg^{1/3}$ , although the predicted value is within one standard deviation of the experimental results.

The LOAD\_BLAST\_ENHANCED results shown in this comparison all used a TNT equivalency of 1.1 times the mass of the PETN charge. A TNT equivalency of 1.1 is an over estimate of the TNT equivalency needed to match the impulses measured by Hargather & Settles. Thus the LOAD\_BLAST\_ENHANCED results over estimate the maximum central plate displacement.

The MM-ALE results consistently under predict the experimental results, although the degree of under prediction lessens as the scaled range increases. A careful investigation of the amount of leakage due to the fluid-structure interaction algorithm might be the cause of the near field MM-ALE under predictions.

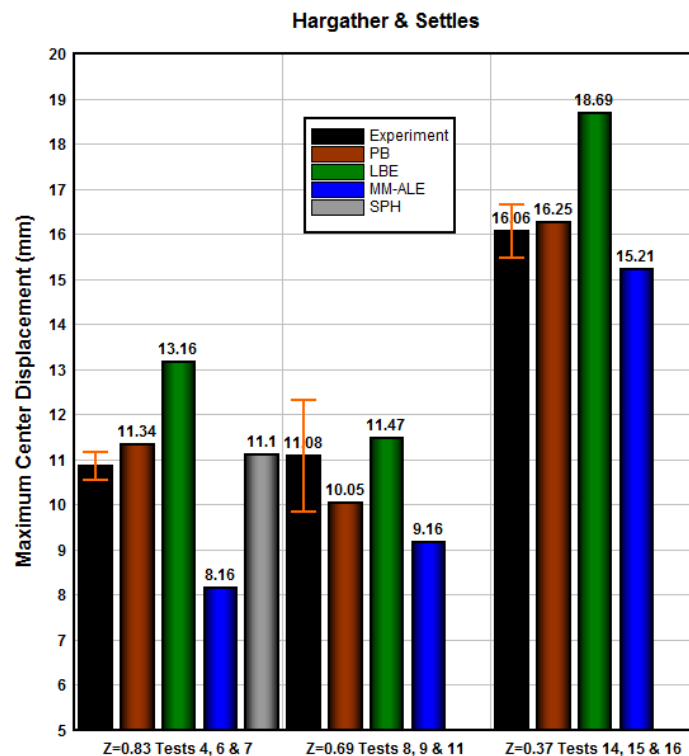


Fig.1: Summary of Hargather & Settles results and simulations.

## 2.2 Neuberger et al. – Near Contact Explosions

Figure 2 is a bar chart summary comparison of the Neuberger et al. near contact explosive experimental results and the corresponding simulation results for the three solution techniques. There are no 'error bars' on the experimental results as there were no repeat tests, nor tests that could be reasonably grouped together. The reader is thus warned not to take the reported experimental results as necessarily being representative of what might have happened with repeat testing.

All the simulation results under predict the experimental maximum plate displacements by about 35% - a significant difference. Somewhat oddly, the solution technique that appears to have the minimum under prediction is LOAD\_BLAST\_ENHANCED. This is odd in that all three scale ranges are less than the recommended lower limit for use of LOAD\_BLAST\_ENHANCED.

Excluding the LOAD\_BLAST\_ENHANCED results, the PARTICLE\_BLAST and MM-ALE results, both axisymmetric and 3D, provide fairly consistent predictions of the maximum displacement; although as already mentioned all are under predictions for these near contact scaled ranges.

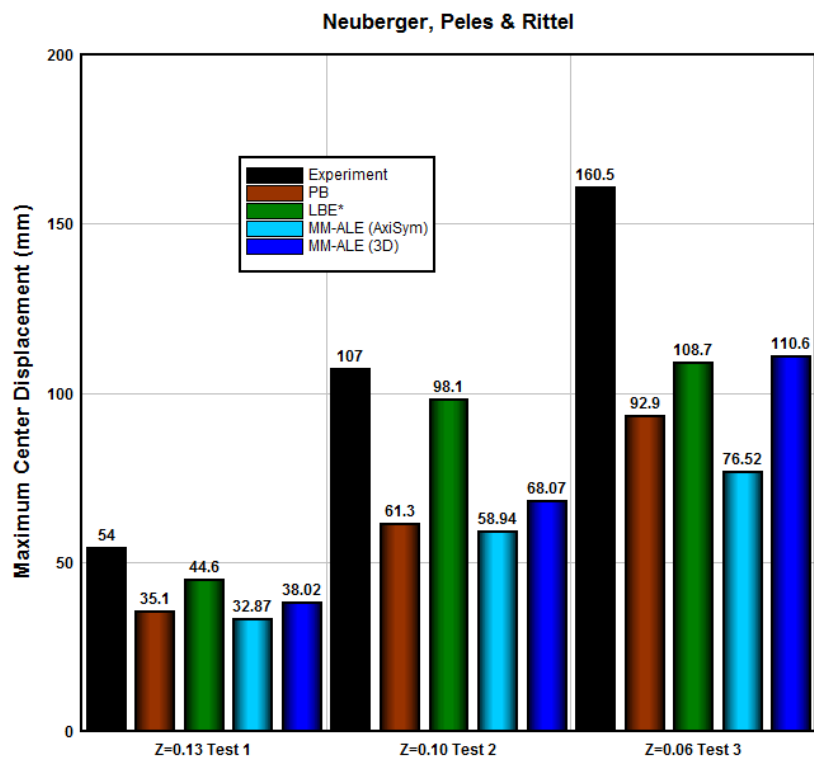


Fig.2: Summary of Neuberger et al. results and simulations.

# ALE/FSI AirBlast Modeling: On the Way to One Billion Elements

Nicolas VAN DORSSELAER<sup>1</sup>, Vincent LAPOUJADE<sup>1</sup>

<sup>1</sup>DynaS+, France

The *Arbitrarian Lagrangian Eulerian* (ALE) method of LS-DYNA® software is the best actual solution to perform AirBlast simulation. Indeed, thanks to its coupling method (ALE/FSI), it allows to the user to model complex blast waves interaction with Lagrangian structures.

Today, due to hardware advances (the computer power highly increased) and LS-DYNA technology enhancement (ALE Mapping, MPP), it becomes possible to consider models with a very large volume of air, while keeping a good accuracy with a small element size. These new possibilities lead to a quantity of elements never reached before, for which LS-DYNA and LS-PrePost® had to adapt.

To be able to perform tests on a realistic case, we modeled a complex ALE/FSI Model with all recent techniques. The case, prepared with the partnership of CEA Gramat (a French Department of Defense Engineering Center), is an air blast simulation with an interaction on a reinforced concrete Lagrangian wall.

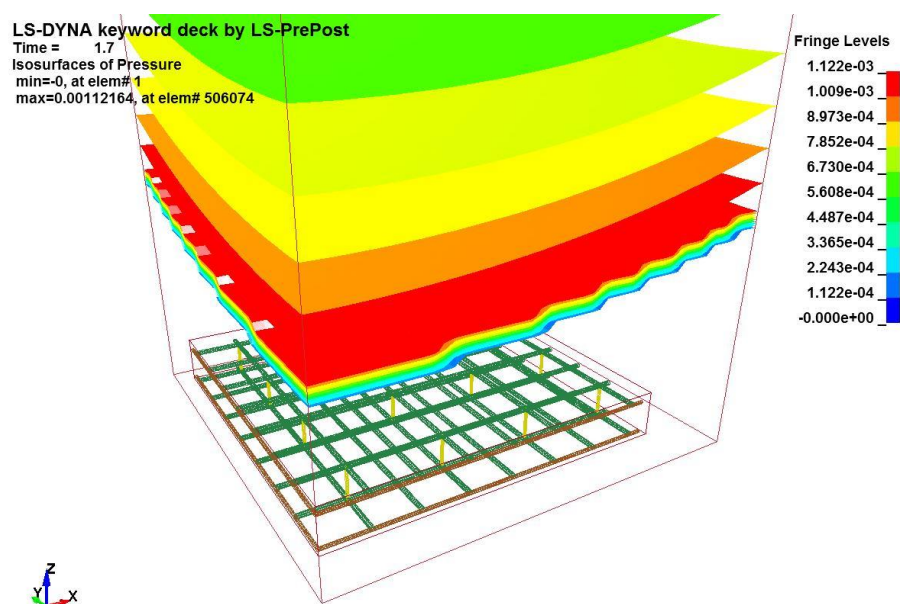


Fig. 1: Blast wave before interaction with the concrete slab.

The chosen case would present no major difficulties if we did it with a “normal” quantity of element, but here, we tested it with three different mesh sizes leading to three big models:

- 50 Millions of elements,
- 100 Millions of elements,
- 200 Millions of elements.

For the creation of big ALE models, a lot of improvements have been made by LSTC to help the user. In LS-PrePost, a “Long Format” has been created to be able to save models containing more than 100 Millions of elements. In LS-DYNA, a new keyword has been created to create the ALE mesh at the beginning of the calculation.

**\*DEFINE\_MMALE\_MESH**

Purpose: This keyword generates structured 3D mesh for Multi-material ALE (MMALE) solver.

This keyword requires a 3D ALE formulation. It is, therefore, incompatible with parts defined using \*SECTION\_ALE2D or \*SECTION\_ALE1D.

Fig.2: New keyword **\*DEFINE\_MMALE\_MESH**

Performing some tests in MPP, we showed that LS-DYNA is perfectly able to run these models in a very reasonable time, even if a difficulty remains concerning decomposition (amount of memory too large for the moment). Concerning post-treatment, some work still need to be done on output format to make easier results using.

Number of Elements	NCPU	Elapsed Time
50M	32	26 h 10 min
50M	64	15 h 22 min
50M	128	9 h 59 min
100M	32	41 h 30 min
100M	64	21 h 26 min
100M	128	11 h 47 min
200M	32	86 h 10 min
200M	64	59 h 59 min
200M	128	35 h 48 min

Table 1: Elapsed Time of all runs

To conclude, setting up a 1 billion ALE / FSI model is headed in the right direction, LSTC and DynaS+ are hardly working on potential solutions that could resolve all problems, for example doing the mesh and decomposition in the same time and creating reduced output data.





**SIMULATION IV**  
**BLAST/PENETRATION**



# An Assessment of ALE Mapping Technique for Buried Charge Simulations

İlker Kurtoğlu<sup>1</sup>

<sup>1</sup>FNSS Savunma Sistemleri A.Ş., Turkey

## 1 Abstract

In this work, the effects of ALE mapping technique developed by LSTC [1] are investigated for buried charge simulations. Before mapping studies, a mesh sensitivity study is performed for the pure ALE simulations to investigate the effect of 3D mesh size on the impulse. The ALE mapping is performed from a 2D axisymmetric model to full 3D model. The mapping time is decided by examining the pressure and velocity results of the 2D model simulations. The effect of different mesh ratios between the 2D and 3D model and the effect of 2D and 3D mesh sizes are also investigated. The impulse on the test plate is compared between all ALE models. Moreover, the normalized displacements at the center of the plates measured in the field tests are compared with the simulation results. A good correlation is obtained between the simulation and test results from the point of displacement.

## 2 Results

The mapping is performed from 4 different mesh size of 2D model to 3 different mesh size of 3D model. The mapping time is decided by investigating the pressure and velocity histories close to the coupled plate.

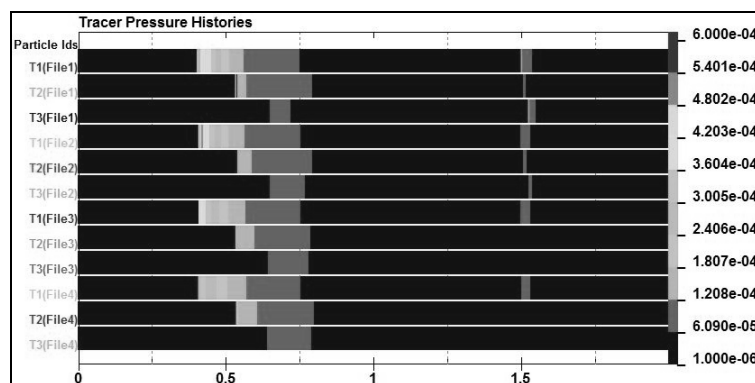


Figure 1 Pressure histories for the tracer points.

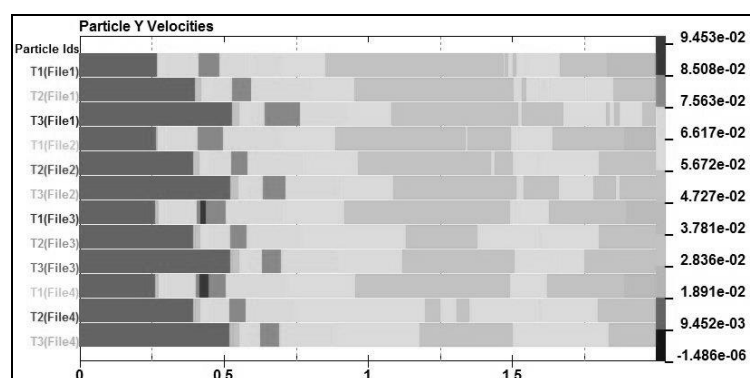


Figure 2 Y-Velocity histories for the tracer points.

The pressure distributions in 2D models, shown in Figure 3, with different mesh sizes are close to each other.

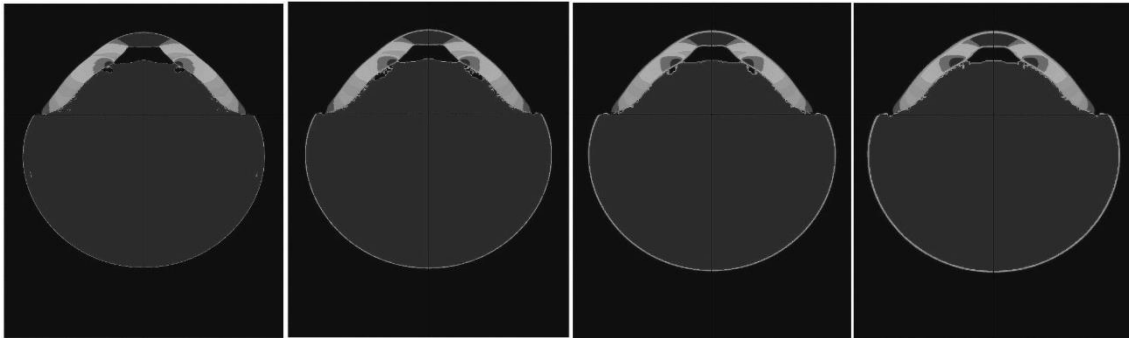


Figure 3 Pressure distributions @400  $\mu$ s for 2D models (1mm – 2mm – 3mm – 4mm).

The mapping results show that by using smaller mesh sizes in the 2D model, the momentum on the plate can be estimated as it is done in the finer 3D model without mapping.

Table 1 3D mapped results compared with no-map model.

	3D Mesh Size	No Map	1mm Map	2mm Map	3mm Map	4mm Map
<b>Momentum (gr-cm/<math>\mu</math>s)</b>	20mm	1911.63	2100.83	2125.55	2151.00	2160.59
	30mm	2010.04	2111.96	2142.54	2115.95	2137.78
	40mm	2048.09	2119.34	2023.61	2054.68	2098.62

The displacement results are also investigated and shown in Table 2. It is observed that using ALE mapping makes the simulation more conservative for the displacements, which is more admissible for the design phase.

Table 2. Normalized midpoint displacements

Model	Results	Model	Results	Model	Results
<b>20mm</b>	0.9195	<b>30mm</b>	0.9613	<b>40mm</b>	0.9789
<b>1mm → 20mm</b>	1.0148	<b>1mm → 30mm</b>	1.0094	<b>1mm → 40mm</b>	1.0685
<b>2mm → 20mm</b>	1.0365	<b>2mm → 30mm</b>	1.0085	<b>2mm → 40mm</b>	0.9962
<b>3mm → 20mm</b>	1.0407	<b>3mm → 30mm</b>	1.0088	<b>3mm → 40mm</b>	1.0013
<b>4mm → 20mm</b>	1.0434	<b>4mm → 30mm</b>	1.0220	<b>4mm → 40mm</b>	1.0126
<b>TEST RESULT</b>					<b>1.0</b>

### 3 References

- [1] Aquelet N., Souli M., 2D to 3D ALE Mapping, 10<sup>th</sup> International LS-DYNA User's Conference, Detroit, USA, 2008.
- [2] AEP-55 Vol.2 Edition 2, Procedures for Evaluating the Protection Level of Armored Vehicles, 2010
- [3] Lapoujade V. (et. al), A Study of Mapping Technique for Air Blast Modeling, 11<sup>th</sup> International LS-DYNA® User's Conference, Detroit, USA, 2010.
- [4] Dobratz B. M., Crawford P. C., LLNL Explosives Handbook – Properties of Chemical Explosives and Explosive Stimulants, Lawrence Livermore National Laboratory, California, USA, 1985.
- [5] LS-DYNA Keyword manual R7.1.

# An Investigation of AA7075-T651 Plate Perforation using Different Projectile Nose Shapes

Buğra Balaban, İlker Kurtoğlu

FNSS Savunma Sistemleri A.S., Turkey

## 1 Abstract

In this study, the ballistic resistance of monolithic and double-layered plates made of AA7075-T651 are evaluated using the non-linear finite element code LS-DYNA®. Plate simulations are carried out using 20 mm diameter, 197g mass hardened steel projectiles with blunt and ogival nose shapes. Penetration simulations of 20 mm monolithic plates made of AA7075-T651 are performed with both Lagrange and ALE methods and the results are compared with literature experimental studies. Simulations are performed with both 2D axisymmetric and 3D solid elements and Modified Johnson Cook constitutive equation is utilized. Moreover, Cockcroft-Latham fracture criterion is used for material behavior of metallic plates. In addition to the material model validation studies, different types of hourglass and element formulations are evaluated and the results are compared under the effects of blunt and ogival projectile nose shapes.

## 2 Results

### 2.1 Lagrange Results

It is observed that residual velocities of perforation studies are quite dependent on mesh configurations. Mesh sensitivity studies are very important to determine optimum mesh configurations for penetration and perforation studies. Moreover 2D axisymmetric elements give consequent results compared with the 3D elements.

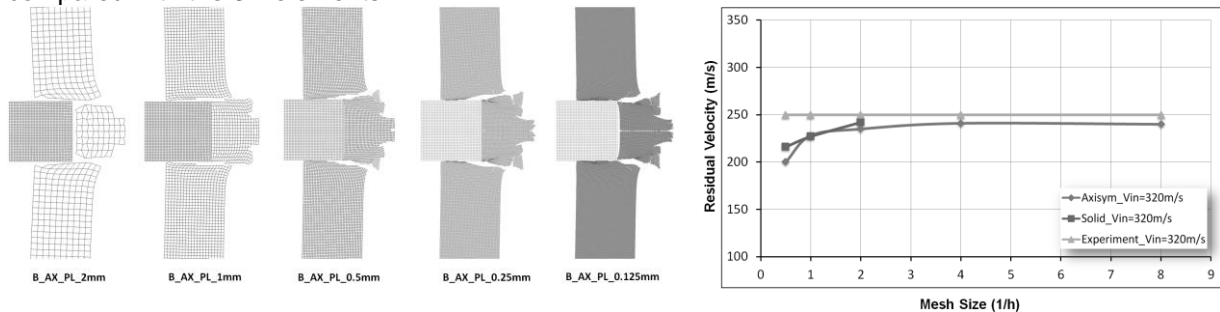


Fig.1: Blunt projectile deformed mesh configurations ( $T=0.07ms$ ) and mesh sensitivity Plots

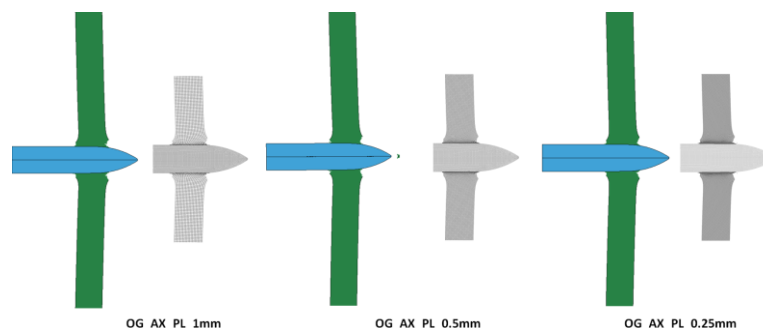


Fig.2: Ogival projectile deformed mesh configurations ( $T=0.07ms$ )

### 2.2 ALE Results

The deformation results for 3 different mesh sizes are shown in the figure below

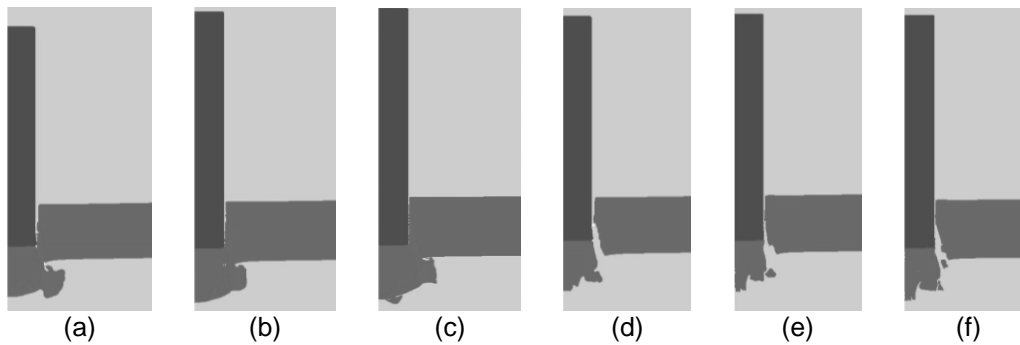


Fig.3: Target plate deformations @0.07ms (a) 0.5mm (b) 0.25mm (c) 0.125mm (SMP solution) (d) 0.5mm (e) 0.25mm (f) 0.125mm (MPP Solution)

It is observed that as the mesh size decreases, the gap between the advection methods increases, but not in significant amount. The exit velocity summary for the blunt projectile is given in table below. Only average values are used.

Mesh Size	SMP (METH – 2)	MPP (METH – 2)	MPP (METH – 3)
<b>0.5mm</b>	229	230	230
<b>0.25mm</b>	232	235	237
<b>0.125mm</b>	236	244	241
<b>Experiment</b>	<b>250</b>	<b>250</b>	<b>250</b>

Table 1: Summary of exit velocity for blunt projectile.

As in the blunt projectile simulations, the deformation results for 3 different mesh sizes are shown in the figure below.

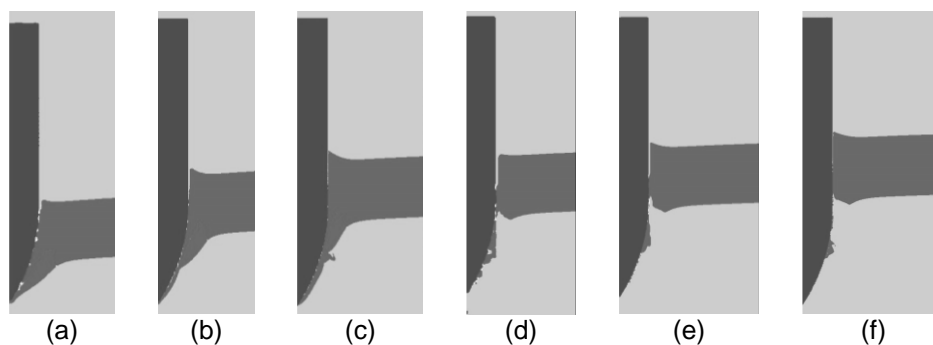


Fig.4: Target plate deformations @0.3ms (a) 0.5mm (b) 0.25mm (c) 0.125mm (SMP solution) (d) 0.5mm (e) 0.25mm (f) 0.125mm (MPP Solution).

As in the case of blunt projectile, method 3 gives lower exit velocities than the method 2. The summary of all results for the ogival projectile is given below.

Mesh Size	SMP (METH – 2)	MPP (METH – 2)	MPP (METH – 3)
<b>0.5mm</b>	-	128	115
<b>0.25mm</b>	-	143	129
<b>0.125mm</b>	-	164	153
<b>Experiment</b>	<b>260</b>	<b>260</b>	<b>260</b>

Table 2: Summary of exit velocity for ogival projectile.

### 2.3 Material Parameter Optimization

Material parameter optimization studies are carried out to determine optimum material parameters and investigate the influence of the parameters on residual velocities. In addition, MAT\_ADD\_EROSION keyword is considered and the maximum shear strain criterion (EPSSH) is utilized. As mentioned

before, Cockcroft-Latham parameter ( $W_{cr}$ ) has the major effect for blunt projectile impact and the EPSSH parameter has the biggest influence for the ogival projectile impacts among the considered parameters.

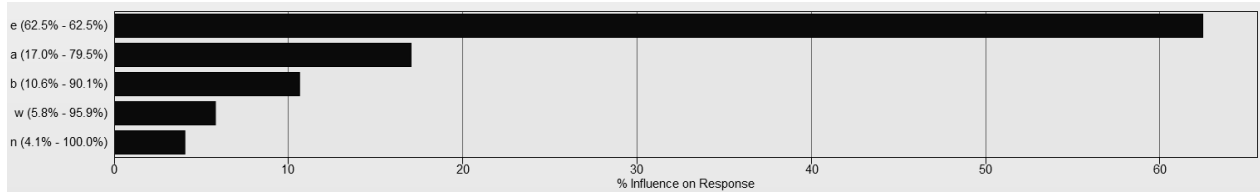


Fig.5: Ogival projectile optimization-2 sensitivity results

## 2.4 Double Layered Plate Simulations

Finally double layered plates are investigated and simulations are performed with the same boundary conditions of monolithic plates. To distinguish between monolithic and layered plates, double layered plates have relatively high ballistic resistance than monolithic plates in case of the blunt projectile penetration. However, for the ogival projectile perforation case monolithic plates show great ballistic performance. This finding supports previous research as mentioned by Dey et al [5].

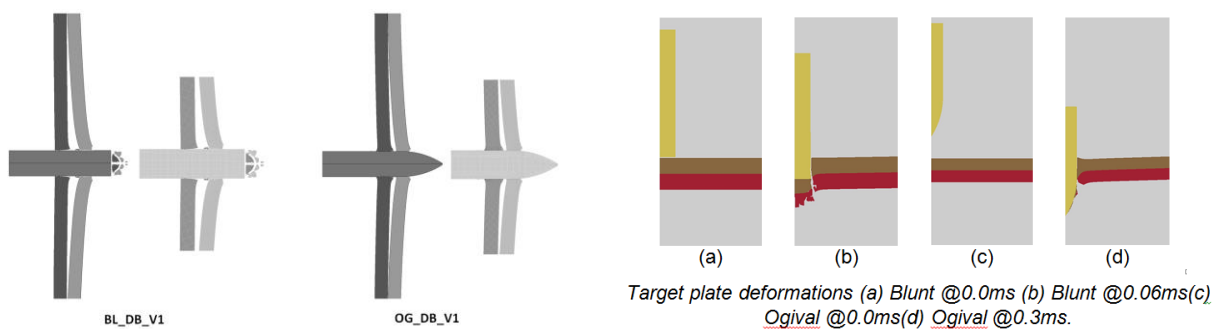


Fig.6: Double layered plate simulations with lagrange and ALE

## 3 Literature

- [1] Børvik T., Hopperstad O.S., Pederson K.O., Quasi-brittle fracture during structural impact of AA7075-T651 aluminum plates. *Int J Impact Eng* 2010;37:537-551
- [2] Børvik T., Hopperstad O.S., Berstad T., Langseth M., A computational model of viscoplasticity and ductile damage of impact and penetration. *Eur.J.Mech A/Solids* 2001;20:685-712
- [3] Schwer L.E., Aluminum plate perforation: A comparative case study using lagrange with erosion, multi-material ALE, and smooth particle hydrodynamics 7<sup>th</sup> European LS-DYNA Conference 2009
- [4] Ls-Dyna Keyword User's Manual, February 2013, Version R7.0, Livermore software Technology Corporation (LSTC)
- [5] Dey S., Børvik T., Teng X., Wierzbicki T., Hopperstad O.S., On the ballistic resistance of double-layered steel plates: An experimental and numerical investigation . *Int.J.Sold.Struc.* 2007;44:6701-6723
- [6] Schwer L.E., A brief look at \*MAT\_NONLOCAL: A possible cure for Erosion illness? 11<sup>th</sup> International LS-DYNA Conference Users Conference,2010.

# Modeling of Ballistic Impact of Fragment Simulating Projectiles against Aluminum Plates

Teresa Fras, Leon Colard, Bernhard Reck

French-German Research Institute of Saint-Louis (ISL), France

In the paper, the ballistic impact test is described in which Fragment Simulating Projectiles (FSPs) have been used against thick plates made of an aluminum alloy. To perforate the plates, the projectiles must have reached velocities higher than 900m/s. The experiment is analyzed by means of LS-DYNA, using an explicit solver of the Lagrangian finite elements.

## 1 Ballistic impact test and its numerical simulation

The Al alloy AA7020-T651 belongs to a group of Aluminum Zinc Magnesium ternary alloys which offer a good resistance to impacts together with a good strength - weight ratio. Due to such properties, the alloy is applied as an important components of many light weight protective structures

To verify ballistic properties of the discussed alloy, the impact test is performed in which Fragment Simulating Projectiles are used. FSPs are standard military penetrators of a non-axi-symmetrical geometry used to simulate artillery shell fragments, [1]. The experimental investigation is performed for the 40 mm thick AA7020-T651 plates in an impact velocity range between 850 m/s and 1500 m/s, Fig. 1.

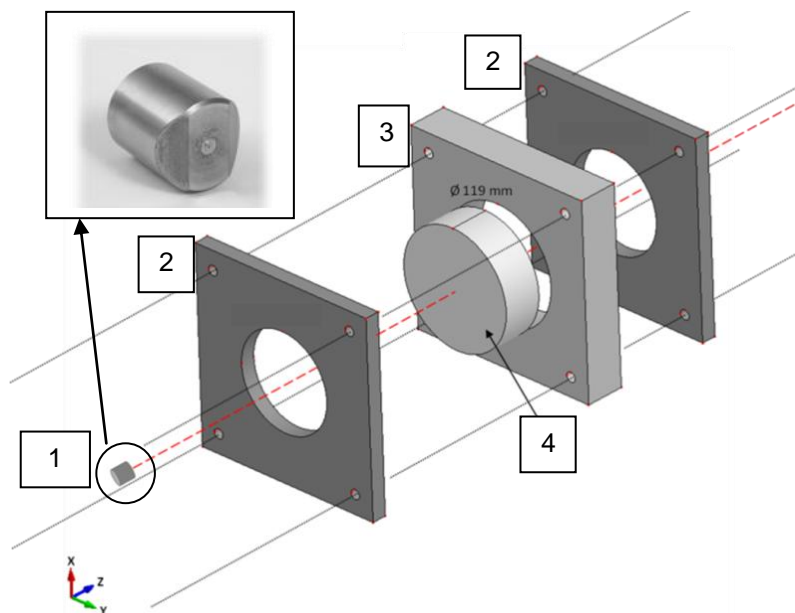


Fig. 1: (a) Experimental configuration for the impact test: 1) projectile, 2) steel frames, 3) aluminum frame, 4) target plate.

For the discussed configuration AA7020-T651/FSP, a ballistic limit curve is determined as a dependence of the initial ( $v_0$ ) and residual ( $v_R$ ) projectile velocities. The ballistic limit velocity, i.e. the



greatest impact velocity the target can withstand without being perforated, is also obtained. With increasing impact velocity, the observed failure modes of the target plates change from plugging ( $v_{\text{impact}} < 1200$  m/s) to discing ( $v_{\text{impact}} > 1200$  m/s), [2].

The aim of the simulation is to examine if the computational model is able to predict the experimentally obtained target responses to the impact. The Johnson - Cook constitutive model coupled with the fracture criterion is applied in the calculations via \*MAT\_107\_MODIFIED\_JOHNSON\_COOK, [3]. The model, which is formulated within the framework of viscoplasticity and continuum damage mechanics, allows large plastic strains, high strain rates and temperature to be accounted for in the calculations. The parameters of the material model are determined basing on the analysis of the mechanical and thermal properties of AA7020-T651 obtained due to our own experimental investigation. Because of the projectile shape, a quarter of the configuration is modeled using 3D solid elements. Contact between the target and projectile is assumed using a contact algorithm which makes possible to tackle with severely distorted elements (\*ERODING\_SURFACE\_TO\_SURFACE).

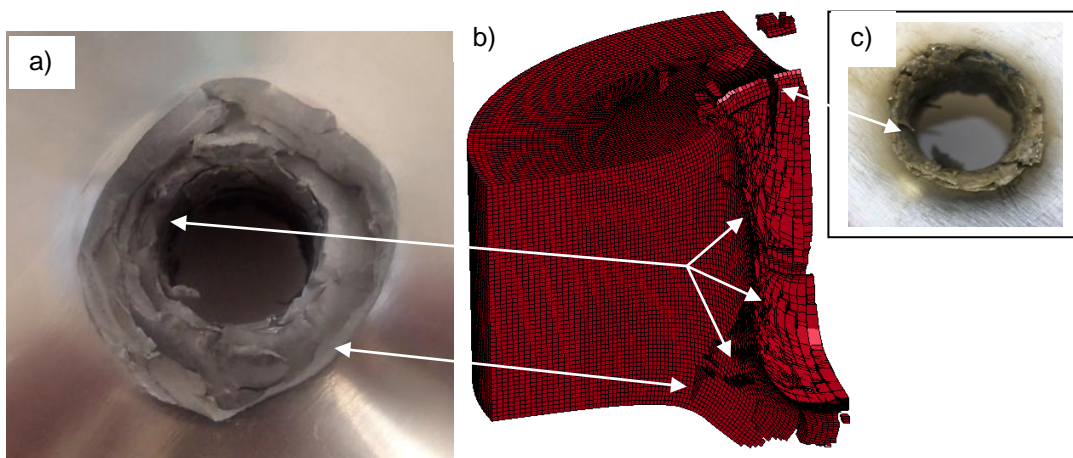


Fig.2: Modeling of a discing failure mode and its comparison with a plate failed due to an impact with an initial velocity 1300 m/s: a) rear plate face, b) numerical results, c) projectile entry.

Fig. 2 shows a comparison between the numerical model of a plate and its experimental equivalent failed due to the impact with an initial velocity of 1300 m/s. Deformation resulting from the impacts is reproduced by the numerical model. Parts of materials from a rear face of the plate are torn away – creating a characteristic shape of the discing failure. Although, the calculations underestimate the expected value of the ballistic limit by 10%, the numerically obtained target response is acceptable.

## 2 Literature

[1] MIL-P-46593A (NOTICE 1), MILITARY SPECIFICATION: PROJECTILE, CALIBERS .22, .30, .50, AND 20MM FRAGMENT-SIMULATING (01-JUN-1996) [S/S BY MIL-DTL-46593B].

[2] Woodward RL. The interrelation of failure modes observed in the penetration of metallic targets. Int J Impact Eng 1984;2.2:121-9.

[3] Børvik T, Hopperstad OS, Berstad T, Langseth M. A computational model of viscoplasticity and ductile damage for impact and penetration. Eur J Mech A/Solids 2001;20:685-712.

# Shock Response Analysis of Blast Hardened Bulkhead in Naval Ship under Internal Blast

Sang-Gab Lee<sup>1</sup>, Hwan-Soo Lee<sup>1</sup>, Jae-Seok Lee<sup>1</sup>, Yong Yook Kim<sup>2</sup>, Gul Gui Choi<sup>2</sup>

<sup>1</sup>Korea Maritime & Ocean University, Marine Safety Technology

<sup>2</sup>Korea Advanced Institute of Science and Technology

## 1 Abstract

It is necessary to restrict the damage area for the enhancement of ship survivability under the internal blast of a Semi-Armor Piercing (SAP) warhead inside a ship's compartment, and to develop design guidance and performance verification technique of Blast Hardened Bulkhead (BHB) for the protection of its damage diffusion to adjoining compartment and continuous flooding. The objective of this study is to develop shock response analysis technique of BHB under the internal blast using MMALE (Multi-Material Arbitrary Lagrangian Eulerian) formulation and FSI (Fluid-Structure Interaction) analysis technique of LS-DYNA code through the verifications of internal blast tests of reduced scale and partial chamber models.

**Keyword Words:** Internal Blast, Blast Hardened Bulkhead (BHB), Reduced Scale and Partial Chamber Models, MMALE (Multi-Material Arbitrary Lagrangian Eulerian), Fluid-Structure Interaction (FSI) Analysis Technique, LS-DYNA code

## 2 Internal Blast Test of Reduced Scale and Partial Chamber Models

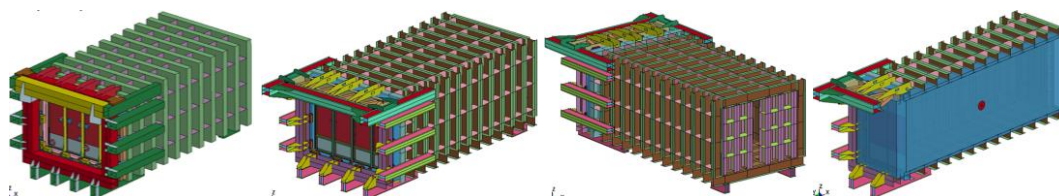


Reduced scale chamber model for internal blast test and damage configurations

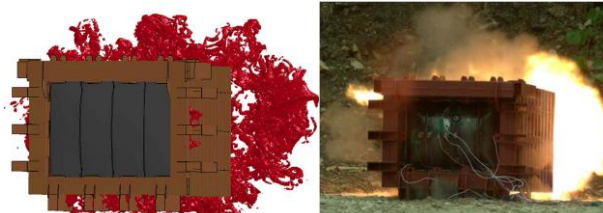


Partial chamber model for internal blast test and damage configurations

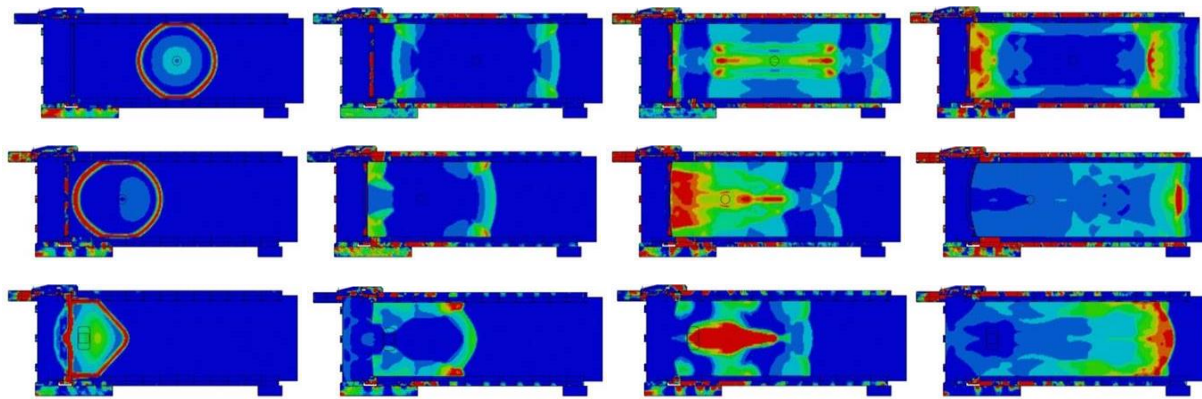
## 3 Modeling & Shock Response Analysis of Chamber Models



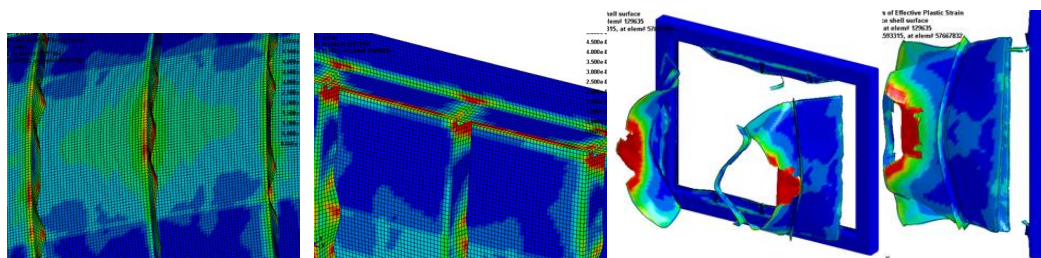
F.E. configurations of reduced scale and partial chamber models



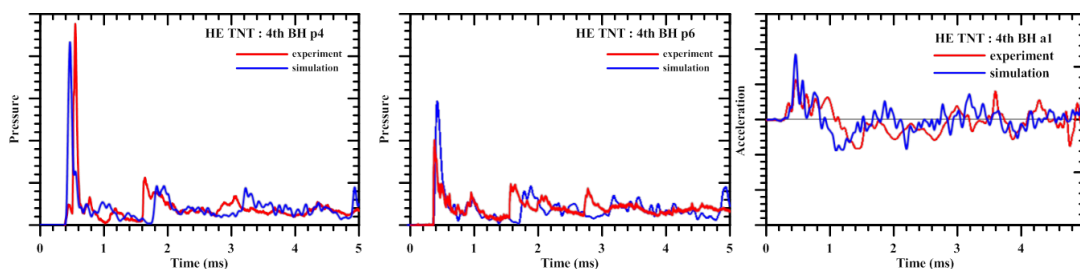
Blast frame in reduced scale chamber model under internal blast of HE TNT charge



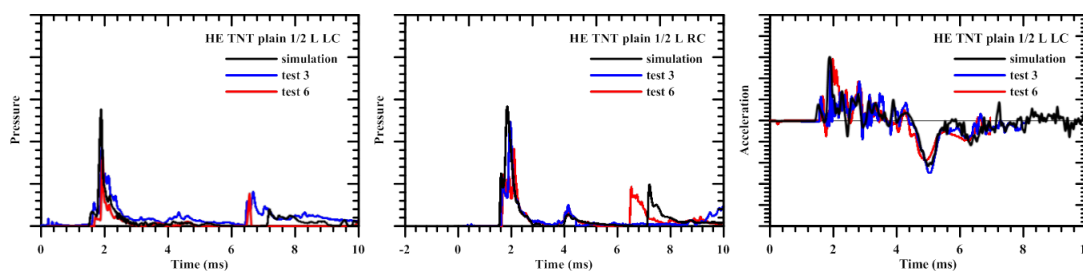
Propagation of shock pressure in part chamber model according to stand-off distance of HE TNT



Damage configurations of partial type bulkhead at stand-off distance 1/2L & 1/16L



Pressure & acceleration responses between experiment & simulation with HE TNT at 4th bulkhead



Pressure & acceleration responses between experiment & simulation with HE TNT at stand-off distance 1/2L

#### 4 Summary

In this study, shock response analysis was carried out for the reduced scale and partial chamber models under the internal blast, and its response analysis technique was verified with the test results of 5 bulkhead models of reduced scale chamber models and 2 types of bulkheads of partial chamber ones according to stand-off distance of HE and LE TNT charges, using MMALE formulation and FSI analysis technique of LS-DYNA code. Shock response characteristics could be also figured out through the verifications of response analysis technique compared with the internal blast test results.

Through the verifications of the internal blast simulations with test results, important factors should be considered carefully, such as FSI analysis techniques, damage mechanism, fracture criterion, and welding effects. It could be found that damage configurations of each bulkhead generally showed good agreement with those of internal blast tests, and that pressure and acceleration responses of shock response analysis, also with those of tests.



# **SIMULATION V**

## **MATERIALS**



# Mechanical Response Modelling of Different Porous Metal Materials

Matej Vesenjak, Matej Borovinšek, Aljaž Kovačič, Miran Ulbin, Zoran Ren

Faculty of Mechanical Engineering, University of Maribor, Slovenia

Porous metals have been increasingly used in modern engineering applications over the past decades due to their multi-functionality and attractive combination of mechanical and thermal properties [1]. The understanding of their mechanical behaviour is of crucial importance for their use in engineering applications. The presentation focuses on geometrical and mechanical analysis of three very different porous materials (Figure): Advanced Pore Morphology (APM) foam [2, 3], open-cell aluminium foam [4, 5] and Metallic Hollow Sphere Structure (MHSS) [6]. The geometrical analysis is based on proper recognition of their internal porous structure reconstructed from micro computed tomography scans, taking into account the statistical distribution of geometrical parameters. The results of conducted geometrical analysis provided means for methodology development for representative 2D and 3D geometrical modelling of irregular porous structures and consequent formation of parametric computational models. These were then used to study the mechanical behaviour of analysed porous structures by means of advanced quasi-static and dynamic nonlinear computational simulations using the LS-DYNA code. Computational results were compared and validated by experimental testing programme.

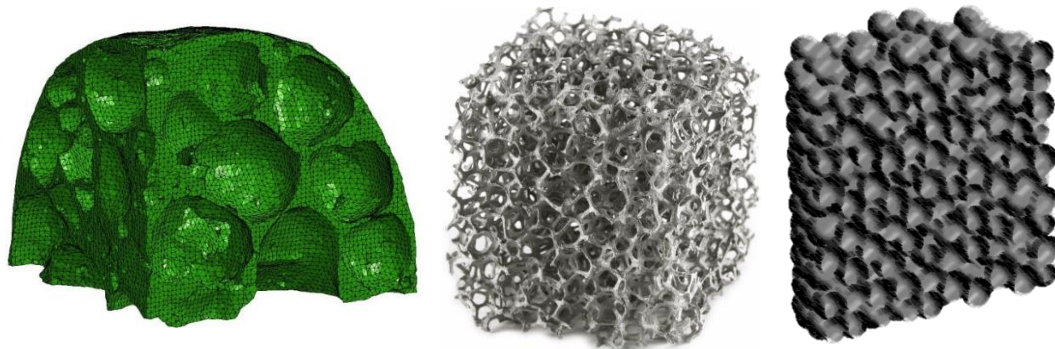


Figure: APM foam element, open-cell foam and MHSS.

## Literature

- [1] M.F. Ashby, A. Evans, N.A. Fleck, et al., Wadley, Metal foams: a design guide, Elsevier Sci., Burlington, Massachusetts, 2000.
- [2] M.A. Sulong, M. Vesenj
- [3] M. Ulbin, M. Borovinšek, Y. Higa, et al., Mater. Lett., 136 (2014) 416-419.
- [4] S. Tanaka, K. Hokamoto, S. Irie, et al., Measurement, 44 (2011) 2185-2189.
- [5] M. Vesenj
- [6] O. Andersen, U. Waag, L. Schneider, et al., Adv. Eng. Mater., 2 (2000) 192-195.

# Development of a Tool for Automatic Calibration of Material Models in LS-DYNA

Aria Mardalizad<sup>1</sup>, Emad Sadeghipour<sup>2</sup>, Markus Lienkamp<sup>2</sup>

<sup>1</sup>Polytechnic University of Turin, Italy

<sup>2</sup>Institute of Automotive Technology, TUM, Germany

## 1 Introduction

LS-DYNA offers a wide range of material models (material keywords or \*MATs) in order to ensure sufficient reliability of the simulation model. However, selecting the most proper material model in LS-DYNA may be confusing. Therefore, a tool is being developed that aims to suggest the proper material keyword for the user's desired application. The algorithm of this tool is based on the information and knowledge from the LS-DYNA keyword user's manual and some published papers. This tool is the beta version of a smart material database for LS-DYNA, which can search for the most proper material keyword with regard to the user's application. The algorithm of this tool is developed and implemented in order to examine its reliability. The Institute of Automotive Technology at TUM (Technische Universität München) intends to develop this database for a community of users and developers from universities and research institutes.

## 2 Approach

The algorithm of the program consists of two steps. The first step is determining the proper mechanical behavior model of the material, called the material keyword. The second step is calibrating the selected keyword with specific mechanical properties or creation of the material card.

The beta version of the tool is developed for four material types commonly used in crash applications: rubber, foam, plastic/metal and composite. First, the material keywords of LS-DYNA are processed in three steps:

1. A list of available material keywords is obtained for each material type. For this, some validated simulation models and some publications were studied to find the most common keywords for each material type in crash simulations.
2. To distinguish the material keywords, the mechanical properties of each material model are analyzed. The minimum mechanical properties required to distinguish the keywords of each material type have been categorized as a list of items with different values.
3. Finally, one table for each material keyword has been developed, which is called the "keyword's profile" here. This profile contains all of the material properties and their relevant items that could be covered through that specific material keyword.

After the material type is selected, the user is asked several questions to detect the desired material properties. Each question addresses a property from the keyword's profile. According to the user's choice, a value will be assigned to the available keywords from the list of the selected material type. The values which are ascertained during the questioning phase will be added together for each material keyword. Finally, the keywords will be sorted from the highest to the lowest value, with the first represented keyword being the most proper material model for the user's application.

The second part of the algorithm is developed to calibrate the selected keyword from the previous section with material properties and creation of a material card. For this aim, a database of material cards is developed, which can be expanded with more cards. The database consists of blocks for each keyword, which contains different material cards.

After selecting the keyword from the user, the algorithm will ask a specific number of questions from the relevant block to find the most proper material cards for the selected keyword. The questions can be skipped if the user does not have enough information. Answers to the questions will be converted into a vector, which will be compared with the vector of stored material cards in the database in order to find the proper material card that covers the desired properties.

## 3 Keywords' Profiles

In this section, the three steps of keyword processing described in section 3.1 is presented for each material type. The first table of each part shows the common keywords that are considered for the relevant material type here. The second table indicates the minimum mechanical properties required to



distinguish the keywords of each material type and the possible values for each item. The third table presents the keywords' profiles, which contain the properties covered by the relevant material keyword.

#### 4 Results of the Program

An example is provided for the purpose of investigating the output of the developed tool. Let us consider a user who searches for an appropriate material card merely by knowing the characteristics provided in Table 1.

Material type	Stress-strain behavior	Damage effect	Lattice structure	Failure criteria	Mass density	Poisson ratio
Metal	Elastoplastic	YES	Isotropic	Basic mode	2730 $\left[\frac{kg}{m^3}\right]$	0.33

Table 1: An example about the desired mechanical characteristics

When the program runs, once the user answers the respective questions, the software reports a sorted list as the first output. The most proper keyword is the first one on the list. It also provides the accuracy percentage of the most proper and second most proper suggested material keyword. According to the outputs, **\*MAT\_081** is the most proper material keyword with 100% accuracy. The reason for this 100% accuracy is that the selected answers are exactly the same as those provided in the profile of this keyword.

Next, to calibrate the material card, the user can simply enter the numbers that are available, which are density and Poisson's ratio in this example. Finally, the software outputs the full list of available material cards from the database along with some extra information, such as their sources.

#### 5 Summary and Discussion

A beta version of a smart material database for LS-DYNA has been developed, which can search for the most proper material keyword with regard to the user's application.

The user has to answer some questions in order to provide enough information for the algorithm. The program attempts to ask questions about minimum required properties in order to specify the material cards. There are several similar characteristics in each sub-unit which the user is not asked about. It should be noted that these questions are based on differences and similarities of the material keywords. Thus, they will not necessarily remain the same, if new material keywords are added to the algorithm. The capability for further development has been considered within all intermediate steps required to obtain the algorithm, so that the final structure can be updated with minimum required effort.

The developed algorithm is implemented in MATLAB and coupled with a database in Microsoft EXCEL in order to examine its reliability. For the next generations of this tool, other programming languages will be used, which are much more powerful for IT applications.

#### 6 Acknowledgment

The project was independently funded by the Institute of Automotive Technology at Technische Universität München (TUM).

The authors would like to express their appreciation to Prof. M. Gola from Polytechnic University of Turin for his support, kind and understanding spirit.

# Verification of the Part-Composite Approach for Modeling the Multi-Layered Structure of a Rolling Truck Tire

Shahram Shokouhfar<sup>1</sup>, Subhash Rakheja<sup>1</sup>, Moustafa El-Gindy<sup>2</sup>

<sup>1</sup> Department of Mechanical and Industrial Engineering, Concordia University, Montreal, Canada

<sup>2</sup> Department of Automotive, Mechanical and Manufacturing Engineering, UOIT, Oshawa, Canada

Accurate modeling of a truck tire for predicting dynamic characteristics requires an adequate representation of its composite plies. This study compares two approaches in modeling the multi-layered structure of a rolling truck tire using LS-DYNA. In the first approach, different layers in the tire structure are modeled using individual elements; whereas, in the second, all layers are represented by a single element with layered configuration managed by the **PART\_COMPOSITE** keyword. The simulation results obtained by the two tire models were compared with each other as well as with the experimental data in terms of load-deflection, cornering and modal characteristics and showed reasonable agreements.

## 1 Introduction

Dynamic performance characteristics of vehicles strongly rely on the forces arising from the tire-road interactions. Widely different tire models have been proposed to predict these forces for applications in vehicle design and dynamic analyses. A number of studies have proposed detailed representations for the multi-layered composite structure of the tire and could yield accurate predictions of the tire dynamic characteristics. However, considering such a high level of complexity resulted in hiring large number of elements and thus expensive computational cost [1]. The purpose of this study is to propose a simplified but still reliable tire model to be used in a virtual tire testing system with reasonable computational demand.

## 2 Methodology

As illustrated by Fig. 1(a), in the Individual-Element (IE) model, the carcass and belt plies are formulated using the Discrete Reinforcement technique [1], where the rubber matrix is represented by solid elements and the reinforcements are discretely modeled using composite shell elements. In the Part-Composite (PC) model, however, the carcass and belt plies are simplified to a single part made of shell elements with layered configuration using the **PART\_COMPOSITE** keyword, as shown in Fig. 1(b). Both of the models use identical material types, thicknesses and fiber orientations for different layers of the carcass and belt. A virtual tire testing environment is created, where the tire is first inflated and then vertically loaded, and finally freely rolls at a constant side-slip situation. Eigenvalue analyses are also performed to compare the natural frequencies of the tire models under the inflation and vertical loads.

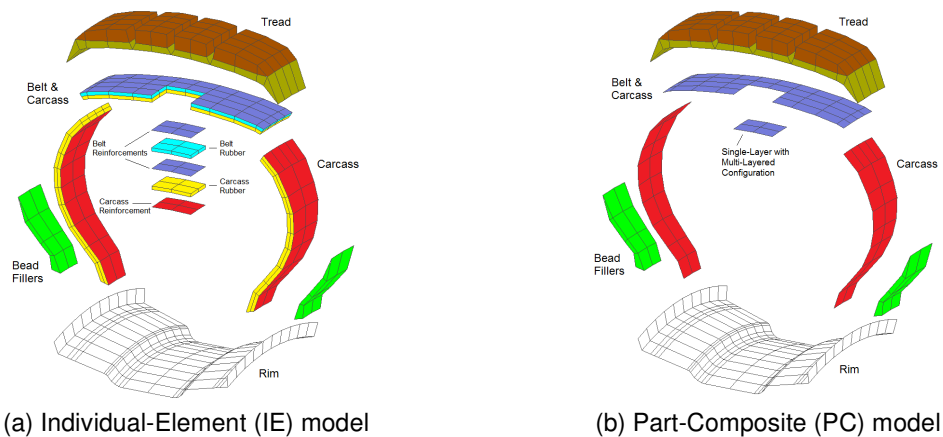
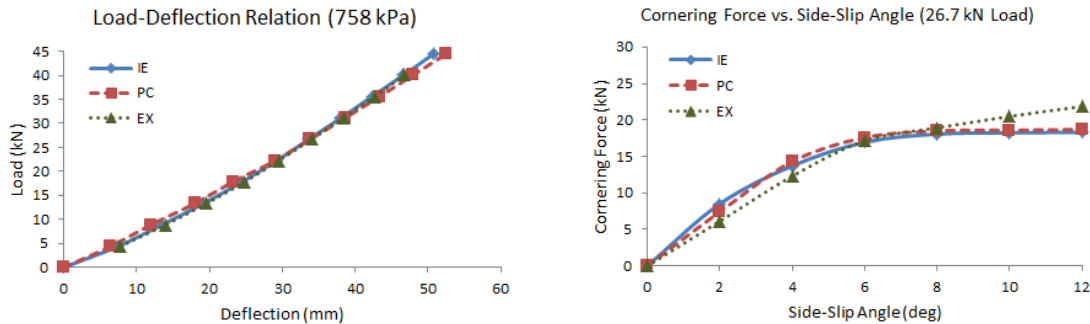


Fig.1: Multi-layered composite structures of the tire models

### 3 Results and Discussions

The static vertical stiffness properties of the two tire models were evaluated through a series of load-deflection tests. The load-deflection properties resulted from the two tire models exhibited perfect agreement with each other as well as with the physical measurements [2], as illustrated in Fig. 2(a). Moreover, the cornering characteristics of the two tire models were evaluated via predicting the cornering forces due to a range of side-slip angles. As shown in Fig. 2(b), the two models showed good agreement with each other, but agreed well with the experimental data only in the mid-range of the side-slip angles. Finally, eigenvalue analyses were performed to compare the modal behavior of the two tire models under inflation and vertical loads. The natural frequencies resulted from the two models showed perfect agreement for the in-plane vibration modes (Fig. 3), while there were some discrepancies (< 7%) between the results for the out-of-plane modes.



(a) Load-deflection relations at 758 kPa pressure (b) Cornering forces at 5 km/h under 26.7 kN load

Fig.2: Simulation results by the IE & PC models and comparisons with the experimental data (EX) [2]

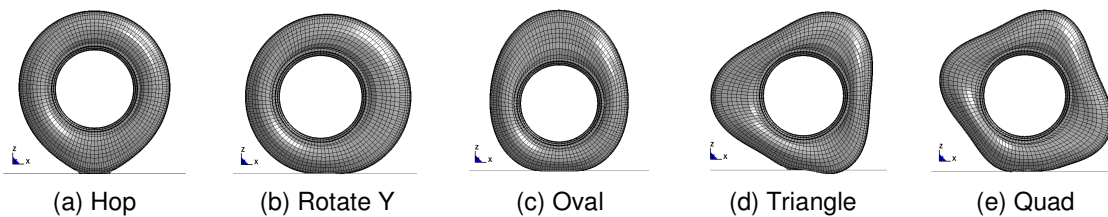


Fig.3: Vibration mode shapes related to in-plane modes

### 4 Summary

The Part-Composite approach in LS-DYNA was verified to be applicable in modeling the multi-layered structure of a rolling truck tire. A simplified tire model using this approach was developed and compared to a much more detailed model which employed individual elements for modeling different layers in the tire structure, while both of the models used the same configuration of layers with identical materials, thicknesses and fiber orientations. The simulation results obtained by the two tire models verified reasonable agreements of the two models with each other as well as with the experimental data in terms of the load-deflection, cornering force/moment and vibration characteristics. Using the Part-Composite (PC) model, the total number of elements was reduced by 63%, which remarkably improved the computational efficiency so that the required CPU time was reduced by 79% in a load-deflection test and by 83% in a cornering simulation.

### 5 Literature

- [1] W. Hall, J. T. Mottram, and R. P. Jones, "Tire modeling methodology with the explicit finite element code LS-DYNA," *Tire Science and Technology*, vol. 32, no. 4, pp. 236–261, 2004.
- [2] S. Chae, *Nonlinear Finite Element Modeling and Analysis of a Truck Tire*. Ph.d. dissertation, Pennsylvania State University, USA, 2006.



# **SIMULATION VI**

## **CRACKS**



# Three-Point Bending Crack Propagation Analysis of Beam Subjected to Eccentric Impact Loading by X-FEM

Toru Tsuda<sup>1</sup>, Yoshihiro Ohnishi<sup>2</sup>, Ryo Ohtagaki<sup>1</sup>, Kyuchun Cho<sup>3</sup>, Takehiro Fujimoto<sup>3</sup>

<sup>1</sup> ITOCHU Techno-Solutions Corp., Japan

<sup>2</sup> ITOCHU Techno-Solutions Corp., Japan

<sup>3</sup> Kobe University, Japan

## 1 Introduction

In this study, we applied FEM with eroding technique and the extended finite element method; X-FEM<sup>[1]</sup> for three-points bending of crack propagation problems of the beam subjected to eccentric impact loading. Then, evaluated problems and the effectiveness of each technique through the comparison with the experiment result<sup>[2]</sup>.

## 2 Impact experiment

Impact three-point bending test of a beam with a pre-crack as shown in Fig.1 was carried out by Cho, et al.<sup>[2]</sup>. The material of specimen used in this test is FC200 (grey cast iron).

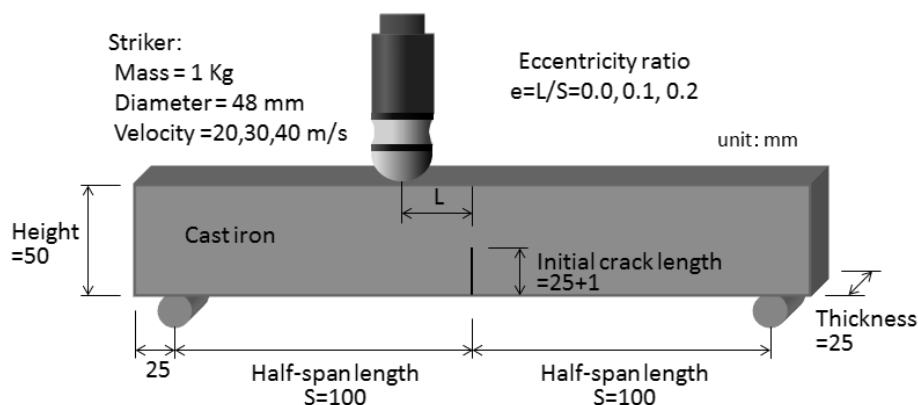


Fig.1: Impact specimen

According to eccentric ratio [0.0, 0.1 and 0.2], the experiments carried out on shifted loading points from the specimen center. And the high speed impact test was conducted under striker shooting velocity [20, 30 and 40m/s]. Table 1 indicates the test case.

Table 1: Test case

		Striker velocity (m/s)		
		20	30	40
Eccentricity ratio $e=L/S$	0.0	case11	-	-
	0.1	case21	case22	case23
	0.2	case31	case32	-

The crack propagation behaviors were observed by ultra-high-speed camera and a crack propagation movie was recorded to measure a crack velocity, fracture path and loading point displacement. The crack propagation images of the case21 as test result are show in Fig. 2.

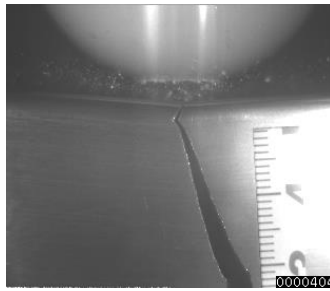


Fig.2: Crack propagation images of case21

### 3 Simulations

We carried out impact three-point bending analysis by using X-FEM.

Figure 3 shows the crack propagation histories of the test (left side) and the simulation (right side) in case21.

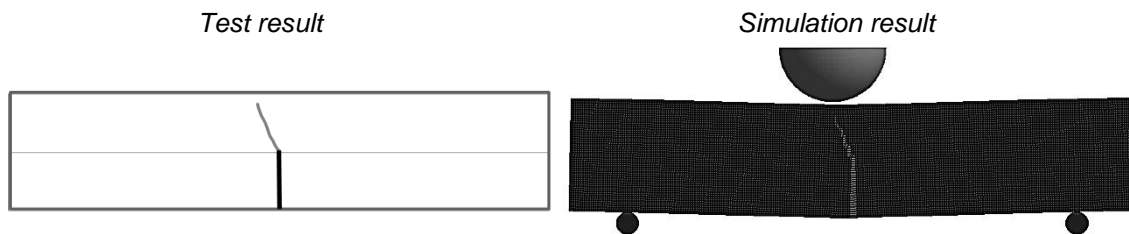


Fig.3: Comparison of propagation path for case21

According to the figure, it is found that the crack propagation path obtained by X-FEM analysis is very similar to the test result.

### 4 Literature

- [1] Moes, N., Dolbow, J., Belytschko, T.: "A finite element method for crack growth without remeshing", Int. J. Numer. Meth. Eng., 46(1), 1999, pp.131-150.
- [2] Cho, K.C., et al.: "Experimental and numerical study on the dynamic fracture characteristics of grey cast iron FC200", The 8th international symposium on impact engineering (ISIE2013), Sep., 2013.



# Keep the Material Model Simple with Input from Elements that Predict the Correct Deformation Mode

T. Tryland<sup>1</sup> and T. Berstad<sup>2</sup>

<sup>1</sup>SINTEF Raufoss Manufacturing, Raufoss, Norway

<sup>2</sup>Department of Structural Engineering, Norwegian University of Science and Technology, Trondheim, Norway

## 1 Background

The 64 km/h frontal offset test is run with a deformable barrier, and the first numerical model of this barrier was made with solid elements to represent the honeycomb blocks. However this required development of a special element formulation to handle the severe deformation of the solid elements together with a special material model that could be calibrated to handle the extreme anisotropy [1]. It is herein important to notice the amount of work, the uncertainties with the test specimens and the test procedure to get a proper representation of the honeycomb material. It was therefore suggested to represent the barrier geometry with shell elements that were able to capture the deformation mode with local and global buckling of the honeycomb structure together with a simple model to represent the material in the 0.076 mm thick aluminium foil [2]. The objective of this study was to investigate whether the same idea can be used to predict cracks when crushing a two chamber aluminium profile.

## 2 Specimen geometry and test procedure

Note that the component that was tested in this study is unlike the situation for real products where the actual combination of geometry and material have to secure robust behaviour for all combinations within the tolerances. Herein the combination of profile geometry, cutting angles, wall thicknesses and material properties was chosen with propose to get an unstable folding pattern and thereby challenge the simulation tool to capture this. The results from the parallel tests shown in figure 1 confirm this.

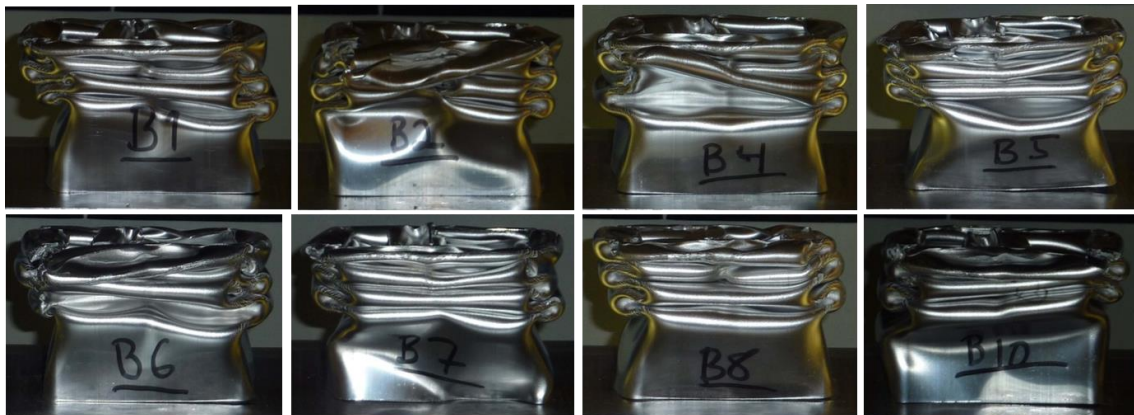


Fig. 1: Parallel tests show specimen 2, 4 and 6 that does not follow progressive folding.

The definition of the cut angles to initiate axial folding was found in the literature [3], and especially this example with a relatively thin mid-wall was found to behave unstable [4], see figure 2. Herein it is interesting to investigate whether this mid-wall represents sufficient stiffness to control the folding mode when the outer part of the profile behaves unstable due to geometrical imperfections. The specimen geometry was represented by both shell and solid elements with aspect ratio about 4 to predict the correct deformation mode [5]. These alternatives may be useful for the practical engineer as they are both fast enough to fit inside for example complete car simulations. Note that this starting point require either shell elements or solids with ELFORM =  $\div 2$ , and smaller solid elements can be used to capture details like the effect of local variation in material properties, see figure 3.

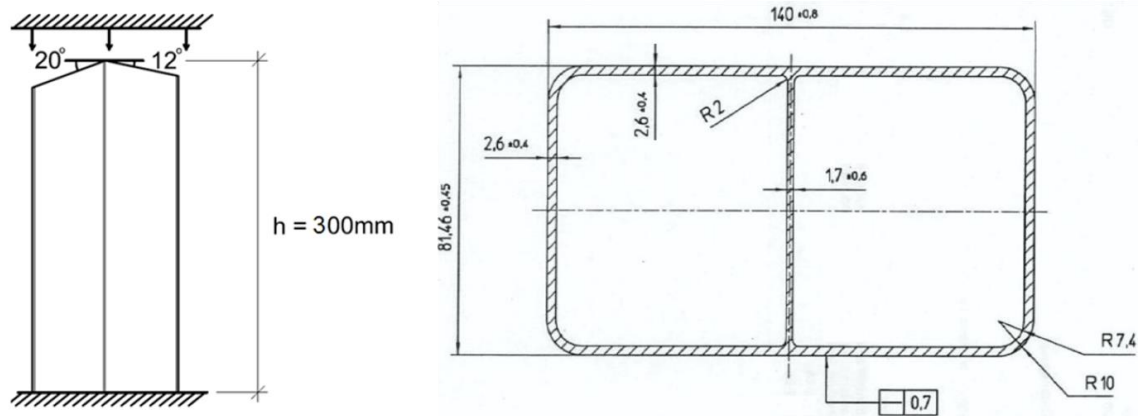


Fig.2: Definition of profile geometry and specimen with cut angles to initiate axial folding [4].

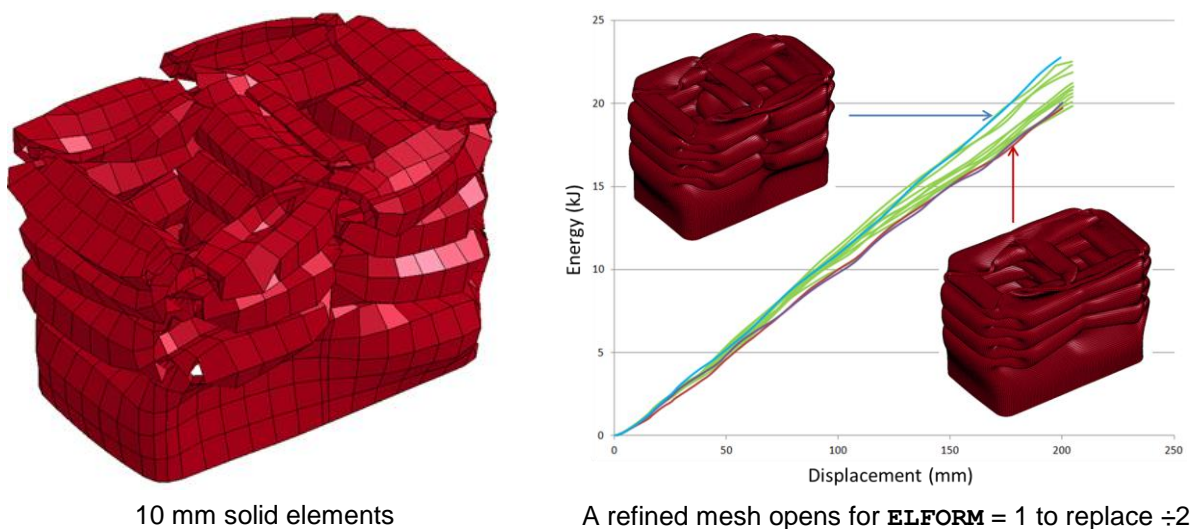


Fig.3: The details are not captured but practical engineers may still prefer 10 mm elements.

### 3 Summary

This study shows that a simple material model like MAT\_107 works well together with a combination of element type and mesh that predict the correct deformation mode. The numerical results show that the relatively thin mid-wall struggle to secure progressive folding, and a more robust folding mode is likely for a profile variant inside the tolerances where all walls has thickness 2.25 mm. The benefit from keeping the material model as simple as possible is reduced cost by calibration based on a simple test specimen and a specimen holder to run the shear test in the same way as a uniaxial tensile test [6].

### 4 Literature

- [1] Kojima, S., Yasuki, T., Mikutsu, S., Takatsudo, T.: "A Study on Yielding Function of Aluminium Honeycomb", 5th European LS-DYNA Users Conference, Birmingham, UK, 2005.
- [2] Tryland, T.: "Alternative Model of the Offset Deformable Barrier", 4th LS-DYNA Forum, Bamberg, Germany, 2005.
- [3] Tryland, T.: "A Simple Compression Test to Evaluate Ductility", 9th Nordic LS-DYNA Users Forum, Gothenburg, Sweden, 2008.
- [4] Olsson, B.: "Testing of Constitutive Models of AA6082-T6 in LS-DYNA", Nordic LS-DYNA Users Forum 2014, Gothenburg, Sweden, 2014.
- [5] Tryland, T.: "Combinations of Meshes and Elements that seems able to Predict the Correct Deformation Mode", 13th LS-DYNA Forum, Bamberg, Germany, 2014.
- [6] Tryland, T., Berstad, T.: "A Simple Shear Test to Evaluate Material Ductility based on Specimens Cut from thin-Walled Sections", 11th LS-DYNA Forum, Ulm, Germany, 2012.

# Damping Modeling in Woven Micro Lattice Materials

Stefan Szyniszewski<sup>1,2</sup>, Stephen Ryan<sup>2</sup>, Seunghyun Ha<sup>2</sup>, Yong Zhang<sup>2</sup>,  
Tim Weihs<sup>2</sup>, Kevin Hemker<sup>2</sup>, James K. Guest<sup>2</sup>

<sup>1</sup>University of Surrey

<sup>2</sup>The Johns Hopkins University

This paper discusses damping measurements and simulations of the woven material under oscillatory loads. Porous metals can enhance energy dissipation [1–3], buckling mitigation [4,5] and bending rigidity (especially for sandwich panels [4]). Multi-physical features of porous metals [6] show even greater promise. In comparison to random porosity of metallic foams (resulting from the foaming technology), metallic woven materials enable a more regular topology [7] that can be optimized by the modification of the weaving pattern, wire diameters and the selection of the wire materials.

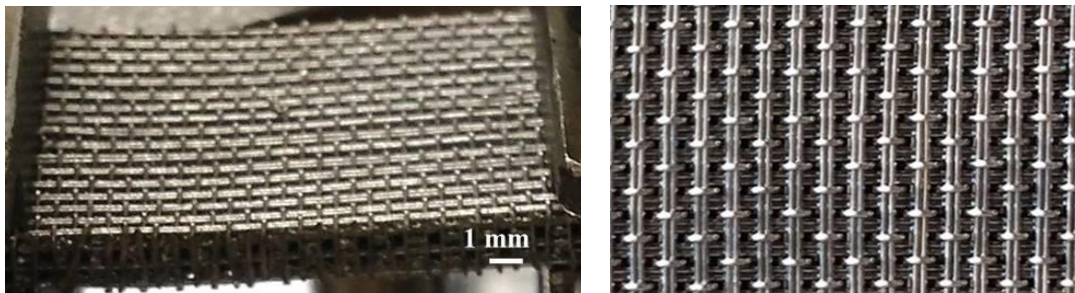


Fig.1: Metallic woven material. The woven micro-lattice design is protected by a pending patent with worldwide coverage.

The experimental results showed high damping with loss coefficient of 0.19-0.25 for copper and NiCr woven micro-lattice materials. LS-DYNA simulations allowed to investigate the importance of gaps between the wires, coefficient of friction and stochastic deviations from regular geometry (resulting from the manufacturing process).

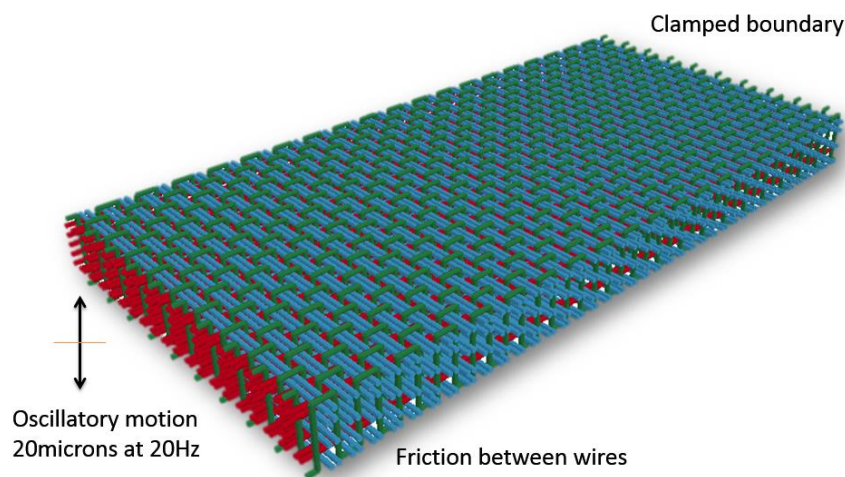


Fig.2: Simulation of the 3D woven metallic sample (clamped at far end, and subjected to oscillatory excitation at the near end). The model employs frictional contact. The modified weave architecture is shown with fill wires shaded blue, the warp wires shaded red, and the z-wires shaded green.

The majority of conventional damping materials with comparable loss coefficients (0.2-0.3), such as polymers, are restricted to significantly lower temperatures, whereas the NiCr wires have a maximum service temperature of 1175°C. A property correlation plot of the damping properties measured in this

work with the maximum service temperatures of the wires is shown in figure 3. If the damping properties are maintained at the maximum service temperatures, 3D woven metallic lattice materials would offer the damping properties of polymers at temperatures in which only high temperature metallic and technical ceramics are applicable.

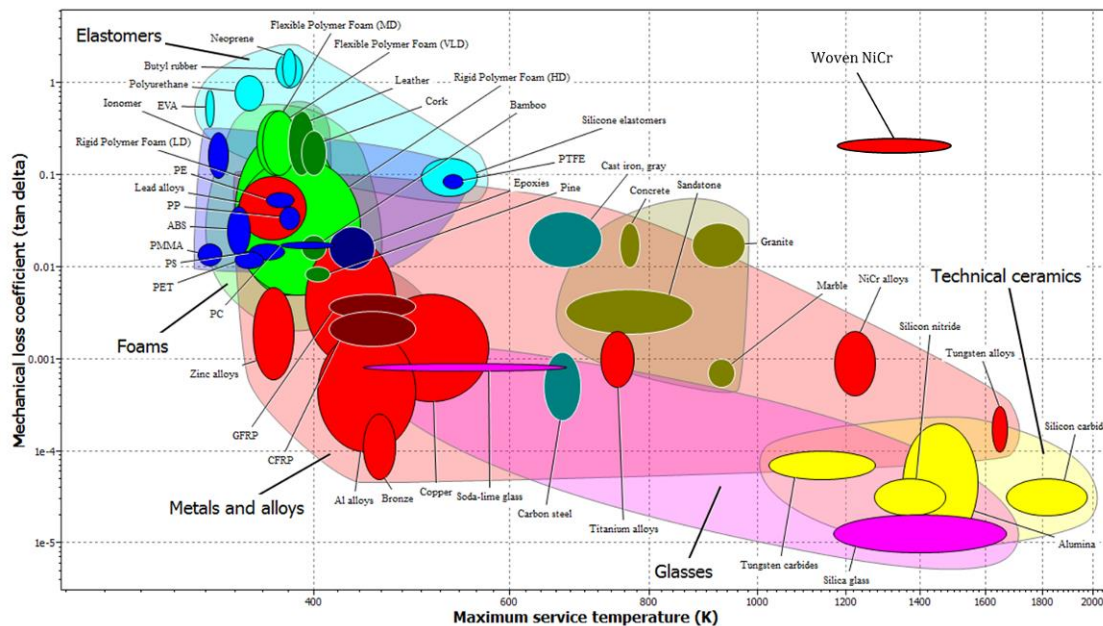


Fig.3: A property correlation plot of the mechanical loss factor,  $\eta$ , and the maximum service temperature for a wide variety of materials and material classes. The measured damping performance of 3D woven NiCr lattice materials combined with the maximum service temperature of NiCr highlight its potential for use in elevated temperature damping environments. Note that the woven materials were all measured in bending.

## Acknowledgments

This study was funded by Defense Advanced Research Projects Agency (DARPA), in the Materials with Controlled Microstructural Architecture (MCMA) program, under award number W91CRB1010004 (Dr. Judah Goldwasser, program manager). The authors would like to thank Dr. Yong Zhang for elastic modulus measurements and Dr. Harold Kahn for dynamic friction measurements. The simulations used the Extreme Science and Engineering Discovery Environment (XSEDE) that is supported by National Science Foundation grant number OCI-1053575.

The woven micro-lattice design is protected by a pending patent with worldwide coverage.

## Literature

- [1] Ashby M. Metal foams : a design guide. Boston: Butterworth-Heinemann; 2000.
- [2] Gibson LJ, Ashby MF, Ashby M. Cellular Solids: Structure and Properties. 2nd ed. Cambridge University Press; 1999.
- [3] Smith BH, Szyniszewski S, Hajjar JF, Schafer BW, Arwade SR. Steel foam for structures: A review of applications, manufacturing and material properties. J Constr Steel Res 2012;71:1–10. doi:10.1016/j.jcsr.2011.10.028.
- [4] Neugebauer R, Hipke T. Machine Tools With Metal Foams. Adv Eng Mater 2006;8:858–63. doi:10.1002/adem.200600095.
- [5] Szyniszewski S, Smith BH, Hajjar JF, Arwade SR, Schafer BW. Local buckling strength of steel foam sandwich panels. Thin-Walled Struct 2012;59:11–9. doi:10.1016/j.tws.2012.04.014.
- [6] Brothers AH, Scheunemann R, DeFouw JD, Dunand DC. Processing and structure of open-celled amorphous metal foams. Scr Mater 2005;52:335–9. doi:10.1016/j.scriptamat.2004.10.002.
- [7] Schaedler TA, Jacobsen AJ, Torrents A, Sorensen AE, Lian J, Greer JR, et al. Ultralight Metallic Microlattices. Science 2011;334:962–5. doi:10.1126/science.1211649.

# Solving Crash Problems of the Fuel Supply Modules in the Fuel Tank

Martin Dobeš<sup>1</sup>, Jiří Navrátil<sup>2</sup>

<sup>1,2</sup>Robert BOSCH spol. s.r.o., Roberta Bosche 2678, České Budějovice 370 04

## 1 Abstract

The first part of this article deals with the experimental measuring of the material data used for explicit computational FEM analyses. The second part of this paper devotes practice application of the FEM simulation in domain of fuel tank and fuel supply modules (FSM). The main focus is on the material computational models, especially material models with strain rate dependence. These computational models are used for polymer materials, like TSCP (Typical Semi-Crystal Polymer). A lot of experiments were used for comparison of the simulation results and reality. Some experiments were proposed directly as appliance for detailed comparison of real deformations in the time of break with focus on the flange part. The flange is the most important part of FSM from the reason of passive safety.

## 2 Introduction

Fuel supply module, which consists of the fuel pump, filter system, rail of the fuel, regulation system and flange belongs between main components of the fuel system of the car. The majority of all parts are made from Polymer materials. The TSCP plastics are familiar as plastics with very significant dependence on the velocity of the loading, likes strain rate dependence. We have to use more sophisticated material models for modeling of the dynamic loadings and stress responses of plastics in these cases. The computational analyses generally help to understand some physical principles in different loading situations. We would like to focus on understanding some principles, which are caused by dynamic loading, especially in fuel tank. We concentrate on the deformation behavior FSM inside the fuel tank during non standard situations, like crash, shock, drop tests etc.

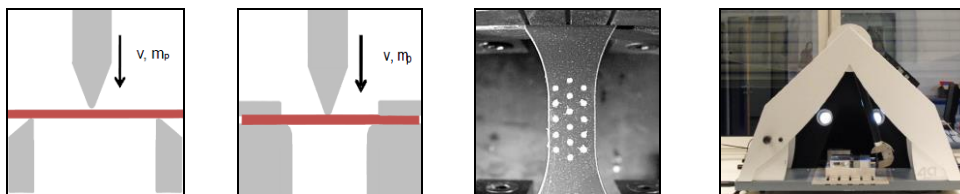


Fig.1: Testing methods for development computational material model for TSCP (4A engineering)

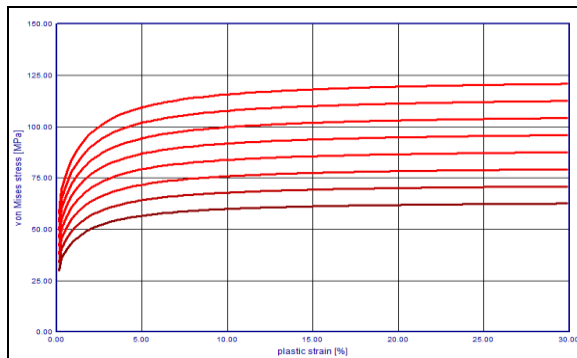
### 2.1 Fuel Supply Module (FSM)

The FSM is one part of the fuel system in a car or motorbike. The basic requests on this product are delivery of the fuel from the tank, measuring of the fuel level, filtering of the fuel, regulation of the pressure, flow and the most important request from our aim is absolute tightness during nonstandard situations, like front or side impact, overturn of the car etc. The flange is the most important part of the FSM from perspective of passive safety, because flange is last part which closes fuel tank. The flange and sub-module (fuel pump, reservoir, filters, fuel level sensor...) are connected by guiding rods (plastic or steel). The weight of the sub-module is approximately between  $m_{sub}=0.7-1.2\text{kg}$ , so this weight loads interfaces on the flange almost in all loading cases, primarily in impact situations. The basic customer request is possible cracking of the flange, but the total tightness of the closed fuel system. Generally FSM has to fulfill a lot of technical requests and stands in real boundary conditions. We solve the interface between guiding rods and flange or designed cracking zones on the guiding rods bosses.

### 3 Computational material model

The company 4A engineering has necessary experimental equipment for measuring of the material mechanical properties. The material model with respecting strain rate dependence was important for

our purposes. This model was fitted for special type of elements 16 fully integrated shell (size 2mm), 10-noded composite tetrahedron (size 0.6mm). The measurement data were validated using other tests for strain range 0-15% and strain rate range 0.001 - 50s<sup>-1</sup>. The breaking points weren't founded for all strain rate levels. This problem was solved in our department, see full manuscript.



$$\sigma = \frac{F}{b \cdot h} \cdot (1 + \varepsilon_l) \quad (1)$$

$$\varepsilon = \log(1 + \varepsilon_l) \quad (2)$$



Fig.2: Computational material model of TSCP material for LS-DYNA (strain rate levels)

#### 4 FE model of the FSM vs. Experiment

We use experiment of the rigid impact to the guiding rods and subsequent cracking of the flange due to effect of the pick-up of the guiding rods from the flange for comparison. FE model is created from shell and solid elements with using of the rigid beam elements for necessary connections between parts. The computational material model is `*MAT_PIECEWISE_LINEAR_PLASTICITY` for plastic parts with strain rate dependence, defined by table (Fig.2). We use in our material model combination of the material limit parameters for definition of eroding elements in card `*MAT_ADD_EROSION`, see full manuscript.

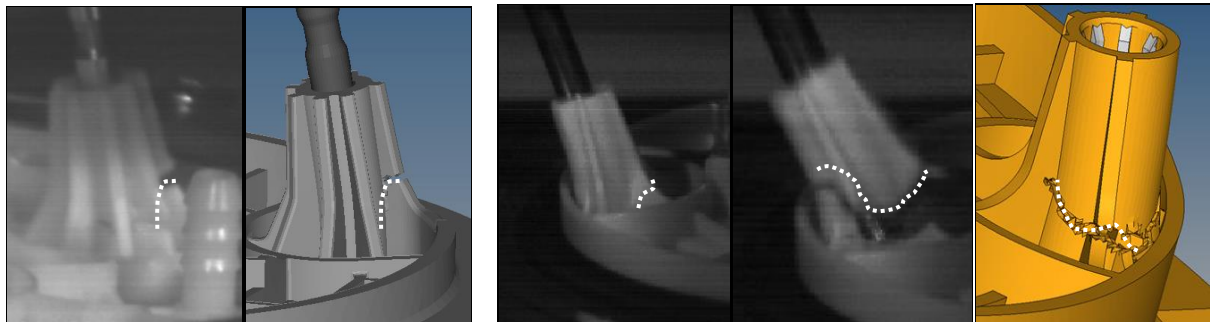


Fig.3: Record of the High-speed cam and Simulation results – initialization of the crack

#### 5 Summary

The results from the experiment and explicit simulation are presented in this paper. The main aim of this work was founding of the correct parameters for computational material model and following eroding of elements. We used rigid impact test for FSM and compared deformation behavior of the real parts and computational model. It is possible to say, that our computational model with founded material parameters has very good agreement. The time step of initial breaking is almost the same as in real condition and propagation of the cracking is very similar too.

#### 6 Literature

- [1] Dobes, M., Navratil, J.: Application of the different computational material models of Polymer material for solution of FEM in LS-DYNA, 22<sup>nd</sup> SVSFEM ANSYS Users' Group Meeting and Conference 2014, Slovakia, pages 10-27
- [2] Hubert, F., Hiermaier, S., Neumann, M.: Materials models for Polymers under crash loads – existing LS-DYNA models and perspective, Proceedings of the 4th LS-DYNA forum, Bamberg, Germany, 2005
- [3] Internal specification of the Loading crash profiles BOSCH (GS-FS/ENG1-Bj)
- [4] Material characteristics of the TSCP, <http://www.basf.com/group/corporate/en/>

## **SIMULATION VII**

### **DROP TEST/BIO**





# Drop Test Simulation and Verification of a Dishwasher Mechanical Structure

Oguzhan Mulkoglu<sup>1</sup>, Mehmet A. Guler<sup>1</sup>, Hasan Demirbag<sup>2</sup>

<sup>1</sup> Department of Mechanical Engineering, TOBB University of Economics and Technology, Turkey

<sup>2</sup> ARÇELİK A.S., Turkey

It is critical for dishwasher manufacturers to design the front door hinge system and the structural components of a dishwasher assembly in terms of appearance and satisfying functional requirements. It is therefore necessary to know the maximum weight of decorative wooden door can be assembled to the built-in front door without endangering the durability on every single opening state

ARÇELİK A.Ş. Dishwasher Plant R & D Structural Design Department decided to design a new door hinge with a new mechanical dishwasher structure to accomplish these requirements and to enhance more robust structure as compared to its current designs. Plastic bottom housing and the required new package module are the critical parts of this new mechanical structure. In this paper, the designs of these parts are analyzed in detail with a finite element model by accomplishing the drop test analyses.

The nonlinear explicit finite element code LS-DYNA® is used for the drop impact simulations. The main purpose of this study is to build a finite element analysis (FEA) model of the drop test of the free-standing dishwasher structure in order to determine the critical regions in the assembly. Drop test experiments are then conducted and the results are compared with the ones obtained from FEA.

Drop tests of dishwashers are generally conducted with three different orientations such as inclined to front, inclined to side and vertical drop test in ARÇELİK group. In this study, inclined to side and vertical drop tests are realized and their finite element simulations are done. LS-DYNA models of these two cases can be seen in Fig. 1.

(a) Vertical drop test FEA model (b) Inclined drop test FEA model

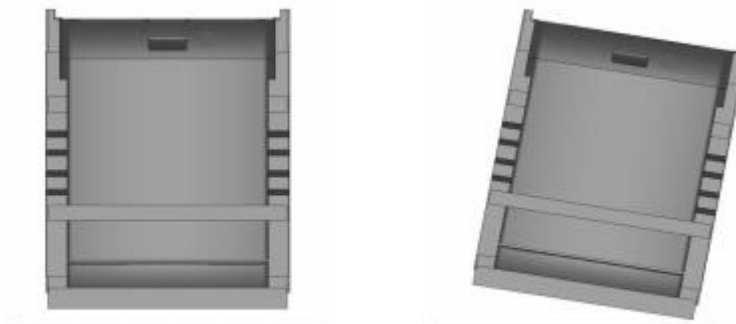


Fig.1: LS-DYNA models (a) Vertical drop test FEA model (b) Inclined drop test FEA model

Vertical and inclined drop tests are successfully simulated in LS-DYNA. The simulation results are compared with experimental drop test images. Plastic bottom housing and the new package module are found to be the critical parts of dishwasher. Results of simulation shows that plastic bottom house of the dishwasher is not affected much compared with packaging module. Therefore, in this paper packaging module is analyzed in detail and verification of the results are done by checking the deformation behavior of packaging module during impact. Deformation behavior of the bottom foam are similar for both FEA and experimental results as shown in Fig. 2.

The FEA model will provide further improvements on the new structure and the packaging module of this new dishwasher platform. ARÇELİK A.Ş dishwasher plant will use this new mechanical structure to whole product range. The optimization of the packaging module will be made for future study.

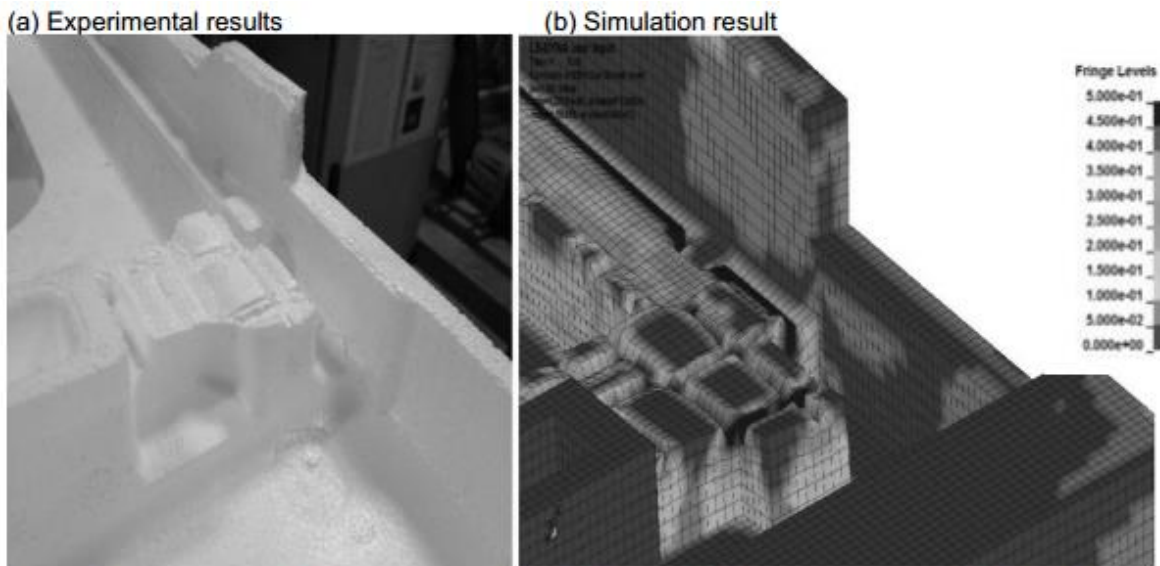


Fig.2: Comparison of bottom foam after vertical drop test (a) Experimental result (b) Simulation result (effective stress contour in MPa)

---

# Impact Simulations on Home Appliances to Optimize Packaging Protection: A Case Study on a Refrigerator

D. Hailoua Blanco\*, A. Ortalda\*, F.Clementi \*\*

\*Enginsoft S.p.a, Italy

\*\* Electrolux Italia S.p.a, Italy

Numerical simulations were used to investigate the impact behavior of complex products such as home appliances. LS-DYNA® is a powerful tool for performing repeat analysis of large assembled parts of the final product, including the packaging. The main goal of the simulations was to verify the performance and suitability of the packaging and its interaction with the structure in case of damage occurring during transportation or delivery. The studies were carried out to guarantee the integrity of the product from factory to customer and therefore to reduce customers service calls.

In particular, impact simulations on a refrigerator and its packaging were performed using LS-DYNA®. The FE model reproduced the testing conditions defined by internal Electrolux regulations. A rear edge drop test was studied and results used to improve current parts.

The paper presents the methodology developed to speed up the product development and to reduce the time to market (TTM). Comparison between the experimental and numerical results are also explored.

# A Variable Finite Element Model of the Overall Human Masticatory System for Evaluation of Stress Distributions during Biting and Bruxism

S. Martinez<sup>1</sup>, J. Lenz<sup>1</sup>, Prof. K. Schweizerhof<sup>1</sup>, Prof. H. J. Schindler<sup>2</sup>

<sup>1</sup>Karlsruhe Institute of Technology

<sup>2</sup>University of Heidelberg

## 1 Introduction

Simulating the masticatory system during chewing, clenching and bruxism, requires the model to capture the dynamical behavior of its different components: the mandibula and maxilla, the temporomandibular joint (TMJ), the teeth, the periodontal ligaments (PDL), and the muscles. A considerable amount of literature has been published on individual components separately [1, 2, 3]. This contribution incorporates this information into a single FE model under conditions close to reality. Within this contribution, the simulation is a transient analysis where the dynamic motion of the jaw is considered and the reaction forces in the teeth and the joints arise from contact instead of nodal forces or constraints.



Fig.1: Finite element model.

## 2 Materials and methods

The TMJ is modeled with geometrical structures and material properties as found in the literature [2] with ensuing additional adjustments. The material properties of the PDL are calibrated to obtain a realistic force-displacement behavior. Geometries for the jaw and teeth were obtained through a segmentation process. Jaw motion is governed by forces from the jaw opening and closing muscles which are positioned following proposals in the literature and are represented by Hill type muscle models. Activation levels of the muscles are employed based on previous works of the authors [3]. Analyses are executed with the FE program LS-DYNA [4] as large motions and complex contact situations have to be analysed. The current model consists of more than 1,900,000 elements (beams, springs, and solid elements) containing 8 different material models.

### 3 Results

The model currently reproduces realistic motions of the jaw during opening and closing. Reaction forces for a variety of biting tasks show good agreement with results found in the literature.

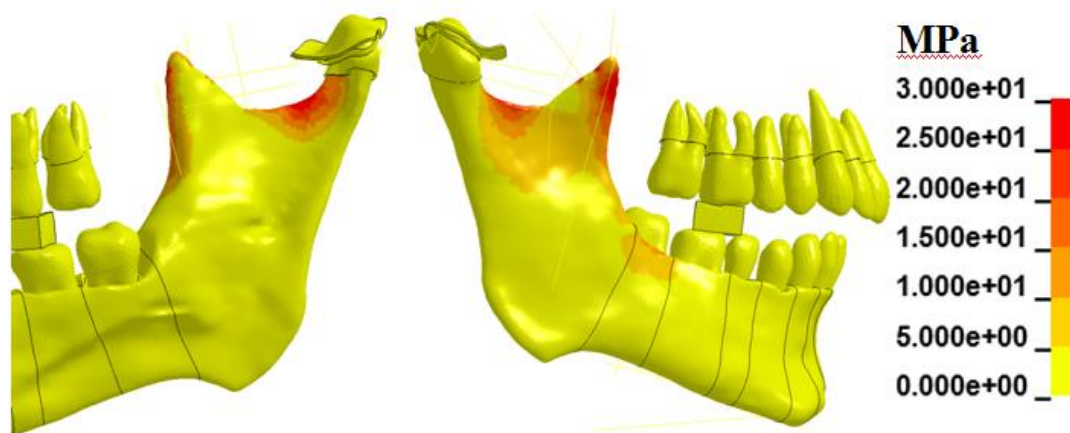


Fig.2: First principal stress during a 300N bilateral molar biting.

The model provides insight into the significance, or lack thereof, of particular structures such as the posterior attachments of the disc and the suprahyoid muscles during various situations. The current and future goals are to determine the stress distributions in the mandible, teeth and PDL during clenching, grinding and chewing with different sized boluses, also when dental implants are incorporated at different positions of the mandible. The models should further help to understand, functioning and/or malfunctioning of various situations to support clinical decisions.

### 4 Literature

- [1] Fill, T.S., Toogood, R.W., Major, P.W and Carey, J.P.: "Analytically determined mechanical properties of, and models for the periodontal ligament: Critical review of literature", Journal of Biomechanics 45, 2012, 9-16
- [2] Koolstra, J. H. and van Eijden, T.M.G.J.: "Combined finite-element and rigid-body analysis of human jaw joint dynamics", Journal of Biomechanics 38, 2005, 2431-2439
- [3] Rues, S., Lenz, J., Türp, J.C., Schweizerhof, K. and Schindler, H.J.: Muscle and joint forces under variable equilibrium states of the mandible", Clin Oral Investig. 15 (5), 2011, 737-47
- [4] Livermore Software technology Corporation: LS-DYNA 6.1 Manual, 2011



# **OPTIMIZATION I**

## **ROBUSTNESS**





# Recent Advances on Surrogate Modeling for Robustness Assessment of Structures with Respect to Crashworthiness Requirements

Fabian Duddeck<sup>1</sup>, Erich Wehrle<sup>1</sup>

<sup>1</sup>Technische Universität München, Chair of Computational Mechanics

Due to the inherent nonlinearity, crashworthiness is one of the most demanding design cases for vehicle structures. Recent developments have enabled very accurate numerical simulations and corresponding optimizations. Therefore, structural concepts are now much better adapted to the specific requirements. This has led to designs in which redundancies are reduced and highly effective car concepts have been derived. Important questions are then the reliability and the robustness of designs. Reliability addresses probabilities that constraints are violated and robustness assures that performance loss is small due to unavoidable variations.

Currently there is neither consensus on the precise definitions of robustness and reliability in the field of crashworthiness nor is there a unique understanding of the appropriate numerical methods. This paper further clarifies these aspects. In addition, an overview of recent research results from PhD theses supervised by the first author is presented. Hereby, special focus is laid on physical surrogate models for robustness assessments.

Crashworthiness is mainly assessed virtually by Finite Element Methods (FEM). Due to high model complexity, full-vehicle computations require several hours even if they are run on a higher number of CPUs and with advanced parallel computing; hereby, it is normally accepted that a single assessment is finished overnight. The computational effort for these *hi-fidelity models* is now one of the main difficulties to be addressed by optimization methods. The same is true for uncertainty assessments where the structural performances are analyzed with respect to unavoidable fluctuations in design and noise parameters. For both, optimization and robustness, we need generally at least 200 or 300 simulations to obtain estimates and up to several thousand computations for more accurate studies. This is clearly not feasible in the standard design process. To reduce this computational effort so-called *surrogate models* are often proposed. Here, the high effort computation is replaced by simpler and faster approaches. Most of the approaches in the literature are based on *mathematical surrogates* where an initial sampling (normally by design of experiment techniques, DoE) is used to construct a mathematical approximation of the response(s). *Physical surrogates* are simplified models, which maintain a base in the physics of the system – albeit with less resolution. They have proven to be a useful alternative to exclusively mathematical surrogates. The paper at-hand focuses on these physical surrogates or *low-fidelity models*.

Physical surrogates enable robustness investigations in early design phases considering mainly uncertainties related to *lack-of-knowledge* (changes, which occur later in the development process). *Solution spaces* derived by simplified models, here surrogate models based on lumped mass approaches, allow decoupled development of components. Robustness is achieved here by maximizing these solution spaces, resulting in high *design flexibility*. Further, an approach for robust design optimization is presented for later development phases based on a trust region and *multi-fidelity approach*. Low-fidelity models (physical surrogates using equivalent static loads and sub-structures) are used in the explorative phase of the analysis. Manufacturing or load case uncertainties are considered. Special criteria are established to switch to high-fidelity models (nonlinear transient finite element models) whenever necessary during optimization. It is hence possible to include robustness into the optimization with reduced numerical effort.

# Robustness Analysis of a Vehicle Front Structure Using Statistical Approach

Masahiro Okamura<sup>1</sup>

<sup>1</sup> JSOL Corporation

## 1 Introduction

In recent years, it has become more and more important to take account of scatter in automotive industry. Liability and performance has been guaranteed by adding safety margin to its target in the past. However, needs in cost reduction and trade-off of conflicting requirements do not allow manufacturers enough amount of safety margin anymore [1].

One way to reduce scatter in product performance is to control production quality. However, too much control increases managing cost, and scatter cannot be reduced more than tolerance allowed by standards. There are some studies showing major scatters in response are sensitive to boundary conditions such as dummy position and offset or angle of barriers [1, 2]. However, these are set up by third parties in hardware tests so that the parameters are beyond control [3].

For the reasons above, realistic approach for the problem is to enhance product design which absorbs scatter in production process and boundary conditions, and several methods have been introduced [4]. However, conventional methods based on design space scanning only visualize non-linear transformation of input/output variables, which illustrate direct relationship of scatters, and the physical mechanisms and how scatters propagate is a black box.

In this paper, scatter propagation mechanism is visualized based on statistical calculation and structural design is enhanced after understanding the scatter initiation and propagation in order to reduce scatter. This time, the front side structure of an automobile is used as an example.

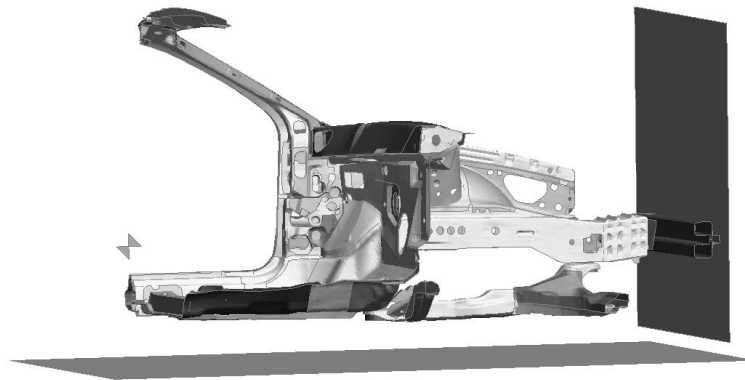


*Fig.1: Study model*

## 2 Robustness analysis with DIFFCRASH

In this study, spotweld strength is varied and 30 simulation runs have been conducted. The results are analyzed by statistical software DIFFCRASH, and trigger of bifurcation have been detected. Countermeasures have been taken by modifying characteristics of spotweld strength. As a result, bifurcations have been suppressed and scatters of the response such as barrier reaction force and floor intrusion have been reduced.

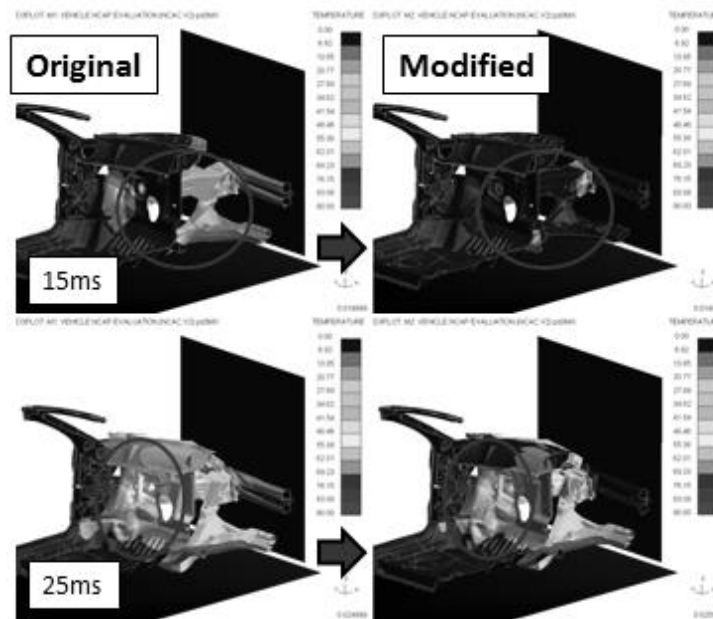


Fig.2: Scatter distribution before and after modification

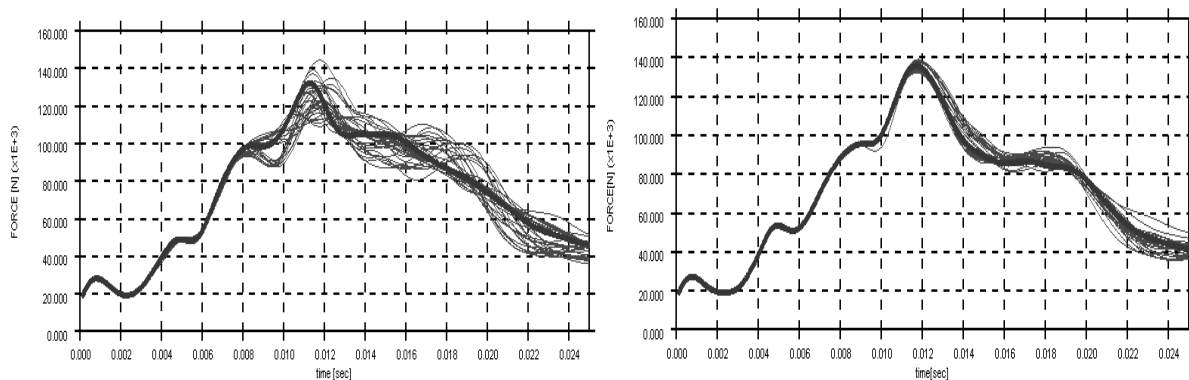


Fig.3: Barrier reaction force before and after modification

### 3 Conclusion

Conventional robust design improvement based on response surface method focus on direct relationship between input variant and output variable so that the analytical results gives only acceptable variable range, but do not give much insight to the mechanisms of scatter. On the other hand, the proposed method adds timing and special information of the scatter initiation and propagation so that it gives more hints for design improvement for suppressing bifurcation and reduce scatter.

### 4 Literature

- [1] Will, J., Baldauf, H.: Integration of Computational Robustness Evaluations in Virtual Dimensioning of Passive Passenger Safety at the BMW AG, VDI Report Nr. 1976, Numerical Analysis and Simulation in Vehicle Engineering, 2006
- [2] Will, J. and Stelzmann, U.: Robustness Evaluation of Crashworthiness using LS-DYNA and OptiSLang, ANSYS Conference & 25th CADFEM Users' Meeting 2007, 2007
- [3] National Highway Traffic Safety Administration, USNCAP test procedure, <http://www.nhtsa.gov/Vehicle+Safety/Test+Procedures/>
- [4] Ortmann, C. and Schumacher, A.: Meta - models in structural optimization - techniques and strategies, Proceedings of the Automotive CAE Grand Challenge 2014, 2014

# Improving Robustness of Chevrolet Silverado with Exemplary Design Adaptations Based on Identified Scatter Sources

Dominik Borsotto<sup>1</sup>, Robin Strickstroch<sup>1</sup>, Clemens A. Thole<sup>1</sup>

<sup>1</sup>SIDACT GmbH, Sankt Augustin, Germany

The investigations described here are related to the unstable behavior of crash-simulations due to minor changes in the model. As a consequence the received simulation results become in some way unpredictable, whereby the causes can be various: e.g. modeling failure, contact issues, numerical instabilities, physical instabilities, etc..

To identify and separate these scatter sources the results are analyzed by means of visualizing the standard deviation of scatter itself and computing scatter-modes for selected parts of interest. Latter computations are based on the principle component analysis (PCA), and deliver new virtual crash results representing the most extreme geometrical shapes of the scatter-modes. This improves and speeds up the process of identifying scatter causes.

For illustration a realistic application case based on the freely available Chrysler Silverado from the National Crash Analysis Center (NCAC) of The George Washington University is analyzed by means of robust design of the crash model. Therefore 25 simulation runs were performed based on small random part thickness changes (representing production tolerances). The part of interest for the investigations is the variance at the fire-wall. As an outcome major scatter sources in the interaction of power-brake and suspension as well as at the longitudinal rail are found which are strongly correlated to the firewall scatter. Approving the software based prediction exemplary design adaptations lead to a significant reduction of scatter on the firewall. The described mathematical methods are part of the software DIFFCRASH, which was used in this study.

Additionally a perspective regarding the integration of these analysis methods into a simulation data management system is given.

# Classification-Based Optimization and Reliability Assessment Using LS-OPT

Anirban Basudhar<sup>1</sup>, Imtiaz Gandikota<sup>1</sup>, Nielen Stander<sup>1</sup>, Åke Svedin<sup>2</sup>, Christoffer Belestam<sup>2</sup>, Katharina Witowski<sup>3</sup>

<sup>1</sup>Livermore Software Technology Corporation, Livermore CA, USA

<sup>2</sup> DYNAmore Nordic, Sweden, <sup>3</sup> DYNAmore GmbH, Germany

Simulation-based design optimization and probabilistic analysis involve repeated calls to potentially expensive (e.g. crashworthiness analysis) design alternative or function evaluations. To avoid the high cost (or computational time) associated with repeated expensive evaluations, the actual function evaluations are substituted with evaluations based on metamodels. Metamodels, trained based on relatively few actual function evaluations, provide an approximation of the system responses and thus act as surrogate models.

Considerable research has been done in the field of metamodel-based design optimization and analysis [1]. Various types of metamodels can be trained based on different criteria for the "best" fit, several of which are also available in LS-OPT [2]. Different sampling schemes have also been developed to globally or locally enhance metamodel accuracy, based on specific applications such as deterministic single-objective design optimization, multi-objective optimization, reliability analysis or reliability-based design optimization [3-6]. For most types of problems, metamodel-based methods have been shown to perform efficiently and accurately. However, the use of metamodels is hampered for certain systems that have discontinuous or binary responses, e.g. buckling, on-off contact, hidden constraints etc [7, 8]. The approximation of response values becomes difficult for such systems.

This paper presents an alternative method, based on the classification of response values, which does not require response approximation [7, 9]. As a result, it is unaffected by the presence of binary or discontinuous responses and provides a straightforward way to solve such problems. The principal idea is to classify the training samples into two classes, using a threshold value or a clustering method, and then construct an "optimal" decision boundary in the design space that separates the samples belonging to the different classes. Thus, this decision boundary can be used as the limit-state in reliability analysis [7] or to constrain feasible design alternatives in optimization [10].

The use of classification methods is quite common in pattern recognition and decision making [11-13], but their use in engineering design is relatively new and has only gained attention over the last decade. A machine learning technique known as support vector machine (SVM) [14] has received special attention due to its ability to minimize generalization error and to define highly nonlinear boundaries needed to solve design problems in the general case. It was first used for reliability assessment in [15] and for deterministic or reliability-based optimization in [7]. Adaptive sampling techniques have also been developed based on the specific application (reliability analysis or optimization) [10, 15-18]. More recently, another classification method known as random forest classification has also gained attention [8]. However, no comprehensive study has been performed to assess the relative efficiency and accuracy of different classification methods. As in the case of metamodels, it is likely that the relative performance of different classifiers is also problem specific. Irrespective of the type of classifier, the basic principles of their application to engineering design remain the same.

The aim of this paper is to give an overview of different applications and advantages of classification in engineering design. A brief overview of the newly implemented MATLAB interface in LS-OPT is also presented. This interface can be used to integrate LS-OPT with open source MATLAB classification codes, but LS-OPT will have the classification algorithms implemented within itself in the near future. A brief overview of the proposed new "Classifier" entity in LS-OPT is also presented. Additionally, a major part of the paper is dedicated to a very recent method for classification-based multiobjective optimization (MOO) [19] developed by the principal author. This method has been compared to existing MOO methods, such as NSGAI [20] and Pareto Domain Reduction (PDR) [21], using several examples up to thirty variables. The SVM classification-based method involves a radical shift from current MOO methods, and is shown to perform significantly better.



## **OPTIMIZATION II**

### **GENERAL**





# Some LS-OPT Applications in the CAE Development of Injection Molded Thermoplastic Parts

A. Wüst

BASF

# Optimization of a Lower Bumper Support regarding Pedestrian Protection Requirements using ANSA and LS-OPT

Isabelle Wetzstein, Beate Lauterbach, Matthias Erzgräber, Lothar Harzheim

Adam Opel AG, Rüsselsheim

## 1 Introduction

A variety of pedestrian protection requirements must be considered during the vehicle development process, in order to improve the protection of vulnerable road users.

The lower bumper support, which is located at the vehicle front, is designed to generate beneficial leg kinematics from early in the impact. For EuroNCAP requirements, the FLEX-PLI leg impactor is used to simulate the leg impact. The leg injury parameters are obtained from the FlexPLI CAE results by calculating knee ligament extension and lower leg bending moments.

## 2 Geometry Optimization for Lower Bumper Support

This presentation deals with the optimization of a glass fiber mat reinforced thermoplastic (GMT) lower bumper support geometry, using ANSA linked with LS-Opt, to meet the EuroNCAP requirements for pedestrian protection.

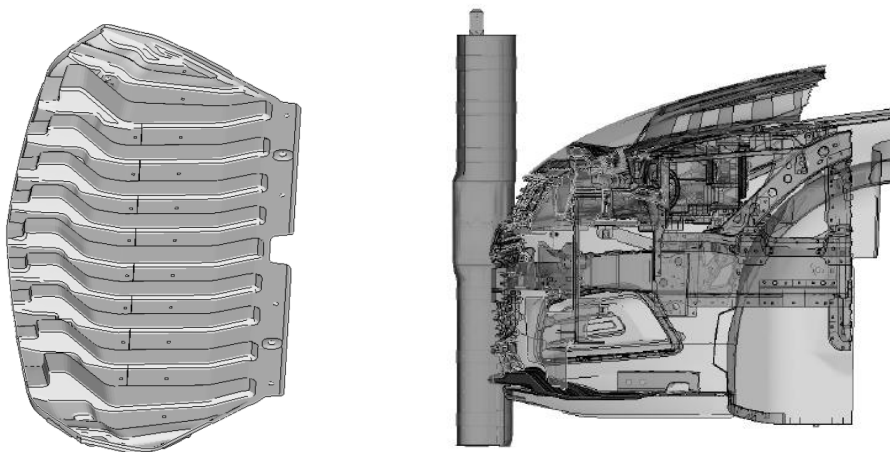
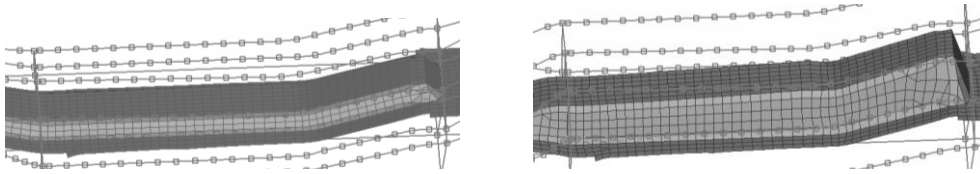


Fig.1: Lower bumper support geometry and it's position within the vehicle

For this work, a parameterized model of the component was built with ANSA-Morphing. LS-Opt was used to find an optimal parameter set for the design variables describing the lower bumper support geometry defined as the width and depth of the component's depressions. A preliminary variance analysis was performed to assess the influence of design variables on the target function. Thus, the number of design variables could be reduced.



*Fig.2: Morphing box for depression height*

The choice of an appropriate target function and a sufficient number of reasonable restrictions is crucial for the obtained optimization result and weather convergence in the optimization procedure is at all achievable. Different approaches for the formulation of the optimization problem to maximize the number of EuroNCAP rating points are demonstrated and discussed.

# X760 Bumper Automation and Optimisation Process

Dr Tayeb Zeguer

Jaguar Landrover

Currently the bumper system is developed through a wide variety of individual virtual test methods, the majority of which also have to be verified with physical testing. This paper will describe a new process that produced a one combined virtual process to encompass the full bumper as a system development method by creating One model for a bumper as one system with multiple attributes and requirements and using only one code “ LS-DYNA and LS-OPT”.

To facilitate this, improvements are required in both CAE prediction confidence and test method interactions for the following requirements: low speed impact, pedestrian leg impact, thermal stability, stone chipping, firmness feel and NVH. The benefit of this approach is to reduce bumper system cost and mass through integrated system design strategy, at early stages, considering all requirements together and have a potential to reduce reliance on physical testing.

# Multi-Scale Material Parameter Identification using LS-DYNA and LS-OPT

Nielen Stander<sup>1</sup>, Anirban Basudhar<sup>1</sup>, Ushnish Basu<sup>1</sup>, Imtiaz Gandikota<sup>1</sup>, Vesna Savic<sup>2</sup>, Xin Sun<sup>3</sup>, Kyoo Sil Choi<sup>3</sup>, Xiaohua Hu<sup>3</sup>, Farhang Pournoghbat<sup>4</sup>, Taejoon Park<sup>4</sup>, Aboozar Mapar<sup>4</sup>, Sharvan Kumar<sup>5</sup>, Hassan Ghassemi-Armaki<sup>5</sup>, Fadi Abu-Farha<sup>6</sup>

<sup>1</sup>Livermore Software Technology Corporation, Livermore CA, USA

<sup>2</sup>General Motors Company, Detroit MI, USA

<sup>3</sup>Pacific Northwest National Laboratory, Richland WA, USA

<sup>4</sup>Michigan State University, East Lansing MI, USA

<sup>5</sup>Brown University, Providence RI, USA

<sup>6</sup>Clemson University, Clemson SC, USA

## 1 Introduction

This paper serves as an introduction to the LS-OPT<sup>®</sup> and LS-DYNA<sup>®</sup> methodology for multi-scale modeling. It mainly focuses on an approach to integrate material identification using material models of different length scales. As an example, a multi-scale material identification strategy, consisting of a Crystal Plasticity (CP) material model and a homogenized State Variable (SV) model, is discussed and the parameter identification of the individual material models of different length scales is demonstrated. The paper concludes with thoughts on integrating the multi-scale methodology into the overall vehicle design.

## 2 New user material models in LS-DYNA<sup>®</sup>

Two constitutive models were implemented as user materials. These two models represent the two length scales respectively.

### 2.1 The MSU Crystal Plasticity model (Michigan State University)

The Combined Constraints Crystal Plasticity model which is based on the principle of maximum dissipation is used to model the large plastic deformation in single crystals.

### 2.2 State Variable model (Pacific Northwest National Laboratory)

PNNL has developed a State Variable model using the phase properties obtained from the CP model. A simple model is used to homogenize the Young's modulus, Poisson ratio, plastic modulus and volume fraction of each phase respectively. Phase stress-strain curves can be provided from the lower length-scale modeling (in this case CP) results or from experimental methods such as in-situ High Energy X-ray Diffraction (HEXRD) test. As for the phase transformation, the Olsen-Cohen model is used as a phenomenological phase transformation kinetics model with the evolution of the austenitic volume fraction defined by:

$$V_{tm} = V_{a0} [1 - \exp\{-b[1 - \exp(-a\bar{\epsilon}_p)]^n\}] \quad (1)$$

where  $a$ ,  $b$ , and  $n$  can be determined by fitting with the experimentally obtained phase transformation kinetics under different loading conditions.

## 3 Integration of the MSU-CP model with the PNNL-SV model in LS-OPT

Because of the interdependency of the material parameters, calibration of the PNNL-SV model relies on the calibrated MSU-CP model parameters as inputs. Therefore, a multi-level process is required to integrate the models. Different stages are required in order to sequence the two parameter identification tasks which are accompanied by multiple test cases to incorporate the four metal phases and five triaxial load cases. Different levels are required because, to calibrate the two models, optimization stages are involved in the process flow and have to be controlled from an outer level.

The process is depicted in Figure 1.

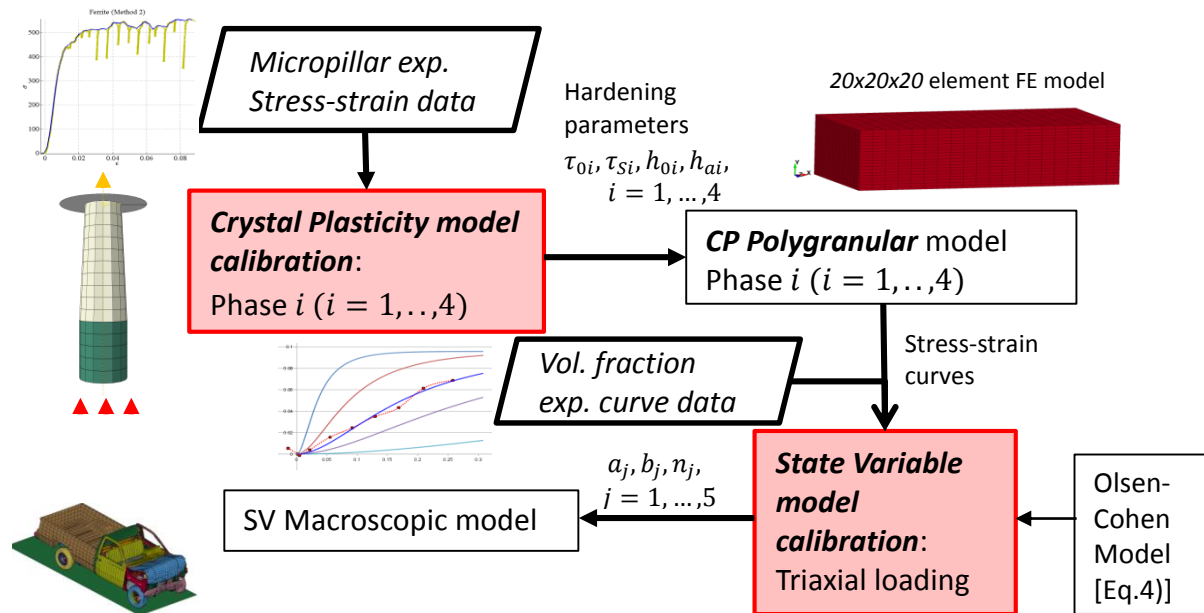


Fig.1: Process flow of the integrated multi-scale calibration of Crystal Plasticity and State Variable models

#### 4 Calibration of the MSU Crystal Plasticity model using LS-DYNA and LS-OPT

To gain an understanding of the calibration of each phase and loading, each calibration was first studied as an isolated individual component.

The calibration of the Crystal Plasticity BCC-24 model was conducted with LS-OPT using the ferrite and martensite phases. The experiments are done on single grain micropillar structures of which tip displacement and force results are extracted. A micropillar constitutes a pure crystal structure representing a single phase and is in the form of a tapered cylinder with measurements in the 1 micron range. BAO QP980 steel was used in the experiments.

#### 5 Calibration of the PNNL State Variable model using LS-DYNA and LS-OPT

The calibration of the State Variable model uses experimental data generated by the in-situ High Energy X-ray Diffraction (HEXRD) test. The experimental data is defined by the retained austenitic volume fraction or the corresponding transformed martensitic volume fraction as a function of equivalent plastic strain. The computed curves are obtained using the Olsen-Cohen model.

#### 6 LS-OPT enhancements required for integration

Several enhancements were added to LS-OPT to facilitate the integration of parameter identification at various levels.

1. A multilevel optimization capability was created by allowing LS-OPT to be defined as a solver or stage type of itself.
2. A class of variables named *response variables* was introduced to allow transfer of data between consecutive stages.
3. Multilevel navigation features were introduced in the GUI to assist the user to monitor progress at any selected level and solver job.

## **OPTIMIZATION III**

### **TOPOLOGY**





# A Weight Balanced Multi-Objective Topology Optimization for Automotive Development

Nikola Aulig<sup>1</sup>, Emily Nutwell<sup>2</sup>, Stefan Menzel<sup>1</sup>, Duane Detwiler<sup>3</sup>

<sup>1</sup>Honda Research Institute Europe GmbH, Offenbach/Main, Germany

<sup>2</sup>Ohio State University SIMCenter, OH, USA

<sup>3</sup>Honda R&D Americas, Raymond, OH, USA

The field of topology optimization refers to algorithms that aim at finding the optimum layout of a lightweight structure. In contrast to shape optimization, which targets fine-tuning of a rather advanced structural design, topology optimization provides the engineer or designer with a structural concept early in the design process. Concretely, topology optimization approaches address the problem of finding the optimal distribution of materials and void within a pre-defined design space [1].

In the field of automotive development topology optimization strives for conceptual car components which are efficiently designed for multiple, partly conflicting loadings. Structures designed to manage crash events typically require a maximization of energy absorption while static loadings typically require a minimization of compliance of the structure.

The complexity due to the nonlinear nature of crash type loads lends itself to heuristic approaches such as the hybrid cellular automata (HCA) approach [2]. The HCA, which aims for a uniform distribution of the internal energy density, offers an efficient solution for the single objective problems but may fail where large energy differences occur in different load cases. Recently, it was demonstrated that a multi-objective optimization can be performed by linearly weighting and careful scaling of the load case energy levels [3]. In this paper, the method is applied and evaluated on a more practical model. The structure developed by this concurrent optimization methodology is compared to a baseline approach of performing the static and dynamic optimization sequentially.

In this work we consider the practical optimization of a vehicle control arm structure LS-Dyna model, which is subject to two compliance load cases and an energy maximization load case. In general, the stiffness of the control arm is important for NVH, durability, and ride comfort and steering response; however, during a load retention scenario, it can be subject to substantial deformation which the structure must efficiently manage. Thus, during normal operation, minimum compliance is required, while during a loading event which results in yielding of the part, energy absorption should be maximized. The control arm and the dynamic load case are illustrated in Fig.1.

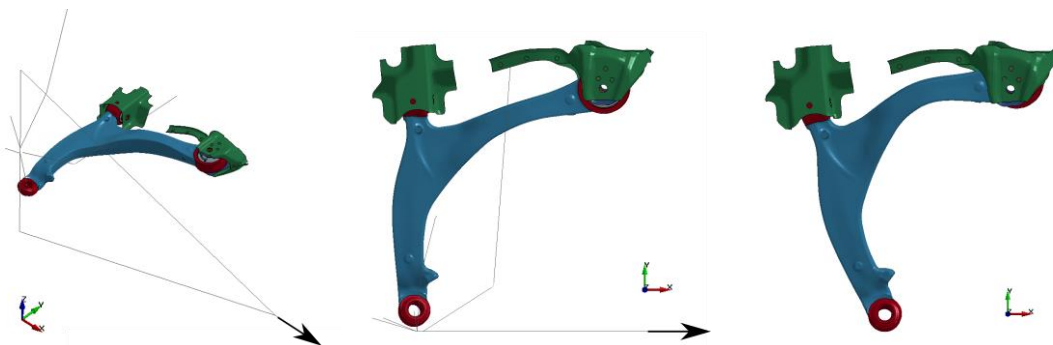


Fig.1: The LS-Dyna model of the nonlinear load case of the control arm. A prescribed displacement is applied to the chain. The rightmost figure shows the deformed structure when the load is applied to the full design space.

The target of the work is to find a conceptual design that balances the different load cases, i.e., the objectives of minimum compliance and maximum energy absorption associated with the respective load requirements. In order to obtain baselines for comparison, each objective was considered separately. Secondly, a sequential approach is applied based on the idea of first optimizing the

compliance objectives, followed by a second optimization for the energy absorbing targets. Finally we apply the multi-objective approach based on scaled weighting from [3]. All experiments implement the software package LS-TaSC [4], the topology optimization software designed to work with LS-DYNA. LS-TaSC provides a straightforward interface to implement the HCA algorithm described, including the capability to weight multiple load case.

Efficient structures are obtained from the optimization, confirming the ability of the HCA algorithm for the targeted optimization objectives of stiffness and energy absorption. The resulting structures from the sequential and concurrent approach are shown in Fig. 2. Similar structures result, that balance the three considered load cases. Results show that both methods are suitable to obtain feasible trade-off solutions, yet the scaled weighting approach provides a slightly better solution without manual interaction step. Furthermore the multi-objective approach provides a regularization of the objectives based on a user preference, as shown in Fig. 3.



Fig.2: Resulting deformed structures of trade-off from running the sequential topology optimization of stiffness and energy absorption (left), and concurrent scaled weighting topology optimization, resulting from an equal preference of compliance and energy absorption (right).

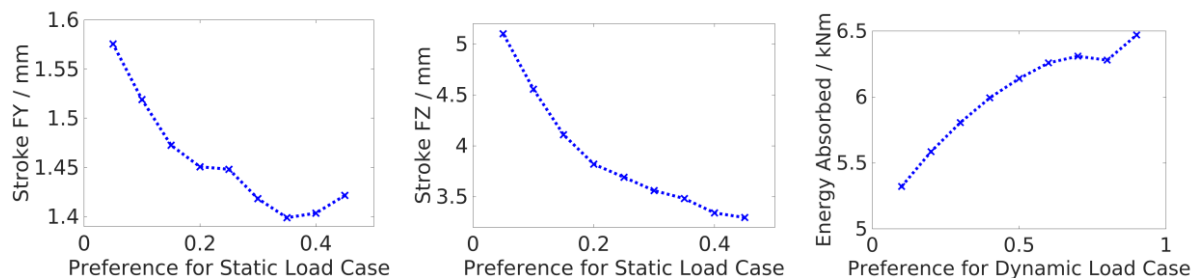


Fig.3: Dependence of the objective value on the preference for the y-directed static load (left), z-directed static load (middle and the dynamic load (right).

## Literature

- [1] Bendsøe, M. and Sigmund, O.: "Topology Optimization Theory, Methods and Applications", 2nd ed., Springer Verlag Berlin, 2004.
- [2] Patel, N. M.: "Crashworthiness design using topology optimization", Ph. D. thesis, University of Notre Dame, 2007.
- [3] Aulig, N., Nutwell, E., Menzel, S., Detwiler, D.: "Towards multi-objective topology optimization of structures subject to crash and static load cases", Engineering Optimization 2014, CRC Press, 2014, 847-852.
- [4] Roux, W.: "Topology design using LS-TaSC™ version 2 and LS-DYNA", 8th European LS-DYNA Users Conference, 2011.

# Topometry and Shape Optimization of a Hood

Yong Ha Han<sup>1</sup>, Katharina Witowski<sup>2</sup>, Nikolay Lazarov<sup>2</sup>, Krassen Anakiev<sup>2</sup>

<sup>1</sup>Hyundai Motor Group

<sup>2</sup>DYNAmore GmbH

## 1 Introduction

To comply with the regulations of pedestrian safety, particularly the head impact requirements, the geometry of the hood panel is significant.

The objective of this research was to develop a standardized automated method to design a hood which meets the pedestrian headform impact safety regulations and additionally the stiffness and fatigue requirements.

The developed method was performed in two steps.

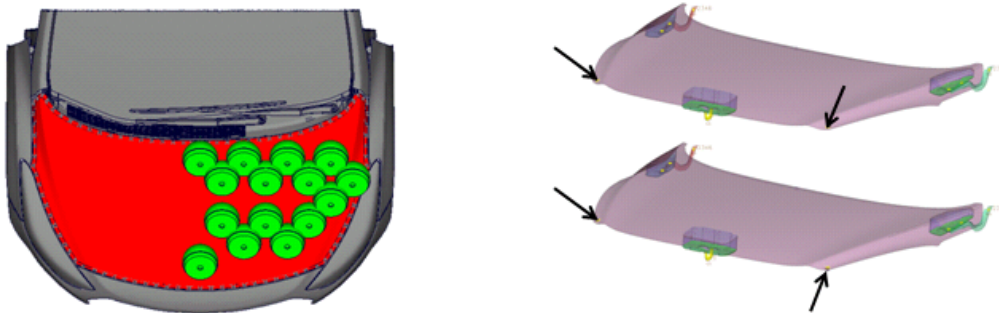


Fig.1: Loadcases for the topometry optimization: position of the 15 head impact points (left), load case "bending" (top right) and load case "torsion" (bottom right).

## 2 Topometry optimization

As a first step, a topometry optimization of the inner hood panel using Genesis from Vanderplaats R&D and the Equivalent Static Load Method (ESL) has been executed. The dynamic simulations were performed with LS-DYNA as the coupling module ESLDYNA of Genesis was used. From the result a preliminary CAD design of the inner hood panel was generated.

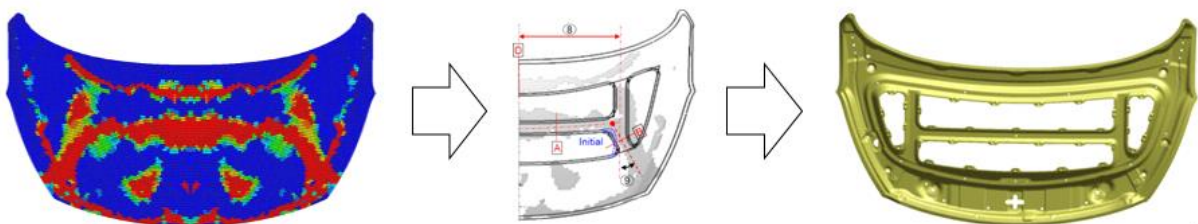


Fig.2: Interpretation of a preliminary CAD design, based on the topometry optimization results.

This design is just one possibility to interpret the result of the topometry optimization. Furthermore, since the ESL method is an interaction of nonlinear dynamic simulations and linear static optimization, nonlinear dynamic quantities such as HIC values cannot be considered directly in the linear static topometry optimization. Hence a second step was necessary to refine the functional requirements.

### 3 Shape optimization

A parametric multi-disciplinary shape optimization with LS-OPT was carried out using the preliminary CAD geometry as a baseline design. The parameters of the optimization with LS-OPT were gauge thicknesses and geometric changes of the inner panel structure. To apply the geometric parameters the ANSA Morphing Tool from BETA CAE Systems S.A. was used.

The method was performed for two different models, a steel and an aluminum hood. As a result, a new design of the hoods with significant improvement of the performance and reduced mass was proposed.

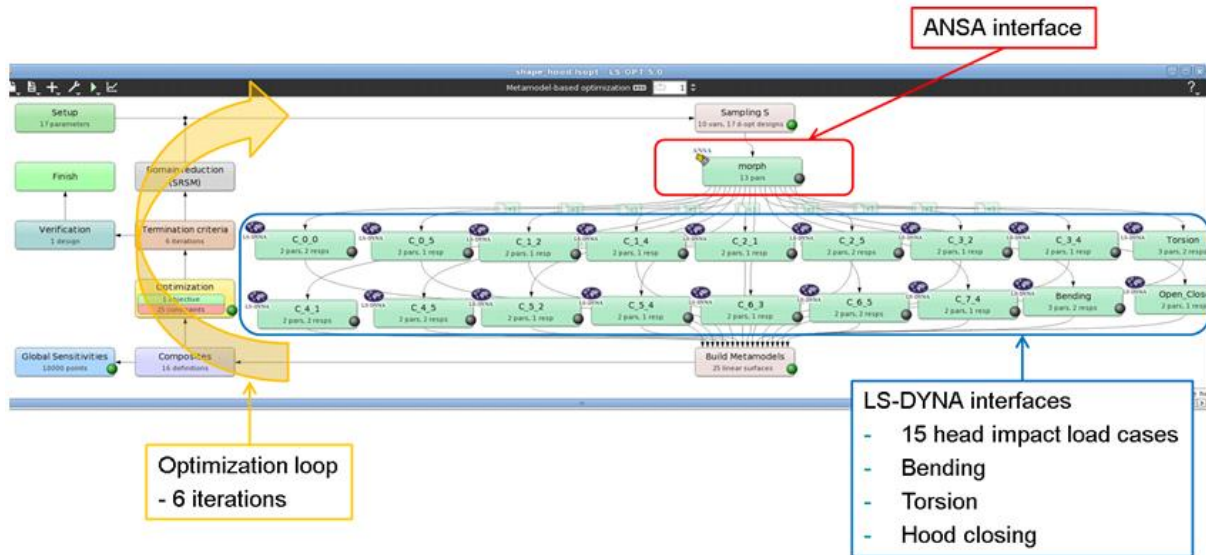


Fig.3: Main LS-OPT GUI window.



Fig.4: Initial design (left), design after topometry optimization (center) and design after shape optimization (right) of the inner aluminum panel.

### 4 Summary

The optimization of the hood has been performed in two steps.

In the first step, a topometry optimization with Genesis/ESL for the design of the supporting structure of an engine hood has been performed. The result was a preliminary CAD design of the inner hood. Since the objectives and constraints have to be defined for the linear optimization in the ESL method, alternative criteria need to be established for nonlinear responses like HIC values. Another challenging task is the translation of the nonlinear LS-DYNA model to a linear Genesis model. The interpretation of the result of the topometry optimization was a design with improved HIC values for four load cases for the steel hood, and for seven load cases for the aluminum hood, respectively.

In the second step, a shape optimization has been performed with LS-OPT, ANSA and LS-DYNA to refine the functional requirements of the model. The mass as well as six HIC values could be further improved. The constraints defined for torsion, bending and the hood closing analysis were not critical.

In total, 10 HIC values could be improved for the steel hood, and 13 HIC values for the aluminum hood, respectively.

# Meta-Model Based Optimization of Spot-Welded Crash Box using Differential Evolution Algorithm

Ahmet Serdar Önal<sup>1</sup>, Necmettin Kaya<sup>2</sup>

<sup>1</sup>Beyçelik Gestamp Kalip ve Oto Yan San, Turkey.

<sup>2</sup>Uludağ University, Mechanical Engineering Department, Turkey

## 1 Introduction

The main goal of this study is to maximize the energy absorption performance of spot-welded crash box using optimization techniques. Maximization of absorbed energy is selected as objective function and the upper bound of maximum initial peak force is defined as constraint function. Design of experiment (DOE) study has been performed with full factorial sampling method, and then polynomial objective and constraint functions were defined to approximate the responses, such as absorbed energy and initial reaction force. A Pascal code based Differential Evolution method was developed for solving optimization problem. Developed optimization software was tested with two test functions, then, optimization problem has been solved.

## 2 Finite Element Model

In order to find optimal crashworthiness of structure, nonlinear finite element method has been used which enables to model complex material models, large deformation and strain rates and frictional contact with acceptable accuracy. In this study, the finite element model of crash box and boundary conditions were prepared using Hypermesh software. An explicit finite element code, Ls-Dyna was used to implement the computations.

The behavior of the crash tubes has been studied by simulating the impact of a rigid barrier traveling at a speed of 10 m/s with a mass of 500 kg for the crash tubes with rectangular cross-section with 1 mm thickness. The material properties of dual phase steel (DP600) were used in the analyses. The crash box consists of two sheet parts and joined with spot welds. Elasto-plastic material model based on Von-Mises plasticity MAT\_100 (MAT\_SPOTWELD\_DAMAGE-FAILURE) was used to model the spot weld connections [3]. The diameter of the spot welds were chosen 4 mm and modeled with by using 4-hexa solid elements. In order to reduce the maximum reaction force, crash initiators are defined on the crash box. An example of 3 crush initiators can be shown in Figure 1 used in this study.

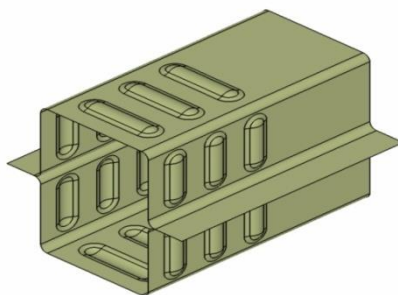


Fig.1: Crush initiators on the crash box

Generating crash behavior databases for all possible numbers of spot weld and crush initiators is an extremely expensive task. Approximation methods such as metamodels will overcome the aforementioned problem, especially in case of crashworthiness design optimization.

## 3 Response Surface Method

Design of Experiment (DOE) simulation was conducted at 9 sampling points by the full factorial design method. In this study, a full factorial design is employed to decide on the analysis points in order to obtain enough information for the approximation. Three levels (3, 5, and 7) for number of spot weld on

one side of crash box and three levels (1, 3, and 5) for number of beads were selected. Curve fitting technique is applied to find the response equation for absorbed energy and initial reaction force respect to number of spot welds and crush initiators.

#### 4 Optimization

The aim of the optimization in this study is to maximize the absorbed energy ( $E$ ) subject to initial reaction force ( $F$ ) lower than 140 kN, Design parameters are number of spot weld and crush initiators. Optimization problem has been solved with Differential Evolution (DE) algorithm. Due to DE algorithm is based on real representation of design parameters, optimum results are real values. Number of spot welds is found as 7 and number of crush initiators is 4.50. Number of crush initiators can be selected as 4 or 5. It is found that number of spot welds for 7 and number of crush initiators for 5 give best results. Alternatively, number of spot welds for 7 and number of crush initiators for 3 is another optimum solution according to DOE study. For optimum design, maximum absorbed energy is 8.308 kJ. Final design undeformed and deformed crush models are given in Figure 2.

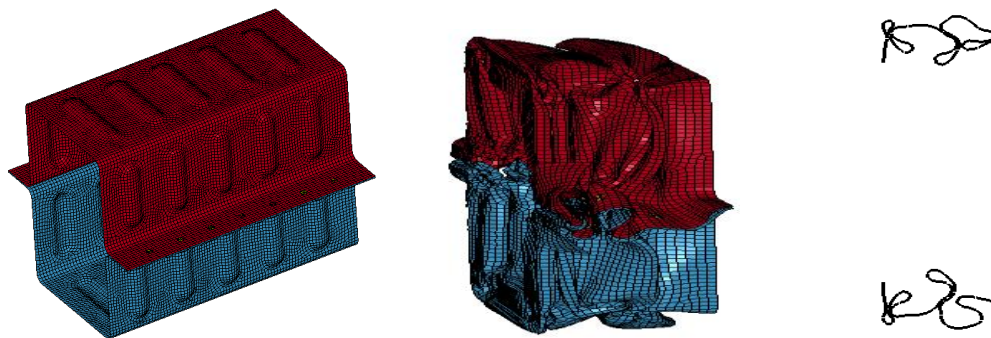


Fig.2: Undeformed, deformation characteristics and section view (deformed time=15 ms)

It is revealed that the with the help of crush initiators maximum reaction force is reduced from 259.38 kN to 141.438 kN. Therefore, crush initiators geometries can be used in crash boxes to reduce the high reaction force effectively. Additionally, it is shown that, the optimization tools can help designers to select best combinations among the candidate designs.

#### 5 Summary

In this study, an optimization study of thin-walled crash box was performed. Maximization of absorbed energy is selected as objective function and the upper bound of maximum peak force is defined as constraint. DOE study has been performed and polynomial objective and constraint functions were defined to approximate the absorbed energy and maximum reaction force. Optimization problem has been defined and solved with Differential Evolution algorithm. By introducing crush initiator geometries and optimization studies, initial reaction force has been reduced without decreasing energy absorption capability of thin-walled and spot welded crash box.

#### 6 Literature

- [1] Chiandussi, G. and Avalue M., Maximisation of the Crushing Performance of a Tubular Device by Shape Optimisation, Computers and Structures, vol. 80, 2002, pp. 2425-2432.
- [2] Kaya, N. and Öztürk F., Multi-objective crashworthiness design optimisation of thin-walled tubes, International Journal of Vehicle Design, Vol. 52, Nos. 1/2/3/4, 2010, pp.54-63.
- [3] Seeger, F., Feucht M., Frank Th., Keding B., Haufe A., An investigation on spot weld modelling for crash simulation with Ls-Dyna. 4. Ls-Dyna Anwenderforum, Bamberg, 2005.
- [4] Hörmann, M., Schulz, A., Rust, W., Structural Optimization using LS-OPT: Basics and Examples, Composite Structures, 21st CAD-FEM Users' Meeting, International Congress on FEM Technology, November 12-14, Berlin, Germany, 2003.
- [5] Price, K.V., Storn R.M. and Lampinen J.A., "Differential Evolution - A practical approach to global optimization", Springer, 2005.

# OPTIMIZATION IV

## TOPOLOGY





# Topology Optimization of Transient Nonlinear Structures—A Comparative Assessment of Methods

E. J. Wehrle<sup>1</sup>, Y. H. Han<sup>2</sup>, F. Duddeck<sup>1</sup>

<sup>1</sup>Chair of Computational Mechanics, Technische Universität München, Germany

<sup>2</sup>Advanced Safety CAE Team, Hyundai Motor Group, Korea

## 1 Topology optimization under transient nonlinear structural-mechanical behavior

Topology optimization considering transient nonlinear behavior of mechanical structures, e.g. automotive crash, remains a challenge in both the implementation as well as computational effort. In recent years, efficient optimization algorithms and increased computer technology has begun to allow the development of methodologies to examine optimal topology of structures undergoing such behavior.

Here, the topology optimization methodologies are categorized by the abstraction of the loads, from fully transient nonlinear structural-mechanical analysis to multiple static replacement loads to a single static replacement load. Several methods are investigated for varying loading conditions and degrees of nonlinear behavior: 1) the use of the algorithms based on hybrid cellular automata with full transient nonlinear finite-element analyses; 2) multiple static replacement loads with updates via transient nonlinear finite-element analysis; 3) multiple static replacement loads without updates; 4) single static replacement load.

## 2 Methods of topology optimization in crashworthiness

Here methods of topology optimization under transient nonlinear loading are categorized in two general types: 1) Reducing or eliminating the number of nonlinear structural analyses and 2) efficient optimization methods. In the first, the number of nonlinear structural-mechanical analyses is greatly reduced or eliminated and instead linear elastostatic replacement loading is used. These methods vary from a single load derived from the nonlinear analysis applied to a structure and then calculated with linear elastostatic finite-element method to several loads that can be further updated throughout the optimization process. The second family includes methods of using full transient nonlinear structural-mechanical analysis in concert with very efficient, gradient-free optimization methods to find optimal topologies will be discussed. Although other, related methods do indeed exist, this section will concentrate on hybrid cellular automata (HCA). Both have advantages and disadvantages, and these will be discussed after a short introduction and example of each method.

## 3 Review and comparison of methods

After studying the use of the methods for topology optimization of transient nonlinear structures on validation cases, a comparison is proposed here. As this study was not exhaustive in all regards of all methods, further investigations are needed to validate and substantiate these findings. From the experience of the optimization results here, amongst others, Table 1 has been created to ascertain the performance of the methods for different design criteria and structural-mechanical behavior.

Future studies are planned and running to verify the statements of Table 1. Further benchmark example will be necessary to further quantify the results as well as the advantages and disadvantages of these methods.

Comparison of methods for topology optimization of transient nonlinear structures. Criteria being very appropriate ++, appropriate: +, neutral: 0, somewhat inappropriate: -, very inappropriate: --, no rating, further investigation must be completed: \*

Category	Method	Number of design variables	Multiple objectives	Constraint flexibility	$\ddot{u}$ as constraint	Highly nonlinear behavior	Light plasticity	Bending	Progressive collapse
Replacement loading	Single replacement	+	++	++	--	--	0	-	--
	Multiple replacement	+	++	++	--	--	+	0	-
	Multiple replacement with update	+	++	++	-	-	++	+	*
Efficient optimization algorithms	HCA in LS-TaSC	++	--	--	++	++	++	++	-
	HCA-TWS	++	-	-	+	++	++	++	+

#### 4 Literature

Barnett, A. R.; Widrick, T. W. and Ludwiczak, D. R. (1995). *Closed-form static analysis with inertia relief and displacement-dependent loads using a MSC-NASTRAN DMAP alter*, World MSC Users' Conference; Los Angeles, CA; USA.

Guyan, R. J. (1965). *Reduction of stiffness and mass matrices*, AIAA Journal 3(2): 380.

Hunkeler, S. (2013). *Topology optimisation in crashworthiness design via hybrid cellular automata for thin walled structures*, PhD thesis, Queen Mary University of London, UK.

Inoue, N.; Shimotai, N. and Uesugi, T. (1994). *Cellular automaton generating topological structures*, Proc. SPIE 2361, 2nd European Conference on Smart Structures and Materials: 47-50.

Liao, L. (2011). *A study of inertia relief analysis*, 52nd AIAA/ASME/ASCE/AHS/ASC Structures, Structural Dynamics and Materials Conference, Denver, CO, USA.

Nelson, M. F. and Wolf, J. A. (1977). *Use of inertia relief to estimate impact loads*, SAE Technical Paper 770604: 149-155.

Pagaldipti, N. and Shyy, Y.-K. (2004). *Influence of inertia relief on optimal designs*, 10th AIAA/ISSMO Multidisciplinary Analysis and Optimization Conference, Albany, NY, USA.

Park, G.-J. (2011). *Technical overview of the equivalent static loads method for non-linear static response structural optimization*, Structural and Multidisciplinary Optimization 43: 319-337.

Patel, N. (2007). *Crashworthiness design using topology optimization*, PhD thesis, University of Notre Dame, IN, USA.

Querin, O.; Steven, G. and Xie, Y. (1998). *Evolutionary structural optimisation (ESO) using a bidirectional algorithm*, Engineering Computations 15: 1031-1048.

Tovar, A. (2004). *Bone remodeling as a hybrid cellular automaton process*, PhD thesis University of Notre Dame, IN, USA.

Volz, K. (2011). *Physikalisch begründete Ersatzmodelle für die Crashtoptimierung von Karosseriestrukturen in frühen Projektphasen*, PhD thesis, Technische Universität München, Chair of Computational Mechanics, Munich, Germany.

Xie, Y. M. and Steven, G. P., (1997). *Evolutionary structural optimization*. Springer, London.

N.N. (2012). *ESLDYNA: Documentation*, <http://www.vrand.com/ESLDyna.html>.

N.N. (2014). *GENESIS analysis manual: Version 13.1*, <http://www.vrand.com/Genesis.html>.

# Multidisciplinary Design Optimisation Strategies for Lightweight Vehicle Structures

Amit Prem<sup>1</sup>, Christophe Bastien<sup>1</sup> and Mike Dickison<sup>2</sup>

<sup>1</sup> Coventry University  
Faculty of engineering and Computing  
Coventry, CV1 5FB, UK

## 1 Introduction

Towards Affordable, Closed-Loop Recyclable Future-Low Carbon Vehicle Structures (TARF-LCV) Project funded by EPSRC [1] is specializing in the field of LCV technology in a number of key areas which has a significant impact on the current automotive industry. The research teams from a number of well renowned UK universities are working together to establish a future LCV structure which meets a number of constraints from ease of dismantling, closed-loop recyclability, advanced material implementation and lightweight structure which meets Euro NCAP crash regulations. This study is primarily focused on the crashworthiness of the TARF structure and predominantly looks into Multidisciplinary design optimization, i.e. the process through which a number of different disciplines are combined within a single optimization phase. The Optimization is governed by a number of performance constraints related to the various disciplines. Frontal offset deformable barrier test, Side impact test, pole impact test and Torsional rigidity test would be simultaneously solved using advanced optimization techniques with the main objective being mass reduction. The TARF vehicle structure was developed through a number of optimization processes, many of which have been engineered and established through previous research at Coventry University [2] [3] [4] [5]. The TARF vehicle structural integrity will be the main focus of the study and not occupant injuries. The TARF vehicle has been setup with instrumentation springs to measure passenger compartment intrusions and also with accelerometers. The main attributes that would be monitored in this study would be the intrusion levels for all the 3 crash loadcases along with vehicle deceleration for the frontal offset deformable barrier impact. The accelerometer output has been filtered using SAE 60Hz. The torsional rigidity of the model would be calculated by dividing the cross sectional moment in the X axis against the change in angle of wheel center points where a load of 1250N has been applied. The following velocities were used for the vehicle crash simulation.

Scenarios	Impact speed (m/s)
Front crash	17.9
Side impact	11.7
Pole impact	8.3

The impact velocity for the side impact is slightly lower due to the type of barrier being used weighing 1306kg instead of 950kg following Euro NCAP Side impact test Protocol v6.0 [9]. The side impact velocity was computed so that the same kinetic energy is observed as per the protocol.

## 2 Methodology

The current vehicle structure and its global behavior to crash loadcases has not been extensively studied. The MDO is the ideal platform to identify and investigate the influences various panels and materials have on crash responses, enabling the fine tuning of the vehicle structure for all the loading scenarios. Metamodel based optimization techniques are therefore employed for design exploration. These metamodels are computationally less intensive in finding the optimum solution for a number of variables as they are based on approximation to the design response within the design space. The metamodel is used instead of actual simulations to find the optimum solution [10]. A study [11] has suggested that polynomial metamodel should be used for low order nonlinearity problems due to their ease of use and high accuracy. Polynomial metamodel has also been recommended to be used first to see if a reasonable fit can be obtained. These models have been found to be ideal for sensitivity analysis studies and were used during the design of experiment (DOE) studies which was used prior to the optimization stage to eliminate redundant variables based on their influence on the responses.

These redundant variables were found using Sobal's Indices as the tool. Radial Basis Function metamodel was used during the single stage optimization phase, Hardy's multi-quadrics function was employed. The Radial Basis neural network consists of a 3-layer topology of which the input layer is linear, the hidden layer is made up of non-linear radial units each of which responds to only a local region of input space and the output layer creates an approximation over the entire design space through input-output mapping after performing a biased weighted sum of these units [12]. Space filling was used for the point distribution throughout the design space for both the DOE and the optimization phase.

### 3 Results

#### 3.1 Design of Experiment (DOE)

The DOE was conducted for a total of 17 variables which consists of 14 panel thickness variables and 3 discrete material variables. 7 feasible design solutions were obtained from a total of 38 simulation points. The feasibility of the solutions was dominated by two models, the frontal ODB and the Torsion model constraints. The DOE study revealed the mass saving potential for the TARF model. The fairly good accuracy of the polynomial metamodel also indicated that it is indeed a good metamodel to choose for sensitivity analysis. The DOE study enabled the elimination of variables whose influence on the responses were minimal. The important variables were identified pertaining to individual loadcases and were fully shared across simulations during the DOE. Certain variable values obtained from the simulation run 1.31 of the DOE were considered as the starting values for the further optimization baseline model. This would however have a negative effect on the torsional stiffness and passenger compartment intrusion but would highlight the significant mass reduction capabilities through MDO. The torsional stiffness lower bound was slightly reduced and the FC2\_Intrusion constraint was increased by 10mm to accommodate the changes. These changes were however reasonable since the rest of the constraints remained unchanged.

#### 3.2 Structural Optimization

The single stage optimization process is best suited if there is a limited simulation budget available. The method is ideal for global exploration studies but requires metamodels which can capture complex responses for automotive application. RBF was chosen as the metamodel for the optimization phase, as it is an ideal metamodel for flexible sample sets. Adaptive simulated annealing with Leapfrog optimizer for constrained minimization was chosen as the algorithm since it is a global stochastic optimization algorithm.

Based on the DOE study certain dominant variables were selected although not all were taken into consideration for the optimization. A total of 8 variables were used, 7 panel thickness variables and 1 discrete material variable. 448 processors were used during the optimization phase of which most were assigned to crash simulation models due to the average run time being 9 hours on 16 processors. The optimization phase led to a significant mass reduction close to 15.58% or 4.47% (if distributed nodal masses are considered) for the optimum result. A mass saving of 14.08kg was obtained from the optimization stage when compared to the optimization baseline model. When compared to the TARF initial baseline model a mass saving of 29.26kg was obtained. Although significant mass savings were possible, the optimum design resulted in the A-pillar T junction to fail. This is due to a lack of reinforcement in this region and predominantly due to the reduction in the gauge of the Lower A-pillar reinforcement, the passenger compartment is however being compromised slightly. The force transferred through the hydroformed upper A-pillar post is at 16.6kN which is well below its critical buckling load, this would further support the increase in the intrusion levels for the frontal Impact ODB. It is to be noted that TARF-LCV structure is still in its infancy but this study has clearly highlighted the mass saving potential of the structure and the use of MDO techniques playing a vital role in accomplishing the objective and constraints.

---

## Literature

- [1] TARF, Towards Affordable Closed-Loop Recyclable Future-Low Carbon Vehicle Structures (2011) EPSRC funded project. <http://gow.epsrc.ac.uk/NGBOViewGrant.aspx?GrantRef=EP/I038616/1>
- [2] LCVTP (2011), Low Carbon Vehicle Technology Project. Re: BG/AM1011, partly funded by ERDF and AWM. Project based on Tata 'Beacon' vehicle layout. Participation of Coventry University for vehicle aerodynamics, HVAC and Vehicle Body Structure
- [3] Bastien, C. (2010) "Topology Optimisation of a Body In White for Low Carbon Vehicle Technology Project", Altair European conference, EHTC 2010, October 2010, Versailles, France
- [4] Bastien, C., Christensen, J. (2011) 'Towards the Light weighting of Low Carbon Vehicle Architectures using Topology Optimisation', EHTC November 2011, Bonn, Germany
- [5] Christensen, J., Bastien, C., Blundell, M. V., Gittens, A., Tomlin, O. (2011) "Lightweight Hybrid Electrical Vehicle Structural Topology Optimisation Investigation Focusing on Crashworthiness", International Journal of Vehicle Structures and Systems, Volume 3, Issue 2.
- [6] Christensen, J., Bastien, C., Blundell, M.V., Kurakins, J., (2012) "Lightweight body in white design using topology-, shape and size optimisation", Electric Vehicle Symposium (EVS26), Los Angeles, California, 2012.
- [7] Christensen, J., Bastien, C. (2011a) 'Effects of Roof Crush Loading Scenario Upon Body In White Using Topology Optimisation', C, J., ICRASH Journal, December 2011.
- [8] Christensen, J., Bastien, C., Grimes, O., Appella, A., Bareham, G., O'Sullivan, K. (2011b) "Generation of Optimised Hybrid Electric Vehicle Body In White Architecture from a Styling Envelope"
- [9] European New Car Assessment Programme: Euro NCAP (2012) Side Impact Testing Protocol V6.0 [www.euroncap.com/en/for-engineers/protocols/adult-occupant-protection/](http://www.euroncap.com/en/for-engineers/protocols/adult-occupant-protection/)
- [10] Ryberg, A.B., Bäckryd, R.D., Nilsson, L.: (2012) "Metamodel-Based Multidisciplinary Design Optimization for Automotive Applications", Linköping University, Technical Report.
- [11] Jin, R., Chen, W., Simpson, T. (2001). "Comparative Studies of metamodelling techniques under multiple modelling criteria". Structural and Multidisciplinary Optimization, 23(1), 1-13.
- [12] Stander, N., Goel, T. (2008). "Metamodel Sensitivity to sequential adaptive sampling in crashworthiness design". 10th International LS-DYNA User's Conference.

# Optimization of Turbine Blade Fir-Tree Root Geometry Utilizing LS-PrePost in Pre- and Postprocessing

Jiří Jankovec<sup>1</sup>

<sup>1</sup>Research and Testing Institute Plzen, Czech Republic

The turbine blade fir-tree root is a type of blade to disc connection, usually used for low pressure steam turbine blades. This part of turbine is exposed to extreme loading conditions caused by centrifugal loading during turbine operation and therefore there is a need to find a design that exhibits lower stresses (see Fig.1), which determine low-cyclic fatigue life of the fir-tree root. This paper describes utilization of LS-Prepost [1] in optimization loop for design of new turbine blade fir-tree root geometry.

The LS-Prepost pre- and post- processor offers a wide range of functionalities for geometry and mesh generation and is well suited for collaboration with the solver of LS-DYNA [2] commercial FE-code and with LS-OPT [3] optimization program. The other inconsiderable advantage of LS-Prepost is that it is delivered free with LS-DYNA and therefore it is not necessary to utilize any commercial Pre- and post-processor to parametrically control geometry of the analyzed problem.

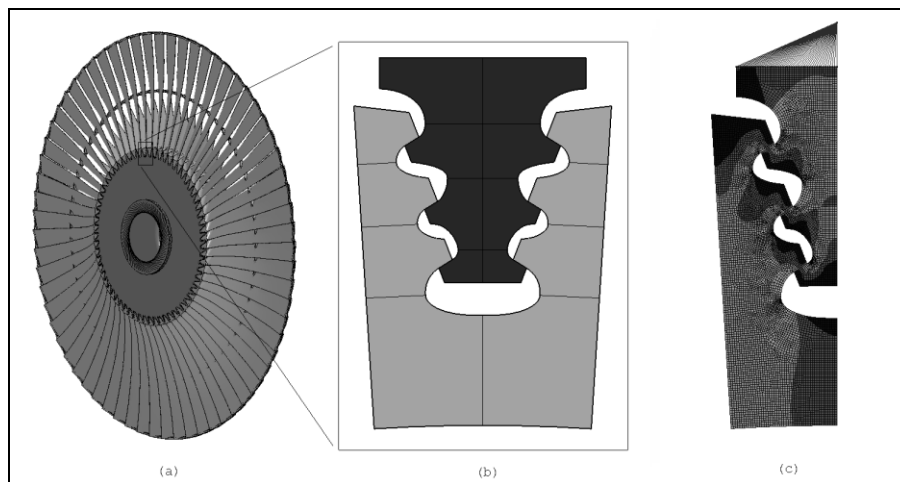


Fig. 1: (a) Whole turbine bladed wheel, (b) detail of blade fir-tree root, (c) analyzed part of the blade fir-tree root structure.

## Literature

- [1] LS-Prepost 4.2 Help Document, <ftp://ftp.lstc.com/outgoing/lsprepost/4.2/doc/win/Document.chm>, 2015
- [2] LS-DYNA Keyword User's Manual, Version 971, Release 4, Livermore Software Technology Corporation, Livermore, 2009
- [3] LS-OPT User's Manual, Version 4.2, Livermore Software Technology Corporation, Livermore, 2012

# MULTIPHYSICS I

## CFD/FSI





# A Numerical Investigation of Turbulent Flow in Circular U-Bend

A. Miloud<sup>1</sup>, M. Aounallah<sup>1</sup>, O.Imine<sup>2</sup> and M. Guen<sup>1</sup>

University of Science and Technology of Oran Mohamed Boudiaf (USTO-MB)

Department of Maritime Engineering

<sup>1</sup>Laboratory Aero-Hydrodynamic Naval

<sup>2</sup>Laboratory Aeronautic and Propulsion Systems  
Algeria

Numerical investigations of turbulent flows through a circular 180° curved bend with defined as the bend mean radius to pipe diameter for a Reynolds number of  $4.45 \times 10^4$  is presented in this study . The computation domain is performed for a U-Bend with full long pipes at the entrance and at the exit. Two turbulence models were tested in this work. The commercial software ANSYS FLUENT is used to solve the steady Reynolds–Averaged Navier–Stokes (RANS) equations. The numerical results were compared with experimental data for presenting their capabilities to capture the formation and extend this turbulence driven vortex. The results of numerical simulations of turbulent flow 3D heat transfer are presented for the case of two channels U turn and rectangular.

The purpose of this investigation was to study the effect of the corrugated walls of the heated portion on the improvement of cooling, in particular the influence of the wave length. The calculations were performed for a Reynolds number of 10,000 set at two values of the number of rotation ( $Ro = 0.0$  to  $0.14$ ) and a report of limited density to  $0.13$ . In these simulations, ANSYS FLUENT code was used to solve the Reynolds equations expressing the relations between the different fields' averaged variables over time. Model performance k-omega SST and model RSM are evaluated through a comparison of the numerical results obtained for each model and the experimental and numerical data. In this thesis, detailed average temperature predictions, the scope of the secondary flow and distributions of the local Nusselt are presented. It turns out that the corrugated configuration further urges the heat exchange provided to reduce the velocity of the coolant within the channel.

# Numerical Investigation of the Nozzle Number on the Performance of Conical Vortex Tube

M.Guen<sup>1</sup>, O.Imine<sup>2</sup>, A.Miloud<sup>1</sup>  
University of Sciences and Technology of Oran  
Mechanical Engineering Faculty  
Marine Engineering Department  
<sup>1</sup>Aero-Hydrodynamic Naval Laboratory  
<sup>2</sup>Aeronautics and Propulsive Systems Laboratory  
Algeria

A three dimensional computational fluid dynamic is used to analyze the mechanisms of flow inside a vortex tube. The vortex tube or Ranque-Hilsch vortex tube is a device which enables the separation of hot and cold air as compressed air flows tangentially into the vortex chamber through inlet nozzles. The SST turbulence model is used to predict the turbulent flow behaviour inside the tube. The vortex tube is an Exair 708 slpm (25 scfm) commercial tube similar to the tube used by Skye in his experiment and in numerical investigation in new configuration (conical shape) by Guen et al. The cold and hot exits areas are 30.2 and 95 mm<sup>2</sup> respectively. The vortex nozzle consists of 6 straight slots; the height and the width of each slot are 0.97 mm and 1.41 mm. The total area normal to the flow associated with six nozzles is therefore 8.15 mm<sup>2</sup>. The performance is related to the nozzle number. Four different nozzles as three, four, five and six were tested in the present study. The commercial software CFX was used to resolve the governing equations for compressible turbulent flow inside the vortex tube which uses the finite-volume method for the discretisation. Only the part of flow domain limited to an angles of 120°, 90°, 72°, 60° are considered due to the symmetry of the problem. The inlet nozzle for the compressed air consists of one of 3, 4, 5, 6 slots. The cold and hot exits are coaxial. The performance curves of the temperature separation versus cold outlet mass fraction were calculated for each nozzle number and compared with experimental study of S. Mohanty et al [33].

# Validation of Fluid Analysis Capabilities in LS-DYNA Based on Experimental Result

Sunao Tokura<sup>1</sup>

<sup>1</sup>Tokura Simulation Research Corporation

## 1 Introduction

The latest LS-DYNA provides several excellent capabilities for modeling of fluid like materials. In this presentation, fluid is modeled using ALE 2D and 3D, SPH 2D and 3D, and ICFD 2D and 3D. The results obtained from each simulation are compared and validated with the result of an experiment known as the "dam break" problem [1].

## 2 Referenced experiment

The experiment of the dam break problem which is used for the validation of simulation methods is shown in Fig.1.

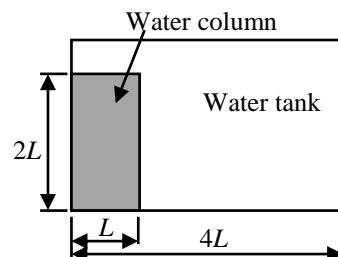


Fig.1: Dimensions of water column,  $L=0.146$  m

## 3 Results

Simulation results are compared with that of experiment in Fig.2. Figure 3 shows the time history of the location of the head of the flow.

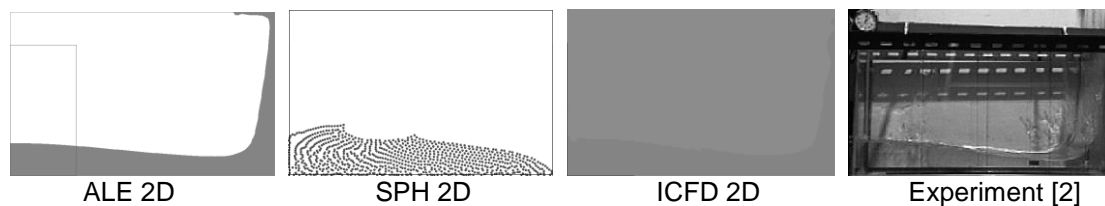


Fig.2: Simulation and experimental results at 0.4 seconds

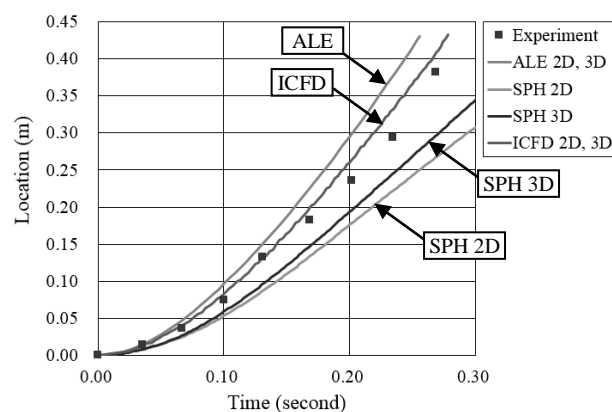


Fig.3: Time history of the location of the head of flow

#### 4 Conclusions

The fluid analysis capabilities in LS-DYNA were examined using the “dam break” model and compared with the experimental result. ALE and ICFD show relatively good results. In contrast SPH in the latest version of LS-DYNA shows viscid behavior. Users should take much care to define proper input parameters and boundary conditions depending on problems to get accurate simulation results using these excellent fluid analysis capabilities.

#### Reference

- [1] Koshizuka, S., Oka, Y., “Moving-Particle Semi-Implicit Method for Fragmentation of Incompressible Fluid”, Nuclear Science and Engineering: 123, 1996, pp.421-434
- [2] Koshizuka, S., “Numerical Analysis of Flow using Particle Method”, Nagare 21, 2002, pp.230-239 (in Japanese)
- [3] Tokura, S., “Key points to use SPH Capability Implemented in Multi Purpose Structural Analysis Software”, Comp. Mech. Div. NewsLetter No.42, Japan Society of Mechanical Engineering, May 2009, pp.16-17 (in Japanese)

## **MULTIPHYSICS II**

### **CFD/FSI**



# Analysis of Unsteady Aerodynamics of a Car Model with Radiator in Dynamic Pitching Motion using LS-DYNA

Yusuke Nakae<sup>1</sup>, Jiro Takamitsu<sup>1</sup>, Hiroshi Tanaka<sup>1</sup>, Tsuyoshi Yasuki<sup>1</sup>

<sup>1</sup> Toyota Motor Corporation

## 1 Introduction

Recently, it is becoming clear that unsteady aerodynamic forces produced due to vehicle dynamic motions affect vehicle dynamic performance attributes such as straight-line stability or handling characteristics. To clarify the impacts of these forces on vehicle dynamic performance attributes and their mechanisms, Nakae et al. [1] have conducted a numerical analysis of unsteady flow fields in dynamic pitching motion of a simplified car model using LS-DYNA ICFD solver. The study concluded that the unsteady aerodynamic forces produced due to vehicle dynamic motions were mostly induced by changes of flow structures around the front wheel house and under the car floor that changed with vehicle motion. However, the previous study has been conducted on the simplified scale car model that had no engine compartment and underside components that seem to affect the flow fields.

In this study, numerical simulations of car models without or with an engine compartment containing a radiator (i.e. porous media) in dynamic pitching motion are performed using new porous media computing function on LS-DYNA ICFD solver. The effects of the cooling-air flow passing through engine compartment on the unsteady aerodynamic forces and the flow fields are discussed. And the necessity for installing engine compartment containing a radiator and underside components onto a car model to get closer to actual car conditions is also shown.

## 2 Object of this study

One of the 1/4 scale car models used in this study is shown in Fig. 1. The model has engine compartment containing a radiator (i.e. porous media), front suspension, and floor tunnel. The behavior of the model is shown in Fig.2. To represent a pitching motion, forced sinusoidal pitching oscillation was imposed on the model body using the center of the wheel base as the center of rotation. The mainstream velocity was 27.78 m/s, and the Reynolds number, which is based on the total length of the model, was  $Re = 1.91 \times 10^6$ .

## 3 Results

Fig. 3 shows the computational results for unsteady aerodynamic force during the pitching motion. The results indicate the phase averaged value for five cycles after sufficient convergence of the computations. This report focuses on the lift coefficient  $C_L$ . The  $C_L$  during nose-down motion showed significant difference while it showed a consistent close correspondence during nose-up motion between the model with engine compartment and that without engine compartment. The  $C_L$  acting on the model with engine compartment showed higher value than that without engine compartment only during nose-down motion ((A), (B) in Fig. 3). This indicates that evaluations using the car model without engine compartment have possibilities of overestimating the amplitude of unsteady aerodynamic forces than the forces acting on a real production car in dynamic motion.

## 4 Discussion

The causes underlying the difference in the  $C_L$  during nose-down motion ((A), (B) in Fig. 3) are examined. Fig. 4 shows the velocity magnitude distribution at the center cross-section and the x-y plane located 24mm above ground level. In case of the model with engine compartment, the flow velocity under the model body was remarkably lower. This originates from under the engine compartment especially the locations where the cooling-air outlets are located (i.e. between rear end of the engine compartment and front end of the floor tunnel : i in Fig. 4, between bottom of the engine block and the front suspension member : j in Fig. 4). This indicates that the cooling-air blowing from engine compartment disturbs the flow under the model body and thus the flow is decelerated and pressure increases under the engine compartment. Moreover, in the engine compartment, pressure is originally higher than that in external flow due to low velocity of the flow in engine compartment. These two factors lead to increasing the surface pressure under the engine compartment and on the front

wheel house. Consequently, the lift force  $C_L$  indicates higher value during nose-down motion. This indicates the flow out from engine compartment greatly affects the aerodynamic characteristics of cars.

**5 Summary**

The numerical simulation of the car model with an engine compartment containing a radiator (i.e. porous media) in dynamic pitching motion was conducted using new porous media computing function on LS-DYNA ICFD solver. As a result of this study, the followings were made clear.

- i. The effects of the cooling-air flow passing through engine compartment and radiator on the flow fields and the unsteady aerodynamic force were clarified.
- ii. The necessity for installing engine compartment containing a radiator and underside components onto a car model to get closer to actual car conditions was shown.

**6 Reference**

[1] Nakae, Y., et al., : " Analysis of Unsteady Aerodynamics of a Car Model in Dynamic pitching Motion Using LS-DYNA R7", 13th International LS-DYNA Users Conference, 2014

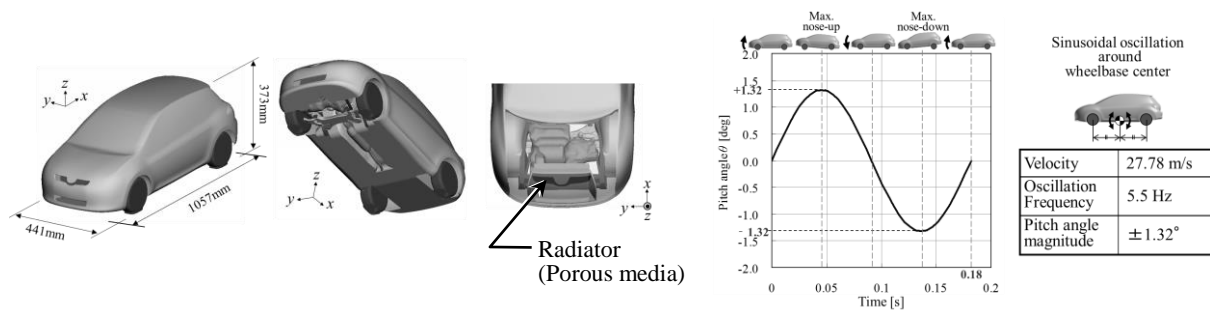


Fig. 1: 1/4 scale car model with Engine Compartment

Fig. 2: Behavior of model

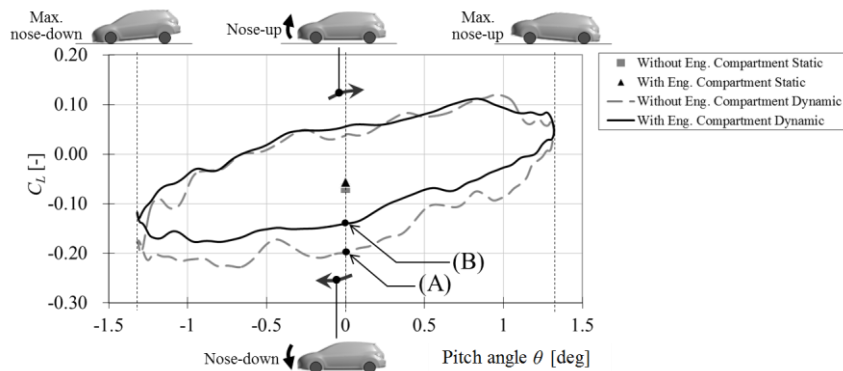
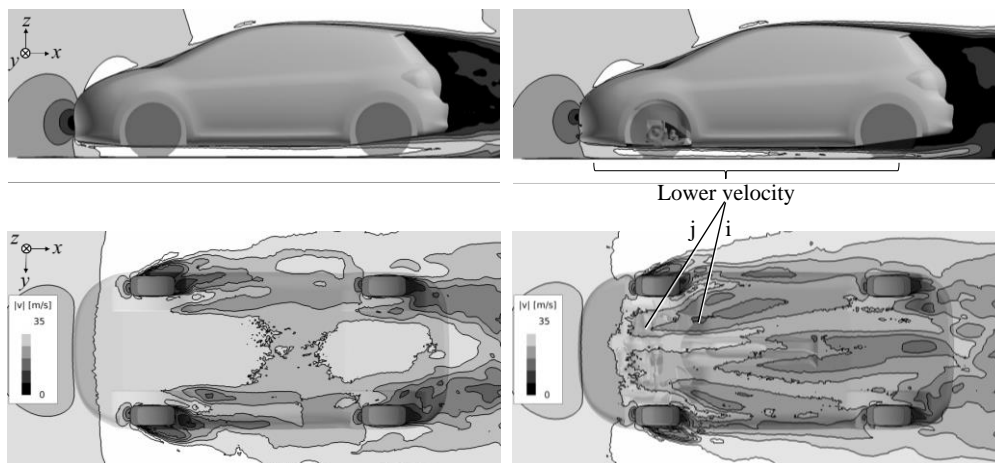


Fig. 3: Unsteady aerodynamic force during pitching motion



(A) Without Eng. Compartment (B) With Eng. Compartment  
Fig. 4: Velocity magnitude distribution at pitch angle 0° during nose-down



# Analysis of an Automobile Roof Panel under Strongly Coupled Fluid Structure Interaction using LS-DYNA

D. Detwiler

Honda R&D Americas

Accurately and efficiently simulating strongly coupled fluid structure interactions has been a challenge. In this presented study, the interaction of a lab-scale experiment using an automotive roof panel with an air flow applied through a pipe from a compressed air tank was analyzed using LS-DYNA multi-physics solver. The purpose of the analysis was the evaluation of the accuracy of deformation, strain, and the pressure distribution on the panel due to the fluid structure interaction. The steel roof panel was modeled with material strain rate properties and the post stamping simulation results applied to take into account the thinning and work hardening effects. These analysis results were compared with those of actual tests and predictive accuracy along with computational costs were summarized.

Accurately and efficiently simulating strongly coupled fluid structure interactions has been a challenge. In this presented study, the interaction of a lab-scale experiment using an automotive roof panel with an air flow applied through a pipe from a compressed air tank was analyzed using LS-DYNA multi-physics solver. The purpose of the analysis was the evaluation of the accuracy of deformation, strain, and the pressure distribution on the panel due to the fluid structure interaction. The steel roof panel was modeled with material strain rate properties and the post stamping simulation results applied to take into account the thinning and work hardening effects. These analysis results were compared with those of actual tests and predictive accuracy along with computational costs were summarized.

# Ground Vehicle Aerodynamics using LS-DYNA

Facundo Del Pin<sup>1</sup>, Iñaki Caldichoury<sup>1</sup> and Rodrigo R. Paz<sup>1</sup>

<sup>1</sup>Livermore Software Technology Corporation

## 1 Abstract

The use of software for the simulation of airflow around ground vehicles plays an important role in the design of a vehicle. Traditionally companies within the automotive industry sector have a Computational Fluid Dynamics department dedicated to the analysis of drag and lift with the objective of improving fuel efficiency, safety, passenger comfort, cooling systems and heat exchangers and minimizing noise. In recent years the increased pressure from government regulators for dramatic improvements in fuel efficiency has pushed the automotive industry to start innovating in lighter materials and hybrid or full electric cars. This has created new challenges in the way that traditional companies operate since the mechanical response of new materials or batteries may be greatly influenced by the fluid temperature and fluid pressure loads which in turns may affect the fluid behavior. forcing companies to overlap efforts between a structural and fluid department. The current paper will show how the use of LS-DYNA may help in reducing the burden of moving results from a CFD / thermal solver to a structural solver, preventing the degradation of the results from mapping variables and the increased cost of licenses for more than one solver, simplifying a queuing system since potentially a single run could provide all the results at once and improving the accuracy since the full non-linear model is being solved. This in turn reduces the communication time between structural and fluid departments where the interaction is sometimes informal and based on "favors" more than following project guidelines. The paper will provide an overview of the tools that LS-DYNA has for CFD analysis and it will show some application examples.

**Keywords:** computational fluid dynamics, turbulent flow, multipysics, coupled problems, conjugate heat, fluid structure interaction.

## 2 Introduction

The study of ground vehicle aerodynamics provides insight to engineers and designers about the fluid forces that the air exerts over the vehicles. The forces are mainly of two types: the ones coming from normal stresses (pressure) and those from tangential stress (viscous forces). There is a large amount of research in the field of vehicle aerodynamics and the mechanics of the problem is very well understood. While engineers may prefer streamlined cars designers or stylists may prefer vehicles that appeal to consumers and finally a compromise between the two is reached.

With the multiphysics capabilities of Ls-Dyna engineers can couple CFD analysis with a thermal or structural solver or both for a more realistic study of not only drag and lift but also the structural response (thermal and mechanical) that in turn may affect the drag and lift.

## 3 The incompressible CFD solver in Ls-Dyna

In recent years LSTC has devoted big efforts in the development of a CFD solver for incompressible flows. The solver is specifically design to tackle coupled problems where low Mach numbers ( $M < 0.3$ ) are involved produceing a scalable parallel solution.

## 4 Coupling possibilities

### 4.1 Thermal coupling

The incompressible CFD solver can be coupled to the heat equation to perform thermal analysis in the fluid. The heat equation for the fluid can also be coupled to the heat equation of the structural problem to perform conjugate heat transfer analysis.

A thermal problem was solved using a model which was provided by GMC for an aerodynamic benchmark. The model includes the engine compartment, exahust, suspension, wheels, radiator, grill and mirrors. The result is shown in Fig.1.

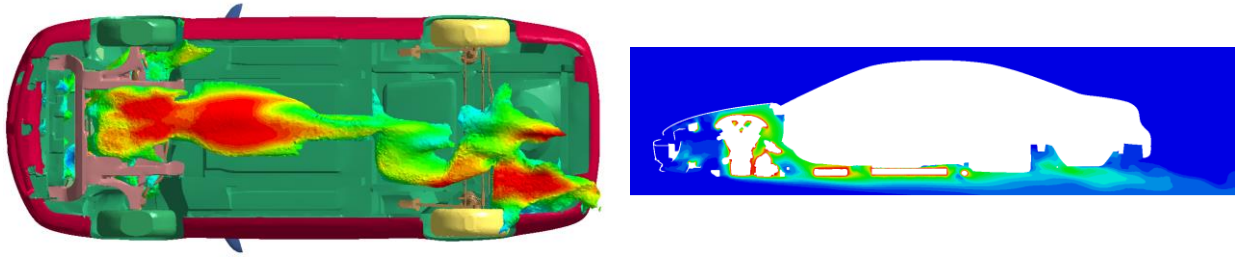


Fig.1: Results for the aerodynamics benchmark on a GMC vehicle. right image shows iso-surface a fluid temperature and left is a cutplane with iso-contours of temperature showing the higher temperature around the engine block and exhaust.

#### 4.2 Fluid structure coupling

The other coupling option which could be combined with the thermal coupling is the one that involves fluid structure interaction (FSI). Strong fluid/structure coupling occurs when the structural and the fluid response are highly dependant of each other. A CFD model which is already working can be used for FSI. The structural part of the model needs to be defined using the standard keywords and format used for structural analysis. The meshes for the fluid and structural model do not need to match at the interfaces although the geometry need to be close enough. Once this is ready a single added keyword on the CFD model will activate the FSI analysis.

In Fig.2 a CFD analysis of a GM Camaro vehicle is shown. After the CFD results were obtained an FSI analysis was requested to study the roof deformation due to the wind speed. Fig.2 shows the post-processing results overlapping CFD and structural deformation for a full non-linear analysis.

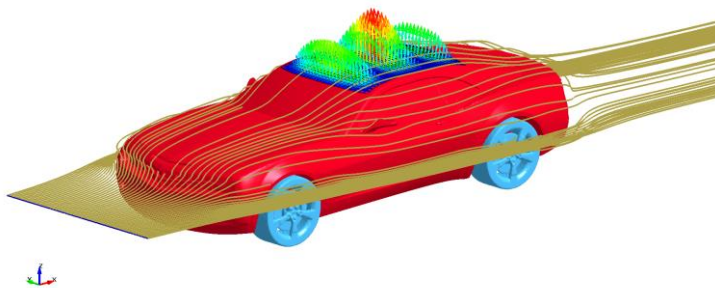


Fig.2: Post-processing of the flow around the vehicle using streamlines and structural displacement of the roof.

### 5 Summary

This paper depicts the possibilities that Ls-Dyna offers in the area of multiphysics regarding CFD, structural and thermal analysis. It was shown that the behavior of turbulent air around a vehicle can be modeled and that the influence that the temperature or structural displacement may have over the flow can be predicted. This opens the possibility for more complete vehicle analysis with little extra cost added. In the case of FSI the extra computational time that is used in the non-linear coupling is much less than the time needed to run two separate analysis, one for CFD and then one for structural analysis using the CFD pressure mappings to achieve only linear coupling performance as it is normally done in the industry.



## **PARTICLE METHODS**

### **SPH/DEM**



---

# Application of the SPH Finite Element Method to Evaluate Pipeline Response to Slope Instability and Landslides

Abdelfettah Fredj<sup>1</sup>, Aaron Dinovitzer<sup>1</sup>, Millan Sen<sup>2</sup>

<sup>1</sup>BMT Fleet Technology, Ottawa, Ontario, Canada

<sup>2</sup>Enbridge Pipelines Inc., Edmonton, Alberta, Canada

Buried pipelines operating on active slopes can be subject to lateral and axial loads resulting from slope instability and landslides. The techniques to predict pipeline displacements, loads, stress or strains are not well described in design standards or codes of practice. Finite element analysis based soil-pipe interaction simulation has developed in recent years and is proving to be a useful tool in evaluating the pipeline behavior in response to slope movement.

A description of the BMT pipe soil interaction modeling techniques, their validation against full scale trails and comparison to spring support models has been previously published. This paper describes the modeling techniques and demonstrates the application and versatility of the LS-DYNA 3D continuum SPH (Smooth Particle Hydrodynamic) model to evaluate pipeline behavior and pipeline strain demand. The effects of key parameters, including soil movement mechanism, pipeline geometry, material grade and soil conditions and properties are considered.

The application and results presented in this paper are used to illustrate an advanced soil structure interaction numerical simulation technique combining the LS-DYNA nonlinear SPH formulation with Lagrangian formulation while satisfying all the principles of continuum mechanism.

# Modeling the Behavior of Dry Sand with DEM for Improved Impact Prediction

S.Sridhar, SushilKumar Vishwakarma

Whirlpool Corporation .

## 1 Abstract

Pumpkin ball impact test is similar to simple pendulum impact test. It represents a rough handling test conducted on user interface parts to check its robustness in case of abuse loading. The objective of this work is to create a standard simulation model that would capture the behavior of sand particles inside a rubber ball and scope is limited to create and validate a finite element model used to replicate a pumpkin ball impact test. Pumpkin ball is a rubber ball filled with dry sand up to 3/4th of its volume. The major challenge in this activity was simulating the real behavior of dry sand inside the rubber ball during the impact. Dry sand granules interact with each other as well as with the inner surface of ball during the course of impact. To capture this behaviour of dry sand granules discrete element method (DEM) was used.

In the current study, the experimental test was conducted on concrete wall and measured acceleration was used for the validation of developed finite element model. The simulation results had shown a close agreement with the experimental results.

**Keywords:** DEM, Console, User interface, Pumpkin ball, accelerometer, dry sand, finite element methods.

## 2 Experimental and simulation test set up

A rubber ball was filled 3/4<sup>th</sup> of its volume with dry sand. The ball was hung from the hinge point by steel pendulum chain, pulled back and released to impact on concrete wall. While testing two accelerometers were attached to ball with glue and tapes to obtain acceleration data with reference to wall during impact. One accelerometer was attached in the impact direction and other to the right adjacent side of the ball.

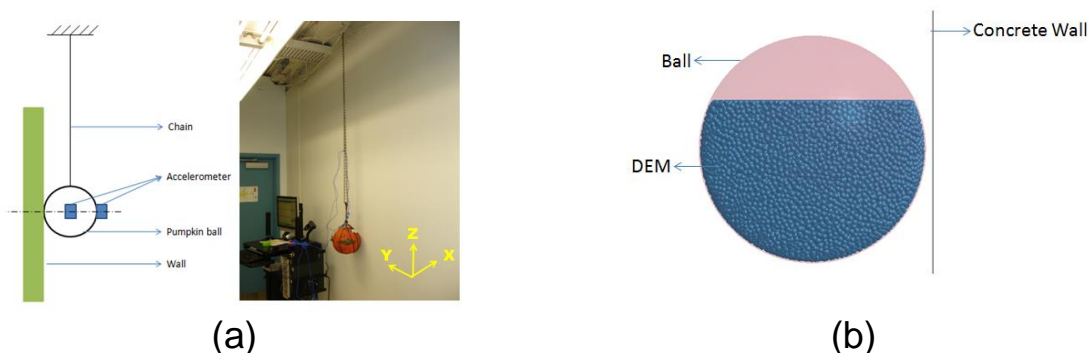


Fig.1: (a) Solid wall concrete set up (b) Finite element model

Shell elements used to model rubber ball and concrete wall, dry sand particles are modeled by DEM technique [1]. The definition of particles was done using the card \*ELEMENT\_DISCRETE\_SPHERE\_VOLUME.

\*MAT\_PIECEWISE\_LINEAR\_PLASTICITY (TYPE 24) material model is used for rubber ball and \*MAT\_ELASTIC (TYPE 001) material model for discrete elements. \*CONTROL\_DISCRETE\_ELEMENT card was defined for self interaction of discrete element spheres and particle-surface interaction is handled by \*DEFINE\_DE\_TO\_SURFACE\_COUPLING contact definition[2][3].



### 3 Simulation result and validation

With above described finite element details the impact test has been simulated in LS-DYNA solver.

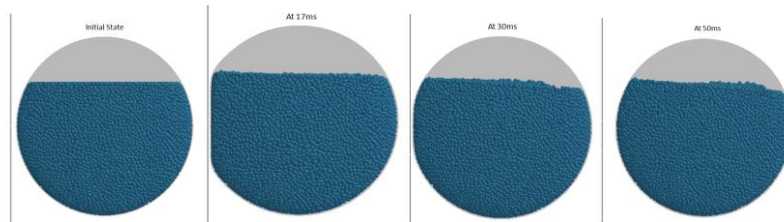


Fig.2: Sand particle behavior during impact

The impact is observed to be highly damped owing to the characteristics of the sand particles. Looking at the impact in the time domain, they are about 0.04 seconds long, and die out almost immediately.

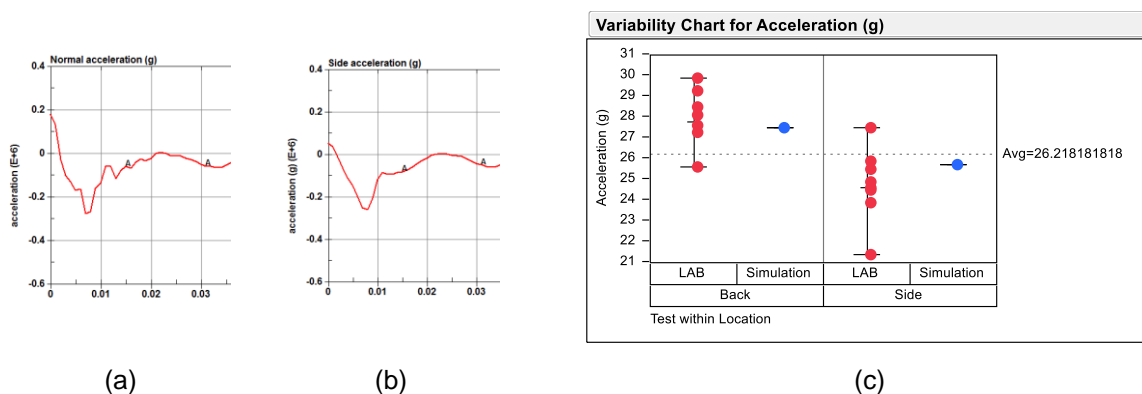


Fig.3: (a) Normal acceleration on ball. (b) Side acceleration on ball (c) Simulation result against experimental lab test.

Acceleration measured in physical test data was used to enhance the behavior and validate the simulation model. Below figure shows the simulation as well as test result data. The simulation results are in close agreement with the experimental test values.

### 4 CONCLUSION

The results from LS DYNA simulation shows good correlation with experimental lab test data. The simulation model created can be further used to verify and optimize design early in the concept stage, instead of depending on physical prototype testing later. Current simulation model can further be improved by better representation of initial shape and material properties of rubber ball.

### 5 REFERENCES

1. J. Koziki, J. Tejchman : Numerical simulations of sand behaviour using DEM with two different descriptions of grain roughness, II International Conference on particle-based methods - Fundamental and Applications, PARTICLES 2011.
2. Nils karajan, Zhidong Han, Hailong, Jason Wang: On the Parameter Estimation for Discrete - Element Method in LS-DYNA, 13th International LS-DYNA User Conference.
3. Frederic V. Donze, Vincent Richefeu, Sophie-Adelaide Magnier: Advances in Discrete Element Method Applied to soil, Rock and Concrete Mechanics. EJGE Bouquet 08.

# Volume-Averaged Stress States for Idealized Granular Materials using Unbonded Discrete Spheres in LS-DYNA

Michael T. Davidson<sup>1</sup>, Jae H. Chung<sup>1</sup>, Hailong Teng<sup>2</sup>, Zhidong Han<sup>2</sup>, Vinh Le<sup>1</sup>

<sup>1</sup> Bridge Software Institute, University of Florida, USA

<sup>2</sup> Livermore Software Technology Corporation, USA

The discrete element method (DEM) permits study of the kinetics of microscopic particles through use of the kinematics of contact mechanics, and has been used by numerous researchers to investigate kinematically admissible deformation fields observed in laboratory tests of Representative Elementary Volumes (REV) of granular masses. In the current study, newly-implemented discrete element analysis features within LS-DYNA are used to simulate three-dimensional (3D) quasi-static stress states for idealized bodies of granules subjected to quasi-static loading conditions. Operating within a 3D Cartesian domain, volume-averages of summed dyadic products of contact forces and branch vectors (obtained from LS-DYNA simulation results) are used to investigate stresses that develop across various regions of uniform, unbonded discrete element sphere (UDES) assemblies, where the contact forces arise due to body forces that are prescribed at the centroid of each sphere. When feasible, averaged local force results (micromechanical stresses) obtained from LS-DYNA simulations are compared to corresponding manual calculations. As demonstration of the LS-DYNA DEM capabilities, and as a means of showcasing a recently implemented stress computation algorithm specific to the use of UDES, volume-averaged stress quantities are investigated at three scales: 1) On an individual sphere within a two-dimensional simple, pyramidal assembly; 2) On an REV associated with laboratory-scale triaxial compression testing; and, 3) On multiple REV's sampled from a megascopic assembly. The as-demonstrated discrete element analysis of the particulate equations of motion can be applied to modeling of in-situ granular soil conditions, where geostatic stress equilibrium conditions can be simulated in relation to micro-mechanical model parameters.

## Literature

- [1] Cundall, P. A., and Strack, O. D.: A discrete element model for granular assemblies. *Geotechnique* **29** (1979), 47-65.
- [2] Livermore Software Technology Corporation (LSTC): *LS-DYNA Keyword User's Manual Vol. I*, (2015), Livermore, California, USA.
- [3] Fortin, J., Millet, O., Saxcé de G.: Construction of an averaged stress tensor for a granular medium, *European Journal of Mechanics A/Solids*, **22** (2003), 567-582.
- [4] ASTM: *Standard test method for consolidate drained triaxial compression test for soils D7181*, ASTM International, (2011), West Conshohocken, Pennsylvania, USA.
- [5] Han, Z., Teng, H., and Wang, J.: Computer Generation of Sphere Packing for Discrete Element Analysis in LS-DYNA, (2012), *12<sup>th</sup> International LS-DYNA Conference*.
- [6] Cil, M. B., and Alshibli, K. A.: 3D analysis of kinematic behavior of granular materials in triaxial testing using DEM with flexible membrane boundary. *Acta Geotechnica*, **9**(2). (2014), 287-298.

# Discrete Element Analysis of Idealized Granular Geometric Packings Subjected to Gravity

Michael A. Faraone<sup>1</sup>, Jae H. Chung\*<sup>1</sup>, Michael T. Davidson<sup>1</sup>

<sup>1</sup>Bridge Software Institute, USA

This paper presents discrete element analysis models for studying quasi-static stress states in idealized granular materials subjected to gravity, and utilizes geometric packings and contact mechanics. The theoretical description of granular materials in assemblies of microscopic particles is a challenging task. The particle assemblies characterize in-situ initial and boundary conditions. In turn, the conditions are used in solving the equations of motion of the particulate system under stress equilibrium states (via a network of particle contact forces and various degrees of dissipative interparticle friction). Using the discrete element analysis model of LS-DYNA [1], the influence of packing on contact stress distributions within an explicit time domain is investigated using idealized assemblies of spherical discrete elements and contact penalty springs. The validity of idealized geometric packings, as to whether uniformity can simulate granular fabrics, is still a matter of debate. However, the present study strictly focuses on the effects of micromechanical structures (idealized by assemblies of spherical discrete elements) in stress states at a macroscopic scale. In this context, the macroscopic scale is associated with the size of samples used for direct shear experiments in laboratory settings).

Modeling of in-situ conditions in geotechnical engineering problems requires simulation of a geostress state known as the “at rest” condition, where stress equilibrium states of granular masses under gravitational body forces vary in phenomenological observations [2]. As a result, force propagations that arise due to externally applied forces are affected by these non-zero stress states. Phenomenologically, this is described by the ratio of horizontal,  $\sigma_h$ , to vertical stress,  $\sigma_v$  :

$$K_o = \frac{\sigma_h}{\sigma_v} = 1 - \sin \varphi \quad (1)$$

where the ratio is termed the coefficient of earth pressure at rest,  $K_o$ . Note that  $K_o$  is defined as a function of the macroscopic characteristics, i.e., the angle of internal friction  $\varphi$  [3]. Alternatively stated, the macroscopic kinematics of a control volume of the granular masses is the controlling phenomenological factor of the geostress equilibrium state at rest. This study is focused on various geometric packings (with uniquely characteristic coordination numbers) as a means of simulating geostatic equilibrium states through use of the discrete element method. The simulation results are discussed regarding selected modeling parameters. Cataloged coordination numbers, considered along with a set of discrete contact properties (interparticle frictional coefficients), are used in a parametric sensitivity study aimed at simulating the effects of granule-to-granule interlocking in the macroscopic characteristics. Macroscopic shear strengths, which vary per packing assembly, are investigated through use of a parametric matrix of direct shear test simulations. Based on the Biot theory and numerical results obtained from constrained chamber test simulations, averaged stresses over a control volume of the assemblies are studied to qualitatively correlate macroscopic shear strengths of packing assemblies with existing semi-empirical methods. Literature

- [1] Livermore Software Technology Corporation (LSTC): *LS-DYNA Keyword User's Manual Vol. I*, (2015), Livermore, California, USA.
- [2] Mitchell, J. K., & Soga, K. (1976). *Fundamentals of soil behavior* (p. 422). New York: Wiley.
- [3] Jaky, J. (1944). The coefficient of earth pressure at rest. *Journal of the Society of Hungarian Architects and Engineers*, 78(22), 355-358.
- [4] Karajan, N., Zhidong, H., Ten, H., and Wang, J.: Interaction Possibilities of Bonded and Loose Particles in LS-DYNA®, (2013), *9th European LS-DYNA Conference*.
- [5] Cil, M. B., & Alshibli, K. A. (2014). 3D analysis of kinematic behavior of granular materials in triaxial testing using DEM with flexible membrane boundary. *Acta Geotechnica*, 9(2), 287-298.

- [6] O'Sullivan, C., Bray, J. D., & Riemer, M. (2004). Examination of the response of regularly packed specimens of spherical particles using physical tests and discrete element simulations. *Journal of engineering mechanics*, 130(10), 1140-1150.
- [7] Rowe, P. W. (1962, October). The stress-dilatancy relation for static equilibrium of an assembly of particles in contact. In *Proceedings of the Royal Society of London A: Mathematical, Physical and Engineering Sciences* (Vol. 269, No. 1339, pp. 500-527). The Royal Society.
- [8] Thornton, C. (1979). The conditions for failure of a face-centered cubic array of uniform rigid spheres. *Géotechnique*, 29(4), 441-459.
- [9] O'Sullivan, C., Cui, L., & Bray, J. D. (2004). Three-dimensional discrete element simulations of direct shear tests. *Numerical Modeling in Micromechanics via Particle Methods*, 373-382.
- [10] Oda, M., & Iwashita, K. (1999). An Introduction mechanics of granular materials. AA BALKEMA, (1), 1-5.
- [11] Hendron Jr, A. J. (1963). *The Behavior of Sand in one Dimensional Compression*. Thesis submitted to the Univ. Of illinois at Urbana-Champaign for partial fulfillment of the requirements of Doctor of Philosophy.

**DEVELOPER I**  
**FREQUENCY DOMAIN**



# Recent Updates in LS-DYNA Frequency Domain Solvers

Yun Huang, Zhe Cui

Livermore Software Technology Corporation

## 1 Introduction

A series of frequency domain features have been implemented to LS-DYNA, since the release of ls971 R6. The frequency domain features include

- FRF (Frequency Response Functions)
- SSD (Steady State Dynamics) and fatigue
- Random vibration and fatigue
- BEM (Boundary Element Method) Acoustics
- FEM (Finite Element Method) Acoustics
- Response Spectrum Analysis

The frequency domain features are developed to provide solutions to the vibration, acoustic and fatigue problems coming from a wide range of industrial areas. A typical application is NVH analysis for automobiles.

A bunch of updates have been made for the frequency domain features, since the last (13th) International LS-DYNA Users' Conference, Detroit, June 8-10 2014. The main updates include

- Incorporation of new boundary conditions in FEM acoustic analysis
- Incorporation of frequency dependent complex sound speed in acoustic analysis
- Acoustic eigenvalue analysis by FEM
- Incorporation of new stress indexes in SSD fatigue analysis
- Incorporation of multi-slope S-N fatigue curve for fatigue analysis
- Introduction of strain output in random vibration analysis

These updates in frequency domain solvers were made to meet the requirements from users, and to improve the capabilities of frequency domain analysis by LS-DYNA.

This paper provides a brief review on the updates.

## 2 FEM Acoustic analysis with new boundary conditions incorporated

For \*FREQUENCY\_DOMAIN\_ACOUSTIC\_FEM, two new boundary conditions are incorporated, in addition to the existing velocity boundary condition. The two new boundary conditions are

- acoustic pressure
- impedance

## 3 Acoustic computation with frequency dependent complex sound speed

To consider the damping in the acoustic medium, a frequency dependent complex sound speed can now be considered in FEM or BEM acoustic computation in LS-DYNA. A new keyword \*FREQUENCY\_DOMAIN\_ACOUSTIC\_SOUND\_SPEED has been implemented so that user can define the frequency dependent complex sound speed.

## 4 Acoustic eigenvalue analysis

To run acoustic eigenvalue analysis, a new option \_EIGENVALUE has been added to the keyword \*FREQUENCY\_DOMAIN\_ACOUSTIC\_FEM. Eigen frequencies and corresponding eigenvectors are provided.

The eigenvectors are saved in the binary plot database D3EIGV\_AC, which is accessible to LS-PrePost.

The acoustic eigenvalue analysis not only provides valuable characteristic information on the acoustic system itself, but also provides basis for modal solution method (comparing to direct solution method) for large scale problems.

## 5 Improved fatigue analysis in a sine sweep test environment

Two new stress indexes (Maximum principal stress, and Maximum shear stress) have been incorporated in the fatigue analysis, in addition to the existing one (Von-Mises stress). The selection of the stress index in SSD fatigue analysis is enabled through the parameter STRTYP in the keyword \*FREQUENCY\_DOMAIN\_SSD\_FATIGUE.

## 6 Incorporation of multi-slope S-N fatigue curve in fatigue analysis

The random vibration fatigue and SSD fatigue features are both based on the materials' S-N fatigue curves. The material's S-N curve is a property of material, and can be defined by the keyword \*MAT\_ADD\_FATIGUE for each material model.

With recent updates on the keyword \*MAT\_ADD\_FATIGUE, user can define an S-N curve with multi slopes, as shown in Figure 1.

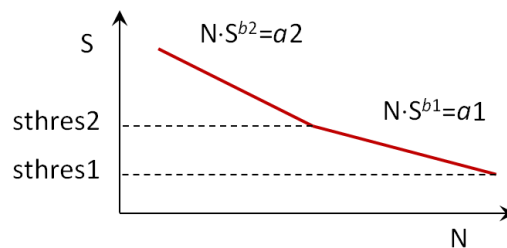


Fig.1: Multi-slope S-N fatigue curve

## 7 Strain results in random vibration analysis

In random vibration analysis, strain results are added to D3PSD and D3RMS. To get strain results in D3PSD and D3RMS for solids, shells and thick shells, one need to set STRFLG=1 in keyword \*DATABASE\_EXTENT\_BINARY; To get beam stresses in D3PSD nad D3RMS, one need to set BEAMIP=1 in keyword \*DATABASE\_EXTENT\_BINARY.

## 8 Summary

A series of updates for the frequency domain features are described in this paper. These updates not only improve the current capabilities of the frequency domain solvers, but also extend greatly the application area of these solvers. Some examples are provided to demonstrate the application of these updated frequency domain solvers.

## 9 Literature

- [1] LS-DYNA Keyword User's Manual, Livermore Software Technology Corporation, 2015.
- [2] Wu, T.W.: "Boundary Element Acoustics: Fundamentals and Computer Codes", Advances in Boundary Elements, Southampton, Boston, WITPress, 2000.



# Statistical Energy Acoustic for High Frequency Analysis

M. Souli<sup>1</sup>, R.Messahel<sup>1</sup>, T. Zeguer<sup>2</sup>, Yun Huang<sup>3</sup>.

<sup>1</sup>Lille University France

<sup>2</sup>Jaguar Land Rover Limited, Coventry UK

<sup>3</sup>LSTC Livermore California USA

## 1 Introduction

For high frequency analysis, Statistical energy analysis (SEA) has proved to be a promising approach to the calculation of sound transmission in complex structures. In automotive industry and also in civil engineering, most of noise transmission is due to high-frequency structural vibrations, where the characteristic wavelength is small compared to the dimensions of the structure. For these applications classical methods of structural analysis, such as the finite element method (FEM), and Boundary Elements Method (BEM), cannot be used due to the large number of degrees of freedom required to model structural deformation. Statistical Energy Analysis (SEA) considers the vibrations of the structure in terms of elastic waves which propagate through the structure and are partially reflected and partially transmitted at structural connections. For the last few year there has been an increase in the application of SEA techniques to study noise transmission in motor vehicles. Numerical results in term of acoustic pressure inside the cavity, are in good agreement compared to analysis using other software published in the literature.

## 2 Theory of SEA

Statistical energy analysis is used to predict sound and vibration transmission of elastic waves which propagate through the structure that are partially reflected and partially transmitted into connected structure through structure discontinuity or line connection. In SEA method systems are considered to be divided into subsystems that are linearly coupled and exchange energy through resonant vibration modes. Subsystems can be plates, beams or acoustic rooms that have modes which are similar in nature, and where the primary variable of interest is energy. The theory of structural vibration transmission has been developed over many years, and detailed theory of SEA is described by Lyons in [1]. The earliest calculations were carried out by Langley et al. [2]. In SEA computation the system can be modeled by the intersection of a number of semi-infinite plates which meet at a single line junction where there must be continuity of displacement, slope and equilibrium of moments and forces. Structural vibration transmission calculations are carried out as part of the calculation of sound and vibration transmission through structures. If two or more plates meet together to form a line junction then the properties of the junction can be given in terms of the transmission coefficient, defined as the ratio of the power transmitted across the junction to the power incident. The power may be transmitted by a transmission wave type that is different from the incident wave in which case there will be energy conversion from one wave type to another. Such applications are be found in automotive industry as well as civil, naval and aerospace engineering for noise transmission in buildings, ships, aircraft and other structures as described in [3], and [4]. In this paper, the plates are assumed to be isotropic, thin and flat and to meet at a continuous line junction.

## 3 Numerical Test.

For comparison to examples that been modeled using other software [4], in this paper we consider the following case that have been modeled by FREE SEA code [4], and the results will be compared to the ones published by the author.

### 3.1 Sound Transmission inside a car

The car example consists of 26 subsystems, 18 Steel plates, 6 glass plates and 2 acoustic rooms, figure 1. The steel plates and glasses are modelled as linear elastic, and the following material properties:

density = 7800 kg/m<sup>3</sup> , Young Modulus = 2.1. 10<sup>11</sup> Pas, Poisson Ration = 0.3

density = 2500 kg/m<sup>3</sup> , Young Modulus = 6.0 10<sup>10</sup> Pas, Poisson Ration = 0.2

A real car would have some sort of a frame, pillars and stiffeners. However with only the information in build a simple SEA model. Input power is applied in bending on the fender left and right front parts of the car as described in figure 1. Sound Pressure in dB units in the passenger compartment is shown in figure 2.

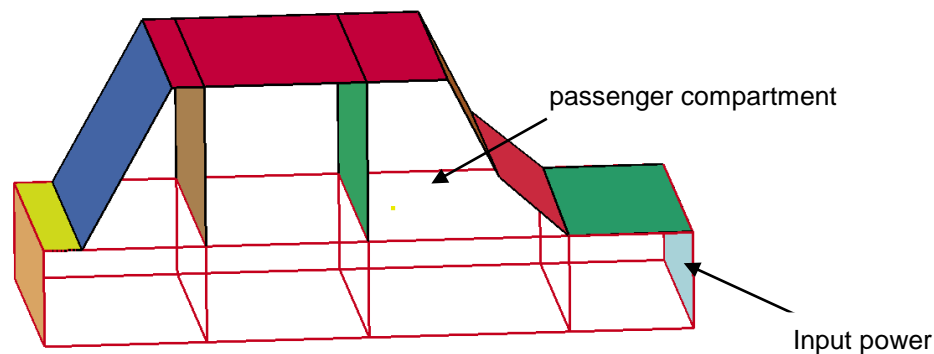


Figure 1. Problem Description of the subsystems

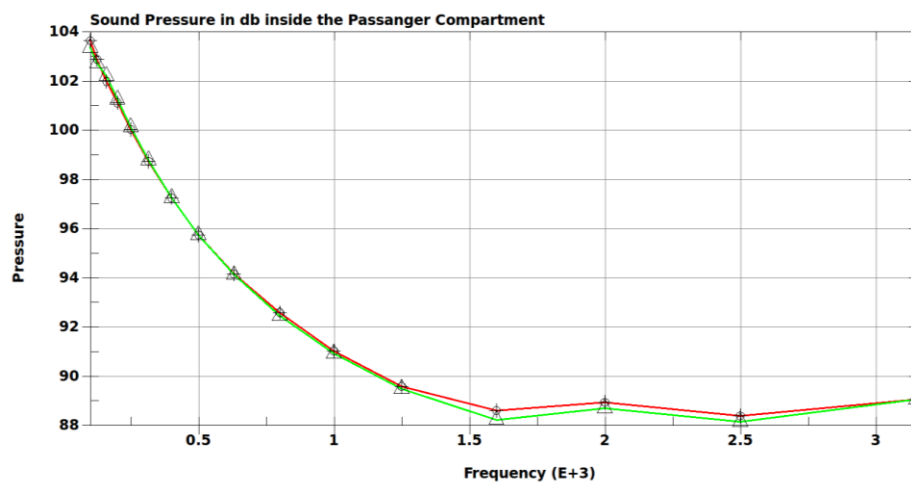


Figure 2. Comparison of acoustic pressure in passenger

#### 4 Literature

- [1] R. S. Langley, K.H Heron  
Elastic Wave Transmission Through Plate/Beam Junction  
Journal of Sound and Vibration (1990) 143(2), 241-253
- [2] R. H. Lyon  
Statistical Energy Analysis of Dynamical Systems: Theory and Applications.  
Cambridge, Massachusetts: MIT Press. 1975
- [3] Daniel Joahansson  
Statistical Energy Analysis software  
Development and implementation of an open source code in Matlab/Octave  
Master's Thesis in the Master's program in Sound and Vibration
- [4] Ennes Sarradj  
Statistical Energy Analysis .Freeware. <http://www.free-sea.de>

# **DEVELOPER II**

## **PREPOST/MAPPING**



---

# Current Status of LS-PrePost and the New Features in Version 4.2

Philip W. Ho

Livermore Software Technology Corporation

## 1 Introduction

The current status of LS-PrePost will be presented along with the new features of the recently released version 4.2 will be introduced. Future development work will also be discussed

## 2 Current Status

LS-PrePost version 4.1 has been released since spring of 2014. Version 4.2 is scheduled to be released in May 2015. Many bugs have been fixed in the 4.2 version. Both versions of LS-PrePost support Windows 7.0/8.0/8.1 in both 32bit and 64bit OS. For Linux versions, the following favors of Linux are supported: Redhat 5.0/6.0 (Centos 5.0/6.0), Suse Enterprise 10/11, OpenSuse 10/11/12/13, and Ubuntu 12. LS-PerPost also supports Apple OSX.

## 3 New Features in version 4.2

The major improvements in LS-PrePost can be categorized in the following areas:

### 3.1 Geometry and Meshing

### 3.2 Read and writing of the long format keyword

### 3.3 New Keyword data support

### 3.4 General Pre-Processing

### 3.5 Post-Processing

#### 3.5.1 *Post-processing for NVH*

#### 3.5.2 *Post-Processing for ICFD*

### 3.6 Plotting, including 3D graph system

### 3.7 Isogeometry element support

### 3.8 DES (Discrete Element Sphere) support

### 3.9 Applications

#### 3.9.1 *Metal Forming EZSetup*

#### 3.9.2 *Jintegral*

#### 3.9.3 *SCL (Scripting Command Language)*

#### 3.9.4 *Metal Forming New Roller Hamming, 3D Drawbeam generation, blanksize/trimline projection*

#### **4 Future Development**

LS-PrePost version 4.3 is already started, will be available for testing soon. Newly requested features will be implemented only in this version. A double precision version that can handle long format keyword file and double precision LS-DYNA results will be available. Pre-processing setup for ICFD applications and NVH. DSM (Die System Module) will also be available. More support for SCL and data center data extraction will be added.

#### **5 Summary**

LS-PrePost has been improved steadily over the past many years. LSTC is committed to continue the development to enhance the robustness and stability of LS-PrePost. We also keep up to support the new features that are being implemented in LS-DYNA such that users do not have to wait for third party pre- and post-processor for the support of those features.

# Non-Linear Fracture Mechanics in LS-DYNA and LS-PrePost

Per Lindström<sup>1,2</sup>, Anders Jonsson<sup>3</sup>, Anders Jernberg<sup>3</sup>, Erling Østby<sup>2</sup>

<sup>1</sup> Department of Engineering Science, University West, Trollhättan, Sweden

<sup>2</sup>DNV GL Materials Laboratory, Høvik, Norway

<sup>3</sup>DYNAmore Nordic AB

## 1 Introduction

Fracture mechanics provides an engineering framework for assessing the consequences of defects in structures. In non-linear fracture mechanics, an energy based criterion is used for assessing the risk for crack growth: if the energy release rate at the crack tip exceeds what is required for creating new surfaces in the material, crack growth will occur. Under certain assumptions the energy release rate at the crack tip can be calculated by a path independent integral, the so-called  $J$ -integral [8]. In modern FE-based fracture mechanics applied to practical design, the structure under consideration is modelled, including cracks at specific locations, and the  $J$ -integral values are used as design criteria. From a numerics viewpoint, the  $J$ -integral has many appealing properties: it can be evaluated from the far-field solution, which reduces numerical errors that may arise close to the crack tip, and the expected path-independence can to some extent be used as a quick check on solution validity.

Evaluation of the  $J$ -integral from LS-DYNA [5] simulation results has been implemented as a post-processing tool in LS-PrePost, including consistent treatment of residual stresses [1]. The implementation covers both 2D (plane stress / plane strain) and 3D applications, using the virtual crack-tip extension [9] (VCE) method. For 3D geometries, both the global  $J$ , corresponding to a uniform virtual crack extension of the entire crack front, as well as the local  $J$  at each node of the crack front is presented. The tool is accessible both via the LS-PrePost GUI and via command file interface. The  $J$ -integral evaluation capability opens for new possibilities to use LS-DYNA within fields where classical fracture mechanics is applied for assessment of structural integrity, for example the nuclear industry, the offshore industry, and general pressure vessel design.

It remains to extend the implementation to also account for higher order solids (20/27 noded hex elements), thermal loadings and material interfaces.

## 2 The $J$ -integral tool in LS-PrePost

The  $J$ -integral tool in LS-PrePost is accessed via the top menu bar: Application>Tools> $J$ -integral. Both the LS-DYNA keywordfile and the `d3plot` results must be loaded into LS-PrePost for the tool to work properly, since for example material properties will be read from the keyword file. Also, the tool will automatically recognize if residual stresses need to be considered, by the presence of `*INITIAL_STRESS` and `*INITIAL_STRAIN` – keywords.

In order to calculate the  $J$ -integral, the user first defines the crack tip node(s), (single node in 2D, all nodes along the crack front in 3D). This is done using the general selection assistant of LS-PrePost, which makes it possible to select crack front nodes by propagating along an edge, or from a node set pre-defined in the keywordfile, which can be very convenient for 3D geometries. The next step is to select a node on the crack surface. This, in combination with the crack opening direction, will define the crack propagating direction, used in the VCE-based calculations. Finally, the user specifies the number of contours for  $J$ -integral computation. The contours are generated automatically by LS-PrePost: the first contour will be the elements neighboring to the crack tip node(s), and after that, the contour  $k + 1$  will be the elements neighboring to contour  $k$ .

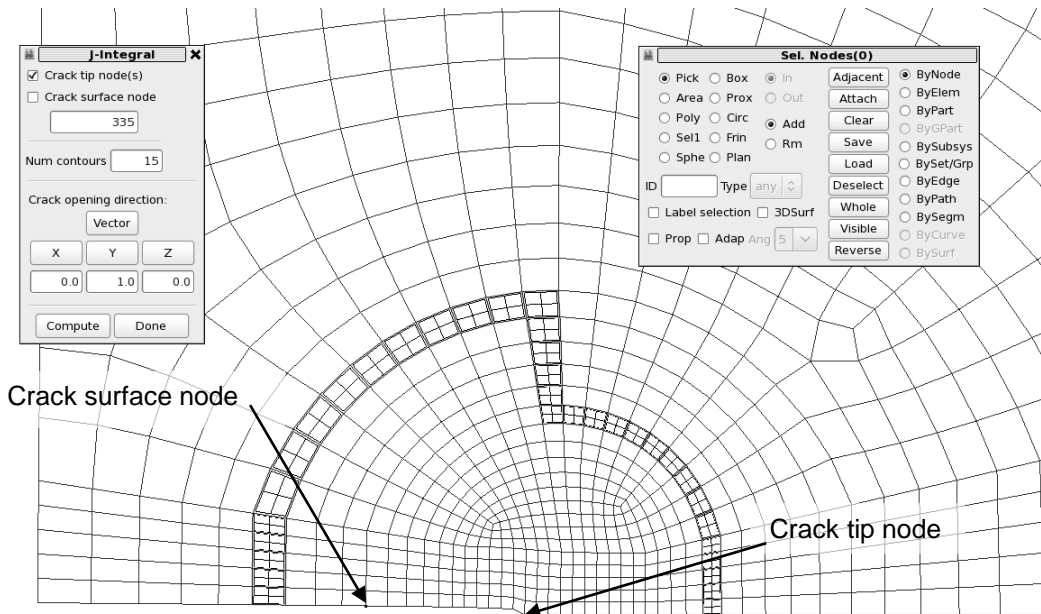


Fig.1: Example of the J-integral GUI in LS-PrePost. The highlighted elements form contour 15.

### 3 Numerical examples

In this section, some examples of  $J$  computed by LS-PrePost from LS-DYNA simulations in both 2D and 3D are presented. In the full paper, more examples are presented, for example a surface crack in a weld [10] is studied.

#### 3.1 Compact tension specimen

Results for two similar compact tension – C(T) – specimen are compared to previous results, for both 2D [2][4] and 3D [3] analyses. The calculated  $J$  results are also compared to the evaluation method of the ASTM standard E1820-13 [6], where  $J$  is evaluated from the global force-displacement curve. The dimensions of the first C(T) – specimen are shown in Fig.2: The thickness is 25 mm and the remaining ligament is  $b_0 = 21.5$  mm.

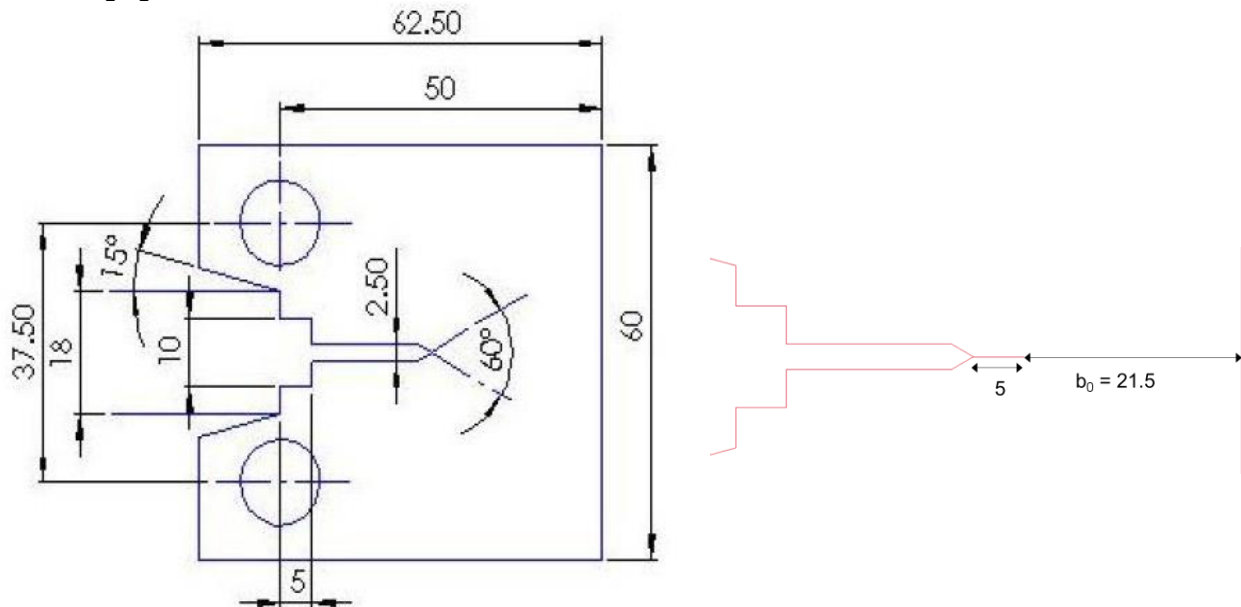


Fig.2: The left image shows the C(T) specimen geometry (from Ref. [4]). The thickness of the specimen is  $B_N = 25$  mm. The right image shows the details of the crack length.

The  $J$  vs. displacement results for the first C(T) – specimen are compared in the left image of Fig.3:. The  $J$  results computed by LS-PrePost are within reasonable agreement (max relative difference 9 %)



to the results obtained by the ASTM evaluation method of Eq. (11). Also, the 2D results from LS-PrePost are within reasonable agreement to the previously presented results of Refs. [2], [4].

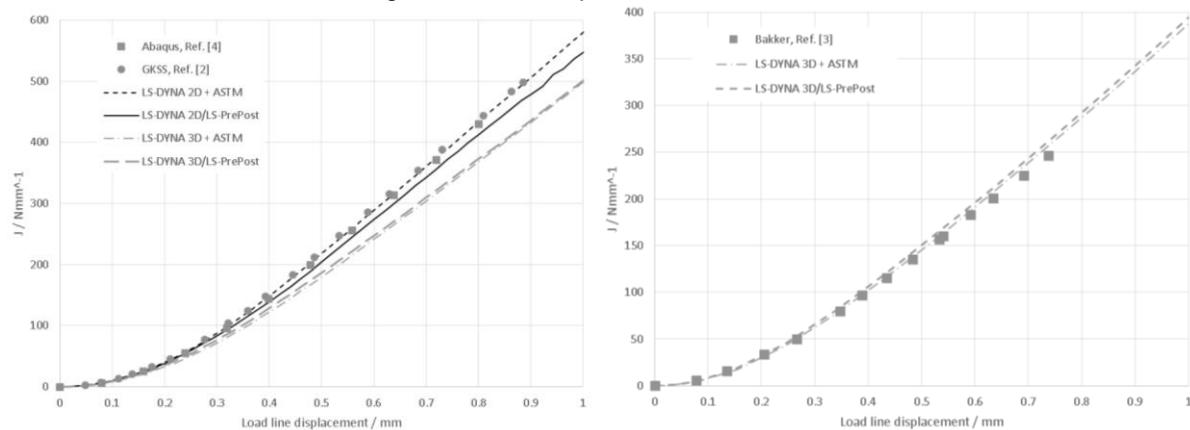


Fig.3: Left: Results comparison for the first C(T) specimen. Both 2D and 3D results. Right: Results comparison for the second C(T) specimen. NOTE: Different scaling on the ordinates!

The geometry of the second C(T) – specimen is only slightly modified compared to the first one: the width is increased to 25.2 mm and the remaining ligament is decreased to  $b_0 = 20.2$  mm. However, a completely different material is used. The results are compared in the left image of Fig.3. Also for the second C(T) specimen, the results from LS-DYNA / LS-PrePost are within reasonable agreement to both the results obtained from the global force-displacement curve by the ASTM – method, and to the previously presented results of Ref. [3].

#### 4 Literature

- [1] Lei, Y., O'Dowd N. P., and Webster, G. A., Fracture mechanics analysis of a crack in a residual stress field, *International Journal of Fracture*, 106, 2000, 195-216.
- [2] Brocks, W., Scheider, I., Numerical aspects of the path-dependence of the J-integral in incremental plasticity, Technical Note GKSS/WMS/01/08, 2001
- [3] Bakker, A., The three-dimensional J-integral, PhD Thesis, TU Delft, 1984
- [4] Abaqus Technology Brief, Fracture mechanic study of a compact tension specimen using Abaqus/CAE, Simulia TB-04-FMCAE-1, 2007
- [5] LS-DYNA Keyword User's manual version 971, Volume I – II, Livermore Software Technology Corporation (LSTC), Livermore CA, 2014
- [6] ASTM Standards, Standard test method for measurement of fracture toughness, ASTM E1820-13, American Society for Testing and Materials, Philadelphia 2013.
- [7] ASTM Standards, Standard test method for plane-strain fracture toughness of metallic material, ASTM 399-90, American Society for Testing and Materials, Philadelphia 1997.
- [8] Rice, J. R., A path independent integral and the approximate analysis of stress concentration by notches and cracks, *Journal of Applied Mechanics*, 35, 1968, 379-386.
- [9] Parks, D. M., "Virtual crack extension: a general finite-element technique for J-integral evaluations", Proc. 1<sup>st</sup> Int. conf Numerical methods in fracture mechanics, Swansea (UK), 1978, 464-478.
- [10] Lindström, P., Improved CWM platform for modelling welding procedures and its effects on structural behaviour, Doctoral thesis, University West, Trollhättan, Sweden, 2015.

# A Fabric Material Model with Stress Map Functionality in LS-DYNA

Thomas Borrvall<sup>1</sup>, Curtis Ehle<sup>2</sup>, Troy Stratton<sup>2</sup>

<sup>1</sup>DYNAmore Nordic AB, Linköping, Sweden

<sup>2</sup>Autoliv OTC, Ogden UT, USA

## 1 Introduction

Woven fabric behavior is generally highly non-linear and non-isotropic. Such behavior is difficult to approximate with typical continuum based material models. As such, woven fiber behavior has generally been simulated employing simple uncoupled non-linear orthotropic behavior based on uniaxial or equi-biaxial input. This approach has been acceptable for system level modeling of airbag-occupant interaction as well as modeling of general inflated shape and volume but insufficient for reasonably accurate prediction of local stress states within the cushion.

LS-DYNA has provided options for modeling of fabric. MAT\_FABRIC, FORM=14 provides non-linear uncoupled fiber behavior. Stress-strain response is based on either uniaxial, equi-biaxial input or some selected strain state in between. This approach can provide approximation of general material stiffness due to fiber coupling but only for the immediate domain of the selected input. MAT\_FABRIC, FORM=-14 was subsequently developed and partially incorporates stiffness effects of fiber coupling over a limited but larger domain. This is accomplished by input of both uni-axial and equi-biaxial input and linearly interpolating between, thereby reasonably approximating fiber coupling for a limited domain near equi-biaxial behavior.

The subject of this paper is new fabric model, MAT\_FABRIC\_MAP which is a general approach to model fiber coupling effects for the entire tension-tension domain while allowing for uncoupled behavior in the compression-tension and compression-compression domains. This is accomplished via direct mapping (tables) of fiber stresses to corresponding a & b fiber strain points throughout the strain domain of simulation. The approach is discussed along with numerical and physical considerations that were addressed to ensure solution stability. Some examples of its use in the airbag industry are provided.

## 2 The Fabric Material Models

### 2.1 FORM=14

FORM=14 is probably the most common option in everyday simulation of material 34 (MAT\_FABRIC). It allows for specification of input curves to define individual stress components' response as function of corresponding strain components

$$S_{XX} = S_{XX}(E_{XX}) \quad (1a)$$

$$S_{YY} = S_{YY}(E_{YY}) \quad (1b)$$

$$S_{XY} = S_{XY}(E_{XY}). \quad (1c)$$

There is no in-plane coupling that separates uniaxial from biaxial response in this model, and the estimation of curves must be made with respect to an assumed combination of the two.

### 2.2 FORM=-14

To account for biaxial stiffening, FORM=-14 was developed. The stress is here determined from a set of uniaxial and biaxial input curves

$$S_{XX} = \left(1 - \alpha\left(\frac{E_{YY}}{E_{XX}}\right)\right) S_{XX}^u(E_{XX}) + \alpha\left(\frac{E_{YY}}{E_{XX}}\right) S_{XX}^b(E_{XX}) \quad (2a)$$

$$S_{YY} = \left(1 - \alpha\left(\frac{E_{XX}}{E_{YY}}\right)\right) S_{YY}^u(E_{YY}) + \alpha\left(\frac{E_{XX}}{E_{YY}}\right) S_{YY}^b(E_{YY}) \quad (2b)$$

while the shear stress is the same as in FORM=14, see (1c). These formula are valid only for  $E_{XX} > 0$  and  $E_{YY} > 0$ , for other combinations of strain (1a) and (1b) are used. The function  $\alpha$  used to interpolate between the uniaxial and biaxial curves can be expressed simply as

$$\alpha(q) = \min(1, q). \quad (3)$$

The curves can be estimated from uniaxial and biaxial tests, and the resulting model is accounting for biaxial stiffening due to interaction between yarns in the warp and weft directions.

### 2.3 Stress Map

The Stress Map Material, as the name suggests, maps a point in strain space to a point in stress space. We have

$$P_{XX} = P_{XX}(e_{XX}, e_{YY}) \quad (4a)$$

$$P_{YY} = P_{YY}(e_{YY}, e_{XX}) \quad (4b)$$

where  $e_{XX}$  and  $e_{YY}$  denote the engineering strain components while  $P_{XX}$  and  $P_{YY}$  are the engineering stress components. This model is a generalization of FORM=14 and the most general elastic model for fabrics currently available, and potentially represents a wide range of biaxial strain states. The shear behavior follows (1c).

### 3 Additional Features

In the context of fabric modelling, a number of features for enhancing robustness and accuracy are discussed. These are hysteresis modelling, fiber compaction and coat induced bending, treated in length in the full paper and briefly summarized here.

#### 3.1 Hysteresis

Incorporating rate independent dissipation has shown to be a necessity for the stability of dynamic analysis of the fiber coupled fabrics, and a tailor made hysteresis model has been developed for this purpose. This model is backed up by thermodynamical arguments, and dynamic simulation of an airbag mushroom is used to show the effects in practice.

#### 3.2 Volumetric Compaction

From a physical standpoint, volumetric compaction prevents the fabric elements to attain zero volume. Instead of modifying the curves in (1), (2) and (4), we suggest an augmented volumetric stress strain relation for this. This can be physically motivated from considering the composite properties of fabric, and it is shown how this affects the well-known picture frame test as an example.

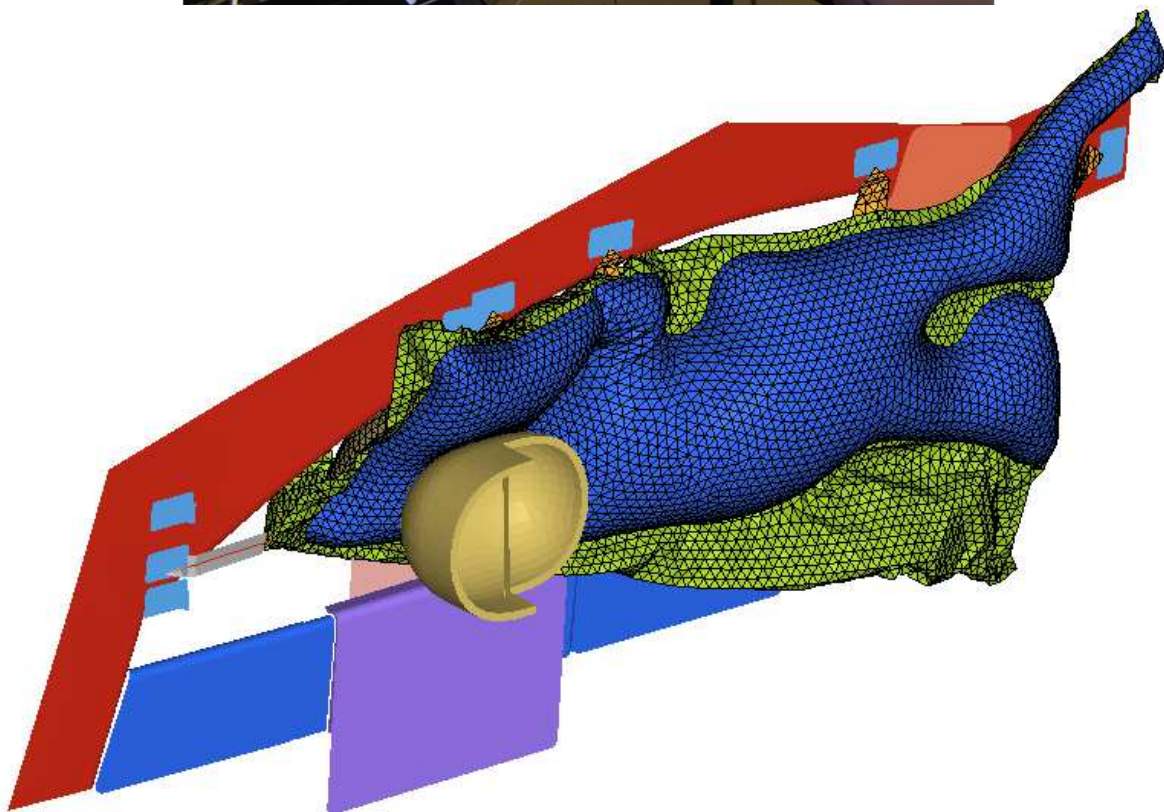
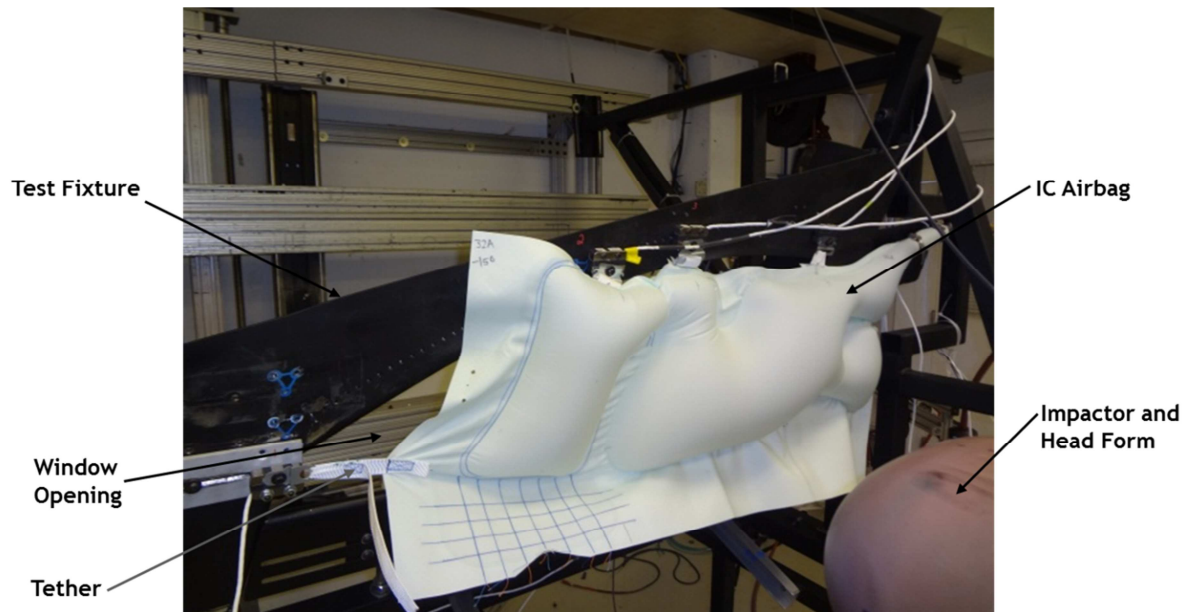
#### 3.3 Bending

Since fabrics are simulated with membrane elements, there is no bending resistance by default which can result in uncontrollable deformation. This can be remedied by adding a thin coat layer on the top and bottom of the fabric elements, consisting of an elastic-plastic polymeric material. This typically results in smoother deformation at little extra cost, and is included in the numerical example that follows.

### 4 Numerical Example

Ejection mitigation (EjM) is occupant protection in the event of a rollover accident. General EjM testing consists of a linear impactor with a head form that is launched at a pressurized ICAB that is suspended from a car body. The linear impactor and head form mass is 18 kg. Two load cases are performed with different initial head form energies and different airbag pressures. The result of an EjM test is the amount of head form excursion. Head form excursion is the distance the head form travels past the window inner surface. FMVSS 226 requires the peak head form excursion to be less than 100 mm to pass government testing. Most OEM's require Autoliv to demonstrate excursions less than 80 mm as an added safety precaution.

In 2013, Autoliv conducted a highly controlled and instrumented series of EjM tests using a small scale cushion and an adjustable test fixture instead of a car body, as seen in the figure below. Initial ICAB pressure was controlled as well as the initial tether tension. A test was repeated several times and an average peak head form excursion of 55 mm was measured. An LS-Dyna model was built to simulate the testing and predict the head form excursion, also shown below. Using MAT\_FABRIC, FORM=14, the peak predicted excursion is 87 mm. Using the equivalent MAT\_FABRIC\_MAP material model with fiber coupling and the coating option for bending stiffness, the peak excursion was reduced to 57 mm. The FORM=14 excursion would not pass the OEM's requirements and require a redesign of the ICAB. Using the more realistic material model produces an excursion prediction that agrees with the test measurement and passes the OEM EjM requirement.



*EJM test setup and simulation model.*

## 5 Summary

A thorough investigation of the most common fabric material modeling options in LS-DYNA has been presented, with emphasis on the new Stress Map material. The Stress Map material allows for general in-plane membrane coupling between the fiber stresses and facilitates the assessment of an airbag design from a constructional point of view. A number of additional features have been discussed, including hysteresis, volumetric compaction and bending, that we find necessary to enhance robustness and accuracy in the present model. Numerical examples highlight the effects of these features and also show the potential advantages of incorporating fiber coupling in the simulation of airbag deployment.

**DEVELOPER III**  
**MULTIPHYSICS**



# Generalized Anisotropic/Isotropic Porous Media Flows in LS-DYNA

Rodrigo R. Paz<sup>1</sup>, Facundo Del Pin<sup>1</sup>, Iñaki Caldichoury<sup>1</sup> and Hugo G. Castro<sup>2</sup>

<sup>1</sup>Livermore Software Technology Corporation, USA.

<sup>2</sup>National Council for Scientific and Technological Research, Argentina.

## 1 Abstract

Among the current needs of large industries and engineering companies is the ability to perform numerical simulations of complex processes that require the coupling of multiple fields, each representing a different physical model and/or phenomena. Processes involving fluid flows through porous media matrices are present in a wide range of these kind of problems.

In the ground vehicles industry, understanding aerodynamics phenomena allows us to optimize the operation of a wide spectrum of road vehicles, that ranges from road passenger transport (cars, buses, trains) to road commercial transport (trucks and trains). Road vehicle aerodynamics is a complex topic due to the interaction between the air flow and the ground and some parts (that play an important role in drag and lift development) could be treated as a porous media (e.g. the radiator, the condenser, air filters, etc). In recent years industries like aerospace and those related to oil production have increased their trustfulness on numerical models and codes for the design, research, production and verification of highly critical parts and production processes. Most of these industries have adopted manufacturing procedures involving composites materials in liquid state, like the Liquid Composite Molding (LCM) and the High Pressure Resin Transfer Molding (HPRTM) methods, where a Newtonian (or Non-Newtonian) fluid flows through highly anisotropic matrices filling an initially empty container. In this article the numerical modeling of the flow through general anisotropic porous media using LS-DYNA is introduced. A generalization of the Navier-Stokes equations that will allow the definition of sub-domains with different permeability/porosity was developed. The SUPG|OSS stabilizing Finite Element Method for the spatial approximation and the second-order Fractional Step Method for the time integration were adopted. Also, the paper will provide some examples showing the use of LS-DYNA in a wide range of low problem. Details about how the users' interface looks like will be given at the conference talk (it also can be found in the LS-DYNA users manual).

## 2 Introduction

The natural generalization of the Navier-Stokes model for the incompressible fluid dynamics is the key point of the multi-physics coupling developed in LS-DYNA. This approach allows to user to model problems of 3D fluid infiltration through a porous media matrix with a moving free surface, like the so called Resin Transfer Molding process (RSM). Infiltration process basically depends on the local porosity, the local orientation of the fibers and on their packing density. In LS-DYNA, such a problem can be modeled with the ICFD+Multi-physics solver using an implicit second-order Fractional-Step time integration. Basically, the porous media solver implements the Ergun Correlation and the Darcy-Forchheimer force models in both the anisotropic and the isotropic forms. The fluid constitutive relation, describing the fluid stresses as function of the fluid velocity field could play an important role in RSM and LCM processes. For this purposes, LS-DYNA implements not only the classical Newtonian model but also a non-Newtonian model based on the power law. The fluid temperature field transport is also coupled to the structural thermal solver through the Conjugate Heat procedure described in previous articles. With the multi-physics capabilities of LS-DYNA engineers can couple CFD analysis with a thermal and/or structural solver in order to solve more complex and realistic problems in industry and general engineering. In particular, the generalization of the Navier-Stokes equations allows the definition of sub-domains with different permeability/porosity. The SUPG|OSS stabilizing Finite Element Method for the spatial approximation and the second-order Fractional Step Method for the time integration were adopted.

## 3 The General Incompressible CFD solver in LS-DYNA.

In recent years LSTC has devoted big efforts in the development of a CFD solver for incompressible flows. The solver is specifically designed to tackle coupled problems where low Mach numbers ( $M < 0.3$ ) are involved and a scalable parallel solution is needed.

## 4 Generalized Anisotropic/Isotropic Navier-Stokes flows through Porous Media.

### 4.1 General Model

A generalization of the Navier Stokes equations (see referece [1]) that will allow the definition of sub-domains with different permeability/porosity by means of the `*ICFD_PART` and `*ICFD_PART_VOL` keywords was implemented. Material parameters are introduced via `*ICFD_MAT` keyword (4<sup>th</sup> CARD, see user's manual). Basically, four different models where implemented so far: **i)** the isotropic Ergun correlation, **ii)** the Darcy-Forchheimer force model, **iii)** a model for the definition of porous parameters using a pressure-velocity curve obtained from experiments, and **iv)** a general Anistropic Darcy-Forchheimer model.

### 4.2 Validation of the model implementation.

The flow of a Newtonian fluid through a rectangular channel with a thick porous layer is considered interchanging mass and momentum through a common interface. This problem was extensively studied by Vafai et.al and is a classical benchmark for 2D/3D NS/Porous flow coupling. 3D LS-DYNA FEM results for the velocity field are compared to a theoretical solution in Figure 1.

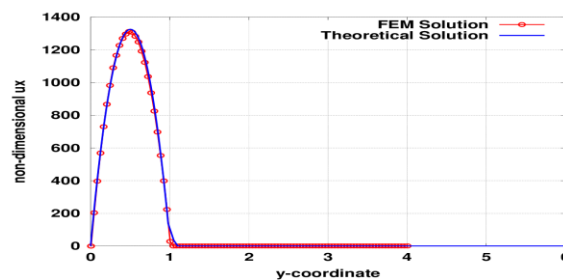


Figure 1: 3D results: FEM vs Theoretical.

### 4.3 Resin Transfer Molding in an Anisotropic Multi-Porous Domain.

The following example is a RTM problem where a Newtonian fluid is injected into a mold at high speed. The porous domains consists in two highly anisotropic regions embedded in an isotropic matrix. In Figure 2 the velocity field and the position of the free surface is shown for a time step.

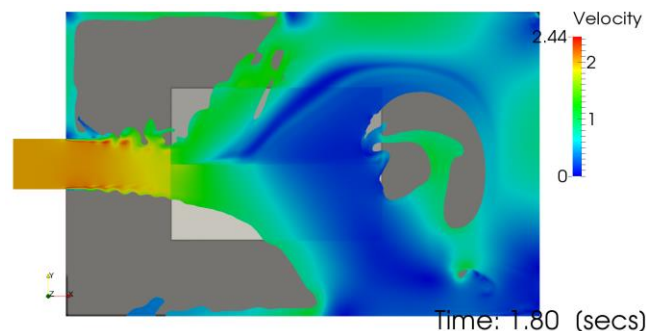


Figure 2: RTM in multi-porous domain.

## 5 Summary

This paper introduced some of the new features that LS-DYNA offers in the area of multi-physics, including general CFD flows, flows through anisotropic or isotropic multi-porous domains, Free-Surface, and thermal analysis. Academic benchmarks and industry/engineering test problems were



# Chemically Reactive Flows in Airbag Inflator Chambers

Kyoung su Im, Grant Cook, Jr., and Zeng-Chan Zhang

Livermore Software Technology Corp.

Airbags are part of an important vehicle safety system, and the inflator is an essential part that generates a specific volume of gas to the airbag for a short duration of time. Recently, we have developed numerical models of automotive airbag inflators in conjunction with the LS-DYNA® chemistry solver. In this study, detailed and comprehensive descriptions for theoretical models are developed for a conventional pyrotechnic inflator (PI) and a compressed, heated gas inflator (HGI). For the model validation, the closed bomb test was executed and compared with an experimental data. In case of pyrotechnic inflator, zero dimensional model in conjunction with a solid propellant grains (e.g.  $\text{NaN}_3/\text{Fe}_2\text{O}_3$ ) is applied and the results are compared with existing data. In HGI model, a 2-dimensional with multi-species chemically reacting flow was calculated in the combustion chamber. Detailed and comprehensive descriptions for constructing the keyword files will be given and the results for the two models will be discussed.

The present study should find wide applications in designing advanced inflator models and predicting airbag performance by coupling to LS-DYNA® airbag solvers (i. e., ALE/ CESE).

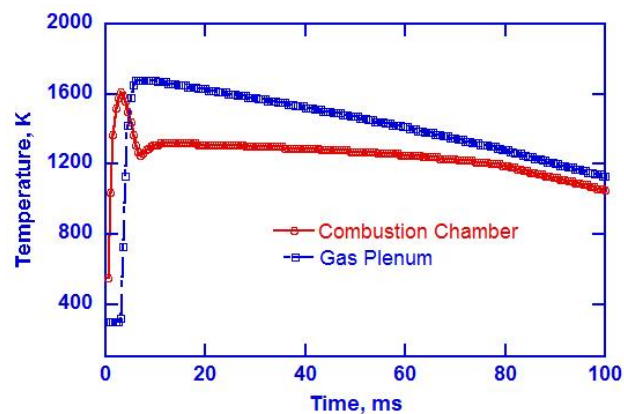


Figure 1 Temperature profiles in the combustion chamber and gas plenum with time.

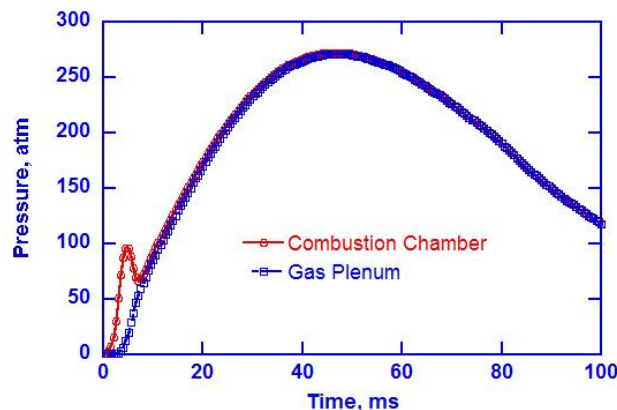


Figure 2 Pressure profiles in the combustion chamber and gas plenum with time.

# Recent Developments in the Electromagnetic Module: A New 2D Axi-Symmetric EM solver

Pierre L'Eplattenier<sup>1</sup>, Iñaki Çaldichoury<sup>1</sup>,

<sup>1</sup>LSTC, Livermore, CA, USA

## 1 Introduction

An electromagnetism module has been developed in LS-DYNA for coupled mechanical/thermal/electromagnetic simulations. More recently, a new 2D axi-symmetric version of this solver was introduced, allowing much faster simulations.

In this solver, the EM equations are solved in a 2D plane, and the 2D EM fields, Lorentz force and Joule heating are then expanded to 3D elements by rotations around the axis. This allows coupling the 2D EM with 3D mechanics and thermal, thus keeping all the LS-DYNA 3D capabilities available. The user needs to provide a 3D mesh with rotational symmetry, either on the full 360 degrees or a small slice.

The 2D-EM eddy-current problems are solved using a coupled FEM-BEM method, both based on differential forms. It can be coupled to different external circuits, including imposed currents, imposed voltage or (R,L,C) circuits. It also allows the coupling of different parts in a single circuit in order to have complex geometries like, e.g., spiral coils. It works both in serial and MPP, and is available for the eddy-current solver. A contact capability has also been introduced.

## 2 Modelling spiral or helix coils using the axisymmetric solver.

Since LS-DYNA is primarily a 3D code, where most of the features are available only in 3D, we decided to couple the EM-2D with the 3D LS-DYNA. This means that the user needs to provide a 3D mesh as well as, for each conducting part, a segment set to define the plane where the EM-2D is done. However, the simulation does not need to be made on a full  $360^\circ$ , but can be made on a slice of the full cylinder. This slice needs to be  $(\frac{1}{2})^p$  times the full cylinder ( $\frac{1}{2}, \frac{1}{4}, \frac{1}{8}, \dots$ ).

As with the 3D solver, one can connect different circuits together, i.e. impose a linear constraint on the global currents of 2 circuits like, for example  $i_1 = i_2$ , using the `*EM_CIRCUIT_CONNECT` card. This allows the simulation in 2D of a spiral or helix coil. This circuit connect feature can even be used when the coil is connected to a R,L,C circuit.

## 3 Figures and Examples

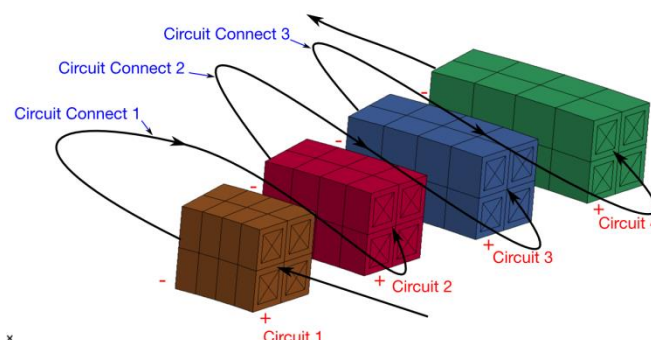


Fig.1: Example of a spiral coil modelled using the axisymmetric solver

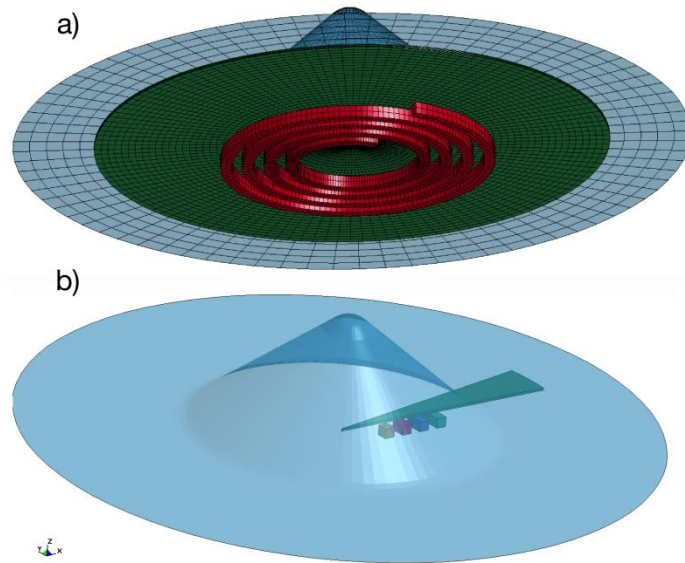


Fig.2: 3D versus 2D metal forming example

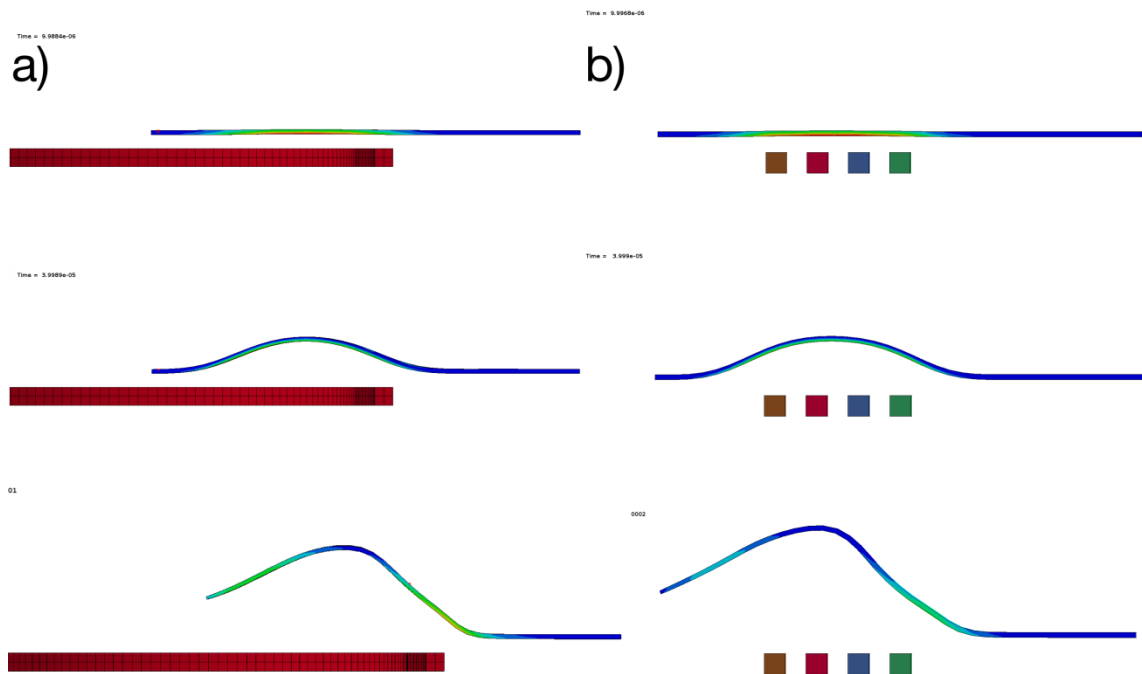


Fig.3: Displacement of the workpiece at different times. Comparison between 3D, a) and 2D b).

(1)



**DEVELOPER IV**  
**MISCELLANEOUS**



# LS-TaSC Product Status

Willem Roux<sup>1</sup>, Katharina Witowski<sup>2</sup>, Peter Schumacher<sup>2</sup>

<sup>1</sup>Livermore Software Technology Corporation

<sup>2</sup>DYNAmore GmbH

## 1 Introduction

The LS-TaSC Version 3.1 topology and shape design tool is presented. The presentation introduces the multi-point numerical derivatives scheme that allows constrained optimization using the mass fractions and load case weights as variables. This allows constrained optimization using any response or mathematical expressions as constraints or objectives. Additionally, the postprocessing of the final design geometry by the creation of iso-surfaces is also reviewed. Application examples illustrate these capabilities.

## 2 Multi-point Optimization

Multi-point optimization is used to solve constrained optimization problems. Two sets of variables are used in a simultaneous iterative process. The global variables, such as the part mass fraction and the load case weights, are used to satisfy the constraints, while the element density variables are used to simultaneously compute the load paths. The two sets of variables are treated differently in the design algorithm: the local variables are computed using a suitable method such as fully stressed design, while the values of the global variables satisfying the constraints are computed using numerical derivatives and mathematical programming. This methodology has the advantage of allowing more general constraints.

Application examples illustrating this method will be presented.

## 3 Iso-surfaces

For solid element designs, a surface containing the final optimal structure can be created and stored in the LS-DYNA input format, Fig. 1.

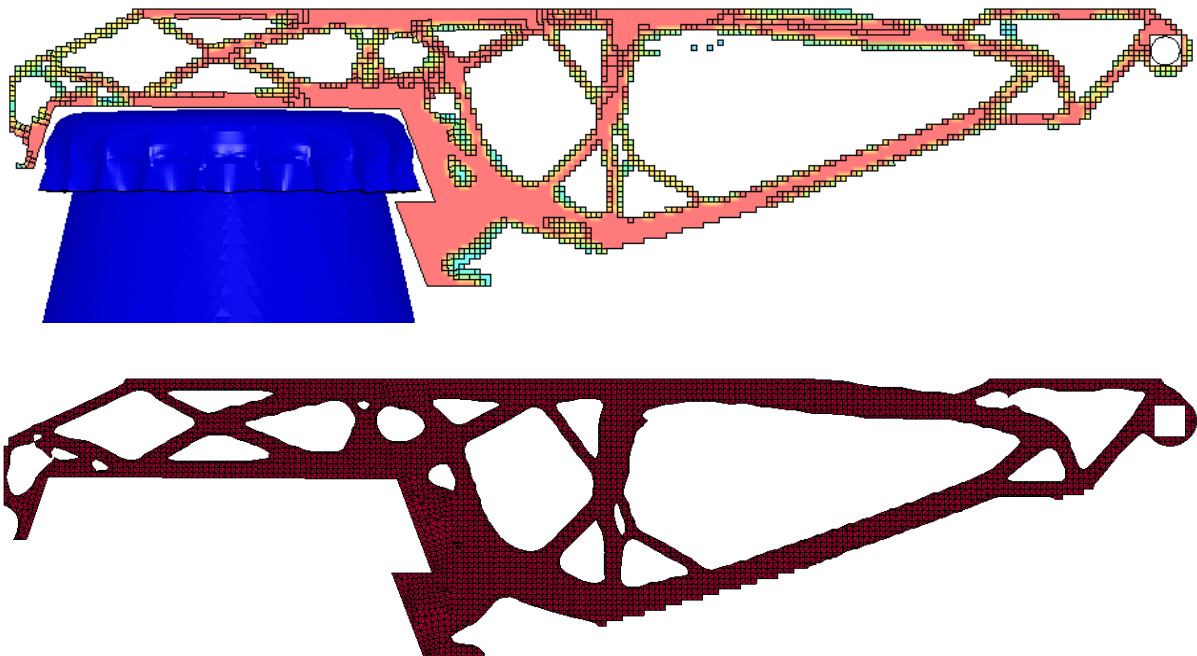


Fig. 1: Example Bottle Opener; Final Design (top) and Iso-Surface (bottom)

# Recent Developments for Thermo-Mechanically Coupled Simulations in LS-DYNA with Focus on Welding Processes

Thomas Klöppel<sup>1</sup>, Tobias Loose<sup>2</sup>

<sup>1</sup>DYNAmore GmbH

<sup>2</sup>Ingenieurbüro Tobias Loose, Germany

## 1 Motivation

Forming, press hardening and welding are well-established production processes in manufacturing industry. Nevertheless predicting the finished geometry and the final material properties of the processed parts is still a major issue. In particular, the deformations caused by welding are often neglected in the virtual process chain, although they have to be compensated for in order to fulfil the requirements on shape tolerance. In this contribution novel developments for thermo-mechanically coupled simulations in LS-DYNA are presented, which are designed to close this gap in the virtual process chain.

## 2 Numerical Implementation

One challenge in welding simulations is to define a heat source. Here, not only the correct amount of energy that is input into system has to be accounted for, but also the power density distribution has to be modelled accurately. In many applications the Goldak double ellipsoidal heat source [1] is a reasonable choice. In LS-DYNA the specific keyword `*BOUNDARY_THERMAL_WELD` provides a convenient way to define this state-of-the-art heat source and is also applicable for curved weld seam geometries, as is exemplarily shown in Fig.1.

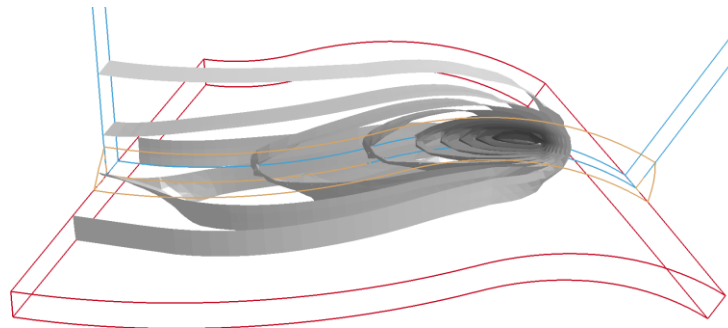


Fig.1: Temperature iso-surfaces during the welding of a curved weld seam.

In general, locally high temperatures and high temperature gradients are characteristic properties of welding processes. Those exceed the melting point of the material and during the solidification phase transformations of the microstructure can be observed during cooling as well as during the heating phase. Numerical models have to account for these effects in order to obtain a comprehensive material behavior and to be able to predict the material properties of the processed part. The LS-DYNA material `*MAT_UHS_STEEL`, initially implemented for press hardening simulations, is able to predict the microstructure and the resulting mechanical properties based on the work of Åkerström [2,3].

It is important to note, that the final microstructure is here not only of interest for the welded structures but even more for the filler material. In welding simulations the weld seams are usually discretized with solid elements in the pre-processing step. However, as long as the filler material has not been affected by the heat source its mechanical properties are negligible. For such applications the ghosting approach first implemented in LS-DYNA material `*MAT_CWM` [4] has been included along with further



enhancements and new features into the formulation of **\*MAT\_UHS\_STEEL** [5]. One of the enhancements is an annealing approach. Plastic strains and other history variables of the material are deleted as the temperature reaches the melting point of the material.

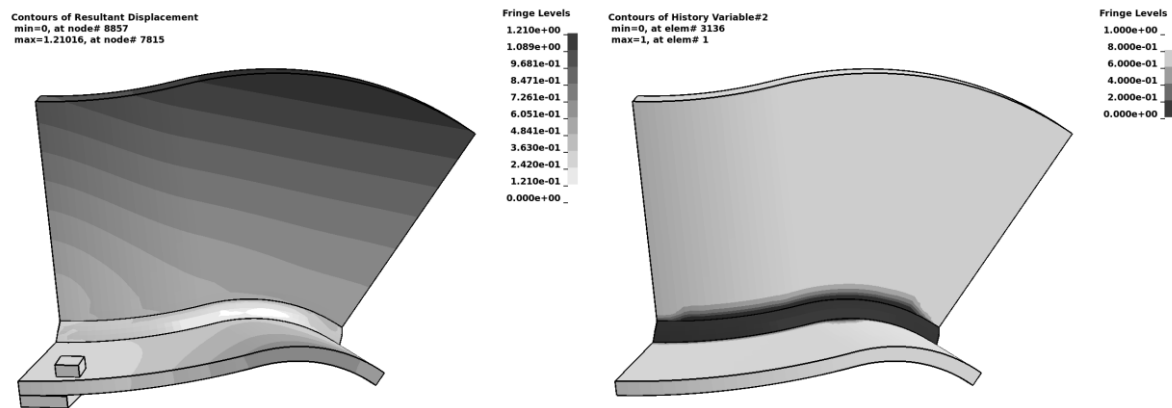


Fig.2: Final displacement field (left) and final ferrite concentration (right) for a welded curved T-joint .

The application of the enhanced material formulation **\*MAT\_UHS\_STEEL** to a curved T-joint can be seen in Fig.2. The final displacements and the final ferrite concentration are depicted here. Initially, the microstructure of the material is assumed to be in a ferrite state, but the phase has been transformed into austenite within the heat affected zone. During the cooling of the structure, the austenite is again decomposed into harder phases

### 3 Summary and Outlook

With the presented new developments and features, it has become possible to accurately simulate a wide range of welding processes. Naturally, these processes can be a single stage in a larger process chain. LS-DYNA easily allows considering data from previous process steps, e.g. residual stresses from a forming stage, within the welding simulations as well as to transfer the stress state and material properties of the welded parts to subsequent stages.

As the name suggests, **\*MAT\_UHS\_STEEL** is limited only to a certain range of materials. Currently, implementation of a more general material formulation for welding and heat treatment simulations is on the way. The new formulation will allow for an arbitrary number of different phases and for each of the possible phase transitions the user can choose from a list of generic transformation models. The current status of the implementation and as well as further possible developments for thermo-mechanically coupled simulations will be discussed.

### 4 Literature

- [1] Goldak, J., Chakravarti, A., Bibby, M.: "A Double Ellipsoid Finite Element Model for Welding Heat Sources", IIW Doc.No., 212-603-85, 1985
- [2] Åkerström P., Oldenburg M.: "Austenite decomposition during press hardening of a boron steel – Computer simulation and test", Journal of Materials Processing Technology, 174, 2006, 399-406
- [3] Åkerström P., Bergman G., Oldenburg M.: "Numerical implementation of a constitutive model for simulation of hot forming", Modeling and Simulation in Materials Science and Engineering, 15: 105-119, 2007.
- [4] Schill, M., Odenberger, E.: "Simulation of residual deformation from a forming and welding process using LS-DYNA", 13<sup>th</sup> International LS-DYNA Conference, Detroit, 2014
- [5] Klöppel, T., Schill, M., Loose, T.: "Recent Developments for Hot Stamping and Welding Processes in LS-DYNA", LS-DYNA Forum 2014, Bamberg, 2014

# Improvements to LS-DYNA Implicit Mechanics

Roger Grimes  
Livermore Software Technology Corporation

## 1 Introduction

LSTC is continually improving the capabilities and performance of Implicit Mechanics especially in the distributed memory computing environment. This talk will review recently added features and performance improvements.

## 2 Gears

The amazing ingenuity of the LS-DYNA User Community discovered two flaws in the treatment of joints including that in Implicit Mechanics. Joints which transfer motion from one rigid body to the second such as gears, rack and pinion, and screw joints implementation assumed that one of the rigid bodies was not moving. The implementation has been enhanced to allow for both translational and rotational motion of the joint assembly without effecting the relative motion between the two rigid bodies.

The second was the treatment of helix and worm gears. This required enhancement of the treatment of gears to account for the gears not being in the same plane. The conference presentation will show videos of these two enhancements.

## 3 Modal Dynamics

In response to user requirements the capabilities for modeling using Modal Dynamics was greatly enhanced in LS971 R7.1. This allows fast simulation of models by replacing the nonlinear model with a linearized model based on eigen modes. The next release of LS971 will allow for the use of prescribed motion constraints on such models. We use the constraint mode feature of \*CONTROL\_IMPLICIT\_MODES to compute the force equivalent of a unit displacement for a particular degree of freedom. Then apply an appropriately scaled force during the modal dynamics simulation.

## 4 Performance Improvements

### 4.1 Reuse of the Symbolic Factorization for the Sparse Linear Equation Solution

As the models used in Implicit simulations grow larger and the use of larger number of parallel processes the Symbolic Factorization phase of the sparse linear equation solution is becoming more of a bottleneck. One user was working with a model with 90M rows in the linear algebra problem using the Hybrid MPP executable of LS-DYNA. He reported that the wall clock time for the numeric factorization using 4096 processes and 6 SMP threads was scaling down to 160 seconds. However the wall clock time for the symbolic factorization was NOT scaling and staying at 2600 seconds.

LSTC is continuing its long term development of a scalable symbolic factorization but that development, requiring new and innovative research, is taking much longer than expected. As a short term fix we have implemented two enhancements. The first enhancement is to monitor the matrix structure from matrix reformation to matrix reformation. If the matrix structure is the same from the last

numeric factorization and the current one we reuse the symbolic factorization. The trade-off with this feature is the additional cost of monitoring of the matrix structure with the up side benefit of reusing the symbolic factorization.

The second enhancement is an MPP only feature. We predict the contact pattern for penalty based (non-tied) contact to allow small changes in the matrix structure due to changes between time steps of contact interface. This has feature can increase the cost of the numeric factorization by adding additional entries to the sparsity of the stiffness matrix. But at the benefit of reusing the symbolic factorization for problems where the contact changes slightly.

#### **4.2 Enhanced Performance of the Numeric Factorization**

For large models the wall clock time is dominated by the numeric factorization of the stiffness matrix.

This numeric factorization is based on the multifrontal algorithm which works on dense submatrices in the context of what is called an elimination tree. As you approach the root of the elimination tree there are fewer submatrices than processes so the dense submatrices have to be distributed across the available processes. Historically this has been a one dimensional distribution. For large submatrices with 16 or more processes we are now distributing the work in a two dimensional pattern to provide more load balancing. Again there are trade-offs of improved load balance but at the cost of increase initialization of the work for each process. Initial testing shows that the trade-off favors the two dimensional distribution when the number of processes involved is 16 or greater and the submatrices is large enough.

### **5 Summary**

This presentation outlines the improvements made in LS-DYNA Implicit. Enhanced and new features for joints and modal dynamics have been described. The performance improvements for large implicit simulations have also been presented.

# MPP Contact: Options and Recommendations

Brian Wainscott

LSTC

## Introduction

There are many different contact algorithms currently implemented in LS-DYNA, each having various options and parameters. I will cover only a few of them. Much of what is discussed will only apply to the MPP version of LS-DYNA, and not to the “soft=2” contact variant.

## Options

The features discussed include:

- IGNORE – a generally useful option to compensate for modeling imperfections and improve stability
- GROUPABLE – a newer version of some contact algorithms with improved scaling
- FORCE TRANSDUCERS – use of these is significantly more efficient than adding extra contact interfaces
- TIEDID – eliminates roundoff problems in penalty offset tied contact
- IPBACK – allows the use of constraint tied contact when other constraints may be present

## Summary

As part of the ongoing development and improvement to the contact capabilities of LS-DYNA, new features and options will continue to be added. When helpful new options are implemented, they are often not enabled by default, due to the desire to preserve the behavior of pre-existing user models. In order to achieve the best behavior, the following settings mentioned in this paper are suggested where applicable:

IGNORE=2  
GROUPABLE=1

# **DEVELOPER V**

## **ELEMENTS**



# Edge-to-Edge Cohesive Shell Elements in LS-DYNA

Jesper Karlsson<sup>1</sup>, Martin Fagerström<sup>2</sup>

<sup>1</sup>Dynamore Nordic AB

<sup>2</sup>Chalmers University of Technology

## 1 Summary

This paper presents a new cohesive element in LS-DYNA for edge-to-edge connection of quadrilateral thin shells.

Cohesive elements are an important tool for simulating the propagation of cracks in materials. For example, to describe failure propagation in a thin walled sheet metal structure along an *a priori* known crack path, e.g. along a weld line, through-the-thickness crack propagation has in the literature been modeled by embedding interface cohesive zone elements in between shells elements, see e.g. References [1-3]. By connecting faces and edges of neighboring elements, the cohesive elements are used to describe the degrading load carrying capacity of the material in the evolving fracture process zone. The elements do not, however, model a physical material in a continuum mechanics sense; instead they model a (non-linear dissipative) spring based force response depending on the separation of the neighboring faces and edges through a cohesive law. Hence, they can remain stable under zero or negative volume.

LS-DYNA has a variety of solid cohesive elements to simulate cracks between solids (element type 19 and 21) and delamination of shells (type 20 and 22). As of Revision 8.0 a new cohesive shell element is now available for edge-to-edge connection of quadrilateral thin shells. The new cohesive element (type 29) accounts for in-plane and out-of-plane separation as well as hinge bending and works with existing cohesive material models.

This paper presents the new element type 29 in detail and shows some relevant benchmark simulations.

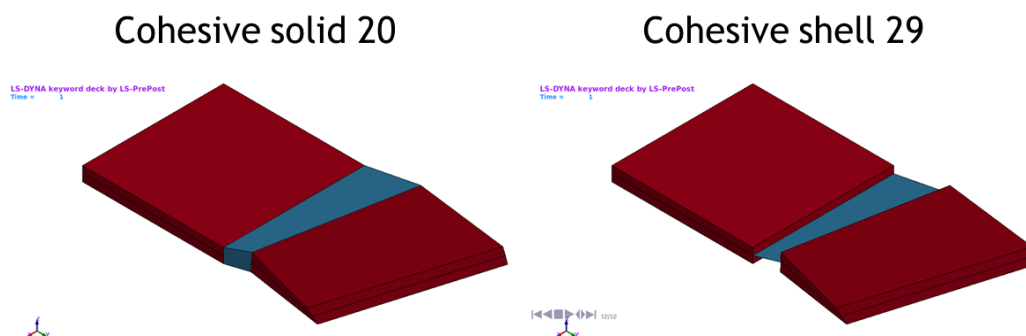


Fig.1: Simple comparison between solid element 20 and shell element 29

## 2 Literature

- [1] Cirak F, Ortiz M, Pandolfi A.: "A cohesive approach to thin-shell fracture and fragmentation", Computer Methods in Applied Mechanics and Engineering, 194, 2005, 2604–2618
- [2] Cornec A.: "Application of the cohesive model for predicting the residual strength of a large scale fuselage structure with a two-bay crack", Engineering Failure Analysis, 16, 2009, 2541–2558
- [3] Scheider I, Brocks W.: "Residual strength prediction of a complex structure using crack extension analyses", Engineering Fracture Mechanics, 76, 2009, 149–163

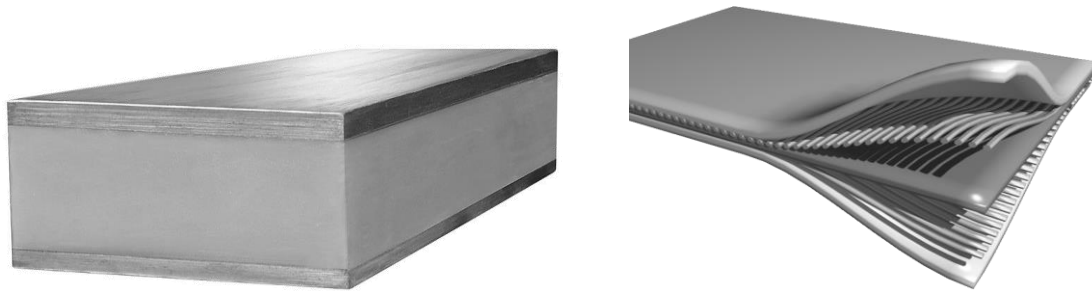
# A New Feature to Model Shell-Like Structures with Stacked Elements

Tobias Erhart

Dynamore GmbH, Stuttgart, Germany

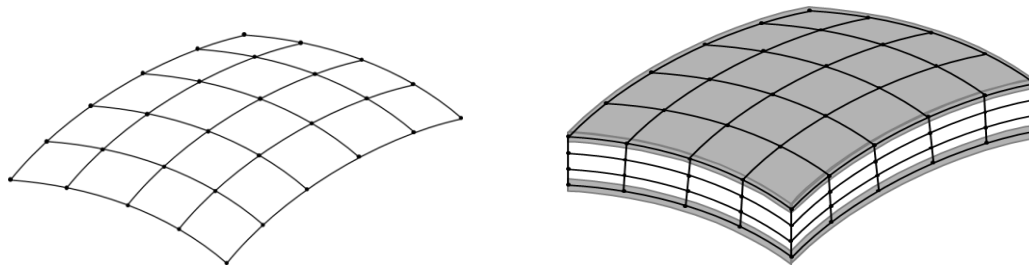
## Abstract

A computational method for the numerical simulation of stacked shell-like structures will be presented. These types of plane load-bearing components possess a thickness which is small compared to its other (in-plane) dimensions, whereas physical properties vary in thickness direction in distinct layers. Examples would be sandwich plate systems (SPS) or composite laminates.

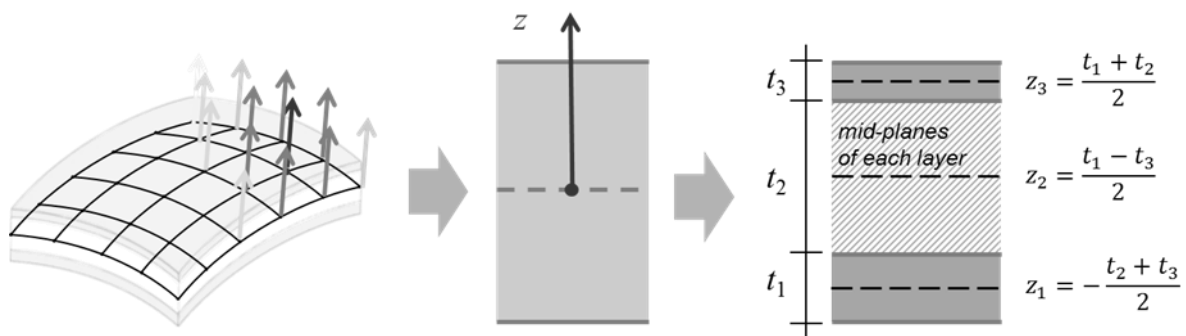


picture credits: Wikipedia

The main idea of this contribution is to create a computational modeling approach for an arbitrary layup sequence of shell and solid elements over thickness for such stacked components. Starting from a pure shell element mesh and a user-defined layup sequence of elements in thickness direction given in new keyword `*PART_STACKED_ELEMENTS`, new nodes and elements are automatically generated.



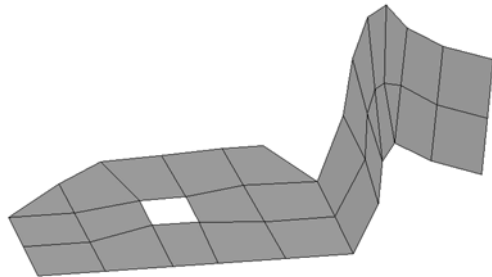
Extrusion methods are used to determine the new node locations, i.e. the description of the out-of-plane geometry. Each layer gets its own predefined properties such as individual thickness, material characteristic and element type.



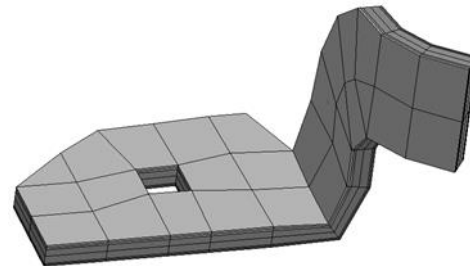


The arrangement of different element types with different properties over the thickness of shell-like structures can already be modeled in graphical pre-processor tools such as LS-PrePost. The advantage of this new approach is that these steps are now automatically taken care of in LS-DYNA itself.

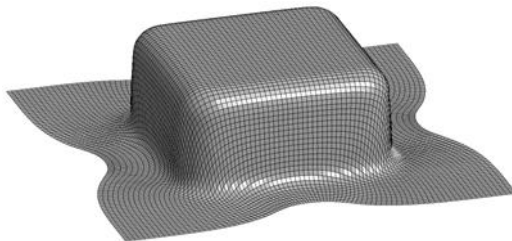
A few numerical examples will illustrate the presented feature. Besides some small verification tests, more practical examples will demonstrate the ability of this approach, e.g. to model sandwich structures or phenomena like delamination in composite materials.



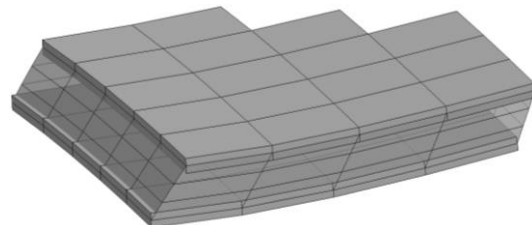
reference shell element mesh



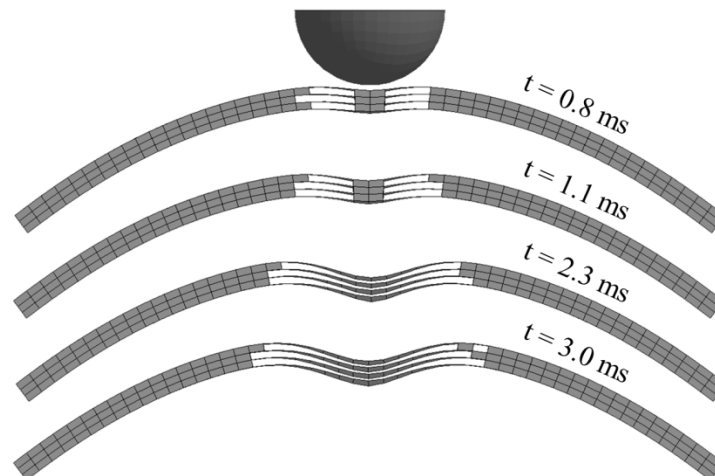
corresponding stacked element model



cup drawing example



deformed sandwich plate system



delamination progress under dynamic impact

In summary, this new feature simplifies the setup of numerical models for stacked shell-like structures by only asking for a minimal amount of user input, such as geometry description (pure shell element mesh) and layer design (number of layers and properties of each layer).

# Isogeometric Analysis in LS-DYNA: Using CAD-Geometry for Numerical Simulation

Dave Benson<sup>1</sup>, Dilip Bhalsod<sup>2</sup>, Stefan Hartmann<sup>3</sup>, Philip Ho<sup>2</sup>,  
Liping Li<sup>2</sup>, Weiguo Li<sup>2</sup>, Atilla Nagy<sup>2</sup>, Isheng Yeh<sup>2</sup>

<sup>1</sup>Professor for Structural Engineering, UC San Diego, CA, USA

<sup>2</sup>Livermore Software Technology Corporation (LSTC), Livermore, CA, USA

<sup>3</sup>DYNAmore GmbH, Stuttgart, Germany

## 1 Introduction

In the last decade numerous research has been done in the area of *Isogeometric Analysis* (IGA). The intention of this rather new technology is the wish to have a stronger integration of *Computer Aided Design* (CAD) and *Finite Element Analysis* (FEA). Its basic idea is to use the same mathematical description for the geometry as well in the design process (CAD) as in the later analysis (FEA). One of the wide spread geometry description methodology in CAD-systems is the usage of *Non-Uniform Rational B-Splines* (NURBS) as basis functions. NURBS-based finite elements have been proven to be very well suited for computational analysis leading to qualitatively more accurate results in comparison with standard finite elements based on Lagrange polynomials. Therefore continuous development of Isogeometric Analysis has been added to LS-DYNA in the last years. The present contribution will give an overview about the current possibilities in LS-DYNA to use NURBS-based CAD-geometry description for numerical simulation and outline future plans for their enhancements.

## 2 NURBS-based shells

Up to now, the main focus of the IGA development in LS-DYNA is set on the implementation of NURBS-based shell elements.

### 2.1 Shell formulations

Basically three different shell formulations are available in LS-DYNA:

- A Reissner-Mindlin shear deformable isogeometric shell [1]
- A large deformation, rotation-free isogeometric shell [2]
- A hybrid version of the first two formulations, called blended isogeometric shell [3]

### 2.2 Regular NURBS-patches

At present, the analysis capability of isogeometric shells in LS-DYNA is limited to the use of so-called regular NURBS-patches. A regular NURBS-patch is represented as a rectangular grid of control-points in the parameter space. Despite this rather crucial restriction it is possible to join various patches within a multi-patch analysis.

#### 2.2.1 Multi-patch analysis: Joining of matching patches

A set of individual NURBS-patch definitions can be easily joined together once they use the same approximation space along their common boundary. This implies equal number and identical positions of control point pairs in the physical space and similar knot-vectors along the common boundaries. Given this requirement, the identical control points of either patch can be merged together.

#### 2.2.2 Multi-patch analysis: Joining non-matching patches

Given the case that two patches should be joined together without having the requirements given in the previous section, a special type of tied contact is currently implemented.

### 2.3 Application of boundary conditions

In NURBS-based finite element, the degrees-of-freedom (DOFs) are located at so-called control points, which are not necessarily part of the actual physical geometry. Therefore special attention is needed for the application of certain boundary conditions.

#### 2.3.1 Contact conditions

For the treatment of contact boundary conditions two possibilities are available in LS-DYNA:

- Standard contact via interpolation elements:  
An additional bi-linear quadrilateral mesh is constructed on the physical surface of either NURBS-patch. This can be thought of something similar to NULL-shells. These so-called interpolation elements do not take part in the actual computation and thus have no contribution to the stiffness of the shell, but their displacements are constrained to the displacements of the underlying NURBS-patch. Basically every standard contact type is available via this concept, so the contact acts between the interpolation shells and the contact forces acting on the interpolation nodes are then transferred to the actual degrees of freedom at the control points of the respective NURBS-patch.
- NURBS-contact:  
A new contact type has been implemented which uses the actual smooth NURBS-surface as the master segment in the contact formulation. With this a natural smooth contact type is available.

### 2.3.2 Nodal forces on the surface

For the application of concentrated nodal force-type boundary conditions, a new keyword has been implemented, which allows to add a massless node at any specific location of a NURBS-surface. The motion of this node is then constrained to the underlying NURBS-patch and the nodal forces applied at this node are distributed to the appropriate degrees of freedom at the control points of the NURBS-patch.

## 2.4 Analysis capabilities

Many of the standard analysis capabilities in LS-DYNA are also available for isogeometric shells

- Implicit and explicit analysis
- Eigenvalue analysis
- Comprehensive material model library
- Conventional mass scaling [4].

## 2.5 Trimmed NURBS

Most of the CAD geometries are so-called trimmed NURBS surfaces. In addition to an underlying regular NURBS-patch (see section 2.2), various trimming curves are defined to further specify if any areas shall be excluded from the actual surface geometry. Various research has been done to find a way to do the analysis on trimmed surfaces. Currently, an approach presented in [5] is being implemented into LS-DYNA.

## 3 NURBS-based solids

The implementation of NURBS-based solid elements has started and preliminary results will be shown in the presentation.

## 4 Pre- and Post-Processing with LS-PrePost

LS-PrePost is capable to read in IGES and STEP geometry files and convert them into an appropriate keyword format for LS-DYNA. Currently work is done to add the trimming capability. For the postprocessing a basic IGA file is already available but additional work is needed in the display of solution variables.

## 5 Summary

The present contribution gives an overview about the present capabilities in the area of isogeometric analysis in LS-DYNA and indicates future effort planned in this field.

## 6 Literature

- [1] Benson, D.J., Bazilevs, Y., Hsu, M.C. Hughes, T.J.R.: "Isogeometric shell analysis: The Reissner-Mindlin shell", *Computer Methods in Applied Mechanics and Engineering*, 199, 2010, 276-289
- [2] Benson, D.J., Bazilevs, Y., Hsu, M.C. Hughes, T.J.R.: "A large deformation, rotation-free isogeometric shell", *Computer Methods in Applied Mechanics and Engineering*, 200, 2011, 1367-1378
- [3] Benson, D.J., Hartmann, S., Bazilevs, Y., Hsu, M.C. Hughes, T.J.R.: "Blended isogeometric shells", *Computer Methods in Applied Mechanics and Engineering*, 255, 2013, 133-146
- [4] Hartmann, S., Benson, D.J.: "Mass scaling and stable time step estimates for isogeometric analysis", *International Journal for Numerical Methods in Engineering*, 102, 2015, 671-687
- [5] Nagy, A.P., Benson, D.J.: "On the numerical integration of trimmed isogeometric elements", *Computer Methods in Applied Mechanics and Engineering*, 284, 2015, 165-185



## IT PERFORMANCE/SCALABILITY I



# Improvement of Domain Decomposition of LS-DYNA R7 and R8

Mitsuhiro Makino

Dynapower corp., Japan

## 1 Motivation

Three type of domain decomposition as show in Fig.1 is tested by LS-DYNA MPP R6.

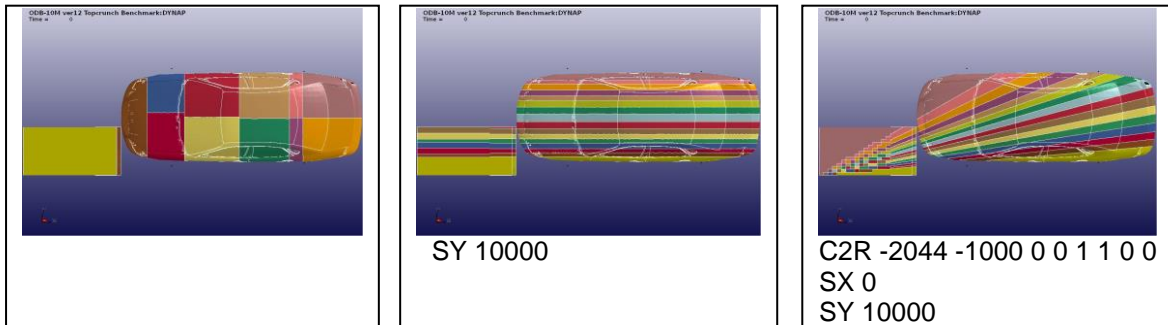


Fig.1: Three type of domain decomposition (a) default, (b) sy and (c) C2R

In the following figures, the performance is the wall clock time of 24cores SY decomposition divided by the each wall clock time, and the abscissa is the number of cores. As shown in Fig.2, the performance of default decomposition ( R6-default) is lower than the other two domain decomposition( R6-SY and R6-C2R).

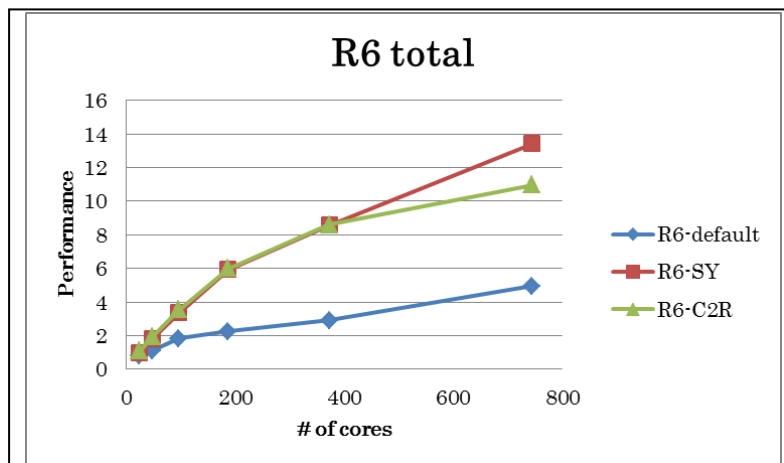


Fig.2: The total performance of R6.

Why the performance of default decomposition is lower than others?

## 2 Element cost evaluation of LS-DYNA MPP R8

User defined element cost for decomposition is developed in LS-DYNA MPP R8.

```

decomp {
  newcost
  shellcosts shell_costs.inc_NEW
  solidcosts solid_costs.inc_NEW
}

```

Fig.3: New costs defined in pfile

Figure 4 shows the result using the new cost evaluation. R8-default-new, which use the new cost for decomposition, is better than R8-defalut and more closer to R8-SY and R8-C2R.

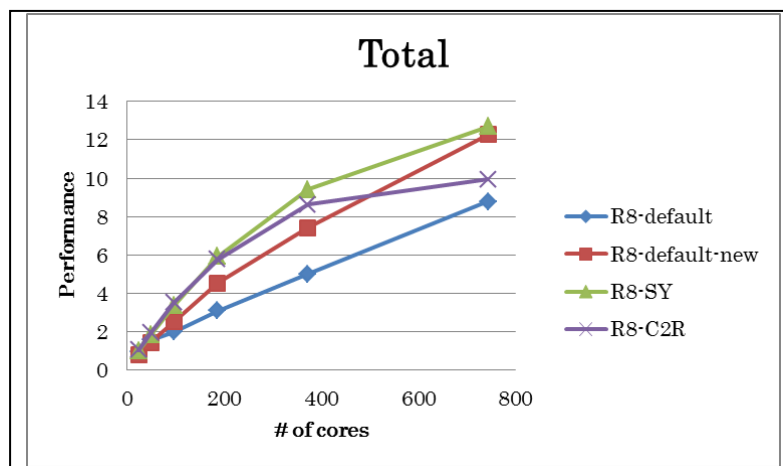


Fig.4: The Total performance of R8.

## 3 Summary

- In LS-DYNA MPP R8, user can define the element cost for domain decomposition.
- LS-DYNA MPP R7 can read the new element cost data shown in Fig.8, however, the new element cost data is created by LS-DYNA MPP R8.
- By using the new element cost data, the performance of default decomposition of ODB-10M is improved. The time step size of LS-DYNA MPP R8, which indicate the load imbalance of element processing, is reduced 28.4% from 47.5%.
- The performance of other decomposition ( SY and C2R ) with new element cost data, which do not shown in this paper, is not improved at this time. Since the time step size of LS-DYNA MPP R8 has 11.9% and 8.8% for SY and C2R, respectively, we need more tuning of element test data, because the set of simple data for element cost is provided by LSTC, and this data is not complete.
- Thick shell element and beam element have not yet to define the new element cost. The new element cost routine will extend to these elements in future.

## 4 Literature

- [1] Makino, M, Yamada, S: "ODB-10M New topcrunch Benchmark Data", 8<sup>th</sup> European LS-DYNA Conference, 2009, session24-2



---

# Performance Optimizations for LS-DYNA with Mellanox HPC-X Scalable Software Toolkit

Pak Lui<sup>1</sup>, David Cho<sup>1</sup>, Gilad Shainer<sup>1</sup>, Scot Schultz<sup>1</sup>, Brian Klaff<sup>1</sup>

<sup>1</sup>Mellanox Technologies, Inc.

From concept to engineering, and from design to test and manufacturing, the automotive industry relies on powerful virtual development solutions. CFD and crash simulations are performed in an effort to secure quality and accelerate the development process. Modern-day engineering simulations are becoming more complex and higher in accuracy in order to model closely to real world scenarios. To accomplish such design simulations virtually on a cluster of computer systems, LS-DYNA<sup>®</sup> decomposes large simulations into smaller problem domains. By distributing the workload and compute requirements across powerful HPC compute nodes that are connected via a high-speed InfiniBand network, the time required to solve such problems is reduced dramatically. To orchestrate such a complex level of communication between compute systems, the solvers of LS-DYNA were implemented with an interface to the Message Passing Interface (MPI) library (the de-facto messaging library for high performance clusters). MPI covers the communications between tasks within an HPC compute cluster. The recently introduced Mellanox HPC-X<sup>™</sup> Toolkit is a comprehensive MPI, SHMEM, and UPC software suite for high performance computing environments. HPC-X also incorporates the ability to offload network collective communication from the MPI processes onto the Mellanox interconnect hardware. In this study, we will review the novel architecture used in the HPC-X MPI library and explore some of the features in HPC-X that can maximize LS-DYNA performance by exploiting the underlying InfiniBand hardware architecture. The newly debuted Mellanox ConnectX<sup>®</sup>-4 HCA, which runs at 100Gb/s EDR InfiniBand and is supported by HPC-X, will be analyzed as well.

# Characterizing LS-DYNA Performance on SGI Systems using SGI MPInside MPI Profiling Tool

Tony DeVarco<sup>1</sup>, Olivier Schreiber<sup>1</sup>, Aaron Altman<sup>1</sup>, Scott Shaw<sup>1</sup>

<sup>1</sup>SGI

## Abstract

SGI delivers a unified compute, storage and remote visualization solution to manufacturing customers reducing overall system management requirements and costs. LS-DYNA integrates several solvers into a single code base. In this paper, the explicit solver is hereby studied for better matching with the multiple computer architectures available from SGI, namely, multi-node Distributed Memory Processor clusters and Shared Memory Processor servers, both of which are capable of running in Shared Memory Parallelism (SMP), Distributed Memory Parallelism (DMP) and their combination (Hybrid) mode.

The MPI analysis tool used is SGI MPInside. SGI MPInside features customary communication profiling. It also features "on the fly" modeling to predict potential performance benefits of the different upgrades available from the latest Intel® Xeon® CPU, interconnect and its middleware, MPI library, and the underlying LS-DYNA source code. We will also describe how the profile-guided mpiplace component is used to minimize inter rank transfer times.

Also outlined in the paper will be the SGI hardware and software components for running LS-pre/post via SGI® VizServer® with NICE Software and how, CAE engineers can now allow multiple remote users to create, collaborate, test, optimize, and verify new complex LS-DYNA simulations without moving their data.

## 1.0 About SGI Systems

SGI systems used to perform the benchmarks outlined in this paper include the SGI® Rackable® standard depth cluster; SGI® ICE™ X integrated blade cluster and the SGI® UV™ 2000 shared memory system. They are the same servers used to solve some of the world's most difficult computing challenges. Each of these server platforms supports LSTC LS-DYNA with its Shared Memory Parallel (SMP) and Distributed Memory Parallel (DMP) modes [1].

### 1.1 SGI® Rackable® Standard-Depth Cluster

SGI Rackable standard-depth, rackmount C2112-4GP3 2U enclosure support four nodes and up to 4TB of memory in 64 slots (16 slots per server). It also supports up to 144 cores per 2U with support of FDR InfiniBand, fourteen-core Intel® Xeon® processor E5-2600 v3 series and 2133 MHz DDR4 memory running SUSE® Linux® Enterprise Server or Red Hat® Enterprise Linux Server for a reduced TCO.

### 1.2 SGI® ICE™ X System

SGI® ICE™ X is one of the world's fastest commercial distributed memory supercomputer. This performance leadership is proven in the lab and at customer sites including the largest and fastest pure compute InfiniBand cluster in the world. The system can be configured with compute nodes comprising Intel® Xeon® processor E5-2600 v3 series exclusively or with compute nodes comprising both Intel® Xeon® processors and Intel® Xeon Phi™ coprocessors or Nvidia® compute GPU's. Running on SUSS® Linux® Enterprise Server and Red Hat® Enterprise Linux, SGI ICE X can deliver over 172 teraflops per rack and scale from 36 to tens of thousands of nodes.

SGI ICE X is designed to minimize system overhead and communication bottlenecks, and offers, for example the highest performance and scalability above 2000 cores for LS-DYNA topcrunch.org benchmarks with top-most positions six years running. SGI ICE X can be architected in a variety of topologies with choice of switch and single or dual plane FDR Infiniband interconnect. The integrated bladed design offers rack-level redundant power and cooling via air, warm or cold water and is also available with storage and visualization options

### 1.3 SGI® UV™ 2000

SGI UV 2000 server comprises up to 256 sockets (2,048 cores), with architectural support for 32,768 sockets (262,144 cores). Support for 64TB of global shared memory in a single system image enables efficiency of SGI UV for applications ranging from in-memory databases, to diverse sets of data and compute-intensive HPC applications all the while programming via the familiar Linux OS [2], without the need for rewriting software to include complex communication algorithms. TCO is lower due to one-system administration needs. Workflow and overall time to solution is accelerated by running Pre/Post-Processing, solvers and visualization on one system without having to move data.

Job memory is allocated independently from cores allocation for maximum multi-user, heterogeneous workload environment flexibility. Whereas on a cluster, problems have to be decomposed and require many nodes to be available, the SGI UV can run a large memory problem on any number of cores and application license availability with less concern of the job getting killed for lack of memory resources compared to a cluster.

### 1.4 SGI® VizServer® with NICE DCV

SGI® VizServer® with NICE DCV gives technical users remote 3D modeling tools through a web-based portal, allowing for GPU and resource sharing and secure data storage.

SGI VizServer with NICE DCV installed on a company's servers can provide LS-PrePost remote visualization capabilities through a software-as-a-service (SaaS) built in the company's private network. The LS-PrePost software is accessed through an easy-to-use web interface, resulting in simplicity for the end user. This solution provides intuitive help and guidance to ensure that less-experienced users can maximize productivity without being hindered by complex IT processes.

SGI VizServer with NICE DCV Components:

- **Engineer-friendly self-service portal:** The self-service portal enables engineers to access the LS-PrePost application and data in a web browser-based setting. It also provides security, monitoring, and management to ensure that users cannot leak company data and that IT managers can track usage. Engineers access the LS-PrePost application and data directly from their web browsers, with no need for a separate software installation on their local client.
- **Resource control and abstraction layer:** The resource control and abstraction layer lies underneath the portal, not visible to end users. It handles job scheduling, remote visualization, resource provisioning, interactive workloads, and distributed data management without detracting from the user experience. This layer translates the user request from the browser and facilitates the delivery of resources needed to complete the visualization or HPC tasks. This layer has a scalable architecture to work on a single cluster or server, as well as a multi-site WAN implementation.
- **Computational and storage resources:** The SGI VizServer with NICE DCV software takes advantage of the company's existing or newly purchased SGI industry-standard resources, such as servers, HPC schedulers, memory, graphical processing units (GPUs), and visualization servers, as well as the required storage to host application binaries, models and intermediate results. These are all accessed through the web-based portal via the resource control and abstraction layer and are provisioned according to the end user's needs by the middle layer.

The NICE DCV and EnginFrame software is built on common technology standards. The software adapts to network infrastructures so that an enterprise can create its own secure engineering cloud without major network upgrades. The software also secures data, removing the need to transfer it and stage it on the workstation, since both technical applications and data stay in the private cloud or data center. These solutions feature the best characteristics of cloud computing—simple, self-service, dynamic, and scalable, while still being powerful enough to provide 3D visualization as well as HPC capabilities to end users, regardless of their location.



## IT PERFORMANCE/SCALABILITY II



# Fast Road Barrier Car Safety Calculation on a Cray XC

Jarosław Cholewiński<sup>1</sup>, Marcin Piechnik<sup>1</sup>, Andreas Findling<sup>2</sup>, Greg Clifford<sup>2</sup>

<sup>1</sup>Stalprodukt S.A.

<sup>2</sup>Cray Computer Deutschland GmbH

EN1317-1 and 2, describing assessment methods for carry on real crash tests evaluating road restraint systems. In the last six years about 100 full scale crash tests were performed according to EN 1317 by Stalprodukt S.A. As a conclusion several standard weakness were found in EN1317 and these include:

Only basic information for impactor models.

Tolerances for test performing.

Raw materials are delivered according to standards proper for steel suppliers have large scope of mechanical properties (from users point of view) it is difficult to use proper parameters. A lot of additional equipment can be installed for road restraint systems like motorcyclist protection and acoustic panels. It is not possible to perform full scale crash tests for all devices in all configurations.

To reduce the problems described above the LS-Dyna software is used with high satisfaction.

There are three main ways for solving problems when using LS-Dyna:

Creation of new products according to Design of Experiment (DOE) method.

When desired properties under impact are not achieved in a full scale crash tests but at the same time the general result of the test is positive it is possible to modify the device in order to achieve the desired properties.

When a road restraint system is used in a specific installation conditions or additional equipment are installed to the barrier.

The need to carry out large amounts of computation was observed during year's 2012, 2013 and 2014. The CRAY XC30 was chosen as solution. Significant reduction of the required time was observed for the validation of a model and designing of new devices. How native LS-Dyna software is supported on the XC30 is explained.

# Cost-Effective Sizing of Your HPC Cluster for CAE Simulations

Nils Henkel<sup>1</sup>, Sebastian Treiber<sup>1</sup>

<sup>1</sup>GNS Systems GmbH

## 1 Abstract

Computer aided engineering (CAE) is a very important part of product development, especially in the automotive industry. At the core of each CAE department stands a compute cluster which is used to run mostly finite element solvers in order to simulate car crashes, airbag inflation and many more physical processes. Almost every software vendor for CAE solvers uses a different license model. Especially the formula for the token scaling (number of tokens as a function of the CPU cores used) is unique for each solver type.

In this work, we present a method to derive the total costs of a single solver run and propose possibilities to increase the efficiency of small to medium sized CAE clusters. Instead of deriving general instructions, we show how specialized analysis of license models, solver behavior and hardware options can be used to maximize efficiency.

## 2 Summary

We used straightforward theoretical considerations in combination with benchmarks for CAE solver jobs in order to derive the total costs of a single CAE solver run. We chose three typical CAE solvers (LS-Dyna, Abaqus, Ansys) to present methods on how the efficiency of small to medium sized CAE clusters can be maximized. The most important results are:

- License costs are higher by roughly a factor of ten than hardware costs
- Using a CPU which fits well to the license model of the solver used, can increase efficiency.
- Under certain conditions, underloading of hardware could be an opportunity to increase efficiency as well and is certainly worthwhile investigating for your specific jobs.



# Cloud-Enabled CAE Solutions: Requirements, Basic Concepts and Usability

Alexander Heine

CPU 24/7 GmbH

Up-to-date, particularly commercial methods of numerical simulation are able to meet requirements of modern product development and optimisation processes. However, essential prerequisite is not only the application software but also the appropriate High Performance Computing (HPC) resources. Specific applications, like simulation of large models with a very high number of grid points, CFD-driven design optimisation with necessary innumerable variations as well as complex, multidisciplinary problems regarding the simulation of iterative interactive effects are typical examples of getting efficient, high-quality, prompt and precise results only through appropriate High Performance Computing.

Recent studies predict an annual growth rate of 7.4 per cent for High Performance Computing between 2013 and 2018, and in the field of computational fluid dynamics (CFD) a rate of 7.3 per cent is forecast for the same period.<sup>1</sup> This development is very evident, and the application of High Performance Computing (HPC), especially for CAE, is likely to rise by 9.4 per cent between 2011 and 2016.<sup>2</sup> Over the past four years there has been an increase of around 10 per cent in the number of companies transferring their HPC workloads to the Cloud.<sup>1</sup>

But not every company is in position to provide such resources in an appropriate amount or – if available at all – to use them continually and efficiently. The necessary infrastructure, especially with regard to technical and personal resources, is cost-intensive and time-consuming. Thus, own HPC infrastructures tie up a lot of capital given also the fact that technology is rapidly changing and improving. So why not renting required computing capabilities, in other words to make use of cloud-enabled CAE solutions?

Cloud-enabled CAE solutions allow users renting high performance computing hardware along with licenses to compute resource-intensive applications for a specified period of time in order to increase feasibility, accuracy and performance as well as efficiency of CAE simulations. Furthermore, cloud-enabled CAE solutions can be seen as a reliable way to absorb project driven peak loads with as little effort as possible enabling companies of every size to activate and make intensive use of scalable computing resources.

But the whole field of outsourcing High Performance Computing resources to a cloud-based infrastructure still meets with considerable skepticism and their usage is still correspondingly limited. This is not surprising given the sensitivity of data that can have a decisive effect on competitiveness. Besides, cloud services focusing on CAE vary significantly regarding their business models. The relatively new and rapidly growing cloud market makes it difficult for engineers to choose the appropriate CAE cloud provider.

From the end user's perspective it is crucial to make these services available in the most transparent, secure and efficient way, e.g. ownership of the hardware, additional communication providers/suppliers, virtualised environments, data transfer export rules etc.

Potential users in the B2B sector are inhibited in particular by various issues and concerns. Data security, cost, usability, adaptability, hardware and software, as well as support and remote connection, were identified as the most important factors.<sup>3</sup>

But these concerns can be handled or even removed if stakeholders understand what finally characterises a CAE cloud from a technical point of view and what happens with processed data.

This paper describes the progress in cloud-enabled CAE solutions. More precisely, it covers their requirements, the basic cloud concepts and their state-of-the-art utilisation in computer-aided engineering. Moreover, the paper shows the risk of non-transparent resource provider models when running simulations on different platforms.

Important criteria and challenges are always the underlying cloud infrastructure, scalability, bottlenecks (data transfer, network interconnection, licenses, etc.), security aspects and offered support models.

The following technical issues will be addressed in detail:

- Data security – Where is the data located and what security measures are being taken?
- Performance – What performance can be expected when running CAE simulation on an HPC cloud infrastructure? What about their scalability?
- Data Transfer – How can data be transferred both efficiently and effectively?
- Access – How are compute resources accessed and applications started? Is it possible to monitor a running calculation or to even analyse calculations results in the cloud?
- Parallel Computations – What is the best partitioning when considering queuing systems in reference to CAE applications?
- Storage – What storage system is the most efficient?
- Support – What about licenses, consulting and customising? What service and support can be expected?

Examples with *LS-DYNA* serve as evidence of all these aspects. Related benchmarks using CPU 24/7 dedicated bare metal servers of various generations indicate reasonable scalability and performance. The paper shows e.g. a downgrade between virtual machines and bare metal providers.

Furthermore, it is shown that application-specific and –optimised HPC platforms are a viable alternative for small and medium sized enterprises to efficiently solve sophisticated CAE problems.

[1] International Data Corporation (IDC), 2014: IDC HPC Update at ISC'14.

[2] Earl Joseph, IDC, 2013: A Worldwide Overview of the HPC Market, Global Trends, Major Changes and Five Year Predictions.

[3] Technical University of Berlin et al, 2015: Abschlussbericht, Capital Cloud Infrastructure (CCI): Vertrauenswürdige Infrastruktur für Capital Cloud.

## IT – CLOUD I



# Collaboration for Future HPC-based Simulation Technologies

Dipl.-Ing. Alexander F. Walser

<sup>1</sup> Automotive Simulation Center Stuttgart e.V.

## 1 Motivation

The use of Numerical Simulation and High Performance Computing (HPC) in vehicle development has already been established for years. Nowadays it is the third pillar of vehicle development along with construction and testing. Computer Aided Engineering (CAE) methods in combination with HPC technologies enable engineers to solve complex problems in a quick and cost-effective way long before hardware prototypes are available. Furthermore it opens up the possibility to analyze not just a single concept idea, but many concept variations parallel. But there are some future challenges in the field of virtual vehicle development. Automotive Original Equipment Manufacturer (OEMs) and suppliers are faced with the need to bring the enormous complexity of interacting system components with the increasing demands on safe, green and smart vehicles with high quality standards in line (Fig.1). In order to minimize the integration costs and reduce time-to-market it is important not only to provide new simulation environments, but also to keep them flexible. New strategies are needed to handle large amounts of data, to facilitate the best possible interplay of soft- and hardware and to optimize the exchange of simulation data along the supply chain. The expectations on numerical simulation software and work flow tools are permanently increasing and therefore the innovation pressure is very high. Just as vehicles must be continuously developed and optimized, a constant adjustment and refinement of CAE methods are necessary to ensure the increasing demand on forecast quality. To stay competitive development tasks should be solved by exploiting the full potential of HPC-simulation technologies. Therefore the development and implementation of new numerical methods are just as important as the change of soft skills of CAE users from a single-domain to a multi-domain simulation expert. The Automotive Simulation Center Stuttgart e.V. – asc(s) is exactly facing these trends. As a non-profit association the asc(s) is working actively on research and development of new CAE methods through bundling the best competences from science and industry in its strong network.

### Safe, green and smart vehicle with high quality product complexity

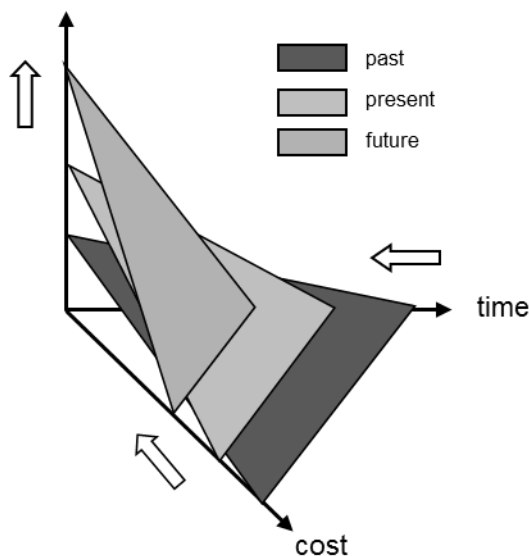


Fig.1: "Magic Triangle" of product development

## 2 Collaboration Platform for Future HPC-based Simulation Technologies

DYNAmore is a founding member of the Automotive Simulation Center Stuttgart e.V. – asc(s). This non-profit association was established in 2008 with tailwind of the German automotive industry as part of the federal HPC-strategy of Baden-Württemberg. It is funded through annual membership fees and third-party contributions. Today more than 20 international members from science and industry are working together to ensure the rapid availability of ISV codes for the next generation of HPC-architecture (Fig.4). The asc(s) boosts the innovative power of automotive industry by bringing automotive manufacturer, suppliers, soft- and hardware vendors, engineering service providers and science together in the pre-competitive research stage for simulation technologies which require high performance computing systems. The business model of the asc(s) is based on the four columns cooperation, competence network, joint project definition and cost-efficient project realisation. Within the asc(s) directly competing companies work together hand in hand acquiring new impulses for the development of their products.

Cooperation - Science and industry cooperate by:

- permanent partnerships and cooperation for joint industrial research
- cooperation at the pre-competitive stage
- fast, commercial availability of high-quality research results

Competence - Use of the competence network by:

- combining simulation expertise from member companies
- avoiding overheads through highest expertise
- solving specific project tasks with the help of national and international experts

Projects - Goal-oriented project handling

- by direct relation to industry
- due to project prioritisation by members
- by taking over the complete project management

Costs - Cost-optimised project implementation by:

- provision of HPC resources for supported projects by the Federal High-Performance Computing Center - HLRS
- provision of CAE licences for joint projects, generally free-of-charge
- application for external funds

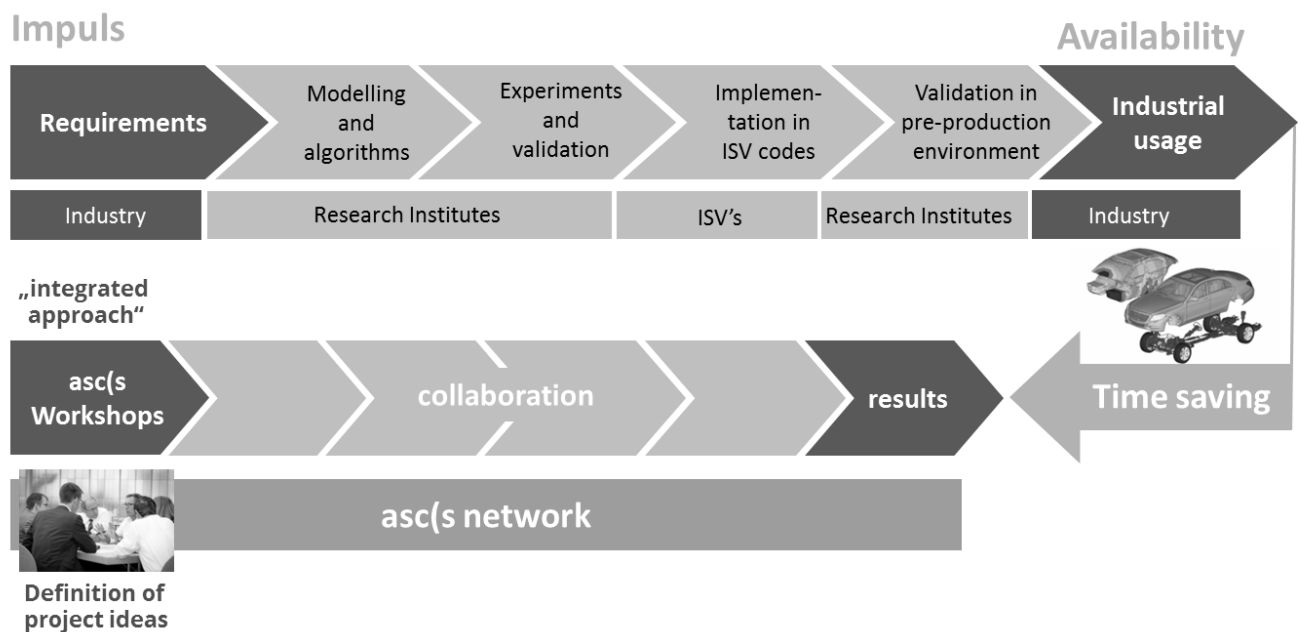


Fig.2: Shortening time to solution through collaboration within the asc(s) network

# CAE as a Service as Cloud Platform for the Full LS-DYNA Simulation Process

Alfred Geiger<sup>1</sup>, Karl-Heinz Hierholz<sup>2</sup>, Christer Neimöck<sup>2</sup>

<sup>1</sup>T-Systems Solutions for Research GmbH

<sup>2</sup>T-Systems international GmbH

## 1 Overview

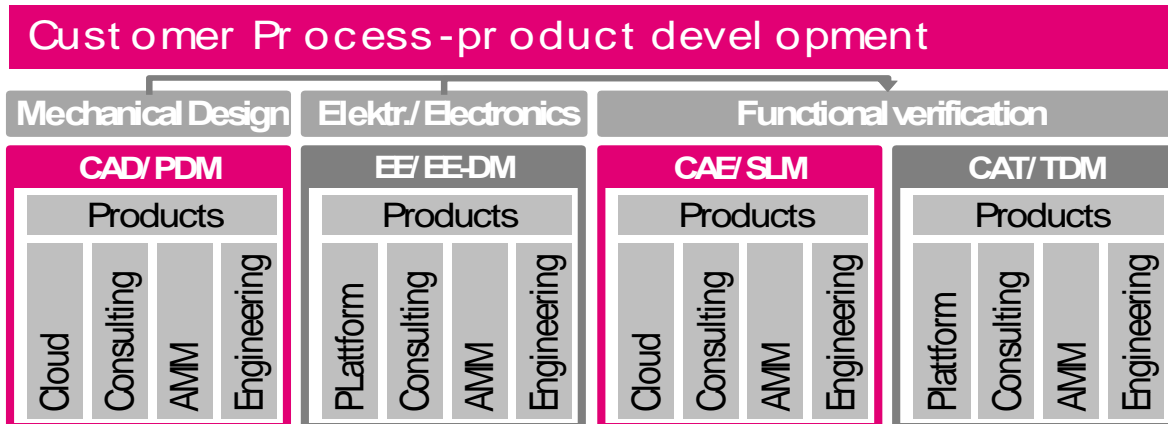
CAE has emerged as important pillar along the marked phases of the product development process - from early predevelopment over the product development and product verification.

T-Systems will subsequently present a Software as a Service and Process as a Service Solution, lowering the entry barriers for CAE usage and replacing high CAE CAPEX with variable costs.

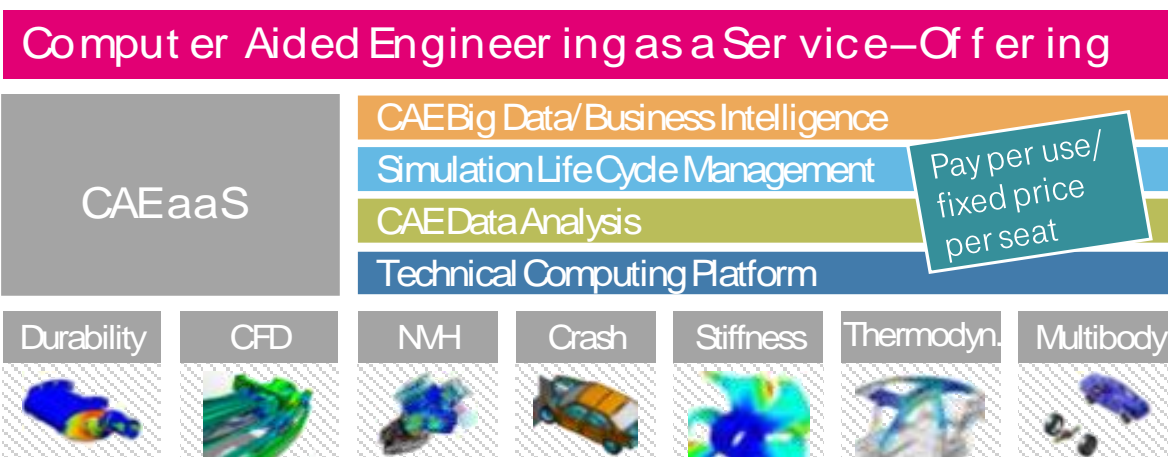
## 2 Cloud based solution concept

T-Systems is the No. 1 automotive IT-Supplier in Germany. It combines it's vast experience in supporting the PLM processes of Automotive, aerospace and manufacturing industries with it's worldwide network of high security and performance datacenters to systematically leverage the customer processes into scalable cloud based Process as a Service / Software as a Service offerings.

T-Systems addresses the standardization and cloudification of it's customer's product development sub processes one by one, starting with CAE and CAD/PLM as a Service:



The CAEaaS Solution addresses the whole CAE process and the infrastructure, platform, software and process level, as shown in the following business architecture overview:



Customer use cases:

1. Technical Compute Platform
  - Scalable capacity for high throughput (via virtualized HPC Cloud-Platform)
  - Scalable capability for large problem sizes (via private-public partnership hww)
2. Simulation Process- and Infrastructure Outsourcing
  - Provides the full PLM subprocess CAE as a service (Platform-, Software-, Process as a Service)
3. Business to Business (OEM/OEM/OES)
  - B2B engineering hub with secured collaboration for OEM/OEM & OEM/OES cooper. Projects

Customer value (relevance of 1/2 depending on specific customer situation):

1. Benefits of faster and improved CAE usage (better accessible CAE)
  - Faster time to market, higher # of variants and reaction to market
  - Reach high maturity level early (frontloading), reduce costs
  - Reduces # of expensive physical prototypes and buildup time
2. Benefits of offered SaaS model
  - Flexible, secured and fast accessible on demand CAE capabilities
  - Replace fix or stepwise fix high CAE costs with "pay per use" costs
  - Cost savings > 20% in infrastructure, licenses, storage & graphics\*

Data security and integrity:

CAE data and environments typically contain highly confidential data of products still to be released. T-Systems ensures highest security, privacy, and integrity for data and processes via its high security Twin-Core Data centers, T-Systems and Deutsche Telekom's German network and cloud security standards. The initial production environment will be the Magdeburg/Biere Twin core cloud data center - one of 11 Twincore Cloud-Data-Centers of T-Systems worldwide. Characteristics:

- o 5.400m<sup>2</sup> Datacenter surface area, 2 x 7 MW IT connected power
- o PUE Factor 1,3 for air cooled systems, Air- and water cooling
- o Redundant and uninterruptible power supply
- o SOX compliant distance of twin cores of >10 miles
- o High distance to risk infrastructure (Airport, water, ...)
- o Optimal connection to supply infrastructure (Energy, grids)
- o Full electromagnetic Shielding
- o Multiple redundant grid connection
- o Optimized Object security

Highest compute power to Solve large problems: Dynamic HPC-Capacities of the hww:

Flagship: Cray XC-40 (HORNET): 3.944 Compute-nodes with 94.656 Intel Haswell Cores, 3,84 Pflop/s (Upgrade in Preparation (> 7 Pflop/s))

Other HPC-Systems: IB-coupled x86-Clusters, Ca. 1.500 nodes intel Xeon (SNB/IVB/HSW)

Application- and user-support solution

The user support starts with a 1<sup>st</sup> level UHD (user help desk) for technical and functional support. It is extended by the 2<sup>nd</sup> and 3<sup>rd</sup> level technical and functional support, in collaboration with the independent Software Providers (ISV's)

**3 CAEaaS as part of the broader T-Systems Cloud-Initiative for the Industry**

CAEaaS is part of a broader T-Systems initiative for cloud based industry solutions also containing "Data Discovery As a service", "Geospatial Analysis as a service", "Genome Analysis as a service".

**4 Summary and vision**

For the manufacturing industry's level 0 core process product development, CAE is one first sub process which is systematically leveraged to a Software as a Service / Process as a Service Solution. Based on the same technology, T-Systems will provide CAD/PLM cloud based solutions and engineering workplaces and environments.

CAEaaS addresses main Market Trends, Business pain Points, IT Pain Points with a scalable Software as a Service / Process as a Service Solution lowering the entry barriers for CAE usage and replacing high CAE CAPEX with variable costs.



# Experiences with LS-DYNA on Cloud-like Infrastructure

Prof. U. Göhner

DYNAmore

# CAE Cluster in Microsoft Azure

T. Karmarkar, N. Greising  
Microsoft

S. Bala  
LSTC

## IT – CLOUD II



---

# Making HPC Accessible for SMEs

Andreas Wierse<sup>1</sup>

<sup>1</sup>SICOS BW GmbH

## 1 Motivation

Numerical computation, often also named simulation, plays in many enterprises an important role in the development process nowadays. Especially in large companies in the automotive or aerospace industry its actually impossible to develop a new product without simulation technology. In recent decades the necessary know-how and personnel has been built up, but there have also been and will be significant investments into the infra structure.

Investments that can be handled easily by large companies, can be a real challenge for an SME. Especially an Return on Investment (ROI) calculation is much more critical for smaller companies. In addition the usage of the infra structure depends stronger on the sequence of projects. For smaller companies it is much more difficult to keep the load well balanced, which in turn makes the technology more expensive. This effect is visible even in larger companies.

A third issue that comes up especially at smaller enterprises: what can be done if a numerical simulation is too big for the available hardware or would block it for days or weeks.

## 2 Usage of a Supercomputer

A solution for the problems mentioned in the introduction could be to buy compute time at an external resource. Even Amazon provides resources today that could be used for this kind of numerical simulations; however compared to computers that are really optimized for numerical simulations these systems do not deliver the performance that specialized computers can provide.

Normally these powerful supercomputers are not available for industrial users. Typically they are installed at research centres and universities and allow only research use, implying a publication of the results. This is not acceptable for enterprises in most cases (except perhaps for pre-competitive issues), especially not for regular productive use.

An exception offers the High Performance Computing Centre Stuttgart (Höchstleistungsrechenzentrum Stuttgart, HLRS): the Cray XC40 (currently with more than 2.7 PetaFLOPS on position 16 in the Top500 list of the worlds fastest computers) is open for industrial users for the simulations. In a long tradition of cooperation between research and industry in the state of Baden-Württemberg high performance computing plays an important role. Porsche for example performs a large part of its computations on HLRS systems since a long time, not the least due the reasons mentioned above, especially the flexibility.

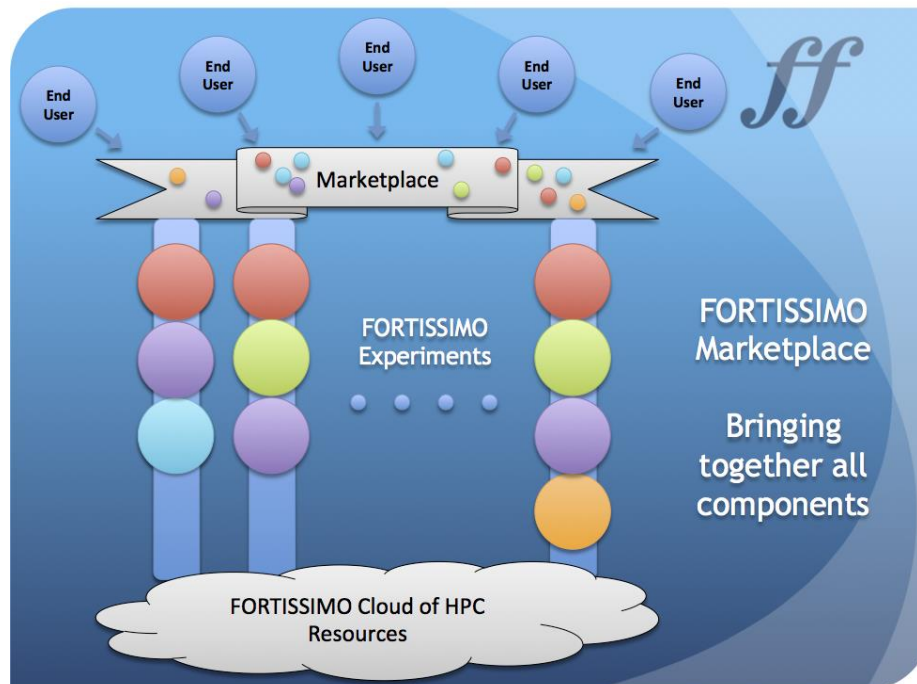
## 3 Access and Security

The access to the HLRS systems is for security reasons obviously restricted; however this is realized in a way that still allows to integrate them into the work flow. Important is a fully encrypted access using Secure Shell (ssh) mechanisms. Users are clearly separated from each other, compute nodes are always exclusive to the current user and access is organized via batch queues (typical for such large systems with many users).

Bandwidth always is an issue, especially in the context of large computations. In most cases the bottle neck is on the users side, since HLRS is connected to the state wide research net with a bandwidth of several 10s of Gbit/s, soon 100 Gbit/s. But also for smaller bandwidths technology is available to support a reasonable access: remote visualisation with tools like VNC allows the users to leave their data sets on the system and just stream the video of a visualisation session; this works well, even with bandwidths in the order of 10 Mbit/s

#### 4 Fortissimo

Fortissimo is an EU-funded project to support especially small and medium sized enterprise to use HPC technology supported by cloud technology. Initially 45 partners, now close to hundred are working to develop the infra structure requirements that allow SMEs to find the right partner for the solution of their simulation problem quickly. A Fortissimo Marketplace will be established, where potential HPC users, HPC experts, Independent Software Vendors (ISVs) and HPC resource providers/computing centres can find each other. In addition tools will be developed to make the usage as easy as possible.



#### 5 Summary

Even if Supercomputing sounds expensive, it is well within the reach of even small and medium sized enterprises. Simulation tools are available as well as fairly easy to use access methods and the costs are very reasonable. SICOS and its shareholders in Karlsruhe and Stuttgart are working continuously to improve the accessibility even further; we are open to support SMEs to learn how to use this important technology to improve their competitiveness.

---

# Scaling LS-DYNA on Rescale – HPC Cloud Simulation Platform

Joris Poort, President & CEO, [Rescale, Inc.](#)

Ilea Graedel, Manager, Rescale, Inc.

## 1 Cloud HPC for CAE Simulations

Engineering and science simulations demand an increasing amount of computing resources. The majority of those resources consist of high performance computing (HPC) hardware, which are adaptable and highly efficient for running simulation software. Enterprises strive to create a lean and agile IT structure that both meets the current and unanticipated future needs of the various internal teams—without creating a cost structure that is unsustainable or disconnected from justifiable activities.

Simulation driven design has become an indispensable tool for product development. Across all industries, simulation is driving a paradigm shift from traditional physical test and design to virtual prototyping, design space explorations and optimizations that evaluate what-if scenarios and trade off studies. As a result, organizations are running engineering simulations that are far more comprehensive and accurate, driving innovation and competitive advantage. The dramatically increasing and highly variable user demand for simulation presents a daunting challenge for traditional IT systems that cannot provision peak demand, resulting in delays and bottlenecks. Providing state-of-the-art HPC resources that carry the computing horsepower and scalability while remaining elastic and flexible are key to deliver on these new IT demands.

## 2 Rescale: Enterprise Cloud HPC Simulation Platform

Rescale is the leading, globally located, highly secure cloud simulation platform specifically designed for computer-aided engineering (CAE) analyses. With a focus on high performance computing (HPC), Rescale provides an innovative solution for enterprise companies to seamlessly execute complex simulations, instantly from anywhere in the world. Lengthy procurement cycles are eliminated, operating and capital expenses are drastically reduced, and engineering and science needs are instantly met.

## 3 Running LS-DYNA Simulations on Rescale's Cloud Simulation Platform

Engineers and scientists access the Rescale cloud simulation platform through a web portal or using Rescale's API tool. Once in their account, they can select the LS-DYNA software, customize hardware configurations, and post-process results. Optimized workflows guide users through the process of setting up simulations in a matter of minutes.

Rescale partners with external data centers around the world to offer enterprise companies access to hundreds of thousand of HPC cores instantly. Data centers are located throughout North and South America, Europe, and Asia. Using the interface, users choose the hardware best suited for every simulation from an extensive list that includes standard CPUs, HPC, InfiniBand connection hardware, and GPUs, among others.

In addition to instantly expanding resources and utilizing customized hardware, engineers and scientists can avoid file transfer times by accessing Desktops, Rescale's remote visualization tool. Users can open a Desktops session, select LS-DYNA Pre/Post and add the simulation they'd like to visualize. From there, users can view and modify files and results directly from Rescale without downloading output files to their local machine.

The screenshot displays the Rescale LS-DYNA web interface. At the top, there's a navigation bar with 'New Job', 'Jobs', 'Desktops', and 'Files'. The main header shows 'LS-DYNA' and a 'Submit' button. Below the header, a workflow diagram illustrates the process: 'Input' leads to 'LS-DYNA' (with 'Hardware Settings' below it), which then goes to 'Post Processing', and finally to 'Output' (with 'Filters' below it). The 'Job Type' is set to 'Basic'. The 'Setup (3/5)' panel on the right includes options for 'Input File(s)', 'Software Settings', 'Hardware Settings' (checked), 'Post Processing (Optional)', and 'Review'. The 'Hourly Price Summary' shows 'Nickel Core (x64)' at \$9.60/hour and 'LS-DYNA' at \$8.25/hour. The 'Specify Hardware Settings' section features a table of core types and a 'Hardware Summary' grid.

Type	Memory	Compute	Interconnect	Storage	Price
Marble Standard	3.8 GB	3.00	Standard	40.0 GB SSD	\$ 0.10
Nickel HPC+	3.8 GB	6.75	10 Gb/s	40.0 GB SSD	\$ 0.15
Onyx HPC++	3.3 GB	7.33	10 Gb/s	36.0 GB SSD	\$ 0.20

The 'Hardware Summary' shows a 4x4 grid of nodes, with a total of 4 nodes selected. Below the grid, the summary table is as follows:

Compute	Memory	Storage
432 CU	240.0 GB	2.6 TB

Fig.1: Figure 1 Customize high performance computing (HPC) hardware

#### 4 Summary

Rescale provides an intuitive cloud simulation platform optimized to run complex LS-DYNA simulations. Enterprise companies can instantly access a range of customizable high performance computing hardware and leverage an elastic, dynamic platform designed to reduce capital and operating expenses while meeting the demands of various engineering and science teams. Users can execute multiple LS-DYNA simulations in parallel, monitor simulation progress in real time, and view results directly in the browser. Lengthy file transfer times are eliminated as users analyze completed LS-DYNA simulations directly in Rescale's platform using the built in remote desktop visualization feature, Desktops. This paper explores in more detail, the full capabilities of Rescale's cloud simulation platform and how enterprise companies can leverage cloud HPC to optimize and accelerate LS-DYNA simulations.



---

# HPC in the Cloud: Gcompute Support for LS-Dyna Simulations

Iago Fernandez<sup>1</sup>, Ramon Díaz<sup>1</sup>

<sup>1</sup>Gcompute (Gridcore GmbH), Stuttgart (Germany)

During the last decades, companies have been introducing CAE simulations as part of their product development with the main objective of improving reliability and reducing the costs of prototyping. It is nowadays demonstrated that introducing simulations during an early step of the product design process reduces the risk of failure as well as the associated costs, when the prototypes need to be redesigned.

Traditionally, enterprises have invested in geographical independent local workstations or clusters that nowadays resulted in non-connected computational units. Besides, CAE Software used for analyzing problems like crash tests or impacts resulted in an essential tool for any Engineer, forcing the growth and development of faster and more powerful computing stations. In order to make the hardware investment more efficient, enterprises are considering new solutions like consolidation of internal resources with Private Enterprise Cloud Environments or External HPC Cloud Services. New challenges arise with this technology such large data transfers and 3D remote visualization over medium to high latency links.

Gcompute has been developing HPC solutions since 2002 to cover these needs both for enterprises and small consultants, offering a complete portfolio that allow users to fulfill all his needs from a unique HPC partner.

# Smart Manufacturing: CAE as a Service, in the Cloud

Wolfgang Gentsch

The UberCloud Inc.

The benefits for small and medium size enterprises (SMEs) of using high performance computing (HPC) technology within their design and development processes can be huge, such as enormous cost savings; reducing product failure during design, development, and production; develop optimized processes; achieve higher quality products to keep existing and gaining new customers; and shorten the time to market. Potentially, all this can lead to increased competitiveness and more innovation.

However, less than 5% of manufacturers are using HPC servers for computer simulations to design and develop their products, according to the two studies, 'Reflect' and 'Reveal', from the US Council of Competitiveness, [1]. The vast majority (about 95%) of the companies perform virtual prototyping or large-scale data modelling still on their desktop computers (workstations or laptops). But, 57% of these companies said that they have application problems that they can't solve with their existing desktop computers, because their desktops are too slow for the problems they want to solve, or because geometry or physics are too complex and need more memory than is available from their desktop. Therefore, most of these companies have a real need for high performance computing.

There are two realistic options today how to acquire additional HPC computing power beyond what is available from the desktop system. One option (which is widely proven to work) is buying an HPC server which is many times faster than what engineers currently have available on their desk. However, for many companies, especially SMEs, buying a large HPC server is often not a viable alternative. One reason for this is the high and complex Total Cost of Ownership, TCO, as demonstrated from IDC [2].

In addition to the high cost of expertise, equipment, maintenance, software, and training, there are often long and painful internal procurement and approval processes, and additional skills and manpower are needed to operate and maintain such a system. Still, buying an HPC server is one possible option for an SME, and several HPC vendors have developed a complete ecosystem of HPC products, solutions, and services, and developed the corresponding go-to-market strategy to sell HPC servers to those SMEs who have decided to buy their own HPC system. Therefore, in this study, we will not discuss this option further, but just investigate the second option, in the following.

The second viable option for SMEs to experience the benefits from HPC without having to buy and operate their own HPC system themselves is recently offered by cloud computing. HPC in the Cloud allows the SME engineers to continue using their own desktop system for daily design and development work, and to submit (burst) the (sometimes much) larger, more complex, more time-consuming jobs into the cloud. Additional benefits of the HPC Cloud solution are on-demand access to 'infinite' resources, pay per use, reduced capital expenditure (CAPEX), greater business agility, higher-quality results to keep existing and gaining new customers, lower risk, lower product failure rate, and dynamically scaling resources up and down as needed.

In the following, we present an overview of the status and trend of HPC in the Cloud for the manufacturing SME market [3] and look at the competitive landscape of current Cloud resource and software providers [4]. We include an outlook on how the UberCloud Experiment [5], [6], [7] can accelerate the process of go-to-market and customer acceptance. Finally we present several UberCloud Experiment case studies, among others one with end-user CaelynX, software provider DYNAmore, and resource provider CPU 24/7, running a full car crash simulation with LS-Dyna in the cloud.

## CAE PROCESSES



# Crashworthy Design of Composite Structures using CAE Process Chain

Madhukar Chatiri<sup>1</sup>, Thorsten Schuetz<sup>2</sup>, Anton Matzenmiller<sup>3</sup>

<sup>1</sup>CADFEM GmbH, Grafing / Munich, Germany

<sup>2</sup>Adam Opel AG, GME Vehicle CAE, Ruesselsheim, Germany, thorsten.schuetz@de.opel.com

<sup>3</sup>Institute of Mechanics, University of Kassel, Kassel, Germany

## 1 Summary

The materials used in automotive industry should play key role in overcoming the current challenging demands such as increased global competition, need for vehicles with highest efficiency, reduction in costs, stringent environmental and safety requirements. This eventual usage of lighter materials mean lighter vehicles and low greenhouse gas emissions. Composites are getting more recognition and hence being used increasingly in the automotive industry due to their excellent weight specific characteristics such as strength and stiffness. Hence the requirements for simulations along the complete production process chain involving reinforced plastics have increased immensely. The main objective of this presentation is to present a workflow for numerical modeling and simulation of carbon fiber reinforced plastic (CFRP) composite structures including computer aided engineering (CAE) process integration. In this regard, a computational constitutive model for anisotropic damage is developed to characterize the elastic-brittle behavior of fiber-reinforced laminated composites. The presented work will introduce and discuss single steps along the process chain with in-house tools and commercial finite element program LS-DYNA.

**Keywords:** CFRP, CAE process chain

## 2 CAE process chain

The various manufacturing technologies of CFRP composite structures have to be represented in the finite element simulations in order to capture possible failure during production processes and exactly map the fiber orientations. This CAE tool chain [1] is explained for thick and thin composite structures. High pressure hydrogen storage system (HSS) for fuel cell vehicles with an operating pressure of 70 MPa is made of CFRP laminate with wall thickness of 40mm to 60mm. Here, three aspects are important. Firstly, the vessel has to fit into the given package space of the vehicle. Secondly, the vessel has to withstand a certain inner pressure and third, the vessel plus integration features have to pass certain vehicle crash acceptance criteria. Thus it is necessary to integrate the high pressure vessel into standard CAE processes in order to work on these aspects in the early phase of a fuel cell vehicle development. The aspect of data importing/exporting interface between individual tools, especially between the wet-winding process simulation and the FEA tools is quite efficiently done in the current tool chain (see **Fehler! Verweisquelle konnte nicht gefunden werden.**).

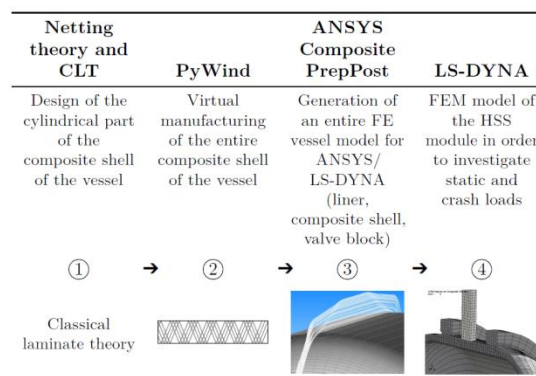


Fig.1: CAE process chain for thick walled composite structures.

### 3 Constitutive modeling of composite structures

A computational constitutive model for anisotropic damage is developed to characterize the elastic-brittle behavior of fiber-reinforced laminated composites. The composite damage model is implemented within LS-DYNA® [2] as user defined material subroutine which can describe progressive failure and damage behavior of carbon fiber reinforced plastic (CFRP) composites [3]. A homogenized continuum is adopted for the constitutive theory of anisotropic damage and elasticity. Damage initiation criteria or first ply failure prediction is based on Puck failure criterion and progressive damage is based on continuum damage mechanics. Internal variables are introduced to describe the evolution of the damage state under loading and as a consequence the degradation of the material stiffness occurs. The corresponding rate equations are subjected to laws of thermomechanics. Emphasis is placed on a suitable coupling among the equations for the rates of the damage variables with respect to different damage modes. The integrated routine is successfully utilized to predict failure and damage of composite laminates which are subjected to impact conditions.

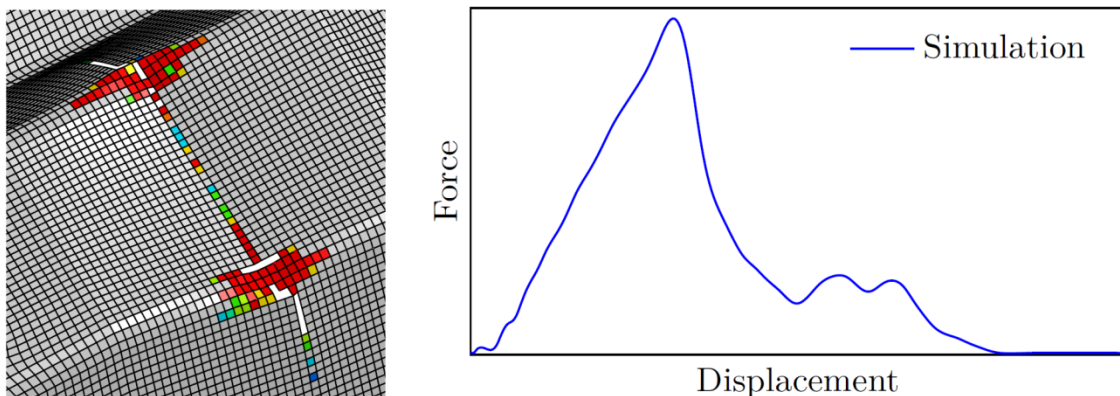


Fig.2: 3-point bending test simulation results: Left, matrix damage and right, force vs. displacement.

### 4 Literature

- [1] Chatiri, M.; Schuetz, T.: Optimized design of Composite Structures Using CAE Process Chain, Nafems Seminar: Simulation of Composites - a closed process chain?, 28<sup>th</sup> – 29<sup>th</sup> . October 2014, Leipzig, Germany.
- [2] Hallquist, J.O.: LS-DYNA Keyword Manual Version 971. Livermore Software Technology Corporation, Livermore, 2013
- [3] Chatiri, M.; Matzenmiller, A.: A Damage-Mode Based Three Dimensional Constitutive Model for Fibre-Reinforced Composites, Computers, Materials & Continua, Vol. 35, No. 3, pp. 255-283, 2013

# New Technologies for Side Impact Model Set up

Thanassis Fokilidis, Athanassios Lioras

BETA CAE Systems S.A.

## 1 Introduction

During the development and design process of a vehicle, Occupant protection in side impact studies has become a standard analysis. One of the most important issues that analysts face in side impact is the adjustment of the passenger's seat and the dummy in the proper position for the laboratory tests. This makes the application of numerical simulations inevitable. Simultaneously, as new legal tests and regulations are continuously introduced, the amount of relative loadcases has been increased dramatically. In order to set up standardized processes that will minimize the complexity and lead time of the numerous side impact CAE simulations, automated and efficient tools are continuously developed by CAE software providers.

## 2 Seat Adjustment in Side Impact

The seat adjustment according to a Side Impact regulation is a very complex procedure, either during a laboratory test or during a CAE simulation process. As far as the CAE simulation is concerned, ANSA pre - processor has implemented an advanced tool that drives the analyst through all the necessary steps a side impact regulation involves. Simultaneously, the corresponding python script code is created, enabling one to parametrize and automate this process. This script can be used for different seats and for all the Side impact regulations. Moreover, the parameterization of the settings of each step, offers the ability for sensitivity analysis considering the definition of different Seating Reference points. Finally, the analyst can have in a short time the final positions for all regulations and for customized applications saved. These positions will be kept throughout the whole process in LS-DYNA files with the use of ANSA Comments. The tool can produce the positions for the Frontal crash regulations as well.

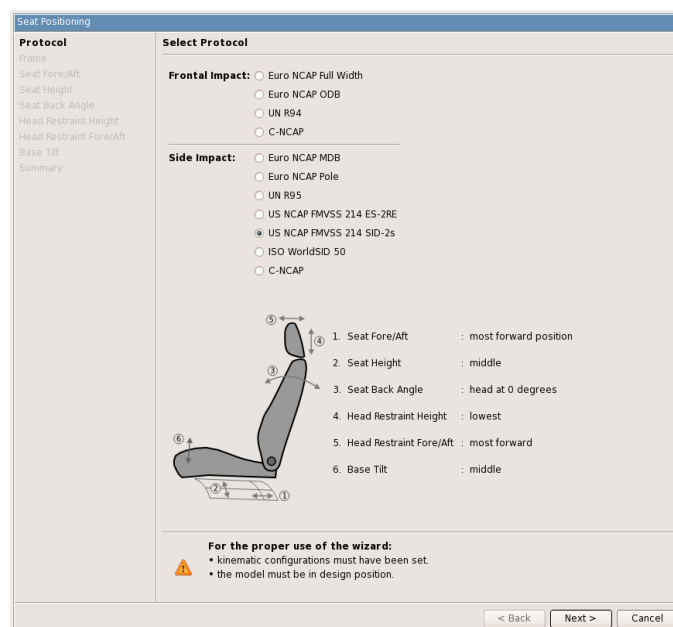


Fig.1: ANSA Seat Positioning tool

## 3 Dummy Handling

A special tool is used in ANSA to position the dummy on the seat positions created by the function explained above. This tool can translate and rotate the whole dummy but also can move its limbs avoiding any penetration between them and the seat structure by using a special 'Contact' algorithm.

Finally all dummy positions for the regulations and the user defined analysis (sensitivity), are saved in LS-DYNA files with the use of ANSA Comments.

#### 4 Seat Depenetration – Seatbelt Application

The dummy depenetration from the seat is a short process in ANSA that needs 3 SET of entities. These SETs contain the entities of the dummy that affect the final shape of the seat, the entities of the seat that will be deformed and some entities that are considered fixed (undeformed). In the current process the depenetration for each dummy – seat position will be applied automatically. Similarly, the seatbelt creation in ANSA is based on ANSA seatbelt entities. The ANSA seatbelt entity offers the flexibility to be created only once, in the design position, and then be reapplied for each dummy – seat position automatically.

#### 5 Automated Massive Loadcase Manager

The final step of the current process is the massive creation of the different LS-DYNA loadcases, for all the saved dummy – seat positions. In ANSA a special tool has been developed for this reason. This tool having as input the files created in the previous steps of the process in combination with the original dummy and seat, moves the seat according to each regulation or user defined position, positions the dummy on it, depenetrates it, reapplies the seatbelt and finally produces the files that will be solved by LS-DYNA. Furthermore, this tool offers the ability for setting a LS-DYNA depenetration loadcase as well.

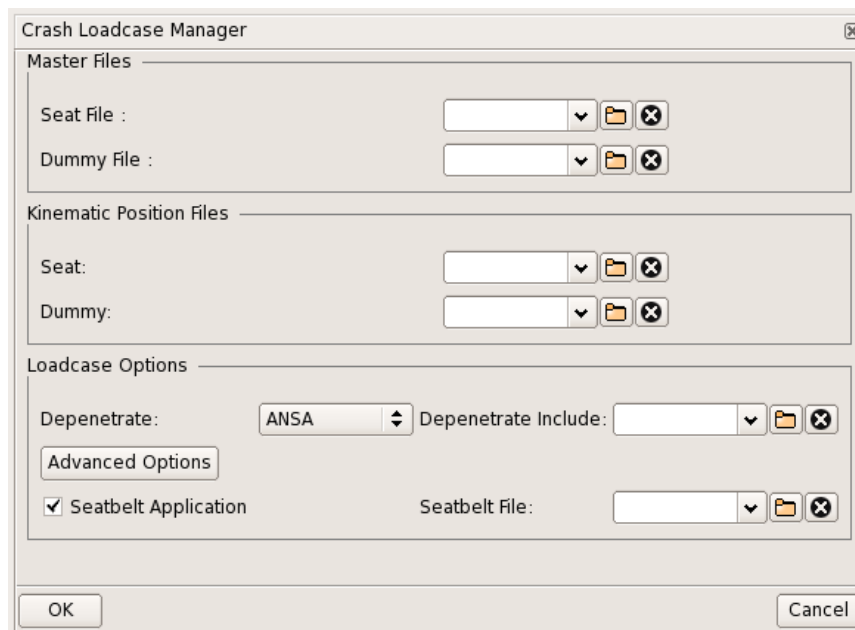


Fig.2: Loadcase Manager tool of ANSA for massive Crash loadcase generation

#### 6 Literature

- [1] ANSA version 15.1.x User's Guide, BETA CAE Systems SA, June 2014
- [2] Halquist, J.o., LS-DYNA Keyword Users Manula Version R7.x, Livermore Software Technology Corporation, Livermore 2014
- [3] carhs, SAFETY COMPANION 2015, 2014



# Speeding up the Pedestrian Protection CAE Process

Gavin Newlands, Chris Archer

Arup

## 1 Introduction

Pedestrian protection is increasingly important to the design and development of the front end of vehicles. The various protocols, impactors and methods relating to pedestrian protection mean that the CAE process can be complex and time consuming. Arup has developed various tools to aid in this process which are used internally within Arup when working on automotive consultancy projects as well as being available externally in the Oasys LS-DYNA® environment software. These tools are available for both head and leg impact analyses. This paper describes the tools and also how they have been used on real world projects.

The tools relate to **Mark-Up, Model Build and Post-Processing.**

## 2 Mark-Up

The mark-up tool within Oasys PRIMER can be used to identify impact zones relating to various protocols (including EuroNCAP v8). The tool will work out the various reference lines that form the bounds of the impact zones. Once the impact zones are determined, the tool can be used to create target points for head/leg impacts in a number of ways:

- Automatically creating a grid of target points over the zones based on specified spacing.
- Manually create target points at specified locations.
- Automatically determine “hard points” below the bonnet based on packaging space and create an appropriate target point on the outer surface of the bonnet based on impactor line of flight.
- Create “robustness points” surrounding specified target points to investigate the sensitivity of impacting at particular locations.

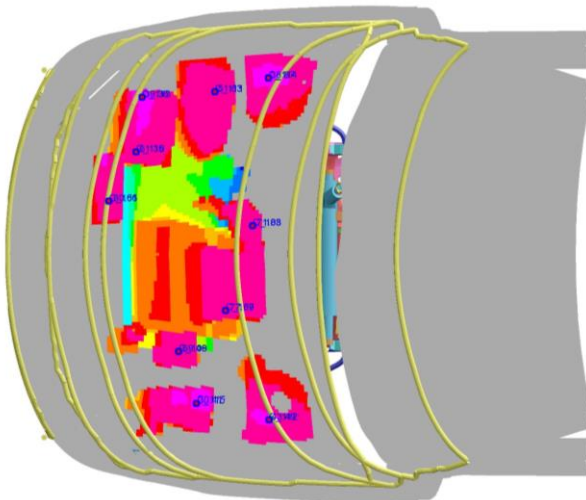


Fig.1: Zone boundary calculation and “hard point” calculation.

## 3 Model Build

Once target points have been specified, the next stage is to build multiple models automatically based on those target points. This is done by:

- Moving the impactor to each target point in turn.

- Depenetrating the impactor according to set rules.
- Outputting models to run in LS-DYNA with \*INCLUDE\_TRANSFORM definitions to move the impactor model to the calculated starting positions.



Fig.2: Multiple build of many LS-DYNA models based on target points.

#### 4 Post-Processing

The final stage is to post-process the many individual LS-DYNA® analyses that are created. Reports can be created automatically using built in templates within Oasys REPORTER. This reduces the time required to manually post-process many runs. Various features are available:

- Produce individual report for each impact.
- Produce a summary report of all individual impacts.
- For EuroNCAP grid method plot results and calculate points scored.
- Create contour plots and “areas of HIC” calculations based on multiple impacts (Head impact - GTR9).

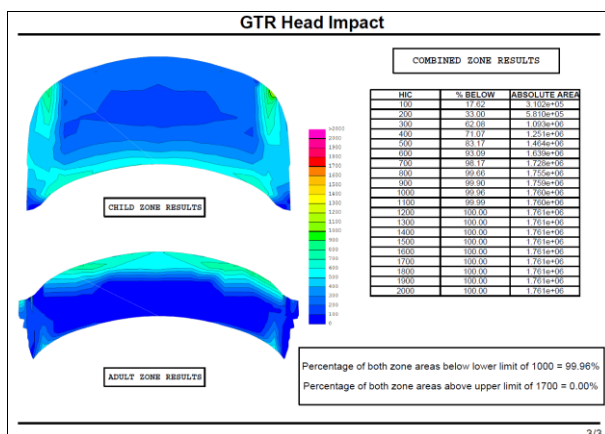


Fig.3: Contour of HIC results.

#### 5 Summary

The pedestrian tools help the user produce models quickly, and spend less time post-processing results. This means input to the design process can be quicker, and the engineer has more time to investigate issues and solutions. The tools are also useful in the initial stages of development for investigating concepts relating to styling, materials, design and packaging.

# Increasing Efficiency of the Design Process with an Isogeometric Analysis Plugin for Siemens NX by Analyzing the CAD Model Directly

M. Breitenberger<sup>1</sup>, B. Philipp<sup>1</sup>, R. Wüchner<sup>1</sup>, K.-U. Bletzinger<sup>1</sup>, S. Hartmann<sup>2</sup>, A. Haufe<sup>2</sup>

<sup>1</sup>Lehrstuhl für Statik, Technische Universität München (TUM), Germany

<sup>2</sup>DYNAMore GmbH, Germany

## 1 Design-through-Analysis process

The bottleneck for today's integrated CAD and CAE tools or for the design-through-analysis process in general is the fact that for each product at least two different geometry representations are used. On the one hand side there is the CAD model and on the other hand side there is the finite element mesh, both representing the same object. The conversion between CAD model and FE model are named meshing and CAD reparameterization, respectively. These operations are error prone, time consuming and cannot fully be automatized. The current approach in industry to close the gap between CAD and CAE is to use more sophisticated and highly specialized tools. In consequence taking benefits out of new algorithms and tools becomes harder and harder.

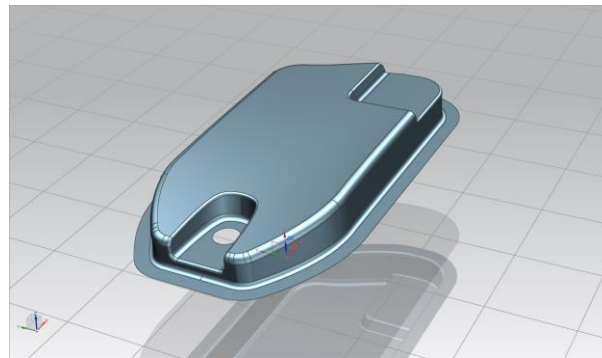


Fig.1: Example of a typical surface CAD model visualized in Siemens NX 9.0 [3]

A completely new approach to overcome the problem of different geometric models is to use one model for both, which means to use the CAD model directly for the analysis. The corresponding approach is called *Analysis in Computer Aided Design (AiCAD)* [2]. The AiCAD concept is based on *isogeometric B-Rep analysis (IBRA)* [2], a new finite element technique. IBRA uses CAD models, especially NURBS based B-Rep models, instead of finite element meshes for approximating solution fields. Thus for IBRA no meshing is necessary (see Fig. 2).

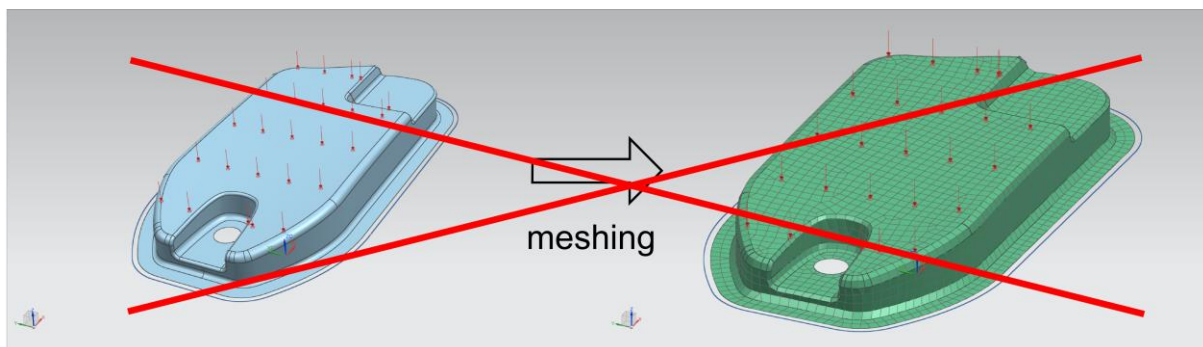


Fig.2: For the proposed AiCAD concept based on IBRA no meshing is necessary

The AiCAD concept is realized in the integrated CAD/CAE/CAM software *Siemens NX 9.0* [3] with a plugin, which extends the CAD tool by the missing analysis functionalities. For the *isogeometric B-Rep analysis* itself the software CARAT++, developed at the Chair of Structural Analysis of the Technische Universität München, is used.

In the following publication the basic steps necessary for the AiCAD concept within *Siemens NX 9.0* are briefly explained. As an example a surface CAD model of an oil sump is used (see Fig. 1).

## 2 Summary

A new approach for unifying CAD and CAE is realized within the integrated CAD/CAE/CAM software *Siemens NX 9.0* [3] using the AiCAD concept [2]. Instead of bridging the gap between CAD and CAE with more sophisticated tools, algorithms, etc. the proposed concept uses just one model for CAD and CAE thus omitting the gap. This can be realized by replacing the classical finite element analysis with the isogeometric B-Rep analysis [2] for the CAE part. IBRA uses CAD models, especially NURBS based B-Rep models, instead of finite element meshes for approximating solution fields.

Fig. 5 shows as an example with a curvature analysis color plot on the deformed CAD geometry. In the same way also stresses can be plotted onto the CAD model.

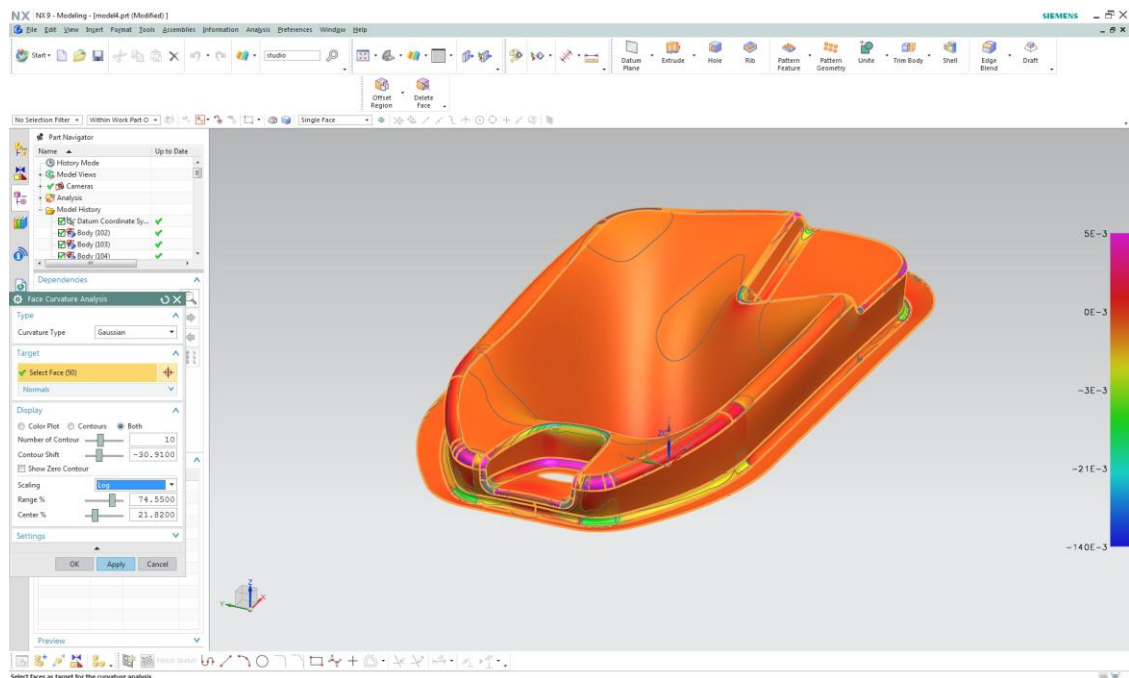


Fig.3: Curvature analysis with color plot on the deformed CAD model

## 3 Literature

- [1] T. Hughes, J. Cottrell, Y. Bazilevs. Isogeometric analysis: CAD, finite elements, NURBS, exact geometry and mesh refinement. *Comput. Methods Appl. Mech. Engrg.* 194 (39–41) (2005) 4135–4195. <http://dx.doi.org/10.1016/j.cma.2004.10.008>
- [2] M. Breitenberger, A. Apostolatos, B. Philipp, R. Wüchner, K.-U. Bletzinger. Analysis in computer aided design: Nonlinear isogeometric B-Rep analysis of shell structures. *Comput. Methods Appl. Mech. Engrg.* 284 (39–41) (2015) 401–457. <http://dx.doi.org/10.1016/j.cma.2014.09.033>
- [3] Siemens NX, <http://www.plm.automation.siemens.com>
- [4] J. Kiendl, K.-U. Bletzinger, J. Linhard, R. Wüchner, Isogeometric shell analysis with Kirchhoff–Love elements, *Comput. Methods Appl. Mech. Engrg.* 198 (49–52) (2009) 3902–3914. <http://dx.doi.org/10.1016/j.cma.2009.08.013>

## SDM & MODEL REDUCTION



---

# Using LoCo for Multi Run Simulations

Richard Luijkx<sup>1</sup>, Marko Thiele<sup>2</sup>

<sup>1</sup>AUDI AG  
<sup>2</sup>SCALE GmbH

## 1 Introduction

For several years now AUDI and DYNAmore (now SCALE) have been working on a new generation of SDM-System called LoadcaseComposer, Short: LoCo. This SDM-System applies several new approaches to Simulation Data Management, such as strict offline capabilities with permanent synchronization of relevant data, consequent and strict version management of all related objects of simulations, novel ontology based approaches for the assembly of components as well as easy customizability and supporting a sustainable process by means of a “continuous integration” approach for frequent upgrades of the entire LoCo deployment.

One of the recent challenges was to enable the user to handle setups for very similar simulations with a minimum of effort and maximum clarity and reusability. In contrary to DOE studies, robustness analyses or optimizations the setup is clearly outlined by regulations such as FMVSS201, ECE-R21 and EuroNCAP testing procedures. Tools such as LS-OPT could have also been used to setup these kind of simulations, however they lag the ease of use, necessary for users to act on a daily basis as well as the tight integration in an SDM system. Furthermore the nature of these setups is such that a later use in design studies or optimizations as a whole will be of interest.

## 2 Setup for Multi Run Simulations

### 2.1 Concepts leading to multi run simulations

LoCo allows process automatization to a huge extent and realizes to some degree a couple of concepts and paradigms known from programming languages.

On the one hand there are includes or components that have to be assembled to complete simulations. They can be compared to data objects of a program. In additions there are the parameters of a setup in LoCo which are rather like variables.

On the other hand there are the attributes in LoCo which to some extend represent conditional statements such as “if”, “than”, “else” and in combination with the RunConfigurations of LoCo these could be interpreted as something similar to the logic of the program or short code fragments.

Having these features, it is already possible to build relatively complex processes for model assemblies, needed to address today’s vehicle development challenges. It is only a logical next step to add the functionality of “loops” to the Simulation Data Management. In the LoCo scope, these loops are implemented in form of “Multi run setups”. By means of a variable (parameter) and corresponding lists the engineer can create loops which will result in the multiple execution (assembly) of a given code fragment (RunConfig) enabling LoCo to reuse all processes and lifecycle management features for each assembly it creates.

The next step already on our road map to complete this analogy will be to provide “multi stage setups” in LoCo. These will allow including one simulation setup within another and could be compared to use “functions” within programming. These will allow engineers to use the complete simulation setup of other departments and disciplines, such as airbag folding or seat assembly, within their own simulation. Referencing to the simulation setup as a whole will allow to dynamically use the already assembled simulation decks of that other department or if necessary run the assembly process, in case there have been parameter changes. Positioning a seat or creating a folded airbag with new parameter sets will be using the process created and approved by the corresponding experts for these topics.

## Setup of simulations

The setup for this kind of "Multiple Run Simulations" and the chosen implementation in LoCo will be discussed in this presentation. Illustrated by an example of a repetitive simulation necessary to develop the protective potential in FMVSS201 lower for a Cockpit Structure. It will be shown the change in the development process enabled by the implementation of the MultiRunSimulation feature in LoCo and how this new paradigm greatly increases the efficiency for simulation engineers who have to deal with these kinds of problems.

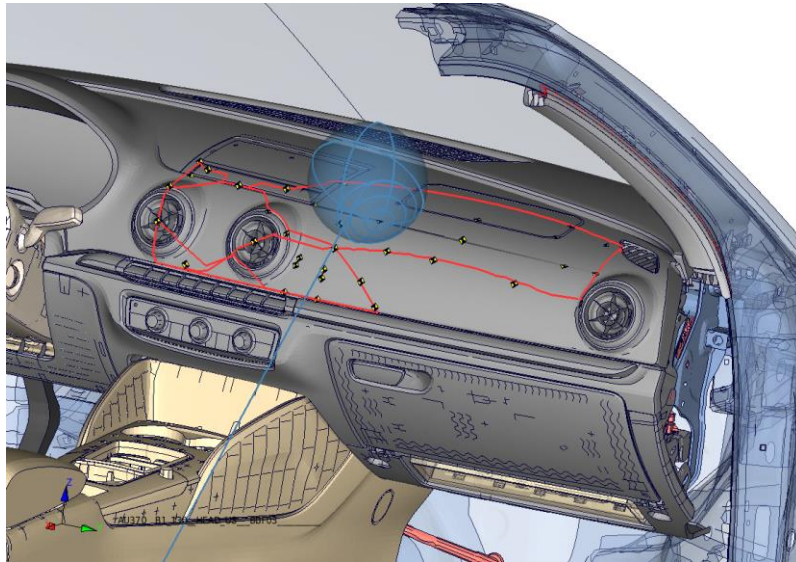


Figure 1: FMVSS201 Area and Impact Points for Head Impact

## 2.2 Post processing

Besides the obvious problem with multiple job assembly as well as job execution there is also the problem that these kinds of simulations need another kind of post processing where the results of all individual simulations are combined to present a complete status for all subloadcases of the underlying problem.

This requires a different approach in post processing of simulation data which is able to take multiple results of different simulation runs into account and generate an overall summarization as an output.

## 3 Summary

With this work we intend to show that in the future, SDM will not only be important in order to effectively handle the large amount of simulation variants and related data but also to provide the means to deal with the continuously growing complexity of the underlying problems engineers are facing nowadays.

These are resulting in more and more complex processes and LoCo is the attempt to give the tools to the engineers necessary to deal with the growing complexity of their daily work.

## 4 Literature

- [1] Sandra Brack, Richard Luijckx (AUDI AG), Marko Thiele, Torsten Landschoff, Heiner Müllerschön (DYNAmore GmbH) „Experience Report on the Application of a Process and Data Management System for CAE at AUDI“, NAFEMS – World Congress, Salzburg 2013



# New Developments in LoCo

Marko Thiele<sup>1</sup>, Torsten Landschoff<sup>1</sup>

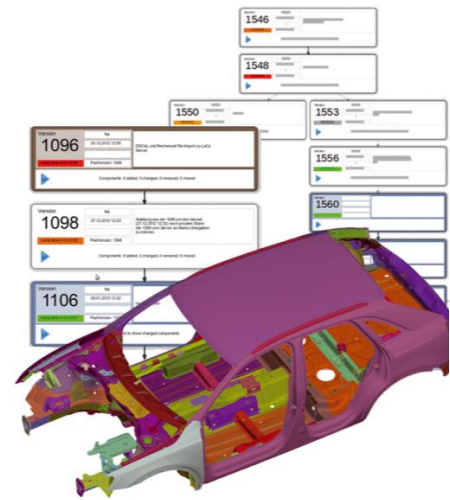
<sup>1</sup>SCALE GmbH

## 1 Introduction

DYNAmore GmbH has founded a new wholly-owned subsidiary known as SCALE GmbH. The aim behind this move is to offer software solutions and IT services for process and data management and for FE methods development in the automotive industry. In the past years, DYNAmore has created a variety of different software products under contract of AUDI. The reason for establishing SCALE GmbH is to further develop and market LoCo and other software products both within the Volkswagen group and beyond it as well. The name SCALE stands for "Scalable Solutions in Simulation Data and Process Management", solutions that can also be used as a shared platform with external development partners.

The core product for simulation and process data management is the innovative software solution LoCo. LoCo is being intensively used at many different simulation units, with currently over 500 users at Audi and at a large number of contracted service providers. LoCo is also being phased in at other brand divisions of the Volkswagen group.

LoCo applies several new approaches to Simulation Data Management, such as strict offline capabilities with permanent synchronization of relevant data, consequent version management of all involved objects by means of simulation models and processes, novel ontology based approaches for the assembly of components as well as easy customizability. LoCo is an open system for the integration of any third party or in-house CAE-product, such as pre-/post processors, FE-solvers, queuing systems, process scripts, etc.



## 2 New Developments in LoCo

The rapidly growing of the user and customer base of LoCo in the past years have led to many additional requirements and new ideas, and consequently to the implementation of new features and concepts. The main focus in the further development of LoCo is to provide a solution which meets best possible all customer requirements and simultaneously keep excellent usability and performance. In the following, already completed features and ongoing developments are listed.

### 2.1 Completed Features

- Completion of the check infrastructure:** Now there are several ways in which users can setup the check infrastructure. New is the possibility to use the solver locally to perform a data check right after modification of include files. This greatly increases the respond time for correcting errors. Engineers are getting notified instantly about errors in their decks and can open the corresponding files right away at the line where the error occurred. On the other hand we introduced functionality where the checks can be done as part of the solving step right before execution on HPC resources. This allows a constant monitoring of the quality of simulation data and measures can be taken in order to prevent users from using faulty decks that might lead to misleading results or excessive use of HPC resources.
- Multi process support:** In order to increase the overall performance of the LoCo rich client now several tasks that are run by LoCo in the background are separated to individual processes each using its own core. By putting the synchronization, the assembly and submit, as well as caching of run objects to dedicated cores of a machine, users can keep having a fluent user experience while working with the GUI.

- **Multi run setups:** Users are now able to easily setup configurations in LoCo where multiple runs with slightly varying setups have to be performed. [1]<sup>1</sup>
- **Advanced searched:** The whole LoCo database can be searched locally and while being offline. Users can search by various properties and combine them to find the desired model data.
- **Preprocessor components:** LoCo now supports the handling of model components in native preprocessor formats such as ANSA database files or Medina BIF files.
- **Copy'n'Paste:** Throughout the whole application the standard mechanisms for Copy'n'Paste such as short cuts or context menu actions, can be used to move data from one point to another.
- **Refactoring of various GUI components:** Various GUI components such as the parameter tables, the assembly dialog and the dialogs for the history comments have been refactored to adapt them to the current needs of the engineers.
- **Import/Export for integrating offline users:** Through this functionality it is now possible to integrate users that are not connected to the network where the LoCo-Server resides. The offline users can still work in the same environment within LoCo just like regular users and their progress is seamlessly integrated into the central LoCo-database by importing their data when it's ready.

## 2.2 Features in Development

- **Encryption for local database:** The encryption of the locally stored includes has been implemented in LoCo since about 2013. This functionality will be completed by extending it to also encrypt the locally used sqlite database. The encryption can be performed by using smart cards allowing for two factor encryption.
- **Data deduplication:** Applying this new compression technology, developed as part of the ongoing VAVID project [3], LoCo will be able to cut down the storage and bandwidth requirements by another factor of 6-8 compared to the actual implementation. Related to uncompressed data this is a factor of compression of about 20-25.
- **Support for SDM-Zip:** In cooperation with SIDACT and AUDI new compression techniques are investigated leading to higher compression factors of about 2-3 for simulation output data compared to actual FEMZIP implementations.

## 2.3 Features on the Roadmap

- **Reducing the visibility:** In order to achieve that using LoCo becomes easier for engineers to be used in big setups with many disciplines, KeyUsers will be enabled to configure what exactly is visible for certain groups of end users.
- **Multi stage setups:** Through this feature user will be able to create setups in which they can reference to the runs of other teams to include their results. This way, for example, it will be possible to include the output of an airbag folding simulation (folded airbag) into another setup for designing a restraint system.
- **Simple client:** Using a whole new GUI-Framework the next generation of LoCo will be started by implementing a simple client. This client will be much easier to use and focus on the core functionality of LoCo while keeping compatible with current data.

## 3 Literature

- [1] Richard Luijckx: "Using LoCo for Multi Run Simulations", 10th European LS-DYNA Conference, Würzburg, Germany
- [2] Wikipedia: "Continuous Integration", [http://en.wikipedia.org/wiki/Continuous\\_integration](http://en.wikipedia.org/wiki/Continuous_integration)
- [3] VAVID - BMBF Big Data research program, <http://www.pt-it.pt-dlr.de/de/3138.php>
- [4] Meister, D., Kaiser, J., Brinkmann, A., Cortes, T., Kuhn, M., & Kunkel, J. (2012, November). A study on data deduplication in HPC storage systems. In Proceedings of the Int. Conf. on High Perf. Computing, Networking, Storage and Analysis (p. 7). IEEE Computer Society Press.
- [5] He, Q., Li, Z., & Zhang, X. (2010, October). Data deduplication techniques. In Future Information Technology and Management Engineering (FITME), 2010 Int. Conf. on Future Information Technology and Management Engineering (FITME) (Vol. 1, pp. 430-433). IEEE.

---

<sup>1</sup> Please consider attending the presentation of Richard Luijckx on the topic „Using LoCo for Multi Run Simulations“ [1]

# Machine Learning Approaches for Repositories of Numerical Simulation Results

Jochen Garcke<sup>1,2</sup>, [Rodrigo Iza Teran](#)<sup>1</sup>

<sup>1</sup>Fraunhofer-Insitut SCAI, Numerical Data-Driven Prediction, Germany

<sup>2</sup>Universität Bonn, Institute for Numerical Simulation, Germany

## 1 Introduction

During the research and development process, engineers easily generate several hundred variants of a detailed finite element model (several million nodes) which simulate different operating conditions of a product. Post-processing software tools are required for the 3D visualization of the geometry and the needed inspection of the associated design variables of each configuration. A detailed comparative analysis of more than a few simulations one by one is time consuming. Data management systems (SDM) alleviate this problem, nevertheless such systems use post processing quantities that are single scalar quantities or vectors assumed to represent the full 3D detailed deformation (or associated quantities like velocity or acceleration). Indeed an efficient analysis of hundreds of designs changes using the full raw data is a challenge.

Approaches that attempt to overcome these limitations have been proposed in recent years, see [1], [2]. In line of this research we propose to use nonlinear dimensionality reduction in the virtual product development process. Methods of machine learning are used that are known to be able to recover the so called intrinsic geometrical structure of the data in the presence of nonlinear correlations in the data, recovering such nonlinear structures can be very effective for analyzing a number of simulations simultaneously (see [2]). In this work we propose to combine machine learning into an SDM system to enable a fast evaluation of complete 3D deformations of thousands of finite element design variants concurrently. This improves considerably the usefulness of an SDM-System supporting a faster improved post processing of many simulation results.

## 2 Nonlinear Dimensionality Reduction

Nonlinear dimensionality reduction is a very active area of research in machine learning in recent years. For our setting each simulation can be treated as a point in a very high dimensional space given by the order of the discretization of the finite element mesh. The principal idea of these methods consist in the assumption that the data dimensionality is actually much lower, methods have been developed precisely to find such a low dimensional parametrization of data sets.

To find such low dimensional structures, this work concentrates on so called kernel methods, which are based on the construction of a similarity matrix with coefficients calculated using a kernel function  $k(x, y)$ . This function is evaluated for all combinations of available datasets so that a matrix of dimension  $m \times m$  is obtained where the number of simulations is  $m$ . The singular value decomposition (SVD) of the matrix is used to extract the eigenvectors corresponding to largest eigenvalues and they are used as low dimensional parametrization for data analysis. In this work we use a specific variant of a kernel method called diffusion map, for details about the method see [3], [4].

A very important observation is that post processing can be speed-up by the use of the method since the task of analyzing many large 3D deformations according to their similarity can be easily done.

## 3 A SDM Approach for Analyzing Numerical Simulation Data

Several steps are necessary to introduce dimensionality reduction into an existent SDM system, some of them can be easily incorporated while others need still need to be developed: 1) **data extraction** – the raw data for the analysis are obtained directly from the simulation, 2) **pre-processing** – transformation of the raw data to allow efficient calculation of step 3, 3) **dimensionality reduction** – in this step a low dimensional representation is obtained, 4) **exploration** – data analysis tasks can efficiently be realized because the information gets parametrized after step 3.

After application of dimensionality reduction, the data exploration in Step 4 should work interactively. A visualization and analysis framework should allow the explorative analysis of all simulations along the parametrized representation. An example of the use of the approach is shown in the next section.

#### 4 Robustness Analysis in Frontal Crash

For this case study we investigate a current and publically available Toyota model with 998,000 nodes and corresponding elements. The position of the bumper was changed along a circle which results in an observably different crash behaviour during a frontal impact with a barrier (see Figure 1 a). A total of 243 numerical simulations were performed using LS-DYNA simulation software. A total of 26 intermediate time steps were saved for each run.

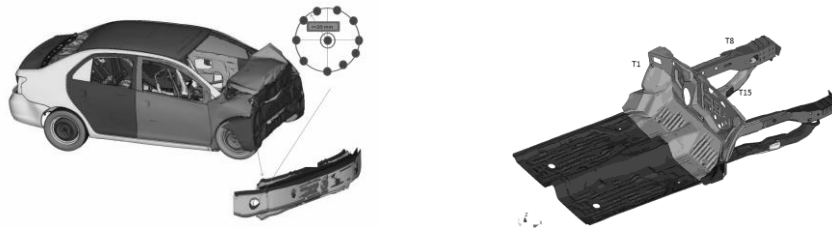


Fig.1: a) Variation of bumper positions along a circle. b) Structure taken for the analysis.

For the analysis, the deformation of the firewall and the lateral beams supporting the frontal crash were extracted (see Figure 1 b for the extracted parts). A total of 243 feature vectors, each of dimension  $N=25748$  were obtained using the total displacements at a specific time step. A method of dimension reduction, diffusion maps, were applied and the resulting low dimensional representation allowed the identification of three different deformation modes (see the clusters on Figure 2 a), each of them corresponding to a different angle (see Figure 2 b (only one of the beams is shown for clarity)).

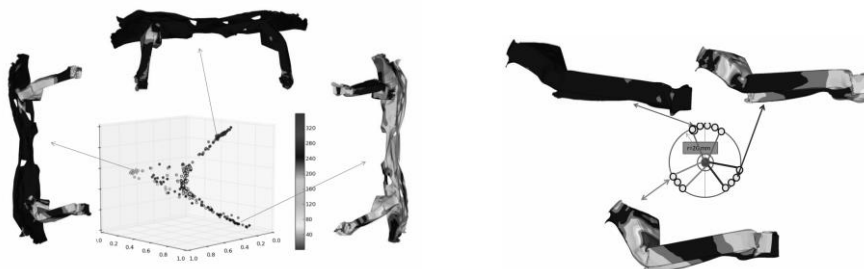


Fig.2: a) Low dimensional representation showing 3 deformation modes. b) Angle dependence of the modes for one of the beams from the structure obtained making use of the embedding in a).

#### 5 Overview and Perspectives

It can be seen, that with the help of these new technologies a conceptually different approach to the analysis of the large data arising in the virtual product development process becomes possible. The approach allows an intuitive and interactive handling of the simulation results and provides to the development engineer simple possibilities for the comparative and concurrent examination of many simulation results.

#### 6 Literature

- [1] Bohn B, Garcke J, Iza Teran R., Paprotny A., Peherstorfer U., Schepsmeier U. and Thole C. A.: "Analysis of car crash simulation data with nonlinear machine learning methods", Proceedings of the ICCS 2013, vol 18, Procedia Computer Science, Elsevier 2013, 621-630
- [2] Iza Teran R.: "Enabling the analysis of finite element simulation bundles", International Journal for Uncertainty Quantification, (1), 2104.
- [3] Coifman R.: "Diffusion Maps", App. Harmonic Analysis, 21 (1), 2006, 5-30
- [4] Wang J., "Geometric Structure of High-Dimensional Data and Dimensionality Reduction", Springer 2011.

# Small-Overlap Crash Simulation Challenges and Solutions

Sri Rama Murty Arepalli, Ganesh Kini, Andrea Gittens

COE Studies, ESI Group

Insurance Institute of Highway Safety, USA, has introduced the small overlap crash test in 2012. As usual this new regulation saw many cars failing to pass the proposed rating. The main reason for failure is no definite crush zone and less protection along outer edge of the car body. Different car companies have come up with several solutions. As it's a new regulation, the simulations face issue of time for identifying the intrusions and IIHS rating. As the regulation calls for more and more simulations there exists always a need of pre and post processors to quickly identifying the IIHS ratings.

LS-DYNA solver is used for the studies. ESI Group has developed tools to handle this challenge. The studies are made on a public domain car model 'Taurus'. A template in Visual-Process Executive sets up a frontal crash model, a macro in Visual-Crash DYNA places different overlap barriers, shapes and offsets and finally a Visual-Viewer template plots all the intrusions and shows the IIHS ratings.

There are several approaches to handle the challenges of the small overlap crash tests. The traditional approach of introducing crush zone may not work always as there is no definite load path. To demonstrate the tools and its capabilities, the current study chose to vary the steel properties of load bearing members. Tools will identify the components that are having higher internal energy and boost up the properties of the components based on pre-set material schemes. Visual-Crash DYNA macros create the required LS-DYNA input. After LS-DYNA solves the problem, results are automatically plotted and reported by Visual-Viewer templates. These reports provide the direction and allow a comparison study.

The study ends up in preparing a summary report of different studies carried out on the car model. The report consists of the changes done in terms of the material, its intrusion plots and the IIHS rating chart.



# WORKSHOPS





---

# WORKSHOPS

**Setting up an ICFD Simulation in LS-DYNA**Room 7, Monday, 15 June, 15:40 – 16:55

---

**Material Parameter Identification with LS-OPT**Room 8, Monday, 15 June, 15:40 – 16:55

---

**Setting up an EM Simulation in LS-DYNA**Room 7, Monday, 15 June, 17:30 – 18:45

---

**Meshing and Postprocessing with LS-PrePost**Room 8, Monday, 15 June, 17:30 – 18:45

---

**Material Failure using GISSMO**Room 8, Tuesday, 16 June, 08:20 – 10:00

---

**Creating Forming Simulations with OpenForm**Room 8, Tuesday, 16 June, 10:30 – 12:10

---

**DEM Modeling in LS-DYNA**Room 7, Tuesday, 16 June, 15:45 – 17:00

---

**New Developments in LoCo– The innovative SDM Solution**Room 8, Tuesday, 16 June, 15:45 – 17:00

---

**Setting up an Implicit Simulation in LS-DYNA**Room 8, Tuesday, 16 June, 17:25 – 18:40

---

**Dynamics Plastic Material Characterization with the 4a/Impetus Pendulum**Room 7, Wednesday, 17 June, 08:30 – 10:10

---

**Welding and Heat Treatment with LS-DYNA**Room 7, Wednesday, 17 June, 10:40 – 12:20

---

**Sheet Metal Forming Simulation with eta/DYNAFORM**Room 8, Wednesday, 17 June, 08:30 – 10:10

---

**Modeling Composites in LS-DYNA**Room 8, Wednesday, 17 June, 10:40 – 12:20

---







DYNAmore Gesellschaft für FEM Ingenieurdienstleistungen mbH

Industriestr. 2  
70565 Stuttgart, Germany  
Tel.: +49 (0)711 - 45 96 00 - 0  
Fax: +49 (0)711 - 45 96 00 - 29  
E-Mail: [info@dynamore.de](mailto:info@dynamore.de)  
[www.dynamore.de](http://www.dynamore.de)

Subsidiaries in Sweden, Italy and Switzerland.



Livermore Software Technology Corp. (LSTC)

7374 Las Positas Road  
Livermore, CA, 94551 USA  
Tel.: +1-925-449-2500  
Fax: +1-925-449-2507  
[www.lstc.com](http://www.lstc.com)